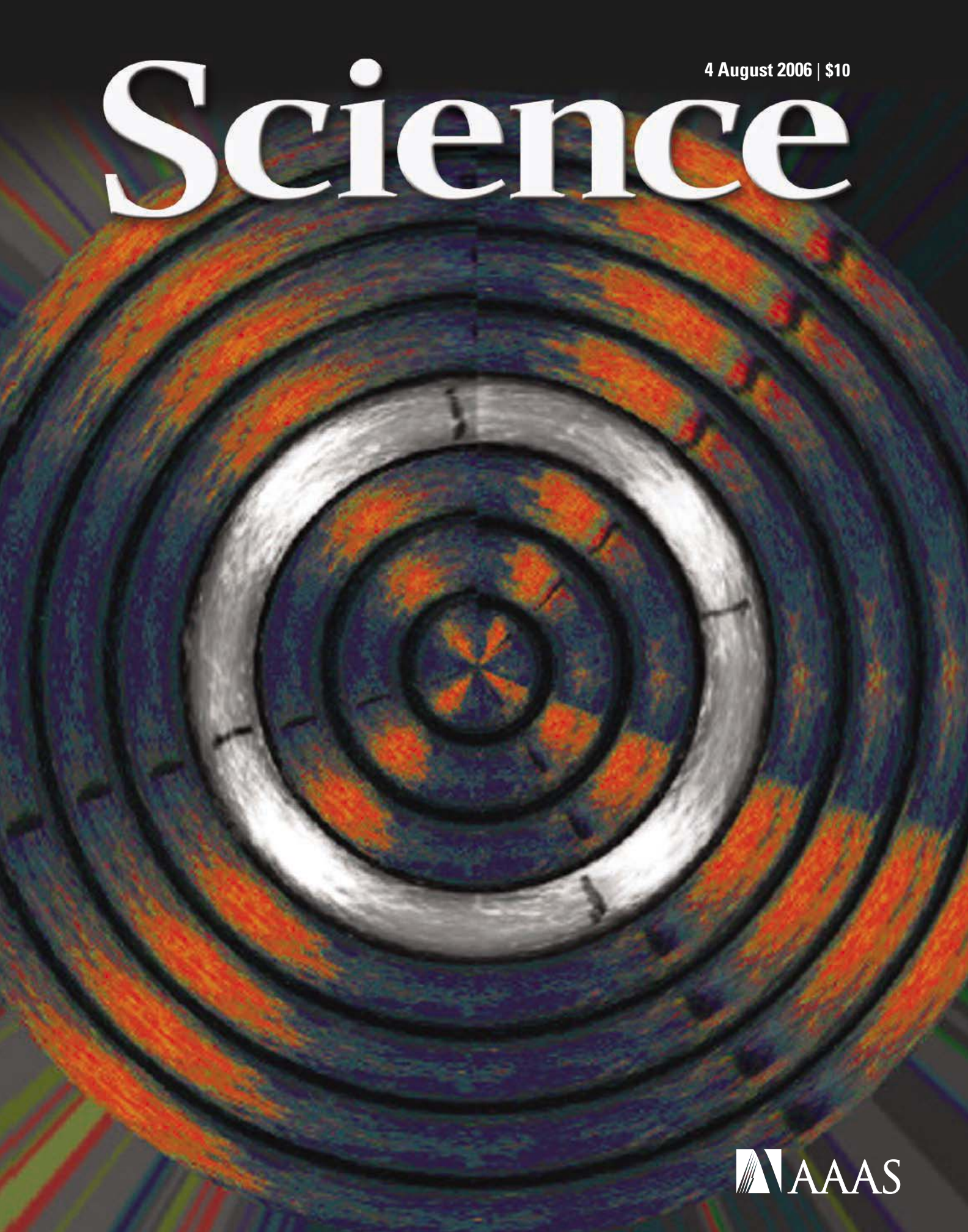


4 August 2006 | \$10

Science



 AAAS

MX3005P™ System
Most Flexible

MX3000P® System
Most Affordable



Performance runs in the family.
Choose the personal QPCR system that's right for you.

Stratagene now offers two affordable, fully-featured quantitative PCR (QPCR) systems. The new five-color Mx3005P™ QPCR System includes expanded features to support a wider range of real-time QPCR applications, such as simultaneous five-target detection and alternative QPCR probe chemistries. The Mx3000P® QPCR System is still the most affordably priced four-color 96-well system available.

- A four- or five-color instrument, with user-selected filters
- Advanced optical system design for true multiplexing capability, and wider application support
- MxPro™ QPCR Software with enhanced data analysis and export functionality

Need More Information? Give Us A Call:

Stratagene US and Canada

Order: 800-424-5444 x3

Technical Service: 800-894-1304 x2

Stratagene Europe

Order: 00800-7000-7000

Technical Service: 00800-7400-7400

Stratagene Japan K.K.

Order: 3-5821-8077

Technical Service: 3-5821-8076

www.stratagene.com

Mx3000P® is a registered trademark of Stratagene in the United States.
Mx3005P™ and MxPro™ are trademarks of Stratagene in the United States.





Astonishingly robust. Want to try some?



Comparison of amplifications using *Taq* DNA Polymerase and GoTaq® DNA Polymerase. B; *Taq* DNA Polymerase in Storage Buffer B. A; *Taq* DNA Polymerase in Storage Buffer A. C; GoTaq® DNA Polymerase in Colorless GoTaq® Reaction Buffer. G; GoTaq® DNA Polymerase in Green GoTaq® Reaction Buffer.

Promega GoTaq® Polymerase delivers better performance and it's more convenient. Plus, you get the same Promega PCR Guarantee as *Taq* in Buffer A or Buffer B. You'll save time, because GoTaq serves as both a loading buffer and tracking dye. This robust enzyme reliably amplifies large or small products.

Here's a sweet deal...try it FREE!

www.promega.com/gotag/

PROMEGA CORPORATION • www.promega.com



Promega

GE Healthcare

as sure as

two bodies of matter attract each other proportional to their masses inversely proportional to the square of the distance between them.

Sir Isaac Newton 1687



Amersham from GE Healthcare. It's not just that **Amersham SPA** is now regarded as the 'gold standard' for biological assay development, cited in over 800 peer-reviewed references.

It's not just that **Amersham Radiochemicals** were first on the market in 1947 for peacetime research, and that we prepared the first compound labelled with ^{14}C .

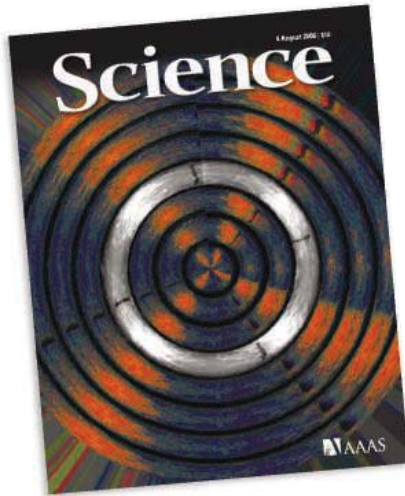
It's that with any Amersham product you get consistently accurate results every time. Leaving the spark of genius up to you. **Life Sciences Re-imagined.**



imagination at work

Amersham

www.gehealthcare.com/lifesciences



COVER

The fungus *Neurospora crassa* expressing spores in a circadian rhythm, distorted into a circle with four parts representing the four stages of the cell cycle. Unanticipated interregulation links the circadian cycle with cell division through modulation of a cell cycle checkpoint kinase, as described on page 644.

Illustration: L. Larrondo

DEPARTMENTS

- 587 *Science Online*
- 588 *This Week in Science*
- 592 *Editors' Choice*
- 594 *Contact Science*
- 595 *NetWatch*
- 597 *Random Samples*
- 611 *Newsmakers*
- 691 *New Products*
- 692 *Science Careers*

EDITORIAL

- 591 *The G8 on Energy: Too Little*
by Martin Rees

NEWS OF THE WEEK

- The Undisclosed Background of a Paper on a Depression Treatment 598
- At Last, Methane Lakes on Saturn's Icy Moon Titan—But No Seas 598
- China Grapples With Seismic Risk in Its Northern Heartland 599
- Singapore-Hopkins Partnership Ends in a Volley of Fault-Finding 600
- The Emotional Brain Weighs Its Options 600
>> Report p. 684
- Hybrid Viruses Fail to Spread 601
- SCIENTESCOPE** 601
- High-Temperature Superconductors Feel the Vibe After All 602
- Physicists See Solid Helium Flow, But Not in the Most Exciting Way 603
>> Science Express Report by S. Sasaki et al.

NEWS FOCUS

- Making Connections 604
Looking for Patterns
- Space Weather Forecasters Plan a Boost in Surveillance Missions 607
- Waiting for the Monsoon 608
- Congress Dials Back Research on Understanding Terrorism 610



608

LETTERS

- Boycott of Israeli Academics Misguided *M. Fainzilber* 612
- Keeping Bandits at Bay? *H. Scales et al.*
Response T. P. Hughes et al.
- Making U.S. Graduate Education More Diverse
C. R. Barrera
- Recognizing Computational Science *J. Bland-Hawthorn*

BOOKS ET AL.

- An Argument for Mind* 616
J. Kagan, reviewed by J. E. Grusec

POLICY FORUM

- Resolving Mismatches in U.S. Ocean Governance 617
L. B. Crowder et al.

PERSPECTIVES

- A New Class of Earthquake Observations 619
F. F. Pollitz
>> Report p. 658
- Caving In to New Chronologies 620
G. M. Henderson
- Solving Laplace's Lunar Puzzle 622
K. Innanen
>> Report p. 652
- How Do Aerosols Affect Cloudiness and Climate? 623
F.-M. Bréon
>> Report p. 655
- Extinguishing a Cell Cycle Checkpoint 624
M. A. Hoyt
>> Report p. 680
- Timing the Sexual Development of Parasites 626
S. L. Hajduk
>> Report p. 667
- Sugar Determines Antibody Activity 627
D. R. Burton and R. A. Dwek
>> Report p. 670

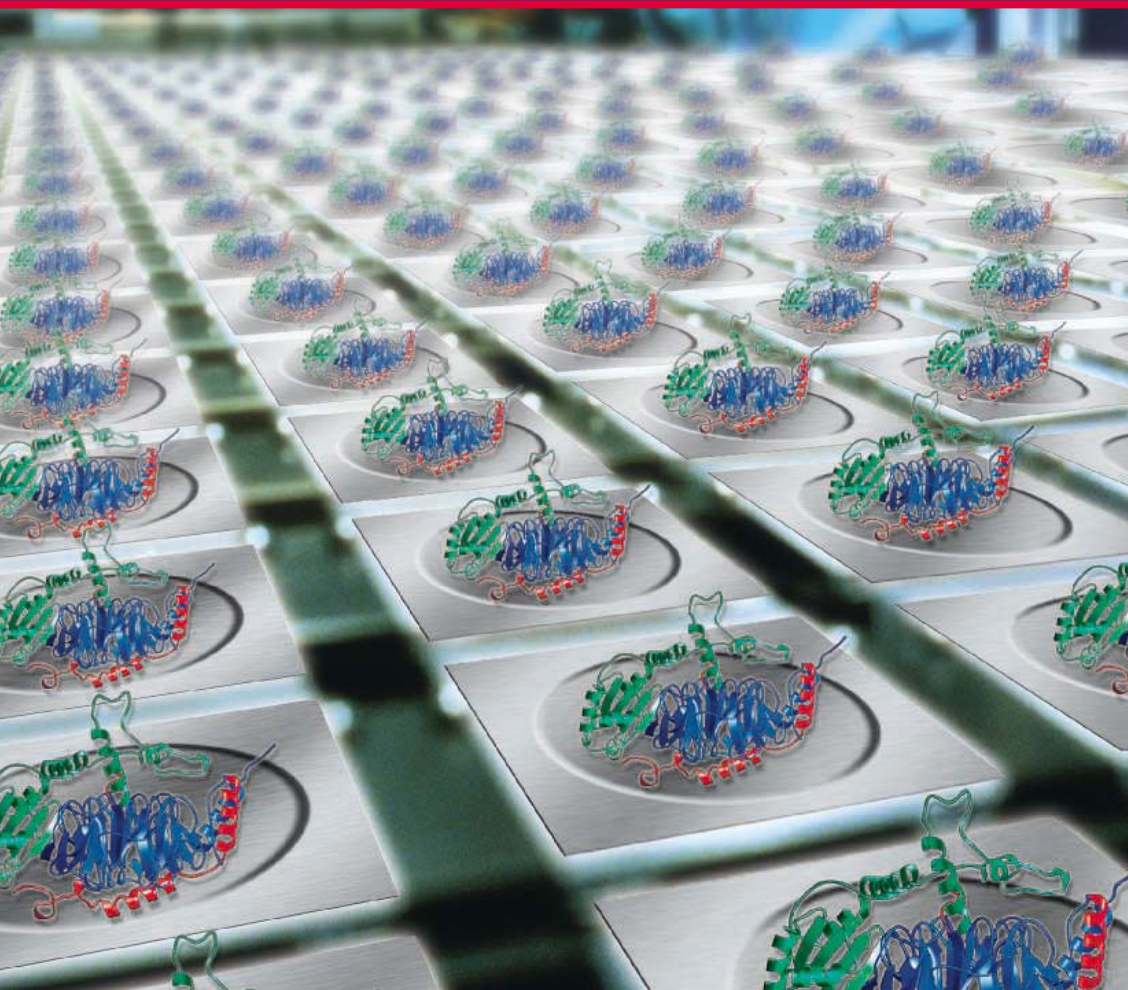


620

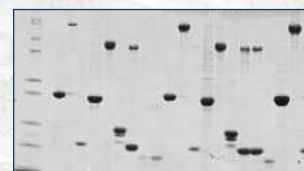
CONTENTS continued >>

Systems Biology — Proteins and Proteomics

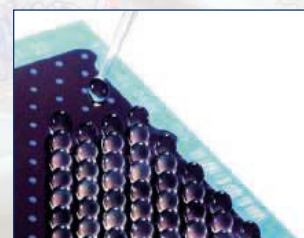
Standardized solutions for proteins



More reproducibility, streamlined crystallization*



More proteins, purer, faster



More peptide matches, more protein hits

Success with proteins — made possible by QIAGEN's expertise!

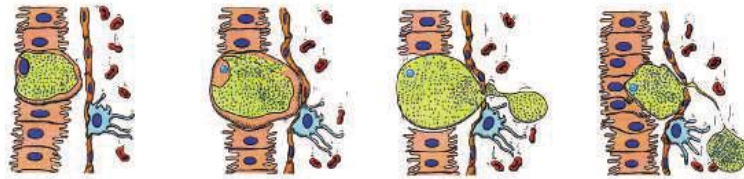
QIAGEN's comprehensive protein portfolio will help you rise to the challenge of working with proteins. QIAGEN provides easy-to-use, integrated solutions to help you succeed with:

- Expression
- Purification
- Detection
- Assay
- Crystallization
- MALDI sample prep
- Proteomics sample prep
- Automation
- Fractionation

Find a standardized solution for your protein challenge at www.qiagen.com/protein !

* Image shows *E. coli* gyrase A C-terminal domain crystals. Courtesy of Alex Ruthenburg from Prof. Verdine's laboratory, Harvard University, Boston, USA. For up-to-date trademarks and disclaimers, see www.qiagen.com . PROTAG0406S1WW © 2006 QIAGEN, all rights reserved.





SCIENCE EXPRESS

www.scienceexpress.org

ASTROPHYSICS

Discovery of a Young Planetary-Mass Binary
R. Jayawardhana and V. D. Ivanov

Two young brown dwarfs, one with a mass 14 times that of Jupiter and the other 7 times as massive, orbit each other, forming a binary system.

10.1126/science.1132128

PHYSICS

Superfluidity of Grain Boundaries and Supersolid Behavior
S. Sasaki, R. Ishiguro, F. Caupin, H. J. Maris, S. Balibar

Experiments show that superfluid flow along grain boundaries in solid ⁴He may explain its supersolid behavior.

>> *News story p. 603*

10.1126/science.1130879

IMMUNOLOGY

Manipulation of Host Hepatocytes by the Malaria Parasite for Delivery into Liver Sinusoids

A. Sturm et al.

The malaria parasite moves from liver to blood during infection by inducing liver cells to die and, in the process, to bud off vesicles containing the parasite that cannot be detected by the immune system.

10.1126/science.1129720

CELL BIOLOGY

Human IRGM Induces Autophagy to Eliminate Intracellular Mycobacteria
S. B. Singh, A. S. Davis, G. A. Taylor, V. Deretic

A small GTP binding protein, associated with innate immunity, is required for cells to use large membrane-bound organelles to sequester and eliminate bacteria that have invaded their cytoplasm.

10.1126/science.1129577

TECHNICAL COMMENT ABSTRACTS

ECOLOGY

Comment on "Post-Wildfire Logging Hinders Regeneration and Increases Fire Risk" 615

M. Newton et al.

[full text at www.sciencemag.org/cgi/content/full/313/5787/615a](http://www.sciencemag.org/cgi/content/full/313/5787/615a)

Comment on "Post-Wildfire Logging Hinders Regeneration and Increases Fire Risk"

B. N. Baird

[full text at www.sciencemag.org/cgi/content/full/313/5787/615b](http://www.sciencemag.org/cgi/content/full/313/5787/615b)

Response to Comments on "Post-Wildfire Logging Hinders Regeneration and Increases Fire Risk"

D. C. Donato et al.

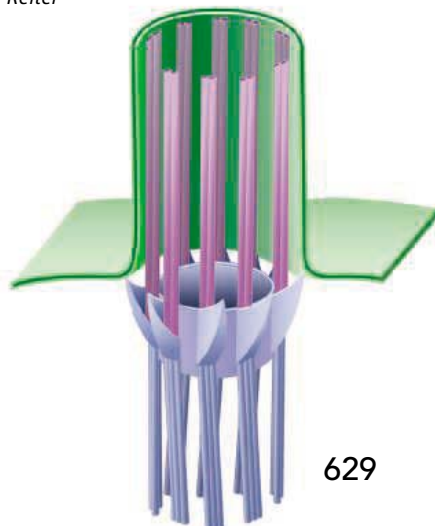
[full text at www.sciencemag.org/cgi/content/full/313/5787/615c](http://www.sciencemag.org/cgi/content/full/313/5787/615c)

REVIEW

CELL BIOLOGY

The Primary Cilium as the Cell's Antenna: Signaling at a Sensory Organelle 629

V. Singla and J. F. Reiter



629

BREVIA

BIOPHYSICS

Fibrin Fibers Have Extraordinary Extensibility and Elasticity 634

W. Liu et al.

The fibrin fibers that support blood clots can be stretched to nearly three times their normal length without losing elasticity and up to six times before rupturing.

RESEARCH ARTICLES

PLANETARY SCIENCE

Spitzer Spectral Observations of the Deep Impact Ejecta 635

C. M. Lisse et al.

The nucleus of comet Tempel 1 is made of minerals and organic compounds from throughout the proto-solar nebula.

DEVELOPMENTAL BIOLOGY

Netrins Promote Developmental and Therapeutic Angiogenesis 640

B. D. Wilson et al.

The netrins, developmental factors that guide axons as they find their targets, also direct the formation of new blood vessels.

CIRCADIAN RHYTHMS

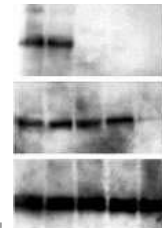
The *Neurospora* Checkpoint Kinase 2: A Regulatory Link Between the Circadian and Cell Cycles 644

A. M. Pregarie et al.

A fungal ortholog of a key regulator for the mammalian cell cycle links cell division with the circadian cycle, gating the ability of DNA damage to reset the clock.

CONTENTS continued >>

LESS
SAMPLE.



MORE
STORY.



Sensitive and sensible, BioSource™ ELISA Kits deliver relevant data from as little as 50 µl. Or fewer than 10,000 cells if you're working with phosphoELISA™ Kits. We offer a wide range of ELISA and phosphoELISA™ Kits for measuring cytokines and phosphorylated proteins— with the exacting sensitivity and reproducibility you need. And faster incubation times. What are you waiting for? See how far your sample can go with BioSource™ ELISA Kits at www.invitrogen.com/elisa.

 **invitrogen™**

REPORTS

PHYSICS

Imaging the Mott Insulator Shells by Using Atomic Clock Shifts 649
G. K. Campbell et al.
 High-resolution spectroscopy reveals the layered electron band structure that produces an insulating, instead of conducting, cloud of cold rubidium atoms.

PLANETARY SCIENCE

Evidence for a Past High-Eccentricity Lunar Orbit 652
I. Garrick-Bethell, J. Wisdom, M. T. Zuber
 The equatorial bulge of the Moon implies that it was in a highly eccentric orbit close to Earth soon after its formation and during its solidification. >> *Perspective p. 622*

ATMOSPHERIC SCIENCE

Smoke and Pollution Aerosol Effect on Cloud Cover 655
Y. J. Kaufman and I. Koren
 A higher concentration of aerosol particles increases cloudiness, but this effect is offset by the amount of sunlight absorbed by the clouds. >> *Perspective p. 623*

GEOPHYSICS

Crustal Dilatation Observed by GRACE After the 2004 Sumatra-Andaman Earthquake 658
S.-C. Han, C. K. Shum, M. Bevis, C. Ji, C.-Y. Kuo
 Changes in Earth's gravity after the 2004 Sumatra-Andaman earthquake reveal that the quake compressed and extended the local crust and mantle, changing their densities.
 >> *Perspective p. 619*

CHEMISTRY

Synthesis of Biaryls via Catalytic Decarboxylative Coupling 662
L. J. Gooßen, G. Deng, L. M. Levy
 A copper catalyst in tandem with palladium can generate useful biaryl compounds from benign carboxylates rather than hazardous organometallics.

SOCIOLOGY

Gender Differences in Patenting in the Academic Life Sciences 665
W. W. Ding, F. Murray, T. E. Stuart
 A longitudinal study shows that women scientists have patented their findings at less than half the rate of men, perhaps because of fewer collaborations and industrial contacts.

MICROBIOLOGY

Regulation of Sexual Development of *Plasmodium* by Translational Repression 667
G. R. Mair et al.
 An essential RNA helicase sequesters mRNAs in the developing malaria parasite until they are needed, presenting a likely target for therapeutics. >> *Perspective p. 626*

IMMUNOLOGY

Anti-Inflammatory Activity of Immunoglobulin G 670
Resulting from Fc Sialylation
Y. Kaneko, F. Nimmerjahn, J. V. Ravetch
 Inflammatory antibodies can be converted to potentially useful anti-inflammatory agents by altering their attached sugar residues.
 >> *Perspective p. 627*

CELL BIOLOGY

N- to C-Terminal SNARE Complex Assembly Promotes Rapid Membrane Fusion 673
A. V. Pobbati, A. Stein, D. Fasshauer
 A preassembled complex of fusion proteins can fuse membranes in vitro as rapidly as is observed during secretion in intact neurons.
 >> *Report p. 676*

CELL BIOLOGY

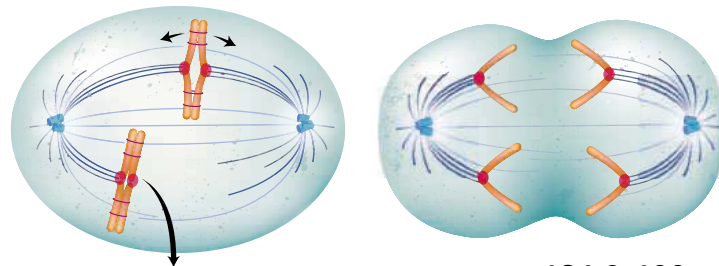
A Clamping Mechanism Involved in SNARE-Dependent Exocytosis 676
C. G. Giraud, W. S. Eng, T. J. Melia, J. E. Rothman
 The protein complexin prevents synaptic vesicles from fusing until calcium is sensed by another protein, synaptotagmin, to initiate fusion. >> *Report p. 673*

CELL BIOLOGY

Anaphase Inactivation of the Spindle Checkpoint 680
W. J. Palframan et al.
 The system that ensures that all chromosomes are properly attached to the spindle poles during cell division is later inactivated by the interaction of two proteins. >> *Perspective p. 624*

NEUROSCIENCE

Frames, Biases, and Rational Decision-Making in the Human Brain 684
B. De Martino, D. Kumaran, B. Seymour, R. J. Dolan
 The framing effect—in which the way a question is posed alters the answer—is a result of biases arising in the amygdala, a brain region involved with emotion. >> *News story p. 600*



624 & 680



ADVANCING SCIENCE. SERVING SOCIETY

SCIENCE (ISSN 0036-8075) is published weekly on Friday, except the last week in December, by the American Association for the Advancement of Science, 1200 New York Avenue, NW, Washington, DC 20005. Periodicals Mail postage (publication No. 484460) paid at Washington, DC, and additional mailing offices. Copyright © 2006 by the American Association for the Advancement of Science. The title SCIENCE is a registered trademark of the AAAS. Domestic individual membership and subscription (51 issues): \$139 (\$74 allocated to subscription). Domestic institutional subscription (51 issues): \$650; Foreign postage extra: Mexico, Caribbean (surface mail) \$55; other countries (air assist delivery) \$85. First class, airmail, student, and emeritus rates on request. Canadian rates with GST available upon request, GST #1254 88122. Publications Mail Agreement Number 1069624. Printed in the U.S.A.

Change of address: Allow 4 weeks, giving old and new addresses and 8-digit account number. Postmaster: Send change of address to AAAS, P.O. Box 96178, Washington, DC 20090-6178. Single-copy sales: \$10.00 current issue, \$15.00 back issue prepaid includes surface postage; bulk rates on request. Authorization to photocopy material for internal or personal use under circumstances not falling within the fair use provisions of the Copyright Act is granted by AAAS to libraries and other users registered with the Copyright Clearance Center (CCC) Transactional Reporting Service, provided that \$18.00 per article is paid directly to CCC, 222 Rosewood Drive, Danvers, MA 01923. The identification code for Science is 0036-8075. Science is indexed in the Reader's Guide to Periodical Literature and in several specialized indexes.

CONTENTS continued >>

For news and
research
with
impact,
turn to
Science



There's only one source for news and research with the greatest impact – *Science*. With over 700,000 weekly print readers, and millions more online, *Science* ranks as one of the most highly read multidisciplinary journals in the world. And for impact, *Science* can't be beat. According to the recently released Thomson ISI Journal Citation Report 2005, *Science* ranked as the No. 1 most-cited multidisciplinary journal with a citation factor of 31. Founded in 1880 by inventor Thomas Edison, and published by the nonprofit AAAS, *Science's* reputation as the leading source for news, research, and leading edge presentation of content continues to grow. Looking for news and research that will impact the world tomorrow? Then look in *Science*.

www.sciencemag.org

To join AAAS and receive your own personal copy of *Science* every week go to www.aaas.org/join





Reducing lab-accident risk.

SCIENCE CAREERS

www.sciencereers.org CAREER RESOURCES FOR SCIENTISTS

SPECIAL FEATURE: Staying Well—Safety in the Lab

J. Austin

Science labs are dangerous places that require vigilance to remove risks for you and your colleagues.

US: NIH Urges Career Training and Tracking

B. Benderly

New provisions of NIH's T32 institutional training grants are intended to foster changes that help postdocs.

EUROPE: Keeping Safe—Some Cautionary Tales

L. Dicks

If you don't work hard at staying safe, in the lab or in the field, somebody will get hurt.

US: Wear Your Safety Goggles

J. Kling

Even when there's no obvious threat to your vision, hidden risks are there.

US: Lab Safety Requires Training and Commitment

J. Borchardt

The risk of accidents in academic labs is 10 to 50 times greater than the risk in industrial labs.

GRANTSNET: August 2006 Funding News

J. Fernandez

Learn about the latest research funding opportunities, scholarships, fellowships, and internships.

SCIENCE NOW

www.sciencenow.org DAILY NEWS COVERAGE

Don't Fear the Hybrid

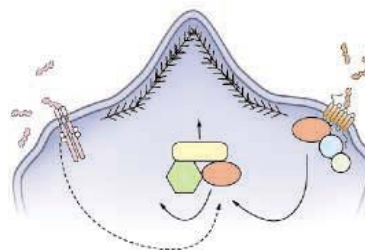
If bird flu and human influenza swapped genes, the results might not be as disastrous as some have expected.

A Shot That Fights Fat

Obesity vaccine curbs weight gain in rats.

Feeling the Earth Move

Team successfully predicts earthquake in western India.



Signals to move.

SCIENCE'S STKE

www.stke.org SIGNAL TRANSDUCTION KNOWLEDGE ENVIRONMENT

PERSPECTIVE: Transducing the Signals—A G Protein Takes a New Identity

D. N. Dhanasekaran

$G\alpha_{13}$ is required for receptor tyrosine kinase signaling.

CONNECTIONS MAPS

Browse the more than 1400 signaling components in this database of cell signaling.

SCIENCE PODCAST



Listen to the 4 August *Science* Podcast to hear about the gender gap in patenting in the life sciences, insights into rational decision-making, the Moon's mysterious bulge, and more.

www.sciencemag.org/about/podcast.dtl

Separate individual or institutional subscriptions to these products may be required for full-text access.

It's All in the Mix

The Deep Impact spacecraft's projectile encounter with comet 9P/Tempel 1 excavated pristine material from deep within its nucleus. Lisse *et al.* (p. 635, published online 13 July) traced its mineral composition of the ejecta in infrared spectra taken with the Spitzer Space Telescope. The mixture of materials seen in the ejecta are usually found in very different environments: highly volatile organic ices; clays and carbonates that form in aqueous environments; and highly crystalline silicates formed at temperatures exceeding 1000 K. These results have implications for the structure and dynamics of the proto-solar nebula 4.5 billion years ago.



Moon Mystery Takes Shape

The peculiar shape of the Moon has puzzled scientists since Laplace drew attention to it in 1799. The Moon's axes have been swelled by spinning and tidal stretching, but the deviations are too large for a body in the current lunar orbit. One explanation is that the Moon's orbit was different early in its history when its shape froze as the lunar magma ocean solidified. However, models have so far failed to fit the precise lunar dimensions. Garrick-Bethell *et al.* (p. 652; see the Perspective by Innanen) show that the Moon's shape can be explained if it had been in an eccentric orbit 100 million years after its formation. If the lunar magma ocean solidified during a period of substantial lunar eccentricity, when the Moon's semimajor orbital axis was about 22 to 28 Earth radii, the "fossil bulge" seen today in the lunar gravity field can be matched. The authors constrain the possible orbits; permitted ones that include a high-eccentricity synchronous orbit, and one with a 3:2 resonance of spin frequency to orbit frequency, as is presently the case for Mercury.

Assessing Aerosol Effects

Most of the uncertainty about how climate will change in coming decades centers on aerosols, largely because of a poor understanding of the effects that they have on the properties and abundance of clouds—estimates of the net radiative effect of aerosols range from 0 to 5 watts per square meter. Kaufman and Koren (p. 655, published online 13 July; see the Perspective by Bréon) address this dilemma by comparing measurements of the attenuation of sunlight by aerosols in the absence of clouds, made by a worldwide network of automatic instruments, to the fraction of time that clouds cover the sites.

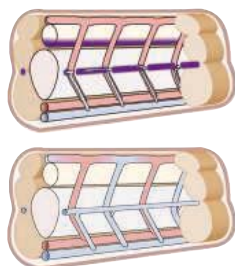
Cloud coverage was positively correlated to the concentration of aerosols in the air, and negatively correlated with how much sunlight was absorbed by the aerosols. This finding was independent of the type of aerosol or location, which suggests that much of the correlation arises from aerosol effects on cloudiness.

Imaging Shells of Cold Atom Insulators

The ability to tune the intersite interaction strength and site occupancy of atomic condensates confined to optical lattices make them ideal systems to explore electronic correlations in condensed matter physics. Campbell *et al.* (p. 649) probed the superfluid–Mott insulator transition of a Bose-Einstein condensate in a three-dimensional optical lattice. Using high-resolution microwave spectroscopy usually associated with atomic clocks, they resolved the layered structure of the Mott shells and directly imaged their spatial distribution.

Netrins Expand Their Repertoire

The axons that neurons extend elaborate a complex interconnected network. Similarly, the circulatory system is a complex interconnected network of vessels. Wilson *et al.* (p. 640, published online 29 June) now show that the blood vessels and axons respond similarly to netrins, which were



originally identified as axonal guidance factors. The receptors that each tissue uses to read the netrin signals, however, are different, and netrins promote angiogenesis through unknown receptors. Netrins stimulated tissues suffering from diabetic or ischemic damage to grow new blood vessels by signaling endothelial cells to manage proliferation and migration.

Gender Gap in Patenting

The reasons for gender disparity in the workplace are a contentious subject. Ding *et al.* (p. 665) present a large-scale study of more than 4000 life scientists and show that women scientists patent their findings at less than half the rate of men. Although the gender gap is decreasing, interviews reveal that professional network differences and traditional views of academic careers are still factors.

Sweet But Not Sticky

Under normal conditions, immunoglobulin G (IgG) antibodies are anti-inflammatory, yet during infection, they can protect the body by recruiting inflammatory cells or pathways. Kaneko *et al.* (p. 670; see the Perspective by Burton and Dwek) now show that IgG can alternate between these states by modifying the sialylation of polysaccharides on the non-variable part of the IgG that is responsible for binding and activating receptors on immune cells. These receptors bind sialylated forms of IgG less strongly, which signals the cell to load its surface with inhibitory proteins. However, under situations of immune challenge, the sialic acid residues are lost, which allows IgG

to bind more tightly and so turn up inflammatory signaling. By switching activity in this way, IgG antibodies may restrict their pro-inflammatory effects to periods of infection and so limit the potential for inadvertent harm resulting from their activity.

Cilia and Signaling

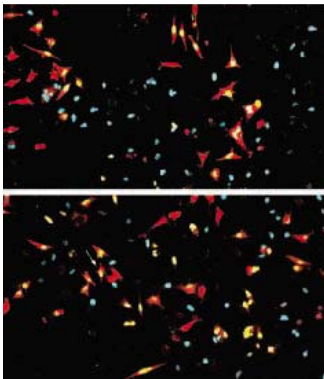
Nearly all vertebrate cells have a primary cilium, a specialized hairlike organelle that projects from the cell surface. The importance of primary cilia in sight, smell, and touch is well established. However, as reviewed by **Singla and Reiter** (p. 629), these organelles have recently been identified as key players in fundamental signal transduction pathways, which may explain why ciliary defects underlie such a wide range of human diseases.

Linking the Clock and the Cell Cycle

The circadian clock is linked to the cell cycle in ways that are not clear. **Pregueiro et al.** (p. 644; published online 29 June; see the cover) investigated the relation between these two fundamental cellular processes in the fungus *Neurospora*. When a gene called *period-4* (*prd-4*) contains a mutation, *Neurospora's* clock runs with a shorter period. The protein PRD-4 is orthologous to checkpoint kinase 2, a mammalian cell cycle regulator, and PRD-4 is both regulated by and regulates the circadian clock. DNA damaging agents can reset the clock in a time-of-day dependent manner, and this circadian-phase resetting is wholly dependent on PRD-4.

Understanding SNARE-Mediated Membrane Fusion

Cellular membrane fusion involves the formation of a four-helix bundle with contributions from vesicle and target membrane SNARE (soluble NSF attachment protein receptor) proteins. SNAREs constitute the minimal fusion machinery and can promote the fusion of liposomes. **Pobbati et al.** (p. 673) dissected the SNARE assembly process in greater detail. In vitro experiments with liposomes showed that SNARE assembly was initiated at the N-terminal region of the four-helix bundle and that was sufficient to drive rapid liposome fusion. **Giraudo et al.** (p. 676, published online 22 June) used a system in which SNARE proteins, which are normally expressed on intracellular membranes, are "flipped" so that they are exposed at the cell surface. Cells expressing such flipped SNAREs fuse spontaneously. By introducing a fusion clamp (complexin) and a calcium sensor (synaptotagmin), cell-cell fusion can be regulated by calcium in a comparable way to the regulation seen during neurotransmitter release.



Emotions, Rationality, and Decision-Making

Theories of economic decision-making traditionally assume that humans are fundamentally rational creatures. However, humans are reproducibly irrational in a number of characteristic ways. One of the most impressive examples is the so-called "framing effect," where merely casting an option in a positive or negative way has a dramatic influence on subsequent choice. **De Martino et al.** (p. 684; see news story by **Miller**) identify the integration of emotional biases arising from an amygdala-based decision-making system as the underlying cause of the framing effect. Most remarkably, they can predict which individuals are most rational, that is, relatively immune to the framing effect.

Malaria Repression

While investigating the mechanisms that control gene expression during the sexual stages of malaria parasites, **Mair et al.** (p. 667; see the Perspective by **Hajduk**) discovered an RNA helicase that binds to and represses a spectrum of parasite messenger RNAs. The helicase is found in cytoplasmic P-granules, ribonucleoprotein complexes containing translationally repressed mRNAs, which are stored ready for activation after fertilization. Parasites that lack the helicase are developmentally defective after gamete fusion. Understanding this key developmental transition in the complex life cycle of the malaria parasite may point to new leads for malaria control.

CREDIT: GIRAUDO ET AL.

Q Who's helping scientists stay one jump ahead?



Photo: Dr. Martin Levy

“ I read my *Science* when I'm at the skatepark with my son. It's great to be out in the fresh air. And an interesting cover picture will often provoke questions and interesting conversations with parents and kids alike. ”

AAAS member Lorraine J. Kuhn, Ph.D.

AAAS is committed to advancing science and giving a voice to scientists around the world. Helping our members stay abreast of their field is a key priority.

One way we do this is through *Science*, which features all the latest groundbreaking research, and keeps scientists connected wherever they happen to be.

To join the international family of science, go to www.aaas.org/join.



ADVANCING SCIENCE. SERVING SOCIETY

www.aaas.org/join

Safety down to a science.

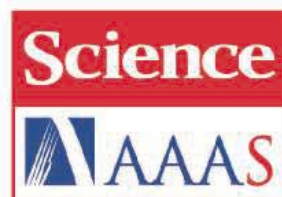


**The all new 2006 Subaru Legacy earns
first-ever IIHS "Top Safety Pick Gold" award.†**

- Insurance Institute for Highway Safety (IIHS)

Subaru's sponsorship of the American Association for the Advancement of Science (AAAS) highlights our advanced design of **symmetrical all-wheel drive** technology to our target markets and underscores Subaru's commitment to further science, engineering and technology education both at the annual meeting and programs throughout the year. Subaru is proud to be the Premier Automotive Sponsor of the AAAS.

In a continuing effort to offer our partners unique and valuable benefits, we provide special offers for AAAS Members, the Subaru VIP Partners Program. AAAS Members can **save up to \$3,000*** off the manufacturer's suggested retail price (depending on model and accessories) on the purchase or lease of a new Subaru from participating dealers. To qualify, you must be a AAAS member in good standing for at least six consecutive months prior to participation in this program. Please contact AAAS Member Services at 202.326.6417 or e-mail membership@aaas.org **BEFORE** visiting your local Subaru dealer. Access subaru.com to find a nearby dealer or learn more about Subaru vehicles.



Think. Feel. Drive.™



*From MSRP to dealer invoice. MSRP does not include tax, title, and registration fees. Limited time offer subject to change without notice. Terms and conditions apply. This offer replaces all other existing offers, cannot be redeemed for cash and is not applicable in Canada and Hawaii. † Based on Insurance Institute for Highway Safety 40 mph offset frontal crash test, 31 mph side impact test, and 20 mph rear impact test.



Martin Rees is president of the Royal Society, the UK national academy of science. He is a professor of Cosmology and Astrophysics at Cambridge University and Master of Trinity College.

The G8 on Energy: Too Little

ENERGY SECURITY WAS A KEY ISSUE AT THE ST. PETERSBURG SUMMIT OF G8 LEADERS LAST MONTH. Their joint communiqué* included many important commitments, but it omitted one crucial pledge: a significant increase in their governments' investments in R&D for energy technologies. The omission of energy R&D by the G8 reflects a worrisome lack of determination to accelerate the development of new energy technologies. The urgent challenge is to meet global demand [scheduled to rise by more than 50% in the next 25 years, according to the International Energy Agency (IEA)] while reducing the impact of greenhouse gas emissions on climate change.

The St. Petersburg communiqué provides a list of future actions focused on private-sector energy funding, but neglects to emphasize the importance of public-sector R&D funding for technologies that are too far from market. It is perhaps not surprising that the communiqué had little to say on government R&D expenditure. A paper published last October concluded that public-sector R&D investment in energy in most industrialized countries has fallen sharply in real terms, from peak levels in the early 1980s, with some stabilization in the 1990s.† That analysis demonstrated that the 11 IEA countries accounting for most of the world's energy R&D had all decreased expenditures as a proportion of gross domestic product between 1975 and 2003. Investments in major energy R&D program areas dropped by 53% between 1990 and 2003. Fossil fuels and nuclear power accounted for more than 90% of the aggregate decline, but there was also an overall drop of 5% for R&D on renewable technologies.

Analyses of these R&D budgets don't tell the whole story, but they do demonstrate that the governments of industrial countries are not facing up to the huge energy challenges that lie ahead. That is disquieting because the IEA is predicting that by 2030, based on current national policies, 80% of the world's primary energy demand will be met by fossil fuels. Meanwhile, nuclear, hydro, biomass, and waste will provide 17%, and other renewables, such as geothermal, solar, and wind energy, will only account for less than 2%.

As a result, the IEA projects that annual energy-related emissions of carbon dioxide will be 52% higher in 2030 than in 2003. Unless there is a radical change, the world will continue to become more reliant on fossil fuels beyond 2030. Without unfeasibly dramatic breakthroughs in carbon sequestration and energy efficiency, this will lead to proportionate increases in atmospheric greenhouse gas concentrations.

To deal with rising energy demands and rising greenhouse gas emissions, more needs to be done to develop new energy technologies that are currently far from market. Governments must play a lead role in stimulating this process by investing more in R&D. One benchmark is set by nuclear fusion, where current publicly funded research runs at around \$1.5 billion per year. But fusion is only one of the technologies that are not yet market-ready. Proportionate support of all other options surely would be a prudent investment in a world where the cost of worldwide energy consumption is measured in trillions of dollars. These R&D expenditures could be funded through carbon taxes or similar economic instruments, levied initially on the countries with the largest emissions.

Such a proposal may seem ambitious, but some commentators have argued that the energy challenge demands a high-profile response analogous to the Manhattan or Apollo project, but on a global, rather than national, scale. An initiative of this type by world leaders would, as happened after the initiation of the Apollo project in the United States, stimulate education and enrollments in science and technology. Will G8 leaders have the vision to announce such an initiative at next year's summit?

– Martin Rees

10.1126/science.1132850

*G8 leaders 2006, *Global Energy Security* (<http://en.g8russia.ru/docs/11.html>). †P. Runci, *Energy R&D Investment Patterns in IEA Countries: An Update* (Pacific Northwest National Laboratory/Joint Global Change Research Institute Technical Paper PNWD-3581, 2005; www.globalchange.umd.edu/energytrends&page=iea).

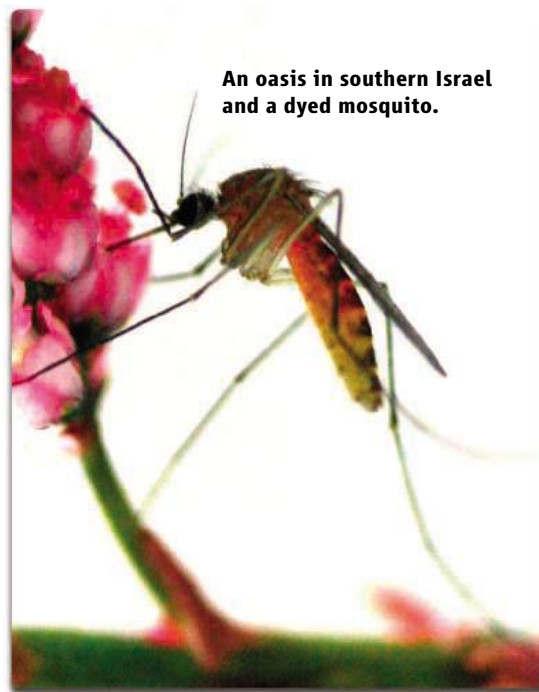


ECOLOGY

The Sweet Taste of Death

Notoriously, female mosquitoes need a meal of blood before laying their eggs. Less well known is that their in-between meals involve snacks of nectar. Müller and Schlein show that in desert areas when there are no other flowering plants available, mosquitoes are attracted to flowering trees. They measured this allure using insect traps baited with flowering and nonflowering branches of various local trees; more than twice as many mosquitoes were caught with flowering branches than with leafy branches or with flowering annual plants. The authors were able to exploit the mosquitoes' thirst for sweets to bring about their demise by spraying acacia trees with a sugar solution that had been spiked with a food dye and the oral insecticide Spinosad, thus almost eliminating them from one oasis. It is possible that this method of localized mosquito control could be used in other types of "nectar deserts," such as rice paddies. — CA

Int. J. Parasitol. **36**, 10.1016/j.ijpara.2006.06.008 (2006).



An oasis in southern Israel and a dyed mosquito.

GEOLOGY

Shaking Clues from the Mississippi

The seismic hazards associated with fault zones removed from plate boundaries are particularly difficult to assess. The New Madrid fault zone in the central United States produced a series of large earthquakes around the year 1812, and trenching has identified an episode of activity starting approximately 1000 years ago (900 C.E.), extending to the 1812 quakes.

However, the earlier activity of the fault zone has been enigmatic, posing a problem in assessing risks.

One major fault in this seismic zone—the Reelfoot thrust fault—straddles the Mississippi River, and Holbrook *et al.* have therefore looked for past changes in the course of the river as an indicator of prehistoric quakes. Large quakes on the fault would have produced uplift to the south, thereby reducing the gradient of the river north of the fault. A lower gradient would then cause the river to straighten its course rather than meander. The river



Mississippi River at New Madrid.

straightened approximately 1000 years ago, coincident with the known seismic activity. The authors also identify a second episode, between 3600 and 4200 years ago, when the river cut off many meandering channels. Thus, two episodes of faulting spanning roughly 1000 years seem to be separated by a several-thousand-year interval of fewer large quakes. The results suggest that another period of more frequent earthquakes could arise after long quiescence. — BH

Tectonophysics **420**, 431 (2006).

ECOLOGY/EVOLUTION

Leaving Out the Details

The species-area relationship (SAR) is a well-studied concept in ecology and biogeography, relating area to the total number of species found within it. The relationship takes the form of a power law $S = cA^z$, where S is the number of species, A is the area, and c is a constant. The exponent z varies from as little as 0.5 to as much as 1.0, according to the group of organism, the scale in question, and the habitat type, but is most commonly found to lie in the range of 0.2 to 0.3. However, the factors underlying this relationship, and the reasons for the variation in z , have remained enigmatic.

In a new theoretical treatment of the question, García Martín and Goldenfeld show that the observed relationship and the value of z flow from the statistical properties of spatial and abundance distributions, such as clustering and mean distance between individuals, rather than directly from any ecological property of organ-

isms and ecosystems (competition, dispersal, etc.) They validate the theory using data from a grassland site in California. — AMS

Proc. Natl. Acad. Sci. U.S.A. **103**, 10310 (2006).

MATERIALS SCIENCE

Hardening Hydrogels

In recent years, preparation methods for biocompatible bonelike materials have grown increasingly sophisticated. One approach has been to mineralize polymeric hydrogels by the addition of calcium salts; however, the chemical functionality of such systems is not easily tuned, nor is the polymer template easily disassembled after mineralization. Schnepf *et al.* replace the polymer with a supramolecular network that self-assembles from water-soluble small-molecule building blocks. They start with an aqueous solution of tyrosine phosphate, N-substituted by an aromatic fluorenylmethoxy-carbonyl (FMOC) group. Enzymatic dephosphorylation induces the assembly of gels composed of nanofilaments held together by tyrosine H-bonding and fluorenyl π -stacking interactions. By exposing the gels to different calcium ion concentrations for different periods of time, the authors achieve controlled degrees of calcium phosphate mineralization.

Nucleation of calcium phosphate along the fibers produced viscoelastic hybrid gels with enhanced thermal stability and stiffness. Furthermore, the shear threshold for a nonlinear response increased by two orders of magnitude relative to the unmineralized sample. Week-long exposure to moderately concentrated

CaCl₂ led to extensively mineralized composites without disrupting the viscoelastic properties of the supramolecular structure; the organic material could then be removed by washing to produce macroporous networks. — MSL

Adv. Mater. **18**, 1869 (2006).

BIOMEDICINE

Batteries Not Required

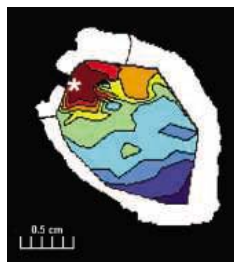
Electronic cardiac pacemakers are small battery-operated devices that are implanted into damaged hearts to correct defects in electrical conduction between the atria and the ventricles. Although these devices are remarkably successful in restoring regular heart rhythm in adults, they can produce complications in children. Thus, new forms of pacemaker therapy are actively being explored.

Choi *et al.* used a tissue engineering approach to create a biologically based artificial pacemaker consisting of skeletal muscle precursor cells from fetal rats cultured in a three-dimensional collagen-based tissue construct. After documenting that the cells within the engineered tissue were coupled

through gap junctions and were capable of propagating an applied electric current, the authors implanted the tissue into the heart of adult rats. The implanted tissue became vascularized and persisted for the entire lifetime of the recipient animals. Importantly, in about one-third of the rats,

it produced a permanent alternative conduction pathway between the right atrium and right ventricle. Whether these tissue constructs would provide adequate pacing support in rats whose native heart rhythm has been blocked remains to be tested. — PAK

Am. J. Pathol. **169**, 72 (2006).



Time course of atrioventricular conduction from site of stimulation (*).

BIOTECHNOLOGY

Labor Relations

Superficially, biosynthetic pathways for natural products might be likened to factory assembly lines where having more workers would mean being able to make more product. When the costs of factory buildings, workers, and excess inventory of parts are factored in, a just-in-time process is a more efficient solution, so that workers are neither overburdened nor idle and

no partially assembled products accumulate. Add in the biological complications of multiple assembly teams using some of the same parts along with feedback, feed-forward, and inter-pathway interactions, and calculating the optimal numbers of workers seems out of reach.

Pfleger *et al.* have instead developed an approach for constructing a library of artificial operons, which in this instance code for a three-enzyme segment of the isoprenoid pathway. By inserting into the intergenic regions variations of posttranscriptional regulatory elements, such as hairpin-forming sequences and ribonuclease sites (and perhaps riboswitches, too), they generate lots of combinations and find that increasing the hairpin-forming propensity of the ribosome binding site in front of the second gene is sufficient to reduce the mRNA levels of the second and third genes, which keeps acetyl CoA concentrations high enough to support vigorous growth and isoprenoid production simultaneously. — GJC

Nat. Biotechnol. **24**, 10.1038/nbt1226 (2006).

CHEMISTRY

Small Yet Selective

Structural diversification of complex molecular frameworks, for example to combat antibiotic resistance, would benefit from an often elusive catalytic combination of specificity (to leave intact biochemically critical functional groups) and versatility (to offer as wide a range of functionality as possible in the components varied for screening). Enzymes have evolved to achieve remarkable selectivity in modifying the structures of intricate organic molecules. The price of this function, however, is a comparatively narrow substrate scope and range of transformations relative to inherently less selective small-molecule catalysts.

Regioselective acylation is a common example of a reaction traditionally left to enzymes. In the absence of a chiral catalyst, acylation of the antibiotic erythromycin A is known to occur preferentially at the 2' and 4" hydroxyl sites. Lewis and Miller show that a pentapeptide catalyst overcomes this kinetic selectivity to acetylate a third site, the 11-OH, with 5:1 selectivity; the same site preference is also observed for the catalyzed addition of longer-chain acyl groups, with selectivities ranging from 3.5 to >10:1. Moreover, an accompanying tautomerization further modifies the adjacent molecular framework. The results suggest that small-molecule catalysts may have unexpected promise for direct functionalization of complex molecules with high regio- and stereoselectivity. — JSY

Angew. Chem. Int. Ed. **45**, 10.1002/anie.200601490 (2006).

Institutional Site License Available

Q

What can *Science STKE* give me?



A

The definitive resource on cellular regulation

STKE – Signal Transduction Knowledge Environment offers:

- A weekly electronic journal
- Information management tools
- A lab manual to help you organize your research
- An interactive database of signaling pathways

STKE gives you essential tools to power your understanding of cell signaling. It is also a vibrant virtual community, where researchers from around the world come together to exchange information and ideas. For more information go to www.stke.org

To sign up today, visit promo.aaas.org/stkeas

Sitewide access is available for institutions. To find out more e-mail stkelicense@aaas.org



1200 New York Avenue, NW
Washington, DC 20005

Editorial: 202-326-6550, FAX 202-289-7562
News: 202-326-6500, FAX 202-371-9227

Bateman House, 82-88 Hills Road
Cambridge, UK CB2 1LQ

+44 (0) 1223 326500, FAX +44 (0) 1223 326501

SUBSCRIPTION SERVICES For change of address, missing issues, new orders and renewals, and payment questions: 866-434-AAAS (2227) or 202-326-6417, FAX 202-842-1065. Mailing addresses: AAAS, P.O. Box 96178, Washington, DC 20090-6178 or AAAS Member Services, 1200 New York Avenue, NW, Washington, DC 20005

INSTITUTIONAL SITE LICENSES please call 202-326-6755 for any questions or information
REPRINTS: Author Inquiries 800-635-7181
Commercial Inquiries 803-359-4578
Corrections 202-326-6501

PERMISSIONS 202-326-7074, FAX 202-682-0816

MEMBER BENEFITS Bookstore: AAAS/BarnesandNoble.com bookstore www.aaas.org/bn; Car purchase discount: Subaru VIP Program 202-326-6417; Credit Card: MBNA 800-847-7378; Car Rentals: Hertz 800-654-2200 CDP#343457, Dollar 800-800-4000 #AA1115; AAAS Travels: Betchart Expeditions 800-252-4910; Life Insurance: Seabury & Smith 800-424-9883; Other Benefits: AAAS Member Services 202-326-6417 or www.aaasmember.org.

science_editors@aaas.org (for general editorial queries)
science_letters@aaas.org (for queries about letters)
science_reviews@aaas.org (for returning manuscript reviews)
science_bookrevs@aaas.org (for book review queries)

Published by the American Association for the Advancement of Science (AAAS), *Science* serves its readers as a forum for the presentation and discussion of important issues related to the advancement of science, including the presentation of minority or conflicting points of view, rather than by publishing only material on which a consensus has been reached. Accordingly, all articles published in *Science*—including editorials, news and comment, and book reviews—are signed and reflect the individual views of the authors and not official points of view adopted by the AAAS or the institutions with which the authors are affiliated.

AAAS was founded in 1848 and incorporated in 1874. Its mission is to advance science and innovation throughout the world for the benefit of all people. The goals of the association are to: foster communication among scientists, engineers and the public; enhance international cooperation in science and its applications; promote the responsible conduct and use of science and technology; foster education in science and technology for everyone; enhance the science and technology workforce and infrastructure; increase public understanding and appreciation of science and technology; and strengthen support for the science and technology enterprise.

INFORMATION FOR CONTRIBUTORS

See pages 102 and 103 of the 6 January 2006 issue or access www.sciencemag.org/feature/contribinfo/home.shtml

EDITOR-IN-CHIEF **Donald Kennedy**

EXECUTIVE EDITOR **Monica M. Bradford**

DEPUTY EDITORS

NEWS EDITOR

R. Brooks Hanson, Katrina L. Kelner Colin Norman

EDITORIAL SUPERVISORY SENIOR EDITORS Barbara Jasny, Phillip D. Szurromi; **SENIOR EDITOR/PERSPECTIVES** Lisa D. Chong; **SENIOR EDITORS** Gilbert J. Chin, Pamela J. Hines, Paula A. Kiberstis (Boston), Marc S. Lavine (Toronto), Beverly A. Purnell, L. Bryan Ray, Guy Riddihough (Manila), H. Jesse Smith, Valda Vinson, David Voss; **ASSOCIATE EDITORS** Jake S. Veston, Laura M. Zahn; **ONLINE EDITOR** Stewart Wills; **ASSOCIATE ONLINE EDITOR** Tara S. Marathe; **BOOK REVIEW EDITOR** Sherman J. Suter; **ASSOCIATE LETTERS EDITOR** Etta Kavanagh; **INFORMATION SPECIALIST** Janet Kegg; **EDITORIAL MANAGER** Cara Tate; **SENIOR COPY EDITORS** Jeffrey E. Cook, Cynthia Howe, Harry Jach, Barbara P. Ordway, Jennifer Sills, Trista Wagoner; **COPY EDITOR** Peter Mooreside; **EDITORIAL COORDINATORS** Carolyn Kyle, Beverly Shields; **PUBLICATION ASSISTANTS** Ramatoulaye Diop, Chris Filiatreau, Joi S. Granger, Jeffrey Hearn, Lisa Johnson, Scott Miller, Jerry Richardson, Brian White, Anita Wynn; **EDITORIAL ASSISTANTS** Lauren Kmec, Patricia M. Moore, Michael Rodewald; **EXECUTIVE ASSISTANT** Sylvia S. Kihara; **ADMINISTRATIVE SUPPORT** Maryrose Police

NEWS SENIOR CORRESPONDENT Jean Marx; **DEPUTY NEWS EDITORS** Robert Coontz, Jeffrey Mervis, Leslie Roberts, John Travis; **CONTRIBUTING EDITORS** Elizabeth Culotta, Polly Shulman; **NEWS WRITERS** Yudhijit Bhattacharjee, Adrian Cho, Jennifer Couzin, David Grimm, Constance Holden, Jocelyn Kaiser, Richard A. Kerr, Eli Kintisch, Andrew Lawler (New England), Greg Miller, Elizabeth Pennisi, Robert F. Service (Pacific NW), Erik Stokstad; Rhipuparna Chatterjee, Diane Garcia, Briahna Gray (Internos); **CONTRIBUTING CORRESPONDENTS** Barry A. Cipra, Jon Cohen (San Diego, CA), Daniel Ferber, Ann Gibbons, Robert Irlan, Mitch Leslie (NetWatch), Charles C. Mann, Evelyn Strauss, Gary Taubes, Ingrid Wickelmaier; **COPY EDITORS** Linda B. Felaco, Rachel Curran, Sean Richardson; **ADMINISTRATIVE SUPPORT** Scherraine Mack, Fannie Groom BUREAU: Berkeley, CA: 510-652-0302, FAX 510-652-1867, New England: 207-549-7755, San Diego, CA: 760-942-3252, FAX 760-942-4979, Pacific Northwest: 503-963-1940 **PRODUCTION DIRECTOR** James Landry; **SENIOR MANAGER** Wendy K. Shank; **ASSISTANT MANAGER** Rebecca Doshi; **SENIOR SPECIALISTS** Jay Covert, Chris Redwood; **SPECIALIST** Steve Forrester **PREFLIGHT DIRECTOR** David M. Tompkins; **MANAGER** Marcus Spiegler; **SPECIALIST** Jessie Mudjtjaba

ART DIRECTOR Joshua Moglia; **ASSOCIATE ART DIRECTOR** Kelly Buckheit; **ILLUSTRATORS** Chris Bickel, Katharine Suttifit; **SENIOR ART SPECIALISTS** Holly Bishop, Laura Creveling, Preston Huey; **ASSOCIATE** Nayomi Kevitiyagala; **PHOTO EDITOR** Leslie Blizard

SCIENCE INTERNATIONAL

EUROPE (science-int.co.uk) **EDITORIAL: INTERNATIONAL MANAGING EDITOR** Andrew M. Sugden; **SENIOR EDITOR/PERSPECTIVES** Julia Fahrenkamp-Uppenbrink; **SENIOR EDITORS** Caroline Ash (Geneva: +41 (0) 222 346 3106), Stella M. Hurlley, Ian S. Osborne, Stephen J. Simpson, Peter Stern; **ASSOCIATE EDITOR** Joanne Baker **EDITORIAL SUPPORT** Alice Whaley; Deborah Dennison **ADMINISTRATIVE SUPPORT** Janet Clements, Phil Marlow, Jill White; **NEWS: INTERNATIONAL NEWS EDITOR** Eliot Marshall **DEPUTY NEWS EDITOR** Daniel Clerly; **CORRESPONDENT** Gretchen Vogel (Berlin: +49 (0) 30 2809 3902, FAX +49 (0) 30 2809 8365); **CONTRIBUTING CORRESPONDENTS** Michael Balter (Paris), Martin Enserink (Amsterdam and Paris), John Bohannon (Berlin); **INTERN** Laura Blackburn

ASIA Japan Office: Asca Corporation, Eiko Ishioka, Fusako Tamura, 1-8-13, Hirano-cho, Chuo-ku, Osaka-shi, Osaka, 541-0046 Japan; +81 (0) 6 6202 6272, FAX +81 (0) 6 6202 6271; asca@os.gulf.or.jp; **ASIA NEWS EDITOR** Richard Stone +66 2 662 5818 (rstone@aaas.org); **JAPAN NEWS BUREAU** Dennis Normile (contributing correspondent, +81 (0) 3 3391 0630, FAX 81 (0) 3 5936 3531; dnormile@gol.com); **CHINA REPRESENTATIVE** Hao Xin, +86 (0) 10 6307 4439 or 6307 3676, FAX +86 (0) 10 6307 4358; haoxin@earthlink.net; **SOUTH ASIA** Pallava Bagla (contributing correspondent +91 (0) 11 2271 2896; pbagla@vsnl.com)
AFRICA Robert Koenig (contributing correspondent, rob.koenig@gmail.com)

EXECUTIVE PUBLISHER **Alan I. Leshner**

PUBLISHER **Beth Rosner**

FULFILLMENT & MEMBERSHIP SERVICES (membership@aaas.org) **DIRECTOR** Marlene Zendell; **MANAGER** Weylon Butler; **SYSTEMS SPECIALIST** Andrew Vargo; **CUSTOMER SERVICE SUPERVISOR** Pat Butler; **SPECIALISTS** Laurie Baker, Tamara Alfson, Karena Smith, Vicki Linton, Latoya Casteel; **CIRCULATION ASSOCIATE** Christopher Refice; **DATA ENTRY SUPERVISOR** Cynthia Johnson; **SPECIALISTS** Tomeka Diggs, Tarrika Hill

BUSINESS OPERATIONS AND ADMINISTRATION DIRECTOR Deborah Rivera-Wienhold; **BUSINESS MANAGER** Randy Yip; **SENIOR BUSINESS ANALYST** Lisa Donovan; **BUSINESS ANALYST** Jessica Tierney; **FINANCIAL ANALYST** Michael LoBue, Farida Yeasmin; **RIGHTS AND PERMISSIONS: ADMINISTRATOR** Emilie David; **ASSOCIATE** Elizabeth Sandler; **MARKETING: DIRECTOR** John Meyers; **MARKETING MANAGERS** Darryl Walter, Allison Pritchard; **MARKETING ASSOCIATES** Julianne Wielga, Mary Ellen Crowley, Catherine Featherston, Alison Chandler, Lauren Lamoureux; **INTERNATIONAL MARKETING MANAGER** Wendy Sturley; **MARKETING/MEMBER SERVICES EXECUTIVE: LINDA RUSK; JAPAN SALES** Jason Hannaford; **SITE LICENSE SALES: DIRECTOR** Tom Ryan; **SALES AND CUSTOMER SERVICE** Mehan Dossani, Kiki Forsythe, Catherine Holland, Wendy Wise; **ELECTRONIC MEDIA: MANAGER** Elizabeth Harman; **PRODUCTION ASSOCIATES** Amanda K. Skelton, Lisa Stanford, Nichele Johnston; **LEAD APPLICATIONS DEVELOPER** Carl Saffell

ADVERTISING DIRECTOR WORLDWIDE AD SALES Bill Moran

PRODUCT (science_advertising@aaas.org); **MIDWEST** Rick Bongiovanni: 330-405-7080, FAX 330-405-7081 • **WEST COAST/W. CANADA** Teola Young: 650-964-2266 **EAST COAST/E. CANADA** Christopher Breslin: 443-512-0330, FAX 443-512-0331 • **UK/EUROPE/ASIA** Tracy Holmes: +44 (0) 1223-326-525, FAX +44 (0) 1223-325-532 **JAPAN** Mashu Yoshikawa: +81 (0) 33235 5961, FAX +81 (0) 33235 5852 **TRAFFIC MANAGER** Carol Maddox; **SALES COORDINATOR** Deandra Simms

CLASSIFIED (advertise@sciencereaders.org); **U.S.: SALES DIRECTOR** Gabrielle Boguslawski: 718-491-1607, FAX 202-289-6742; **INSIDE SALES MANAGER** Daryl Anderson: 202-326-6543; **WEST COAST/MIDWEST** Kristine von Zedlitz: 415-956-2531; **EAST COAST** Jill Downing: 631-580-2445; **CANADA, MEETINGS AND ANNOUNCEMENTS** Kathleen Clark: 510-271-8349; **SALES COORDINATORS** Erika Bryant; Rohan Edmonson, Allison Millar, Joyce Scott, Shirley Young; **INTERNATIONAL SALES MANAGER** Tracy Holmes: +44 (0) 1223 326525, FAX +44 (0) 1223 326532; **SALES** Christina Harrison, Svetlana Barnes; **SALES ASSISTANT** Helen Moroney; **JAPAN:** Jason Hannaford: +81 (0) 52 789 1860, FAX +81 (0) 52 789 1861; **PRODUCTION: MANAGER** Jennifer Rankin; **ASSISTANT MANAGER** Deborah Tompkins; **ASSOCIATES** Christine Hall; Amy Hardcastle; **PUBLICATIONS ASSISTANTS** Robert Buck; Mary Lagnaudi

AAAS BOARD OF DIRECTORS **RETIRING PRESIDENT, CHAIR** Gilbert S. Omenn; **PRESIDENT** John P. Holdren; **PRESIDENT-ELECT** David Baltimore; **TREASURER** David E. Shaw; **CHIEF EXECUTIVE OFFICER** Alan I. Leshner; **BOARD** Rosina M. Bierbaum; John E. Dowling; Lynn W. Enquist; Susan M. Fitzpatrick; Alice Gast; Thomas Pollard; Peter J. Stang; Kathryn D. Sullivan



ADVANCING SCIENCE. SERVING SOCIETY

SENIOR EDITORIAL BOARD

John I. Brauman, Chair, Stanford Univ.
Richard Losick, Harvard Univ.
Robert May, Univ. of Oxford
Marcia McNutt, Monterey Bay Aquarium Research Inst.
Linda Partridge, Univ. College London
Vera C. Rubin, Carnegie Institution of Washington
Christopher R. Somerville, Carnegie Institution
George M. Whitesides, Harvard University

BOARD OF REVIEWING EDITORS

Joanna Aizenberg, Bell Labs/Lucent
R. McNeill Alexander, Leeds Univ.
David Altshuler, Broad Institute
Arturo Alvarez-Buylla, Univ. of California, San Francisco
Richard Amasino, Univ. of Wisconsin, Madison
Meinrat O. Andreae, Max Planck Inst., Mainz
Kristi S. Anseth, Univ. of Colorado
Cornelia I. Bargmann, Rockefeller Univ.
Brenda Bass, Univ. of Utah
Ray H. Baughman, Univ. of Texas, Dallas
Stephen J. Benkovic, Pennsylvania St. Univ.
Michael J. Bevan, Univ. of Washington
Ton Bisseling, Wageningen Univ.
Mina Bissell, Lawrence Berkeley National Lab
Peer Bork, EMBL
Robert W. Boyd, Univ. of Rochester
Dennis Bray, Univ. of Cambridge
Stephen Buratowski, Harvard Medical School
Jillian M. Burkiak, Univ. of Alberta
Joseph A. Burns, Cornell Univ.
William P. Butz, Population Reference Bureau
Doreen Cantrell, Univ. of Dundee
Peter Carmeliet, Univ. of Leuven, VIB
Gerbrand Ceder, MIT
Mildred Cho, Stanford Univ.
David Clapham, Children's Hospital, Boston
David Clary, Oxford University
J. M. Claverie, CNRS, Marseille

Jonathan D. Cohen, Princeton Univ.
F. Fleming Crim, Univ. of Wisconsin
William Cumberland, UCLA
George O. Daley, Children's Hospital, Boston
Caroline Dean, John Innes Centre
Judy DeLoache, Univ. of Virginia
Edward DeLong, MIT
Robert Desimone, MIT
Dennis Discher, Univ. of Pennsylvania
W. Ford Doolittle, Dalhousie Univ.
Julian Downward, Cancer Research UK
Denis Duboule, Univ. of Geneva
Christopher Dye, WHO
Richard Ellis, Cal Tech
Gerhard Ertl, Fritz-Haber-Institut, Berlin
Douglas H. Erwin, Smithsonian Institution
Barry Everitt, Univ. of Cambridge
Paul G. Falkowski, Rutgers Univ.
Ernst Fehr, Univ. of Zurich
Toni Fenchel, Univ. of Copenhagen
Alain Fischer, INSERM
Jeffrey S. Flier, Harvard Medical School
Chris D. Frith, Univ. College London
R. Gadagkar, Indian Inst. of Science
John Gearhart, Johns Hopkins Univ.
Jennifer M. Graves, Australian National Univ.
Christian Haass, Ludwig Maximilians Univ.
Dennis L. Hartmann, Univ. of Washington
Chris Hawkesworth, Univ. of Bristol
Martin Heimann, Max Planck Inst., Jena
James A. Hendler, Univ. of Maryland
Ove Hoegh-Guldberg, Univ. of Queensland
Ary A. Hoffmann, La Trobe Univ.
Evelyn L. Hu, Univ. of California, SB
Olli Ikkala, Helsinki Univ. of Technology
Meyer B. Jackson, Univ. of Wisconsin Med. School
Stephen Jackson, Univ. of Cambridge
Daniel Kahne, Harvard Univ.
Bernhard Keimer, Max Planck Inst., Stuttgart
Elizabeth A. Kelly, Univ. of Missouri, St. Louis
Alan B. Krueger, Princeton Univ.
Lee Kump, Penn State

Mitchell A. Lazar, Univ. of Pennsylvania
Virginia Lee, Univ. of Pennsylvania
Anthony J. Leggett, Univ. of Illinois, Urbana-Champaign
Michael J. Lenardo, NIAID, NIH
Norman L. Letvin, Beth Israel Deaconess Medical Center
Olle Lindvall, Univ. Hospital, Lund
Richard Losick, Harvard Univ.
Ke Lu, Chinese Acad. of Sciences
Andrew P. MacKenzie, Univ. of St. Andrews
Raul Madariaga, Ecole Normale Supérieure, Paris
Rick Maizels, Univ. of Edinburgh
Michael Malim, King's College, London
Eve Marder, Brandeis Univ.
William McGinnis, Univ. of California, San Diego
Virginia Miller, Washington Univ.
Yasushi Miyashita, Univ. of Tokyo
Edward Morse, Norwegian Univ. of Science and Technology
Andrew Murray, Harvard Univ.
Naoto Nagao, Univ. of Tokyo
James Nelson, Stanford Univ. School of Med.
Roeland Nolte, Univ. of Mijmegen
Helga Nowotny, European Research Advisory Board
Eric N. Olson, Univ. of Texas, SW
Erin O'Shea, Univ. of California, SF
Elinoir Ostrom, Univ. of Pennsylvania
Jonathan T. Overpeck, Univ. of Arizona
John Pendry, Imperial College
Philippe Poulin, CNRS
Mary Power, Univ. of California, Berkeley
David J. Read, Univ. of Sheffield
Les Res, Emory Univ.
Colin Renfrew, Univ. of Cambridge
Trevor Rees, Univ. of Cambridge
Nancy Ross, Virginia Tech
Edward M. Rubin, Lawrence Berkeley National Labs
Gary Ruvkun, Mass. General Hospital
J. Roy Sambles, Univ. of Exeter
David S. Schimel, National Center for Atmospheric Research
George Schulz, Albert-Ludwigs-Universität
Paul Schulz Letert, Max Planck Inst., Cologne
Terence J. Sejnowski, The Salk Institute
David Sibley, Washington Univ.

George Somero, Stanford Univ.
Christopher R. Somerville, Carnegie Institution
John Steitz, Yale Univ.
Edward I. Stiefel, Princeton Univ.
Thomas Stocker, Univ. of Bern
Jerome Strauss, Univ. of Pennsylvania Med. Center
Tomoyuki Takahashi, Univ. of Tokyo
Marc Tatar, Brown Univ.
Glenn Telling, Univ. of Kentucky
Marc Tessier-Lavigne, Genentech
Craig B. Thompson, Univ. of Pennsylvania
Michiel van der Klis, Astronomical Inst. of Amsterdam
Derek van der Kooy, Univ. of Toronto
Bert Vogelstein, Johns Hopkins
Christopher A. Walsh, Harvard Medical School
Christopher T. Walsh, Harvard Medical School
Graham Warren, Yale Univ. School of Med.
Colin Watts, Univ. of Dundee
Julia R. Weertman, Northwestern Univ.
Daniel M. Wegner, Harvard University
Ellen D. Williams, Univ. of Maryland
R. Sanders Williams, Duke University
Ian A. Wilson, The Scripps Res. Inst.
John Workman, Stowers Inst. for Medical Research
John R. Yates III, The Scripps Res. Inst.
Martin Zatz, NIMH, NIH
Walter Zieglschberger, Max Planck Inst., Munich
Huda Zoghbi, Baylor College of Medicine
Maria Zuber, MIT

BOOK REVIEW BOARD

John Aldrich, Duke Univ.
David Bloom, Harvard Univ.
Linda Schieberger, Stanford Univ.
Richard Sweder, Univ. of Chicago
Ed Wasserman, DuPont
Lewis Wolpert, Univ. College, London



EXHIBITS

Baby Monitor

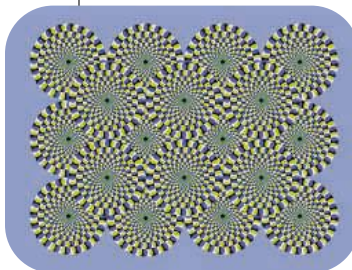
Anesthesiologist Virginia Apgar (1909–1974; above) isn't a household name, but her protocol for quickly gauging a newborn's condition helped reform medical procedures in the delivery room. Read more about Apgar's life and contributions at this new exhibit from the U.S. National Library of Medicine's Profiles in Science series.

The first female full professor at Columbia University College of Physicians and Surgeons, Apgar grew worried about the high death rate for newborns even in modern hospitals. She proposed a list of standard criteria for recognizing that a baby is in trouble: heart rate, respiration, muscle tone, response to stimulation, and color. Today, the Apgar score still dictates whether a youngster receives emergency treatment. Along with a biography, the site offers a cache of Apgar's letters and publications, including the 1953 paper in which she first described her assessment system. >> profiles.nlm.nih.gov/CP

RESOURCES

Gone to Seed

The early stages of a plant's life are the bailiwick of the Seed Biology Place, a primer from botanist Gerhard Leubner of Freiburg University in Germany. From the site's 10 chapters, visitors can reap the latest information on seed evolution, dormancy, and other topics. Numerous diagrams will fertilize your understanding of seed anatomy and plant hormones' role in germination. Chapters also sprout abundant links to abstracts and full-text articles by members of Leubner's lab and other researchers. Right, a magnetic resonance image of a barley grain 15 days after pollination. >> www.seedbiology.de/index.html



IMAGES

<< Get Disillusioned

If these circles appear to be spinning, you don't need to update your eyeglass prescription. Instead, take a look at this Web site on optical illusions from psychologists at the Autonomous University of Barcelona in Spain. Here you can follow step-by-step explanations of some common physical, physiological, and cognitive *trompe l'oeil*. The site allows visitors to manipulate the illusions until their secrets are transparent. You can battle perspective to predict line lengths in Ponzo's illusion or play with the brightness in the spinning wheels trick. The circles appear to revolve because their luminance differs from that of the background. >>

psicol93.uab.es/ilusions

Send site suggestions to >> netwatch@aaas.org Archive: www.sciencemag.org/netwatch

Q What's the quickest link to advances in the world of science?

AAAS

AAAS Advances—the free monthly e-newsletter exclusively for AAAS members.

Each month, AAAS members keep up with the speed of science via a quick click on the newsletter Advances.

Look for the next issue of Advances delivered to your inbox mid month. Look up archived issues at aaas.org/advances.

Features include:

- A special message to members from Alan Leshner, AAAS CEO
- Timely news on U.S. and international AAAS initiatives
- Just-released reports and publications
- Future workshops and meetings
- Career-advancing information
- AAAS members-only benefits

All for AAAS members only.

aaas.org/advances



Advances

Advances – The Monthly Newsletter for AAAS Members

- Message to Members: [R&D Funding Trends](#)
- AAAS in Action: [News to Note](#)
- AAAS at Work: [Programs at the Forefront](#)
- AAAS Science Careers: [Events, Tools, Advice](#)
- AAAS Announcements: [Items of Interest](#)
- Read On, Online: [Science Sites](#)

**Message to Members
R&D FUNDING TRENDS**

Dear AAAS Member,
As a continuing service to scientists, engineers, and others, AAAS provides timely, comprehensive, and in-depth analyses of R&D funding in the U.S. federal budget. A new AAAS analysis of the proposed Fiscal Year 2007 shows that R&D funding for most nondefense areas is projected to decline significantly over the next five years, but a few will in fact increase. Funding for the physical sciences, NSF, the Department of Energy, and the National Science Foundation will increase, as will funding for space and technology. At the same time, the National Institute of Health budget is slated to continue a decline over the next few years. For continuously updated coverage of the U.S. Congress and Executive Branch, go to aaas.org. A book-length report on R&D in the FY 2007 budget was released at the AAAS Forum on S&T Policy and the AAAS continues to speak out, both directly and indirectly, in public forums, urging sound science policy, investment in critical areas such as the physical sciences, health, and energy resources, which is necessary for innovation to benefit global society. We thank you for supporting these critical actions.

Sincerely,
Alan I. Leshner, CEO, AAAS

P.S. Symposium proposals are due 8 March 2007. Meeting, "Science and Technology for the Future," 10-12 February in San Francisco.



BOOK FROM A BOG

The finding last week of an ancient Christian psalm book, thought to be perhaps 1200 years old, has stunned archaeologists, who have already drawn comparisons to the Dead Sea Scrolls.

A bulldozer working in a bog in the Irish midlands uncovered the ancient book, written on vellum. Archaeologists from the National Museum of Ireland excavated the book, which is still in its original binding, and surrounding material. "This is an exceptional find," says museum head Ragnall Ó Floinn. "The last find of a pre-1000 A.D. manuscript was in the 1790s." He adds that although ancient bodies have been found in bogs, preserved by the peat, this is a first for a manuscript.

The book has 40 sheets of vellum, comprising 80 pages, and contains psalms written in a Latin script used by scribes in early Christian Ireland. The script resembles the rounded letters in the 1200-year-old Book of Kells, an illuminated manuscript of the Gospel, says Ó Floinn. The text of Psalm 83 is visible, and experts think the book may contain all the psalms as well as clues to Irish religious practices of that period.

Scholars around the world are looking forward to studying the find once it has been safely dried out and preserved. Dáibhí Ó Cróinín, a professor of history at the National University of Ireland, Galway, says, "It is very rare to have a full manuscript, and biblical scholars will be salivating."

Nice Song—I'll Have Another

Owners of bars with disappointing revenues may want to change their CD collections. A study published in the current *International Journal of Hospitality Management* suggests that replacing Top 40 pop fare with classic drinking songs may inspire increased consumption.

Several previous studies have indicated that music influences customer drinking choices; one paper showed that people took home more expensive bottles when a wine store played classical music, and another showed that music from Germany or France made the enophiles more likely to pick up German or French wines.

For the new study, Céline Jacob of the Research Center in Economics and Management at the Université de Rennes 1 in France asked the owner of a small bar in a French coastal town to play one of three types of popular music during the afternoon: current hits, songs from animated movies such as *Snow White and the Seven Dwarfs*, or classic French drinking songs. For each genre, about 30 patrons were secretly monitored and their tabs tallied. With the drinking songs playing, customers stayed an average of 21 minutes—compared to 13 minutes with the Top 40 hits and 14 with the cartoon songs. They also spent 50% more, averaging €4.96 apiece.

Psychologist Alexandra Logue of the City University of New York calls the outcomes "very interesting." She says drinking songs may cause physical reactions that promote drinking, just as thinking of food can raise insulin levels.

EYE ON THE IBIS

The northern bald ibis, once the bird of the pharaohs and now the Middle East's rarest bird, might take a step back from the brink of extinction with a new tagging program.

There are about 227 of the birds in the wild, mostly in Morocco and Turkey. Most ibises are sedentary, but 6 years ago, scientists discovered a tiny group in Syria that left their breeding grounds every summer, returning in February. Several wildlife organizations have now teamed up with the Syrian Agriculture Ministry to find out where they spend the rest of the year.

Last month, three of the ibises were outfitted with transmitters allowing them to be tracked by satellite. The seven-member colony "has not been growing, which means there must be problems on migration or wintering grounds," says researcher Jeremy Lindsell of the U.K.'s Royal Society for the Protection of Birds. Scientists now hope to find out why. Since the birds took off on 18 July, they have traveled southward nearly 3200 kilometers, reaching the Yemeni border last Friday. Updates on their progress can be seen at www.rspb.org.uk/tracking/northern_bald_ibis.asp.



Ibis as the head of King Toth.



<< A CLOSE-UP OF HISTORY

This vintage 1830 microscope, used by Gregor Mendel, the progenitor of genetics, is one of the items that will be on display starting 15 September at the Field Museum in Chicago, Illinois. Mendel, an Augustinian friar, did his groundbreaking research on pea plants in the garden of the Abbey of St. Thomas in Brno, then

part of the Austrian Empire. He used the instrument, which magnified pollen 179 times, to facilitate pollination of a plant with a single grain—something Darwin and others had said was impossible. The exhibit includes photographs, manuscripts, and Mendel's gardening tools, as well as videos and interactive displays.

Breakdown in
Singapore

600

Seeing
supersolidity

603

SCIENTIFIC PUBLISHING

The Undisclosed Background of a Paper on a Depression Treatment

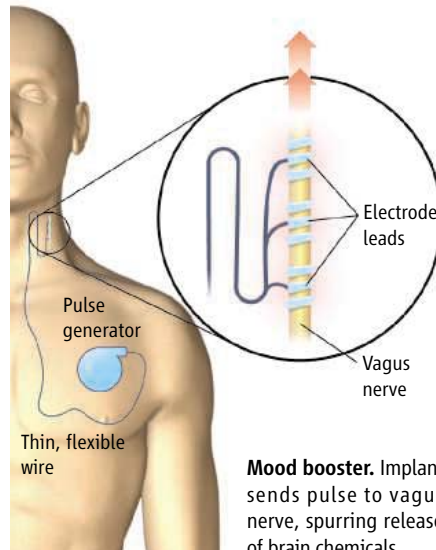
Last month, a group of scientists published a review of research on vagus nerve stimulation (VNS), a controversial treatment for depression. But the article, published in the journal *Neuropsychopharmacology*, omitted an important detail: All the authors are paid advisers to the company that manufactures a device for VNS that was approved last year by the U.S. Food and Drug Administration.

The episode has raised a stir at the American College of Neuropsychopharmacology (ACNP), publisher of the journal, which has promised an investigation as soon as lead author Charles B. Nemeroff—who is also editor-in-chief of the journal—returns from a vacation in South Africa. Nemeroff, chair of the psychiatry department at Emory University in Atlanta, Georgia, says he and his co-authors informed the journal about their ties to Cyberonics in Houston, Texas, manu-

facturer of the device. He says the failure to mention those ties in the article, as required by journal policy, was a simple “oversight.” A prominent depression researcher with his thumb in many commercial pies, Nemeroff heads the “mechanism of action” advisory board at Cyberonics.

The paper, authored with seven other board members and a Cyberonics employee, reviews research on use of the Vagus Nerve Stimulator—an implanted device that sends impulses by wire to the vagus nerve in the neck—to treat severe depression. The article speculates on the mechanisms of action, which are as yet unclear.

Some observers find this episode particularly troubling because not only is Nemeroff the journal’s editor but also the first draft of the paper was prepared by a professional writer, hired by Cyberonics, who



Mood booster. Implant sends pulse to vagus nerve, spurring release of brain chemicals.

was not listed among the authors. (She was named in the acknowledgements.) The matter attracted considerable press coverage in late July, thanks in large part to the efforts of Bernard Carroll, former chair of psychiatry at Duke University and now at the Pacific Behavioral Research Foundation in ▶

PLANETARY SCIENCE

At Last, Methane Lakes on Saturn’s Icy Moon Titan—But No Seas

Team members poring over radar data returned on 21 July by the Cassini spacecraft believe they now have very strong evidence for methane lakes on Saturn’s haze-shrouded moon Titan. That would make Titan the only

says planetary radar specialist Donald Campbell of Cornell University.

When Cassini was launched, most planetary scientists expected that it would find Titan covered by seas of methane liquefied by the moon’s -183°C temperatures. But those hydrocarbon seas were nowhere to be seen on Cassini’s arrival, and Cassini’s Huygens lander later bumped down on methane-damp water ice rather than splashing down in a frigid sea or even a puddle. Yet methane clouds, high methane humidity, and river-cut valleys in the icy surface spoke of methane cycling on Titan much the way water cycles through oceans, clouds, and rain on Earth.

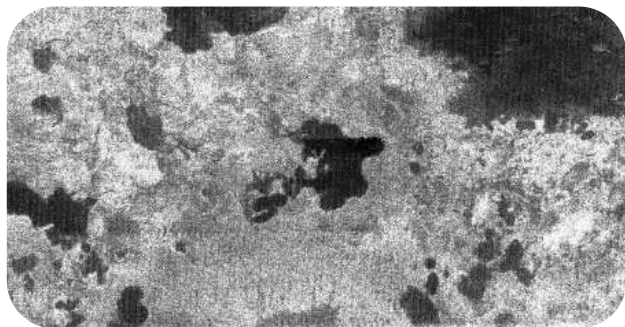
On its latest pass by Titan, Cassini’s surface-scanning radar detected places that fail to reflect any detectable signal back to Cassini, says team member Jonathan Lunine of the University of Arizona,

Tucson. That is just the way a radar beam striking a smooth, liquid surface would behave; the signal would just bounce away from Cassini into space.

These “radar-black” areas ranging from 1 or 2 kilometers to 30 kilometers in size meet other expectations of lakes, says Lunine. The putative shorelines are sharp boundaries between radar-black and radar-gray, and some possible tributaries are radar-black as well. And the lakelike features reside poleward of 70°N , where weather models predict that there should be substantial rain in northern Titan winter to fill them. Equatorward of 70°N , where it shouldn’t be raining much, the same sort of topography has no lakelike features.

Team members think they have finally found the last link in the methane cycle of Titan. To be absolutely certain, the Cassini team decided to scan some of the same “lakes” during an October flyby from a slightly different angle. If there’s wind on the lakes, Cassini radar may catch signs of waves.

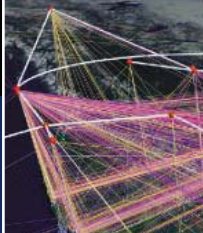
—RICHARD A. KERR



A likely lake. The black blotch in the center of this radar image returned by Cassini is so black that it is probably a pool of liquefied methane.

other body in the solar system known—or ever likely to be known—to have standing bodies of liquid. The new radar images “looked quite convincing; I was impressed,”

CREDITS (TOP TO BOTTOM): (BASE ANATOMY IMAGE) 3D CLINIC/CORBIS; NASA/JPL



Carmel, California. Last month, Carroll broadcast an e-mail to colleagues and the press accusing Nemeroff of running a “slick public relations disinformation campaign,” hiring a “ghostwriter,” and “incestuously” placing the article in his own journal.

ACNP initially responded by acknowledging a “serious omission” and saying that corrections were being made online and in print. In Nemeroff’s defense, it pointed out that he had recused himself from the journal’s editorial process and said, “The charge the paper was ‘ghostwritten’ does not appear to be valid.” Last week, however, ACNP Executive Director Ronnie Wilkins said the ACNP council plans a

“thorough investigation” of the matter, including a comparison of the original and final drafts of the manuscript.

Nemeroff insists he is guilty of “an oversight and nothing more. ... I provided all of the financial disclosure information to *Neuropsychopharmacology*, ... but it was not all included in the printed version of the paper,” he said in an e-mail to *Science*. “These things are being hypermagnified beyond their importance,” says Alan Schatzberg, chair of psychiatry and behavioral sciences at Stanford University in Palo Alto, California, who calls Carroll’s accusations “outlandish.”

Others are more worked up. Psychiatrist Irwin Feinberg of the University of California, Davis, calls Nemeroff’s actions “inexcusable.” And Drummond Rennie, an editor at the *Journal of the American Medical Association*, adds, “It is very bad scientific and ethical practice to have a nonauthor write the first draft.”

Many acknowledge that, whatever the final outcome of the ACNP’s investigation, appearances are everything. This has “sorely devalued” both the journal and ACNP, says psychiatrist Richard Wurtman of the Massachusetts Institute of Technology in Cambridge. “And I’m afraid this perception won’t disappear for a long time.”

—CONSTANCE HOLDEN

EARTH SCIENCE

China Grapples With Seismic Risk in Its Northern Heartland

BEIJING—Last week, ceremonies marked the 30th anniversary of the deadliest earthquake in 400 years: the Tangshan earthquake, which killed at least 244,000 people in China’s Hebei Province. But as the 1976 cataclysm fades into history, a scientific puzzle endures: The magnitude-7.5 temblor struck along a fault that no one knew existed.

Tangshan is a striking example of the enigmatic tectonics of northern China—a problem now getting long overdue attention. In one project, China is installing a seismometer array across the North China Plain, and this fall the Natural Sciences Foundation of China (NSFC) is expected to unveil a \$20 million, 5-year initiative to probe the region’s geology and seismic risk. The twin efforts, described here last week at the 2006 Western Pacific Geophysics Meeting, “will treat north China as a natural laboratory for studying earthquakes,” says geophysicist Zhou Shiyong of Peking University. He says that the Chinese Earthquake Administration (CEA), tasked with quake prediction, views north China as an analog of the Parkfield segment of the San Andreas fault in California, the most closely observed earthquake zone in the world.

The stakes are high: North China is “the political, economic, and scientific center of China,” Zhou says. Seismic risk is of paramount political concern. Moments after a magnitude-5.1 quake rattled Beijing on 4 July, Premier Wen Jiabao phoned the CEA director to ask for a detailed report, says Mian Liu, a geophysicist at the University of Missouri, Columbia.

Most puzzling is why north China is a seismic hotbed. Much of the region sits atop a craton, a chunk of ancient crust that, by definition, should shake little. But some 150 million years ago, the North China Craton became restive. “No other cratons behave like this. North China is unique,” says Liu. Intraplate faults



Solemn vigil. Ruins from the Tangshan earthquake.

themselves are not novel: A prime example is the New Madrid fault in Missouri. But deformation in north China is an order of magnitude larger than that of New Madrid, Liu says. The result has been a parade of devastating quakes in northern China, including Tangshan and the worst in history: the Shaanxi earthquake in 1556, which claimed some 830,000 lives.

To help shed light on this tectonic anomaly, the Deep Earth Lightning project—involving CEA, the Chinese Academy of Sciences, and

NSFC—is wiring north China with nearly 800 portable broadband seismometers. The array will image the crust and upper mantle to map faults and explore craton evolution and dynamics. The initiative is setting up a data center modeled after the Incorporated Research Institutions for Seismology (IRIS) consortium in Washington, D.C., says Chen Yong of CEA’s Institute of Earthquake Science in Beijing.

Complementing that effort is NSFC’s Great North China Initiative. GNCI, a top priority in NSFC’s strategic plan, evolved from discussions between top Chinese geoscientists and a U.S.-based association of Chinese expatriates, the International Professionals for the Advancement of Chinese Earth Sciences.

Both initiatives mark a tectonic shift of a different sort. In the past, Western scientists often hired Chinese counterparts as guides or assistants. Now the Chinese are calling the shots. “This is a fundamental change in collaborating with the Chinese scientific community,” says Liu. U.S. scientists, he says, “should take advantage of this new funding environment.”

Either way, the initiatives should be revelatory, says Liang Xiaofeng of Peking University: “There are too many unknown structures beneath our feet.”

—RICHARD STONE

INTERNATIONAL SCIENCE

Singapore-Hopkins Partnership Ends in a Volley of Fault-Finding

Singapore's government and Johns Hopkins University in Baltimore, Maryland, are shutting down a joint research and education program that Singapore has funded for 8 years at a cost of more than \$50 million. As news of the closure leaked last week, the partners blamed each other for failing to achieve goals on recruiting faculty, enrolling students, and transferring technology to local industry, among other issues.

The collaborative effort, supported by Singapore's Agency for Science, Technology, and Research (A*STAR), has a troubled history. According to a chronology of events released by A*STAR, Singapore and Johns Hopkins agreed to set up an international clinic as well as an educational and research scheme in 1998. Although the clinic proved successful, the joint educational and research efforts were struggling; in February 2004, they were restructured into the Division of Biomedical Sciences Johns Hopkins in Singapore (DJHS), reporting to the dean of medicine at Johns Hopkins's Baltimore campus.

Early this year, A*STAR concluded that DJHS was still failing to meet goals. After unsuccessful negotiations between the agency and the university, on 20 June, the

director of A*STAR's Biomedical Research Council, Andre Wan, and DJHS Director Ian McNiece jointly sent a private notice to



Trouble in Biopolis. Singapore is pulling the plug on a training and research program cosponsored by Johns Hopkins University.

all staff and faculty members that DJHS was being “wound down.”

Few knew about it until the news appeared in Singapore's *The Straits Times* newspaper on 22 July. The article quoted an unnamed Johns Hopkins University spokesperson as saying the university had done its part to recruit faculty members and graduate students and accusing A*STAR of failing to meet its financial and educational obligations. According to the newspaper, the Johns Hopkins spokesperson called it a “reputa-

tional issue for Singapore and A*STAR.”

A*STAR responded with a barrage of letters to editors and public statements, including charts giving the history of the collaboration and snippets of e-mails between agency and university officials. Among other things, A*STAR claims DJHS failed to meet eight of 13 agreed “key performance indicators.” DJHS was supposed to attract 12 senior investigators with an international standing to the faculty in the first 2 years of the new agreement. A*STAR alleges that there is only one faculty member meeting those criteria; others are entry-level academics or do not reside full-time in Singapore. A*STAR also claims that by February this year, DJHS was to have enrolled eight Ph.D. students but had none. Wan says A*STAR responded strongly “to make it clear that Singapore had lived up to our financial obligations and had been more than generous with support and opportunities for the project to succeed.”

DJHS directed queries to Johns Hopkins's Media Relations office in Baltimore, which, as *Science* went to press, had not replied to requests for an interview or to e-mailed questions.

Wan describes the joint effort as “an experiment that didn't give us the results hoped for.” But he notes that Singapore is collaborating with other universities. In July, a separate agency announced plans for a new joint research center with the Massachusetts Institute of Technology. “We have multiple avenues for young Singaporeans to pursue scientific training,” Wan says.

—DENNIS NORMILE

NEUROSCIENCE

The Emotional Brain Weighs Its Options

Faced with a decision between two packages of ground beef, one labeled “80% lean,” the other “20% fat,” which would you choose? The meat is exactly the same, but most people would pick “80% lean.” The language used to describe options often influences what people choose, a phenomenon behavioral economists call the framing effect. Some researchers have sug-

Choice meat. The brain's emotional areas react to the language describing a choice—80% lean, for example.



gested that this effect results from unconscious emotional reactions.

Now a team of cognitive neuroscientists reports findings on page 684 that link the framing effect to neural activity in a key emotion

center in the human brain, the amygdala. They also identify another region, the orbital and medial prefrontal cortex (OMPFC), that may moderate the influence of emotion on decisions: The more activity subjects had in this area, the less susceptible they were to the framing effect. “The results could hardly be more elegant,” says Daniel Kahneman, an economist at Princeton Uni-

versity who pioneered research on the framing effect 25 years ago (*Science*, 30 January 1981, p. 453).

In the new study, a team led by Benedetto De Martino and Raymond Dolan of University College London used functional magnetic resonance imaging (fMRI) to monitor the brain activity of 20 people engaged in a financial decision-making task. At the beginning of each round, subjects inside the fMRI machine saw a screen indicating how much money was at stake in that round: £50, for example. The next screen offered two choices. One option was a sure thing, such as “Keep £20” or “Lose £30.” The other option was an all-or-nothing gamble. The odds of winning—shown to the subjects as a pie chart—were rigged to provide the same ▶

CREDITS (TOP TO BOTTOM): MUNSHI/AHMED PHOTOGRAPHY; K. BUCKHEIT/SCIENCE

average return as the sure option. In interviews after the experiment, participants said they'd quickly realized that the sure and gamble options were equivalent, and most said that they had split their responses 50–50 between the two choices.

But they hadn't. When the sure option was framed as a gain (as in "Keep £20"), subjects played it safe, gambling only 43% of the time on average. If it was framed as a loss, however, they gambled 62% of the time.

When the researchers examined the fMRI scans, the amygdala stood out. This brain region fired up when subjects either chose to keep a sure gain or elected to gamble in the face of a certain loss. It grew quiet when subjects gambled instead of taking a sure gain or took a sure loss instead of gambling. De Martino suggests that the amygdala activity represents an emotional signal that pushes subjects to keep sure money and gamble instead of taking a loss.

De Martino says he expected to find that subjects with the most active amygdalas

would be more likely to keep sure gains and gamble when faced with a certain loss. But no such correlation turned up. Instead, activity in OMPFC best predicted individuals' susceptibility to the framing effect. De Martino speculates that OMPFC integrates emotional signals from the amygdala with cognitive information, such as the knowledge that both options are equally good. "People who are more rational don't perceive emotion less, they just regulate it better," he says.

"It's a nice, strong correlation between individual differences in behavior and individual differences in the brain," says Russell Poldrack, a neuroscientist at the University of California, Los Angeles. Yet Elizabeth Phelps, a cognitive neuroscientist at New York University, cautions that fMRI studies alone can rarely prove a brain region's causal role. She suggests examining people with damage to the amygdala or OMPFC to clarify how these regions contribute to the framing effect.

—GREG MILLER

AVIAN INFLUENZA

Hybrid Viruses Fail to Spread

Experts have long worried that if a human influenza virus and the H5N1 avian influenza strain now circulating across much of the globe were to combine their genes, the result could be a disaster—a lethal virus that spreads easily among people. But scientists at the U.S. Centers for Disease Control and Prevention (CDC) in Atlanta, Georgia, who in controversial experiments have created such potential pandemic viruses in the lab, report this week that the hybrid viruses are, at least in ferrets, relatively benign.

That doesn't mean the world can let down its guard against H5N1. "I'm cautious about using the word 'reassuring,'" CDC Director Julie Gerberding told reporters, noting that the study looked only at simple combinations of one human flu virus and a single H5N1 strain. But it would have been bad news if a so-called reassortant had spread easily among ferrets, according to virologist Albert Osterhaus of Erasmus Medical Center in Rotterdam, the Netherlands. We can be a "little bit" relieved, he says.

To Osterhaus, Gerberding, and others, the new study, published online this week in the *Proceedings of the National Academy of Sciences*, confirms the value of reassortant experiments, which some bioweapons experts have said should not proceed without more review, if at all (*Science*, 30 July 2004, p. 594). CDC says the work also establishes



Mixed up. CDC scientists tested hybrids of the H5N1 influenza virus (above) and a human flu virus.

ferrets, which have a respiratory tract that makes them similar to humans in their susceptibility to the influenza virus, as an important new animal model in which to test how flu strains spread.

Since 1997, the H5N1 virus has infected at least 232 people, mostly in Asia, 134 of whom have died. So far, the virus has not assumed a form that passes easily among humans. That could happen if H5N1 were to develop the needed mutations, as likely happened with the 1918 Spanish influenza. Or an H5N1 flu ►

Pandemic Vaccine Shows Promise

For the first time, a vaccine against the avian influenza strain H5N1 has shown promise at low doses, making it a possible candidate for use in a pandemic. In a statement issued last week, GlaxoSmithKline (GSK) said that a trial involving 400 healthy volunteers in Belgium revealed that two vaccine shots of just 3.9 micrograms each were enough to elicit antibodies against the flu strain.

Previously tested pandemic vaccines, which have consisted of killed copies of a genetically engineered virus, were efficacious only at much higher doses of up to 90 micrograms injected twice (*Science*, 12 August 2005, p. 996). Because most flu vaccines are still produced using chicken eggs, production is difficult to scale up; that's why experts say a so-called dose-sparing vaccine such as GSK's is essential to protect large numbers of people in a pandemic. GSK declined to reveal the nature of the so-called adjuvant, an immune-boosting ingredient, in its vaccine. "We need to see more data," says Frederick Hayden, an influenza expert at the World Health Organization in Geneva, Switzerland, "but it looks like an encouraging result."

—MARTIN ENSERINK

Go Deep

CAMBRIDGE, U.K.—The United Kingdom should permanently dispose of its radioactive waste in a deep geological repository, says a government-appointed panel of experts after more than 2 years of study. The U.K. government must dispose of 470,000 cubic meters of waste already in temporary storage from existing plants. Among its key points, the committee recommends research into interim storage—because it may take as long as a century to complete a deep storage site—and the immediate creation of a body to get the process rolling. Given the opposition to earlier proposed sites, the committee calls for localized incentives for potential host communities. "It will take a long time to put in place all the component parts, so now it's time to get on with the job," says Gordon MacKerron of the University of Sussex, the panel's chair.

Geoffrey Boulton, chair of the Royal Society's working group on radioactive-waste management, welcomed the recommendations. "There is considerably less scientific uncertainty in this approach than with other options," he said in a statement.

—DANIEL CLERY

virus that has infected a person could swap some of its eight genes with those of a human flu virus—keeping its H5 hemagglutinin surface protein, to which people have no immunity. Known as reassortment, this process led to two milder flu pandemics in 1957 and 1968.

So, CDC researchers and collaborators used a lab technique called reverse genetics to make combinations of H3N2, a seasonal human flu strain, and the 1997 strain of H5N1. To model the virus's spread in people, they housed ferrets inoculated with the reassortants in cages adjacent to healthy ferrets, which would allow the infected animals to pass on the virus through the air.

The hybrids with H3N2 proteins on the outside and H5N1 internal proteins replicated well in cells but didn't transmit as easily in ferrets as H3N2 itself, the CDC team found. And the potentially most dangerous combinations—viruses containing genes for H5N1's surface proteins and for internal human virus proteins—not only didn't grow as well as H5N1 but also didn't spread at all between ferrets. Any reassortant would likely need more genetic changes, such as ones that made the 1957 and 1968 strains better able to bind to human respiratory tract epithelial cells, the CDC team suggests. “The picture is more complex” than just mixing avian and human flu

genes, says co-author Jacqueline Katz of CDC.

The CDC team also infected a ferret with an H5N1 outer/H3N2 inner hybrid, allowed the virus time to mutate, and then inoculated another ferret with virus from the first animal, repeating this cycle four more times. The virus still didn't become transmissible, however.

CDC and other labs are now conducting reassortment studies with more recent H5N1 strains and more human flu strains. “I don't think we should underestimate the virus,” says flu researcher Yoshihiro Kawaoka of the University of Tokyo and the University of Wisconsin, Madison.

—JOCELYN KAISER

With reporting by Martin Enserink.

PHYSICS

High-Temperature Superconductors Feel the Vibe After All

Tiny vibrations could shake up physicists' understanding of high-temperature superconductors. In ordinary superconductors, quantized vibrations, or “phonons,” provide the glue that binds electrons in pairs, and they then zip through the material unimpeded. But for various reasons, most physicists believe phonons have little to do with high-temperature superconductors' ability to conduct electricity with zero resistance at temperatures up to 138 kelvin. Now, ultraprecise measurements may nudge researchers to reconsider that assumption.

“I'm very happy that these results seem to be consistent with what we have been saying,” says Zhi-Xun Shen, an experimenter at Stanford University in Palo Alto, California, who has reported other evidence of electron-phonon interactions in high-temperature superconductors. However, some researchers argue that the vibrations seen in the new work are an experimental artifact.

To spot the shaking, J. C. Séamus Davis of Cornell University and colleagues employed a fingerlike probe called a scanning tunneling microscope (STM). The STM's tip hovered above the surface of the superconductor, bismuth strontium calcium copper oxide, and electrons jumped between the two. At different points above the material, the team varied the voltage between tip and surface and recorded the rate at which the current changed. That revealed the number of channel-like quantum states into which the electrons could jump.

As the researchers ramped up the voltage, they observed a deep dip in the number of states; this so-called superconducting gap arises when the electrons form pairs. On either side of the gap, they also saw wiggles,

or “inflection points,” as they report this week in *Nature*. These were signs that something was interacting with the electrons. The researchers proved it was phonons by showing that the energy of the

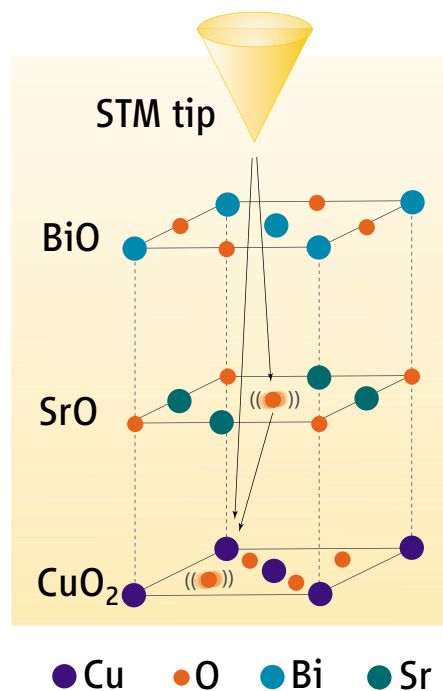
change the maximum temperature at which a given high-temperature superconductor works. That's one reason many researchers have doubted that phonons cause the pairing of electrons within them.

Others had observed electron-phonon interactions by, for example, using x-rays to measure the speed of the electrons, which decreases above a certain energy as phonons essentially drag on the electrons. But Davis and colleagues also show a correlation between the energy of the phonon and the width of the superconducting gap, both of which vary almost from atom to atom across the surface. That suggests that the electron-phonon interaction isn't an extraneous detail but actually affects the superconductivity, Davis says. The phonons alone still may not provide the glue for pairing, he says, but “more and more people are concluding that you can't ignore these lattice vibrations.”

Some researchers are skeptical, however. Davis's team believes the shaking atoms lie in the planes of copper and oxygen in the layered superconductor along which the paired electrons glide. But to reach such a plane, an electron from the STM might first hop onto an oxygen in the layer of atoms above and set it vibrating, notes Manfred Sigrist, a theorist at the Swiss Federal Institute of Technology in Zurich. That could generate a very similar signal, Sigrist says. But Thomas Devereaux, a theorist at the University of Waterloo in Canada, says if that effect were so strong, it should have shown up in other STM experiments, too.

In spite of the skepticism, it's clear that phonons are now a hot topic in high-temperature superconductivity.

—ADRIAN CHO



Spot the signal. Do the observed vibrations come from an electron jumping straight to the copper oxide layer, or from it stopping in the strontium oxide layer en route?

features decreased in samples in which they replaced the common isotope oxygen-16 with heavier oxygen-18. That's exactly what should happen if the wiggles were produced by vibrating oxygen atoms.

Ironically, changing isotopes does not

PHYSICS

Physicists See Solid Helium Flow, But Not in the Most Exciting Way

If seeing is believing, then a new experiment dispels all doubt that, bizarrely, solid helium can flow like the thinnest conceivable liquid. Physicists have literally watched solid helium flow when tugged on by gravity, they report online in *Science* this week (www.sciencemag.org/cgi/content/abstract/1130879). The direct observation confirms less conclusive evidence of “supersolidity” from 2 years ago. Ironically, it may also undermine the most tantalizing explanation of the phenomenon.

In 2004, Eunseong Kim, now of the Korea Advanced Institute of Science and Technology in Daejeon, and Moses Chan of Pennsylvania State University in State College reported the first evidence of supersolidity, and others confirmed their results this year (*Science*, 24 March, p. 1693). Some theorists believe the flow occurs when atoms in an orderly crystal crowd into a single quantum wave in a process called Bose-

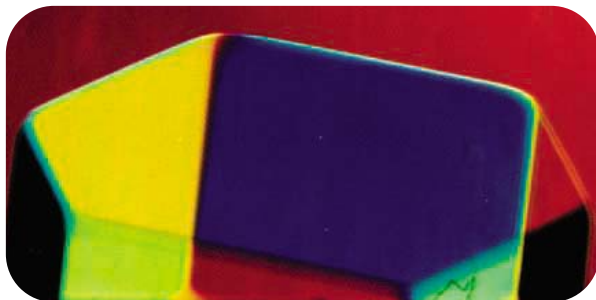
Einstein condensation. Others say that’s impossible, and one group of experimenters claims that signals of the sort Kim and Chan reported vanish when solid helium is gently heated to eliminate flaws in the crystal.

Now, Sébastien Balibar of the École Normale Supérieure in Paris and colleagues have seen the flow of solid helium—but only in imperfect crystals consisting of several distinct “grains.” That suggests a less exotic explanation for the flow: On the boundaries between grains, the helium remains inherently liquid, and superfluid liquid helium, which also flows without resistance, seeps along the interfaces. “Balibar’s experiment says, ‘Wait a minute folks; this might not be as astonishing as we thought,’” says Robert Hallock, an experimenter at the University of Massachusetts, Amherst.

To see the flow, Balibar and colleagues placed an inverted test tube in a container of liquid helium and compressed the helium to more than 28 times atmospheric pressure to make some of it solidify. The denser solid filled the bottom of the container and grew up into the tube. The physicists then quickly melted some of the helium surrounding the tube. If the solid could flow through itself, then the level

inside the tube should fall to match that of the surrounding solid. And that’s precisely what the researchers saw—sometimes.

On two occasions, the level inside the tube fell at a steady rate rather than slowing, a crucial detail that indicates the flow encountered no resistance. In 10 cases, the level inside the tube remained fixed. In fact, the solid flowed only if its surface showed cusplike ridges of the sort that would form when the boundaries between grains poke through the surface. That suggests “this effect is not due to the crys-



Price of perfection. Does the faultlessness of this crystal of solid helium stop it from flowing?

talline part but to the space between the crystallites,” Balibar says.

However, Balibar’s experiment differs from Chan’s in a key way, say John Beamish, an experimenter at the University of Alberta in Edmonton, Canada. Chan chills and squeezes his helium so much that only solid helium can exist. Balibar and colleagues study helium at a temperature and pressure at which solid and liquid coexist, like ice and water in glass. The solid is on the verge of melting, Beamish says, and “when a crystal melts, it melts along the grain boundaries, so at some point you would expect to have flow along them.”

Kim and Chan also see evidence of flow in helium crammed into porous glass. That would be hard to explain in terms of grain boundaries, which would have to wend through the pores. All this suggests an intriguing explanation. “It’s entirely possible that Balibar and company have discovered an interesting effect that doesn’t have anything to do with the work of Kim and Chan,” says theorist Anthony Leggett of the University of Illinois, Urbana-Champaign. As with skinning a cat, perhaps there is more than one way to make solid helium flow.

—ADRIAN CHO

Monkey Business Decried

NEW DELHI—The Indian government is investigating charges that the topflight Indian Institute of Science (IISc) in Bangalore acted too hastily in releasing 20 macaques into a protected forest last month. Activists say the long-captive monkeys will likely die in the wild, and the governmental Committee for the Purpose of Control and Supervision of Experiments on Animals (CPCSEA) opened a probe this week. IISc’s primate lab is a “good facility,” says CPCSEA member Sanobar Bharucha, but she says that the release was done “prematurely.” In September, CPCSEA will weigh penalties including limits on experiments and even prison time for the facility’s head. IISc says it followed research guidelines, freeing only healthy animals.

—PALLAVA BAGLA

Climate Squall Peters Out

Congressional hearings on what’s wrong with the science of global warming have quietly segued into less threatening channels. Last year, global-warming skeptic Representative Joe Barton (R-TX) launched an investigation of the so-called hockey-stick climate record, which portrays dramatic warming starting in the late 19th century. Scientists feared that Barton was going to politicize the science, but the matter culminated innocuously enough in two hearings late last month. He has asked the U.S. Government Accountability Office to examine data-sharing policies, “especially as they related to climate change research.” He also plans to ask the National Research Council to examine questions including whether climate science peer review may be too inbred.

—RICHARD A. KERR

“Open” Journal to Open

TORONTO, CANADA—A new competitor journal has emerged as the *Canadian Medical Association Journal (CMAJ)* has reformed itself. Following last winter’s battle over editorial independence (*Science*, 24 March, p. 1695), *CMAJ* last month restored ownership to the association and bolstered oversight; officials say the journal is enjoying a stream of top submissions. Amir Attaran of the University of Ottawa, who helped *CMAJ* review its governance of the journal, calls the new reforms “a very good basis” for a fresh start.

But former *CMAJ* senior editor Anne Marie Todkill says the reforms don’t go far enough, calling for “a fully independent” alternative. She and five other former *CMAJ* editors plan this fall to launch *Open Medicine*, styled after open-access titles published by the Public Library of Science.

—PAUL WEBSTER

Social network analysis made news as a possible tool for scanning phone records for security threats, but the field is exerting a broader impact in business, biology, computer networks—and movie titles

Making Connections

LINTON FREEMAN, A PROFESSOR OF sociology at the University of California, Irvine, has just offered the perfect alibi for murder. A colleague was known to attend every one of the talks in a weekly seminar series. At the end, as part of an experiment, Freeman's students asked the other attendees if he'd been at the last meeting. Those who attended regularly assumed that he must have been, because he'd been to every other session. Those who attended irregularly had no assumptions, and many correctly guessed that he had not been. "If you ever want to do a murder, don't show up where you always are; you'll get away with it," advises Freeman.

Freeman's real point is not to offer a tutorial in crime but to underscore that his specialty—social network analysis (SNA)—is good at uncovering unexpected outcomes in what may seem like obvious situations. Or more complicated ones. SNA made headlines in May, when newspaper reports fueled speculation that the U.S. National Security Agency was using it to scan phone records.

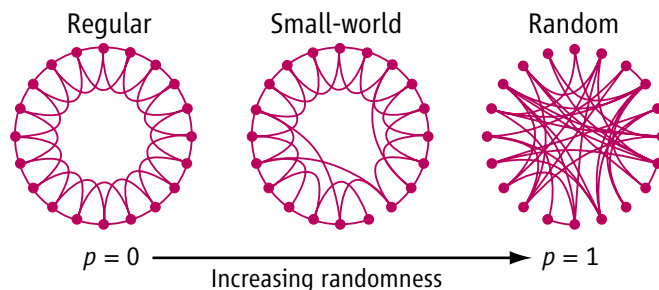
But those in the field are quick to point out that SNA isn't simply some diabolical data-mining scheme. SNA has proven its worth in arenas as far-flung as business, biology, social

policy, epidemiology, and computer networks. It also spawned the catch phrase "six degrees of separation" and a related trivia game involving actors who have worked with the film star Kevin Bacon. There's even an upcoming television show called *Six Degrees*. Unfortunately, its practitioners add wryly, almost everything that people outside the field think they know about it is wrong.

SNA is a full-fledged field of research that dates back at least 70 years. Broadly speak-

can seem trivial to analyze when only a few individuals are involved can grow to frightening complexity in larger networks, especially because one individual can have multiple kinds of connections. To tackle such problems, network analysts bring to bear techniques from statistics, graph theory, and theoretical modeling; a subset of the field, cognitive analysis, looks at people's perceptions, as in Freeman's murder tutorial. "Network analysis with a cognitive twist studies the individual's perceptions of social structure," says statistician Stanley Wasserman of Indiana University, Bloomington, "such as your view of who the cliques are versus the actual cliques."

The results are often counterintuitive. For example, suppose you need to reach an executive in an unfamiliar corporation. You might start by contacting a "hub" person: someone with links to everyone else in the company. But not necessarily, SNA experts are fond of pointing out: The hub person may be so busy that you would be better off going through someone who isn't quite so central. In fact, Freeman says, corporations are increasingly using SNA to ascertain who actually *talks* to whom, rather than who merely reports to whom on their organization charts. Being able to correctly trace an indi-



Sliding scale. A seminal 1998 paper showed that networks come in different degrees of randomness and connectedness. Later work modified the rings into multi-dimensional lattices and explained how even big networks can be easy to search.

ing, it's the study of the structure of connections among individuals, organizations, and nations. Social network analysts directly observe or interview people ("nodes") going about their daily routines, then graph their connections ("paths") and analyze the data to find unsuspected structure. Connections that

vidual's social network, freed from the trap of conventional wisdom, is essential for public health and public policy planning, says Gery Ryan of the RAND Corp., who is working on a study of the social connections of homeless women in order to understand how best to provide support services.

Social networks and the life sciences

SNA has traditionally been an interdisciplinary field, but in the late '90's, two models, both conceived by physicists, drew in even more disciplines. The first, by Duncan Watts and Steve Strogatz of Cornell University, modeled the "small world problem." It was published in *Nature* in 1998, with a follow-up *Nature* paper in 2002. The second, on "scale-free networks," by Albert-László Barabási of the University of Notre Dame in Indiana and his then-graduate student Réka Albert, who is now a professor at Pennsylvania State University in State College, appeared in *Science* in 1999 (15 October 1999, p. 509).

Everyone has had a "small world" experience: The man you sit next to at your distant cousin's wedding turns out to be your former boss's ex-husband, that sort of thing. In 1967, Harvard University professor Stanley Milgram decided to see whether there was more to the phenomenon than just anecdotes. He asked Midwestern volunteers to send packages to strangers in Boston. The Midwesterners were not allowed to mail the packages directly but had to relay them through personal contacts. Milgram reported that the average number of intermediaries for completed chains was five, which made for a six-linked chain—the basis for the popular phrase "six degrees of separation."

Watts and Strogatz wondered what mathematical conditions would be needed to create a "small world" like Milgram's. Purely random sampling wouldn't produce the tight clusters of mutual friends that most of us belong to. But if the world were completely clustered, how could we all be "six degrees" apart? They concluded that networks must exist on a sliding scale between clustered and random, producing tightly knit groups of friends but also short paths that reach throughout the whole network.

Their 1998 paper famously showed that the same mathematical technique could model a power grid, a film actor's collaborators, and the neural network of *Caenorhabditis elegans*. It introduced the "clustering coefficient," a mathematical way to model the friends-of-friends effect: If John knows Mary, and Mary knows Sue, the clustering coefficient weights the likelihood of John also

knowing Sue. The concept has become widely used in biological network analysis from neuroscience to bioinformatics. For example, says Albert, the clustering coefficient can be used as an objective criterion for whether two genes are considered coexpressed.

The paper attracted enormous fanfare, but the model overlooked a crucial insight. Jon Kleinberg of Cornell University pointed out in *Nature* in 2000 that it could explain how Milgram's Midwesterners got near their tar-

could do it in a short hop if they shared an interest in, say, hiking.

Despite how often the 1998 and 2002 papers are cited, Watts despairs that the full model is not accurately understood. It's not, as the famous 1998 diagram suggests, a one-dimensional ring but a multidimensional lattice. If you think of relationships in one dimension, it's hard to imagine the "short paths" necessary to get six degrees of separation. But on a multidimensional lattice, draw a line from the neuroscientist network, down through another grid, the hiking network, and on that grid it's a short hop to a farmer in Vermont who hikes.

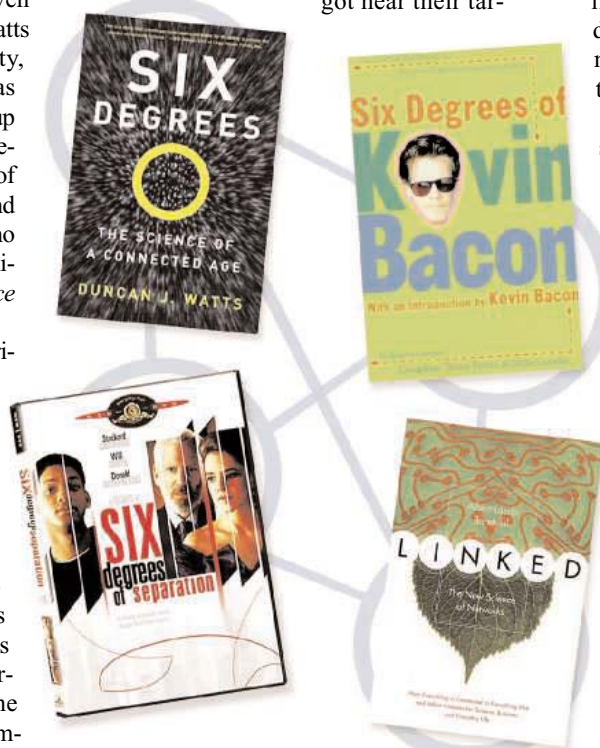
Timing was on Watts and Strogatz's side. "[In 1998], there was a collision of a number of factors: massive computing and storage, a genuine social movement to put information on the Internet, which was simultaneously exciting to mathematicians and social scientists," says Kleinberg. "The Watts-Strogatz paper really crystallized the spirit behind that and brought various communities that traditionally had not interacted closer together."

Those communities included biologists and neuroscientists, who had already begun to examine the network properties of cellular and neuronal processes. They would be further inspired by Barabási and Albert's model when it came out a year later in *Science*.

Barabási was uncomfortable with the idea that networks could be completely random: "There's no way all these computers on the Internet would be randomly connected. There's no way all these molecules in the cells could be randomly connected. There must be some structure in this network."

Borrowing a term from physics, Barabási and Albert modeled what they called "scale-free" networks. Scale-free networks follow power laws. "Unlike the more familiar Gaussian 'bell curve,'" explains Wasserman, "a power-law distribution is a very skewed distribution." Applied to networks, this means there are highly connected hubs that get the majority of the connections. In a dynamic, growing network controlled by power laws, there will be "preferential attachment," essentially a rich-get-richer idea: One is more likely to attach where there are already many links.

After the paper was published, scientists seemed to find power laws everywhere. Their effect on biology has been profound, as



Vogue words. Basic ideas of social network analysis have diffused into popular culture.

gets, but not how they ultimately found them. "Truly random connections are good for getting you halfway around the world, but they're not good for getting you the last 100 miles; you can't aim at the target," says Kleinberg.

In his *Nature* paper, Kleinberg proposed a model that showed how in very large networks the paths to the target could be found with only a modest amount of computation; it became the basis of many computer search algorithms. "Neither we, nor anyone else in fact, understood that searchability was important; that's what Jon taught us," says Watts.

In a 2002 *Science* paper (17 May 2002, p. 1302), Watts and collaborators Mark Newman and Peter Dodds further refined the model, having realized that the key was multiple interests: A neuroscientist at the California Institute of Technology (Caltech) in Pasadena might never reach a farmer in Vermont through his network of neuroscientists, but he

Looking for Patterns

The U.S. National Security Agency's analysis of telephone databases likely combines social network analysis with probabilistic models developed by Soviet-era Russian mathematicians that were later refined in Cold War American intelligence projects.

Probabilistic models allow researchers to estimate the statistical likelihood of certain events occurring. They have been used to determine, for example, whether the pattern of purchases on a credit card is so unusual that the card has likely been stolen. But they are also used along with social network analysis to crack more sophisticated kinds of theft. For example, says fraud expert Malcolm Sparrow of Harvard University, sometimes credit-card fraud is a well-planned attack by a network of thieves. One ring member working in, say, a luxury hotel duplicates victims' credit cards, and weeks later, the cards are used in a foreign country for purchases that can easily be converted to cash. Although it would not be unusual for one wealthy person to travel abroad and buy jewelry, two dozen people buying jewelry in the same foreign city on the same day, who can't be connected through a tour group or family event, triggers alarms: "These are things you would never find by looking at one account or its behaviors," says Sparrow.

The underlying math for the most popular



Connect the dots. Russian mathematicians Markov (top) and Kolmogorov paved the way for modern pattern-recognition algorithms.

probabilistic models was first developed by Andrey Andreyevich Markov, a mathematician who taught at the University of St. Petersburg in Russia. Andrei Nikolaevich Kolmogorov, winner of the Lenin Prize, extended Markov's pioneering probability work, laying the foundation for its application in fields as diverse as fraud detection and bioinformatics.

A Markov chain allows you to "chain" probabilities together, with each link affecting the next forward link in the chain. Go through a yellow traffic light, and it has a "transition probability" of turning red before you're fully through the intersection. If it does turn red, then the probability you could receive a ticket increases.

A more complex version, known as the Hidden Markov Model (HMM), was developed in the 1960s as part of classified research at the Institute for Defense Analyses in Princeton, New Jersey. An HMM allows you to discover the unknown cause of a current state. "Whereas a Markov chain just has states, an HMM has both 'hidden states' and 'observations': the observations are what you see, and the hidden states are the 'unknown causes,'" says mathematician Jon Kleinberg of Cornell University.

Take office couture. "The outfits that your colleague wears are the observations, and the hidden state is what she's done that day," says Kleinberg. "For example, hiking boots as part of an observed outfit may mean that the hidden state—what she did that day—includes hiking." They can also help you predict a likely outcome, such as whether your friend is going hiking tomorrow. But most importantly, HMMs can help you trace the source of an anomaly. If your colleague always wears a different outfit, then the same outfit 2 days in a row stands out. Both gossips and mathematicians can work back from that observation to the "hidden state": What is the probability she spent the night in someone else's apartment? What is the probability she worked all night?

Combining aspects of social network analysis with Markov models provides the analytical power to probe interconnections in the genome or, say, several billion phone records.

—K.H.

researchers such as Marc Vidal of the Dana-Farber Cancer Institute in Boston find that in cell signaling networks there are hub proteins that are heavily interconnected and "spoke" proteins that just touch a few other proteins.

But some remain skeptical. The novelty and significance of Barabási's idea has been challenged by Evelyn Fox Keller of the Massachusetts Institute of Technology in Cambridge in an article in *Bioessays*. Engineer and mathematician John Doyle of Caltech, who has published a paper challenging Barabási's concept of Internet architecture, says Barabási "used methodologies that are standard in physics but inevitably lead to errors when applied to technological or biological systems."

But Watts, who, like Barabási, wrote a popular book, thinks that much of the backlash derives not so much from the flaws of the scale-free model as from the aggressive manner in which it was promoted as a

"universal theory" of networks. (Barabási's book is *Linked*; Watts's is *Six Degrees*.)

At the moment, however, Barabási is more intrigued with network dynamics, trying to understand how the architecture of a network constrains the activities on it. He has also begun to work with more traditional social scientists, including political scientist David

Lazer of Harvard's Kennedy School of Government, combining a physicist's expertise with large data sets and a social scientist's expertise on human behavior.

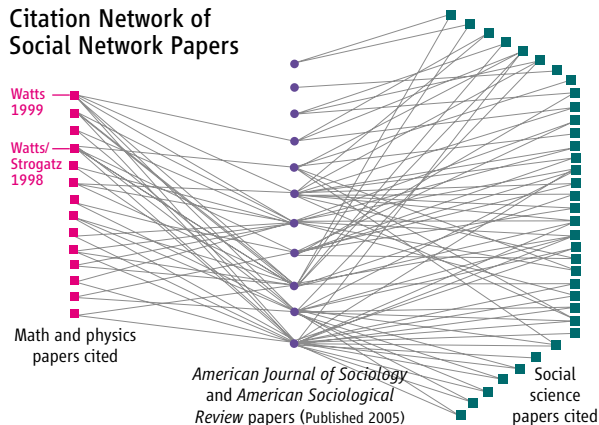
In fact, the most striking example of "six degrees" seems to be the amount of collaboration that goes on in SNA, even between those who disagree with each other. Barabási and Watts recently co-edited a book called *The Structure and Dynamics of Networks* with Newman. Wasserman speaks for many of the SNA old guard when he complains about "Johnny-come-lately physicists," reinventing the wheel. But he still shares two grants with Barabási. One funds the development of a new network-analysis software, the "NetworkBench." The other was to organize the NetSci2006 conference, which drew more than 200 sociologists, physicists, mathematicians, computer scientists, and biologists.

Lazer points to the emergence of the term "network science" to capture the attempt to bridge the analysis of human and nonhuman networks by researchers across the spectrum. SNA, in other words, is rapidly extending its own nodes and paths.

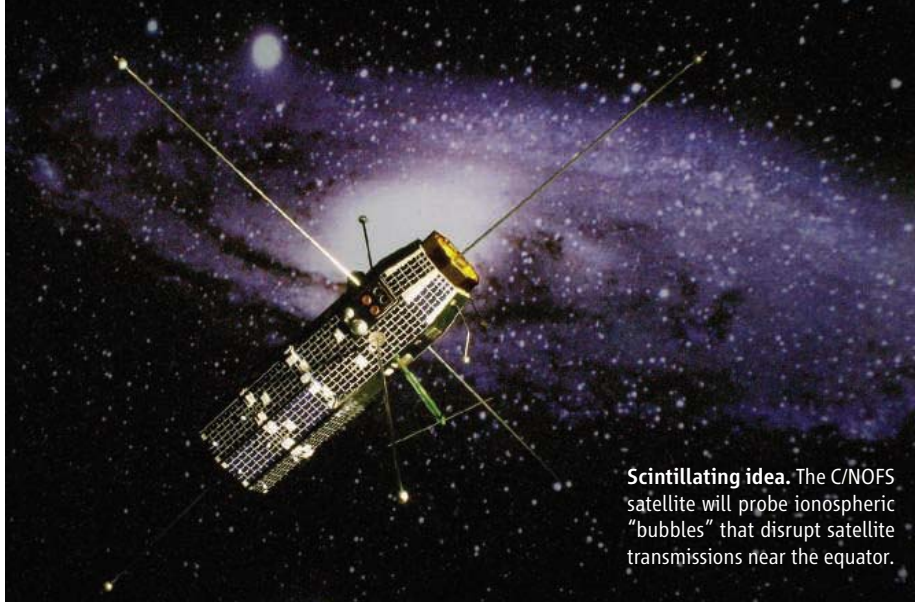
—KAREN HEYMAN

Karen Heyman is a writer in Santa Monica, California.

Citation Network of Social Network Papers



Middle way. A network plot of references in published papers highlights how social network analysis draws on insights from both physical and social sciences.



Scintillating idea. The C/NOFS satellite will probe ionospheric “bubbles” that disrupt satellite transmissions near the equator.

SOLAR PHYSICS

Space Weather Forecasters Plan A Boost in Surveillance Missions

Two new missions to track solar outbursts, radio scintillation, and geomagnetic storms could prove vital now that older satellites are running on fumes

BEIJING—Whether it’s a thunderstorm supercell spawning a tornado or warm ocean waters feeding a hurricane, turmoil in the lower atmosphere follows predictable rhythms. Not so space weather. Although it’s known that solar outbursts spark geomagnetic storms, Earth can be blindsided by devastating but low-profile events. Two missions described here last week at the 2006 Western Pacific Geophysics Meeting aim to fill critical gaps in space weather surveillance.

First on the lineup is a probe to monitor disturbances in the upper atmosphere that blight satellite communication and Global Positioning System navigation. To study and forecast this phenomenon, the U.S. military plans to launch the Communication/Navigation Outage Forecasting System (C/NOFS) satellite in 2008. China meanwhile is planning a major solar observatory, dubbed KuaFu, with a launch target of 2012, which would track solar outbursts and geomagnetic storms in fine detail. “These two missions are very important and promising for space weather forecasting,” says Kazuo Shiokawa, a solar physicist at Nagoya University in Japan.

Geomagnetic storms occur when surges in the solar wind warp Earth’s magnetosphere, sending energy and charged particles into the upper atmosphere. The fiercest storms occur during crests in the sun’s 11-year activity cycle, marked by powerful solar flares and blizzards of charged particles called coronal mass ejections (CMEs). Strong storms can

short-circuit satellites and power grids. They also pose a risk for space travel. For example, if the Apollo 17 moon mission in December 1972 had been launched 4 months earlier, “the astronauts would probably have been killed” by a barrage of energetic particles from an extraordinary series of superflares and CMEs, says Rainer Schwenn, a solar physicist at the Max Planck Institute for Solar System Research in Katlenburg-Lindau, Germany. Future travelers to the moon or Mars would face the same hazard.

Geomagnetic storm forecasting took a giant leap forward 10 years ago, after the Solar and Heliospheric Observatory (SOHO)—a joint NASA and European Space Agency mission—began orbiting Lagrangian point L1, an interplanetary doldrums where balanced gravitational forces keep SOHO in a fairly stable perch between sun and Earth. At the meeting, speakers showed a movie of a SOHO camera lit up by a hail of CME particles in October 2003, the precursor to one of the biggest storms ever seen. SOHO gave several hours’ warning, ample time to limit damage by powering down satellites. Still, “a significant number of storms cannot be predicted,” says Nandita Srivastava of the Udaipur Solar Observatory in India.

Nor are geomagnetic storms the only hazard. Satellite transmissions to Earth can be disrupted—an effect called radio scintillation—by “bubbles” in the ionosphere, the ionized upper part of Earth’s atmosphere. The

origins of these patches of low-density plasma, which can be hundreds of kilometers across and usually occur between dusk and midnight near the equator, are a mystery. “Satellite TV may suddenly disappear when a bubble is passing above,” says Shiokawa. The \$100 million C/NOFS mission, run by the U.S. Air Force Research Laboratory and the Department of Defense’s Space Development and Test Wing in Kirtland, New Mexico, will be the first to sample plasma density continuously in search of bubbles. “It will be a fantastic mission for improving our ability to forecast these hazards as well as understand the basic mechanisms responsible for creating them,” says space scientist Michael Liemohn of the University of Michigan, Ann Arbor.

Although C/NOFS’s primary objective is to give early warning to the U.S. military, “data will not be restricted,” says Guan Le, a C/NOFS project scientist at NASA’s Goddard Space Flight Center in Greenbelt, Maryland. Originally planned for launch on a Pegasus XL rocket in 2004, technical problems have delayed the launch to mid-2008.

Further in the future, KuaFu could become China’s most ambitious space science effort yet. Named after a character in a Chinese legend who chases the sun, KuaFu would consist of a trio of satellites. A probe at L1 would image solar flares and CMEs and give up to 3 days’ warning of impending geomagnetic storms. And two satellites in the magnetosphere would provide round-the-clock monitoring of auroras in the Northern Hemisphere, tracking storms as they develop. “KuaFu has numerous firsts, if it goes,” says Eric Donovan, a mission collaborator at the University of Calgary in Canada.

China would build and launch the KuaFu satellites. Although Canadian and European institutions are taking the lead in defining scientific objectives, officials at the China National Space Administration (CNSA) insist that homegrown scientists play a significant role in developing the instruments, says mission chief Tu Chuanyi of Peking University. “With this mission,” says Schwenn, a KuaFu collaborator, “China wants to join the international space science club.”

CNSA expects to complete a review of KuaFu by spring and give a final go-ahead in 2009. With SOHO and another L1 probe, NASA’s Advanced Composition Explorer, having long surpassed their design lives, KuaFu could prove vital. “Within a few years, we might be completely blind again to mass ejections,” Schwenn says. And that could be as ruinous as turning a blind eye to tornadoes or hurricanes.

—DENNIS NORMILE AND RICHARD STONE

Waiting for the Monsoon

No one can predict the heavy summer rains that bring the Sahel back to life each year. A new 10-year data research program aims to improve forecasting and model building

MALBOROU, NIGER—On a hot afternoon in July, a chanting, dancing, drumming crowd has formed on the main road that crosses the village, half an hour's drive north of the border with Benin. The villagers have begun the rain dance. They want to bring on the monsoon that drenches the earth every year from June to August; it's now several weeks late. The millet crop needs 3 months to ripen, and time is running out for planting the seed.

The people who live on the flat, reddish-brown, dusty landscape of southern Niger depend heavily on the West African monsoon: In 2001, 39% of the Nigerian gross domestic product came from agriculture, which employs 90% of the workforce and involves virtually no irrigation. Niger's neighbors throughout the Sahel, the strip of Africa that stretches across the continent directly south of the Sahara, face similar circumstances. From the 1970s to the 1990s, the Sahel suffered severe drought, leading to some of the worst famines in recent history. Precipitation levels began to rise beginning in the late '90s, but crops were once more devastated by drought in 2005; 2006 did not begin well.

Climate scientists cannot say what has delayed the monsoon this year or whether the delay is part of a larger trend. Nor do they fully understand the mechanisms that govern rainfall over the Sahel. Most frustrating,

perhaps, is that their prognostic tools—computer simulations of future climate—disagree on what lies ahead. “The issue of where Sahel climate is going is contentious,” says Alessandra Giannini, a climate scientist at Columbia University. Some models predict a wetter future; others, a drier one. “They cannot all be right.”

One obvious problem is a lack of data. Africa's network of 1152 weather watch stations, which provide real-time data and supply international climate archives, is just one-eighth the minimum density recommended by the World Meteorological Organization (WMO). Furthermore, the stations that do exist often fail to report.

To fill the gap, a European-led consortium of more than 140 European, American, and African institutions has set out to monitor and thoroughly describe the West African monsoon over a 10-year period. Launched in 2001, the African Monsoon Multidisciplinary Analysis (AMMA) has brought together more than 400 researchers. This summer, they are undertaking the most intense data collection to date. From January through September, they plan to monitor not only rainfall but also every aspect of the monsoon: the structure of clouds and their water content, the amount, movement, and characteristics of particles suspended in the air, the distribution of water in river systems, and sea surface



Holding on. Farm villagers depend on a millet crop—and an annual blast of rainwater—for survival.

temperatures in the Gulf of Guinea and across the Atlantic, as well as temperature, humidity, pressure, and wind speeds at various altitudes across the region.

This effort is badly needed, because what happens in Africa—particularly in the Sahara and Sahel regions—affects the entire planet. It is one of the most important sources of heat in the atmosphere. Dust from the Sahara is a significant contributor to global aerosols. Weather systems above the Sahel during the monsoon give rise to some of the hurricanes that sweep across the Atlantic each year. Yet this critical piece of the climate system remains out of focus.

The hope is that AMMA's data-gathering effort will not only improve regional forecasts but the performance of global climate models as well. They need all the help they can get: Even the latest climate models used by the Intergovernmental Panel on Climate Change (IPCC) vary in what they predict for the Sahel over the coming century, ranging from drought to a significant increase in rainfall. “The Sahel remains one of the toughest challenges for modeling,” says Richard Washington, a climate scientist at the University of Oxford in the U.K. who co-authored a 2004 G8 report on African climate science. “The debate on the Sahel has hinged on models, ... but they are not a particularly sharp tool in that region.”

Flawed and divergent

Several recent studies have underlined the disharmony in the models. In May 2005, Martin Hoerling and James Hurrell of the U.S. National Oceanic and Atmospheric Administration (NOAA) and the National Center for Atmospheric Research presented results at the American Geophysical Union annual meeting that seemed encouraging for



Extremes. Much of the land of the West African Sahel is parched and unproductive—until it is drenched by midsummer storms.

CREDITS: CATHERINE BRAHIC

the Sahel. Using averaged results from a group of the latest atmospheric general circulation models, they found that they predicted more rain in the Sahel in the first half of the 21st century.

In November, Isaac Held of NOAA published results from a new model that reproduced 20th century climate variations in the Sahel better than any other. Looking forward, however, he wrote in the *Proceedings of the National Academy of Sciences* that the model predicted more drought for the Sahel.

More recently, Kerry Cook and Edward Vizzy of the Department of Earth and Atmospheric Sciences at Cornell University combined approaches in a paper in press at the *Journal of Climate*. Of the 18 models being used in the IPCC's fourth assessment, they selected three that best reproduced 20th century climate and compared their predictions for the 21st century. Whereas one model simulated severe drying across the Sahel late in this century, another predicted wet conditions for the entire century. The third projected "modest" drying.

"There must be something in the models' physics that is causing them to respond differently," says Giannini. Deciphering the problem, she says, "is a scientific priority that requires really getting into the [models'] bowels."

Making repairs

There are telltale signs that the algorithms that drive these models are flawed, some researchers say. For instance, they point out that many models show cooler present-day sea surface temperatures close to the Americas and warmer ones by the African coast, when in fact observation shows that the gradient should be the other way around. Cook and Vizzy, meanwhile, say that some models place the maximum monsoon rainfall over the Gulf of Guinea instead of over West Africa, where it should be.

Jan Polcher, a climate modeler at France's research agency, CNRS, suggests that the problem lies in a wide variation in sensitivity to factors such as land or sea surface temperatures. Others point to lack of resolution: Small turbulences can play an important role in the distribution of energy inside a cloud system, but the models resolve areas of 100 square kilometers or more.

"One thing is clear," says Washington. "If we carry on with the models as they are, we are just going to get different answers all the time, so we need to fix their basics."

A solution suggested by Cook and Vizzy is to assess the likelihood of the scenarios generated by the models by looking for obvious

flaws (such as placing maximum rainfall over the ocean instead of over land). Using this method, they concluded that the third model they examined, which predicted modest drying of the Sahel, was most likely to be accurate.

For Polcher, however, continually modifying and assessing the models so that they match observed climate—without understanding the underlying mechanisms—is a moot exercise. That's why he's leading AMMA's vast initiative to fill the West African climate data gap, together with Thierry Lebel of the French Institut de Recherche pour le Développement, Jean-Luc Redelsperger of the Centre Nationale des Recherches Météorologiques, Chris Thorncroft of the University of Albany in New York, and Douglas Parker of the University of Leeds, U.K.

The effort will cost \$50 million over 10 years; weather instruments and equipment are costly to buy and operate. Remote sensing

provide basic data on temperature, humidity, and pressure. The African section of this global grid fell into disrepair during the 1980s. By the late 1990s, the 8 million square kilometers of West Africa had only eight WMO reporting stations—the same number as France.

Through negotiations with West African governments and meteorological agencies, AMMA has restored the network to 17 stations releasing balloons up to eight times a day. Each balloon takes measurements every 2 to

4 seconds and relays the information, along with a GPS reading of its location, to a data collection center via satellite.

The balloons cost about €1000 and are rarely returned to experimenters. (Earlier this year, one landed in a Nigerian village, where it remains closely guarded.) After a decade of collecting data on the monsoon,

AMMA aims to show which stations are critical to support weather forecasting and climate modeling over the long term. AMMA hopes international agencies will see the value of the network and help underwrite it.

Turning point

Three weeks ago, in the savanna that surrounds Niamey, Niger's capital, a tantalizing night storm brought out dozens of seasonal ponds and a cacophony of frogs. Everywhere, men began to hoe the ground, with children trailing behind: two strikes to lift the earth just enough to drop a few seeds in before moving over a meter and starting again. Just 5 kilometers away, the ground remained dry. The rain had come from a small cloud that quickly dumped its 30 mm and moved on.

But now, fears that 2006 would once more bring famine to the region have abated. The monsoon rains arrived at the end of July. For farmers, any later would have been too late. More data might make it possible to know whether the delay is a symptom of long-term climatic change or simply a seasonal variation.

—CATHERINE BRAHIC

Catherine Brahic is a writer for SciDev.Net.



Ground truth. A European-led research project is funding a 10-year study in West Africa that will gather water data, monitor the atmosphere, and feed information into climate models.

through satellites will be useful only if information gathered from the images is validated with initial ground observations.

Central to AMMA's effort is a plan to rebuild a network of stations that release radiosondes, atmospheric sensors carried aloft by helium-filled balloons. WMO members have agreed to launch and track balloons two to seven times a day across a worldwide grid to

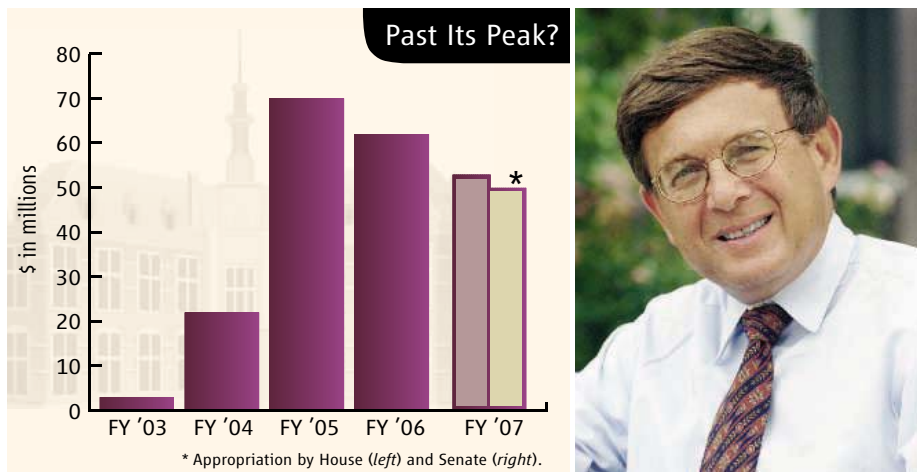
Congress Dials Back Research on Understanding Terrorism

Legislators cite shoddy management in cutting the 2007 budget for university research within the Department of Homeland Security

Arie Kruglanski spends a lot of time thinking about what drives terrorists. A social psychologist at the University of Maryland (UM), College Park, Kruglanski believes that basic research on human behavior can fill an important niche in the fight against terrorism. “The intelligence community can address the mosquito,” he says, referring to the pursuit of suspected or actual terrorists. “Academic researchers can help to dry out the swamp.”

Congress endorsed that argument in 2002 when it included a robust science

Funding for the university program, which peaked in 2005 at \$70 million (see graphic, below), would decline for 2007 to \$50 million in the House version and \$52 million in the Senate. (The differences will be worked out in the weeks ahead.) The two bodies have proposed even larger cuts—24% and 18%, respectively—in the agency’s overall research and development budget, which emphasizes applied work for securing airports and ports and minimizing the risks of biological, chemical, and explosive attacks. The legislators cited poor financial



Downward slope. DHS’s Melvin Bernstein says that the expected cuts to the university program will prevent the agency from funding any new centers.

director within the U.S. Department of Homeland Security (DHS) that was created after the 11 September 2001 terrorist attacks. In short order, the directorate began funding a network of centers at universities around the country—including one that Kruglanski co-directs at UM—to generate knowledge aimed at thwarting future terrorist attacks. But only 2 years after the first center was created, Congress has become so unhappy with DHS’s management of its research portfolio that it is poised to levy a double-digit funding cut next year across the department’s \$1.2 billion science and technology directorate, including the centers program. A Senate panel last month labeled the directorate “a rudderless ship without a clear way to get back on course.”

management, the absence of a research plan, and the lack of progress in developing technologies to protect the nation. In addition, senators would prohibit DHS from funding any center for more than 3 years. Congress expected DHS to spread the wealth, establishing a center and then letting the university find alternative sources of funding after 3 years. The Senate language does not prevent a university-based center from entering a subsequent competition, a staffer added.

The reduced funding would freeze the university program at seven centers—including one announced last week—rather than the 10 that the department had hoped to support. And agency officials say the 3-year rule will change the character of the centers, moving them away from exploring fundamental research questions toward work on

short-term problems. “We’d have to choose narrower topics instead of open-ended problems that reach into more fundamental aspects of homeland security,” says program director Melvin Bernstein. The shorter timeline would also tilt training toward master’s degree students rather than Ph.D.s.

Legislative aides say that members felt they had no choice but to crack down on DHS’s research activities after finding what the House appropriations committee calls “financial reporting deficiencies, including serious difficulties maintaining accurate financial records related to obligations and disbursements.” In short, says one congressional staffer, “the directorate [has failed] to answer how it is executing its programs and what it has done with its money.”

One example is some \$67 million within the university program, which includes fellowships and other initiatives, that Congress awarded over the past 4 years but DHS had not obligated. Bernstein said last week that the money has “now been fully accounted for,” although he declined to provide a breakdown of how or when it will be spent. “When we started, it took us anywhere from 6 to 8 months to start a center, so the money came in a lot faster than we were able to spend it,” he says. “Now we have a steady state.” However, Bernstein says these newly committed funds won’t allow DHS to add to its stable of centers or to award new fellowships next year.

Shaun Kennedy, deputy director of the DHS-funded National Center for Food Protection and Defense (NCFPD) at the University of Minnesota, Twin Cities, says it’s hard for his and other centers to find other federal backers because their work is so multidisciplinary. NCFPD’s goal of reducing the potential for contamination in the nation’s food supply and minimizing the effects of an attack on it, he notes, requires cross-fertilization across disciplines as diverse as epidemiology, food microbiology, economics, and risk communication. “DHS is the only agency whose mission justifies funding this type of work,” he says.

UM’s Kruglanski and other center directors are hoping that legislators eventually drop the 3-year funding limit when they reconcile the two spending bills, even if they don’t restore funding to the program. “Our center is investigating the causes, motivations, and recruitment mechanisms that drive terrorism,” he says. “We need to integrate all the knowledge on terrorism from the past 30 years and carry out a broad set of studies. It doesn’t make sense for us to think short-term.”

—YUDHIJIT BHATTACHARJEE



Three Q's

University College London epidemiologist **Michael Marmot**, 61, whose landmark “Whitehall studies” of British civil servants showed that status and income strongly influence health, chairs the World Health Organization’s Commission on Social Determinants of Health set up last year. Its report is due in 2008.

Q: Why a new commission? Isn’t the link between social conditions and health well known?

It is, but we want to offer a concrete set of evidence-based tools for governments and international bodies that want to do something about health inequalities. A number of things have come together recently: There is more evidence, some countries have started to apply it, and the international health and development communities are interested in how this type of evidence can help.

Q: Why did you take this assignment?

I have been studying the social determinants of health all my life. I saw an opportunity to put the research into practice and change things for the better.

Q: A background paper for your commission criticized the market reforms advocated by the World Bank and the International Monetary Fund in the 1980s and ’90s and warned that industry might resist your recommendations. Do you worry about being seen as left wing? We’re concerned for the health of the disadvantaged. If that seems to be a left-wing position, then so be it.

AWARDS

YOUNGER CROP. The Lemelson Foundation wants its prizewinners to have a little less gray hair. In June, the Oregon-based foundation announced that it is restricting its annual \$500,000 Lemelson-MIT Prize to inventors 45 years old or younger. The average age of the 13 past winners is 61.

The move fits with the foundation’s overall goal of inspiring young people to become inventors, says Merton Flemings of the Massachusetts Institute of Technology, who directs the program. “We want to present inventors as role models for kids, like rock stars,” he says.

The foundation has also converted its \$100,000 lifetime achievement award into a prize to recognize inventors whose ideas can become “sustainable solutions to real-world problems,” such as improving crop yields or energy efficiency. Nominations for next year’s award are due 6 October (web.mit.edu/invent).

DEATHS

HARMONY AND DISCORD. National Medal of Science winner George Wetherill, who died 19 July at age 80, helped unify the planetary sciences in work that got him excommunicated from his church.

As a newly minted Ph.D. in physics, Wetherill joined the Carnegie Institution’s

Department of Terrestrial Magnetism (DTM) in 1953, where he and colleagues soon worked out techniques to date rocks using the slow radioactive decay of various elements. Wetherill took on the so-called uranium-lead technique that had been giving researchers fits. “George was the guy who figured out how to interpret other people’s data,” says astrophysicist Alan Boss of DTM. “When they plotted the data the way George said to, it made sense.” Wetherill called his way of graphing them a “concordia plot.”

Wetherill’s insight let researchers date rocks back to the formation of the solar system. But, as

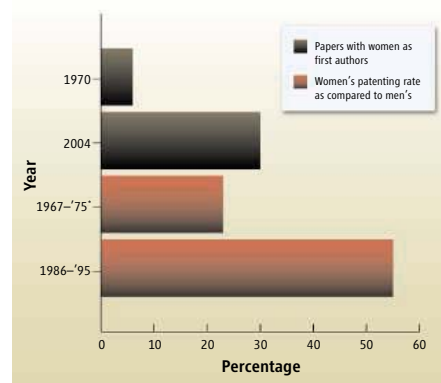
Wetherill often recorded, his work did not sit well with the Lutheran Church—Missouri Synod, an officially creationist church with a long history of using the word “concordia.” Wetherill, a Lutheran at the time, was thrown out of the denomination, which Boss says made him “quite proud. ... He chose very important questions and tackled them single-mindedly.”



Data Point >>

NETWORK, NETWORK. Two new studies show that women in the life sciences are doing a lot better at publishing and patenting than they did 3 decades ago. But they still trail men on both measures of professional success.

In the patenting study (p. 665), researchers led by Waverly Ding of the University of California, Berkeley, found that women who earned Ph.D.s between 1986 and 1995 received patents at 55% of the rate of men in the same cohort, compared with a rate of only 23% for women who earned their doctorates between 1967 and 1975. The publishing study, by Reshma Jagsi of Harvard Medical School in Boston in the 20 July *New England Journal of Medicine*, found that the number of women lead authors in six major medical journals has risen fivefold in 30 years. But even that 30% rate falls far short of their majority status among medical students.



* Cohort that earned Ph.D.s in this period.

The gap in patenting—especially among senior women—may be the result of “limited commercial networks” and “traditional views of academic careers,” Ding speculates. Jagsi suggests that family responsibilities could be a significant factor behind the women’s lower rate of first-authorship. Mentoring programs and better work-family policies could help on both fronts, says Jong-on Hahm, former director of the National Academies’ Committee on Women in Science and Engineering.

On psychology
and biology

616



Climate records
from caves

620



LETTERS | BOOKS | POLICY FORUM | EDUCATION FORUM | PERSPECTIVES

LETTERS

edited by Etta Kavanagh

Boycott of Israeli Academics Misguided

THE RECENT MOTION BY THE U.K.'S LARGEST UNIVERSITY UNION (NAFHE) recommending a boycott of all Israeli academics who "do not publicly dissociate themselves" from Israeli policies has reignited the debate around this issue ("Over protests, U.K. union endorses boycott of Israeli academics," E. Marshall, *News of the Week*, 2 June, p. 1289).

Despite the fact that the NAFHE decision is only "advisory," it is likely that many will view it as an inducement to act along the lines of the motion. As an Israeli academic, I find myself wondering just which Israeli policies these anonymous potential boycotters would like me to publicly dissociate myself from?

Should I dissociate myself from the policy to encourage joint Palestinian-Israeli science projects, the policy to admit students and faculty to our universities regardless of their race or religion, or the policy to continue withdrawals from occupied territory if the Palestinians will only stop using such territory as launching

"How will the boycotters decide who has and who has not publicly dissociated themselves from Israeli policies?"

—Fainzilber

pads for further attacks on us? Or perhaps the boycotters would like me to dissociate myself from the security barrier that has markedly reduced the number of deaths of Israeli civilians from homicide bombers? If the latter, unfortunately, it seems the boycotters would like to see us choose between death and damnation.

How will the boycotters decide who has and who has not publicly dissociated themselves from Israeli policies? In the absence of a "public dissociation commissar" to categorize myself and my colleagues in Israeli academia into those who are boycottable versus those who are not, I would like to issue the following challenge to

those currently quietly supporting this boycott from the safety of their anonymity. I hereby publicly identify myself as an Israeli academic who has not dissociated himself from the Israeli government policies described above, and challenge the boycott supporters to reciprocate by publicly identifying themselves as supporting this boycott. After all, if they want to support a boycott policy that is the antithesis

of academic freedom and is reminiscent of the darkest days of Lysenkoism in Soviet academia, at the very least they should have the courage to stand behind their misguided convictions.

MIKE FAINZILBER

Department of Biological Chemistry, Weizmann Institute of Science, Rehovot 76100, Israel.

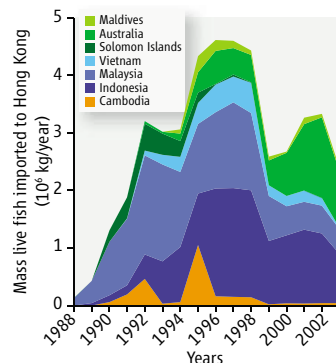
Keeping Bandits at Bay?

IN THEIR POLICY FORUM "GLOBALIZATION, roving bandits, and marine resources" (17 Mar., p. 1557), F. Berkes and colleagues highlight the serious ecological and management consequences of sequential exploitation of biological resources by mobile agents with no attachment to place. Such "roving bandits" (either legal or illegal) deplete stocks and move on faster than local institutions can be developed to regulate them. Here, we quantify the dynamics of a roving bandit system: the live reef fish trade (LRFT) supplying luxury seafood restaurants, mainly in Hong Kong, with large predatory fish (1–4).

We compiled annual statistics on the mass of live reef fish imported to Hong Kong from individual source nations (1988–2003; see graph) from the Hong Kong Census and

Statistics Department (5). Analyzing the start-up dates of the trade from these nations reveals that the LRFT has been spreading away from Hong Kong at an accelerating pace, starting at about 100 km yr⁻¹ in the 1970s and reaching over 400 km yr⁻¹ in the late 1990s (see map) (6). Of 19 exporting nations (7), 10 clearly

show a pattern of boom and bust. Moreover, booms appear to be increasingly ephemeral, with the time between the start and peak of the trade being significantly shorter for more distant countries (see graph) (8). The progressive deterioration of LRFT fisheries in most source nations has also led to what may be termed



Imports of live reef food fish to Hong Kong over time, excluding countries for which the trade volume is too low to be visible and countries detailed in (7). Color-coded by region in ascending chronological order of entry into the LRFT, with minor data gaps extrapolated. The drop in catches in 1999 is a consequence of the global economic downturn that impacted demand for luxury food.

"fishing down the price list." Analyzing LRFT imports by species (9) instead of countries shows that species were depleted serially in order of price (10, 11).

As the accelerating wave with its quickening boom-and-bust pattern spreads out, do local actors have time to react to the threat of roving bandits, or, as

Register to receive print and video interviews. Participate in live conference call symposia.

INTERVIEWS



Discovery of Novel Splice Variations Improves Glial Tumor Classification. Read the interview with Pim French, Ph.D., and Justine Peeters, M.Sc., Erasmus Medical Center, Rotterdam, Netherlands.



Desktop Data Analysis for Large-Scale Studies. Read the interview with Tom Downey, M.Sc., President, Partek, Inc.

CONFERENCE CALL SYMPOSIA



Reduction in Tamoxifen-induced CYP3A2 Expression and DNA Adducts Using Antisense Technology. Participate in a conference call symposium with

Brinda Mahadevan, Ph.D., Oregon State University.
Thursday, August 24, 2006, 9:00am PDT



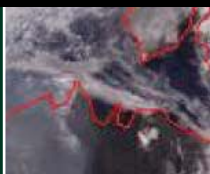
Gene Expression During Long-Term Memory Storage.

Participate in a conference call symposium with Ted Abel, Ph.D., University of Pennsylvania.

Thursday, August 31, 2006, 9:00am PDT

REGISTER TODAY

www.affymetrix.com/workshop



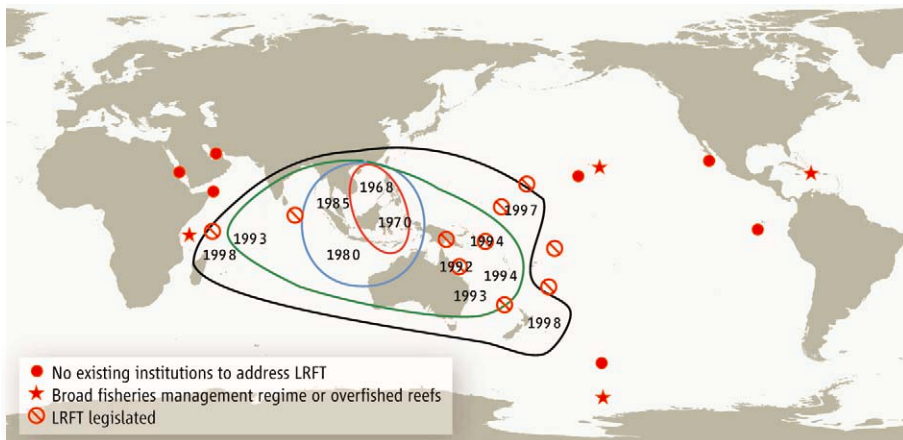
More aerosols;
more clouds

623



Malaria parasite
development

626



The global spread of the LRFT, showing the start-up year for the trade in several areas. Color contours represent the area covered by the trade before 1970 (red), 1985 (blue), 1995 (green), and present (black).

feared by Berkes *et al.*, are they simply too slow? A surprisingly positive answer comes from the Pacific Ocean, an area that, because of its comparatively healthy and sustainably exploited reefs (12), offers perhaps most scope for the expansion of the LRFT. Increasing caution about the trade has led several Pacific nations to start to introduce small-scale trial fisheries and LRFT management plans along the edge of the expanding wave (see map). These efforts are coordinated through the Pacific Regional LRFT Initiative of the Secretariat of the Pacific Community (SPC) (4, 13). But what about areas that are not part of the SPC? Some (e.g., Hawaii) might nevertheless be protected by effective general fisheries regulations, while others (such as the Caribbean and Western Indian Ocean) might simply be ignored because their reefs are already overfished. Of greater concern are areas such as the Red Sea, Persian Gulf, and eastern Pacific, at potentially high risk through a combination of relatively healthy reefs and a lack of effective local institutions or regional coordination (see map).

HELEN SCALES,¹ ANDREW BALMFORD,¹ MIN LIU,²
YVONNE SADOVY,² ANDREA MANICA^{1*}

¹Department of Zoology, University of Cambridge, Downing Street, Cambridge CB2 3EJ, UK. ²The Swire Institute of Marine Science, Department of Ecology and Biodiversity, University of Hong Kong, Pokfulam Road, Hong Kong SAR, China.

*To whom correspondence should be addressed. E-mail: am315@cam.ac.uk

References and Notes

1. R. E. Johannes, M. Riepen, "Environmental, economic, and social implications of the live fish trade in Asia and

the West Pacific" (Nature Conservancy, Arlington, VA, 1995).

- C. Lee, Y. Sadovy, *NAGA* **21**, 38 (1998).
- P. Chan, *SPC Live Reef Fish Inf. Bull.* **7**, 3 (2000).
- Y. J. Sadovy *et al.*, *While Stocks Last: The Live Food Reef Fish Trade* (Asian Development Bank, Manila, 2003).
- Data on gross annual mass of marine fish imports carried by air (all imports) and by sea (foreign vessels only) into Hong Kong (provided by the Hong Kong Census and Statistics Department). Hong Kong is the major market for the LRFT, and these imports represent most of the global trade.
- Quadratic regression of distance from Hong Kong (km) versus start year [for 14 countries, from (1, 4, 14)]: $R^2 = 0.92$, $F(1,12) = 71.9$, $P < 0.001$.
- Excluding Mainland China, Singapore, and Taiwan, which receive large amounts of fish from other countries; Thailand and Bangladesh, which mostly export farmed fish; and the Philippines, due to a major temporal shift from largely unreported, illegally operating vessels to mainly reported air exports (1, 14).
- Time to peak versus distance from Hong Kong: $F(1,8) = 9.3$, $P = 0.016$, $R^2 = 0.48$. Note that there is no confounding effect of reef area – time to peak versus area [from (15)]: $F(1,8) = 0.4$, NS.
- Data from 1997 to 2002. These include imports by all foreign vessels (including catches that were problematic to assign geographically, such as those from Taiwan and Mainland China) and from voluntary reports by locally registered vessels (collected by the Hong Kong Agriculture, Fisheries and Conservation Department).
- Time to peak versus 2002 wholesale prices [from (4)]: $r = -0.66$, $n = 9$ species, $P = 0.050$.
- See Supporting Online Material on Science Online at www.sciencemag.org/cgi/content/313/5787/612c/DC1.
- K. Warren-Rhodes, Y. Sadovy, H. Cesar, *Ambio* **32**, 481 (2003).
- A. J. Smith, *SPC Live Reef Inf. Bull.* **3**, 47 (1997).
- N. Bentley, "Fishing for solutions: Can the live trade in wild groupers and wrasses from Southeast Asia be managed?" (Traffic Southeast Asia, Kuala Lumpur, Malaysia, 1999).
- M. D. Spalding, C. Ravilious, E. P. Green, *World Atlas of Coral Reefs* (University of California Press in association with UNEP-WCMC, Berkeley, CA, ed. 1, 2001).

Response

SCALES ET AL. PROVIDE AN IMPORTANT ANALYSIS of the live reef fish trade. The loss of these local fish resources creates long-term social and economic hardship, while the profits flow from impoverished countries to a luxury market. We advocated addressing this phenomenon on various fronts: reforming markets, using the precautionary principle, establishing property rights, and building multi-level institutions from local to global that can learn from experience. Scales *et al.* argue that some of these policy changes have begun for the live reef fish trade, although we contend that their efficacy in preventing local stock depletion remains to be demonstrated.

A critical issue for coping with “roving bandits” is that local policy responses need to be largely based on lessons learned elsewhere. International agencies such as the Secretariat of the Pacific Community (SPC) can play a critical role in providing good governance and training, and in strengthening local capabilities for monitoring and enforcement. However, the majority of the 22 member nations and territories of the SPC have not yet implemented legislation to regulate the live reef fish trade.

Scales *et al.* attribute the temporary decline in live reef fish imports to Hong Kong in 2000 to a change in demand rather than supply. This observation supports our argument that reforming markets is an important strategy for coping with roving bandits. The regional-scale monitoring of international trade reported by Scales *et al.* is crucial for revealing the market demands for live reef fish that have been stimulated by global trade liberalization and by uneven economic development. Unfortunately, their analysis shows no significant change to market drivers, other than a flexibility to substitute species and locations, characteristic attributes of “roving bandits.” Action to date has instead concentrated on harvesting restraints at the local level, encouraged by international agencies such as the SPC. Multilevel action, from the local to the international, is needed to establish institutions that are able to learn from experiences with roving bandits, develop decision-making skill in an environment of uncertainty and complexity, and respond quickly to shifts in demand from global markets.

As well as the trial fisheries and live fish management plans that have been initiated in some places, there are encouraging signs that licensing, monitoring, and enforcing can be effective, at least on a local scale. However, the social inequity arising from exportation of the dwindling coral reef resources of developing tropical nations is a strong argument for banning the international trade of live fish entirely,

unless sustainability can be demonstrated. Once those resources are destroyed and forgotten, it is the local people who bear the costs of reduced options for future development.

T. P. HUGHES,¹ F. BERKES,² R. S. STENECK,³
J. A. WILSON,⁴ D. R. BELLWOOD,¹ B. CRONA,^{5,6}
C. FOLKE,^{5,6} L. H. GUNDERSON,⁷ H. M. LESLIE,⁸
J. NORBERG,⁶ M. NYSTRÖM,^{5,6} P. OLSSON,⁵
H. ÖSTERBLÖM,⁶ M. SCHEFFER,⁹ B. WORM¹⁰

¹Australian Research Council Centre of Excellence for Coral Reef Studies, James Cook University, Townsville, QLD 4811, Australia. ²Natural Resources Institute, University of Manitoba, Winnipeg, MB R3T 2N2, Canada. ³School of Marine Sciences, University of Maine, Walpole, ME 04573, USA. ⁴School of Marine Sciences, University of Maine, Orono, ME 04469, USA. ⁵Centre for Transdisciplinary Environmental Research, ⁶Department of Systems Ecology, Stockholm University, 106 91 Stockholm, Sweden. ⁷Department of Environmental Studies, Emory University, Atlanta, GA 30322, USA. ⁸Department of Ecology and Evolutionary Biology, Princeton University, Princeton, NJ 08544, USA. ⁹Aquatic Ecology and Water Quality Management Group, Department of Environmental Sciences, Wageningen University, 6700 DD Wageningen, The Netherlands. ¹⁰Biology Department, Dalhousie University, Halifax, NS B3H 4J1, Canada.

Making U.S. Graduate Education More Diverse

INCREASING THE PARTICIPATION OF MINORITY students in science and engineering, at all levels, remains a daunting challenge in the United States despite concerted efforts over the past 30 years (“Diversity remains elusive for flagship NSF program,” J. Mervis, *News of the Week*, 9 June, p. 1454). The issue is more critical than ever before, but we seem to keep trying the same things and expecting different results. Most programs seek to better prepare undergraduates, but the problem is that few are admitted to doctoral programs. The basic problem is therefore admission, not a lack of minority students who have the ability to succeed. If indeed one of the major goals of the Integrative Graduate Education and Research Traineeship program (IGERT) is to increase the number of women and minorities in science, then individual IGERT programs that fail to do that should not be renewed. There is no question that the science that is being done through these IGERT programs is laudable, but if the aim of the program is not being met, investigators should be funded through other programs. I agree that productive faculty often do not have spare time to seek and recruit these students. They rely on the traditional model in which students actively seek participation in graduate research, either on their own or with the assistance of faculty mentors. Such students are self-confident in the pursuit of graduate education in research universities. Although some minority students do fall into this category, the numbers are relatively small. A central, national office to assist

in recruiting minority students will no doubt help, but faculty simply have to make the commitment and find the time to actively seek minority students who might not have that self-confidence but who nonetheless are highly qualified. Wherever one finds a successful program, one will always find a faculty member or department head that does this, and we should do more to enable and reward their efforts. After all, it is individual faculty members who ultimately decide who gets admitted to graduate programs.

CECILIO R. BARRERA

Associate Dean, Graduate College, Texas State University—San Marcos, 601 University Drive, San Marcos, TX 78666, USA.

Recognizing Computational Science

THERE ARE PRESTIGIOUS INTERNATIONAL awards that recognize the role of theory and experiment in science and mathematics, but there are no awards of a similar stature that explicitly recognize the role of computational science in a scientific field. In my view, this is a serious omission.

In 1945, John von Neumann (*1*) noted that “many branches of both pure and applied mathematics are in great need of computing instruments to break the present stalemate created by the failure of the purely analytical approach to nonlinear problems.” In the past few decades, great strides in mathematics and in the applied sciences can be linked to computational science, and perhaps one can debate to what extent these advances are due to terraflop performance rather than human ingenuity in harnessing this power. Advances may be easier to recognize when simulations are supported by controlled experiments (*2*). But for some disciplines (e.g., atmospheric physics, space weather, cosmology), progress is made through passive observation, where “discovery” may be harder to quantify.

Nonetheless, in many different fields of science where great advances are being made, the

Letters to the Editor

Letters (~300 words) discuss material published in *Science* in the previous 6 months or issues of general interest. They can be submitted through the Web (www.submit2science.org) or by regular mail (1200 New York Ave., NW, Washington, DC 20005, USA). Letters are not acknowledged upon receipt, nor are authors generally consulted before publication. Whether published in full or in part, letters are subject to editing for clarity and space.

central apparatus is a computer rather than a lab experiment, and this should be recognized by a prestigious international award. The role of computational science in scientific discovery is taken largely for granted. Without it, however, we would still be contemplating von Neumann's stalemate of 60 years ago.

JOSS BLAND-HAWTHORN

Head of Instrument Science, Anglo-Australian Observatory,
167 Vimiera Road, Epping, NSW 2121, Australia. E-mail:
jbh@ao.gov.au

References

1. P. Lax, *SIAM News*, 1 March 2005
(<http://www.siam.org/news/news.php?id=39>).
2. J. Cohen, *PLoS Biol.* **12**, 2017 (2005).

TECHNICAL COMMENT ABSTRACTS

COMMENT ON "Post-Wildfire Logging Hinders Regeneration and Increases Fire Risk"

**M. Newton, S. Fitzgerald, R. R. Rose,
P. W. Adams, S. D. Tesch, J. Sessions, T. Atzet,
R. Powers, C. Skinner**

Donato *et al.* (Brevia, 20 January 2006, p. 352) concluded that logging after wildfire kills natural regeneration and increases fire risk. We argue that their paper lacks adequate context and supporting information to be clearly interpreted by scientists, resource managers, policy makers, and the public.

Full text at www.sciencemag.org/cgi/content/full/313/5787/615a

COMMENT ON "Post-Wildfire Logging Hinders Regeneration and Increases Fire Risk"

B. N. Baird

Based on limited sampling 2 years after the 2002 Biscuit Fire in Oregon, Donato *et al.* (Brevia, 20 January 2006, p. 352) concluded that postfire logging reduced seedling regeneration by 71%. Analysis of the study methodology and raw data suggest that this estimate is statistically flawed and misleading and says nothing about the impacts of more prompt postfire harvest.

Full text at www.sciencemag.org/cgi/content/full/313/5787/615b

RESPONSE TO COMMENTS ON "Post-Wildfire Logging Hinders Regeneration and Increases Fire Risk"

**D. C. Donato, J. B. Fontaine, J. L. Campbell,
W. D. Robinson, J. B. Kauffman, B. E. Law**

We reported that postfire logging 2 to 3 years after the 2002 Biscuit Fire was associated with significant mortality in natural conifer regeneration and elevated potential fire behavior in the short term as a result of increased surface fuel loads. We underscore the strength of our study design and statistical conclusions, provide additional details of the research setting and scope, and address comments pertinent to forest development and fire ecology.

Full text at www.sciencemag.org/cgi/content/full/313/5787/615c

Save Your Back Issues



Preserve, protect and organize your **Science** back issues. Slipcases are library quality. Constructed with heavy bookbinder's board and covered in a rich maroon leatherette material. A gold label with the **Science** logo is included for personalizing. Perfect for the home or office. Great for Gifts!

One - \$15 Three - \$40 Six - \$80

Add \$3.50 per slipcase for P & H.

Send orders to:

**TNC Enterprises Dept. SC
P.O. Box 2475
Warminster, PA 18974**

Please send _____ add \$3.50 per slipcase for postage and handling. PA residents add 6% sales tax. You can even call **215-674-8476** to order by phone. USA orders only.

Name _____

Address _____

City, State, Zip _____

Credit Card Orders:

Visa, MC, AmEx

Card No. _____

Exp. Date _____

Signature _____

Email Address _____

**To Order Online: www.tncenterprises.net/sc
Unconditionally Guaranteed**

PSYCHOLOGY

Reflections on Mind

Joan E. Grusec

In *An Argument for Mind*, a distinguished developmental psychologist reflects on his career and his discipline. Jerome Kagan (an emeritus professor at Harvard University) provides a summary of changes that have occurred in psychology over the past 50 years, shares some of his personal history and research contributions, and offers a critique of contemporary social science. He also manages to insert the occasional general commentary on the state of American society.

The book should appeal to a wide audience. For developmental psychologists it is, among other things, an overview of the field's history and a primer on how to do good research. For others who might be curious about the empirical study of children, it also provides an excellent view of the way developmental researchers study psychology's most basic question—how nature and nurture interact in the complex dance that constitutes the developmental process. Understanding this interaction requires a grasp of the content and methodology of both life and social sciences. Kagan, a master of both, uses his knowledge to paint a broad picture of where developmental psychology has been and where it is going.

At the beginning of Kagan's career, psychology was dominated by behaviorism and psychoanalysis, with their respective messages of extreme environmentalism and the impact of early experience on the development of adult personality. As Kagan documents, approaches have changed substantially. It is now evident that biological underpinnings and predispositions combine with experience and that the effects of early experience are not necessarily irreversible. As well, psychologists have repeatedly demonstrated that events must be evaluated and understood in the developmental, cultural, and historical context in which they appear. For example, harsh corporal punishment during Puritan times, the historically frequent practice of being sent to live with a wet nurse, and the terror aroused by an enraged father in Japan can be construed in their time and

place as signs of love and caring rather than parental rejection.

Kagan uses descriptions of his career, anecdotes, and overviews of his research as a framework within which to offer broader ideas and conceptions that have guided his thinking over the years. As an example, the uniquely human moral sense, which results in pleasure at having done good, is a topic that reappears throughout the book. Indeed, Kagan suggests that it is this sense that determines the relative usefulness of an action (in contrast to relative cost or inclusive fitness). He specifically devotes one chapter to the topic of morality. Paralleling his approach in other chapters, it includes a survey of empirical evidence for children's early development of



schematic concepts for prohibited actions, empathic concern for others that restrains harmful actions, sense of shame and guilt, and understanding of good and bad. From this empirical base, Kagan reflects on the current state of American society, with its emphasis on personal freedom and self-interest to the detriment of group loyalty and altruism. Yet the latter values, he believes, are naturally more dominant because they reflect the strong biological urge humans have for caring and cooperation.

Over the course of the book, Kagan touches on many other topics. A major one is temperament—the object of much of his research (*I*)—and the development through the life course of those individuals who display either high or low reactivity to novelty. He writes about the practice of good science, arguing for careful use of language and avoidance of excessive commitment to theory. He relates how his attempts during the 1970s to

study the impact of day care experience on the children of working-class African Americans ran into political difficulty when there were complaints that any result would fuel racist ideas: If day care experience made no difference, then not even Harvard professors could help these families; if such experience made a difference, it revealed the inadequacy of African American mothers. Kagan describes the behavior of 18-month-old children who show distress when they infer they ought to imitate the actions of others but cannot do so, and he discusses the implications of this behavior for early conceptions of right and wrong action. He suggests that the human love of novelty explains the current attractiveness of spirituality because we are less excited by scientific discoveries as they become more routine.

The author's most impassioned remarks are reserved for “the dark shadow hovering over this . . . stage in the history of psychology,” the belief that understanding the brain brings with it a complete understanding of the mind. Kagan is very much a psychologist, and this book is very much a celebration of the mind.

Hence his dismay at those who would reduce, without remainder, phenomena now described in psychological terms to the activity of neurons, receptors, and activated neural circuits. He cites as an example of such misguided activity the attribution by researchers of the smaller vocabularies of children with less well-educated parents to compromised functioning of the brain area involved in language. The more useful explanation, surely, is that these children are read and talked to less. Distinct vocabularies are needed for mind and brain because the referents for psychologists are reports of feelings and observed behavior, whereas for the neuroscientist they are brain circuits: “Looking for the place in the brain where a person's feeling of fear is located is as fruitless as Diogenes' search for an honest man.”

It is difficult to capture the nature of *An Argument for Mind* in a short review, at least in part because the book has no single defining theme. Nevertheless, Kagan's account can be characterized as entertaining and enlightening reading, filled as it is with wisdom gathered over many years of scholarly activity.

Reference

1. J. Kagan, N. Snidman, *The Long Shadow of Temperament* (Harvard Univ. Press, Cambridge, MA, 2004). Reviewed by P. Costa, *Science* **308**, 500 (2005).

An Argument for Mind

by Jerome Kagan

Yale University Press, New Haven, CT, 2006. 301 pp.

\$27.50, £17.50. ISBN 0-300-11337-4.

The reviewer is at the Department of Psychology, University of Toronto, 100 St. George Street, Toronto, Ontario M5S 3G3, Canada. E-mail: grusec@psych.utoronto.ca

10.1126/science.1129914

CREDIT: LUCIDIO STUDIO INC./CORBIS

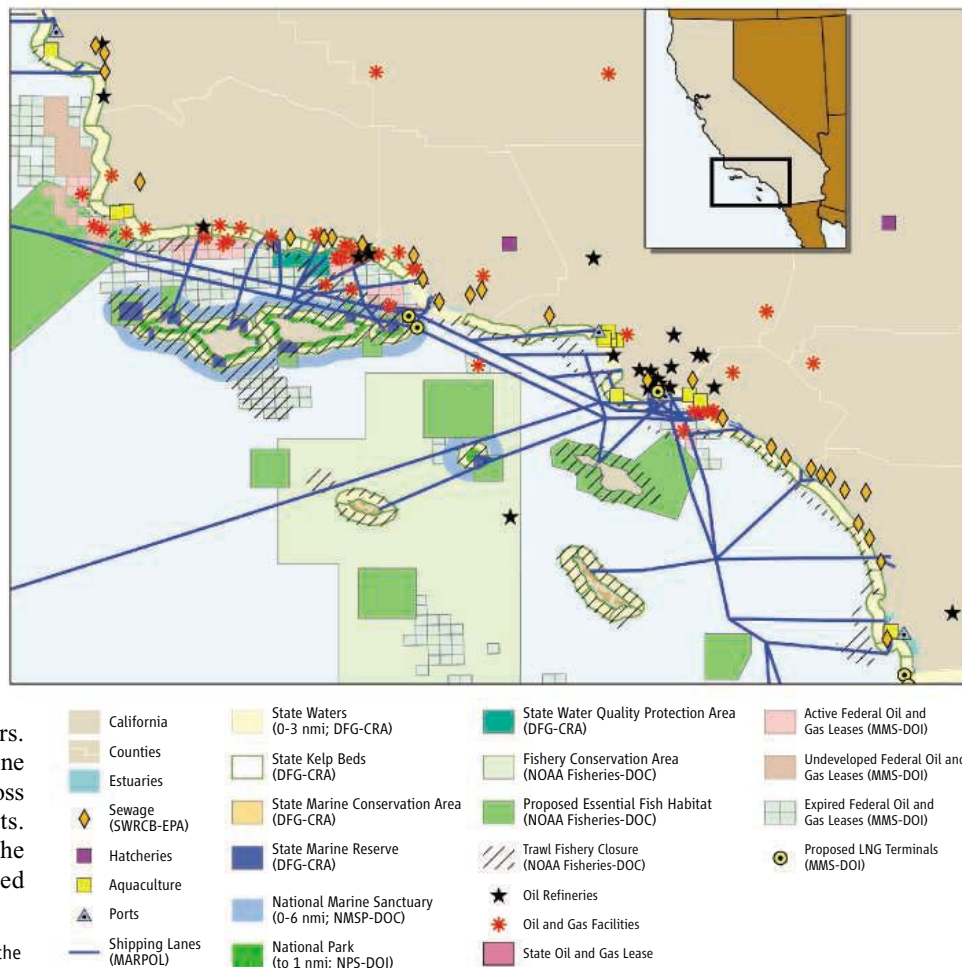
SUSTAINABILITY

Resolving Mismatches in U.S. Ocean Governance

L. B. Crowder,^{1*} G. Osherenko,² O. R. Young,³ S. Aïramé,² E. A. Norse,⁴ N. Baron,⁵ J. C. Day,⁶ F. Douvère,⁷ C. N. Ehler,⁷ B. S. Halpern,⁵ S. J. Langdon,⁸ K. L. McLeod,⁹ J. C. Ogden,¹⁰ R. E. Peach,¹¹ A. A. Rosenberg,¹² J. A. Wilson¹³

That the oceans are in serious trouble is no longer news. Fisheries are declining, formerly abundant species are now rare, food webs are altered, and coastal ecosystems are polluted and degraded. Invasive species and diseases are proliferating and the oceans are warming (1). Because these changes are largely due to failures of governance, reversing them will require new, more effective governance systems.

Historically, ocean management has focused on individual sectors. In the United States, at least 20 federal agencies implement over 140 federal ocean-related statutes. This is like a scenario in which a number of specialist physicians, who are not communicating well, treat a patient with multiple medical problems. The combined treatment can exacerbate rather than solve problems. Separate regimes for fisheries, aquaculture, marine mammal conservation, shipping, oil and gas, and mining are designed to resolve conflicts within sectors, but not across sectors. Decision-making is often ad hoc, and no one has clear authority to resolve conflicts across sectors or to deal with cumulative effects. Many scientists are now convinced that the solution can be found in ecosystem-based



Fragmentation of management for human uses of marine areas in southern California.

management (2). Ecosystem-based management focuses on managing the suite of human activities that affect particular places. This is a marked departure from the current approach. The time has come to consider a more holistic approach to place-based management of marine ecosystems, comprehensive ocean zoning (3).

Management regimes for individual sectors operate under different legal mandates and reflect the interests of different stakeholders, so governance is riddled with gaps and overlaps (4). Fishing has a larger impact on biological diversity than any other human activity (5), but the Magnuson-Stevens Act,

Problems in ocean resource management derive from governance, not science. Ocean zoning would replace mismatched and fragmented approaches with integrated regulatory domains.

which governs fisheries, contains no mandate to maintain biodiversity. Ecosystem-based fisheries management (6) is only a partial solution—it does not account for impacts on nontarget species or manage other activities that degrade fisheries, such as pollution or wetlands loss (7). The problem of fragmented governance is growing, as new place-based activities in the sea [e.g., aquaculture, wind farms, liquefied natural gas (LNG) terminals] are increasing the potential range and severity of conflicts across sectors.

California's Channel Islands illustrate the potential for conflict and fragmentation of management authority (see figure, above).

¹Center for Marine Conservation, Nicholas School of the Environment and Earth Sciences, Duke University Marine Laboratory, Beaufort, NC 28516, USA. ²Marine Science Institute, University of California, Santa Barbara, CA 93106–6150, USA. ³Donald Bren School of Environmental Science and Management, University of California, Santa Barbara, CA 93106–5131, USA. ⁴Marine Conservation Biology Institute, Bellevue, WA 98004, USA. ⁵National Center for Ecological Analysis and Synthesis, Santa Barbara, CA 93101, USA. ⁶Great Barrier Reef Marine Park Authority, Townsville, QLD 4810, Australia. ⁷Man and the Biosphere Program, UNESCO, 75732 Paris Cedex 15, France. ⁸Department of Anthropology, University of Alaska, Anchorage, AK 99508, USA. ⁹Department of Zoology, Oregon State University, Corvallis, OR 97331, USA. ¹⁰Florida Institute of Oceanography, St. Petersburg, FL 33701, USA. ¹¹Kennedy School of Government, Harvard University, Cambridge, MA 02138, USA. ¹²Institute for the Study of the Earth, Oceans, and Space, University of New Hampshire, Durham, NH 03824, USA. ¹³School of Marine Sciences, University of Maine, Orono, ME 04469, USA.

*Author for correspondence. E-mail: lcrowder@duke.edu

In 2003, California established a network of fully protected marine reserves and conservation areas that allow limited take in the state waters (0 to 3 nautical miles) of the Channel Islands National Marine Sanctuary. This followed a 5-year multiagency, multi-stakeholder process. Yet federal agencies still have not implemented the proposed reserves in federal sanctuary waters (3 to 6 nautical miles) because the roles of the two National Oceanic and Atmospheric Administration agencies (Fisheries and National Marine Sanctuaries) are unclear.

Spatial mismatches between scales of governance and ecosystems are common. Current subdivisions of state, federal, and international waters are understandable in historical and political terms. But it makes little ecological sense for managing highly migratory fishes or for LNG terminals, which can be built in state or federal waters.

Spatial mismatches typically arise from jurisdictional boundaries too small for effective management. Leatherback and loggerhead sea turtles forage over much of the Pacific, but bycatch reduction efforts required in U.S. fisheries are not used in foreign fisheries, which potentially contributes to ongoing declines (8). Western and Eastern substocks of Atlantic bluefin tuna migrate, so the high catches in the East may cancel the potential benefits of restricted catches in the West (9).

Sometimes, the causes of the problems are too far removed from the effects. Farming in the Mississippi River watershed contributes to nutrient loading and hypoxia in the Gulf of Mexico, displacing fishes and other marine organisms (10). Jurisdictions can also be too large. Cod management in the northwest Atlantic focused on the whole region as local stocks experienced serial depletion (11).

Temporal mismatches between biological systems and human institutions can also degrade marine ecosystems. Annual appropriations and 2- or 4-year voting cycles drive many policy processes. But problems affecting marine systems can occur on time scales that are too fast for these policy rhythms (e.g., sudden collapses of fish populations, outbreaks of invasive species or harmful algal blooms) or too slow (e.g., increases in ocean temperatures, acidification, or the cumulative loss of wetlands). The white abalone fishery in California expanded and crashed rapidly in the early 1970s, 20 years before the management agency restricted fishing (12). Longline tuna fisheries in the Gulf of Mexico reduced oceanic whitetip sharks by 99.7% over five decades, but the change was so gradual that managers failed to notice or prevent it (13).

Problems generated by fragmentation and mismatches become particularly severe in systems that include multiple, interactive, and cumulative stressors. Just as stressed humans are more susceptible to opportunistic infections, stressed ecosystems lack robustness and resilience. On the U.S. West coast, the combination of degraded spawning habitat, shifting ocean temperatures, and overfishing led to population declines and endangered species listings for salmon. This did not occur in Alaska, because of better river conditions, protection of spawning habitat, and a spatial fisheries permit system (14).

These governance problems are difficult to alleviate even after they become well understood (15). Incremental improvements in sectoral governance can reduce some problems (e.g., overfishing of target species), but they generally cannot address fragmentation and mismatches.

Marine spatial planning with comprehensive ocean zoning can help address these problems. Although property rights and management arrangements in the sea differ from those on land, spatial planning could be initiated with cooperation among federal, state, tribal, and local authorities. Zoning would not replace existing fishing regulations or requirements for oil and gas permits, but would add an important spatial dimension by defining areas within which compatible activities could occur.

Key elements of successful zoning include locating and designating zones based on the underlying topography, oceanography, and distribution of biotic communities; designing systems of permits, licenses, and use rules within each zone; establishing compliance mechanisms, and creating programs to monitor, to review, and to adapt the zoning system. Not only does comprehensive ocean zoning directly address fragmentation and spatial mismatches, zoning also facilitates efforts to adjust governance to the rhythms of human institutions and the dynamics of spatially bounded ecosystems.

Of course, establishing an effective system of ocean zoning in the United States will present a formidable challenge. But other countries, including Belgium, China, Germany, the Netherlands, and the United Kingdom, have already begun implementing or experimenting with marine spatial planning (16–18). Massachusetts is considering legislation to develop and implement an ocean management plan (19). A striking example of comprehensive, multiple-use zoning of marine resources is Australia's Great Barrier Reef Marine Park. It provides specific areas with high levels of pro-

tection, while allowing other uses, including fishing, to continue elsewhere (20).

The transition to comprehensive ocean zoning in the United States will not be easy. Critics point to the contentiousness of efforts to introduce zoning, the difficulties of developing legislation acceptable to all stakeholders, and failures to achieve desired results even after zoning is established. But our current approach simply cannot address the critical issues in the oceans. Recovering ocean ecosystems will require a better understanding of the consequences of interconnections among ecosystem components, as well as a systemic change in the way we consider issues and make choices regarding ocean use.

References and Notes

1. Millennium Ecosystem Assessment (MEA), *Living Beyond Our Means: Natural Assets and Human Well-Being* (MEA, United Nations Environment Programme, Nairobi, Kenya, 2005).
2. K. L. McLeod *et al.*, *Scientific Consensus Statement on Marine Ecosystem-based Management* (Communication Partnership for Science and the Sea, Washington, DC, 2005).
3. E. A. Norse, in *Marine Conservation Biology: The Science of Maintaining the Sea's Biodiversity*, E. A. Norse and L. B. Crowder, Eds. (Island Press, Washington, DC, 2005), pp. 422–444.
4. O. R. Young, *Institutional Dimensions of Environmental Change: Fit, Interplay, and Scale* (MIT Press, Cambridge, MA, 2002).
5. J. B. C. Jackson *et al.*, *Science* **293**, 629 (2001).
6. E. K. Pikitch *et al.*, *Science* **305**, 346 (2004).
7. A. A. Rosenberg, K. L. McLeod, *Mar. Ecol. Prog. Ser.* **300**, 270 (2005).
8. R. Lewison *et al.*, *Ecol. Lett.* **7**, 221 (2004).
9. B. A. Block *et al.*, *Nature* **434**, 1121 (2005).
10. J. K. Craig, L. B. Crowder, *Mar. Ecol. Prog. Ser.* **294**, 79 (2005).
11. J. A. Hutchings, J. D. Reynolds, *BioScience* **54**, 297 (2004).
12. G. D. Davis *et al.*, *Trans. Am. Fish. Soc.* **125**, 42 (1996).
13. J. K. Baum, R. A. Myers, *Ecol. Lett.* **7**, 135 (2004).
14. R. Hilborn *et al.*, *Proc. Natl. Acad. Sci. U.S.A.* **100**, 6564 (2003).
15. O. R. Young, *Matching Institutions and Ecosystems: The Problem of Fit* [Institut du Développement Durable et des Relations Internationales (IDDRI), Paris, 2002].
16. F. Douvère *et al.*, *Mar. Policy* (2006), in press.
17. Department for Environment, Food, and Rural Affairs, *A Marine Bill* (www.defra.gov.uk/corporate/consult/marinebill/consult.pdf).
18. Dynamic and Interactive Assessment of National, Regional and Global Vulnerability of Coastal Zones to Climate Change and Sea-Level Rise (www.pik-potsdam.de/DINAS-COAST/).
19. The Commonwealth of Massachusetts, Senate, No. 2308, reported out of the committee on Environment, Natural Resources, and Agriculture, 15 December 2005 (www.mass.gov/legis/).
20. J. C. Day, *Ocean Coastal Manage.* **45**, 139 (2002).
21. Supported by the National Center for Ecological Analysis and Synthesis, University of California at Santa Barbara; Working Group on Ocean Ecosystem Management; the David and Lucile Packard Foundation; the Gordon and Betty Moore Foundation; and the Center for Marine Conservation, Nicholas School of the Environment and Earth Sciences, Duke University, Beaufort, NC 28516, USA.

GEOPHYSICS

A New Class of Earthquake Observations

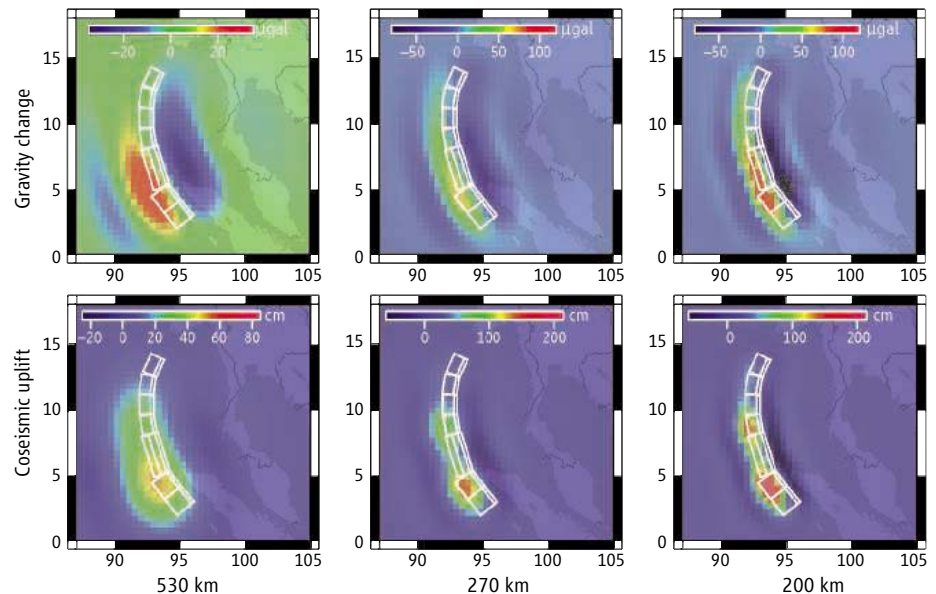
Fred F. Pollitz

A leap in observational geodesy—the science of measuring the size and shape of Earth—occurred 20 years ago with the establishment of several satellite-based measurement systems, including satellite laser ranging (SLR), very long baseline interferometry (VLBI), and the Global Positioning System (GPS). Geodesists exploited these systems to measure crustal deformation and tectonic motion to an accuracy of about 1 cm or better (1). Another leap came in the early 1990s with the development of synthetic aperture radar combined with interferometric processing (InSAR) (2), which provided centimeter-level accuracy and high spatial resolution. The combined accuracies of GPS for horizontal motions and InSAR for vertical motions have been generally sufficient to capture earthquakes of magnitude $M \geq 5$, allowing the quantification of earthquake ruptures at a level of detail not possible before the mid-1980s.

Geodesists have long anticipated a similar leap in remote sensing of earthquakes by means of gravity signals. This advance was realized with the March 2002 launch of the Gravity Recovery and Climate Experiment (GRACE) twin satellites. This mission is a partnership between NASA and DLR (Deutsche Forschungsanstalt für Luft- und Raumfahrt) and is designed to measure every 30 days the time-variable gravity caused by movement of water mass (3). It is based on ranging measurements between two identical satellites that fly in the same low Earth orbit, separated by about 200 km. Because their orbital height is only 500 km, GRACE measures global gravity at unprecedentedly small scales (4). Applications of this powerful system include the detection of monthly-variable snow and ice levels on the polar caps, surface water flux on continents, and seafloor pressure fluctuations (5, 6). Soon after it was launched, this new system was also deemed capable of detecting gravity changes associated with $M \approx 9.0$ earthquakes (7). On page 658 of this issue, Han and colleagues (8) demonstrate an unequivocal observation of the gravity change from an earthquake with satellite-based measurements.

The author is with the U.S. Geological Survey, Menlo Park, CA 94025, USA. E-mail: fpollitz@usgs.gov

Advances in satellite technology have improved measurements of Earth's properties. Now changes in local gravity resulting from large earthquakes can be detected.



Mapping gravity. Gravity change and uplift at Earth's surface (18) computed on the spherical Preliminary Reference Earth Model (19) (including an ocean layer) using a refinement of the Banerjee *et al.* (9) coseismic slip model of the Sumatra-Andaman earthquake (fault planes are indicated by white outlines). The gravity and uplift fields are filtered at progressively smaller half-wavelengths: 530 km (left), 270 km (middle), and 200 km (right). The left image is comparable to the GRACE gravity observations and model presented by Han *et al.* (8).

The earthquake investigated by Han *et al.* is the magnitude 9.2 Sumatra-Andaman earthquake that occurred on 26 December 2004. Having ruptured about 1500 km of the megathrust zone (the long and wide boundary between tectonic plates) of the Sumatran trench, this earthquake is the longest ever recorded. The authors take advantage of the technical capabilities of the GRACE satellites (in particular their onboard GPS receivers and accelerometers) to correct satellite-to-satellite distance measurements for the effects of non-gravitational acceleration. By further differencing the gravity fields estimated before and after the earthquake, they isolate the effects of the Sumatra-Andaman earthquake on Earth's gravity field, which range from -15 to $+15$ microgals, well above the uncertainty in the measurement. (For comparison, gravitational acceleration at Earth's surface is 980 gals.) The processes contributing to this gravity change are (i) the vertical motions of the solid Earth, which rearranges the internal stratification in intrinsic density—for example, bringing relatively high-density rock to a level previously occupied by low-density rock—and

(ii) a change in the intrinsic density of the surrounding material, which is induced by permanent dilatation or contraction of the material by the earthquake. At relatively short wavelengths of the static deformation field, the first effect dominates because of the large effect of vertical offset of the seafloor caused by the earthquake (see the figure). However, at longer wavelengths the second effect gains in importance because it is compounded over a volume of large dimensions. At wavelengths greater than 800 km, where the expected signal is well above the measurement error, Han *et al.* find that both effects contribute about equally to the net measured gravity change.

Global static deformation from the Sumatra-Andaman earthquake has been accurately measured by GPS (9–12), and corresponding dislocation models of net slip have been constructed with these sets of displacements. As is the case for most earthquakes, gaps in coverage by GPS instruments lead to uncertainties in the details of rupture (e.g., depth extent of slip, horizontal variations in slip, etc.). Vertical offsets of the seafloor near the Sumatran trench but away from Sumatra

and smaller land areas (where GPS instruments are placed) would likely go undetected by GPS instruments but could, in principle, be seen by GRACE measurements. Although not yet investigated, the Aceh basin off the coast of northern Sumatra could provide such a target in order to test the intriguing hypothesis that 15 to 20 m of slip on a secondary thrust structure (13) occurred simultaneously with known slip on the megathrust. This secondary thrust is suspected of having contributed to the tsunami that devastated northern Sumatra (13).

The successful detection of gravity changes caused by the Sumatra-Andaman earthquake opens the door to the detection of related geophysical phenomena. Gravity fields mapped by GRACE can reveal details at a resolution of about 400 km, but the relatively large observational errors at finer resolution demand large sources with sufficiently large spatial dimensions. Future observations might include detection of postglacial readjustment of Earth's ductile mantle (14) at continent-wide scales, strain

accumulation at megathrust zones (15), and postseismic relaxation of the mantle after a Sumatra-sized earthquake, as has already been detected by GPS (16). These processes affect volumes of material extending to several hundreds of kilometers in depth, and high-resolution global gravity measurements should provide good and unique constraints on the depth-dependent nature of the associated mantle flow fields. The detection threshold of these processes will be dramatically improved if the follow-on to GRACE provides data with errors smaller by one to two orders of magnitude (17), which would lower the detection threshold of earthquakes to $M \approx 7.5$ (7).

References

1. D. E. Smith, D. L. Turcotte, *Contributions of Space Geodesy to Geodynamics: Technology* (American Geophysical Union, Washington, DC, 1993).
2. R. Bürgmann, P. A. Rosen, E. J. Fielding, *Annu. Rev. Earth Planet. Sci.* **28**, 169 (2000).
3. B. D. Tapley, S. Bettadpur, J. C. Ries, P. F. Thompson, M. Watkins, *Science* **305**, 503 (2004).
4. B. D. Tapley, S. Bettadpur, M. M. Watkins, C. Reigber, *Geophys. Res. Lett.* **31**, L09607 (2004).
5. J. Wahr, S. Swenson, V. Zlotnicki, I. Velicogna, *Geophys. Res. Lett.* **31**, L11501 (2004).
6. O. B. Andersen, J. Hinderer, *Geophys. Res. Lett.* **32**, L01402 (2005).
7. W. Sun, S. Okubo, *J. Geophys. Res.* **109**, B04405 (2004).
8. S.-H. Han, C. K. Shum, M. Bevis, C. Ji, C.-Y. Kuo, *Science* **313**, 658 (2006).
9. P. Banerjee, F. F. Pollitz, R. Bürgmann, *Science* **308**, 1769 (2005).
10. S. Jade, M. Ananda, P. Kumar, S. Banerjee, *Curr. Sci.* **88**, 1980 (2005).
11. C. Vigny *et al.*, *Nature* **436**, 201 (2005).
12. C. Subarya *et al.*, *Nature* **440**, 46 (2006).
13. G. Plafker, S. Nishenko, L. Cluff, M. Syahrial, *Seismol. Res. Lett.* **77**, 231 (2006).
14. I. Velicogna, J. Wahr, *J. Geophys. Res.* **107**, 10.1029/2001JB001735 (2002).
15. V. Mikhailov, S. Tikhotsky, M. Diamant, I. Panet, V. Ballu, *Earth Planet. Sci. Lett.* **228**, 281 (2004).
16. F. F. Pollitz, P. Banerjee, R. Bürgmann, *Geophys. J. Int.*, in press.
17. M. Stephens *et al.*, paper presented at the Sixth Annual NASA Earth Science Technology Conference, 27 to 29 June 2006, College Park, MD.
18. F. F. Pollitz, *Phys. Earth Planet. Inter.* **99**, 259 (1997).
19. A. Dziewonski, D. Anderson, *Phys. Earth Planet. Inter.* **25**, 297 (1981).

10.1126/science.1131208

CLIMATE

Caving In to New Chronologies

Gideon M. Henderson

When you check the weather forecast on TV, you do not expect it to be completely accurate. But you do expect a degree of certainty about when the forecast is for: It would not be very useful to hear that it will probably be rainy, but with a thousand-year uncertainty about when. Yet this is the situation faced by those studying past climate. Records of climate from sediment or ice cores are not time series but depth series, and converting depth to age generally carries a substantial uncertainty.

This is unfortunate because the timing of climatic changes can provide fundamental information about the mechanisms driving that change. A climate change in one region, for instance, could not have been caused by change at a later time in another region. This situation presents paleoclimatologists with a dilemma. Often, the



Stalagmite tales. Stalagmites such as those shown here can provide highly accurate climate records for the past 400,000 years.

best way to constrain the chronology of a poorly dated record is to line up events in that record with those in a better dated record. But to do so discards information about the phasing of change and therefore about the links between climate in different regions, or between climate and the forces that drive it.

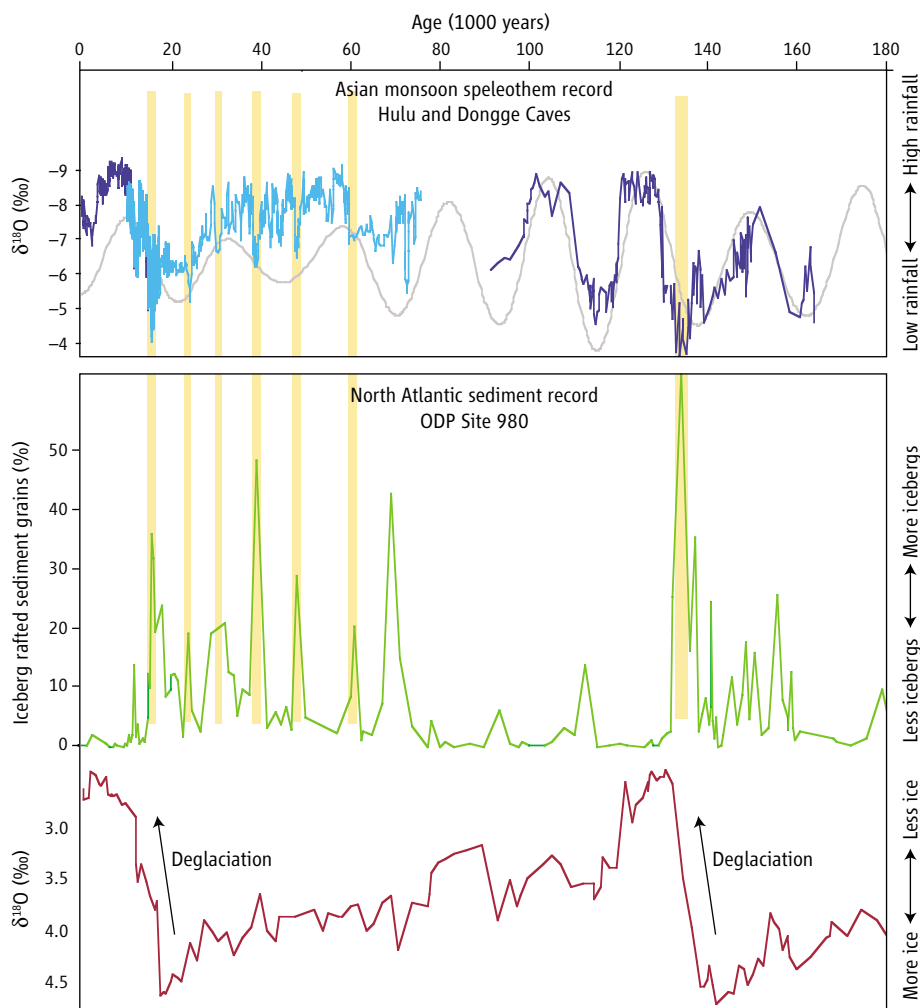
The question of paleoclimate chronology has been given fresh focus by the burgeoning field of climate reconstruction from speleoth-

ems—formed in caves, such as stalagmites, can be dated precisely and are increasingly providing detailed and accurate records of past climates.

ems—the general term for carbonates found in caves, such as stalagmites (see the first figure). Speleothem climate records can be dated by measuring the growth of thorium-230 from the radioactive decay of uranium, yielding climate chronologies for the past 400,000 years at unprecedented precision. When and how can other climate records be correlated to these well-dated speleothem records?

Some of the best stalagmite records come from regions influenced by the Asian monsoon (1, 2). These records show abrupt changes in monsoon strength on millennial time scales, with a pattern similar to those seen in records from ice and sediment cores from the North Atlantic region. Extreme cold events in the North Atlantic are caused by increases in the flux of fresh water (sometimes from icebergs that carry and deposit coarse-grained sediments as evidence of their past presence). This freshwater flux decreases the rate of deep-water formation and hence the northward transport of heat, leading to cold

The author is in the Department of Earth Sciences, University of Oxford, Oxford OX1 3PR, UK. E-mail: gideonh@earth.ox.ac.uk



Precise dating. Climate records from Asian caves (**top**) (10) and a North Atlantic sediment core (**bottom**) (11) show millennial variability (yellow bars) and longer period variability associated with changing insolation (upper gray curve). Speleothem records have precise chronologies based on radiometric dating; North Atlantic records can only be well dated for the past 30,000 to 40,000 years. Comparison of the records for this time period demonstrates that periods of low Asian rainfall coincide with periods of iceberg release and cold conditions in the North Atlantic. Assuming that this relation between the records also holds further back in time, the speleothem chronology can be imported into older parts of the sediment record where direct dating is not possible.

conditions. Assessing how rainfall changes in the Asian region during these Atlantic cold events would tell us how atmospheric processes link the two regions and provide information about possible future change.

For the past 30,000 years, such an assessment is possible because there are good, independent chronologies for both regions from precise uranium/thorium dating of Asian speleothems and from counting of annual layers in Greenland ice cores. This comparison indicates that chilly conditions in the North Atlantic correlate with dry periods in Asia, probably because cooling of the northern continents prevents rainfall associated with the intertropical convergence zone from penetrating so far into the monsoon regions of Asia. A future shut-down in deep-water formation in the North Atlantic, such as might be caused by

ice-melting and higher ocean temperatures as the planet warms, could therefore cause substantial change to rainfall thousands of miles away in Asia.

Given this link at the millennial time scale, is it reasonable to transfer monsoon chronologies onto longer duration changes in the North Atlantic? A pivotal issue here is the timing of glacial-interglacial cycles involving the growth and collapse of continental ice sheets, principally around the North Atlantic. Over the past 1 million years, deglaciations have occurred relatively rapidly about every 100,000 years and represent the largest amplitude climate changes observed during this period. They are associated with substantial increases in atmospheric carbon dioxide concentration (3) and with dramatic change to almost every aspect of Earth's surface envi-

ronment. Traditional thinking holds that deglaciations are driven or at least initiated by changes in summer insolation (incoming solar radiation) at northern mid-latitudes, where the ice sheets were found. Others have suggested a more noisy link between insolation and deglaciation (4) and an inconsistent phasing between the two.

If we can use well-dated speleothem records to better constrain the timing of deglaciations, we could test these ideas and learn more about the causes of glacial-interglacial cycles. But care is needed to tackle this issue. In contrast to the 100,000-year glacial cycle, the monsoon beats regularly with the 21,000-year cycle of orbital precession, which governs the strength of summer heating of the Asian continent (see the second figure). At these longer time scales, the mechanisms driving change in monsoon rainfall and North Atlantic temperature may be very different from those causing the tight linkage at millennial time scales.

Cheng *et al.* (5) tackled this problem by using the linkage at millennial time scales to line up longer duration records from the two regions. They correlate an extreme dry period in the monsoon with a pulse of iceberg release in the North Atlantic that occurred almost synchronously with the penultimate deglaciation (see the second figure). Their analysis shows that the midpoint of deglacial melting occurred some 4000 years before the abrupt change to wetter monsoon conditions; the latter change is well dated in the speleothem records at 129,000 years. The resulting age for the deglaciation of ~133,000 years agrees with attempts to directly date this event (6) and is significantly earlier than the 128,000 to 130,000 years predicted by direct forcing from Northern Hemisphere insolation change (7, 8). The speleothem chronology thus supports the idea of a more complex link between insolation and the glacial cycle.

This example illustrates the huge potential of speleothem records to provide chronologies for climate change at very high resolution—a potential that may make speleothems the new ice cores. Drilling into high-latitude and high-altitude ice sheets has revolutionized our understanding of climate, particularly at time scales of millennia and shorter. Such records have taught us how abruptly climate can change; they have provided unique records of past atmospheric composition; and they will doubtless continue to enlighten us.

But ice cores do have limitations. They are found far from major human populations, they do not capture variability in major climate systems such as the monsoons or El Niño, and they are difficult to date accurately. In contrast,

speleothems are scattered over most continental areas and provide exceptional chronology. They will allow investigation of spatially variable changes as climate fronts move across continental regions, and enable direct comparison of climate in distant regions, as recently demonstrated in a study of rainfall in the southern and northern Tropics (9).

For paleoclimate, the past two decades

have been the age of the ice core. The next two may be the age of the speleothem.

References and Notes

1. Y. L. Wang *et al.*, *Science* **294**, 2345 (2001).
2. D. Fleitmann, *et al.*, *Science* **300**, 1737 (2003).
3. U. Siegenthaler *et al.*, *Science* **310**, 1313 (2005).
4. P. Huybers, C. Wunsch, *Nature* **434**, 491 (2005).
5. H. Cheng *et al.*, *Geology* **34**, 217 (2006).
6. G. M. Henderson, N. C. Slowey, *Nature* **404**, 61 (2000).
7. J. Imbrie *et al.*, in *Milankovitch and Climate*, A. Berger, J. Imbrie, J. Hays, G. Kukla, B. Saltzman, Eds. (Reidel, Dordrecht, 1984), pp. 269-305.
8. D. G. Martinson *et al.*, *Quat. Res.* **27**, 1 (1987).
9. X. Wang *et al.*, *Nature* **432**, 740 (2004).
10. D. X. Yuan *et al.*, *Science* **304**, 575 (2004).
11. J. F. McManus, D. W. Oppo, J. L. Cullen, *Science* **283**, 971 (1999).

10.1126/science.1128980

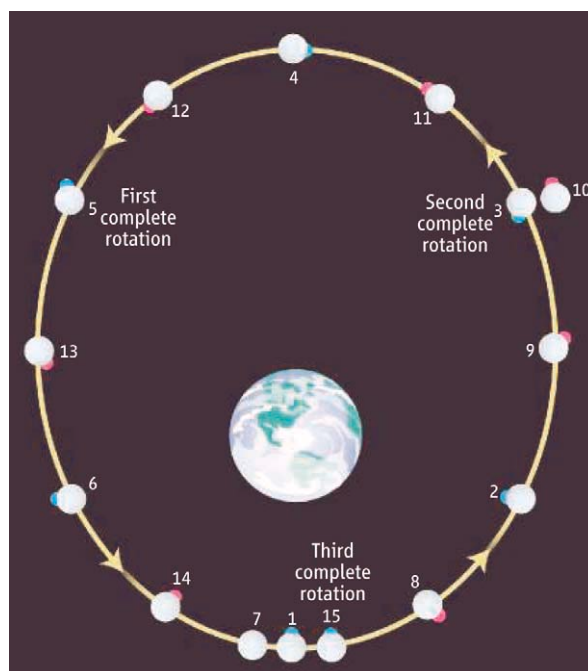
PLANETARY SCIENCE

Solving Laplace's Lunar Puzzle

Kimmo Innanen

About two centuries ago, the eminent mathematician Pierre-Simon Laplace noted something unusual about the Moon's gravity (1). With a mass ratio of about 80:1, Earth and its Moon are unique in the solar system and are sometimes referred to as a double planet. As the Moon revolves around Earth in about a month, this double planet itself revolves around the Sun in a year. Both orbits are slightly elliptical, with the lunar orbit tilted a few degrees to Earth's solar orbit. The result is a three-dimensional example of what is called the gravitational three-body problem. Adding to the complexity is that both bodies are pear-shaped, with the Moon locked into a synchronous orbit with one face toward Earth. One can thus envision this choreography: a pair of slightly flexible (one covered with oceans), spinning, bulgy gyroscopes in mutual gravitational motion, with the pair in concurrent motion around the Sun. Laplace's problem was that he could not reconcile the observed orbital properties of the Moon with its shape and expected motion. Very simply, there is excess bulge material in the Moon's equatorial region. On page 652 of this issue (2), Garrick-Bethell *et al.* present an ingenious method to fill a gap in our knowledge of the earlier history of the Moon's orbit without using a full computer simulation of the entire complex system. Their results now offer a credible solution to Laplace's problem.

Following Newton's exact solution of the two-body problem (in the form of ellipses, with the center of gravity at one focus), the search for a complete analytical solution to the general three-body problem preoccupied and frustrated the best mathematical minds



A long time ago but not so far away. Schematic illustration of the Moon's orbit 100 to 200 million years after formation (with exaggerated eccentricity). In this orbit, the Moon rotates 1.5 times during each orbit (starting from position 1; the red and blue dots indicate the orientation), much like the orbit of Mercury around the Sun. The present-day orbit is nearly circular with a radius 2.5 times larger, and the near side of the Moon is always facing Earth. [Adapted from (8)]

for more than three centuries. Newton himself is said to have suffered severe headaches in his own attempts to provide a more complete theory of the Moon's motion. Two of the most famous mathematicians of the 18th and early 19th centuries were Leonard Euler and Laplace. Euler made fundamental contributions (now known as Euler's equations) to the dynamics of solid and fluid bodies, introducing the concept of the three basic moments of inertia A , B , and C of symmetri-

cal bodies with equatorial bulges. The moments of inertia capture the rotational properties of a body much the way its mass quantifies its inertia for motion in a straight line. Euler also applied his results in attempts to understand the Moon's motion. Laplace used Euler's work and his own mathematical skills to identify the most important secular perturbation terms and thereby to show that the lunar moments cannot be in equilibrium with its present orbit. In the solar system, many of the mutual interactions (perturbations) between the planets, including their satellites, are of short term (say hundreds or thousands of years) and average to zero. Secular perturbations do not average out to zero, but accumulate significantly over much longer times, over, say, hundreds of thousands or millions of years. Something interesting must therefore have happened during the Moon's early history to "lock in" this disequilibrium,

perhaps as it cooled and solidified, when it was much closer to Earth. The theoretical work on the Moon's orbit culminated in the late 19th and early 20th century with the analyses of Delaunay, Hill, and Brown (3). Their work used the perturbation method: Beginning with the elliptical orbit as a reference, they added perturbing terms to take account of the other physical influences affecting the system. The result was a list of more than 300 perturbing terms, each with

perhaps as it cooled and solidified, when it was much closer to Earth. The theoretical work on the Moon's orbit culminated in the late 19th and early 20th century with the analyses of Delaunay, Hill, and Brown (3). Their work used the perturbation method: Beginning with the elliptical orbit as a reference, they added perturbing terms to take account of the other physical influences affecting the system. The result was a list of more than 300 perturbing terms, each with

The author is in the Department of Physics and Astronomy, York University, Toronto, ON M3J 1P3 Canada. E-mail: kiminn@yorku.ca

its own periodic effect. (It is a testament to the care of Delaunay, Hill, and Brown that only a handful of modest errors have been discovered in this work by means of modern computer algebraic methods that have added many more terms.) Nevertheless, this huge list was enough to discourage later generations of mathematicians and astronomers from studying the problem.

Modern computer analyses of the general three-body problem (4, 5) have shown its incredible complexity, so that statistical approaches become viable. There are also additional important longer-period complexities in the problem: To conserve angular momentum (which is not affected by friction), the frictional energy losses due to Earth's ocean tides sloshing near the coastal shorelines cause the Earth's spin to slow down and the Earth-Moon distance to increase by 3.8 cm each year, to a present distance of some 60 Earth radii. (In comparison, geosynchronous communication satellites revolve around Earth at the same rate as it spins, at a distance of about 6 Earth radii.) This very slow lunar recession is known from two sources: the timing and location of ancient solar eclipses, and from accurate measurement of the Earth-Moon distance with lasers on Earth and reflectors left on the Moon's surface by the Apollo astronauts. It is therefore possible to run the Moon's position backward in time. In addition, the moments of inertia of both the Moon and

Earth have been accurately determined from artificial satellite motions.

In the work of Garrick-Bethell *et al.*, the central issue is the Moon's own nonspherical shape, which, together with its orbit, lead the authors to an interesting conclusion about its past history: Its orbit around Earth in the distant past must have been much closer and also more eccentric than it is now (see the figure). In fact, their optimum solutions locate the young Moon at a time 100 to 200 million years after its formation, when it was at a distance of some 24 to 27 Earth radii. At this time it would have passed through the 3:2 spin-orbit resonance, reminiscent of the present-day behavior of the planet Mercury, which rotates three times about its own axis for every two revolutions about the Sun. They show that the distance and eccentricity at this time would have been optimal for the bulge to "freeze" into the solidifying Moon, a fossil bulge we observe to this day. These results appear to dovetail in a reasonable way with the most viable contemporary theory of the Moon's own origin through a giant impact of a Mars-like object with Earth, from which debris the primordial Moon formed at some 4 Earth radii (6, 7).

This work should provide impetus for renewed analytical interest in the fascinating history of our still mysterious cosmic companion. In particular, there arise the questions of how the Moon passed through the

geosynchronous and 3:2 resonances and arrived at its present orbit. At 24 Earth radii, the Earth-Moon proximity would certainly have had dramatic effects on the Earth as well. Suppose that Earth's rotation period then was 12 hours, so that the true lunar month would have been 18 hours. Ignoring their small motion around the Sun, the Moon's phases would have gone through a full cycle in just 18 hours. Perhaps even more dramatically, the Moon's tidal effects on the Earth would have been some 10 times today's amplitudes with about 6 hours between maxima. The magnitude and frequency of this sort of powerful tidal machine would require complex modeling.

References and Notes

1. P.-S. Laplace, *Traité de Mécanique Céleste* (Duprat, Courcier, and Bachelier, Paris, 1798–1827), vol. 2, book 5, chap. 2.
2. I. Garrick-Bethell, J. Wisdom, M. T. Zuber, *Science* **313**, 652 (2006).
3. C. D. Murray, S. F. Dermott, *Solar System Dynamics* (Cambridge Univ. Press, Cambridge, UK, 1999).
4. M. Valtonen, H. Karttunen, *The Three-Body Problem*, (Cambridge Univ. Press, Cambridge, UK, 2006).
5. C. D. Murray, in *Chaotic Motion in the Solar System in Encyclopedia of the Solar System*, T. Johnson, P. Weissman, L. McFadden, Eds. (Academic Press, Orlando, FL, 1998).
6. E. Belbruno, J. R. Gott, *Astron. J.* **129**, 1724 (2005).
7. D. Mackenzie, *The Big Splat* (Wiley, New York, 2003).
8. www.solarviews.com/eng/mercury.htm
9. I acknowledge support of the Natural Sciences and Engineering Research Council of Canada.

10.1126/science.1131113

CLIMATE

How Do Aerosols Affect Cloudiness and Climate?

François-Marie Bréon

What is the net impact of anthropogenic aerosol emissions on Earth's climate? Is it similar in magnitude to that of greenhouse gases? Do aerosols mostly affect the amount of solar radiation reflected back into space, or do they also have a substantial effect on the hydrological cycle? Many recent studies have tried to answer these questions, but the picture gets ever more complex. On page 655 of this issue, Kaufman and Koren (1) bring some clarity to the issue by quantifying the positive impact of aerosol

load on the cloud cover and demonstrating the opposite effect in the presence of absorbing aerosols.

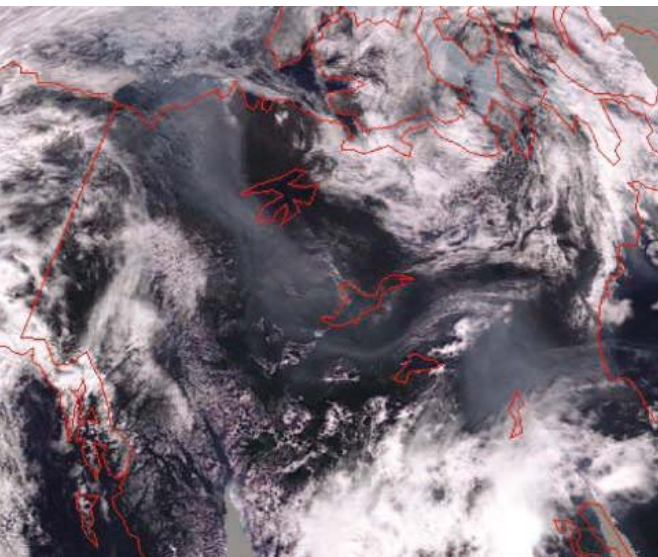
Aerosols were long thought to affect climate mainly by reflecting incoming solar radiation back to space, thus cooling Earth's surface. But in the late 1990s, it was shown that some aerosols can absorb substantial amounts of solar energy, thereby increasing solar heating, particularly when aerosol layers are located above cloud decks. Even worse news for attempts to quantify the effect of aerosols on climate came with the identification of the so-called indirect effects, through which aerosols change the optical properties and the life cycle of clouds.

Anthropogenic aerosol emissions may increase cloud cover by up to 5%, resulting in a substantial net cooling of Earth's atmosphere.

In the first indirect effect, the presence of aerosols leads to the formation of more numerous and smaller cloud droplets (2, 3), resulting in brighter clouds that reflect more solar energy back into space. This reduction in cloud droplet size tends to reduce precipitation and, together with other aerosol-cloud processes, changes the geographical extent of cloudiness (the second indirect effect) (4). Both processes lead to an increase in the solar energy reflected back to space, and thus a net cooling of climate.

However, the opposite effect has been observed above the Indian Ocean (5) and over the Amazon Basin (6): Aerosols that can absorb substantial amounts of solar energy—

The author is at the Laboratoire des Sciences du Climat et de l'Environnement, 91191 Gif-sur-Yvette, France. E-mail: francois-marie.breon@cea.fr



Aerosol-cloud interaction. Forest fires inject large amounts of smoke into the atmosphere over western Canada, generating aerosol layers that extend over hundreds of kilometers and show as a gray-blue haze from Hudson Bay to the Arctic Ocean. Aerosols may either increase the cloud lifetime (and thus the cloud cover) or increase the atmosphere's temperature (which tends to decrease the cloud cover). The image is a true-color composite of three successive passes of the PARASOL satellite on 23 August 2005 from an altitude of about 700 km.

particularly black carbon, which is produced by incomplete combustion (see the figure)—tend to warm the atmosphere and inhibit cloud formation. Aerosols may also alter convective cloud dynamics (7). The net impact of aerosols on cloud cover may thus depend not only on local atmospheric conditions, but also on the magnitude of the aerosol absorption.

To address these issues, Kaufman and Koren performed a statistical analysis of ground-based remote sensing data from around the globe. The analysis confirms a positive and robust correlation between aerosol load and cloud cover, with a mean slope that gets smaller as aerosol absorption increases. On the basis of these results, the authors estimate that anthropogenic aerosols increase the global cloud cover by 5%. Assuming a typical cloud albedo of 0.5, this corresponds to an increase of the reflected solar flux by 5 W m^{-2} —a forcing on climate that is larger than, and of opposite sign to, that of greenhouse gases.

These estimates are based on global average cloud reflectance, aerosol load, and absorption. Furthermore, the statistical analysis is limited to specific cloud cover conditions. Many regions have overcast skies or a meteorology that is not suitable for the formation of clouds, even in the presence of large aerosol loads. The figures above are therefore

probably overestimates, and considerable uncertainties remain.

More accurate estimates of the effect of aerosols on climate require global monitoring of aerosol absorption. Unfortunately, this parameter is difficult to estimate from satellite data; current values rely on ground-based remote sensing measurements made at a few locations (8). Furthermore, aerosol-cloud interaction depends on the vertical distribution of the aerosols, which is poorly known. This may change with the recent completion of the A-Train, a series of remote-sensing satellites that provide a three-dimensional view of the atmosphere (9).

There is a strong need to better understand and model the effect of aerosols on climate. Many studies have shown that aerosol and greenhouse gas forcings have the same order of magnitude, but it may be much easier to curb the aerosol load than to limit the growth of greenhouse gas concentrations. Anthropogenic aerosols typically remain in the atmosphere for a few days, whereas carbon dioxide released today may linger in the atmosphere for centuries. Furthermore, new technologies are being implemented to reduce

particulate matter emissions from fuel use, whereas future efforts to sequester carbon dioxide will probably be limited to large power plants. On the other hand, a reduction of particle emissions may increase global warming (10). We may have to choose between an aerosol-loaded air, with its adverse effects on human health, and a rapid and strong climate change.

References and Notes

1. Y. J. Kaufman, I. Koren, *Science* **313**, 655 (2006); published online 13 July 2006 (10.1126/science.1126232).
2. F.-M. Bréon, D. Tanré, S. Generoso, *Science* **295**, 834 (2002).
3. J. E. Penner, X. Q. Dong, Y. Chen, *Nature* **427**, 231 (2004).
4. D. Rosenfeld, *Science* **287**, 1793 (2000).
5. A. S. Ackerman *et al.*, *Science* **288**, 1042 (2000).
6. I. Koren, Y. J. Kaufman, L. A. Remer, J. V. Martins, *Science* **303**, 1342 (2004).
7. I. Koren, Y. J. Kaufman, D. Rosenfeld, L. A. Remer, Y. Rudich, *Geophys. Res. Lett.* **32**, L14828 (2005).
8. H. Yu *et al.*, *Atmos. Chem. Phys.* **6**, 613 (2006).
9. A. L. Anderson *et al.*, *Bull. Am. Meteorol. Soc.* **86**, 1795 (2005).
10. M. O. Andreae, C. D. Jones, P. M. Cox, *Nature* **435**, 1187 (2005).
11. After the paper by Kaufman and Koren (1) had been accepted, the first author was hit by a car and died as a result of his injuries. Yoram Kaufman will be remembered as a brilliant scientist and charismatic leader who collaborated with scientists around the world to advance our understanding of Earth's climate system.

10.1126/science.1131668

CELL BIOLOGY

Extinguishing a Cell Cycle Checkpoint

M. Andrew Hoyt

The steps in cell division are precisely orchestrated. A key checkpoint is inactivated after it has performed its function so that the next steps can take place.

The faithful ordering of the events that accomplish the division of a eukaryotic cell is enforced by checkpoints, mechanisms that block the initiation of key events until an upstream event has been successfully completed. A well-studied example is the spindle checkpoint, which prevents the mitotic spindle from segregating replicated chromosomes into progeny nuclei until all the chromosomes have achieved proper attachment to spindle fibers (1). Cells defective for spindle checkpoint genes

segregate chromosomes with reduced fidelity, causing aneuploidy, a hallmark of many cancer cells (2).

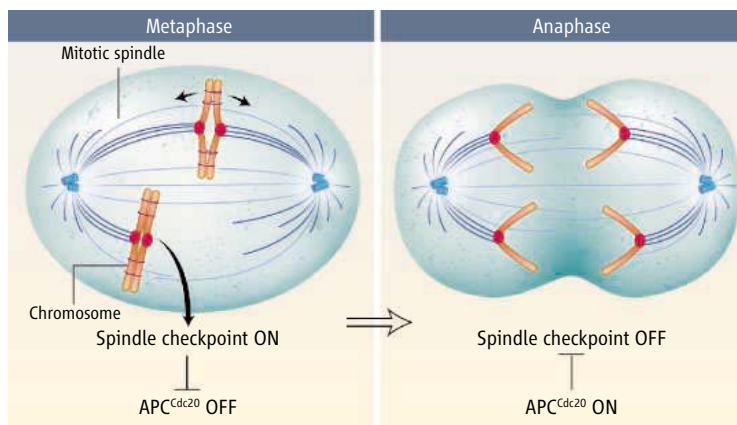
Specialized sites on chromosomes called kinetochores attach to spindle fibers in metaphase of mitosis. When all attachments are proper, the spindle checkpoint permits anaphase, the stage at which chromosomes separate. Paradoxically, the mechanism responsible for separation of the chromosomes at anaphase itself creates chromosome attachments that the checkpoint would normally recognize in metaphase as improper. Yet, the cell cycle proceeds naturally unimpeded; these improper chromosome attachments fail to activate the cycle-blocking

The author is in the Department of Biology, Johns Hopkins University, 3400 North Charles Street, Baltimore, MD 21218, USA. E-mail: hoyt@jhu.edu

activity of the spindle checkpoint after anaphase onset. From a clever series of experiments reported on page 680 of this issue by Palframan *et al.* (3), we now know why. In anaphase cells, the actions of the spindle checkpoint are extinguished by the very same protein complex that previously was the target of its anaphase-inhibitory activity.

Chromosome attachment to spindle fibers is complete in metaphase, when all chromosomes assume a bipolar (or amphitelic) orientation. That is, all replicated chromosomes attach to the spindle such that paired sister kinetochores are connected to opposite spindle poles. Tension is created across kinetochores by spindle action that pulls each sister kinetochore poleward, but is resisted by a “chromosome glue”—the protein cohesin—that binds the sisters together (see the figure). By a mechanism that is still unclear, the conserved proteins of the spindle checkpoint detect kinetochores that are not properly attached and/or are not subject to bipolar tension (4). Activated by these improperly attached kinetochores, the checkpoint elicits a protein-based signal that blocks chromosome separation at anaphase. The inhibited target here is a form of the anaphase-promoting complex (APC^{Cdc20} ; the complex is bound to the protein Cdc20), a multisubunit enzymatic complex with ubiquitin ligase activity. Its specific actions select key proteins for degradation, permitting the onset of anaphase. An important indirect target of APC^{Cdc20} action is cohesin, whose destruction allows sister chromatids to be pulled apart by the mitotic spindle. Therefore, when all chromosomes are bioriented and under tension, the spindle checkpoint is satisfied, its inhibition of APC^{Cdc20} is relieved, cohesin is destroyed, and chromosomes move to the poles.

Chromosomes separated at anaphase, however, cannot be under tension, and even kinetochores that are detached during anaphase fail to arrest cell-cycle progression (3). Whether anaphase actually creates a condition that permits kinetochores to once again signal their lack of tension is debatable. Nonetheless, Palframan *et al.* clearly demonstrate that the spindle checkpoint is inactivated in anaphase and that artificial reactivation at this stage will



Regulatory factors that dominate mitosis. (Left) In metaphase, sister chromatids (orange) of a chromosome are held together by cohesin (purple) and attached to spindle microtubule fibers (blue) at their kinetochores (red). The two sister chromatids of the top chromosome are properly attached in a bipolar fashion, and therefore the kinetochores are under tension (arrows). The bottom chromosome has not yet achieved bipolar attachment so its kinetochores signal the spindle checkpoint to inhibit APC^{Cdc20} . (Right) When all chromosomes achieve a bipolar connection, inhibition of APC^{Cdc20} is relieved, allowing the degradation of cohesin and chromosome segregation to the spindle poles in anaphase. In anaphase, APC^{Cdc20} mediates the inhibition of spindle checkpoint proteins, thereby preventing its reactivation by the presence of kinetochores not under tension.

block cell-cycle progression. The authors attempted to reactivate the spindle checkpoint in anaphase cells of the yeast *Saccharomyces cerevisiae* by artificially overexpressing the checkpoint protein Mps1, a condition known to activate the spindle checkpoint before anaphase (5). They observed that expression of Mps1 in anaphase did indeed reactivate the checkpoint. In a manner dependent upon the actions of the downstream checkpoint protein Mad2, APC^{Cdc20} was inhibited, and cells were blocked from exiting mitosis. This study and others showed that APC^{Cdc20} is required not only for the metaphase-to-anaphase transition but also for subsequent passage through anaphase and out of mitosis. The important new finding here is that APC^{Cdc20} can be inhibited in anaphase by the spindle checkpoint proteins provided they are activated. Therefore, whether or not anaphase kinetochores signal their lack of tension, spindle checkpoint action must be extinguished in anaphase for cell division to proceed.

Palframan *et al.* also reveal that the spindle checkpoint is attenuated in anaphase by proteolysis, a cell cycle-regulatory mechanism commonly used presumably because it is irreversible. They show that Mps1 is normally unable to inhibit cell-cycle progression in anaphase simply because it is no longer present (making the issue of whether anaphase kinetochores are capable of signaling their lack of tension moot). Strikingly, this study demonstrates that Mps1 is degraded

in anaphase by the actions of APC^{Cdc20} , the target that the spindle checkpoint proteins inhibit before anaphase. Therefore, APC^{Cdc20} and spindle checkpoint proteins share a mutually antagonistic relationship: When active in metaphase, the spindle checkpoint directly inhibits APC^{Cdc20} [and also somewhat destabilizes Cdc20 (6)], whereas in anaphase, at least one spindle checkpoint protein, Mps1, is destabilized by APC^{Cdc20} .

The antagonistic relationship between APC^{Cdc20} and spindle checkpoint proteins may create a bistable switch mechanism in which flipping between alternate states can be achieved by a subtle change in balance that is rapidly reinforced by inhibition of the other state. In metaphase, the spindle checkpoint must be tuned so sensitively as to respond to a single improperly attached kinetochore by causing inhibition of APC^{Cdc20} . Following attachment of the last kinetochore, a rapid and irreversible flip to the APC^{Cdc20} -mediated anaphase state is enhanced by the degradation of Mps1 (and possibly other spindle checkpoint proteins). Indeed, Palframan *et al.* were able to predictably switch cells between these two biochemical states. For example, even transient overexpression of Mps1 in anaphase yeast cells could cause a prolonged switch to a metaphase-like state; the spindle checkpoint was activated and exit from mitosis was prevented long after the expression of Mps1 was shut down. Similarly, an artificial reduction of Cdc20 expression in anaphase cells stabilized Mps1 and produced the same effect.

We can now appreciate the basic mechanism that causes the spindle checkpoint to be shut off. On to the next seemingly more difficult issue of how an improperly attached kinetochore turns it on.

References

1. D. J. Lew, D. J. Burke, *Annu. Rev. Genet.* **37**, 251 (2003).
2. V. M. Draviam, S. Xie, P. K. Sorger, *Curr. Opin. Genet. Dev.* **14**, 120 (2004).
3. W. J. Palframan, J. B. Meehl, S. L. Jaspersen, M. Winey, A. W. Murray, *Science* **313**, 680 (2006); published online 6 July 2006 (10.1126/science.1127205).
4. B. A. Pinsky, S. Biggins, *Trends Cell Biol.* **15**, 486 (2005).
5. K. G. Hardwick *et al.*, *Science* **273**, 953 (1996).
6. J. Pan, R.-H. Chen, *Genes Dev.* **18**, 1439 (2004).

10.1126/science.1131625

Timing the Sexual Development of Parasites

Stephen L. Hajduk

The protozoan parasite *Plasmodium* infects a wide range of warm-blooded hosts and causes malaria in humans. These parasites undergo complex developmental changes in both a mosquito vector and host, including asexual and sexual cycles (see the figure). Asexual reproduction occurs most often in a host's red blood cells. Multiplication eventually causes red blood cells to rupture, and although most of the released parasites invade other red blood cells, a few develop in the bloodstream into male and female gamete-

The myriad of developmental events that any single organism experiences during its life is controlled by multiple levels of gene expression regulation. In multicellular eukaryotes, tissue- and developmental-specific regulation most often involves the hierarchical expression of diverse transcription factors that bind to specific DNA elements, thus activating or suppressing the expression of specific genes. Generally, in an early developing embryo, nuclear transcription—the synthesis of protein-encoding messenger RNA (mRNA) from

Like other eukaryotes, the malaria parasite stores maternal RNA in the female gamete for later use in directing early development. An RNA helicase is a key regulator of this process.

female gametocyte mRNAs, P25 and P28, are translationally repressed (4, 5). That is, the female gametocyte stably stores these mRNAs and activates their translation upon ingestion by the insect. These transcripts encode unique *Plasmodium* proteins that appear to be necessary for parasite infection of the insect, though their actual functions remain unknown.

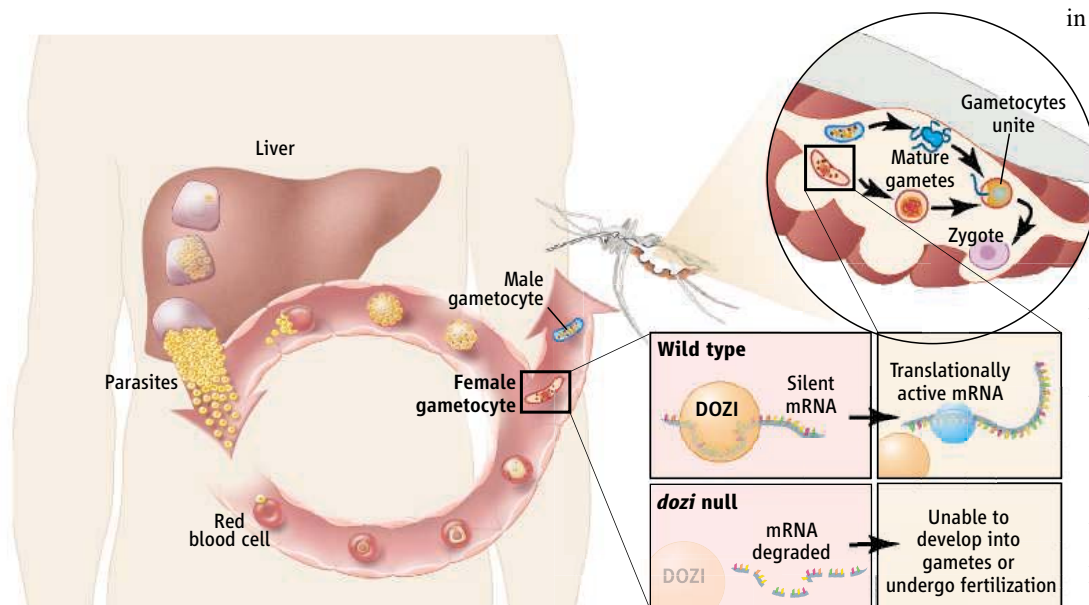
To identify the factors controlling translational repression in gametocytes, Mair *et al.* searched the gametocyte sex-specific suite of proteins, or proteomes, for those whose expression is up-regulated

in the female gametocytes. The authors found DOZI, a protein with homology to the DDX6 family of RNA helicases. These enzymes catalyze the unwinding of an RNA helix (6). The DDX-helicase family is closely linked to translational repression in many multicellular eukaryotes and in yeast, possibly by facilitating the binding of other proteins that repress translation.

To determine whether DOZI is associated with mRNPs in female gametocytes of *Plasmodium*, the authors generated a *Plasmodium* line expressing DOZI fused to green fluorescent protein (DOZI: GFP). This fusion protein localized to the cytoplasm of female gametocytes. Moreover, fluorescent *in situ* hybridization analysis of the *p25* and *p28* mRNAs

revealed localization of both transcripts with DOZI:GFP in cells. DOZI:GFP could also be biochemically isolated in a complex with mRNPs that contained P25 and P28 transcripts.

Does DOZI function in the sexual development of *Plasmodium*? Mutant parasites that do not express the *dozi* gene develop normally in the asexual bloodstream stages and produce gametocytes and gametes, but do not develop fertilized zygotes. As predicted by the authors, the expression of *p25* and *p28* mRNAs was dramatically reduced in the DOZI-null mutant, supporting the function of DOZI in storing translationally



***Plasmodium* gametocyte development.** Male and female gametocytes develop during bloodstream infections and mature to gametes within the mosquito gut. Female bloodstream gametocytes store translationally silent mRNAs in cytoplasmic bodies containing DOZI and activate the translation of these mRNAs in the insect. Female gametocytes are then able to develop into mature gametes and undergo fertilization.

cytocytes. When ingested by a mosquito, these gametocytes mature into gametes and the sexual reproductive phase of the life cycle begins. Gametes undergo fertilization to produce zygotes. These eventually become sporozoites, the parasitic form that collects in the insect's salivary gland, poised to infect the next host. On page 667 of this issue, Mair *et al.* (1) report the mechanism underlying the regulation of gene expression during the sexual cycle of this parasite.

genomic DNA—is very limited, and transcription-dependent mechanisms play a relatively minor role in modulating gene expression. By sequestering mRNAs into quiescent messenger ribonucleoprotein particles (mRNPs), translation of mRNAs into proteins is repressed. The release of translationally silent mRNAs from storage in mRNPs thus controls the timing and location of protein expression (2, 3).

Very little is known about the control of gene expression in *Plasmodium*, and the mechanisms underlying the activation of gamete maturation and fertilization have been complete mysteries. It has been known that two major

The author is at the Josephine Bay Paul Center, Woods Hole, MA 02543, USA. E-mail: shajduk@mbl.edu

repressed mRNAs. In addition, by microarray analysis, Mair *et al.* found that the expression of 370 other transcripts was also reduced in the DOZI-null mutant. Surprisingly, a large number of transcripts were also increased in abundance in the DOZI-null mutant. As the authors point out, these results suggest that the putative RNA helicase plays a critical role in maintaining steady-state levels of gametocyte-specific transcripts.

This work further substantiates the phenomenon of translational repression in *Plasmodium* and its importance in regulating sexual development of these parasites. Given the widespread occurrence of translational repression and its role in both temporal and spatial gene expression, this should perhaps not be so sur-

prising. The finding raises a number of provocative questions, however. How do translationally silent mRNPs undergo assembly-disassembly cycles? What triggers this process in the insect gut? When released from mRNPs, how do the once-silent mRNAs move from the cytoplasmic mRNPs to cytoplasmic polysomes for expression? The discovery that hundreds of mRNAs are influenced by the mutation of DOZI suggests that the putative helicase plays a pivotal role in control of sexual development in these important parasites. It may also be that closely related parasites, such as *Toxoplasma*, use a similar mechanism. The recent completion of several protozoan parasite genomes reveals a surprising lack of canonical transcription factors indicating that post-transcriptional

mechanisms, like translational repression, may play a disproportionate role in gene regulation in these important pathogens. It may also be that closely related parasites, such as *Toxoplasma*, *Pneumocystis*, *Cryptosporidium*, and *Babesia*, may use a similar mechanism for regulating expression of their genes.

References

1. G. R. Mair *et al.*, *Science* **313**, 667 (2006).
2. L. J. Colegrove-Otero, N. Minshall, N. Standart, *Crit. Rev. Biochem. Mol. Biol.* **40**, 21 (2005).
3. E. R. Gavis, R. L. Lehmann, *Nature* **369**, 315 (1994).
4. M. G. Paton *et al.*, *Molec. Biochem. Parasitol.* **59**, 263 (1993).
5. E. G. Abraham *et al.*, *J. Biol. Chem.* **279**, 5573 (2004).
6. S. M. Khan *et al.*, *Cell* **121**, 675 (2005).

10.1126/science.1131299

IMMUNOLOGY

Sugar Determines Antibody Activity

Dennis R. Burton and Raymond A. Dwek

Antibodies come in many flavors to confront the bewildering array of pathogens to be encountered in one's lifetime. At the structural level, this is achieved by an extensive variability in the sites that interact with foreign pathogen-associated molecules (antigens) that typically elicit an immune response. The remainder of the antibody molecule is much more conserved, as befits its primary role in binding to a limited set of effector molecules that control inflammatory responses and trigger antigen elimination. Differences in the amino acid sequences of conserved parts of the antibody molecule lead to different antibody classes [e.g., immunoglobulin G (IgG), IgA, IgM, etc.] and subclasses (e.g., IgG1 to IgG4 in humans) that bind different effector molecules. A new study by Kaneko *et al.* on page 670 of this issue (1) suggests that another type of difference between antibody molecules, determined by the sequences of attached oligosaccharides, may be crucial for antibody function. The

results may have far-reaching implications for understanding antibody responses and provide further support for a critical role for glycosylation in immunity.

The IgG molecule consists of two Fab arms, involved in antigen binding, that are connected via a flexible hinge region to an Fc region, which binds to effector molecules (see the figure). The Fc region has two tightly interacting or paired Ig domains and also, in contrast, two domains that are separated and do not interact but have two oligosaccharide chains interposed between them. These chains cover the hydrophobic faces that would normally lead to domain pairing. The oligosaccharides are heterogeneous—about 30 structures, or glycoforms, are known, with certain residues being conserved and others highly variable. Differences in the sequences of the oligosaccharide chains lead to differences in orientation of the chains on the protein surface, spacing between the unpaired domains, and exposure of key sugar residues. In the three IgG structures shown (see the figure), one lacks terminal galactose and sialic acid on two arms of a sugar chain and exposes *N*-acetylglucosamine, one lacks sialic acid but places one of the terminal galactoses in a “pocket” on the Fc protein and the other in the interstitial space between the two unpaired domains (this represents the predominant glycoform of IgG under normal conditions), and the third fully exposes terminal sialic acid residues.

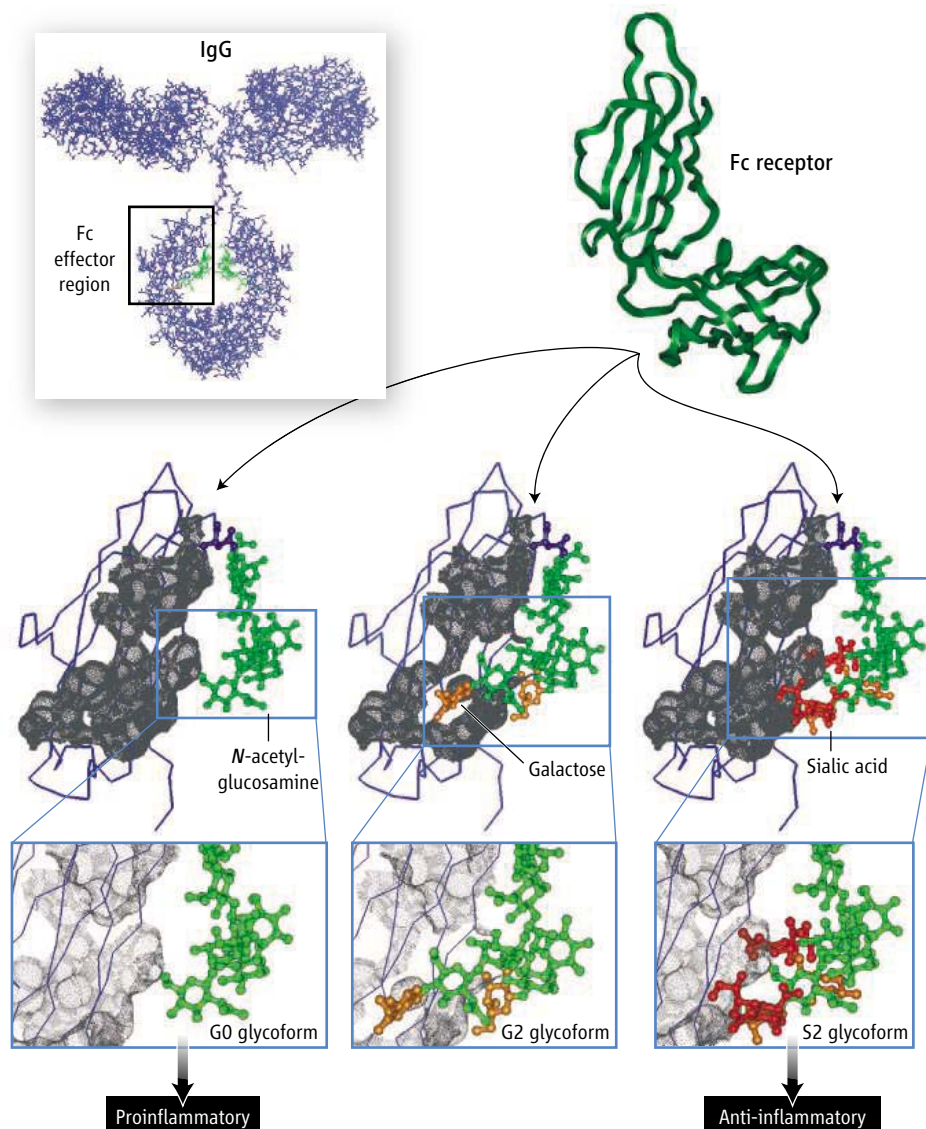
Understanding the functional consequences of the identity and sequence of the sugars attached to antibodies may be useful in designing therapies for a range of disorders.

The first indications that differences in glycosylation might affect antibody function came from studies associating rheumatoid arthritis with glycoform prevalence (2). The percentage of G0 glycoforms (no galactoses) is raised in rheumatoid arthritis, increases with disease progression, and returns to normal when patients go into remission. Pathology appears to result from interaction of exposed *N*-acetylglucosamine residues on the G0 glycoform with the manose-binding lectin, which subsequently activates a series of reactions (the complement cascade) in the blood with cellular destructive activities (3). Other studies have shown that the presence of fucose on Fc carbohydrate chains can influence binding of the IgG to Fc receptor molecules (4, 5). Fc receptor proteins are present on a variety of immune cells, and IgG binding can activate or inhibit inflammatory responses through respective Fc receptors (6). This control by sugar modification can be quite complex: A recent study (7) shows that human IgG-Fc receptor interactions depend upon sugar structures on both the Fc region of the IgG and on Fc receptors to permit discrimination of IgGs among Fc receptors.

Kaneko *et al.* focused on the role of Fc sialic acids in the interaction of IgG and Fc receptors and in inflammatory responses in a number of mouse models. By lectin affinity chromatography, they enriched for monoclonal IgGs (even monoclonal antibodies are heterogeneous with respect to sugars) bear-

Enhanced online at
www.sciencemag.org/cgi/content/full/313/5787/627

D. R. Burton is in the Departments of Immunology and Molecular Biology, Scripps Research Institute, 10550 North Torrey Pines Road, La Jolla, CA 92037, USA. E-mail: burton@scripps.edu R. A. Dwek is at the Glycobiology Institute, Department of Biochemistry, University of Oxford, South Parks Road, Oxford OX1 3QU, UK. E-mail: raymond.dwek@exeter.ox.ac.uk



Different glycoforms of IgG. Typical Fc receptors bind to all three glycoforms of IgG shown at a site near the top of the Fc stem of the IgG molecule. The G2 glycoform has terminal galactose residues and represents a major form in normal IgG. The S2 glycoform has two terminal sialic acid residues and (possibly together with the S1 glycoform that has one sialic acid) has a lower Fc receptor binding affinity. This glycoform has anti-inflammatory activities (1). Only the G0 glycoform binds to the mannose-binding lectin through terminal *N*-acetylglucosamine residues. This interaction triggers processes that activate inflammation. The gray color is the surface of the IgG that is in contact with the sugar moiety. Red, sialic acid; orange, galactose.

ing terminal sialic acids and showed that this fraction had lowered affinity for a number of Fc receptors. The net effect of increased sialylation was decreased ability of specific antibodies to clear platelets in a mouse model, although precisely how this is linked to Fc receptor affinity was unclear.

The authors hypothesized that sialylated IgG might be involved in the effects of a polyclonal human IgG preparation known as IVIG (intravenous Ig) that is widely used to treat inflammatory diseases such as immune-mediated thrombocytopenia. In support of this notion, enzymatic treatment of IVIG to remove sialic acids eliminated the protective

effect of the IgG in a mouse model of arthritis. The protective effect of sialylated IgG was associated with the induced expression of an inhibitory Fc receptor (8). If this finding can be extended to humans, then one could imagine the far more efficient use of anti-inflammatory IgG because current IVIG preparations contain but a small fraction of sialylated IgG. However, there is a lack of correspondence between mouse and human IgG subclasses and Fc receptors, and this demands that phenomena such as those described be carefully investigated in humans (9).

Finally, Kaneko *et al.* looked at sialylation changes in IgG after mouse immuniza-

tion with a test antigen. A lower sialic acid content of IgG after immunization was observed; those of IgM and a control protein were unaffected. The authors suggest that the sialylation change in IgG might be beneficial in switching from a steady anti-inflammatory state upon immunization.

Evidence mounts that the immune system discriminates between different antibody glycoforms. Mannose-binding lectin, linked to the complement cascade, recognizes terminal *N*-acetylglucosamine residues on IgG. Fc receptors, key molecules in mediating inflammation, sense the presence on IgG of both fucose and sialic acid residues. The sequences of IgG oligosaccharides are determined by the levels of glycosyltransferases or glycosidases in antibody-producing cells. A topic for further research is likely to be how and which external stimuli control the levels of these enzymes, and how this integrates with the overall control of immune responses. An intriguing possibility is that IgG-secreting immune cells may have receptors for factors such as inflammatory cytokines, which may modulate the cell's glycosylation machinery. With regard to antibodies for therapy, glycosylation can be controlled by cell engineering (10).

The molecular basis for Fc receptor discrimination of sialylated IgG glycoforms presents an intriguing problem because the sialic acid moieties are distant from Fc receptor binding sites on the Fc region of an IgG. Closer proximity of the critical unpaired Fc domains to each other as the oligosaccharide chains are shortened, which reduces binding to Fc receptors (11), may not be responsible here, as sialylated and desialylated Fc regions have relatively similar spacing between unpaired domains (12). Other problems relate to the molecular mechanism by which sialylated IgG induces inhibitory Fc receptors. The story of sugar in immunity is far from crystallized.

References

1. Y. Kaneko, F. Nimmerjahn, J. V. Ravetch, *Science* **313**, 670 (2006).
2. R. B. Parekh *et al.*, *Nature* **316**, 452 (1985).
3. R. Malhotra *et al.*, *Nat. Med.* **1**, 237 (1995).
4. R. L. Shields *et al.*, *J. Biol. Chem.* **277**, 26733 (2002).
5. R. Niwa *et al.*, *J. Immunol. Methods* **306**, 151 (2005).
6. F. Nimmerjahn, J. V. Ravetch, *Science* **310**, 1510 (2005).
7. C. Ferrara, F. Stuart, P. Sondermann, P. Brunker, P. Umama, *J. Biol. Chem.* **281**, 5032 (2006).
8. P. Bruhns, A. Samuelsson, J. W. Pollard, J. V. Ravetch, *Immunity* **18**, 573 (2003).
9. J. M. Woof, *Science* **310**, 1442 (2005).
10. L. G. Presta, *J. Allergy Clin. Immunol.* **116**, 731 (2005).
11. Y. Mimura *et al.*, *J. Biol. Chem.* **276**, 45539 (2001).
12. S. Krapp, Y. Mimura, R. Jefferis, R. Huber, P. Sondermann, *J. Mol. Biol.* **325**, 979 (2003).

The Primary Cilium as the Cell's Antenna: Signaling at a Sensory Organelle

Veena Singla and Jeremy F. Reiter*

Almost every vertebrate cell has a specialized cell surface projection called a primary cilium. Although these structures were first described more than a century ago, the full scope of their functions remains poorly understood. Here, we review emerging evidence that in addition to their well-established roles in sight, smell, and mechanosensation, primary cilia are key participants in intercellular signaling. This new appreciation of primary cilia as cellular antennae that sense a wide variety of signals could help explain why ciliary defects underlie such a wide range of human disorders, including retinal degeneration, polycystic kidney disease, Bardet-Biedl syndrome, and neural tube defects.

Eukaryotic cilia and flagella are cell surface projections familiar to school-children everywhere for the elegant swath they cut as they propel protozoa through pond water. Although assigned different names to reflect their different beating motions, cilia and flagella are structurally similar (the two names are used interchangeably here) and they show remarkable conservation from protozoa to humans.

Cilia can be viewed as specialized cellular compartments or organelles. All cilia are generated during interphase from a plasma membrane-associated foundation called the basal body (Fig. 1A). At the heart of the basal body is a centriole (Fig. 1B), an important component of the mitotic spindle apparatus in dividing cells. During interphase, however, the centriole moves to the plasma membrane and templates the nucleation of the axoneme, the structural core of the cilium. Construction of the axoneme requires intraflagellar transport (IFT), a bidirectional transport system discovered in the green alga *Chlamydomonas* [reviewed in (1)] (Fig. 1C). Because no protein synthesis occurs within cilia, IFT needed to move the organelle's structural components from the cell body to the ciliary tip (the anterograde direction) where axoneme synthesis occurs. This anterograde movement of the IFT complex is driven by the heterotrimeric motor Kinesin-2 (2) and, at least in the nematode *Caenorhabditis elegans*, by the kinesin OSM-3 (3). IFT returns proteins from the cilium to the cell body by means of a retrograde movement driven by a dynein motor (4). IFT also brings signaling proteins to the cilium. For example, adhesion of the flagella of

two *Chlamydomonas* gametes activates an IFT-dependent signaling pathway, resulting in cell fusion (5).

Structural elements contribute to the specialization of the ciliary environment. Among these elements are the terminal plate at the distal end of the basal body and the transitional fibers at the base of the cilium, which may physically restrict entrance of proteins into the cilium (6) (Fig. 1B). The most prominent structural element is the axoneme, consisting of nine doublet microtubules that originate at the triplet microtubules of the basal body centriole and extend the length of the cilium. Most motile cilia have an additional central microtubule pair (the 9+2 microtubule arrangement). Primary cilia are usually immotile, and they lack this central pair (the 9+0 arrangement). The motile primary cilia present on the node, a specialized signaling structure in the early mammalian embryo, are an exception (Fig. 1D). The twirling of these primary cilia creates a leftward flow of the surrounding fluid and this flow is essential for the development of the left-right axis (7).

The developmental and physiological roles of motile cilia have been reviewed elsewhere (8, 9). Here, we discuss the established and emerging functions of the single, immotile primary cilia that are present on almost all vertebrate cell types (10) (Fig. 1, D to L).

Cilia Are Sensory Organelles: Smell and Sight

The role of cilia in sensing the extracellular environment is best understood in the context of olfaction and photoreception. In the first step of olfaction, an odorant interacts with a G protein-coupled receptor (GPCR) (11) on the ciliary membrane of an olfactory sensory neuron (12), producing the second messenger cyclic adenosine monophosphate (cAMP) within the cilium (13). Elevated levels of cAMP then depolarize the cell by opening a cyclic nucleotide-gated channel also located in the ciliary membrane

(14). Other important regulators of olfactory signaling such as GPCR kinase 3 (GRK3), β -arrestin-2, Phosphodiesterase 1C, and Ca^{2+} /calmodulin-dependent kinase II are all present in cilia (15), suggesting that these organelles are sites of both odorant reception and signal amplification. Indeed, olfactory neurons lacking either cilia or odorant receptors on their cilia cannot respond to odorants (16, 17).

Photoreception occurs through a cilium-based signaling pathway broadly similar to that of olfaction. The rod and cone cells of the vertebrate retina possess a primary cilium equipped with an expanded tip called the outer segment, which is specialized for the reception and transduction of light. At the outer segment, opsin GPCRs respond to photons of light by increasing hydrolysis of a different cyclic nucleotide, cyclic guanosine monophosphate (cGMP), thereby closing cGMP-gated channels. Signal initiation and termination components such as the heterotrimeric G protein transducin and GRK1 (Rhodopsin Kinase) also localize to the outer segment (18, 19).

Maintenance of the photoreceptor signaling machinery requires continuous IFT-mediated transport of prodigious quantities of both lipids and proteins into the cilium. The retinal protein Opsin, for example, moves through the cilium at a rate of about 2000 molecules per minute (20). Mutations affecting IFT components or the anterograde Kinesin-2 motor cause the accumulation of Opsin and membranes outside of the cilium, which ultimately leads to cell death (21). Inherited defects in this transport system are one cause of human retinal degeneration. For example, mutations in Rhodopsin that disrupt its transport to the cilium cause retinitis pigmentosa, a common form of retinal degeneration (22).

The link between cilia function and the senses of sight and smell is underscored by Bardet-Biedl syndrome, a polygenic disorder associated with basal body and ciliary defects. Patients with Bardet-Biedl syndrome display retinal degeneration and cannot smell (23). Other characteristics of this multifaceted disorder include polydactyly, diabetes, obesity, hearing loss, and polycystic kidney disease, suggesting that primary cilia may play additional roles in human physiology (24, 25).

Cilia Link Mechanoreception and Polycystic Kidney Disease

In addition to sensing odorants and light, cilia can sense movement. These functions have been well characterized in model organisms. Cilia are the sites at which the vanilloid family of transient receptor potential (TRP) ion channels function as mechanosensors in the fruit fly *Drosophila* and the nematode *C. elegans*. In *Drosophila*, two TRP channels on the cilia of auditory sensory neurons mediate reception of sound vibrations at the antenna (26). Similarly, two *C. elegans* TRP channels localize to sen-

Program in Developmental and Stem Cell Biology, and Diabetes Center, University of California, San Francisco, CA 94143-0525, USA.

*To whom correspondence should be addressed. E-mail: jreiter@diabetes.ucsf.edu

sory neuron cilia, where they respond to nose touch and high osmolarity (27). Other cilia-associated TRP channels in sensory neurons play a different role in *C. elegans*: the mating behavior of males requires PKD-2, a member of the polycystin family of TRP channels, and its binding partner LOV-1 (28).

The vertebrate homologs of LOV-1 and PKD-2 are polycystin-1 (PC1) and polycystin-2 (PC2). Mutations in either of the polycystin genes cause PKD in humans (29). In PKD, loss of PC1 or PC2 function results in clonal expansion of kidney epithelial cells. These cells then form cysts that crowd out normal nephrons, causing kidney failure. PC1 and PC2 localize to primary cilia of kidney epithelial cells (30), suggesting that the functional link between these proteins and cilia is conserved from nematodes to mammals.

Insight into how these proteins participate in cyst formation has come from studies showing that PC1 and PC2 comprise a mechanosensory complex that translates deflection of the primary cilium of kidney epithelial cells into signals associated with the control of growth and differentiation. Also present in this complex are the transcription factor STAT6 and its coactivator P100, which are retained in the cilium by binding to the cytoplasmic tail of PC1 (31) (Fig. 2A). During normal kidney function, urine flows over kidney epithelial cells, bending their primary cilia. This bending results in a PC1- and PC2-dependent increase in intracellular Ca^{2+} concentration and the inhibition of the regulated intramembrane proteolysis (RIP) of PC1 (32–34) (Fig. 2A). Insults to the kidney that disrupt urine production or flow allow the cilium to straighten, blocking Ca^{2+} flux and activating the RIP of PC1. RIP releases a portion of the PC1 cytoplasmic tail, which translocates to the nucleus together with STAT6 and P100 where they activate transcription (Fig. 2B). These observations suggest that in PKD, defects in ciliary mechanosensation result in the cell activating this “no flow” response even in the presence of normal urine production, leading to unregulated cell proliferation and cyst formation. Consistent with this model, complete loss of primary cilia in the mouse kidney also produces cysts (35).

Primary Cilia Coordinate the Mammalian Hedgehog Signal-Transduction Machinery

A clue that vertebrate cilia may be involved not only in sensing environmental inputs but

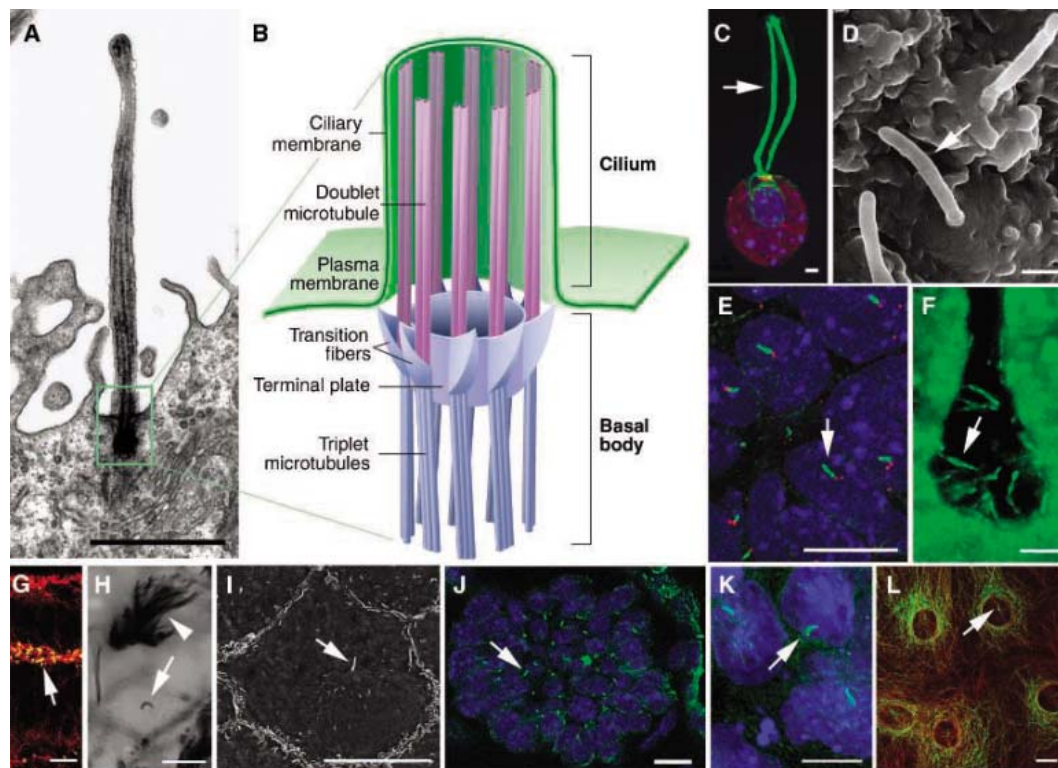


Fig. 1. Primary cilia are highly structured and are found in many organisms and on many cell types. (A) Electron micrograph of the primary cilium of a canary brain radial glia (69). (B) Schematic showing structure of the basal body and primary cilium [modified from (6, 70)]. (C) The green alga *Chlamydomonas* showing flagella (green, arrow) and basal body (red). Nuclei are blue. [(D) to (L)] Scanning electron and immunohistological images of primary cilia (arrows) of (D) the mouse node, (E) the mouse neural tube, emanating from basal bodies (red), (F) the *Xenopus* neural tube, (G) the zebrafish neural tube, (H) a mouse neurogenic astrocyte, (I) a mouse embryonic epidermal cell, (J) a mouse somite, (K) mouse embryonic stem cells, and (L) mouse astrocytes expressing glial fibrillary acidic protein (red). Also shown in (H) are motile ependymal cell cilia (arrowhead). Scale bars, 1 μ m [(A), (C), and (D)] and 10 μ m [(E) to (L)].

also in transducing intercellular signals came from the surprising finding that mutations in genes encoding IFT components cause defects in mammalian Hedgehog (Hh) signal transduction (36). Hh family members are secreted lipoproteins that regulate tissue patterning, cell proliferation, and many other biological processes [reviewed in (37)]. Defects in Hh signaling can cause human birth defects and cancer [reviewed in (38)].

Hh signaling culminates in the conversion of Gli transcription factors from repressors to activators. Central to this conversion are two transmembrane proteins, Smoothed (Smo) and the Hh receptor Patched (Ptc). In the absence of Hh signals, Ptc maintains Smo in an inactive state, and Gli transcription factors are processed to their repressor forms. Upon binding Hh, Ptc loses the ability to repress Smo, leading to the generation of Gli transcriptional activators that execute the Hh transcriptional program.

How do IFT proteins participate in mammalian Hh signal transduction? An answer is suggested by recent studies demonstrating that several Hh pathway components, including Smo and Gli proteins, are present at the primary cilium (39, 40) (Fig. 3A). Smo moves to the cilium in response to Hh signaling (Fig.

3B). Disrupting the transport of Smo to the cilium blocks Hh signal transduction, suggesting that Smo activates the downstream pathway at the primary cilium. Analysis of limb bud patterning in mouse IFT mutants indicates that IFT proteins are not only essential for Gli activator function but also for Gli repressor function (41), implying that both the “on” and “off” states of the mammalian Hh pathway depend on the presence of a primary cilium. Together, these data begin to suggest a dynamic model describing how primary cilia coordinate the mammalian Hh signaling machinery. Without Hh stimulation, Smo is present on intracellular vesicles and Gli proteins are processed to their repressor form at the ciliary tip (Fig. 3A). Hh signals alter Ptc regulation of Smo, allowing Smo to move to the cilium (Fig. 3B), where it interacts with the Gli processing machinery to promote Gli activator formation. Gli activators then move down the cilium, enter the nucleus, and turn on Hh-dependent genes.

Interestingly, the primary cilium is not critical to Hh signaling in all metazoans. Although Hh signal transduction in both mice and frogs is disrupted by loss of cilia, mutations in the *Drosophila* homologs of IFT genes do not

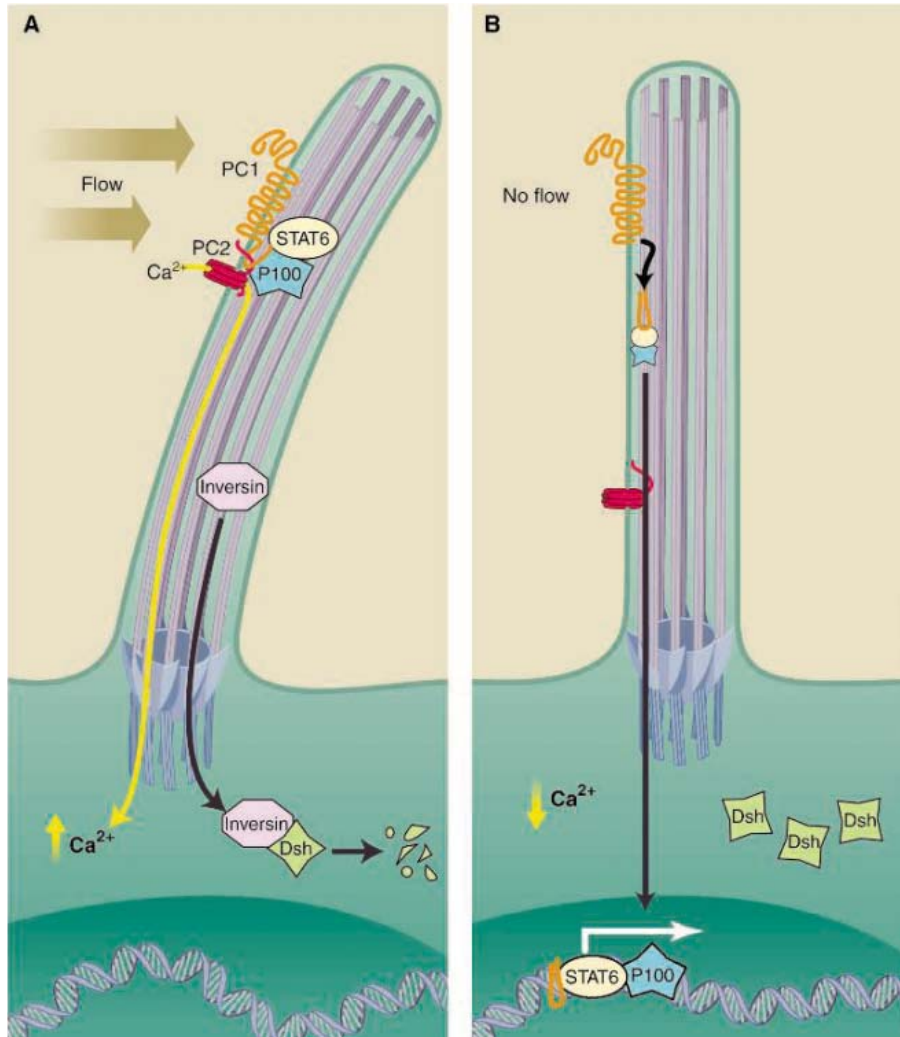


Fig. 2. Primary cilia of kidney epithelial cells sense urine flow and control cell proliferation. **(A)** Deflection of the primary cilium caused by flow within the nephron tubule is detected by PC1 (orange) and PC2 (red), two transmembrane proteins. Flow induces Ca^{2+} influx through PC2 and maintains STAT6 (yellow) and P100 (turquoise) in a complex bound to the tail of PC1. Flow also leads to up-regulation of Inversin (purple), which targets cytoplasmic Dsh (green) for degradation by the proteasome. **(B)** In the absence of flow, Ca^{2+} influx is reduced and the tail of PC1 is cleaved, allowing P100 and STAT6 to translocate to the nucleus and activate transcription. Lack of flow also reduces Inversin levels, stabilizing Dsh levels and permitting β -catenin to initiate transcription of canonical Wnt pathway target genes. The same pathways may be activated in the absence of PC1, PC2, or the cilium itself, leading to unregulated cell proliferation and formation of cysts.

disturb embryonic development (42, 43). The involvement of the microtubule binding protein Cos2 specifically in *Drosophila* Hh transduction suggests that the Hh signal transduction machinery may be coordinated by other microtubular structures.

Primary Cilia, Wnt Signaling, and Planar Cell Polarity

Like Hh, Wnt family members are secreted lipoproteins that regulate both cell proliferation and differentiation [reviewed in (44)]. However, unlike Hh, Wnt proteins activate several distinct signaling pathways, classified as either β -catenin dependent (the so-called canonical pathway) or β -catenin independent (the noncanonical path-

ways). The protein Dishevelled (Dsh) acts as a switch between the canonical and noncanonical pathways. Plasma membrane-localized Dsh is essential for noncanonical signaling, whereas a cytoplasmic pool of Dsh functions in canonical signaling (45).

Similar to loss of the cilium, constitutive activation of the canonical Wnt pathway in the mouse kidney causes cyst formation (46), raising the possibility that overactivity of this pathway contributes to human PKD. Recent investigations into the function of the primary cilium-associated protein Inversin support this hypothesis. Mutations in the gene encoding Inversin both disrupt mouse left-right axis formation and cause one form of human PKD, two processes

linked to cilia function (47, 48). Reduction of Inversin in embryos of the frog *Xenopus laevis* causes a third defect—disruption of convergent extension movements (49) (Fig. 4A). These coordinated cellular movements are essential for both vertebrate gastrulation and neural tube closure, and they are regulated by the planar cell polarity (PCP) pathway, one form of noncanonical Wnt signaling. PCP is the orientation of cells along an axis orthogonal to the apical-basal axis and is manifested in ways that, in addition to convergent extension, include *Drosophila* bristle orientation and stereocilia orientation in the vertebrate inner ear [reviewed in (50)]. Mice lacking Inversin develop misoriented hair pattern, a defect similar to that seen in mice lacking the PCP regulator Frizzled-6 and superficially similar to the wing bristle misorientation displayed by *Drosophila* PCP mutants (49, 51).

Biochemical analyses have shown that Inversin participates in the Dsh-mediated switch between the canonical and noncanonical Wnt pathways. Specifically, Inversin targets the cytoplasmic pool of Dsh for degradation, inhibiting the canonical pathway (49). Inversin does not degrade the plasma membrane-localized pool of Dsh and thus does not inhibit non-canonical signaling. Indeed, Inversin appears to actively promote PCP signaling during *Xenopus* convergent extension. Inversin displays some homology to the *Drosophila* PCP protein Diego, which protects Dsh from the PCP antagonist Prickle (52). Perhaps Inversin acts similarly, given that both Diego and Inversin can interact with Prickle, as well as another conserved PCP protein, Van Gogh (49, 53).

Studies of other known regulators of PCP and cilia further support a functional connection between the two. In addition to their roles in ciliary function, the products of two Bardet-Biedl genes, *Bbs4* and *Bbs6*, function in vertebrate PCP (24). Similarly, proteins with conserved roles in PCP can also be required for ciliogenesis; homologs of Fuzzy and Inturned, two proteins that participate in *Drosophila* PCP, are essential for *Xenopus* ciliogenesis (54).

This involvement of several proteins in both cilia and PCP raises the question of how the two are mechanically connected. One possibility is that these proteins act in a single process fundamental to both PCP and ciliogenesis, such as the orientation of microtubule growth, as suggested by Park *et al.* (54). Oriented microtubules form the heart of the cilium and are essential for the asymmetric localization of PCP determinants (55). In support of this possibility, *Bbs4* participates in the ordering of microtubules outside of the cilium (23, 56). Alternatively, the primary cilium could be directly involved in the execution of the PCP program. Interestingly, a mammalian Van Gogh protein localizes to the cilium and basal body, suggesting that some components of the PCP pathway may function at the primary cilium (24). This model predicts that any fundamental disruption

of cilia structure will disrupt PCP by interfering with the functions of ciliary proteins such as Van Gogh and Inversin. Consistent with a link between cilia and PCP is the observation that Meckel syndrome, a human disorder associated with neural tube defects, is caused by mutations in genes implicated in ciliary function (57, 58).

PCP defects may also contribute to the pathogenesis of PKD. Notably, during kidney tubule elongation, the mitotic apparatus of cells is precisely oriented to direct cell division parallel to the axis of the tubule (Fig. 4B). Decreased expression of the ciliary protein Pkhd1 results in both PKD and disoriented kidney cell mitosis (59) (Fig. 4C). Given that the non-canonical Wnt pathway performs similar roles in the orientation of mitosis in *Drosophila*, *C. elegans*, and zebrafish (60–62), it will be

interesting to assess whether Pkhd1 participates in the known PCP pathway or orients the mitotic spindle through a different mechanism.

Together with the finding that fluid flow modestly up-regulates Inversin and represses canonical Wnt pathway activity in ciliated kidney cells (49), these results suggest an attractive model of kidney cyst pathogenesis. Normally, flow sensation by the primary cilium acts through Inversin to repress the canonical Wnt pathway, preventing inappropriate cell proliferation. Either ciliary defects or loss of Inversin disinhibits the canonical pathway which, together with the PC1- and PC2-dependent defects in Ca^{2+} signaling and STAT6 activity, leads to unregulated cell proliferation. Ciliary defects or loss of Inversin may also disrupt PCP, resulting in the mis-orientation of mitoses. Thus, ciliary defects may

have two consequences—inappropriate cell proliferation and disorganization of tissue growth—which act in concert to generate cysts.

An Evolutionarily Conserved Role for Cilia in Signaling?

Although all metazoans appear to have primary cilia, two of the most widely studied model organisms, *Drosophila* and *C. elegans*, have cilia in only a small set of cells. Does this indicate that our last common ancestor used the cilium in a similarly limited fashion?

As noted above, many protozoa use flagella for propulsion, including the closest known

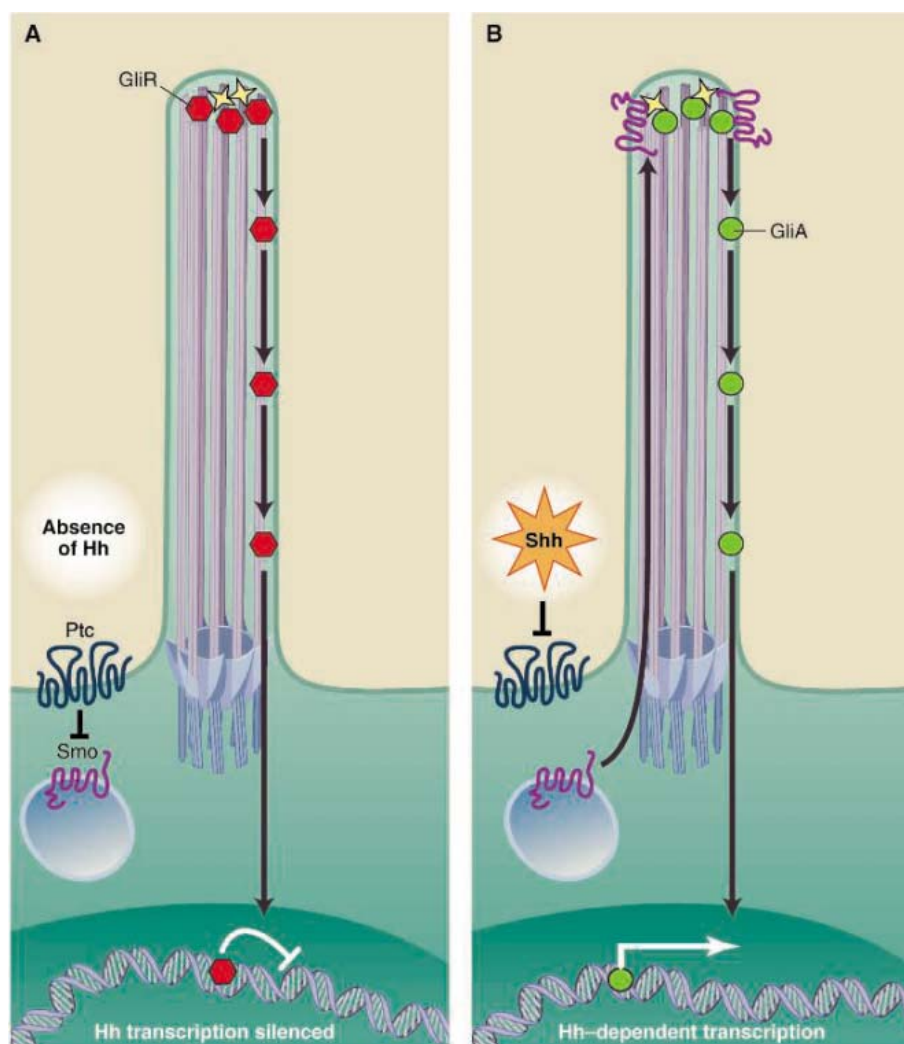


Fig. 3. A model of vertebrate Hh signal transduction. **(A)** In the absence of Hh, Ptc (blue) represses the function of Smo (purple), which is predominantly on intracellular vesicles. Gli proteins are processed at the cilium into their transcriptional repressor forms (red). These repressors move down the cilium to the nucleus and bind regulatory elements to maintain the silence of the Hh transcriptional program. **(B)** In the presence of Hh proteins such as Shh (orange), the inhibition of Smo by Ptc is blocked and Smo moves to the cilium. There, it presumably interacts with the Gli processing machinery (yellow) to promote formation of transcriptional activator forms (green). Gli activators then enter the nucleus where they activate Hh-dependent transcription.

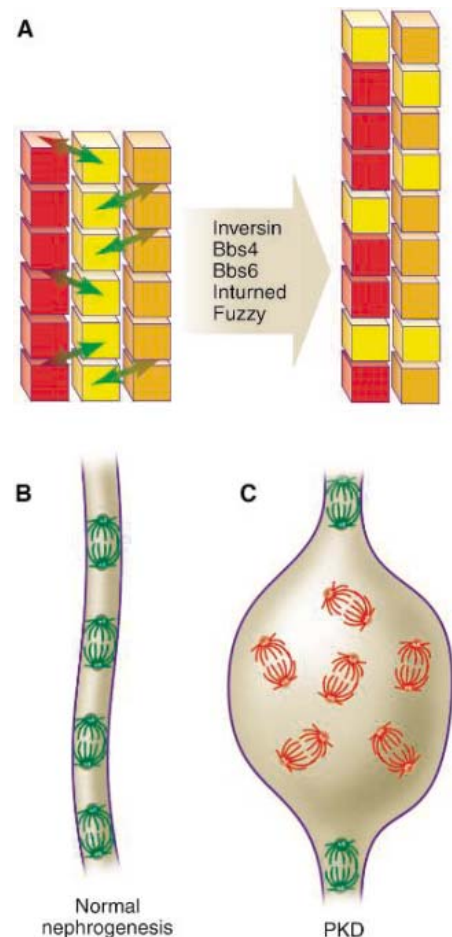


Fig. 4. Noncanonical Wnt signaling in vertebrates may be modulated by ciliary function. **(A)** One form of noncanonical Wnt signaling regulates convergent extension, the coordinated intercalation of cells (green arrows) that narrows and lengthens a tissue. Inversin, Bbs4, Bbs6, Inturned, and Fuzzy all participate in both cilia function and convergent extension, suggesting that the two are mechanistically related. **(B)** During normal kidney tubule growth, the mitotic spindle (green) is aligned with the axis of the nephron. In other systems, noncanonical Wnt signaling can control the orientation of mitosis. **(C)** In some forms of PKD, misorientation of the mitotic spindle (red) may act in concert with deregulated cell proliferation to trigger cyst formation.

relatives of animals, the choanoflagellates [reviewed in (63)]. Some protozoa also use cilia for signaling. For example, when *Paramecium tetraurelia* swims into an object, the force bends its motile cilia, opening mechanosensitive Ca²⁺ channels (64). The subsequent increase in intracellular Ca²⁺ concentration reverses ciliary beat direction and, consequently, swimming direction. This is reminiscent of kidney epithelial cells in which mechanical deformation of primary cilia opens mechanosensitive Ca²⁺ channels.

Other unicellular eukaryotes may use the cilium to sense their environment in additional ways. Proteins involved in *Chlamydomonas* light reception and interpretation are present on flagella (65, 66). Similar to *Chlamydomonas*, dinoflagellates also use flagella and an eyespot for phototaxis (67). Interestingly, several dinoflagellate species do not absorb light at the eyespot. Instead, the eyespot is adapted to focus and reflect light onto a flagellum, the presumptive photoreceptor location (68). This mechanism is similar to light reception by the human eye; a lens focuses light on cilia called rods and cones where the light is absorbed, translated into biochemical signals, and communicated to the cell body. This “ciliocentric” view suggests that the ancestral organelle for the detection and reception of light was a cilium and that cilia may have ancient and widespread roles in sensing information from the extracellular environment, whether that information takes the form of light, movement, or signals from other cells.

Conclusions

The primary cilium has several characteristics that make it an ideal cellular location for sensing and transducing signals. It extends into

the extracellular space, affording access to environmental signals. Its elongated geometry provides a high surface-to-volume ratio that may promote interaction of transmembrane receptors with downstream signaling machinery. Finally, the regulated entry of proteins into the cilium confers the advantages of specialization and compartmentalization. Evolution appears to have made use of these characteristics to adapt the cilium for the interpretation of information both from the environment and from other cells.

We have discussed established and emerging mechanisms by which cilia participate in several types of signal reception and transduction. Ciliary defects can cause diverse human diseases (Table 1), which may well reflect the involvement of cilia in diverse sensory modalities and signaling pathways. The unexplained phenotypic manifestations of these diseases raise the possibility that cilia have additional, unexplored roles in skeletal development, brain function, diabetes, and obesity.

References and Notes

- J. L. Rosenbaum, G. B. Witman, *Nat. Rev. Mol. Cell Biol.* **3**, 813 (2002).
- K. G. Kozminski, P. L. Beech, J. L. Rosenbaum, *J. Cell Biol.* **131**, 1517 (1995).
- J. J. Snow *et al.*, *Nat. Cell Biol.* **6**, 1109 (2004).
- G. J. Pazour, C. G. Wilkerson, G. B. Witman, *J. Cell Biol.* **141**, 979 (1998).
- J. Pan, W. J. Snell, *J. Cell Sci.* **116**, 2179 (2003).
- R. G. Anderson, *J. Cell Biol.* **54**, 246 (1972).
- S. Nonaka *et al.*, *Cell* **95**, 829 (1998).
- L. Eley, L. M. Yates, J. A. Goodship, *Curr. Opin. Genet. Dev.* **15**, 308 (2005).
- H. J. Yost, *Curr. Biol.* **13**, R808 (2003).
- Primary Cilium Resource Page, List of Cells (www.bowserlab.org/primarycilia/cilialist.html).
- L. Buck, R. Axel, *Cell* **65**, 175 (1991).
- J. Krieger *et al.*, *Eur. J. Biochem.* **219**, 829 (1994).
- I. Boekhoff, E. Tareilus, J. Strotmann, H. Breer, *EMBO J.* **9**, 2453 (1990).
- T. Nakamura, G. H. Gold, *Nature* **325**, 442 (1987).
- B. P. Menco, *J. Neurocytol.* **34**, 11 (2005).
- A. A. Bronshtein, A. V. Minor, *Tsitologiya* **19**, 33 (1977).
- R. Benton, S. Sachse, S. W. Michnick, L. B. Vosshall, *PLoS Biol.* **4**, e20 (2006).
- R. V. Elias, S. S. Sezate, W. Cao, J. F. McGinnis, *Mol. Vis.* **10**, 672 (2004).
- K. J. Strissel *et al.*, *J. Biol. Chem.* **280**, 29250 (2005).
- J. C. Besharse, C. J. Horst, in *Ciliary and Flagellar Membranes*, R. A. Bloodgood, Ed. (Plenum Press, New York, 1990), pp. 389–417.
- J. R. Marszalek *et al.*, *Cell* **102**, 175 (2000).
- T. Li, W. K. Snyder, J. E. Olsson, T. P. Dryja, *Proc. Natl. Acad. Sci. U.S.A.* **93**, 14176 (1996).
- H. M. Kulaga *et al.*, *Nat. Genet.* **36**, 994 (2004).
- A. J. Ross *et al.*, *Nat. Genet.* **37**, 1135 (2005).
- P. L. Beales, *Curr. Opin. Genet. Dev.* **15**, 315 (2005).
- Z. Gong *et al.*, *J. Neurosci.* **24**, 9059 (2004).
- D. Tobin *et al.*, *Neuron* **35**, 307 (2002).
- M. M. Barr *et al.*, *Curr. Biol.* **11**, 1341 (2001).
- M. Bisceglia, C. A. Galliani, C. Senger, C. Stallone, A. Sessa, *Adv. Anat. Pathol.* **13**, 26 (2006).
- S. M. Nauli *et al.*, *Nat. Genet.* **33**, 129 (2003).
- S. H. Low *et al.*, *Dev. Cell* **10**, 57 (2006).
- V. Chauvet *et al.*, *J. Clin. Invest.* **114**, 1433 (2004).
- H. A. Praetorius, K. R. Spring, *J. Membr. Biol.* **184**, 71 (2001).
- K. Hanaoka *et al.*, *Nature* **408**, 990 (2000).
- F. Lin *et al.*, *Proc. Natl. Acad. Sci. U.S.A.* **100**, 5286 (2003).
- D. Huangfu *et al.*, *Nature* **426**, 83 (2003).
- L. Lum, P. A. Beachy, *Science* **304**, 1755 (2004).
- M. Pasca di Magliano, M. Hebrok, *Nat. Rev. Cancer* **3**, 903 (2003).
- K. C. Corbit *et al.*, *Nature* **437**, 1018 (2005).
- C. J. Haycraft *et al.*, *PLoS Genet.* **1**, e53 (2005).
- A. Liu, B. Wang, L. A. Niswander, *Development* **132**, 3103 (2005).
- P. Chang, T. H. Giddings Jr., M. Winey, T. Stearns, *Nat. Cell Biol.* **5**, 71 (2003).
- R. Sarpal *et al.*, *Curr. Biol.* **13**, 1687 (2003).
- R. Nusse, *Development* **130**, 5297 (2003).
- J. D. Axelrod, J. R. Miller, J. M. Shulman, R. T. Moon, N. Perrimon, *Genes Dev.* **12**, 2610 (1998).
- S. Saadi-Kheddouci *et al.*, *Oncogene* **20**, 5972 (2001).
- E. A. Otto *et al.*, *Nat. Genet.* **34**, 413 (2003).
- D. Morgan *et al.*, *Nat. Genet.* **20**, 149 (1998).
- M. Simons *et al.*, *Nat. Genet.* **37**, 537 (2005).
- T. J. Klein, M. Mlodzik, *Annu. Rev. Cell Dev. Biol.* **21**, 155 (2005).
- N. Guo, C. Hawkins, J. Nathans, *Proc. Natl. Acad. Sci. U.S.A.* **101**, 9277 (2004).
- A. Jenny, J. Reynolds-Kenneally, G. Das, M. Burnett, M. Mlodzik, *Nat. Cell Biol.* **7**, 691 (2005).
- G. Das, A. Jenny, T. J. Klein, S. Eaton, M. Mlodzik, *Development* **131**, 4467 (2004).
- T. J. Park, S. L. Haigo, J. B. Wallingford, *Nat. Genet.* **38**, 303 (2006).
- Y. Shimada, S. Yonemura, H. Ohkura, D. Strutt, T. Uemura, *Dev. Cell* **10**, 209 (2006).
- J. C. Kim *et al.*, *Nat. Genet.* **36**, 462 (2004).
- U. M. Smith *et al.*, *Nat. Genet.* **38**, 191 (2006).
- M. Kyttila *et al.*, *Nat. Genet.* **38**, 155 (2006).
- E. Fischer *et al.*, *Nat. Genet.* **38**, 21 (2006).
- Y. Bellaiche, M. Gho, J. A. Kaltschmidt, A. H. Brand, F. Schweisguth, *Nat. Cell Biol.* **3**, 50 (2001).
- A. Schlesinger, C. A. Shelton, J. N. Maloof, M. Meneghini, B. Bowerman, *Genes Dev.* **13**, 2028 (1999).
- Y. Gong, C. Mo, S. E. Fraser, *Nature* **430**, 689 (2004).
- N. King, *Dev. Cell* **7**, 313 (2004).
- R. Eckert, Y. Naitoh, K. Friedman, *J. Exp. Biol.* **56**, 683 (1972).
- K. Huang, T. Kunkel, C. F. Beck, *Mol. Biol. Cell* **15**, 3605 (2004).
- C. Iomini, L. Li, W. Mo, S. K. Dutcher, G. Piperno, *Curr. Biol.* **16**, 1147 (2006).
- W. Hand, J. Schmidt, *Protozoology* **22**, 494 (1975).
- G. Kreimer, *Protist* **150**, 311 (1999).
- A. Alvarez-Buylla, J. M. Garcia-Verdugo, A. S. Mateo, H. Merchant-Larios, *J. Neurosci.* **18**, 1020 (1998).
- E. T. O'Toole, T. H. Giddings, J. R. McIntosh, S. K. Dutcher, *Mol. Biol. Cell* **14**, 2999 (2003).
- Q. Liu, J. Zuo, E. A. Pierce, *J. Neurosci.* **24**, 6427 (2004).
- We regret that space limitations precluded our acknowledgment of numerous other contributors to this topic. We thank R. Bloodgood, K. Corbit, and W. Marshall for helpful comments and A. Alvarez-Buylla, Y.-G. Han, J. Garcia-Verdugo, Z. Mirzadeh, J. Feldman, P. Scherz, D. Stainier, and J. Wallingford for providing images used in Fig. 1. Supported by NIH grant R21DK69423, the March of Dimes, NSF (V.S.), and the UCSF Fellows Program (J.F.R.).

10.1126/science.1124534

Fibrin Fibers Have Extraordinary Extensibility and Elasticity

W. Liu,^{1*} L. M. Jawerth,^{2*} E. A. Sparks,¹ M. R. Falvo,³ R. R. Hantgan,⁶
R. Superfine,⁴ S. T. Lord,^{5†} M. Guthold^{1†}

Blood clots stem the flow of blood, which is essentially a mechanical task. Hence, there has been a longstanding interest, initiated by Ferry *et al.* (1), in elucidating the mechanical properties of clots. The macroscopic properties are well known (2), and these can be related to clotting disorders. Nevertheless, the underlying microscopic mechanisms that give rise to these macroscopic properties are not understood (3). Clots form when soluble fibrinogen is converted to fibrin monomers that polymerize to form a branched network of fibrin fibers. The mechanical properties of any branched network depend on the network architecture and the mechanical properties of the individual fibers. The fibrin network architecture has been well-characterized in microscopy images (2). In contrast, aside from the bending modulus for small strains (4) and the radius dependence of the rupture force in air (5), the mechanical behavior of single fibrin fibers is unknown. Yet, exactly this knowledge is needed to construct and test mechanical models of blood clots.

We have developed an atomic force–fluorescence microscopy technique to study the mechanical properties of single fibrin fibers (6) (fig. S1). The tip of the atomic force microscope (AFM) was used to stretch fibers that were suspended across 12 μm -wide channels; the fluorescence microscope was used to image this stretching process. We selected and analyzed fibers that bridged the grooves at an approximate right angle and that were well anchored on the ridges (i.e.,

strain was not due to fiber slipping). Thus, our experimental design yielded a well-defined geometry. We determined the extensibility and elastic limit of fibers formed in the presence and absence of factor XIIIa (FXIIIa) (6). FXIIIa induces covalent cross-links between the γ chains [along the fiber axis (7)] and between the α chains. In this study, γ - γ cross-linking was 50 to 75% complete, and α - α cross-linking was 25 to 35% complete. Samples without FXIIIa showed no cross-linking.

All fibers showed extremely large extensibilities and recovered elastically from very large strains [definitions in (6)]. Figure 1, A to D (movie S1), depicts the rupture of a fiber. The fiber did not break at the AFM tip, indicating that the fiber ruptured due to stretching between the tip and the anchoring point. Uncross-linked fibers extended $226 \pm 52\%$ (36 fibers), and cross-linked fibers extended $332 \pm 71\%$, or 4.32 times their original length (29 fibers). The most extreme fibers could be extended over six times their length [over 500% strain (movie S3)]. These extensibilities are the largest of any protein fiber (table S1). After rupture, the fiber arms contract to nearly their original length, indicating mainly elastic deformations.

We tested the elastic limit by stretching fibers to a certain strain and releasing the applied force (Fig. 1, E to K, and movie S2). Uncross-linked fibers could be stretched 2.2 times their length (120%) and recover elastically. Remarkably, cross-linked fibers could be stretched over 2.8

times their length (180% strain) and still recover without permanent damage (movies S4 and S5).

Fibrin fibers displayed extreme and different mechanical properties relative to other protein polymers (table S1). Highly regular, nearly crystalline fibers, such as actin filaments and microtubules, show small extensibilities. Despite the nearly crystalline arrangement of fibrin monomers along the fiber axis, fibrin fibers show extraordinarily large extensibilities. This apparent conflict suggests the fibrin monomers can extend substantially and reversibly while maintaining the most important fibrin-fibrin interactions within a fiber.

Furthermore, the effect of cross-linking is unusual in fibrin. In collagen, spider silk, and keratin fibers, cross-linking makes fibers stiffer and less extensible. The increased extensibility and elasticity we observed for cross-linked fibrin indicates the cross-links are directional, along the fiber axis. Thus, in physiological conditions, the fast-forming γ - γ cross-links along the axis may enhance elasticity and prevent rupture of the nascent fibers.

Whereas fibers have over 330% extensibility, whole fibrin film networks have extensibilities of “only” 100 to 200% (1). Because a network has two mechanisms to extend, first aligning then stretching fibers, it is extraordinary that individual fibrin fibers have the larger extensibility. These data suggest clot rupture does not arise from the rupture of individual fibers, as previously assumed. Rather, the branch points yield first. Further analysis may nevertheless show that the remarkable extensibility and elasticity of individual fibers influence the mechanical behavior of clots formed *in vivo*.

References and Notes

1. J. D. Ferry, P. R. Morrison, *J. Am. Chem. Soc.* **69**, 388 (1947).
2. E. A. Ryan, L. F. Mockros, J. W. Weisel, L. Lorand, *Biophys. J.* **77**, 2813 (1999).
3. J. W. Weisel, *Biophys. Chem.* **112**, 267 (2004).
4. J. P. Collet, H. Shuman, R. E. Ledger, S. T. Lee, J. W. Weisel, *Proc. Natl. Acad. Sci. U.S.A.* **102**, 9133 (2005).
5. M. Guthold *et al.*, *Biophys. J.* **87**, 4226 (2004).
6. Materials and Methods are available on Science Online.
7. P. A. McKee, P. Mattock, R. L. Hill, *Proc. Natl. Acad. Sci. U.S.A.* **66**, 738 (1970).
8. We thank M. C. Stahle, J. L. Moen, O. V. Gorkun, and L. Carroll for advice and technical assistance. We acknowledge support from NIH grant nos. P41 EB002025 (R.S.), R01 HL31048 (S.T.L.), R41 CA10312 (M.G.); Research Corporation grant no. RI0826 (M.G.); and American Cancer Society grant no. IRG-93-035-6 (M.G.).

Supporting Online Material

www.sciencemag.org/cgi/content/full/313/5787/634/DC1

Materials and Methods

Fig. S1

Table S1

Movies S1 to S5

13 March 2006; accepted 30 May 2006

10.1126/science.1127317

¹Department of Physics, Wake Forest University, Winston-Salem, NC 27109, USA. ²Department of Physics, Harvard University, Cambridge, MA 02138, USA. ³Curriculum in Applied and Materials Science, ⁴Department of Physics and Astronomy, ⁵Department of Pathology and Laboratory Medicine, University of North Carolina, Chapel Hill, NC 27599, USA. ⁶Department of Biochemistry, Wake Forest University School of Medicine, Winston-Salem, NC 27157, USA.

*These authors contributed equally to this work.

†To whom correspondence should be addressed. E-mail: gutholdm@wfu.edu (M.G.); stl@med.unc.edu (S.T.L.)

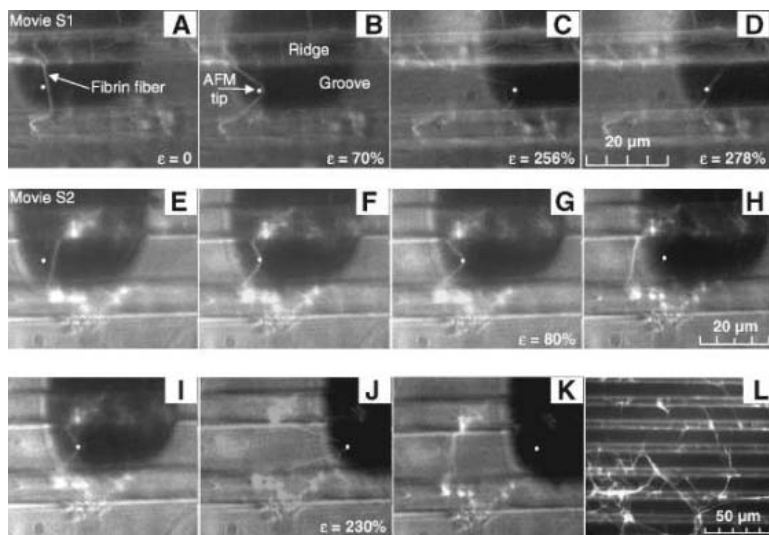


Fig. 1. (A to D) Extensibility. A fiber suspended between two ridges (brighter horizontal bands) is stretched with the AFM tip (white dot) until rupture. The AFM cantilever appears as a dark, 35- μm -wide rectangle. The lower and upper segments of the fiber break at 183% strain and 278% strain, respectively. (E to H) Elastic deformation. A fiber was strained 80%, from which it snapped back to its original length. (I to K) Permanent deformation. The same fiber was strained to 230% (I), suffering some permanent lengthening (K). (L) Representative clot used for fiber manipulations.

Spitzer Spectral Observations of the Deep Impact Ejecta

C. M. Lisse,^{1,2*} J. VanCleve,³ A. C. Adams,³ M. F. A'Hearn,² Y. R. Fernández,⁴ T. L. Farnham,² L. Armus,⁵ C. J. Grillmair,⁵ J. Ingalls,⁵ M. J. S. Belton,⁶ O. Groussin,² L. A. McFadden,² K. J. Meech,⁷ P. H. Schultz,⁸ B. C. Clark,⁹ L. M. Feaga,² J. M. Sunshine²

Spitzer Space Telescope imaging spectrometer observations of comet 9P/Tempel 1 during the Deep Impact encounter returned detailed, highly structured, 5- to 35-micrometer spectra of the ejecta. Emission signatures due to amorphous and crystalline silicates, amorphous carbon, carbonates, phyllosilicates, polycyclic aromatic hydrocarbons, water gas and ice, and sulfides were found. Good agreement is seen between the ejecta spectra and the material emitted from comet C/1995 O1 (Hale-Bopp) and the circumstellar material around the young stellar object HD100546. The atomic abundance of the observed material is consistent with solar and C1 chondritic abundances, and the dust-to-gas ratio was determined to be greater than or equal to 1.3. The presence of the observed mix of materials requires efficient methods of annealing amorphous silicates and mixing of high- and low-temperature phases over large distances in the early protosolar nebula.

Before 2005, the best understanding we had of a comet's nucleus was obtained by studying the material emitted from the surface into the surrounding gravitationally unbound atmosphere (the coma). This understanding of the solar system's most primitive bodies, however, assumed that the information obtained from the coma could be extrapolated back to the surface and subsurface regions of the nucleus. There is now increasing evidence that comets evolve from their initial state, because of the effects of solar insolation, until their surfaces become devolatilized, hiding the pristine solar system material under a processed surface layer.

On 4 July 2005, NASA's Discovery mission Deep Impact (hereafter DI) sent a 364-kg impactor into the nucleus of comet 9P/Tempel 1 (hereafter Tempel 1) at 10.2 km s⁻¹. The impactor burrowed below the processed surface layers of the nucleus, releasing copious amounts of subsurface material in a prominent ejecta cone (1). The vast majority of the ~10⁶ kg of material released in the impact [see the supporting online material (SOM)] was removed from the comet in an extremely gentle fashion, at low overpressures (<1 kPa) (2, 3) and temperatures,

thereby preserving the mineralogical nature of the component material at the micrometer-scale level, although deaggregation of large (>100 μm) fractal particles clearly occurred.

Here we describe Spitzer Space Telescope (SST) (4) infrared measurements of the solid materials excavated from the comet at the impact site. We used the highly sensitive Infrared Spectrograph (IRS) low-resolution ($R \sim 100$) modules of the SST (5, 6), obtaining four 60-s spectra over 5.2 to 14.5 μm and eight 30-s spectra over 14.0 to 38.0 μm at each pointing during the period from 2 to 5 July 2005. Basic data processing was performed using the IRS pipeline at the Spitzer Science Center (version S11.5). One-dimensional sky-subtracted spectra were extracted from these products, as described in (7). IRS peak-up (PU) images, used to center the comet in the 10"-wide spectrometer slit, were also used to obtain imaging photometry of the comet in a passband from 13 to 18.5 μm. At each pointing (Table 1),

we obtained two 16-μm PU images before obtaining spectra, allowing us to monitor the development of the impact ejecta (7).

Imaging observations. Pre-impact mid-infrared (IR) (16-μm) comet images obtained with the SST IRS peakup camera showed a normally active comet streaming dust from its nucleus into interplanetary space (Fig. 1, first panel). The dust seemed typical as compared to that seen in previous apparitions (8). About the size of fine sand (particles with an effective radius of 10 to 100 μm), it initially flows into space in all directions but then gets pushed back by the pressure of the Sun's light into the comet's tail.

After impact [05:52 universal time (UT), 4 July 2005], things changed dramatically (Fig. 1, right four panels). A stream of material was seen to flow outward from the nucleus toward the SW, in the downrange direction of the impact. A concomitant change was also seen in the SST PU light curves. In a 10" × 10" aperture, the 16-μm brightness of the comet's continuum shows a sharp, doubly inflected rise to a total excess of 25%. Similarly, a 5- to 35-μm spectrum of the comet taken 45 min after impact shows a flux density of about 5 janskys (Jy), 25% higher than the pre-impact coma signal of about 4 Jy. At the same time, the DI spacecraft observed a huge fog of fine particles with high optical depth and an abundance of dust so large that it completely obscured the impact site (1). The ejecta spectral signatures were detected from the time of impact through at least 41 hours afterward, but by 121 hours after impact, all spectral signatures above the pre-impact levels were absent.

Spectral observations. Using 5- to 35-μm time-resolved IRS spectra, we searched for the signature of fresh new subsurface dust in the 8- to 13-μm and 18-μm silicate emission bands, and their change as a function of time from pre-impact quiescence, through crater excavation, to post-impact active emission. From Infrared Astronomy Satellite (IRAS) observations of Tempel 1

Table 1. SST observations at 1 – 2 days to 1 + 2 days, with 5- to 35-μm spectroscopy and 2" imaging at 16 μm. All observations are four-slit IRS low-resolution + PU imaging except for pointing no. 3, which is in the special high-time-resolution Instrument Engineering Request (IER) mode. Schedule calculations assume a heliocentric distance = 1.51 AU; an SST-to-comet distance = 0.75 AU; a 41-hour nucleus rotation period; an encounter time of 4 July 2005 06:00 UT; and a start time of observation –0.6 hours before the midpoint of observation, except for pointing no. 4, which is the long-duration (4.7 hours) IRS four-order observation with continual cycling between orders.

Pointing no.	Time since impact of pointing/length of pointing	No. of nucleus rotations since impact	Observation start time	Ground-based contemporaneous imaging site
1	–41.00 hours/1.18 hours	–1.00	2 July 12:23	–
2	–22.55 hours/1.18 hours	–0.55	3 July 06:50	Hawaii
3	–0.08 hour/0.55 hour	0.00	4 July 05:47	Hawaii
4	0.50 hour/4.7 hours (four complete spectra)	0.012	4 July 06:20	Hawaii
5	10.25 hours/1.18 hours	0.25	4 July 15:39	–
6	20.50 hours/1.18 hours	0.50	5 July 01:54	Chile
7	41.82 hours/1.18 hours	1.02	5 July 23:13	Chile

¹Planetary Exploration Group, Space Department, Johns Hopkins University Applied Physics Laboratory, 11100 Johns Hopkins Road, Laurel, MD 20723, USA. ²Department of Astronomy, University of Maryland, CSS 2341, College Park, MD 20742, USA. ³Ball Aerospace and Technologies Corporation, 1600 Commerce Street, Boulder, CO 80306, USA. ⁴Department of Physics, University of Central Florida, Post Office Box 162385, Orlando, FL 32816–2385, USA. ⁵Spitzer Space Science Center, California Institute of Technology, Pasadena, CA 91125, USA. ⁶Belton Space Exploration Initiatives, 430 Randolph Way, Tucson, AZ, 85716, USA. ⁷Institute for Astronomy, University of Hawaii, 2680 Woodlawn Drive, Honolulu, HI 96822, USA. ⁸Department of Geological Sciences, Brown University, Providence, RI 02912–1846, USA. ⁹Space Exploration Systems, Lockheed Martin, Denver, CO 80201, USA.

*To whom correspondence should be addressed.

in 1983 (8), we expected a relatively featureless continuum before impact, with little silicate emission feature strength or deviation from local thermal equilibrium (LTE) blackbody behavior. This is because of the predominance of large dust particles in the natural coma emission, typical of other low-activity short-period comets. The SST pre-impact spectra revealed this near-LTE behavior with a color temperature of ~ 235 K (Fig. 2).

The immediate post-impact spectra showed a remarkable change in the outflowing material, with at least 16 strong spectral features, varying in strength from 20 to 140% of the ambient signal. The features directly correlate with those seen in the Infrared Space Observatory (ISO) spectrum of the extraordinarily active comet C/1995 O1 (Hale-Bopp) (Fig. 2) (9, 10) and those found in the spectrum of the very young stellar object (YSO) HD100546 (11).

Modeling and interpretation of the spectra.

The spectra for the first 10 hours showed near-identical structure. Thus we focus here on the observations made during the first four pointings: the three taken before impact and the one taken at impact (I) + 30 to I + 60 min after impact. After isolating the ejecta emission from the normal coma and nucleus emission by subtracting the pre-impact spectrum, and removing the instrument artifacts and gross temperature effects by dividing the result by the pre-impact spectrum scaled to the best-fit ejecta continuum temperature (SOM), we found the emissivity spectrum of Fig. 3. Some strong characteristic emission features stand out immediately: carbonates at 6.5 to 7.2 μm , pyroxenes at 8 to 10 μm , olivines at 11 μm , and sulfides at 27 to 29 μm .

Next, the observed emissivity spectrum was compared to a linear combination of emission spectra of over 80 candidate mineral species, selected for their reported presence in YSOs, solar system bodies, dusty disk systems, and interplanetary dust particles (IDPs). When doing this comparison, the detailed properties of the ejected dust—the particle composition, size distribution, temperature, and porosity—all had to be addressed, because they can strongly affect the observed infrared flux. An accurate, thorough treatment without arbitrary simplifying assumptions is critical to the accuracy of our findings, and we describe our methodology at length in the SOM.

What is presented here are the results from a minimalistic model of the majority ejecta species, built from the fewest and simplest components possible. We do not claim to have found the exact mineral species with our technique; rather, we claim to have found the important mineral classes present in the ejecta and their gross atomic abundance ratios. A set of components was tested exhaustively before the addition of a new species was allowed, and only species that dropped the reduced chi-squared value χ^2_{ν} below the 95% confidence limit (CL) were kept. Current compositional models of cometary dust [such as the five-component model of Malfait *et al.* (11) and the three-component mixture of Harker *et al.* (12)] were tested, and none of them resulted in an acceptable fit at the 95% confidence level—more components were required. It is important to emphasize that although the number of parameters [composition, temperature, and particle size distribution (PSD)] may seem large, there were actually very few detected species for the 334 independent spectral points and 16 strong

features obtained at high signal-to-noise ratio by the SST/IRS over the 5- to 35- μm range. It was, in fact, extremely difficult to fit the observed spectrum within the 95% CL of $\chi^2_{\nu} = 1.13$.

The best-fit model reveals a spectrum dominated by compositional signatures in different wavelength regimes: water ice and gas, carbonates, and polycyclic aromatic hydrocarbons (PAHs) at 5 to 8 μm ; silicates at 8 to 11 μm ; carbonates, silicates, and PAHs at 11 to 20 μm ; silicates and phyllosilicates at 20 to 35 μm ; and sulfides at 27 to 29 μm (Fig. 3). The derived compositional abundances from our best-fit dust model with $\chi^2_{\nu} = 1.05$ are given in Table 2 (13). For the best-fit model, the relative atomic abundance we found in the ejected dust is H:C:O:Si:Mg:Fe:S:Ca:Al = 15:0.53:11:1.0:0.88:0.74:0.28:0.054: ≤ 0.085 (for Si = 1.0). The Si:Mg:Fe:Ca:Al ratios are consistent with solar system abundances determined from the Sun and from C1 chondrites, giving us confidence in our solution (14, 15).

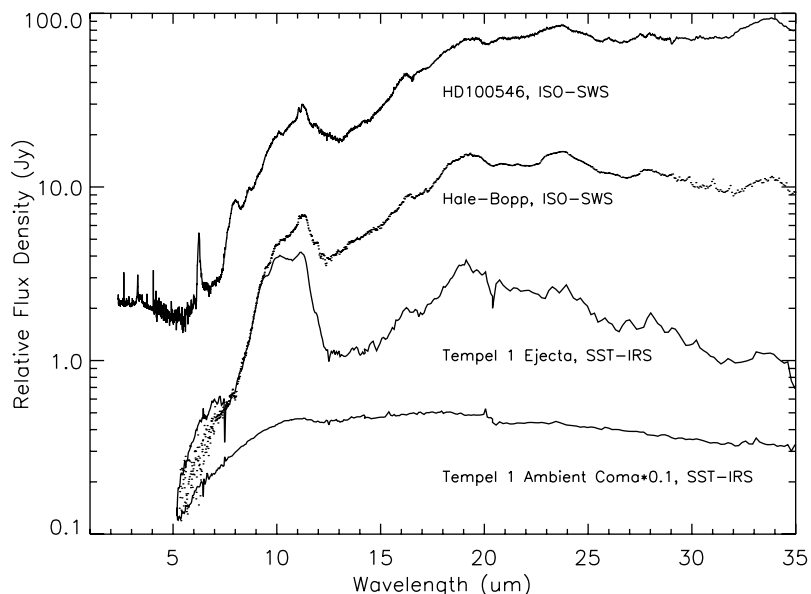


Fig. 2. SST 5- to 35- μm spectra of Tempel 1. From bottom to top, the traces are as follows: (i) spectrum of the ambient coma, taken 23 hours before impact; (ii) spectrum of the ejecta at I + 0.75 hours after impact; (iii) ISO spectrum of C/Hale-Bopp [after (9)]; (iv) ISO spectrum of YSO HD100546 [after (12)]. Note the logarithmic scale.

Fig. 1. IRS PU 16- μm imagery of the DI encounter. The first panel shows a total flux image of the comet, taken at I - 23 hours. There is appreciable signal throughout the field of view. The right four panels show the ratio of total flux image to the image at I - 23 hours. The green box shows the effective size of the IRS spectrometer entrance slit.



Compositional results. Here we discuss the 12 mineral species (plus PAHs and water ice and gas) found by our modeling, with emphasis on the plausibility of each detection and the constraints they place on the nature of the protosolar nebula (PSN).

Olivines. The dominant olivine species is Mg-rich forsterite, consistent with the results of numerous previous comet studies (16). New in our spectrum is a detection of fayalite, or Fe-rich olivine, in the ejecta. Some Fe is expected in the crystalline olivine component, as it is found in the amorphous olivine, but Nuth and Johnson (17) argue, however, that Fe may be preferentially in the amorphous silicates because the annealing of the amorphous Fe-rich olivine into crystalline fayalite requires high temperature (~1400 K). Forsterite, on the other hand, requires annealing only at ~1100 K. Our results indicate that the crystalline forsterite:fayalite abundance ratio is 3.9 by mole fraction and that there is about half as much crystalline fayalite as total amorphous olivines. This suggests that the effective annealing temperature for the olivines incorporated into the comet was between 1100 and 1400 K and that the crystallization process was relatively efficient, because about 72% of the olivines are crystalline.

Pyroxenes. Tempel 1 was sufficiently bright after impact for the SST to detect the crystalline pyroxenes in the ejecta, and we found a pyroxene:olivine abundance ratio of about unity. In our spectrum, we found the majority of pyroxene as Fe-rich ferrosilite, with minority fractions of orthoenstatite and diopside. This suggests that much of the Fe that was not incorporated into Mg-rich olivines wound up instead in Fe-rich pyroxenes and sulfides. The mechanism for crystallizing the pyroxenes was almost complete: >90% of the pyroxenes were in crystalline form, which is consistent with the lower (versus olivines) pyrox-

ene annealing temperatures of 800 to 900 K. The presence of pyroxenes, both amorphous and crystalline, in comets was recently confirmed in comet Hale-Bopp (16).

Phyllosilicates. We found that ~8% of all silicates (by surface area) occurred in the form of phyllosilicates; the best match in our spectrum is the Fe-rich Na-bearing nontronite, a smectite-group mineral formed as an aqueous alteration product of basic rock. We did not find good fits with Mg-rich saponite or serpentine. The existence of hydrated silicates in comets is provocative, because it would suggest the presence of abundant amounts of reactive water in the formation region of the comet or in the cometary parent body. On the other hand, Brownlee (18) noted that there is a minority component of phyllosilicates in IDPs of likely cometary origin.

Smectite has a band near 2.35 μm , but no such feature has yet been reported in the DI spacecraft data. It was suggested as the cause of a near-IR feature seen in a spectrum of comet 124P/Mrkos (19). An absorption feature at that wavelength was also seen in a DS-1 spectrum of comet 19P/Borrelly's surface (20). The only major reservoir of Na in the observed dust was the nontronite; it would be relatively labile upon dehydration and ultraviolet (UV) processing of the phyllosilicate, which is consistent with an extended dust source for the Na tails of comets (21).

Carbonates. In our SST spectrum (Figs. 2 and 3), there is a strong, broad, and persistent feature at 6.5 to 7.2 μm , arguing for a solid-state source. Carbonate species have a characteristic emission feature at these wavelengths. The carbonates magnesite (Mg-rich) and siderite (Fe-rich) fit the spectrum best; Ca-rich calcite and aragonite do not match the spectrum well. We also find the predicted secondary features at 11 to 12 μm and 13 to 14 μm in the data after removal of the silicate features (Fig. 4). The

amount of carbonates is about 5% of the total surface area of dust detected. The presence of carbonates is provocative because, like the phyllosilicates, liquid water was thought to be required to form carbonates from CO_2 in the presence of silicates. However, recent work by Toppani *et al.* (22) suggests that carbonates can be grown from the vapor phase in the presence of silicates, water, and carbon dioxide vapor.

Studies demonstrating the presence of carbonates in IDPs (23) suggest that our identification of cometary carbonates is plausible. Furthermore, Bradley (24) and Flynn *et al.* (25) have stated that in an analysis of their IDP sample libraries, carbonates and the 6.8- μm spectral feature are seen at the few-percent level in the anhydrous (cometary) IDPs. Reports of a (C, O, Mg) class of particles detected by the Giotto Particle Impact Analyzer (PIA) dust spectrometer during the 1P/Halley flyby in 1987 (26, 27) were interpreted as probably due to magnesite. Bregman *et al.* (28) observed comet 1P/Halley in 1987 with the Kuiper Airborne Observatory, detecting a transient 6.8- μm feature in one of the three resulting spectra.

PAHs. Using the PAH emission models of Li and Draine (29) for a mix of PAHs with average radius = 3 \AA ($\text{C}_{14}\text{H}_{10}$) and standard deviation 1 \AA , the spectral signature of PAHs at 6.2, 7.7, 8.6, and 11 μm was found in the I + 45 min spectra at the level of a few percent by total surface area [10^4 parts per million (ppm)] (Fig. 4). The emission line at 12.3 μm is much more subtle, because it is small compared to the strong silicate emission features at 8 to 12 μm . Confirmation of the PAH detection was provided by the hot PAH lines seen at 5.2, 5.8, 6.2, 7.7, and 8.2 μm in our high-time-resolution, transient SST spectra taken using an experimental mode (IER) of the IRS instrument during the first half hour after the impact.

Table 2. Composition of the best-fit model to the I + 45 min SST T1-DI ejecta spectrum. MW, molecular weight; N , number; T_{max} , maximum temperature.

Species	Weighted surface area	Density (g cm ⁻³)	MW	N_{moles}^* (relative)	Model T_{max} (°K)	Model χ^2_{v} if not included
Amorphous olivine (MgFeSiO ₄)	0.17	3.6	172	0.35	340	5.92
Forsterite (Mg ₂ SiO ₄)	0.31	3.2	140	0.70	340	4.28
Fayalite (Fe ₂ SiO ₄)	0.086	4.3	204	0.18	340	1.40
Amorphous pyroxene (MgFeSi ₂ O ₆)	0.041	3.5	232	0.06	340	1.38
Ferrosilite (Fe ₂ Si ₂ O ₆)	0.33	4.0	264	0.50	295	9.30
Diopside (CaMgSi ₂ O ₆)	0.115	3.3	216	0.18	340	1.86
Orthoenstatite (Mg ₂ Si ₂ O ₆)	0.10	3.2	200	0.16	340	1.70
Smectite nontronite (Na _{0.33} Fe ₂ (Si,Al) ₄ O ₁₀ (OH) ₂ * 3H ₂ O)	0.14	2.3	496	0.07	340	3.76
Magnesite (MgCO ₃)	0.030	3.1	84	0.11	340	1.30
Siderite (FeCO ₃)	0.051	3.9	116	0.17	340	1.83
Niningerite (Mg ₅₀ Fe ₅₀ S)	0.15	4.5	72	0.92	340	2.51
PAH (C ₁₀ H ₁₄), ionized	0.039	1.0	<178>	0.022	N/A	1.58
Water ice (H ₂ O)	0.049	1.0	18	0.27	220	1.40
Water gas (H ₂ O)	0.028	1.0	18	23.7†	220	1.22
Amorphous carbon (C)	0.068	2.5	12	1.45	390	13.3

* $N_{\text{moles}} \sim$ density/molecular weight \times surface area weighting; \pm 10% errors on the abundances (2 σ).

†Determined using a g factor of 2.2×10^{-4} , normalization of 5.8×10^5 kg of total water gas, and 7.8×10^5 kg of total dust mass in the beam.

PAHs have been suspected to be cometary constituents since their detection in the interstellar medium (ISM) and in YSOs (30–32). To date, no direct detection of PAHs in comets has been made; the strongest claim was produced by Bockelee-Morvan *et al.* (33), who examined the 3.2- to 3.6- μm emission in seven comets, and by removing the known species, found a small residual near the 3.28- μm aromatic C-H stretch wavelength. The amount of PAHs suggested by the residual, however, was quite small, on the order of 1 ppm versus water.

The emitting characteristics of PAH molecules, triggered by the stochastic absorption of one UV photon, allow them to emit in the mid-IR even when “normal” dust grains in LTE do not emit appreciable flux. The relative strengths of the different PAH features depend on the molecules’ size and charge state. Our best-fit model shows a clear preference for the ionized rather than neutral PAH signature, implying that the rate of PAH ionization is fast enough that the majority of PAHs are ionized within 45 min of exposure to sunlight at 1.5 astronomical units (AU).

Sulfides. It is clear that there are two emission peaks from 27 to 29 μm that are not due to silicates (Fig. 4). The Fe-S stretch feature is at $\sim 30 \mu\text{m}$, and the Mg-S stretch is at 25 to 40 μm ; however, these features are highly dependent on the crystal structure and Mg/Fe stoichiometry of the system (34–36). We can rule out crystalline troilite and pyrite as contributing significantly to the observed spectrum, as well as the more oxidized cognate sulfate species. On the other hand, the MgFeS ningerite fit could be improved, and nonstoichiometric pyrrothite or pentlandite, as suggested by the preliminary STARDUST results, have features at 24.5 μm , consistent with one of the apparent (but noisy) peaks in our residuals. We conclude that the actual sulfide phase in the ejecta has yet to be properly identified; a problem similar to that faced by Hony *et al.* (37) in studying iron sulfides formed and ejected from carbon stars.

The presence of metal sulfides in cometary dust is plausible; iron sulfides are found in abundance in IDPs (38). Sulfur is half as abundant as Fe or Mg in the solar system but appears depleted in cold dense molecular clouds with embedded young stellar objects, indicating that most of it probably resides in solid grains. Schulze and Kissel (39) found strong evidence for Fe-rich sulfides from the PIA in situ measurements at comet 1P/Halley.

Water ice. Water ice is present in low but detectable quantities (3% by surface area) in the SST spectra, as a broad feature at 10.5 to 15 μm . The spectral signature of water ice is attenuated and reddened as compared to those of the other ejecta solids, because the ice is at much lower temperatures than the rest of the dust. Thus, the water ice spectral signature is subtle and required detailed modeling to detect the shoulder longward of the strong 8- to 12- μm silicate emission peak.

Detection of water ice was expected, because water is the major volatile species in comets, and Sunshine *et al.* (40), using the DI High Resolution Instrument (HRI)-IR spectrometer, demonstrated the presence of significant amounts of water ice in the ejecta at I + 14 min. The presence of fragile, labile water ice in the ejecta confirms the relative absence of processing by the DI collision. The mean icy grain particle temperature found from our fits, 220 K, is somewhat above the expected pure ice grain temperature controlled by sublimation, which argues that we were observing dirty, crystalline water ice grains.

Water gas. Water gas does not suffer from the thermal damping effect, and the broad, relatively strong H₂O ν_2 out-of-plane molecular vibration is the source of the small but significant 6- μm emission feature seen in the SST data (41). The amount of water detected in the SST beam is $\sim 5.8 \times 10^5 \text{ kg}$, assuming a g factor for the ν_2 band of water at 6.27 μm of $2.2 \times 10^{-4} \text{ s}^{-1}$ (42). Compared with the minimum dust mass required by the Spitzer spectrum, $7.8 \times 10^5 \text{ kg}$ (table S1), this implies a dust/gas ratio of the ejecta of at least 1.3.

Amorphous carbon. The final constituent found in the comet consists of optically dark,

highly absorbing particles of amorphous carbon. Abundant amorphous solid carbon is found in IDPs and is a well-known species in comets, and the presence of abundant carbon grains in the ISM has been inferred from the 2200 \AA feature in the interstellar extinction law. It is this component, when fractionated into small individual pieces, that gives rise to the bulk of the “superheat,” or positive deviation from LTE, at short wavelengths (3 to 8 μm) in cometary dust spectra. These particles are very hot, efficiently absorbing sunlight while poorly reemitting long-wavelength thermal radiation.

The total amount of carbonaceous material (carbonates, amorphous carbon, and PAHs) detected in our I + 45 min spectra is 20% of the amount of silicates found. “Typical” comets studied in our survey have abundances of 33 to 50%, so Tempel 1 seems to be somewhat depleted in carbonaceous material as compared with the typical comet; A’Hearn *et al.* (43), in their survey of 85 comets, found Tempel 1 to be typical, but near the low end of typical, in terms of its C₂ abundance (8).

PSN implications and parent-body evolution. From our results, comet Tempel 1 appears to contain high-temperature crystalline silicates formed by annealing at temperatures

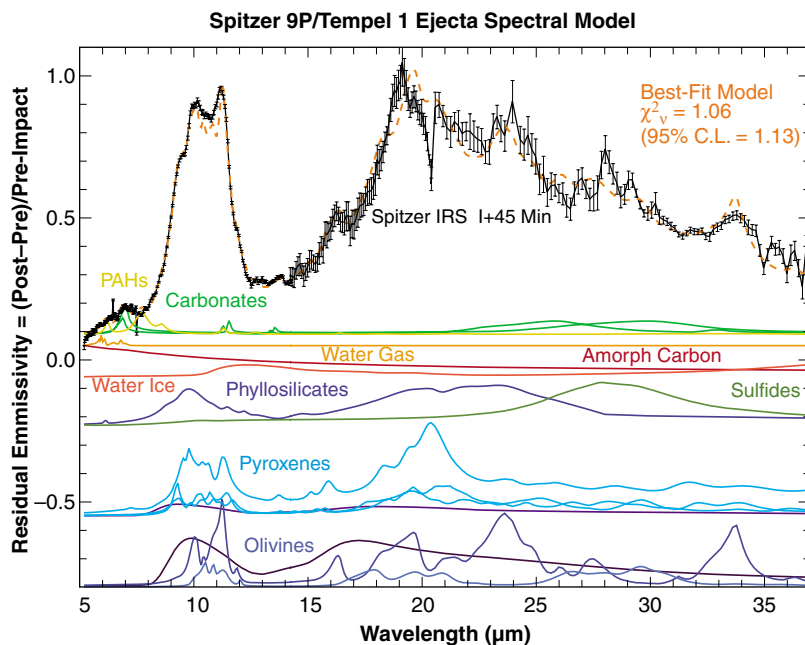


Fig. 3. Emissivity spectrum for the Tempel 1 ejecta, measured at I + 45 min. Silicates dominate the observed emission. The black line shows the SST ejecta spectrum, divided by the pre-impact spectrum normalized to a 235 K blackbody. Error bars are $\pm 2\sigma$. The orange dashed line shows the best-fit model spectrum. The colored curves show emission spectra for the constituent species, scaled by the ratio $B_{\lambda}[T_{\text{dust}}(a)_i]/B_{\lambda}(T_{\text{post-impact}})$, where the temperature T is for a particle of radius a and composition i , and $T_{\text{post-impact}} = 390 \text{ K}$ is found from the best fit of a blackbody B_{λ} to the post-impact continuum. The best-fit model individual species curves have been scaled by a factor of 2 versus the data for emphasis. Dark purples, amorphous silicates of pyroxene or olivine composition. Light blues, crystalline pyroxenes: ferrosilite, diopside, and orthoenstatite, in order of 20- μm amplitude. Dark blues, crystalline olivines: forsterite, and fayalite, in order of 20- μm amplitude. Red, amorphous carbon. Deep orange, water ice. Light orange, water gas. Yellow, PAHs. Bright greens, carbonates: siderite and magnesite, by order of 7- μm emissivity amplitude. Olive green, sulfides, represented here by ningerite.

>1000 K, combined with mid-temperature phyllosilicates and sulfides formed at temperatures ~600 K, plus water ice, which is stable up to ~200 K, and highly volatile gas species such as CO, CO₂, and CH₄, present as ices, which are stable only at temperatures less than 100 K. The presence of such diverse species in the interior of comet 9P/Tempel 1 has important implications for the state of the PSN at the time of the comet's formation, ~4.5 billion years ago, and its evolutionary history since its formation.

PSN mixing. There is now strong evidence (44) that there must be a mechanism for crystallizing silicates in the PSN, because they come from the ISM as amorphous material. If this was done by thermal heating of material near the young Sun (temperatures >1000 K were reached only inside the present orbit of Mercury), then there must also have been a method for efficiently transporting the silicates out to the formation region of the comet. Tempel 1, a Jupiter family comet, was originally formed in the trans-neptunian region of the PSN, at its outer edges. The same mechanism may have been responsible for taking carbonates and phyllosilicates, formed in the regions of the PSN with abundant water vapor (0.5 to 3.0 AU), out to the region of cometary formation. The implication of strong mixing—that the cometary bodies should be relatively similar in composition to the bulk PSN—is consistent with the near-solar atomic abundances found from the SST spectra. (Another annealing mechanism, shock waves due to the formation of the giant planet cores or the young Sun's turbulence, is

not consistent with the fluffy, porous, ISM-like aggregate dust found in the ejecta; it is more likely to create chondrule-like objects by total disruption of the local material, followed by recondensation. It is also not consistent with the high crystalline forsterite:fayalite ratio of 3.9:1 and the near 1:1 abundance of crystalline pyroxenes, which argues for a well-defined dust annealing temperature of no less than 900 K and no more than 1200 K.)

The PSN mixing cannot have been perfect, however, or else the solar system would be highly homogenous and asteroids would merely be comets with few to no volatiles. This is clearly not the observed case. Trends in compositional diversity are evident in the asteroid belt, with the most primitive asteroids being in the outer regions. The density, porosity, and tensile strength measurements from the DI mission for Tempel 1 are in disagreement with similar measurements for asteroids (45). A likely possibility is that the mixing occurred early on, in a relatively warm PSN, and then turned off, allowing sufficient time for significant small body evolution afterward. A natural time scale is the 5 million to 10 million years after nebula formation, when the giant planet cores formed and inhibited further radial transport across their orbits (46, 47). This would create a quantity of nebular crystalline silicates, phyllosilicates, and carbonates that was time-dependent, resulting in variability in the comet compositional spectrum (48).

Parent-body alteration. The ejecta material from comet Tempel 1 is a good representation of the material from which the comet was formed, unless changes have occurred in the parent body

over 4.5 billion years. For example, the aqueous alteration suggested by the detection of phyllosilicates and carbonates could have been caused in two ways: suddenly, by producing abundant warm water during impacts, or slowly, by a thermal wave from the Sun penetrating into the depths of the comet and heating a boundary layer between the cold icy core and the warm gaseous coma at the nucleus surface.

The thermal layer mechanism would make a thin altered region all over the comet, wherever sublimation was occurring. Even though the DI experiment sampled material from only one location, the match between the Tempel 1 spectrum and the C/1995 O1 (Hale-Bopp) spectrum argues for a global mechanism: The material from Hale-Bopp was emitted from at least five strong jets, well spaced over the surface of the comet (49). The work of Sarid *et al.* (50) casts doubts on the intrinsic liquid water layer model; it is more likely that there are regions of strong water vapor flow. The impact mechanism would alter compositions in the vicinity of an impact site and has the advantage of providing high transient temperatures and pressures as well. The location of the DI impact site lay between two established impact craters, in a depression apparently excavated by the heating incurred during repeated perihelion passages of the comet (1). Consistent with this model, new laboratory work by Toppani *et al.* (22) has demonstrated the ability to grow carbonate crystals from hot silicate, water, and carbon dioxide vapors. However, there must be limits to this processing; it is difficult to understand how the material excavated by DI could have been impact-processed to the ~1200 K crystalline silicate annealing temperature indicated by the SST spectra, while at the same time retaining the low density, low tensile strength, high porosity, and evidence of volatile ices determined for the interior material by DI (1).

The match between the Tempel 1 ejecta spectrum (Fig. 2) and the HD100546 dusty disk spectrum argues for a similar origin of the comet and YSO material. Ceccarelli *et al.* (51) and Chiavassa *et al.* (52) have also found that half of all YSOs in the ISO Long Wavelength Spectrometer survey display emission due to carbonates. If parent-body processes are the origin of the altered species, then there must also be a mechanism for reemitting large amounts of the species into the surrounding nebula in significant quantities (such as jets or collisional fragmentation).

References and Notes

1. M. F. A'Hearn *et al.*, *Science* **310**, 258 (2005).
2. D. Stoffler *et al.*, *J. Geophys. Res.* **80**, 4062 (1975).
3. H. J. Melosh, in *Impact Cratering: A Geologic Process* (Oxford Monographs on Geology and Geophysics, No. 11, Clarendon Press, Oxford, 1989).
4. M. W. Werner *et al.*, *Astrophys. J. Suppl.* **154**, 1 (2004).
5. J. R. Houck *et al.*, *Astrophys. J. Suppl.* **154**, 18 (2004).
6. The SST is the most sensitive mid-infrared observing platform ever built, due to its location in a stable space environment orbit above the terrestrial atmosphere and to its operations at superfluid helium temperatures. The background level at 5 μm for the SST IRS was 6 orders of

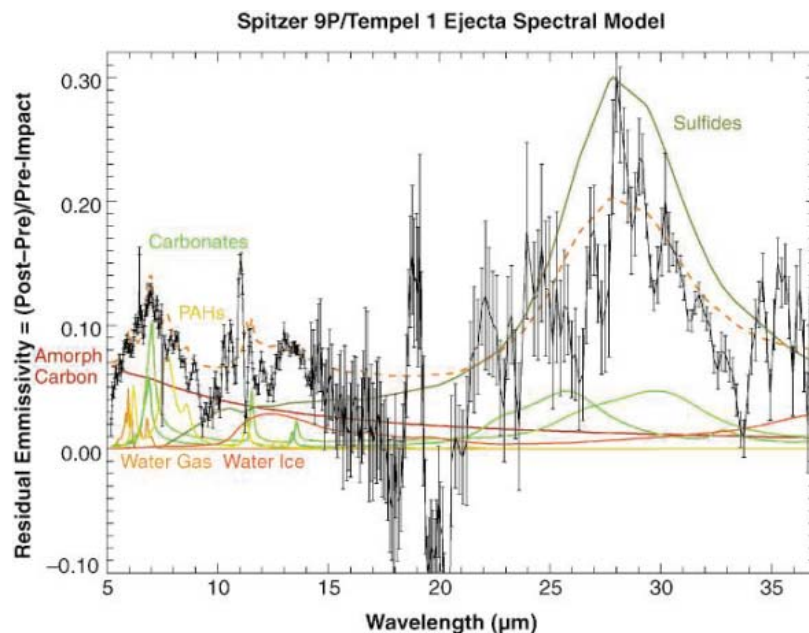


Fig. 4. Enhanced nonsilicate emissivity spectrum. Same as in Fig. 3, except with the silicate emission contributions removed. Left are the residual emission features due to PAHs, carbonates, amorphous carbon, water ice and gas, and sulfides. Error bars are 2σ . The best-fit model individual species curves have been scaled by a factor of 2 versus the data for emphasis. The large residual at 21 μm is due to problems with matching the spectra between the orders and slits.

- magnitude less per pixel than for the DI HRI-IR passively cooled spectrometer, resulting in SST spectra taken at 0.75 AU from the comet with precisions rivaling those obtained by the HRI-IR, taken at 1000 km (6.8×10^{-6} AU) from the comet.
7. C. M. Lisse *et al.*, *Astrophys. J. Lett.* **625**, L139 (2005a).
 8. C. M. Lisse *et al.*, *Space Sci. Rev.* **117**, 161 (2005b).
 9. J. Crovisier *et al.*, *Science* **275**, 1904 (1997).
 10. E. Lellouch *et al.*, *Astron. Astrophys.* **339**, L9 (1998).
 11. K. Malfait *et al.*, *Astron. Astrophys.* **332**, L25 (1998).
 12. D. E. Harker *et al.*, *Science* **310**, 278 (2005).
 13. As a test of the robustness of our best-fit model, the last column in Table 2 also gives the best-fitting χ^2_{ν} , we could find if we deleted a particular species while keeping the rest.
 14. E. Anders, N. Grevesse, *Geochim. Cosmochim. Acta* **53**, 197 (1989).
 15. H is very deficient, as expected for small primitive bodies' inability to retain solar nebula H_2 . C is deficient by a factor of 10, due to its majority partitioning into the comet's labile icy volatiles (CH_4 , C_2H_6 , CO, and CO_2). E. K. Jessberger *et al.* (53) found a C/Mg ratio (atom/atom) in 79 selected large particles during the flythrough of the coma of 1P/Halley that was an order of magnitude greater than in typical IPDs. O is less deficient than C, depleted by only a factor of ~ 2 , due to its more lithophilic chemistry and majority presence in the relatively involatile H_2O . S appears deficient by a factor of 1.5, suggesting that we may not have well characterized the sulfide constituents or that a significant fraction of S was present in volatile species such as H_2S .
 16. D. Wooden *et al.*, *Astrophys. J.* **517**, 1034 (1999) and references therein.
 17. J. A. Nuth, N. M. Johnson, *Icarus* **180**, 243 (2006).
 18. D. Brownlee, personal communication.
 19. J. Licandro *et al.*, *Astron. Astrophys.* **398**, L45 (2003).
 20. L. A. Soderblom *et al.*, *Icarus* **167**, 100 (2004).
 21. J. K. Wilson *et al.*, *Geophys. Res. Lett.* **25**, 225 (1998).
 22. A. Toppani *et al.*, *Nature* **437**, 1121 (2005).
 23. S. Sandford, *Science* **231**, 1540 (1986).
 24. J. Bradley, personal communication.
 25. G. J. Flynn *et al.*, in *Dust in Planetary Systems*, proceedings of the conference held 26 to 28 September 2005, Kaua'i, Hawaii (Lunar and Planetary Institute Contribution No. 1280, 2005), p. 48.
 26. B. C. Clark *et al.*, *Astron. Astrophys.* **187**, 779 (1987).
 27. Also reported by M. N. Fomenkova *et al.* (54), based on the fact that F. K. Rietmeijer (55) had reported carbonates and layer silicates as minor phases in anhydrous chondritic porous IPDs.
 28. J. D. Bregman *et al.*, *Astron. Astrophys.* **187**, 616 (1987).
 29. A. Li, B. T. Draine, *Astrophys. J.*, in press.
 30. K. Tomeoka, P. R. Buseck, *Science* **231**, 1544 (1986).
 31. L. Deutsch *et al.*, *Astrophys. Space Sci.* **224**, 89 (1995).
 32. M. S. Hanner *et al.*, *Astrophys. J.* **502**, 871 (1998).
 33. D. Bockelee-Morvan *et al.*, *Icarus* **116**, 18 (1995).
 34. Y. Kimura *et al.*, *Astron. Astrophys.* **442**, 507 (2005).
 35. L. P. Keller *et al.*, *Nature* **417**, 148 (2002).
 36. L. P. Keller *et al.*, *Lunar Planet. Sci. Conf.* **XXXI**, abstract 1860 (2000).
 37. S. Hony *et al.*, *Astron. Astrophys.* **393**, L103 (2002).
 38. J. P. Bradley, in *Astrominerology*, vol. 609 of *Lecture Notes in Physics*, T. Henning, Ed. (Springer-Verlag, Berlin-Heidelberg-New York, 2002), pp. 217–235.
 39. H. Schulze, J. Kissel, *Meteoritics* **27**, 286 (1992).
 40. J. S. Sunshine *et al.*, *Science* **311**, 1453 (2006).
 41. Due to an O-H bending mode, the broad 6.0- μ m feature is similar to the broad 3- μ m water ice absorption feature. It had not been positively detected in comets before DI, although Bregman *et al.* (28) allude to a "deficit versus the best fit greybody at 6.0 μ m" in the December 1985 spectrum of comet 1P/Halley.
 42. J. Crovisier, personal communication.
 43. M. F. A'Hearn *et al.*, *Icarus* **118**, 223 (1995).
 44. C. Kemper *et al.*, *Astrophys. J.* **609**, 826 (2004).
 45. A. Cheng, *Adv. Space Res.* **33**, 1558 (2004).
 46. A. P. Boss, *Astrophys. J.* **616**, 1265 (2004).
 47. H.-P. Gail, *Astron. Astrophys.* **413**, 571 (2004).
 48. J. A. Nuth *et al.*, *Nature* **406**, 275 (2000).
 49. S. M. Lederer, H. Campins, *Earth Moon Planets* **90**, 381 (2002).
 50. G. Sarid *et al.*, *Pub. Astron. Soc. Pacific* **117**, 796 (2005).
 51. C. Ceccarelli *et al.*, *Astron. Astrophys.* **395**, L29 (2002).
 52. A. Chiavassa *et al.*, *Astron. Astrophys.* **432**, 547 (2005).
 53. E. K. Jessberger *et al.*, *Nature* **332**, 691 (1988).
 54. M. N. Fomenkova *et al.*, *Science* **258**, 266 (1992).
 55. F. J. Rietmeijer, *Earth Planet. Sci. Lett.* **102**, 148 (1991).
 56. This paper was based on observations taken with the NASA SST, operated by the Jet Propulsion Laboratory (JPL)/CalTech, under JPL contracts 1274400 and 1274485. The authors thank S. Bajt, J. Bradley, D. Brownlee, N. Chabot, B. Clark, N. Dello-Russo, G. Flynn, W. Glaccum, C. Grady, E. Gruen, D. Harker, K. Hibbits, W. Jackson, D. Joswiak, L. Keller, D. Lauretta, A. Li, J. Nuth, W. Reach, A. Rivkin, and D. Wellnitz for valuable discussions; G. Flynn and M. Sitko for their invaluable reviews; and J. Jackson and S. Kido for their help with the graphics.

Supporting Online Material

www.sciencemag.org/cgi/content/full/1124694/DC1

SOM Text

Fig. S1

Table S1

References and Notes

6 January 2006; accepted 13 June 2006

Published online 13 July 2006;

10.1126/science.1124694

Include this information when citing this paper.

Netrins Promote Developmental and Therapeutic Angiogenesis

Brent D. Wilson,^{1,2*} Masaaki Ii,^{7*†} Kye Won Park,^{1,3*} Arminda Sulji,^{4*} Lise K. Sorensen,² Frédéric Larrieu-Lahargue,¹ Lisa D. Urness,^{1,2} Wonhee Suh,^{1,‡} Jun Asai,⁷ Gerhardus A.H. Kock,⁷ Tina Thorne,⁷ Marcy Silver,⁷ Kirk R. Thomas,^{1,5} Chi-Bin Chien,^{4,6||} Douglas W. Losordo,^{7||} Dean Y. Li^{3||}

Axonal guidance and vascular patterning share several guidance cues, including proteins in the netrin family. We demonstrate that netrins stimulate proliferation, migration, and tube formation of human endothelial cells *in vitro* and that this stimulation is independent of known netrin receptors. Suppression of *netrin1a* messenger RNA in zebrafish inhibits vascular sprouting, implying a proangiogenic role for netrins during vertebrate development. We also show that netrins accelerate neovascularization in an *in vivo* model of ischemia and that they reverse neuropathy and vasculopathy in a diabetic murine model. We propose that the attractive vascular and neural guidance functions of netrins offer a unique therapeutic potential.

Neuronal pathfinding is directed by a series of extracellular guidance cues that either attract or repulse growing axons. All of the four major families of neural guidance cues—ephrins, semaphorins, slits, and netrins—have been shown to direct patterning in the vascular system (1–4). The netrins are the prototypical axonal attractants, first identified as extracellular factors secreted from the floor plate that attract spinal commissural axons toward the midline (5). This family includes netrin-1, netrin-2 (netrin-3 in mouse), netrin-4, and the netrin-related molecules, netrin-G1 and netrin-G2.

The signaling pathways for netrin-1 are best understood. Receptors in the deleted in colo-

rectal cancer (DCC) subfamily (DCC and neogenin) mediate axon attraction toward netrin-1 (2), although this signal can be converted from an attractive to a repulsive cue by binding of netrin to the Unc5b receptor (6). The adenosine 2b receptor (A2b) reportedly binds to netrin-1 (7), but its role in netrin-mediated axonal extension has been questioned (8).

Netrins have roles that extend beyond axonal guidance. The netrins are expressed in Schwann cells, are required for regeneration and maintenance of the central nervous system (9, 10), and have been implicated in the development of mammary gland, lung, pancreas, and blood vessel (11–14). Although others have reported that

netrin-1 inhibits endothelial migration and blocks filopodial extension through the repulsive netrin receptor Unc5b (14), we have suggested that netrin-1 functions as a proangiogenic factor (13).

Netrins are endothelial mitogens and chemoattractants. To further elucidate the activity of netrins, we first evaluated the effects of purified netrin proteins on the behavior of human microvascular endothelial cells (HMVECs) *in vitro*. Netrin-1, -2, and -4 all stimulated migration of HMVECs in a dose-dependent fashion (Fig. 1), inconsistent with a published report concluding that netrin-1 inhibited migration of endothelial cells (14). To exclude the possibility of contamination in our netrin preparations, we used mass

¹Program in Human Molecular Biology and Genetics, ²Division of Cardiology, ³Department of Oncological Sciences, ⁴Department of Neurobiology and Anatomy, ⁵Division of Hematology, ⁶Brain Institute, University of Utah, Salt Lake City, UT 84112, USA. ⁷Division of Cardiovascular Research, Caritas St. Elizabeth's Medical Center, Tufts University School of Medicine, Boston, MA 02135, USA.

*These authors contributed equally to this work.

†Present address: Stem Cell Translational Research, Institute of Biomedical Research and Innovation/RIKEN Center for Developmental Biology, Kobe 650-0047, Japan.

‡Present address: Department of Medicine, Samsung Medical Center, Samsung Biomedical Research Institute, Sungkyunkwan University School of Medicine, 50 Ilwon-dong, Kangnam-Ku, Seoul 135-710, Korea.

§Present address: Department of Cardiology, Thoraxcenter, University Medical Center Groningen, University Groningen, 30.001 Groningen, Netherlands.

||To whom correspondence should be addressed. E-mail: dean.li@hmbg.utah.edu (D.Y.L.); douglas.losordo@tufts.edu (D.W.L.); chi-bin.chien@neuro.utah.edu (C.B.C.)

spectroscopy and SDS–polyacrylamide gel electrophoresis (SDS–PAGE) to show that they were >95% pure. Moreover, depletion of the media by antibody to netrin removed all promigratory activity (fig. S1). Because the previous report used conditioned media containing netrin-1 (1 $\mu\text{g}/\text{ml}$) (14), we also considered the possibility that netrin could be inhibiting an induced migratory behavior of endothelial cells. We therefore examined the effect of the netrins on vascular endothelial growth factor (VEGF)–induced migration (Fig. 1B) and found that, even at the published concentrations, netrins did not inhibit endothelial migration toward VEGF. Netrin-1, -2, and -4 were also found to stimulate endothelial proliferation and tube formation (Fig. 1, C and D) but, despite their structural similarities to the laminin family of extracellular matrix proteins, did not promote endothelial cell adhesion. The chemotactic and mitogenic effects of the netrins were reproduced in two different laboratories using similar but not identical protocols. These effects were observed on HMVECs and other endothelial cell lines, including human umbilical vein endothelial cells (HUVECs), human umbilical artery endothelial cells (HUAECs), human coronary artery endothelial cells (HCAECs), and murine endothelial cells (MS1s) (fig. S2).

Because of the suggestion that Unc5b mediates signaling by netrin-1 in the endothelium (14), we examined expression of Unc5b and the other known netrin receptors in the endothelial cell lines used in our cell biology assays (Fig. 2A). By using quantitative, real-time reverse transcription

polymerase chain reaction (RT–PCR), we detected high concentrations of the endothelial receptors roundabout 4 (Robo4), platelet endothelial cell adhesion molecule (PECAM), and VEGF receptor–2 (VEGFR-2 or Flk-1) but did not detect significant expression of Unc5b or the other known netrin receptors. Western blots using antibodies directed against DCC, neogenin, or Unc5b were similarly negative. We then used co-immunoprecipitation to test whether netrin-4 binds Unc5b and the other netrin receptors. Although netrin-1 bound as predicted to all known netrin receptors, netrin-4 did not bind to DCC, neogenin, or the Unc5 receptors (Fig. 2B and fig. S3), despite having activity similar to that of netrin-1 in endothelial cell assays and in vitro axon extension experiments (15, 16). We also revisited the possibility that A2b could serve as an endothelial netrin receptor (1, 2, 17, 18). We found that netrin-1 and netrin-4 did not bind to A2b (Fig. 2C) or stimulate A2b-mediated cyclic adenosine monophosphate (cAMP) production (Fig. 2, D and E) and that adenosine antagonists did not inhibit netrin's biologic effect (fig. S3). Together, the expression, binding, and signaling experiments indicate that the proangiogenic response of cultured human endothelial cells to netrins, especially netrin-4, is not mediated by known netrin receptors.

Zebrafish netrin1a is required for parachordal vessel formation. The effects of exogenous netrins on cultured endothelial cells led us to examine the required roles of endogenous netrin by using *fli:egfp* zebrafish embryos, whose

endothelium expresses enhanced green fluorescent protein (EGFP) (19) (Fig. 3). From <24 to 32 hours postfertilization (hpf), the netrin-1 ortholog, *netrin1a*, was expressed strongly in the ventral neural tube, weakly in the somites, and strongly in muscle pioneer cells in the horizontal myoseptum (HMS), which divides ventral from dorsal somites (20) (Fig. 3H). It was reported that injecting a translation-blocking antisense morpholino oligonucleotide (MO) at the one-cell stage leads to ectopic vascular sprouting at 48 hpf (14). In our studies, this MO caused severe defects during gastrulation at even moderate doses, suggesting a requirement for maternally transcribed *netrin1a*. To avoid these confounding defects, we used a splice-blocking MO targeting the *netrin1a* exon1–intron1 boundary, which abolished normal mRNA splicing but did not grossly affect overall trunk morphology (Fig. 3, A and B, and fig. S4). In *netrin1a* MO-injected embryos (morphants), the intersegmental vessels (ISVs) and the dorsal longitudinal anastomotic vessels (DLAVs) formed normally. However, formation of the parachordal vessels (PAVs) was strongly inhibited (Fig. 3, C and G). In *netrin1a* morphants at 50 to 54 hpf, 60% (29/48) of hemisegments lacked all *fli:egfp*-positive cells at the presumptive position of the PAV, a condition almost never seen in uninjected wild types (1%, 1/99) or control morphants (4%, 5/128). After 24 hpf, the posterior cardinal vein (PCV) normally gives rise to secondary sprouts, which grow dorsally (21) (Fig. 3, C and I) and by ~36 hpf contribute to the PAV, which becomes

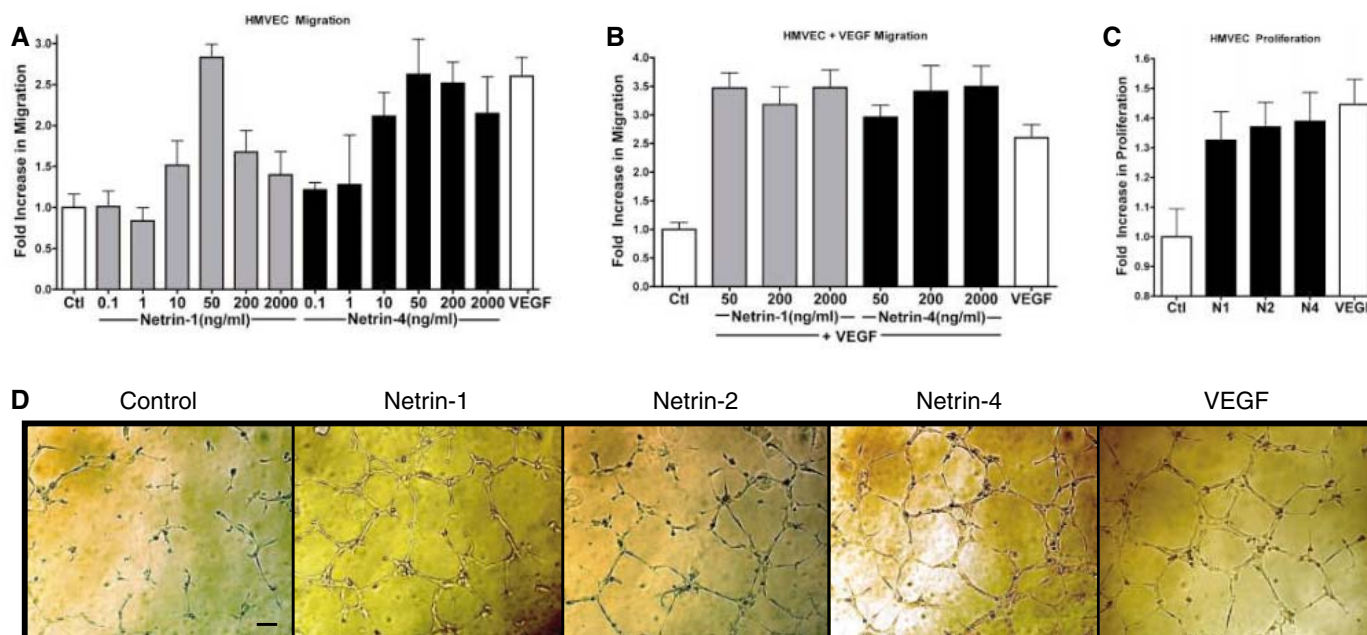


Fig. 1. Netrin function in vitro. **(A)** Migration of HMVECs toward netrins. Migration was measured in a Boyden chamber containing varying concentrations of netrin-1 or netrin-4 in the lower well. The number of migrating cells was normalized to a 0.1% bovine serum albumin (BSA) control (Ctl); the positive control was 13 ng/ml VEGF. Note that 50 ng/ml netrin-1 or -4 and 13 ng/ml VEGF are equimolar (0.625 nM). Bars represent mean \pm SEM of 24 separate determinations. **(B)** Migration of HMVECs

toward 50 to 2000 ng/ml netrin-1 and netrin-4 in the presence of 13 ng/ml VEGF. **(C)** Proliferation of HMVECs over 72 hours in the presence of 0.1% BSA (Ctl); 50 ng/ml netrin-1 (N1), -2 (N2), or -4 (N4); or 13 ng/ml VEGF. Number of cells is normalized to plates containing only BSA. **(D)** Tube formation of HUVECs stimulated by netrin-1 and -4 (200 ng/ml) as well as VEGF (13 ng/ml) compared with stimulation by control (0.1% BSA). Scale bar, 200 μm .

visible as *fli:egfp*-positive cells at the HMS, coincident with domains of strong *netrin1a* expression (21) (Fig. 3H). In *netrin1a* morphants at 36 hpf, 66% (79/120) of hemisegments lacked *fli:egfp*-positive cells at the HMS, which was never seen in uninjected controls (0/115). Secondary sprouts from the PCV seemed to form normally in *netrin1a* morphants at 36 hpf (Fig. 3D); at 50 hpf, secondary sprouts at the HMS occasionally extended ectopic projections as though searching to form a PAV (Fig. 3G) (14). The absence of PAVs in *netrin1a* morphants, together with the strong expression of *netrin1a* messenger RNA (mRNA) by muscle pioneers that prefigures the PAV, are most consistent with a proangiogenic role for *netrin1a*.

Netrins promote neovascularization in mammalian models. The cell biology and zebrafish data led us to hypothesize that netrins could induce neovascularization in vivo. We therefore compared netrins with VEGF in their ability to promote angiogenesis and reperfusion in a murine model of hindlimb ischemia (22). The iliac artery of FVB/NJ mice was ligated, resulting in severe vascular perfusion defects. Blood flow was measured with laser Doppler imaging and quantitated as the ratio of ischemic to nonischemic limbs. Expression of netrin-1, netrin-4, and VEGF complementary DNA molecules (cDNAs) was driven by a cytomegalovirus (CMV) enhancer and a Rous sarcoma virus (RSV) promoter that were characterized previously in preclinical and clinical trials of VEGF (23–27). The base expression vector (empty vector) was used as a control. All constructs were delivered locally into the ischemic gastrocnemius muscle at 0, 7, 14, and 21 days after induction of ischemia. Imaging revealed that hindlimb perfusion was significantly improved 7 days postsurgery in mice injected with netrin-1, netrin-4, or VEGF constructs compared with those of mice injected with empty vector (Fig. 4A). Serial Doppler measurements demonstrated continued improvement in limb perfusion, with the greatest effect at 28 days after induction of ischemia. Histological analysis after day 28 showed a significantly greater (>twofold) capillary density and reduced fibrosis in the netrin-1-, netrin-4- and VEGF-treated animals (fig. S5). Interestingly, more vessels stained positive for smooth muscle α -actin in netrin-1-treated animals than in netrin-4- or VEGF-treated animals, suggesting a greater number of vessels with medial layers.

The dual role of netrin in guiding nerves and blood vessels suggests that netrins may have unique therapeutic potential. In diabetes and related metabolic syndromes, neural and vascular compromise appear together clinically (28, 29). Reduced nerve conduction velocity is an early marker of neuropathy in diabetic models, such as *db/db* mice, and is secondary to a combination of pathologic effects on neuronal cells and compromise to perineural vascular beds (vasa nervosa). To examine whether netrins reverse diabetic vasculopathy and neuropathy in *db/db*

mice, we delivered netrin-1 and netrin-4 expression constructs into their hindlimbs every 7 days for a total of 28 days. After 7 days of treatment with vectors expressing netrin-1, netrin-4, or VEGF, both motor and sensory sciatic nerve conduction velocities in *db/db* mice returned to nondiabetic amounts and were significantly better than empty vector-injected controls (Fig. 4). At 14 days, the conduction velocities in netrin-1-treated mice continued to improve beyond nondiabetic values, whereas those measured in either netrin-4- or VEGF-treated animals remained near normal nondiabetic conduction ve-

locities. The improvement in conduction velocities in *db/db* mice treated with netrin-1, netrin-4, or VEGF was associated with increased capillary density of the vasa nervosa surrounding the sciatic nerve (fig. S6). The increased capillary density was correlated with endothelial proliferation as measured by 5-bromo-2'-deoxyuridine (BrdU) incorporation and lectin staining. The amounts of endothelial proliferation in netrin-1-, netrin-4-, and VEGF-treated animals were similar, although animals exposed to netrin-1-containing vectors showed proliferation of cells that also expressed the Schwann cell marker

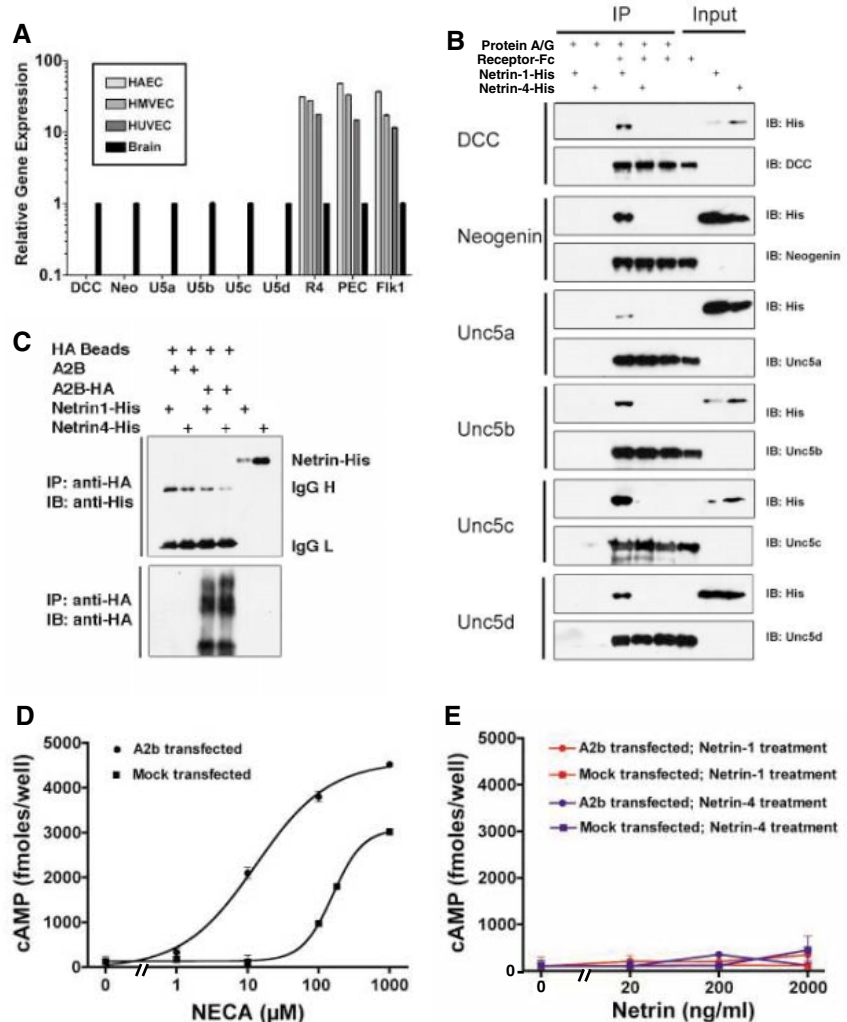


Fig. 2. Angiogenic effects of netrin-1 and netrin-4 are not mediated by known or postulated netrin receptors. (A) Quantitative real-time RT-PCR of DCC receptors (DCC and neogenin), Unc5 receptors (U5a to U5d), Robo4 (R4), PECAM (PEC), and VEGF receptor (Flk1). Expression amounts were measured relative to that of glyceraldehyde-3-phosphate dehydrogenase (GAPDH) and compared with transcript amounts in brain tissue (normalized to 1). The absence of bars indicates values less than 0.1. (B) Co-immunoprecipitation (co-IP) of purified receptor-Fc fusion proteins (N-terminal) and 10X-His-tagged netrin proteins (C-terminal). Immunoblotting (IB) performed with antibody to His or receptor-specific antibody. (C) Co-IP of purified netrin-1-His and netrin-4-His incubated with lysates of A2b-hemagglutinin (HA)-transfected human embryonic kidney (HEK) 293T cells. Precipitation and immunoblot were carried out by using antibodies against HA and His, respectively. (D and E) Stimulation of cAMP accumulation by 5'-(N-ethylcarboxamido) adenosine (NECA) and netrins. HEK cells were transfected with vectors expressing A2b or the G protein-coupled receptor, arginine vasopressin receptor-2 (mock), and exposed to increasing concentrations of NECA (D) or netrin-1 or netrin-4 (E). Error bars indicate SEM.

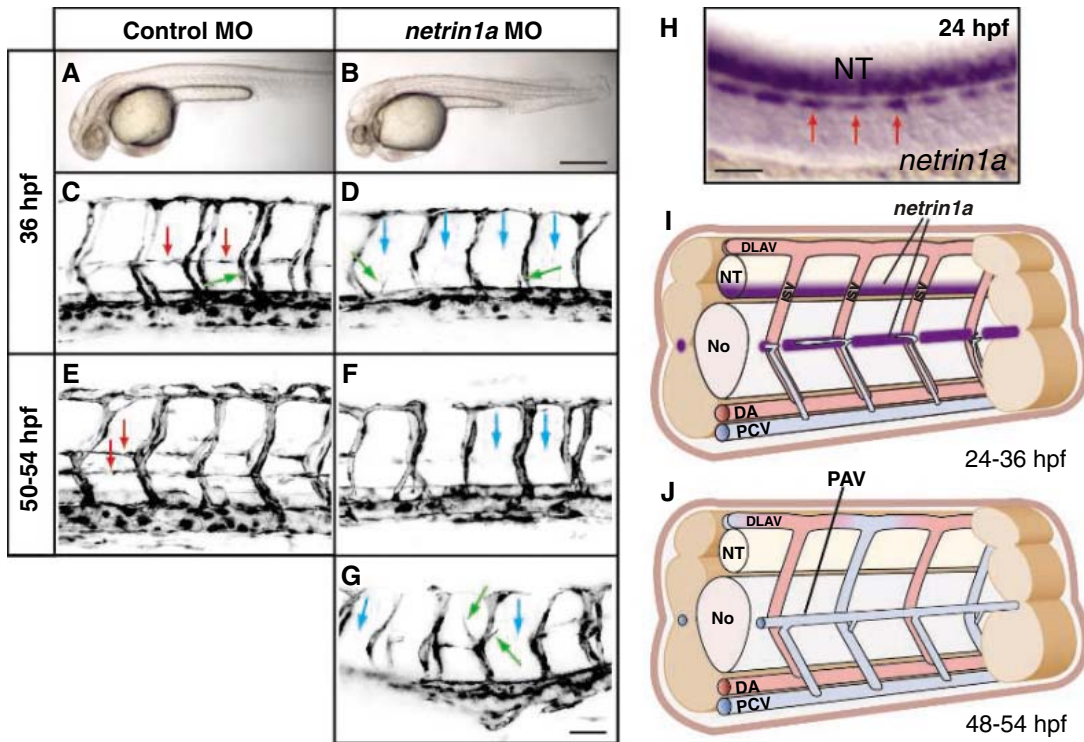


Fig. 3. Knockdown of zebrafish *netrin1a* prevents formation of a specific vessel, the PAV. *fli:egfp* zebrafish embryos were injected at the one- to two-cell stage with a control MO or a splice-blocking *netrin1a* MO and analyzed at 36 to 54 hpf. (A and B) Brightfield images. Scale bar, 400 μ m. (C to G) Confocal projections showing lateral views of somites 7 to 11; anterior to the left. Embryo in (E) is tilted to visualize both sides. Red arrows indicate PAV in control embryos; blue arrows indicate absence of PAVs in morphants; green arrows indicate secondary sprouts growing dorsally from the PCV in controls and morphants. Scale bar, 50 μ m. (G) Secondary sprouts occasionally give rise to short branches at the presumptive location of the PAV (green arrows). (H) In situ hybridization for *netrin1a* shows strong staining at the HMS (red arrows). 24 hpf, lateral view of somites 7 to

14. Scale bar, 50 μ m. NT, neural tube. (I) Schematic, 24 to 36 hpf. *Netrin1a* is expressed at the horizontal myoseptum through 32 hpf; weak expression in somites not shown. By 36 hpf, secondary sprouts (blue) arise from the PCV and begin to form the PAV at the myoseptum. DA, dorsal aorta; No, notochord. (J) Schematic, 48 to 54 hpf. By this time, ISVs have started to acquire arterial or venous fates. The PAV is mature and connected to the veins by shunts. Without *netrin1a* function, the PAV does not form.

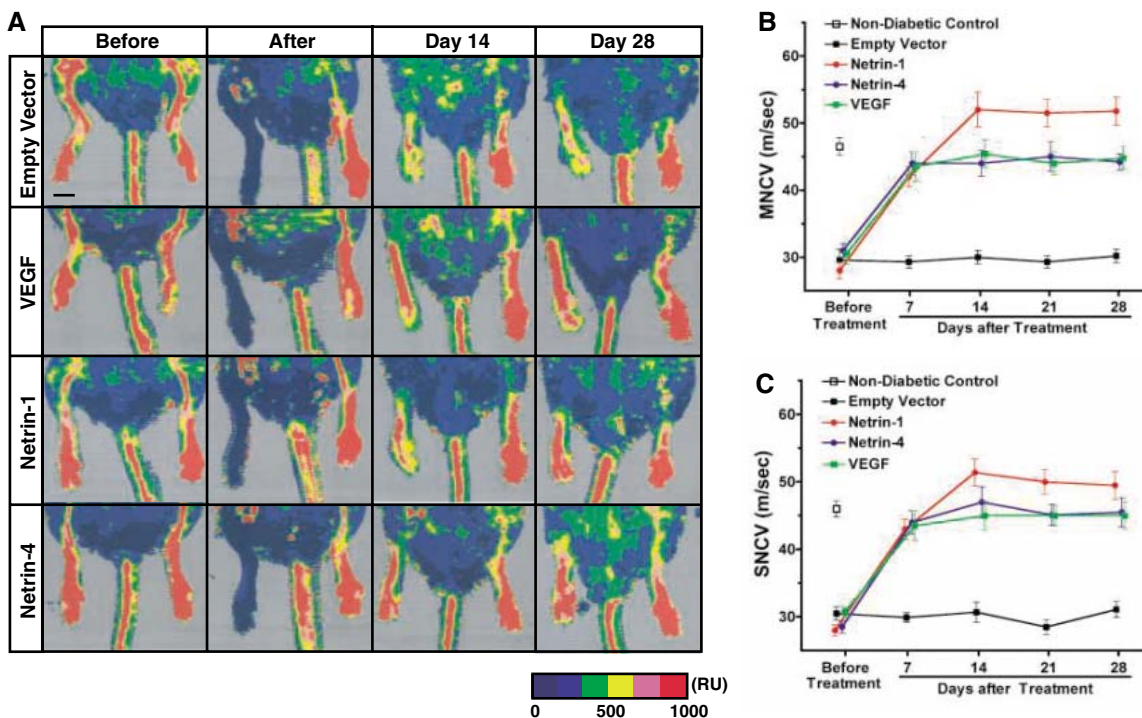


Fig. 4. Local delivery of VEGF, netrin-1, or netrin-4 expression constructs promotes revascularization and restoration of nerve conduction velocity. (A) Hindlimb ischemia was surgically induced in FVB/NJ mice by ligation and excision of the proximal femoral artery as described previously (22). VEGF, netrin-1, netrin-4, and empty vector DNA expression plasmids (50 μ g of DNA in 100 μ l of saline in each group) were locally injected into the right gastrocnemius muscle immediately, 7, 14, and 21 days after surgery. Laser Doppler perfusion imaging was used to record serial blood flow measurements over the course of 4 weeks post-operatively, as previously described (32). In these digital color-coded images,

red indicates regions with maximum perfusion, yellow depicts medium perfusion, and blue identifies low perfusion. Scale bar, 3 mm. Color bar in lower right corner displays absolute values in readable units (RU). (B) Motor nerve conduction velocities (MNCVs) in *db/db* mice 7 days after injection with VEGF, netrin-1, or netrin-4. (C) Sensory nerve conduction velocities (SNCVs) in *db/db* mice 7 days after injection with VEGF, netrin-1 (NT1), netrin-4 (NT4), or empty vector constructs. Uninjected, nondiabetic mice serve as controls in both (B) and (C). Error bars indicate SEM.

S100. These data suggest that netrin-1 reverses vascular and neural pathology in *db/db* mice by stimulating both endothelial and Schwann cells and may account for the superior recovery of nerve conduction seen in netrin-1-treated *db/db* mice.

Conclusion. By using zebrafish and mammalian systems, loss-of-function and gain-of-function strategies, and in vivo and in vitro assays, we have shown that netrins stimulate angiogenesis. First, netrin-1, -2, and -4 induce migration, proliferation, and tube formation in multiple endothelial cell lines. Surprisingly, we could identify none of the known netrin receptors as being responsible for these behaviors. Second, the inhibition of *netrin1a* mRNA in zebrafish reveals a requirement for netrin signaling in formation of PAVs. Lastly, netrins can activate blood vessel formation and accelerate revascularization and reperfusion of ischemic tissue in two murine disease models.

It has been proposed that netrin signaling in the vasculature can be mediated by the repulsive Unc5b receptor and that the experimental attenuation of either netrins or Unc5b results in increased branching of vessels in zebrafish and mice (14). However, we could not detect significant amounts of Unc5b in any of the responsive cell lines, nor could we detect any binding of Unc5b to netrin-4, despite the fact that netrin-4 elicits an endothelial response identical to that of netrin-1 in all of our in vitro and in vivo assays. Moreover, we were unable to find any evidence that netrins can inhibit vascular growth in vivo. Knocking down *netrin1a* mRNA in zebrafish by using a splice-blocking MO prevents formation of the PAV, implying a proangiogenic role. PAVs are absent in both *netrin1a* and *unc5b* morphants in the published work of others [figure 2 of Lu *et al.* (14)]. These authors did not remark upon these findings and focused on ectopic sprouting in their morphants at 48 hpf. We also observed ectopic sprouting, but this occurred in a minority of *netrin1a* morphants and appeared secondary to loss of the PAV at 36 hpf. The temporal sequence of events during zebrafish embryogenesis is most consistent with a role of netrin as a positive regulator of angiogenesis. We also generated mice carrying a targeted deletion of exons 4 to 13 of the Unc5b locus (figs. S7 and S8). Embryos homozygous for this mutation show normal branching of cranial, intersomitic, hindbrain, and yolk sac vessels; whether this is due to allelic difference or strain background (shown to modify the Unc5b phenotype) is currently under investigation.

The ability of netrins to promote the growth of both neurons and vasculature has made them a promising therapeutic target for treating a number of degenerative diseases. Our studies demonstrate that netrins promote neovascularization and reperfusion in a murine model of peripheral vascular disease. In fact, vectors expressing netrin-1 and netrin-4 are comparable in effectiveness to vectors expressing VEGF that

are currently being tested in phase II clinical trials. A potential advantage of netrin-1 over VEGF is that it enhances capillary density and stimulates smooth muscle cells to form a vascular media in both in vitro (13) and in vivo studies (fig. S5). Microvascular disease and polyneuropathy are morbid complications of long-standing diabetes whose onset is delayed but not prevented by intensive blood glucose control with insulin or oral agents (30, 31). Here, we show that the netrins restore nerve function and vascular supply in a murine model of diabetes. Although netrin-1 has proangiogenic effects similar to those of VEGF and netrin-4 in this model, our data suggest that netrin-1 is superior in restoring nerve conduction velocity, possibly because it has potent effects on both endothelial and neural biology. This report provides proof of concept for a novel therapeutic strategy aimed at using the dual vascular and neural regenerative properties of guidance molecules to treat diabetic complications that result from vasculopathy and neuropathy and sets the stage for further investigation.

References and Notes

1. M. Klagsbrun, A. Eichmann, *Cytokine Growth Factor Rev.* **16**, 535 (2005).
2. P. Carmeliet, M. Tessier-Lavigne, *Nature* **436**, 193 (2005).
3. A. Eichmann, F. Le Noble, M. Autiero, P. Carmeliet, *Curr. Opin. Neurobiol.* **15**, 108 (2005).
4. B. M. Weinstein, *Cell* **120**, 299 (2005).
5. T. Serafini *et al.*, *Cell* **78**, 409 (1994).
6. K. Hong *et al.*, *Cell* **97**, 927 (1999).
7. V. Corset *et al.*, *Nature* **407**, 747 (2000).
8. E. Stein, Y. Zou, M.-m. Poo, M. Tessier-Lavigne, *Science* **291**, 1976 (2001).
9. F. Cebria, P. A. Newmark, *Development* **132**, 3691 (2005).
10. R. D. Madison, A. Zomorodi, G. A. Robinson, *Exp. Neurol.* **161**, 563 (2000).
11. K. Srinivasan, P. Strickland, A. Valdes, G. C. Shin, L. Hinck, *Dev. Cell* **4**, 371 (2003).
12. M. Yebra *et al.*, *Dev. Cell* **5**, 695 (2003).

13. K. W. Park *et al.*, *Proc. Natl. Acad. Sci. U.S.A.* **101**, 16210 (2004).
14. X. Lu *et al.*, *Nature* **432**, 179 (2004).
15. Y. Yin, J. R. Sanes, J. H. Miner, *Mech. Dev.* **96**, 115 (2000).
16. M. Koch *et al.*, *J. Cell Biol.* **151**, 221 (2000).
17. H. Arakawa, *Nat. Rev. Cancer* **4**, 978 (2004).
18. P. Mehlen, C. Furne, *Cell. Mol. Life Sci.* **62**, 2599 (2005).
19. N. D. Lawson, B. M. Weinstein, *Dev. Biol.* **248**, 307 (2002).
20. J. D. Lauderdale, N. M. Davis, J. Y. Kuwada, *Mol. Cell. Neurosci.* **9**, 293 (1997).
21. S. Isogai, N. D. Lawson, S. Torrealday, M. Horiguchi, B. M. Weinstein, *Development* **130**, 5281 (2003).
22. T. Couffinhal *et al.*, *Am. J. Pathol.* **152**, 1667 (1998).
23. A. Kawamoto *et al.*, *Circulation* **110**, 1398 (2004).
24. J. P. Reilly *et al.*, *J. Interv. Cardiol.* **18**, 27 (2005).
25. P. Schratzberger *et al.*, *J. Clin. Investig.* **107**, 1083 (2001).
26. D. W. Losordo *et al.*, *Circulation* **105**, 2012 (2002).
27. D. H. Walter *et al.*, *Circulation* **110**, 36 (2004).
28. M. Li *et al.*, *Circulation* **112**, 93 (2005).
29. Y. S. Yoon *et al.*, *Circulation* **111**, 2073 (2005).
30. Diabetes Control and Complications Trial Research Group, *Ann. Intern. Med.* **122**, 561 (1995).
31. UK Prospective Diabetes Study Group, *Lancet* **352**, 837 (1998).
32. T. Murohara *et al.*, *J. Clin. Investig.* **101**, 2567 (1998).
33. We thank K. Whitehead, P. Lindblom, and H. Gerhardt for technical expertise and assistance; I. Shepherd, L. Hinck, and D. Grunwald for reagents; the Mass Spectroscopy Core Facility at the University of Utah; and D. Lim for graphics. D.Y.L. is supported by grants from NIH, American Cancer Society, American Heart Association (AHA), Flight Attendants Medical Research Institute, and Burroughs Wellcome Fund. C.B.C. is supported by grants from NIH. D.W.L. is supported by grants from NIH and AHA. B.D.W. is an American College of Cardiology Foundation/Pfizer Fellow in Cardiovascular Medicine.

Supporting Online Material

www.sciencemag.org/cgi/content/full/1124704/DC1

Materials and Methods

SOM Text

Figs. S1 to S8

6 January 2006; accepted 23 May 2006

Published online 29 June 2006;

10.1126/science.1124704

Include this information when citing this paper.

The *Neurospora* Checkpoint Kinase 2: A Regulatory Link Between the Circadian and Cell Cycles

Antônio M. Pogueiro,¹ Qiuyun Liu,³ Christopher L. Baker,¹ Jay C. Dunlap,^{1*} Jennifer J. Loros^{1,2*}

The clock gene *period-4* (*prd-4*) in *Neurospora* was identified by a single allele displaying shortened circadian period and altered temperature compensation. Positional cloning followed by functional tests show that PRD-4 is an ortholog of mammalian *checkpoint kinase 2* (*Chk2*). Expression of *prd-4* is regulated by the circadian clock and, reciprocally, PRD-4 physically interacts with the clock component FRQ, promoting its phosphorylation. DNA-damaging agents can reset the clock in a manner that depends on time of day, and this resetting is dependent on PRD-4. Thus, *prd-4*, the *Neurospora Chk2*, identifies a molecular link that feeds back conditionally from circadian output to input and the cell cycle.

Many core components of cellular circadian clocks constitute molecular feedback loops (1–4). Additional circuits, although not required for circadian function, can

connect the clock to its outputs or even feed back to affect the core loops or input to them (5–7). In mammals, one prominent circadian output leads to regulation of the cell cycle (8–10).

¹Department of Genetics, ²Department of Biochemistry, Dartmouth Medical School, Hanover, NH 03755, USA. ³The Key Laboratory of Gene Engineering of Ministry of Education and Biotechnology Research Center, Zhongshan University, Guangzhou 510275, P. R. China.

*To whom correspondence should be addressed. E-mail: jay.c.dunlap@dartmouth.edu (J.C.D.); jennifer.loros@dartmouth.edu (J.L.)

Fig. 1. Cloning and identification of *prd-4*. (A) Genetic map of part of the right arm of linkage group I showing the location of *prd-4* with respect to mapped markers (37). (B) Genetic and physical map between *os-1* and *arg-13* (13, 14) showing predicted genes (15). (C) Sequencing of the region shown in (B) (light pink box) from diverse *prd-4* mutant (*prd-4^m*) strains revealed a single C to T transition associated with the *prd-4^m* phenotype. (D) Western blotting with antisera directed against PRD-4 (see Methods in SOM) identifies an ~80-kD protein (arrow) in *prd-4^m* but not in the *prd-4* deletion strain (Δ *prd-4*). Asterisk, nonspecific band. (E and F) Expression of the allele bearing the single base change in the predicted *prd-4* gene phenocopies the characteristic shortening of period length seen in *prd-4^m* (E) and the partial loss of temperature compensation (F). Period lengths are average \pm SD. Each data point in (F) corresponds to three or more race tubes (>20 individual circadian period estimates; see SOM).

The *period-4* (*prd-4*) strain, a circadian clock mutant in *Neurospora*, was isolated more than 25 years ago in a genetic screen for mutants that failed to show an appropriate circadian phase shift in response to a light pulse (11, 12). The mutant displayed a period 3 hours shorter than wild type at 25°C that, unlike other

short-period clock mutants, became even shorter as the ambient temperature rose. Heterokaryons bearing wild-type and mutant *prd-4* nuclei have an intermediate period, indicating semidominance of this allele (13). Genetic mapping placed *prd-4* on the right arm of linkage group I between *os-1* and *arg-13* (Fig. 1A) (13, 14).

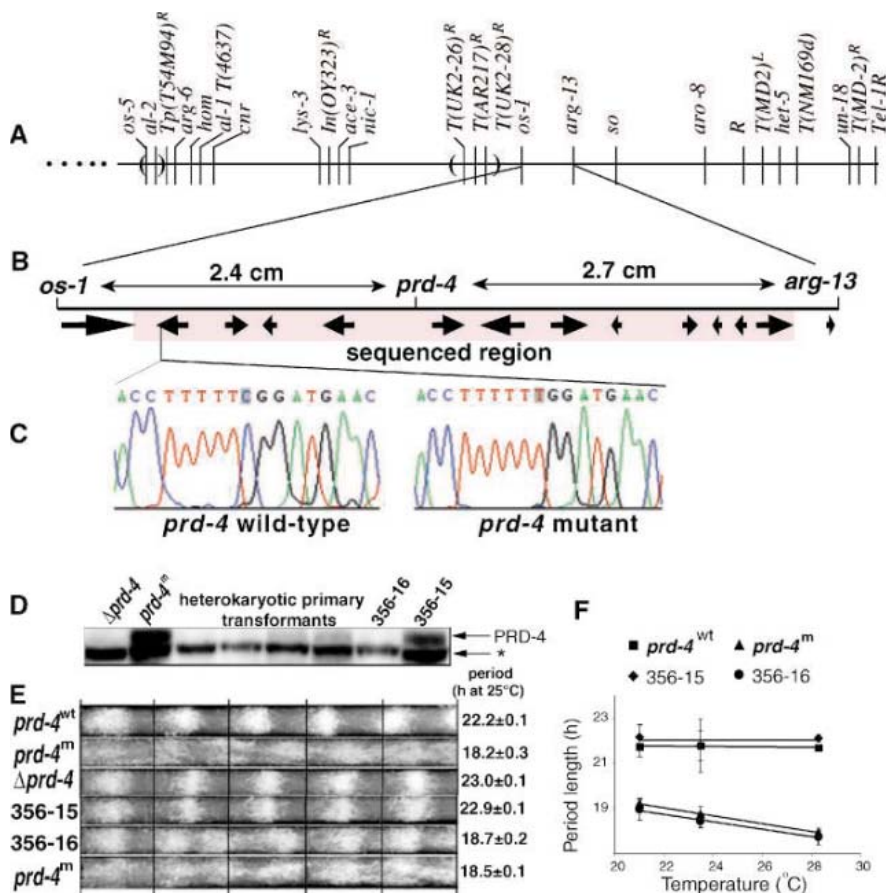
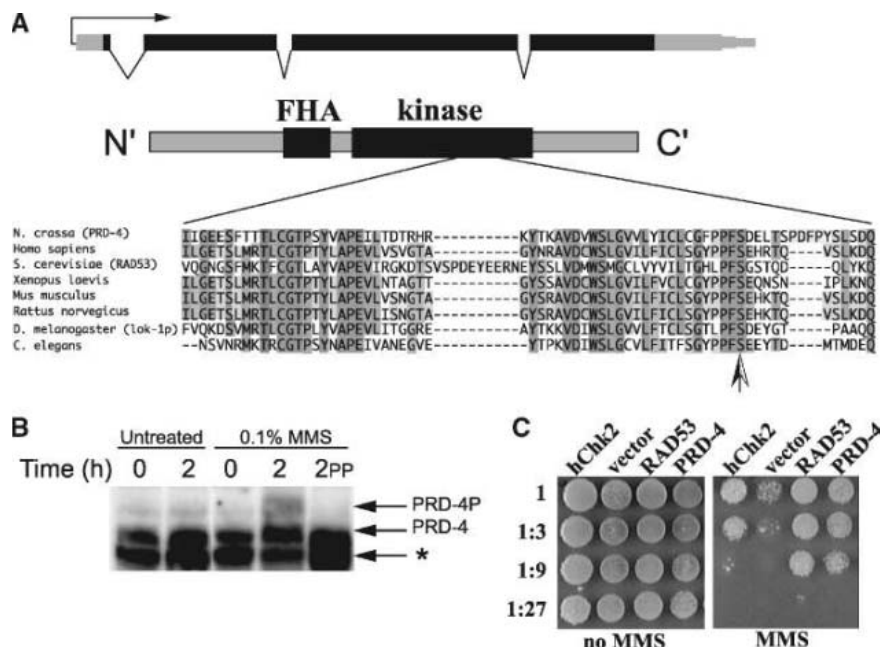


Fig. 2. *prd-4* is the *Neurospora crassa* Chk2. (A) Intron-exon structure of the *prd-4* transcript (top) reveals untranslated regions (light blocks), the ORF (dark blocks), and introns (diagonal lines). Variation in polyadenylation sites is depicted by differences in light block height. Locations of the FHA and kinase domains in PRD-4 (middle panel) and a portion of the alignment of the kinase domain of eight representative Chk2s (bottom panel) are shown. (Full alignments of FHA and kinase domains are in fig. S1.) Arrow, serine 493, mutated to leucine in the canonical *prd-4^m* strain. (B) PRD-4 is phosphorylated in response to treatment with the DNA-damaging agent MMS. Protein extracts made from *Neurospora* treated with 0.1% MMS were used for Western blotting (see SOM for Methods). Arrows, PRD-4 and phosphorylated PRD-4 (PRD-4P); asterisk, nonspecific band. Treatment with lambda phosphatase (2PP) restores the mobility of PRD-4 to that of the untreated control and confirms that mobility shifts caused by MMS are due to phosphorylation of PRD-4. (C) *prd-4*, like *hChk2*, complements loss of RAD53 in yeast. *S. cerevisiae* strain W2105-7b (*MATa leu2 sm1Δ::URA3 rad53Δ::HIS3 RAD5 W303*) (25) was transformed with empty plasmid vector (pBJ245), human Chk2 (pMH267) (18), or pBJ245 containing *S. cerevisiae* RAD53 or *Neurospora prd-4*, each under a galactose-inducible promoter.



Cloning and identification of the *prd-4* gene. A chromosomal walk from *arg-13* to *os-1* identified cosmids spanning the interval (13, 14), but the semidominance of the mutation, combined with inherent variability among heterokaryotic primary transformants, made it impossible to use transformation to identify *prd-4* (13). The DNA sequence spanning the interval between *arg-13* and *os-1* (15) revealed about 39 thousand base pairs (kbp) containing 12 predicted coding sequences (Fig. 1B). DNA sequencing of this interval from strains bearing the *prd-4* mutation consistently identified a single base-pair change in an open reading frame (ORF) close to *os-1* (Fig. 1, B and C). The ORF was deleted by homologous gene replacement [(16), see Methods in Supporting Online Material (SOM)], and this strain was used as the recipient in DNA transformation experiments to confirm that the point mutation was indeed responsible for the *prd-4* phenotype: We cloned the genomic fragment containing the gene and its promoter from the canonical *prd-4* mutant strain and transformed this fragment into a neutral chromosomal site in the knockout strain (Fig. 1D and SOM). Because primary transformants are heterokaryons having both transformed and nontransformed nuclei, we backcrossed a primary transformant to the deletion mutant and isolated homokaryotic progeny, some of which expressed the mutant PRD-4 protein (for example, strain 356-16) and thus carried the transgene (Fig. 1D). Such strains recapitulated both the short period length and altered temperature compensation phenotypes of *prd-4* (Fig. 1, E and F), which indicated that the transforming DNA contained the gene.

The semidominance of the original *prd-4* mutation is consistent with altered function or gain of function, as was the appearance of PRD-4 protein in the mutant. However, to our surprise, the *prd-4* deletion mutant displayed a period length similar to wild type's (Fig. 1E). This suggested the existence of functionally redundant gene(s), whose actions could compensate for the loss of PRD-4, or that the gain-of-function *prd-4* mutation might cause PRD-4 to acquire a novel function, specificity, or regulation with respect to the clock. Because *prd-4* null mutants are fully rhythmic, the gene is clearly not essential for basic clock function, but PRD-4 might connect other cellular processes to the circadian pacemaker.

***Neurospora crassa* PRD-4 protein is an ortholog of Chk2.** After processing to remove three introns, *prd-4* mRNA encodes a 702-amino acid protein bearing a forkhead-associated (FHA) domain followed by a serine-threonine protein kinase domain (Fig. 2A); this is an arrangement uniquely characteristic of a class of checkpoint kinases (17). BLAST searches identified PRD-4 as a *checkpoint kinase 2* (Chk2), with human checkpoint kinase 2 (hChk2) being the closest homolog (BLAST

score of e^{-72}). The sequences show 38% identity and 51% similarity over the FHA domain and 43% identity and 62% similarity over the kinase domain (fig. S1). A reciprocal search of the *Neurospora crassa* genome with different Chk2 sequences also identifies PRD-4 as the highest-scoring homolog. The mutation responsible for the *prd-4* phenotype results in a

change from serine to leucine at position 493 (S493L) within a highly conserved portion of the kinase domain (Fig. 2A and fig. S1).

In mammals, Chk2 links the DNA damage-activated kinases ATM (ataxia telangiectasia mutated) and ATR (ATM and Rad3-related) with checkpoint effectors in the cell cycle and DNA-repair machinery (18, 19). In addition, mutations

Fig. 3. PRD-4 participates in signaling DNA damage to the circadian clock via modification of FRQ. (A) Mutation of *prd-4* results in early phosphorylation of FRQ. Western blots of FRQ over 24 hours in the dark in *prd-4*⁺ and *prd-4*^{S493L} backgrounds. Electrophoresis was extended to accentuate the normal cycle in FRQ phosphorylation-induced mobility shifts (26). Light gray boxes highlight the largest difference in FRQ mobility between wt and *prd-4*^{S493L}. (B) Time course of FRQ phosphorylation after transfer in darkness from 4°C to 25°C to initiate synthesis of FRQ. FRQ mobility is decreased earlier in samples harvested from strains expressing PRD-4^{S493L}, which indicates premature phosphorylation of FRQ. Coom, Coomassie blue-stained gel (loading control). (See also fig. S2A.) (C) MMS-induced phosphorylation of FRQ requires PRD-4 and varies with circadian phase. *prd-4*⁺ (wt) and Δ *prd-4* (ko) strains were grown in liquid medium, in constant light at 25°C for 24 hours, before addition (+) or mock addition (–) of 0.1% MMS for 2 hours. In early evening (DD2) and subjective midday (DD16), FRQ is phosphorylated in response to MMS, which results in a mobility shift, but this is not seen in the Δ *prd-4* (ko) background. Note that after 6 hours in the dark (DD6, mid-subjective night), FRQ is normally highly phosphorylated, and MMS results in no additional shift.

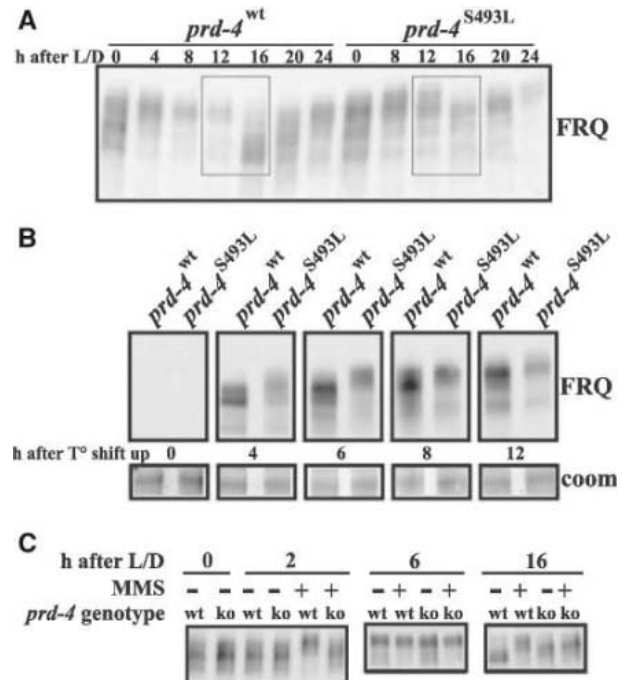
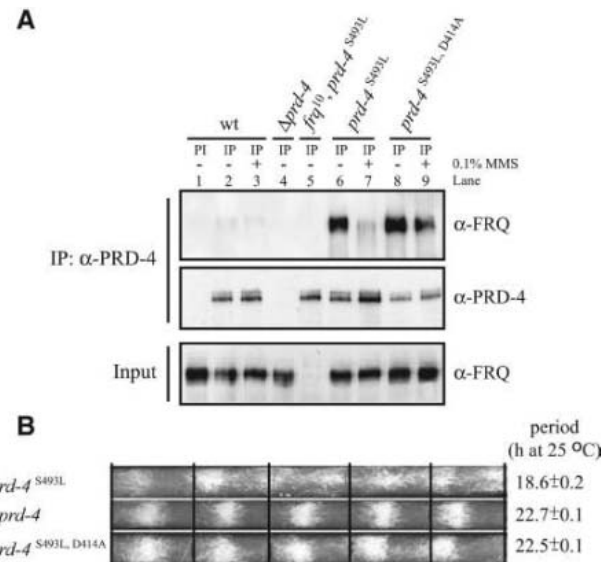


Fig. 4. PRD-4 interacts with FRQ in vivo. (A) Antisera recognizing PRD-4 specifically immunoprecipitate PRD-4 complexes containing FRQ from extracts made from clock-wild type (*prd-4*⁺) cultures following 2 hours treatment with and without 0.1% MMS. The FRQ-PRD-4 interaction is increased in *prd-4*^{S493L} and in the kinase-dead double mutant (*prd-4*^{S493L, D414A}). Immunoprecipitations from Δ *prd-4* and *frq* null (*frq*¹⁰, *prd-4*^{S493L}) provide negative controls. Input; total extract from wild type representing 3% of that used for immunoprecipitation (IP); PI, preimmune serum. (B) Race tubes of relevant strains. Although FRQ-PRD-4 interaction is preserved in the kinase-dead strain (A, lane 8), the period shortening effect on the clock is lost. Period estimates (\pm SD) are from three to six race tubes, each with five or six cycles.



in *Chk2* have been associated with human tumors, which qualifies the gene as a tumor suppressor (20). In many systems, *Chk2* acts by phosphorylating the phosphatases *Cdc25A* and *Cdc25C* (17). The phosphorylation of human *Cdc25C* on Ser²¹⁶ prevents it from dephosphorylating and thereby activating the *Cdc2*-cyclin B complexes required for entry into mitosis. *Chk2* can also phosphorylate, and thereby stabilize, *p53* (21, 22), which allows it to transactivate *p53* target genes and leads to sustained G₁ and G₂ arrest and/or apoptosis (17). To bring about these actions, *Chk2* is phosphorylated in response to DNA damage caused by ionizing radiation and by radiomimetic drugs like methylmethane sulfonate (MMS) (18, 23). Therefore, we treated *Neurospora* with 0.1% MMS and confirmed that, like other *Chk2*s, PRD-4 is phosphorylated in response to DNA

damage (Fig. 2B). In *Saccharomyces cerevisiae*, the sensitivity to MMS seen in *rad53Δ sml1Δ* double mutants (24, 25) is rescued by transformation with human *Chk2*, and this sensitivity has been used to show that RAD53 and hChk2 are homologs (18). We applied this functional test by expressing *prd-4* in a *rad53Δ sml1Δ S. cerevisiae* strain grown on media with and without MMS. As expected (18), the *rad53Δ sml1Δ* strain containing the plasmid vector alone is severely impaired by the presence of MMS in the medium (Fig. 2C, lane 2), but *Neurospora* PRD-4, like yeast Rad53 and human *Chk2*, can complement the *rad53* loss of function (Fig. 2C, lanes 1, 3, and 4), which demonstrates that PRD-4 can functionally substitute for Rad53. Thus, on the basis of strong sequence similarity, regulation, and both functional and physiological tests,

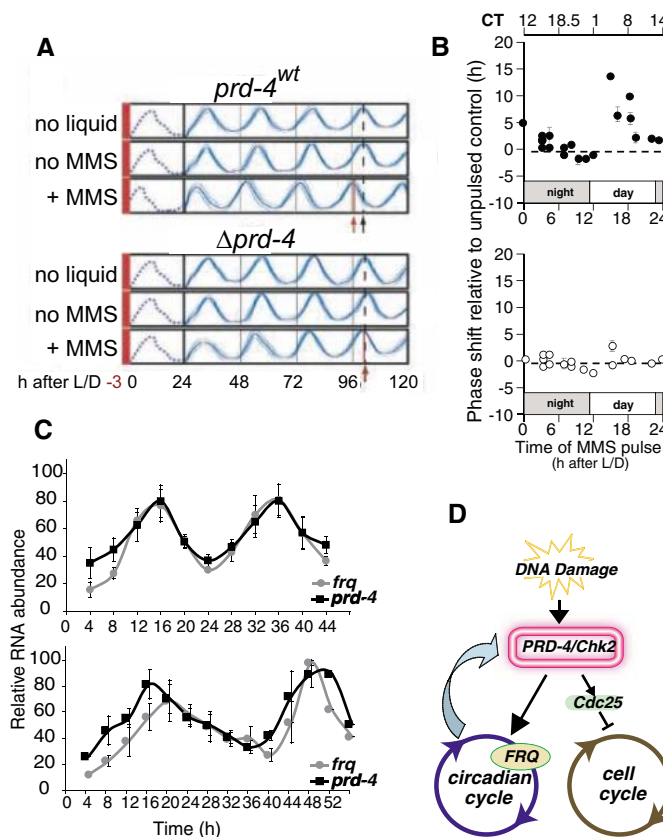
prd-4 encodes an ortholog of the cell cycle regulator *Chk2*.

PRD-4 signals DNA-damage information to the circadian clock. The semidominance of the original *prd-4^{S493L}* allele suggests that it could encode an inappropriately active kinase, and an obvious candidate for a clock-relevant substrate is the clock protein FRQ (1, 4). The phosphorylation profile of FRQ changes in a well-defined and characteristic manner through the day (26), but this characteristic pattern is altered in the *prd-4^{S493L}* mutant: FRQ is precociously phosphorylated during its daily cycle after a light-to-dark transfer (Fig. 3A), as well as after cycling is initiated by a temperature step (Fig. 3B and fig. S2A). Because the kinetics of FRQ phosphorylation and turnover determine period length (27), this early phosphorylation could account for the shortening of the FRQ cycle and the resulting short circadian cycle. A working model—activation of the checkpoint pathway via DNA damaging agents such as MMS might transmit a signal to the clock via FRQ—allows several predictions. First, treatment of *Neurospora* with γ radiation or a radiomimetic like MMS should result in activation of PRD-4, causing enhanced phosphorylation of FRQ; second, MMS-induced FRQ phosphorylation should be PRD-4-dependent and perhaps time-of-day dependent, because it would be superimposed on the daily circadian cycle of FRQ phosphorylation; and third, and most salient, activation of PRD-4/*Chk2* should reset the clock.

To test the first prediction, cultures were treated with MMS at three different times (Fig. 3C and fig. S2B). After 2 hours in darkness (DD2), FRQ is abundant but not fully phosphorylated, and treatment with MMS results in clearly enhanced FRQ phosphorylation; this is not seen in the Δ *prd-4* background which indicates that PRD-4 is required to mediate this effect. In the subjective night at DD6, FRQ is maximally phosphorylated just before its degradation (26), and addition of MMS has no further apparent effect, presumably because FRQ is already maximally phosphorylated. In the mid-subjective day (DD16), when FRQ is newly synthesized but has yet to be significantly phosphorylated, addition of MMS again results in a significant increase in FRQ phosphorylation that is dependent on PRD-4 function (Fig. 3C).

Immunoprecipitation was used to test whether PRD-4 physically interacted with FRQ (Fig. 4A). FRQ weakly associates with PRD-4 in clock wild-type vegetative cultures before and after MMS treatment (lanes 2 and 3), and association of FRQ with PRD-4^{S493L} is increased compared with wild type before DNA damage (lane 6). The interaction between FRQ and PRD-4 is attenuated after addition of MMS in the mutant, although it is difficult to determine whether this change is the same for the wild-type because of the weak interaction. A

Fig. 5. PRD-4 establishes a link between clock and cell cycle checkpoints. (A) MMS interferes with clock phasing in a PRD-4-dependent manner. Strains were treated (+0.1% MMS) or mock treated (no MMS) for 2 hours, allowed 1 hour to recover, and inoculated onto race tubes at 25°C in the dark. Strains never grown in liquid (no liquid) controlled for effects caused by manipulations (six race tubes per treatment). Densitometric scans are aligned by the 24-hour marks (solid vertical black lines). A dashed vertical line marks the peaks of the rhythm in controls on day 4, and a red line, the corresponding peak in the MMS-treated sample. Red bar shows the time of MMS-treatment recovery and dashed curve, growth before the first growth mark. **(B)** MMS resets the clock in a PRD-4-dependent and circadian phase-specific manner. The treatment described in (A) was carried out at different times of the subjective day for *prd-4*⁺ (top) and Δ *prd-4* (bottom) strains. Darkness from 0 to 11 hours corresponds to subjective night and from 11 to 22 hours to subjective day. Circadian times (CT) are indicated above. Data points represent phase \pm 1 SD, estimated from three to six race tubes compiled from four independent experiments. **(C)** *prd-4* is regulated by the circadian clock. Average relative level (\pm 2 SEM; for three to five independent time series) of *prd-4* (black) and *frq* mRNA (internal control, gray) determined by reverse transcriptase-polymerase chain reaction (RT-PCR) from samples collected over 2 days from both *frq*⁺ (top) (period length, 22 hours) and *frq*⁷ (bottom) (period length, 29 hours) cultures. **(D)** PRD-4 (as *Chk2*) is assumed to act through *Cdc25* in *Neurospora* as part of the well-established eukaryotic checkpoint pathway that senses DNA damage and signals arrest to the cell cycle. PRD-4 also signals DNA damage information to the clock, in part by modifying FRQ and shifting the rhythm. The circadian clock established by the FRQ negative-feedback loop regulates the circadian cycling of *prd-4* products, which establishes *prd-4* as an output or clock-controlled gene and describes a nested feedback loop closing around the circadian clock.



similar pattern of association before activation and diminution of binding following DNA damage has been reported for PML and BRCA1 in a mammalian system (28). These data, together with the short-period phenotype and precocious FRQ phosphorylation, suggest that the S493L mutation results in basal kinase activity that can be further stimulated by DNA damage resulting in hyperphosphorylation of its substrate (FRQ) and subsequent reduced association. Consistent with this, the association of PRD-4 with FRQ after MMS treatment is stronger when the D414A mutation (Asp⁴¹⁴ replaced by Ala, which eliminates kinase activity) is introduced into the S493L background (lanes 7 and 9), although it is clear that MMS treatment still results in reduced association between PRD-4 and FRQ. Effects on circadian timing (Fig. 4B) are also consistent with the molecular data and the working model: Strains bearing the PRD-4^{S493L, D414A} double mutations (increased association but catalytically inactive) have a wild-type clock, which strongly suggests that it is the precocious phosphorylation of FRQ (not just the increased interaction) that results in the characteristic short period of PRD-4^{S493L}. Additionally, these data establish a direct association between FRQ and PRD-4 (Chk2), which confirms the first and second predictions and leads to the third. Because changes in FRQ phosphorylation are known to affect the clock (4, 27), these data indicate that MMS might also do so.

To directly test the effect of a DNA-damaging agent on the circadian clock, *Neurospora* cultures were exposed to MMS for 2 hours immediately before the light to dark (L/D) transfer that normally sets the clock to subjective dusk and initiates circadian cycling. These cultures exhibited a 4-hour phase advance of the rhythm (with no effect on period) (Fig. 5A), consistent with an MMS-derived premature phosphorylation of FRQ; this clock effect was not seen in the *Aprd-4* strain (Fig. 5A). Next, strains were systematically exposed to MMS for short intervals at times scanning a full circadian cycle (Fig. 5B). MMS yielded large phase advances during the subjective day, beginning at the time FRQ first appears (26) and decreasing over the course of the day, in line with the normal course of FRQ phosphorylation as predicted from the previous data (Fig. 3C); that is, clock effects are seen only when MMS can result in enhanced FRQ phosphorylation. The phase of the rhythm was unaffected by MMS in the *Aprd-4* strain. Taken together, these data establish that DNA-damaging agents can act as strong clock-resetting cues and that PRD-4 (Chk2) is essential for mediating the effect of one of these, MMS, on the clock.

These results suggest that PRD-4 acts only when there is DNA damage and that it is an essential mediator of the effects of DNA damage on the clock. Although there is no precedent

for chemical mutagens resetting the clock, a growing body of knowledge supports a role for the clock in DNA-damage responses and tumor suppression (29) and for interrelationships between checkpoint kinases and clock components. For example, the human Timeless protein interacts with the cell cycle checkpoint protein Chk1 and the ATR-ATRIP complex (30), so this type of regulation may exist broadly in circadian systems.

In mammals, the clock protein Per2 regulates expression of tumor suppressor genes including p53; thus it may modulate sensitivity to DNA-damaging radiation and apoptosis in a circadian fashion (29). In addition, the gene encoding the cyclin B1-Cdc2 kinase regulator Wee1 is directly under circadian control in regenerating mouse liver (31). In fact, Chk2 in mammals controls cell cycle progression through regulation of Cdc25C, the same protein whose phosphorylation status and activity are modulated by the clock-controlled protein Wee1 (31). This parallel suggests that *prd-4* might be similarly clock-regulated: In fact, *prd-4* expression is regulated by the circadian clock, peaking in the subjective morning in parallel with *frq* (Fig. 5C).

This regulation of *prd-4* by the clock closes a loop: Circadian regulation of *prd-4* expression as an output of the clock could provide a time-of-day specific gate, albeit a weak one, for the ability of DNA-damaging agents to affect the clock (Fig. 5D). Strains bearing PRD-4^{S493L}, however, have partially bypassed the need for activation of the kinase and have lost the loop from output to input closing around the core FRQ/WCC circadian feedback loop. This explains the circadian regulation of *prd-4* expression, the PRD-4-dependent phase shift in response to MMS, and the effects of *prd-4*^{S493L} on the period length of the clock. The possibility of a cell cycle-related circadian output feeding back onto the clock can perhaps also be seen in hindsight in studies where inhibitors suggested a role for cyclin-dependent kinases in the *Bulla gouldiana* circadian system (32). Regulation through Chk2 is consistent with the increased incidence of tumors in Per2 mutant mice, because this connection seems to be mediated through effectors like p53, another protein regulated by Chk2. Altogether, a variety of data implicate Chk2 as an important upstream link between the clock and cell cycle checkpoints. Thus, as previously suggested (9, 29), the clock has a protective role in addition to its pacemaker functions: Corroborative experimental and medical evidence show a higher incidence of mammary tumors in rats subjected to constant light (33) and of breast cancer among shift workers (34), as well as circadian variations in effectiveness of anticancer treatments (35, 36). The suggestive coordination of the clock and cell division through cell cycle checkpoints might further support the

presumed ancient origin of clocks and their integral role in basic cell biology.

Note added in proof: Gery *et al.* (38) now report that, reminiscent of FRQ and PRD-4, the mammalian clock protein Per1 interacts with Chk2 and ATM both prior to and after DNA damage-induced activation, and that Per1 is needed for and promotes Chk2 activation. Although not therein examined, this result would be consistent with an effect on the mammalian clock initiated by DNA damage and effected via CHK2-mediated modification of clock proteins. Each study suggests that core clock proteins could act in tumor suppression, both through transcriptional control of cell cycle-related genes and through apparently conserved direct interactions with cell cycle checkpoint pathway proteins. All these data are consistent with an emerging role of circadian regulation in cancer.

References and Notes

- M. W. Young, S. A. Kay, *Nat. Rev. Genet.* **2**, 702 (2001).
- U. Schibler, P. Sassone-Corsi, *Cell* **111**, 919 (2002).
- J. C. Dunlap, in *Chronobiology: Biological Timekeeping*, J. C. Dunlap, J. J. Loros, P. Decoursey, Eds. (Sinauer Associates, Sunderland, MA, 2004), pp. 210–251.
- J. C. Dunlap, J. J. Loros, *J. Biol. Rhythms* **19**, 414 (2004).
- N. Preitner *et al.*, *Cell* **110**, 251 (2002).
- K. Lee, J. J. Loros, J. C. Dunlap, *Science* **289**, 107 (2000).
- C. Heintzen, J. J. Loros, J. C. Dunlap, *Cell* **104**, 453 (2001).
- L. Cardone, P. Sassone-Corsi, *Nat. Cell Biol.* **5**, 859 (2003).
- C. C. Lee, *Methods Enzymol.* **393**, 852 (2005).
- H. Okamura, *J. Biol. Rhythms* **19**, 388 (2004).
- G. F. Gardner, J. F. Feldman, *Plant Physiol.* **68**, 1244 (1981).
- J. F. Feldman, G. F. Gardner, R. A. Dennison, in *Biological Rhythms and their Central Mechanism*, M. Suda, Ed. (Elsevier, Amsterdam, 1979), pp. 57–66.
- Q. Liu, dissertation, Dartmouth (1991).
- B. D. Aronson, K. A. Johnson, Q. Liu, J. C. Dunlap, *Chronobiol. Int.* **9**, 231 (1992).
- J. Galagan *et al.*, *Nature* **422**, 859 (2003).
- H. Colot *et al.*, *Proc. Natl. Acad. Sci. U.S.A.* **103**, 10352 (2006).
- J. Bartek, J. Falck, J. Lukas, *Nat. Rev. Mol. Cell Biol.* **2**, 877 (2001).
- S. Matsuoka, M. Huang, S. J. Elledge, *Science* **282**, 1893 (1998).
- A. Sancar, L. A. Lindsey-Boltz, K. Unsal-Kacmaz, S. Linn, *Annu. Rev. Biochem.* **73**, 39 (2004).
- S. Matsuoka *et al.*, *Cancer Res.* **61**, 5362 (2001).
- N. H. Chehab, A. Malikzay, M. Appel, T. D. Halazonetis, *Genes Dev.* **14**, 278 (2000).
- A. Hirao *et al.*, *Science* **287**, 1824 (2000).
- J. Falck, N. Mailand, R. G. Syljuasen, J. Bartek, J. Lukas, *Nature* **410**, 842 (2001).
- B. A. Desany, A. A. Alcasabas, J. B. Bachant, S. J. Elledge, *Genes Dev.* **12**, 2956 (1998).
- X. Zhao, E. G. Muller, R. Rothstein, *Mol. Cell* **2**, 329 (1998).
- N. Garceau, Y. Liu, J. J. Loros, J. C. Dunlap, *Cell* **89**, 469 (1997).
- Y. Liu, J. Loros, J. C. Dunlap, *Proc. Natl. Acad. Sci. U.S.A.* **97**, 234 (2000).
- J. Ahn, M. Urist, C. Prives, *DNA Repair (Amst.)* **3**, 1039 (2004).

29. L. Fu, H. Pelicano, J. Liu, P. Huang, C.-C. Lee, *Cell* **111**, 41 (2002).
30. K. Unsal-Kacmaz, T. E. Mullen, W. K. Kaufmann, A. Sancar, *Mol. Cell. Biol.* **25**, 3109 (2005).
31. T. Matsuo *et al.*, *Science* **302**, 255 (2003).
32. N. A. Krucher, L. Meije, M. H. Roberts, *Cell. Mol. Neurobiol.* **17**, 495 (1997).
33. L. E. Anderson, J. E. Morris, L. B. Sasser, R. G. Stevens, *Cancer Lett.* **148**, 121 (2000).
34. J. Hansen, *Epidemiology* **12**, 74 (2001).
35. W. J. Hrushesky, *J. Control. Release* **74**, 27 (2001).
36. G. A. Bjarnason, R. Jordan, *Prog. Cell Cycle Res.* **4**, 193 (2000).
37. www.fgsc.net/fgn47/lgi.htm.
38. S. Gery, N. Komatsu, L. Baldjyan, A. Yu, D. Koo, H. P. Koeffler, *Mol. Cell* **22**, 375 (2006).
39. Supported by grants from the NIH (MH44651 to J.C.D. and J.J.L. and R37GM34985 to J.C.D.), NSF (MCB-0084509 to J.J.L.), and the Norris Cotton Cancer Center core grant to Dartmouth Medical School. We thank R. Rothstein for yeast strain W2105-7b, S. Elledge for plasmid pMH267, and both for helpful discussions.

Supporting Online Material

www.sciencemag.org/cgi/content/full/1121716/DC1
Materials and Methods
Figs. S1 and S2
References

24 October 2005; accepted 11 May 2006
Published online 29 June 2006;
10.1126/science.1121716
Include this information when citing this paper.

REPORTS

Imaging the Mott Insulator Shells by Using Atomic Clock Shifts

Gretchen K. Campbell,^{1*} Jongchul Mun,¹ Micah Boyd,¹ Patrick Medley,¹ Aaron E. Leanhardt,² Luis G. Marcassa,^{1†} David E. Pritchard,¹ Wolfgang Ketterle¹

Microwave spectroscopy was used to probe the superfluid–Mott insulator transition of a Bose-Einstein condensate in a three-dimensional optical lattice. By using density-dependent transition frequency shifts, we were able to spectroscopically distinguish sites with different occupation numbers and to directly image sites with occupation numbers from one to five, revealing the shell structure of the Mott insulator phase. We used this spectroscopy to determine the onsite interaction and lifetime for individual shells.

The Mott insulator (MI) transition is a paradigm of condensed matter physics, describing how electron correlations can lead to insulating behavior even for partially filled conduction bands. However, this behavior requires a commensurate ratio between electrons and sites. If this condition for the density is not exactly fulfilled, the system will be conductive. For neutral bosonic particles, the equivalent phenomenon is the transition from a superfluid to an insulator for commensurate densities. In inhomogeneous systems, as in atom traps, the condition of commensurability no longer applies: For sufficiently strong interparticle interactions, it is predicted that the system should separate into MI shells with different occupation number, separated by thin superfluid layers (1–3).

The recent observation of the superfluid-to-MI transition with ultracold atoms (4) has stimulated a large number of theoretical and experimental studies [(5) and references therein]. Atomic systems allow for a full range of control of the experimental parameters, including tunability of the interactions and defect-free preparation, making them attractive systems for studying condensed matter phenomena. The MI

phase in ultracold atoms has been characterized by studies of coherence, excitation spectrum, noise correlations (4, 6, 7), and molecule formation (8). Recently, by using spin-changing collisions, Gerbier *et al.* selectively addressed lattice sites with two atoms and observed the suppression of number fluctuations (9).

In this study, we combined atoms in the MI phase with the high-resolution spectroscopy used for atomic clocks and used density-dependent transition frequency shifts to spectroscopically resolve the layered structure of the Mott shells with occupancies from $n = 1$ to $n = 5$ and to directly image their spatial distributions.

Bosons with repulsive interactions in an optical lattice can qualitatively be described by the Hamiltonian (10, 1),

$$\hat{H} = -J \sum_{\langle i,j \rangle} \hat{a}_i^\dagger \hat{a}_j + \frac{1}{2} U \sum_i \hat{n}_i (\hat{n}_i - 1) + \sum_i (\epsilon_i - \mu) \hat{n}_i \quad (1)$$

where the first two terms are the usual Hamiltonian for the Bose-Hubbard model, the last term adds in the external trapping potential, and J is the tunneling term between nearest neighbors, \hat{a}_i^\dagger and \hat{a}_i are the boson creation and destruction operators at a given lattice site. $U = (4\pi\hbar^2 a/m) \int |w(x)|^4 d^3x$ is the repulsive onsite interaction, where \hbar is Planck's constant divided by 2π , m is the atomic mass, a is the s-wave scattering length, $w(x)$ is the single particle Wannier function localized to the i th lattice site, and $\hat{n}_i = \hat{a}_i^\dagger \hat{a}_i$ is the number operator for bosons

at site i . The last term in the Hamiltonian is due to the external trapping confinement of the atoms, where $\epsilon_i = V_{\text{ext}}(r_i)$ is the energy offset at the i th site due to the external confinement and μ is the chemical potential.

The behavior of this system is determined by the ratio J/U . For low lattice depths, the ratio is large and the system is superfluid. For larger lattice depths, the repulsive onsite energy begins to dominate, and the system undergoes a quantum phase transition to a MI phase. For deep lattices, the atoms are localized to individual lattice sites with integer filling factor n . This filling factor varies locally depending on the local chemical potential $\mu_i = \mu - \epsilon_i$ as

$$n = \text{Mod}(\mu_i/U) \quad (2)$$

where Mod is the modulo and decreases from the center to the edge of the trap.

To prepare the atoms in the Mott insulating phase, we first created a ⁸⁷Rb Bose-Einstein condensate in the the $|F = 1, m_F = -1\rangle$ state (where F and m_F are the quantum numbers for the total spin and its t component, respectively) by using a combination of an Ioffe-Pritchard magnetic trap and an optical dipole trap. The optical trap was oriented perpendicular to the long axis of the magnetic trap, creating a more isotropic trapping potential that was better matched to the optical lattice. The laser beam for the optical trap had a $1/e^2$ waist $\approx 70 \mu\text{m}$ and was retroreflected. However, the polarization of the retroreflected beam was rotated such that the interference between the two beams had minimal contrast. The resulting trap had radial and axial trap frequencies of $\omega = 2\pi \times 70 \text{ Hz}$ and $\omega = 2\pi \times 20 \text{ Hz}$, respectively, where the axial direction is now parallel to the optical trap. A three-dimensional (3D) optical lattice was created by adding two additional retroreflected laser beams derived from the same laser at $\lambda = 1064 \text{ nm}$. The lattice was adiabatically ramped up by rotating the polarization of the retroreflected optical trapping beam to increase the interference contrast along that axis and by increasing the laser power in the other two axes. The lattice depth was increased by using an exponential ramp with a 40-ms time constant. After ramping on the lattice, all three beams were linearly polarized orthogonal to each other and

¹MIT-Harvard Center for Ultracold Atoms, Research Laboratory of Electronics, Department of Physics, Massachusetts Institute of Technology, Cambridge, MA 02139, USA. ²JILA, Boulder, CO 80309, USA.

*To whom correspondence should be addressed. E-mail: gcampbel@mit.edu

†Permanent address: Instituto de Física de São Carlos, University of São Paulo, São Paulo 13560-970, Brazil.

had different frequency detunings generated by using acousto-optic modulators. The lattice depth was up to $40E_{\text{rec}}$, where $E_{\text{rec}} = \hbar^2 k^2 / 2m$ is the recoil energy and $k = 2\pi/\lambda$ is the wave vector of the lattice light. At $40E_{\text{rec}}$, the lattice trap frequency at each site was $\omega_{\text{lat}} = 2\pi \times 25$ kHz, and the external trap frequencies increased to $\omega = 2\pi \times 110$ Hz and $\omega = 2\pi \times 30$ Hz in the radial and axial directions, respectively.

Zeeman shifts and broadening of the clock transition from the $F = 1$ to the $F = 2$ state were avoided by using a two-photon transition between the $|1, -1\rangle$ state and the $|2, 1\rangle$ state, where at a magnetic bias field of ~ 3.23 G both states have the same first-order Zeeman shift (11). The two-photon pulse was composed of one microwave photon at a fixed frequency of 6.83 GHz and one radio frequency (rf) photon at a frequency of around 1.67 MHz. The pulse had a duration of 100 ms, and when on resonance the fraction of atoms transferred to the $|2, 1\rangle$

state was less than 20%. After the pulse, atoms in the $|2, 1\rangle$ state were selectively detected with absorption imaging by using light resonant with the $5^2S_{1/2}|2, 1\rangle \rightarrow 5^2P_{3/2}|3, 1\rangle$ transition. For observing the spatial distribution of the Mott shells, we imaged the atoms in the trap. For recording spectra, we released the atoms from the trap and imaged them after 3 ms of ballistic expansion in order to reduce the column density.

When the two-photon spectroscopy is performed on a trapped condensate without a lattice, the atoms transferred to the $|2, 1\rangle$ state have a slightly different mean field energy because of the difference between a_{21} and a_{11} scattering lengths, where a_{21} is the scattering length between two atoms in states $|2, 1\rangle$ and $|1, -1\rangle$ and a_{11} is the scattering length between two atoms in the $|1, -1\rangle$ state. This difference in scattering lengths leads to a density-dependent shift to the resonance frequency, $\Delta\nu \propto \rho(a_{21} - a_{11})$, where ρ is the condensate density (11). This collisional

shift is commonly referred to as the clock shift (12) because of its importance in atomic clocks, where cold collisions currently limit the accuracy (13, 14). When performed on a condensate with peak density ρ_0 in a harmonic trap in the limit of weak excitation, the line shape for the two-photon resonance is given by (15):

$$I(\nu) = \frac{15h(\nu - \nu_0)}{4\rho_0\Delta E} \sqrt{1 - \frac{h(\nu - \nu_0)}{\rho_0\Delta E}} \quad (3)$$

where ν_0 is the hyperfine transition frequency and the mean field energy difference is

$$\Delta E = \frac{\hbar^2}{\pi m} (a_{21} - a_{11}) \quad (4)$$

In the case of ^{87}Rb , $a_{21} = 5.19$ nm and $a_{11} = 5.32$ nm (16). Both the frequency shift and the linewidth increase with the condensate density. As the lattice is ramped on, the peak density of the condensate in a given lattice site increases as

$$\rho_0(r) = \left(\mu - \frac{1}{2} m \omega_{\text{trap}}^2 r^2 \right) / U \quad (5)$$

where ω_{trap} is the external trap frequency for the combined magnetic and optical trap, and, by using the Thomas-Fermi approximation μ , the chemical potential, is given by

$$\mu = \left[\frac{15}{16} \frac{(\lambda/2)^3 m^{3/2} N U \omega_{\text{trap}}^3}{\sqrt{2\pi}} \right]^{2/5} \quad (6)$$

where N is the total atom number. For low lattice depths, the system is still a superfluid, delocalized over the entire lattice. However, the two-photon resonance line is shifted and broadened because of the increased density, with the center of the resonance at $\nu = \nu_0 + 2\rho_0\Delta E/3h$. For deep lattices in the MI regime, the repulsive onsite interaction dominates, number fluctuations are suppressed, and each lattice site has a sharp resonance frequency determined by the occupation number in the site. The separation between

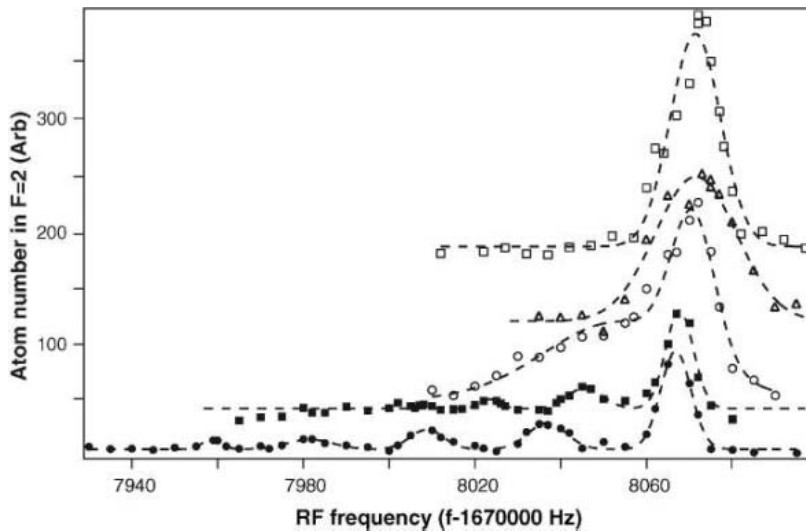
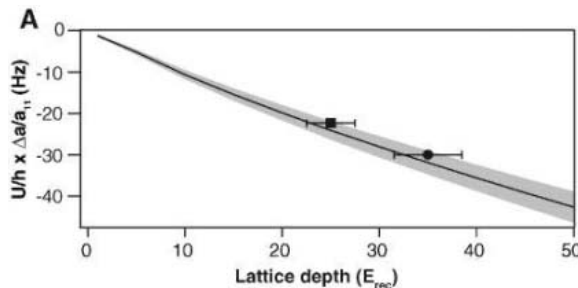


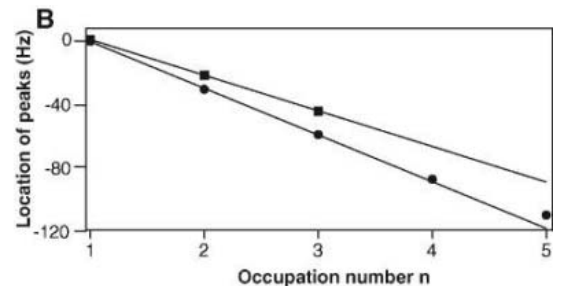
Fig. 1. Two-photon spectroscopy across the superfluid-to-MI transition. Spectra for 3D lattice depths of $0E_{\text{rec}}$ (open squares), $5E_{\text{rec}}$ (open triangles), $10E_{\text{rec}}$ (open circles), $25E_{\text{rec}}$ (solid squares), and $35E_{\text{rec}}$ (solid circles) are shown. The spectra are offset for clarity. The shift in the center of the $n = 1$ peak as the lattice depth is increased is due to the differential AC Stark shift from the lattice. The dotted lines show Gaussian fits of the peaks.

Fig. 2. Probing the onsite interaction energy.

(A) The separation between the $n = 1$ and $n = 2$ peaks is shown for lattice depths of $V = 25E_{\text{rec}}$ (square) and $V = 35E_{\text{rec}}$ (circle). As the lattice depth was increased, the separation increased from 22(1) Hz to 30(1) Hz. The shaded



area gives the expected value determined from a band structure calculation, including the uncertainty in the scattering lengths. The uncertainty in the measured separation is indicated by the size of the points. (B) Location of resonances for all MI phases relative to the $n = 1$ phase for $V = 25E_{\text{rec}}$ and $V = 35E_{\text{rec}}$. For low site occupation (n values



from 1 to 3), the separation between the resonances is roughly constant, implying constant U . For $V = 35E_{\text{rec}}$, the separation between the $n = 4$ and $n = 5$ peaks was 22(2) Hz, a 27% decrease from the 30(1) Hz separation between the $n = 1$ and $n = 2$ peaks. The slope of the lines is fit to the separation between the $n = 1$ and $n = 2$ peaks.

the resonance frequencies for the n and $n - 1$ MI phases is given by

$$\delta\nu = \frac{U}{h}(a_{21} - a_{11})/a_{11} \quad (7)$$

The linewidth of the resonances is no longer broadened by the inhomogeneous density and should be limited only by the bandwidth of the two-photon pulse.

The resonance transitioned from a broadened line to several sharp lines as the lattice depth was increased (Fig. 1). At a lattice depth of $V = 5E_{\text{rec}}$, the line was broadened and the line center was shifted slightly because of the increased density. At $V = 10E_{\text{rec}}$, the line was shifted and broadened further, and in addition the line shape became asymmetric as the atom number in lattice sites with small occupation was squeezed. For deeper lattice depths, the system underwent a phase transition to a MI phase, and discrete peaks appeared, corresponding to MI phases with different filling factors; for $V = 35E_{\text{rec}}$, MI phases with occupancies of up to five were observed.

When the lattice depth was increased inside the MI regime (from $V = 25E_{\text{rec}}$ to $V = 35E_{\text{rec}}$), the separation between the resonance peaks increased, presumably because of the larger onsite interaction energy as the lattice trap was increased. As given in Eq. 7, the separation between the peaks provides a direct measurement of the onsite interaction energy, U . Our results are in good agreement with calculated values of U (Fig. 2A). Although the separation between the $n = 1$, $n = 2$, and $n = 3$ peaks is roughly constant, for higher filling factors the separation between the peaks decreases; the effective onsite interaction energy becomes smaller for higher filling factors (Fig. 2B). This result shows that for low occupation numbers the atoms occupy the ground state wave function of the lattice site, whereas for larger occupation numbers, the repulsive onsite interaction causes the wave function to spread out, lowering the interaction energy. From a variational calculation of the wave function similar to (17), we

find that the onsite energy for the $n = 5$ shell should be $\sim 20\%$ smaller than that for the $n = 1$ shell, in agreement with the measured value (Fig. 2B).

The peaks for the different occupation numbers were spectrally well separated. Therefore, on resonance, only atoms from a single shell were transferred to the $|2, 1\rangle$ state. An image of these atoms (without any time of flight) shows the spatial distribution of this shell. Figure 3B shows absorption images for $n = 1$ to $n = 5$ shells. As predicted (1), the $n = 1$ MI phase appears near the outer edge of the cloud. For larger n , the radius of the shell decreases, and the $n = 5$ sites form a core in the center of the cloud. The expected radius for each shell was obtained from Eq. 2 by using the measured values for the onsite interaction. The observed radii were in good agreement except for the $n = 1$ shell, which may have been affected by anharmonicities in the external trap. Absorption images taken with rf values between the peaks show a small signal, which may reflect the predicted thin superfluid layers between the insulating shells; however, this needs to be studied further with improved signal-to-noise ratio. The expected absorption

image of a shell should show a column density with a flat distribution in the center and raised edges. However, because of limitations (resolution and residual fringes) in our imaging system, these edges were not resolved.

Because we were able to address the different MI phases separately, we could determine the lifetime for each shell. For this, the atoms were first held in the lattice for a variable time τ before applying the 100-ms two-photon pulse. For the $n = 1$ MI phase and ignoring technical noise, the lifetime should only be limited by spontaneous scattering from the lattice beams. Even for the deepest lattices, the spontaneous scattering rate is less than 10^{-2} Hz. For the $n = 2$ MI phase, the lifetime is limited by dipolar relaxation, which for ^{87}Rb is slow, with a rate $< 10^{-2}$ Hz. For sites with $n \geq 3$, the lifetime is limited by three-body recombination with a rate equal to $\gamma n(n-1)(n-2)$ (18), with $\gamma = 0.026$ Hz for our parameters. This gives three-body lifetimes of τ_{3B} of 6.2 s, 1.6 s, and 0.6 s for the $n = 3$, $n = 4$, and $n = 5$ MI phases, respectively. This calculation of γ assumes for the density distribution the ground state of the harmonic oscillator potential, so for higher filling factors the actual lifetime could be higher. We

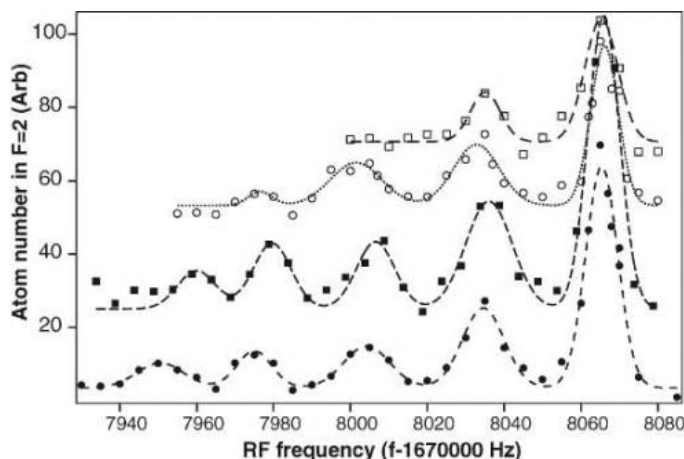


Fig. 4. Lifetime of individual MI shells. The lifetime for each MI phase can be measured independently by adding a hold time before applying the two-photon pulse. Spectra are shown for hold times of 0 ms (solid circles), 100 ms (solid squares), 400 ms (open circles), and 2000 ms (open squares). The lattice depth was $V = 35E_{\text{rec}}$ except for the 100-ms hold time, for which it was $V = 34E_{\text{rec}}$. The lines show Gaussian fits to the peaks, and the spectra were offset for clarity.

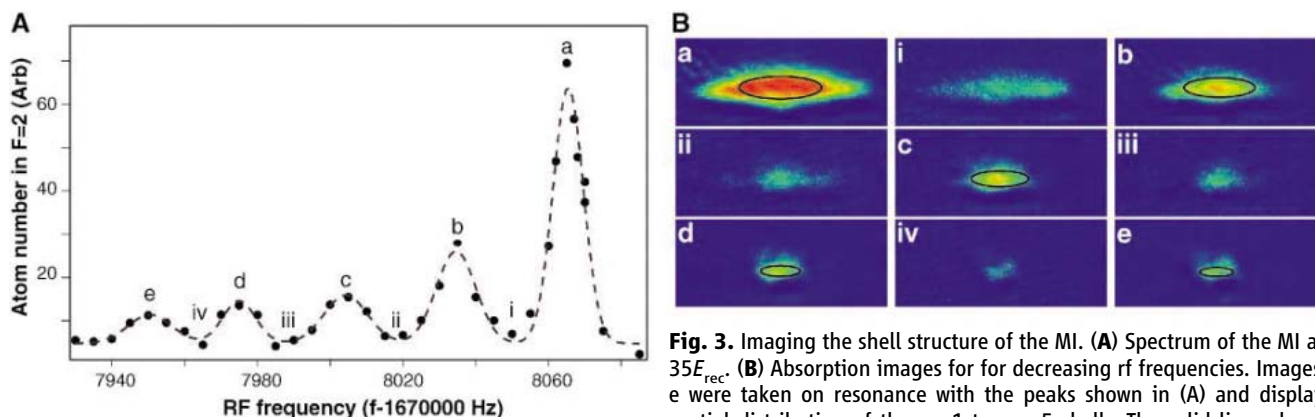


Fig. 3. Imaging the shell structure of the MI. (A) Spectrum of the MI at $V = 35E_{\text{rec}}$. (B) Absorption images for decreasing rf frequencies. Images a to e were taken on resonance with the peaks shown in (A) and display the spatial distribution of the $n = 1$ to $n = 5$ shells. The solid lines show the predicted contours of the shells. Absorption images taken for rf frequencies between the peaks (images i to iv) show a much smaller signal. The field of view was $185 \mu\text{m}$ by $80 \mu\text{m}$.

show relative populations as a function of the hold time and derive lifetimes as τ almost equal to 1 s, 0.5 s, and 0.2 s for the $n = 3$, $n = 4$, and $n = 5$ MI phases, respectively (Fig. 4); this is shorter than predicted, which is possibly due to secondary collisions. For $n = 1$ and $n = 2$, lifetimes of over 5 s were observed.

We expect that this method can be used to measure the number statistics as the system undergoes the phase transition. One would expect that the spectral peaks for higher occupation number become pronounced only at higher lattice depth; an indication of this can be seen already in Fig. 1. For low lattice depths, the tunneling rate is still high, but one can suddenly increase the lattice depth and freeze in populations (19), which can then be probed with high-resolution spectroscopy. Fluctuations in the atom number could identify the superfluid layers between the Mott shells. In addition, by applying a magnetic gradient across the lattice, tomographic slices could be selected, combining full 3D resolution with spectral resolution of the site occupancy. These techniques may address questions about local properties that have been raised in recent theoretical simulations (20). The addressability of

individual shells could be used to create systems with only selected occupation numbers (e.g., by removing atoms in other shells). Such a preparation could be important for the implementation of quantum gates, for which homogenous filling is desirable. For atoms other than rubidium, atomic clock shifts are much larger, e.g., for sodium, larger by a factor of 30. Therefore, it should be easier to resolve the MI shells, unless the collisional lifetime of the upper state of the clock transition sets a severe limit to the pulse duration.

Note added in proof: After submission of this work, the vertical profile of an $n = 2$ MI shell was obtained by using spin-changing collisions and a magnetic resonance imaging technique (21).

References and Notes

1. D. Jaksch, C. Bruder, J. I. Cirac, C. W. Gardiner, P. Zoller, *Phys. Rev. Lett.* **81**, 3108 (1998).
2. G. G. Batrouni *et al.*, *Phys. Rev. Lett.* **89**, 117203 (2002).
3. B. Marco, C. Lannert, S. Vishveshwara, T. C. Wei, *Phys. Rev. A* **71**, 063601 (2005).
4. M. Greiner, O. Mandel, T. Esslinger, T. W. Hänsch, I. Bloch, *Nature* **415**, 39 (2002).
5. I. Bloch, *Nature Phys.* **1**, 23 (2005).
6. T. Stöferle, H. Moritz, C. Schori, M. Köhl, T. Esslinger, *Phys. Rev. Lett.* **92**, 130403 (2004).

7. S. Fölling *et al.*, *Nature* **434**, 481 (2005).
8. T. Volz *et al.*, published online 8 May 2006 (<http://arxiv.org/abs/cond-mat?paperum=0605184>).
9. F. Gerbier, S. Fölling, A. Widera, O. Mandel, I. Bloch, *Phys. Rev. Lett.* **96**, 090401 (2006).
10. M. P. A. Fisher, P. B. Weichman, G. Grinstein, D. S. Fisher, *Phys. Rev. B* **40**, 546 (1989).
11. D. M. Harber, H. J. Lewandowski, J. M. McGuirk, E. A. Cornell, *Phys. Rev. A* **66**, 053616 (2002).
12. K. Gibble, S. Chu, *Phys. Rev. Lett.* **70**, 1771 (1993).
13. C. Fertig, K. Gibble, *Phys. Rev. Lett.* **85**, 1622 (2000).
14. Y. Sortais *et al.*, *Phys. Scr.* **195**, 50 (2001).
15. J. Stenger *et al.*, *Phys. Rev. Lett.* **82**, 4569 (1999).
16. E. G. M. van Kempen, S. J. J. M. F. Kokkelmans, D. J. Heinzen, B. J. Verhaar, *Phys. Rev. Lett.* **88**, 093201 (2002).
17. G. Baym, C. J. Pethick, *Phys. Rev. Lett.* **76**, 6 (1996).
18. M. W. Jack, M. Yamashita, *Phys. Rev. A* **67**, 033605 (2005).
19. M. Greiner, O. Mandel, T. W. Hänsch, I. Bloch, *Nature* **419**, 51 (2002).
20. O. Gygi, H. G. Katzgraber, M. Troyer, S. Wessel, G. G. Batrouni, *Phys. Rev. A* **73**, 063606 (2006).
21. S. Fölling, A. Widera, T. Mueller, F. Gerbier, I. Bloch, published online 23 June 2006 (<http://arxiv.org/abs/cond-mat?paperum=0606592>).
22. The authors thank I. Bloch and S. Fölling for insightful discussions. This work was supported by NSF. L.G.M. also acknowledges support from Fundação de Apoio a Pesquisa do Estrado de São Paulo.

23 May 2006; accepted 7 July 2006
10.1126/science.1130365

Evidence for a Past High-Eccentricity Lunar Orbit

Ian Garrick-Bethell,* Jack Wisdom, Maria T. Zuber

The large differences between the Moon's three principal moments of inertia have been a mystery since Laplace considered them in 1799. Here we present calculations that show how past high-eccentricity orbits can account for the moment differences, represented by the low-order lunar gravity field and libration parameters. One of our solutions is that the Moon may have once been in a 3:2 resonance of orbit period to spin period, similar to Mercury's present state. The possibility of past high-eccentricity orbits suggests a rich dynamical history and may influence our understanding of the early thermal evolution of the Moon.

The Moon is generally thought to have accreted close to the Earth and migrated outward in a synchronously locked low-eccentricity orbit. During the early part of this migration, the Moon was cooling and continually subjected to tidal and rotational stretching. The principal moments of inertia $A < B < C$ of any satellite are altered in a predictable way by deformation due to spin and tidal attraction. The moments are typically characterized by ratios that are easier to measure, namely, the libration parameters $\beta = (C - A)/B$ and $\gamma = (B - A)/C$, and the degree-2 spherical-harmonic gravity coefficients $C_{20} = (2C - B - A)/(2Mr^2)$ and $C_{22} = (B - A)/(4Mr^2)$, where M and r are the satellite mass and radius. Of these four values

β , γ , and C_{20} can be taken as independent. Using the ratio $(C - A)/A$, Laplace was the first to observe that the lunar moments are not in equilibrium with the Moon's current orbital state (1). He did not, however, address the possibility of a "fossil bulge," or the frozen remnant of a state when the Moon was closer to the Earth. Sedgwick examined the lunar moments in 1898, as did Jeffreys in 1915 and 1937, and both authors effectively showed that β is too large for the current orbit, suggesting that the Moon may carry a fossil bulge (2–5). However, Jeffreys showed that the fossil hypothesis might be untenable because the ratio of $\gamma/\beta = 0.36$ does not match the predicted ratio of 0.75 for a circular synchronous orbit (equivalently, $C_{20}/C_{22} = 9.1$, instead of the predicted ratio of 3.33). Indeed, using data from (6), none of the three independent measures of moments represent a low-eccentricity synchronous-orbit hydrostatic form; $C_{20} = 2.034 \times 10^{-4}$ is 22 times too large for the current state, and $\beta =$

6.315×10^{-4} and $\gamma = 2.279 \times 10^{-4}$ are 17 and 8 times too large, respectively (7, 8).

The inappropriate ratio of γ/β or C_{20}/C_{22} has led some to dismiss the fossil bulge hypothesis as noise due to random density anomalies (9, 10). However, the power of the second-degree harmonic gravity field is anomalously high when compared to the power expected from back extrapolating the power of higher harmonics (7, 11). This suggests that the bulge may be interpreted as a signal of some process. Degree-2 mantle convection has been proposed as a means of deforming the Moon (12, 13), but the dissimilarity of all three principal moments violates the symmetry of any simple degree-2 convection model (12). The Moon's center-of-mass/center-of-figure offset influences the moment parameters slightly, but that problem is geophysically separate and mathematically insignificant to the degree-2 problem (8, 14).

Because C_{20} is due primarily to rotational flattening, and C_{22} is due to tidal stretching, the high C_{20}/C_{22} ratio seems to imply that the Moon froze in its moments while rotating faster than synchronous. However, in such cases no constant face would be presented to the Earth for any C_{22} power to form in a unique lunar axis. This apparent dilemma can be avoided by considering that in any eccentric orbit with an orbit period to spin period ratio given by $n:2$, with $n = 2, 3, 4, \dots$, the passage through pericenter results in higher C_{22} stresses throughout a single elongated axis (hereafter called the pericenter axis). When the stresses experienced over one orbit period are time-averaged, the highest stresses

Department of Earth, Atmospheric and Planetary Sciences, Massachusetts Institute of Technology, 77 Massachusetts Avenue, Cambridge, MA 02139, USA.

*To whom correspondence should be addressed. E-mail: iang@mit.edu

will still appear in the pericenter axis, despite the shorter dwell time near pericenter. This is because, with respect to orbital distance, the tidal forces acting near pericenter increase faster than the decrease in time spent near pericenter.

Higher average stresses can form a C_{22} semipermanent bulge through the pericenter axis because higher stresses lead to increased strain rate. Therefore, for lunar material having both viscous and elastic properties (e.g., approximated as a Maxwell material), any higher time-averaged stresses will accumulate as higher strains, as long as the material's relaxation time is substantially longer than the period of the orbit. Because the young lunar surface must at some point cool from a liquid to a solid, it will certainly pass through a state in which the relaxation time exceeds the orbit period. This pericenter axis deformation process will also take place for a high-eccentricity synchronous orbit, where strong librational tides move the location of the C_{22} bulge over the lunar sphere, but on average the pericenter axis still attains the highest stresses.

Eventually, a semipermanent bulge that is stable on time scales of the lunar orbit must be made permanent over billions of years. The lithosphere's ability to support degree-2 spherical harmonic loads for >4 billion years is well established by theoretical calculations (15), and the overcompensation of large-impact basins suggests that the Moon has supported substantial lithospheric loads from an early time (16). The transition between the state of short and long relaxation time must also happen relatively quickly for the shape to record a particular orbital configuration. Recent isotope studies have indicated that the lunar magma ocean crystallized about 30 to 100 million years after lunar formation (17), and Zhong and Zuber showed that a degree-2 deformation on a 100-million-year-old lithosphere will relax only 20% of its initial deformation after 4 billion years (15). Therefore, a conservatively late estimate of the start of bulge freeze-in, if it took place, would be between 100 and 200 million years after lunar formation. We can obtain a rough estimate of the location of the Moon at this time by using established equations for the evolution of zero-eccentricity synchronous orbits (18, 19). With a current Earth potential Love number of $k \approx 0.3$, and the quality factor for a modern oceanless Earth, $Q_{\text{Earth}} = 280$ (20), the Moon reaches a semimajor axis of $24 r_E$ (Earth radii) by ~ 100 million years and $27 r_E$ by 200 million years. Therefore, over a 100-million-year time scale for fossil freeze-in, the orbit does not appreciably evolve. It will also be shown that these semimajor axis estimates are consistent with the observed libration parameters and second-degree gravity harmonics, and that our solutions permit an average fossil

to develop during orbit evolution. Without better constraints on k and Q for the early Moon and Earth, and the evolution of eccentric and higher resonance orbits, no existing data rule out the development of a strong lithosphere on the relevant time scales.

To calculate eccentric orbits that may generate the time-averaged values of the three independent parameters β , γ , and C_{20} , we write the time-averaged tidal potential in each of three principal axes

$$\begin{aligned} \langle U_{t,\hat{a}} \rangle &= \frac{-GMr^2}{a^3} \left(\frac{3}{4} X_{-3,p,q}(e) + \frac{1}{4} \right) \\ \langle U_{t,\hat{b}} \rangle &= \frac{GMr^2}{a^3} \left(\frac{3}{4} X_{-3,p,q}(e) - \frac{1}{4} \right) \\ \langle U_{t,\hat{c}} \rangle &= \frac{GMr^2}{2a^3} X_{-3,0,0}(e) \end{aligned} \quad (1)$$

where G is the gravitational constant; M is the Earth mass; r is the mean lunar radius (1738 km); a is the orbital semimajor axis; and \hat{a} , \hat{b} , and \hat{c} refer to the principal lunar axes with respective moments $A < B < C$. The parameter $X_{l,p,q}(e)$ is the eccentricity-dependent Hansen function that arises from time averaging the orbit (21). A 1:1 resonance is represented by $p = 2$ and $q = 2$, whereas 3:2 and 2:1 resonances are represented by $p = 2$, $q = 3$, and $p = 2$, $q = 4$, respectively. The instantaneous potentials are recovered by replacing a with R , and $X_{l,p,q}(e)$ with $\cos(2f - 2\omega t)$, where f is the true anomaly, ω is the lunar rotational velocity, and t is the time since passage of pericenter. The rotational potentials in the principal axes can be written (18)

$$U_{r,\hat{a}} = U_{r,\hat{b}} = -\frac{1}{2} U_{r,\hat{c}} = -\frac{1}{6} \omega^2 r^2 \quad (2)$$

The lunar radii due to these potentials can be expressed by $r_{\hat{a},\hat{b},\hat{c}} = -h_2 \langle U_{\hat{a},\hat{b},\hat{c}} \rangle r^2 / Gm$, where h_2 is the lunar secular displacement Love number, and m is the lunar mass (22). Without better constraints, we approximate the young Moon as a strengthless homogeneous body, for which $h_2 = 5/2$. After summing the centrifugal and tidal potentials, we may obtain $r_{\hat{a},\hat{b},\hat{c}}$ for any orbit. Given the moment relations $A \propto r_b^2 + r_c^2$, $B \propto r_a^2 + r_c^2$, $C \propto r_a^2 + r_b^2$, the gravity harmonic $C_{20} = [r_c - \frac{1}{2}(r_a + r_b)] / 5r^2$ (23), and the definitions of β and γ given previously, we obtain for a 3:2 resonance

$$\begin{aligned} C_{20} &= \frac{Mr^3}{ma^3} \left(-\frac{1}{2} X_{-3,0,0}(e) - \frac{11}{8} \right) \\ \beta &= \frac{5}{2} \frac{Mr^3}{ma^3} \left(\frac{1}{2} X_{-3,0,0}(e) + \frac{3}{4} X_{-3,2,2}(e) + \frac{11}{8} \right) \\ \gamma &= \frac{15}{4} \frac{Mr^3}{ma^3} X_{-3,2,2}(e) \end{aligned} \quad (3)$$

Similarly, for synchronous rotation, we obtain

$$\begin{aligned} C_{20} &= \frac{Mr^3}{ma^3} \left(-\frac{1}{2} X_{-3,0,0}(e) - \frac{3}{4} \right) \\ \beta &= \frac{5}{2} \frac{Mr^3}{ma^3} \left(\frac{1}{2} X_{-3,0,0}(e) + \frac{3}{4} X_{-3,2,2}(e) + \frac{3}{4} \right) \\ \gamma &= \frac{15}{4} \frac{Mr^3}{ma^3} X_{-3,2,2}(e) \end{aligned} \quad (4)$$

These equations approximate the tidal and rotational effects for nonchanging orbits of arbitrary eccentricity.

We searched the a - e space of Eqs. 3 and 4 to find minimum-error solutions to the observed values of β , γ , and C_{20} . For synchronous rotation we find one solution at $a = 22.9 r_E$, $e = 0.49$; and for 3:2 resonance we find two solutions at $a = 24.8 r_E$, $e = 0.17$, and, $a = 26.7 r_E$, $e = 0.61$. One means of visualizing how closely these solutions match the observed values is to plot the a - e solutions for each parameter in a - e space (Figs. 1 and 2). For a Moon frozen instantaneously into the average potentials of a given orbit, the values of the solution curves of β , γ , and C_{20} will intersect at a single point. The insets in Figs. 1 and 2 show that the calculated solutions intersect quite near each other. That is, the Moon's observed moments closely satisfy a specific set of orbital constraints on the ratio of β , γ , and C_{20} . To see this effect more clearly, imagine, for example, if the value of the observed C_{20} was smaller by 20%, i.e., closer to producing the value of 3.33 for the ratio C_{20}/C_{22} . In this case the curves would no longer intersect so closely, and the results would be more inconclusive (Fig. 1). Currently, altering either β or C_{20} by about 2%, or γ by 8%, will bring the lines into a perfect intersection, a much smaller difference than the discrepancies discussed in the first paragraph.

The Moon may have relaxed somewhat since freeze-in, but because β , γ , and C_{20} would have relaxed equally, the observed solution would merely be a horizontal displacement in semimajor axis from an earlier three-way intersection. For example, Fig. 2 shows a 3:2 resonance solution for the values of 2β , 2γ , and $2C_{20}$ ($a = 19.6 r_E$, $e = 0.17$), i.e., if the current values are relaxed by 50%. More generally, the Moon need not have frozen instantaneously to produce the moments we observe. The average of the values of β , γ , and C_{20} for any two solutions in a - e space produces a valid third solution, so that an evolving orbit may produce not a single true fossil, but a combination (14, 24). For example, in the case of 3:2 resonance, if the Moon started freezing its figure at $a = 23 r_E$, $e = 0.2$, the observed values of β , γ , and C_{20} would be higher by a factor of 1.28, 1.43, and 1.27, respectively. Later, if the Moon evolved to an orbit at $a = 27 r_E$, $e = 0.12$, and completed its

freeze-in there, we would have at that location 0.73β , 0.57γ , and $0.78C_{20}$ (Fig. 2). These final and initial parameters average very close to the observed values, but they are not uniformly lower by a single factor, as would be expected for parameters changed by relaxation alone.

Therefore, the requirement that the Moon changed rapidly from a state of short relaxation time to long relaxation time is not a stringent one. Combining relaxation and multiple averages over an evolving orbit, a rich history is permitted by the single observed solution.

We also find solutions for 2:1 resonance at $a = 28.6 r_E$, $e = 0.39$, and $a = 29.0 r_E$, $e = 0.52$. No one solution for any orbital state is better constrained over the others by the values β , γ , and C_{20} . However, we may interpret which state is more likely in the context of what we presently know about the orbital evolution of the Moon and Mercury. Past high-eccentricity orbits for the Moon have been considered possible for some time (22, 25), and it is interesting to note that the Moon's eccentricity is the highest of all solar system satellites with radius > 200 km. In general, torques on a satellite from tides raised on the primary body will increase eccentricity, whereas energy dissipation in the satellite due to tides raised by the primary body will decrease eccentricity. Peale gives an expression for the energy dissipation rate in a low-eccentricity synchronous orbit (26), but there are no readily available expressions for orbits with higher-order resonances. Deriving new expressions and interpreting plausible orbital histories are not possible in the limited space here, but we note that for any combination of e , k , and Q of the Earth and Moon, there will be a critical initial eccentricity above which eccentricity may start to increase. Touma and Wisdom have also studied in detail the process by which a synchronously rotating Moon can be excited into high eccentricity ($e = 0.5$) at $a = 4.6 r_E$, in a resonance known as the evection (27). Numerical models of lunar accretion give initial eccentricities that range from 0 to 0.14 (28).

It has long been considered that the Moon may have passed through resonances higher than synchronous (22, 29, 30), and it is believed that Mercury passed through resonances higher than 3:2 (29, 31). Among the solar system satellites, the Moon has one of the highest capture probabilities into 3:2 resonance (30). Formation by giant impact would leave the Moon to form near $4 r_E$ (28), where synchronous orbital periods would be greater than 10 hours. The initial spin period of the Moon may be as low as 1.8 hours before reaching rotational instability (30), leaving open the possibility of sufficient angular momentum to permit greater than synchronous resonances.

The probability of capture into resonance generally decreases with the order of the resonance (29), so capture in the 3:2 resonance is more likely than the 2:1 resonance. As for the high- e solutions for synchronous rotation and 3:2 resonance, these orbits dissipate energy faster and would change orbital parameters faster than their low- e counterpart. The low- e 3:2 solution may therefore have the slowest evolving orbit, which may be more compatible with freeze-in. The k and Q values for the very young Moon and Earth, possible formation of the Moon nearer the evection point, and variations in initial eccentricity all affect the probability of achieving a 3:2 resonance. In any case, the Moon must have eventually escaped any past 3:2 state, possibly through eccentricity

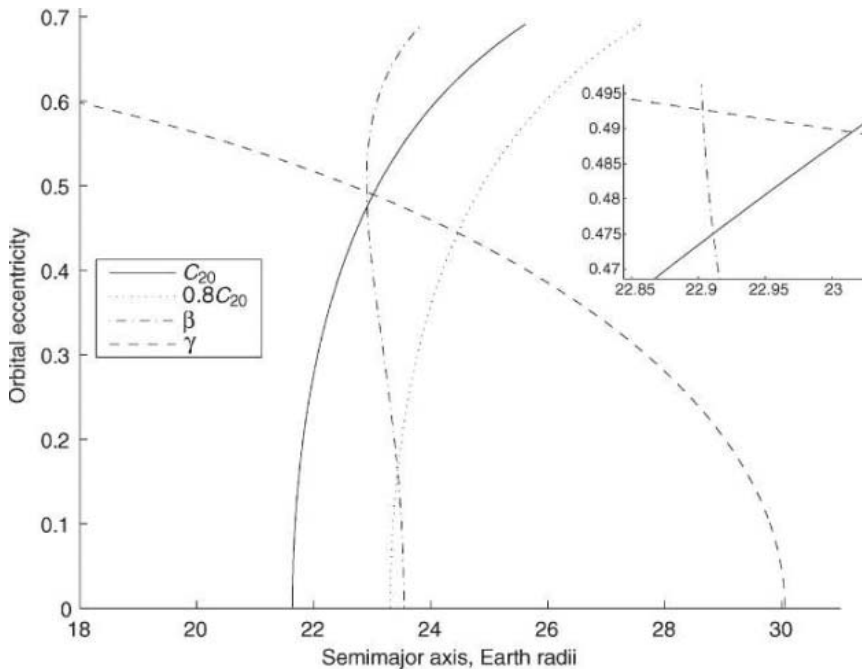


Fig. 1. Synchronous orbit solutions in a and e that give the observed values of β , γ , and C_{20} (Eq. 4). Valid a - e solutions to a hypothetical $0.8C_{20}$ are plotted to show the uniqueness of the observed parameters β , γ , and C_{20} . (Inset) Close-up of the intersection.

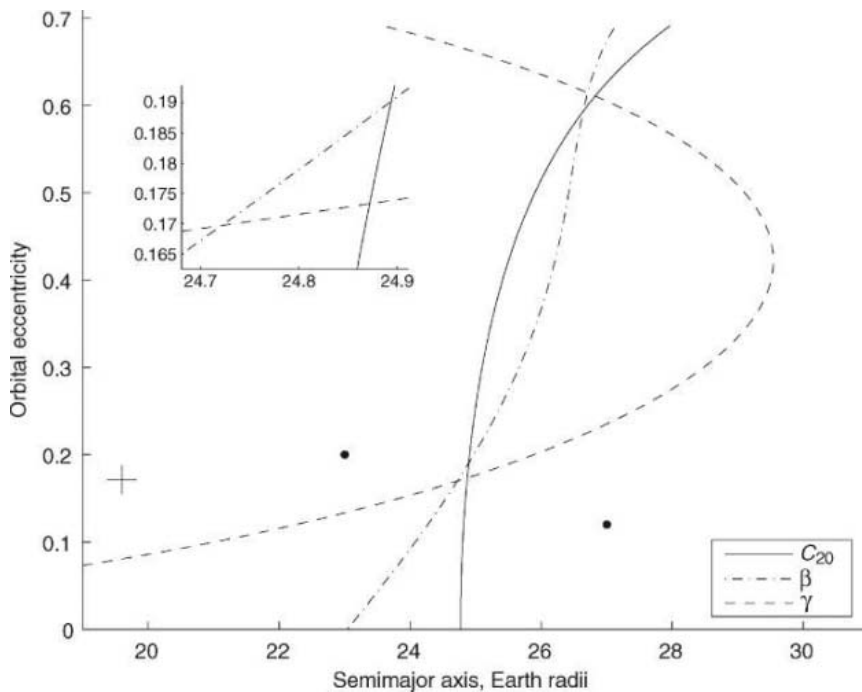


Fig. 2. 3:2 resonance solutions in a and e that give the observed values of β , γ , and C_{20} (Eq. 3). The cross at $r_E = 19.6$, $e = 0.17$, shows an orbit solution if the current values of β , γ , and C_{20} are from a fossil bulge that has relaxed by 50%. The two dots show solutions that average to the observed values of β , γ , and C_{20} . (Inset) Close-up of the bottom intersection.

damping. None of the above processes in early lunar evolution are well explored.

References and Notes

1. P.-S. Laplace, *Traité de Mécanique Céleste* (Paris Duprat, Bachelier 1798-1827), vol. 2, book 5, chap. 2.
2. W. F. Sedgwick, *Messenger Math.* **27**, 171 (1898).
3. H. Jeffreys, *Mem. R. Astron. Soc.* **60**, 187 (1915).
4. H. Jeffreys, *Mon. Not. R. Astron. Soc. Geophys. Suppl.* **4**, 1 (1937).
5. H. Jeffreys, *The Earth* (Cambridge Univ. Press, Cambridge, 1970).
6. A. S. Konopliv et al., *Science* **281**, 1476 (1998).
7. J. G. Williams, D. H. Boggs, C. F. Yoder, J. T. Ratcliff, J. O. Dickey, *J. Geophys. Res.* **106**, 27933 (2001).
8. Z. Kopal, *Proc. R. Soc. London Ser. A* **296**, 254 (1967).
9. P. Goldreich, A. Toomre, *J. Geophys. Res.* **74**, 2555 (1969).
10. M. Lefftz, H. Legros, *Phys. Earth Planet. Inter.* **76**, 317 (1993).
11. K. Lambbeck, S. Pullan, *Phys. Earth Planet. Inter.* **22**, 29 (1980).
12. S. K. Runcorn, *Nature* **195**, 1150 (1962).
13. P. Cassen, R. E. Young, G. Schubert, *Geophys. Res. Lett.* **5**, 294 (1978).
14. D. J. Stevenson, *Proc. Lunar Planet. Sci. Conf. XXXII*, abstract 1175 (2001).

15. S. Zhong, M. T. Zuber, *J. Geophys. Res.* **105**, 4153 (2000).
16. G. A. Neumann, M. T. Zuber, D. E. Smith, F. G. Lemoine, *J. Geophys. Res.* **101**, 16841 (1996).
17. T. Kleine, H. Palme, K. Mezger, A. N. Halliday, *Science* **310**, 1671 (2005).
18. C. D. Murray, S. F. Dermott, *Solar System Dynamics* (Cambridge Univ. Press, Cambridge, 1999).
19. J. Touma, J. Wisdom, *Astron. J.* **108**, 1943 (1994).
20. R. D. Ray, R. J. Eanes, F. G. Lemoine, *Geophys. J. Int.* **144**, 471 (2001).
21. The Hansen functions, $X_{l,p,q}(e)$, satisfy $(\frac{d}{dt})^l \cos(pf) = \sum_q X_{l,p,q}(e) \cos(qM)$ (32), where f is the true anomaly and M is the mean anomaly. For our purposes, $l = -3$. The Hansen functions are also called Hansen coefficients, and the expansions in e to fourth order can be found in table 3.2 of (33), albeit with a different subscript convention.
22. S. J. Peale, P. Cassen, *Icarus* **36**, 245 (1978).
23. C. F. Yoder, in *Global Earth Physics*, T. J. Ahrens, Ed. (American Geophysical Union, Washington, DC, 1995), p. 1.
24. The simple average of two different sets of parameters β , γ , and C_{20} may take place during the transition from the state of low relaxation time to the state of long relaxation time. During this time, the Moon is plastic enough to accommodate changes in form, yet stiff enough to retain some signature of its state when freeze-in started. Indeed, the

Moon is necessarily a sum of different orbits, however close or far apart, if the fossil bulge hypothesis is valid.

25. P. Goldreich, *Mon. Not. R. Astron. Soc.* **126**, 257 (1963).
26. S. J. Peale, *Celest. Mech. Dyn. Astron.* **87**, 129 (2003).
27. J. Touma, J. Wisdom, *Astron. J.* **115**, 1653 (1998).
28. E. Kokubo, S. Ida, J. Makino, *Icarus* **148**, 419 (2000).
29. P. Goldreich, S. J. Peale, *Astron. J.* **71**, 425 (1966).
30. S. J. Peale, in *Satellites*, J. A. Burns, Ed. (Univ. of Arizona Press, Tucson, 1978), p. 87.
31. Mercury's unnormalized coefficients $C_{20} = 6 \times 10^{-5} \pm 2.0$ and $C_{22} = 1 \times 10^{-5} \pm 0.5$ (34) are not reproduced by any orbit-spin resonance at Mercury's current semimajor axis.
32. H. C. Plummer, *An Introductory Treatise on Dynamical Astronomy* (Dover, New York, 1960).
33. W. M. Kaula, *Theory of Satellite Geodesy* (Dover, New York, 1966).
34. J. D. Anderson, G. Colombo, P. B. Esposito, E. L. Lau, G. B. Trager, *Icarus* **71**, 337 (1987).
35. We are grateful to B. Hager and B. Weiss for helpful comments. This work was supported by NASA Planetary Geology and Geophysics Program grants (to M.T.Z. and J.W.).

3 April 2006; accepted 8 June 2006
10.1126/science.1128237

Smoke and Pollution Aerosol Effect on Cloud Cover

Yoram J. Kaufman¹ and Ilan Koren^{2*}

Pollution and smoke aerosols can increase or decrease the cloud cover. This duality in the effects of aerosols forms one of the largest uncertainties in climate research. Using solar measurements from Aerosol Robotic Network sites around the globe, we show an increase in cloud cover with an increase in the aerosol column concentration and an inverse dependence on the aerosol absorption of sunlight. The emerging rule appears to be independent of geographical location or aerosol type, thus increasing our confidence in the understanding of these aerosol effects on the clouds and climate. Preliminary estimates suggest an increase of 5% in cloud cover.

Aerosol particles originating from urban and industrial pollution or smoke from fires have been shown to affect cloud microphysics, cloud reflection of sunlight to space, and the onset of precipitation (1, 2). Delays in the onset of precipitation can increase the cloud lifetime and thereby increase cloud cover (3, 4). Research on the aerosol effect on clouds and precipitation has been conducted for half a century (5). Although we well understand the aerosol effect on cloud droplet size and reflectance, its impacts on cloud dynamics and regional circulation are highly uncertain (3, 5–9) because of limited observational information and complex processes that are hard to simulate in atmospheric models (10, 11). Indeed, global model estimates of the radiative forcing due to the aerosol effect on clouds range from 0 to -5 W/m^2 . The reduction of this uncertainty is a major challenge in improving climate models.

Satellite measurements show strong systematic correlations among aerosol loading, cloud cover (12), and cloud height over the Atlantic Ocean (13) and Europe (14), making the model estimates of aerosol forcing even more uncertain. However, heavy smoke over the Amazon forest (15) and pollution over China (16) decrease the cloud cover by heating the atmosphere and cooling the surface (17) and may balance some of this large negative forcing. Global climate models also show a reduction in cloud cover due to aerosol absorption (τ_{abs}) outside (18) and inside the clouds (19). In addition, the aerosol effect on slowing down the hydrological cycle by cooling parts of the oceans (1) may further reduce cloud formation and the aerosol forcing. Understanding these aerosol effects on clouds and climate requires concentrated efforts of measurement and modeling of the effects.

There are several complications to devising a strategy to measure the aerosol effect on clouds. Although clouds are strongly affected by varying concentrations of aerosol particles, they are driven by atmospheric moisture and stability. Local variations in atmospheric moisture can affect both cloud formation and aerosol humidification, resulting in apparent correlations between aerosol column concentration and cloud cover (12, 13, 20).

In addition, chemical processing of sulfates in clouds can affect the aerosol mass concentration for aerosol dominated by sulfates.

We attempt to address these issues by introducing an additional measurement dimension. We stratified the measurements of the aerosol effect on cloud cover as a function of τ_{abs} of sunlight, thus merging in one experiment both the aerosol enhancement and inhibition of cloud cover. Because the concentration of the absorbing component of aerosols is a function of the aerosol chemical composition, rather than aerosol humidification in the vicinity of clouds, this concentration can serve as a signature for the aerosol effect on clouds. A robust correlation of cloud cover with aerosol column concentration and τ_{abs} in different locations around the world can strengthen the quantification of the aerosol effect on cloud cover, though a direct cause-and-effect relationship will await detailed model simulations.

Table 1. Slopes and intercepts of $\Delta f_{\text{ci}}/\Delta \ln \tau$ versus τ_{abs} (Fig. 3A) for the complete data set (All data), continental data dominated by air pollution aerosol, coastal stations, and stations dominated by biomass burning. Results are given for (i) absolute change of the independent cloud fraction Δf_{ci} versus the optical depth $\Delta f_{\text{ci}}/\Delta \ln \tau$ and for (ii) partial change $\delta f_{\text{ci}}/\delta \ln \tau$ from a multiple regression of Δf_{ci} with $\ln \tau$ and total precipitable water vapor.

	Slope versus τ_{abs}		Intercept for $\tau_{\text{abs}} = 0$	
	$\Delta f_{\text{ci}}/\Delta \ln \tau$	$\delta f_{\text{ci}}/\delta \ln \tau$	$\Delta f_{\text{ci}}/\Delta \ln \tau$	$\delta f_{\text{ci}}/\delta \ln \tau$
All data	-3.5	-2.6	0.17	0.13
Continental	-3.2	-2.6	0.16	0.13
Coastal	-3.4	-1.9	0.17	0.11
Biomass burning	-4.0	-3.5	0.18	0.14

¹NASA/Goddard Space Flight Center, 613.2, Greenbelt, MD 20771, USA. ²Department of Environmental Sciences and Energy Research, Weizmann Institute, Rehovot 76100, Israel.

*To whom correspondence should be addressed. E-mail: ilan.koren@weizmann.ac.il

The satellite analysis (12–16) may be affected by potential cloud artifacts (21). Therefore, instead of satellite data, we use measurements obtained by Aerosol Robotic Network (AERONET) sunphotometers (22, 23) in 17 sites with long data records and representing different aerosol and climatic regimes (Fig. 1). AERONET measures the aerosol attenuation of sunlight in cloud-free conditions. Although the sunphotometer was not designed to measure cloud cover, clouds affect the interval between consecutive aerosol measurements. We distinguished aerosols from clouds by using spectral variability of three consecutive measurements within 1 min (24). The interval is usually 15 min, but it is too variable to derive the actual cloud cover; however, we can use a systematic variation in the intervals with the aerosol optical thickness τ to derive the change in the cloud cover.

To develop the relationship between the cloud cover and the interval of measurements, let N_0 be the instrumental average rate of measurements per unit of time in the absence of clouds and N be the rate of measurements for a given cloud fraction f_c so that

$$N = N_0(1 - f_c) \quad (1)$$

where f_c is the fraction of the time in which the sunphotometer will detect the cloud and not report aerosol data. The intervals in the sunphotometer measurements are correspondingly $T = 1/N$ and $T_0 = 1/N_0$, where T is the interval between measurements for f_c and T_0 is the interval between measurements for a cloud-free sky. Therefore

$$f_c = 1 - \frac{T_0}{T} \quad (2)$$

Differentiating with respect to the logarithm of τ , a measure of the aerosol column concentration, gives

$$\frac{df_c}{d\ln\tau} = \frac{T_0}{T^2} \frac{dT}{d\ln\tau} \quad \text{or, using Eq. 2:}$$

$$\frac{df_c}{d\ln\tau} = \frac{1}{T} (1 - f_c) \frac{dT}{d\ln\tau} \quad (3)$$

where $df_c/d\ln\tau$ and $dT/d\ln\tau$ are the derivatives of f_c and T , with respect to the logarithm of τ . As the cloud field expands because of an increase in the size or lifetime of the cloud, an overlap among the clouds will mask part of the aerosol effect proportionally to the cloud fraction. This distorts the aerosol effect, particularly for high cloud cover. Therefore, we defined the independent cloud cover change df_{ci} as

$$df_{ci} = \frac{df_c}{(1 - f_c)} = \frac{dT}{T} \quad (4)$$

and used it instead of df_c in this paper. We also tested the AERONET-derived cloud cover against total sky pyranometer measurements (fig. S1).

Figure 2 shows three scatterplots of the interval between adjacent AERONET measurements as a function of τ for different values of τ_{abs} . For each site, 3 to 5 years' worth of data

are separated for every 2 calendar months. We also used the AERONET measurements of τ_{abs} (25, 26). τ_{abs} is accurate within ± 0.01 for a single calibration data set and within ± 0.003 for 5 years of data with approximately six independent calibrations (25, 26). We used τ_{abs} rather than a single scattering albedo because τ_{abs} has very small sensitivity to possible cloud contam-

ination and aerosol humidification. Subvisible clouds, although affecting the scattering in the atmosphere, have almost no effect on absorption and therefore have little influence on τ_{abs} . As the aerosol concentration increases, both the scattering and absorption increase, competing for their effects on the cloud cover. We provide the average values of τ_{abs} for each data set (Figs. 2 and 3),

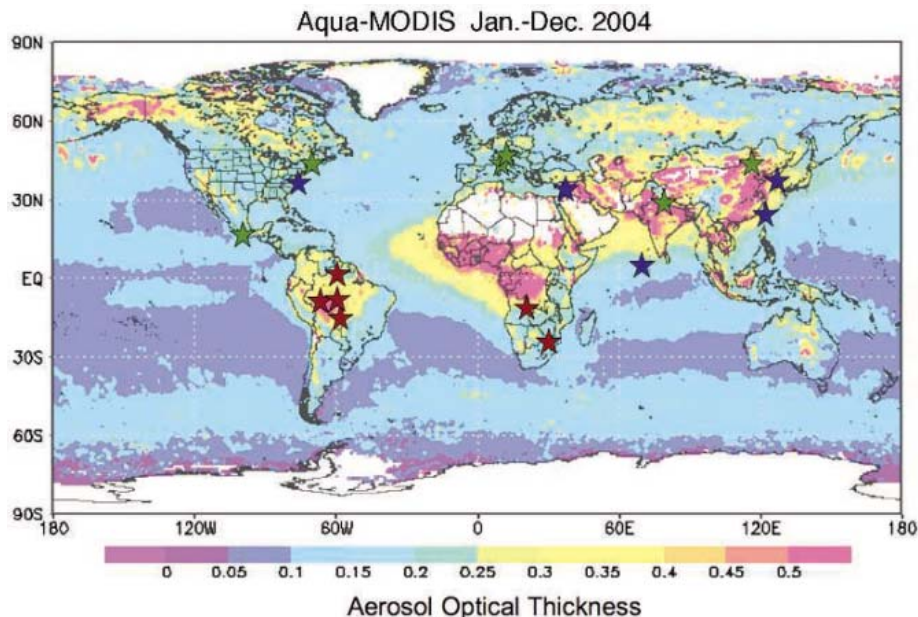
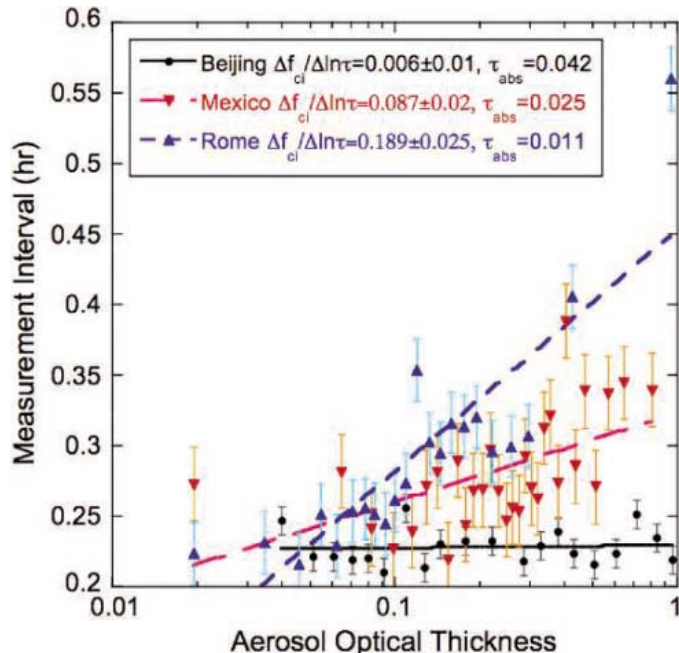


Fig. 1. Global distribution of the AERONET sunphotometers used in the analysis. The background is the average τ (a measure of the aerosol column concentration) for the year 2004 measured by MODIS on the Terra satellite. Green stars, continental sites in North America, Europe, and Asia; blue stars, marine locations in North America, the Mediterranean region, and Asia; red stars, biomass-burning sites in Africa and South America.

Fig. 2. Scatterplots of the time interval between two adjacent AERONET aerosol measurements that were not obscured by clouds, as a function of the average τ around the interval. The three examples are for low τ_{abs} (blue line and triangles; Rome, Italy from September to October; $\tau_{abs} = 0.011$), medium τ_{abs} (red line and triangles; Mexico City, Mexico from July to August; $\tau_{abs} = 0.025$), and high τ_{abs} (black line and circles; Beijing, China from September to October; $\tau_{abs} = 0.042$). Four years of data were used for each site for the 2 calendar months. The data were sorted by τ and averaged in groups of 100. The error bars are the standard error for each point. The corresponding changes in the cloud cover, $\Delta f_{ci}/\Delta \ln\tau$, are shown.



representing the value of absorption that competes with the number of potential cloud condensation nuclei in determining the cloud fraction.

In order to study the effect of pollution and smoke aerosols, we restricted the data to locations and periods with minimal dust influence. To have enough points for each time increment, we also restricted the data to cloud systems that passed over the site during no more than 3 hours (27). As a result, the observations were weighted toward meteorological systems with broken clouds.

The results for the change in cloud cover Δf_{ci} with a change in $\Delta \ln \tau$ are shown in Fig. 3 (see also table S1). Every point represents an analysis of ~ 3000 measurements. A linear fit to all of the data shows that

$$\frac{\Delta f_{ci}}{\Delta \ln \tau} = (0.17 \pm 0.01) - (3.5 \pm 0.5)\tau_{abs} \quad (5)$$

with a correlation of $r = 0.69$.

Uncertainties are represented by the standard errors in the average values, and the 95% confidence level range of the slopes is between -2.6 and -4.4 . There is a smooth transition from aerosol enhancement of cloud cover to aerosol decrease of the cloud cover (Fig. 3).

Does Eq. 5 represent the aerosol effect on cloud cover, cloud processing of aerosols, or coincidental variations of clouds and aerosol with the meteorological field? To address this question, we subdivided the data in Fig. 3A into three geographical regions (colored stars in Fig. 1): continental Northern Hemisphere sites with pollution aerosols, coastal marine sites, and biomass-burning sites in Africa and South America (25, 26, 28). These regions differ in aerosol and cloud properties; however, the slope of $\Delta f_{ci}/\Delta \ln \tau$ versus τ_{abs} for these regions varies within the uncertainty range of Eq. 5.

The fact that we have the same relationship for smoke and pollution aerosol is of special importance. Pollution aerosol is strongly hygroscopic, and thus variation in the humidity from 0% to 85% can triple the value of τ (29). Smoke is much less hygroscopic; an increase in the humidity to 85% increases τ by only 20% (30). The similarity in the regressions shows that it is unlikely that aerosol humidification in conditions that favor cloud formation is responsible for the increase of cloud cover with either an increase in aerosol concentration or its decrease with the introduction of τ_{abs} . The same can be said about cloud processing, which affects pollution aerosol

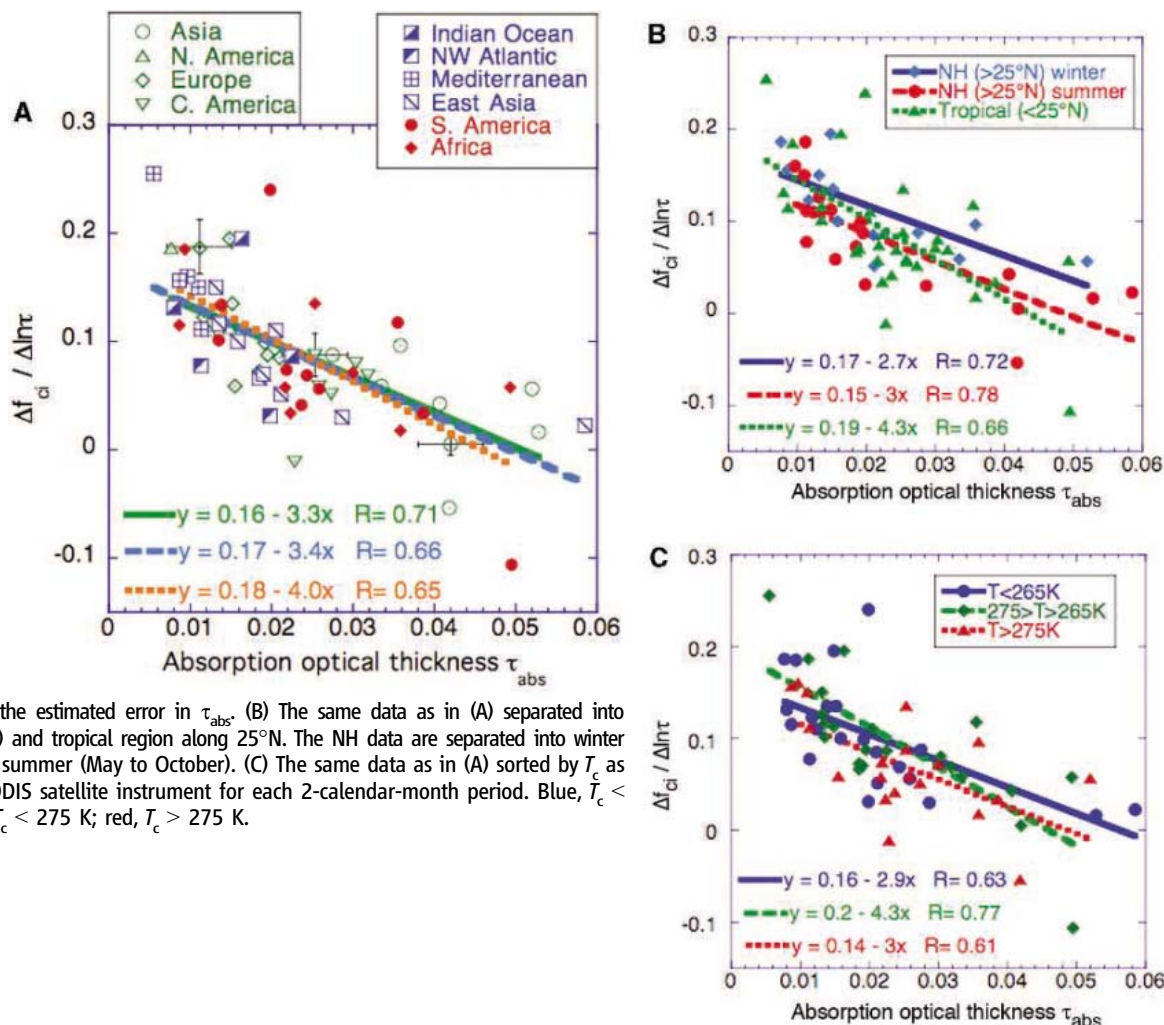
through sulfate production, which is not important for aerosols produced by biomass burning.

To address possible effects from seasonal variability, we subdivided the data in Fig. 3B based on season (winter to spring and summer to fall) in the Northern Hemisphere and year-long data in the Tropics. Alternatively in Fig. 3C, we separated the data by the cloud-top temperature (T_c) obtained from Moderate Resolution Imaging Spectroradiometer (MODIS) satellite data (31, 32). In all of these cases, the slopes of $\Delta f_{ci}/\Delta \ln \tau$ versus τ_{abs} varied within the uncertainty of Eq. 5.

To what degree can the relationship in Eq. 5 be influenced by atmospheric dynamics? Convergence zones and updrafts can increase the depth of the boundary layer, the column concentration of aerosols, and total precipitable water vapor. They can also promote cloud cover (33). Analysis of aerosol and water vapor separately for each location and season shows significant correlations between τ and the total precipitable water vapor (Fig. 3), which is a possible indication of the effect of convergence. The results, summarized in Table 1, show that $\sim 25\%$ of the relationship of Δf_{ci} with τ may be associated with variation of the precipitable water vapor. As expected, the effects are stronger for

Fig. 3. Regional (A), seasonal (B), and T_c (C) analyses of the AERONET data for the effect of aerosols on cloud cover. $\Delta f_{ci}/\Delta \ln \tau$ was plotted as a function of τ_{abs} . Each point represents an analysis of ~ 3000 measurements from a given location and 2 calendar months averaged over 3 to 5 years. (A) Green symbols indicate continental sites, blue symbols indicate marine sites, and red symbols indicate biomass-burning sites. For distribution of the sites, see Fig. 1. Error bars are printed for three representative points and indicate the average uncertainties in the least-squares fit used

for individual points and the estimated error in τ_{abs} . (B) The same data as in (A) separated into Northern Hemisphere (NH) and tropical region along 25°N . The NH data are separated into winter (November to April) and summer (May to October). (C) The same data as in (A) sorted by T_c as determined from the MODIS satellite instrument for each 2-calendar-month period. Blue, $T_c < 265$ K; green, $265 \text{ K} < T_c < 275$ K; red, $T_c > 275$ K.



pollution aerosol in the Northern Hemisphere than for biomass burning in the tropics, where the dry season is associated with smaller meteorological variability (34).

We found a consistent relationship between an increase in the cloud fraction and an increase in τ (representing column concentration), as well as a decrease in τ_{abs} . The relationship is invariant to the location or to the aerosol type. About 25% of the relationship of clouds to aerosol can be explained by the variation of total precipitable water vapor and may be associated with atmospheric convergence. What are the consequences of this systematic effect of aerosol on the cloud cover?

We used the limited global sample of aerosol interaction with clouds from Fig. 3 to roughly estimate the global average anthropogenic aerosol impact on cloud cover over the oceans. For a global average aerosol (excluding dust) single scattering albedo of 0.92 ± 0.05 (25, 26) and an average total optical depth value of $\tau = 0.093 \pm 0.02$ over the oceans [composed of $\tau = 0.06 \pm 0.01$ (for baseline natural aerosol) and $\tau = 0.033 \pm 0.01$ (for anthropogenic aerosols) (35, 36)], we obtained a τ_{abs} value of 0.007 ± 0.005 . From Table 1, we acquired a $\delta f_{\text{ci}}/\delta \ln \tau$ value of 0.11 ± 0.02 . Anthropogenic aerosol increases the fine τ over the oceans, which provide most of the cloud condensation nuclei, from baseline values of 0.03 ± 0.01 to 0.065 ± 0.02 (35, 36). For an average cloud cover of 0.6, the increase in τ corresponds to a change in cloud cover of

$$\begin{aligned} \Delta f_c &= \Delta f_{\text{ci}}(1 - f_c) = 0.11 \Delta \ln \tau (1 - 0.6) \\ &= 0.03 \pm 0.01 \end{aligned} \quad (6)$$

The spatial distributions of aerosol over the oceans and their absorption properties are highly heterogeneous. Consequently, the estimated average impact is uncertain and should be viewed as a first approximation. The clouds sampled by the AERONET procedure do not include extended cloud systems that are sensitive to aerosol effect. The analysis applies to urban industrial pollution and aerosol produced by biomass burning rather than land-use-generated dust.

The relationship between cloud cover and aerosol given by Eq. 5 can serve as a constraint on models of the aerosol and cloud interaction, independently of the cause-and-effect relationship. The robustness of the effect of aerosols on clouds, presented here, makes it more likely that most of the observed changes in the cloud cover are due to the aerosol impact. The large effect of elevated aerosol concentration on cloud cover, an increase of 0.03 (5%) in average cloud cover (Eq. 6), can have a profound effect on the hydrological cycle and climate.

References and Notes

- V. Ramanathan *et al.*, *Science* **294**, 2119 (2001).
- J. Haywood, O. Boucher, *Rev. Geophys.* **38**, 513 (2000).
- B. A. Albrecht, *Science* **245**, 1227 (1989).
- L. D. Rotstajn, Y. G. Liu, *Geophys. Res. Lett.* **32**, 10.1029/2004GL021922 (2005).
- R. Gunn, B. B. Phillips, *J. Meteorol.* **14**, 272 (1957).

- S. Menon *et al.*, *J. Atmos. Sci.* **59**, 692 (2002).
- K. M. Lau, M. K. Kim, K. M. Kim, *Clim. Dyn.* 10.1007/s00382-006-0114 (2006).
- D. Rosenfeld, *Science* **287**, 1793 (2000).
- M. O. Andreae *et al.*, *Science* **303**, 1337 (2004).
- A. S. Ackerman *et al.*, *Science* **288**, 1042 (2000).
- J. E. Penner *et al.*, *Climate Change 2001: The Scientific Basis*, J. T. Houghton *et al.*, Eds. (Cambridge Univ. Press, New York, 2001), pp. 289–348.
- Y. J. Kaufman, I. Koren, L. A. Remer, D. Rosenfeld, Y. Rudich, *Proc. Natl. Acad. Sci. U.S.A.* **102**, 11207 (2005).
- I. Koren, Y. J. Kaufman, L. A. Remer, D. Rosenfeld, Y. Rudich, *Geophys. Res. Lett.* **32**, 10.1029/2005GL023187 (2005).
- A. Devasthale, O. Kruger, H. Grassl, *IEEE J. Trans. Geosci. Remote Sens.* **2**, 333 (2005).
- I. Koren, Y. J. Kaufman, L. A. Remer, J. V. Martins, *Science* **303**, 1342 (2004).
- O. Kruger, H. Grassl, *Geophys. Res. Lett.* **31**, 10.1029/2001GL014081 (2004).
- G. Feingold, H. L. Jiang, J. Y. Harrington, *Geophys. Res. Lett.* **32**, 10.1029/2004GL021369 (2005).
- J. Hansen, M. Sato, R. Ruedy, *J. Geophys. Res.* **102**, 6831 (1997).
- M. Z. Jacobson, *J. Phys. Chem. A* **110**, 6860 (2006).
- M. Sekiguchi *et al.*, *J. Geophys. Res.* **108**, 10.1029/2002JD003359 (2003).
- J. Zhang, J. S. Reid, B. N. Holben, *Geophys. Res. Lett.* **32**, 10.1029/2005GL023254 (2005).
- B. N. Holben *et al.*, *Remote Sens. Environ.* **66**, 1 (1998).
- B. N. Holben *et al.*, *J. Geophys. Res.* **106**, 12067 (2001).
- Y. J. Kaufman, G. P. Gobbi, I. Koren, *Geophys. Res. Lett.* **33**, 10.1029/2005GL025478 (2006).
- O. Dubovik *et al.*, *J. Atmos. Sci.* **59**, 590 (2002).
- Y. J. Kaufman, O. Dubovik, A. Smirnov, B. N. Holben, *Geophys. Res. Lett.* **29**, 10.1029/2001GL014399 (2002).
- The locations were selected outside of the African dust range. We used only periods with average Ångström exponent $\text{Å} > 1$, $\tau > 0.10$, and at least 1000 points. These conditions also excluded Asian dust. The requirement of 1000 points ensured that, for the variation of $\ln \tau$ of 0.7 and the measured average standard deviation of Δf_{ci} of 0.6, we get uncertainty in variation of $\Delta f_{\text{ci}}/\Delta \ln \tau < 0.03$. Individual AERONET data points were selected for solar zenith angle $< 60^\circ$, $\tau < 1$, and measurement interval < 3 hours.
- L. A. Remer, Y. J. Kaufman, *Atmos. Phys. Chem.* **6**, 237 (2006).
- R. A. Kotchenruther, P. V. Hobbs, D. A. Hegg, *J. Geophys. Res.* **104**, 2239 (1999).
- Y. J. Kaufman *et al.*, *J. Geophys. Res.* **103**, 31,783 (1998).
- M. D. King, Y. J. Kaufman, P. Menzel, D. Tanré, *IEEE J. Trans. Geosci. Remote Sens.* **30**, 2 (1992).
- Giovanni MODIS Online Visualization and Analysis System (MOVAS) (<http://lake.nascom.nasa.gov/movas/>).
- M. D. Chou, P. K. Chan, M. H. Wang, *J. Atmos. Sci.* **59**, 748 (2002).
- Y. J. Kaufman, R. S. Fraser, *Science* **277**, 1636 (1997).
- Y. J. Kaufman, A. Smirnov, B. N. Holben, O. Dubovik, *Geophys. Res. Lett.* **28**, 3251 (2001).
- Y. J. Kaufman *et al.*, *Geophys. Res. Lett.* **32**, 10.1029/2005GL023125 (2005).
- We thank T. Eck, B. Holben, L. Remer, J. Lu, E. Wilcox, and many others, including anonymous reviewers, for comments on the work; the AERONET project for maintaining consistent high data quality and easy availability and use of the data worldwide; and the numerous AERONET site principal investigators for their efforts in establishing and maintaining the sites. I.K. is the incumbent of the Benjamin H. Swig and Jack D. Weiler Career Development Chair.

Supporting Online Material

www.sciencemag.org/cgi/content/full/1126232/DC1

Materials and Methods

Fig. S1

Table S1

14 February 2006; accepted 21 June 2006

Published online 13 July 2006;

10.1126/science.1126232

Include this information when citing this paper.

Crustal Dilatation Observed by GRACE After the 2004 Sumatra-Andaman Earthquake

Shin-Chan Han,^{1*} C. K. Shum,¹ Michael Bevis,¹ Chen Ji,² Chung-Yen Kuo¹

We report the detection of an earthquake by a space-based measurement. The Gravity Recovery and Climate Experiment (GRACE) satellites observed a ± 15 -microgalileo gravity change induced by the great December 2004 Sumatra-Andaman earthquake. Coseismic deformation produces sudden changes in the gravity field by vertical displacement of Earth's layered density structure and by changing the densities of the crust and mantle. GRACE's sensitivity to the long spatial wavelength of gravity changes resulted in roughly equal contributions of vertical displacement and dilatation effects in the gravity measurements. The GRACE observations provide evidence of crustal dilatation resulting from an undersea earthquake.

The devastating 26 December 2004 Sumatra-Andaman undersea earthquake, with a moment magnitude (M_w) between 9.1 and 9.3, ruptured more than 1000 km of a locked subduction interface near northern Sumatra, Nicobar, and the Andaman islands (*I*). Measurements from global seismic network and Global Positioning System (GPS) stations have been used to infer the coseismic slip history of this event (*I–A*). The earthquake permanently changed the mass distribution within Earth and has consequently perturbed the motion of Earth-orbiting

satellites by an amount that is measurable from the ranging instrument onboard the Gravity Recovery and Climate Experiment (GRACE) satellites (5). GRACE consists of two identical satellites co-orbiting at low altitude (~ 450 km), separated by

¹Geodetic Science, Department of Geological Sciences, Ohio State University, 275 Mendenhall Laboratory, 125 South Oval Mall, Columbus, OH 43210–1398, USA.

²Department of Earth Sciences, University of California at Santa Barbara, Santa Barbara, CA, USA.

*To whom correspondence should be addressed. E-mail: han.104@osu.edu

~220 km and linked with the K-band microwave ranging (KBR) satellite-to-satellite tracking (SST) system (6). Minute changes in the distance between the GRACE satellites (measured by KBR) reflect mass anomalies within the Earth system and manifest as changes in Earth's gravity field (5).

Some of the better known time-variable gravity signals observed by the GRACE satellites, including tides (of the solid earth, ocean, atmosphere, and pole) and atmospheric and ocean barotropic mass variations, have been removed from GRACE observations using a priori models (5–7). Although the solid-earth mass transport induced by earthquakes is abrupt and permanent, climate-related signals such as hydrological (8–10) and ocean mass fluxes (11) are periodic, with primarily seasonal and possibly interannual or longer time scales. In order to eliminate signals other than those associated with the earthquake, we took differences of the gravity solutions (from the same months in various years), using measurements obtained before and after the earthquake. By doing so, we suppressed the normally dominant gravity variations driven by seasonal changes. By using multiple months of data, we can further enhance the tectonic signal-to-noise ratio (SNR) in the GRACE gravity solutions.

Our method is based on the direct use of KBR SST data to measure the range changes between the centers of mass of the GRACE

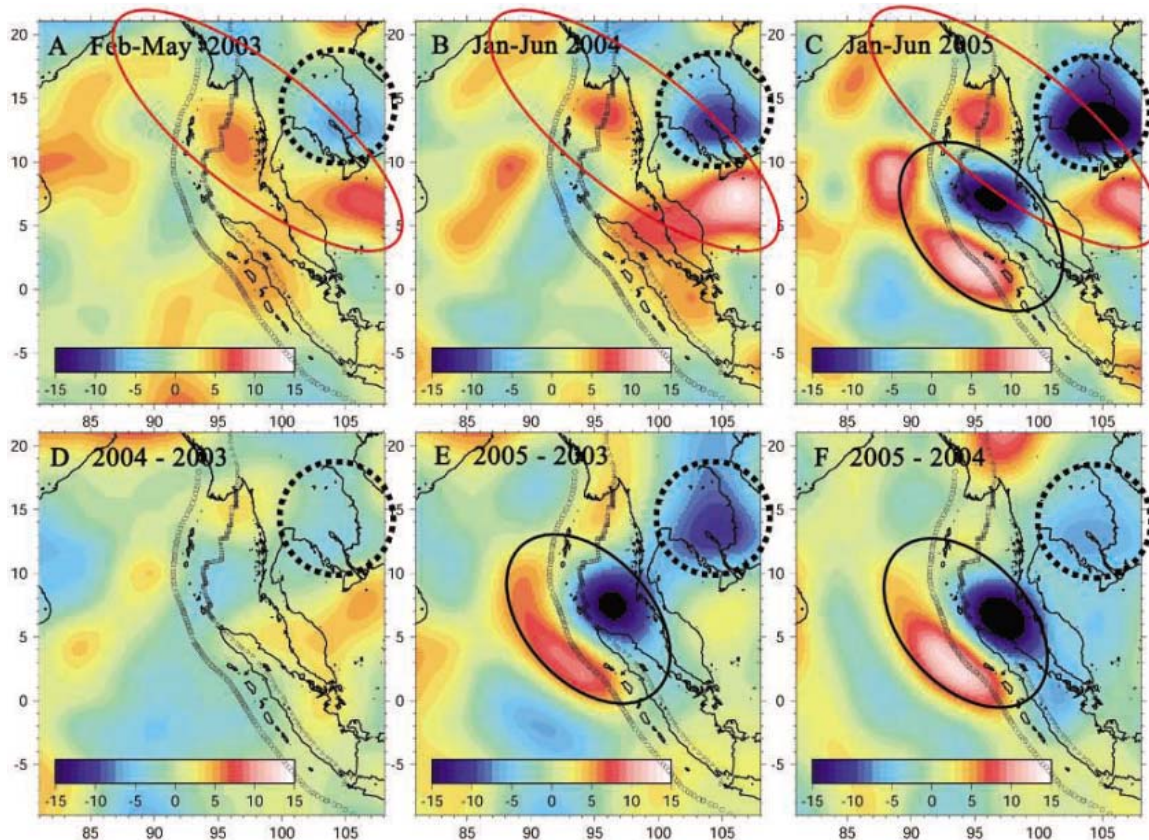
satellites and accelerometer and attitude data to measure and remove the effect of nongravitational forces acting on the satellites. We used the energy conservation principle and regional gravity field inversion to enhance the spatial and temporal resolutions (12, 13). The technique has been demonstrated by successful analysis of various geophysical phenomena, including hydrological variations in the Amazon (10) and ocean tides underneath the Antarctica ice shelves (14), with improved spatial (500 km) and temporal (5 days) resolutions. The data for the first 6 months of the years 2003, 2004, and 2005 were used, except for January and June 2003 and the last half of January 2004, during which there are no available data. The gravity changes in each year were computed using data from the available months (that is, February to May 2003 and January to June 2004 and 2005) with respect to a reference gravity model GGM01C (6) (Fig. 1, A to C).

We find that (Fig. 1) (i) the gravity anomalies appearing along the coastal area of the Bay of Bengal and the east of Thailand exist in all years; (ii) the negative gravity anomalies are observed to be getting larger near the south of the Mekong River, Cambodia/Vietnam, every year; and (iii) the gravity anomalies appear north of the Sumatra Islands and Andaman Sea with a 30- μ Gal peak-to-peak variation only in 2005. The gravity variation in 2004 with re-

spect to 2003 (Fig. 1D) is insignificant, whereas the variation in 2005 with respect to 2003 or 2004 shows strong negatives in the Andaman Sea and positives along the west of the Sumatra, Nicobar, and Andaman Islands (Fig. 1, E and F), indicating the occurrence of a strong earthquake during 2004. The other dominant anomaly found south of the Mekong River implicates hydrologic variations. The anomalies in all differenced pairs are negative, and the magnitude is larger in the 2-year differenced pair of 2005 and 2003 than in the 1-year differenced pairs (2005 and 2004 or 2004 and 2003). This implies negative interannual variation or mass decreasing every year, which could result from the droughts occurring during the same time period in southeastern Asia. To retain only the anomalies relevant to the earthquake, we filtered the average of two pairs, 2005/2003 and 2005/2004 (Fig. 2). The gravity anomalies outside a spherical cap centered at the earthquake epicenter (3.5°N, 96°E), with a spherical radius of 7°, were further filtered by downweighing the anomalies with a factor of inverse square of distance away from the edges of the spherical cap.

We analyzed the GRACE gravity observations using a seismically derived dislocation model for the Sumatra-Andaman (26 December 2004) and the Nias (28 March 2005) earthquakes (15). The geometry (size, orientation, and location) of the fault planes is assumed

Fig. 1. Cumulative gravity changes (in μ Gal) in the Bay of Bengal and the Andaman Sea with respect to a reference model GGM01C (6) for the periods from (A) February to May 2003, (B) January to June 2004, and (C) January to June 2005. (D) Gravity changes between 2004 and 2003, inferred by differencing (B) and (A). (E) Gravity changes between 2005 and 2003, inferred by differencing (C) and (A). (F) Gravity changes between 2005 and 2004, inferred by differencing (C) and (B). Red circles indicate gravity changes that exist in all years. Black dotted circles indicate an increasing hydrology-related negative anomaly near the south of the Mekong River. Black solid circles indicate gravity change induced by the Sumatra-Andaman earthquake and appear in 2005 only. Java trenches, Sagaing and Sumatra transform faults, and Andaman ridges are depicted with circles, triangles, and squares, respectively.



to be known. Assuming an elastic half-space (16, 17), the fault slip data were used to model the uplift and subsidence at the sea floor and at the Moho (18), where large density contrasts exist. The computed topography changes for both levels were used to predict the gravity changes at sea level (Fig. 3, A to C) [see the supporting online material (SOM) for the formalism of computing gravity changes due to vertical displacement at sea level]. We then

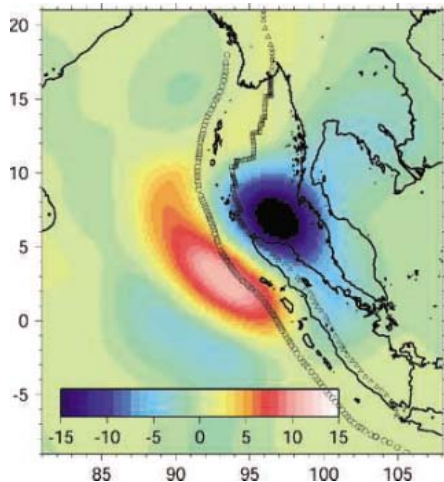
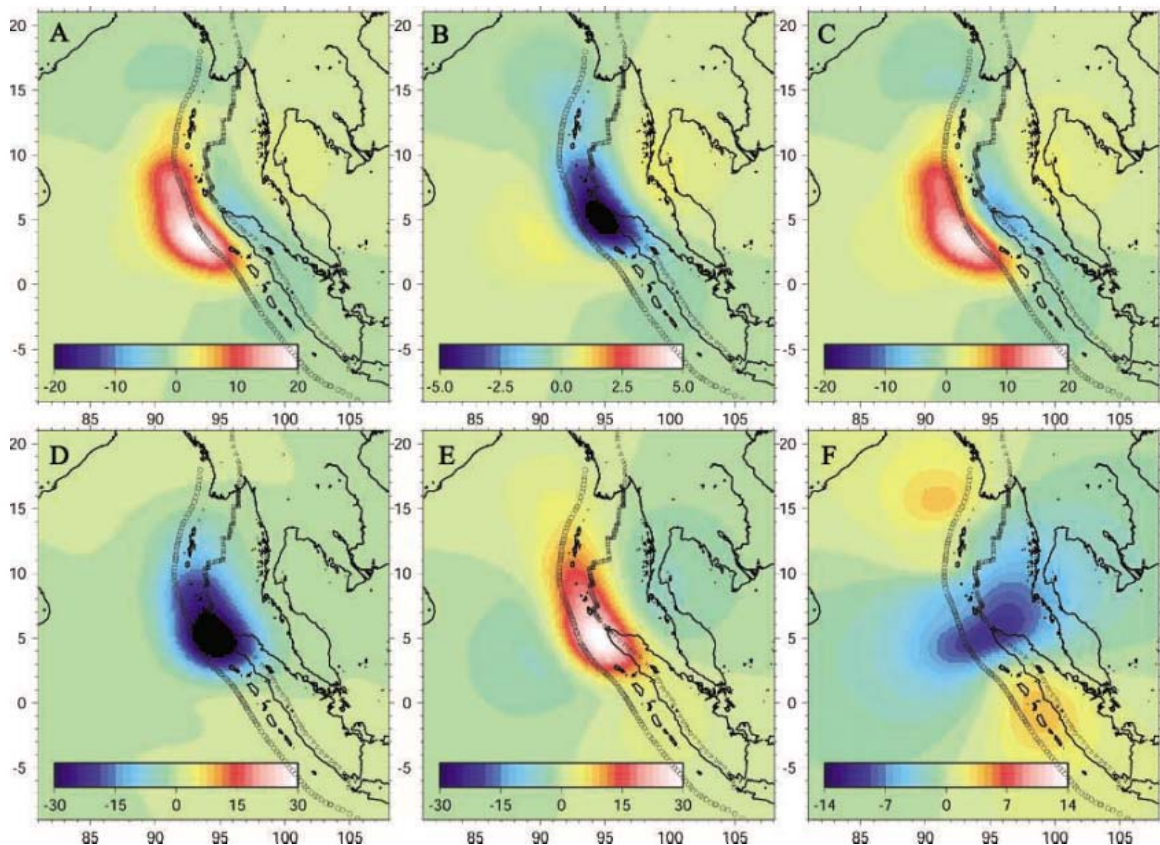


Fig. 2. Gravity changes (in μGal) after the Sumatra-Andaman earthquake, computed from averaging and filtering the two gravity changes between two different time periods (Fig. 1, E and F).

Fig. 3. Predicted gravity changes (in μGal) from a seismically derived dislocation model (15), caused by (A) uplift and subsidence at the sea floor, (B) uplift and subsidence at the Moho, (C) the total effect of vertical displacement [that is, (A) + (B)], (D) expansion within the crust, (E) compression within the mantle, and (F) the total effect of dilatation [that is, (D) + (E)]. Smoothing radii of 300 km in longitude and 200 km in latitude were used.



applied Gaussian smoothing to the computed gravity from the model (15), with averaging radii of 300 km in longitude and 200 km in latitude (19), to be commensurate with the spatial resolution of the GRACE observations.

The larger positive gravity change (Fig. 3A) is due to the dominant up-warping of the hanging wall and the density contrast at the sea

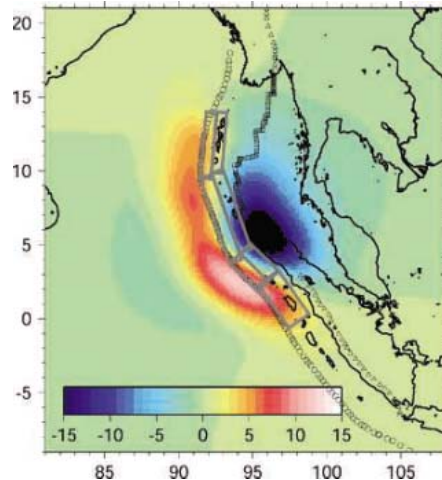


Fig. 4. Predicted coseismic gravity changes (in μGal) from the seismic model (15), inferred by combining vertical displacement (Fig. 3C) and dilatation (Fig. 3F). The seven fault planes used in the seismic model are shown (see fig. S4 for a detailed description).

floor, which is three to four times larger than that at the Moho. The negative gravity change is due to the (smaller) down-warping of the hanging wall (Fig. 3A) and subsidence of the foot wall at the Moho (Fig. 3B). The resulting largely positive gravity change due to vertical displacement (Fig. 3C) cannot fully explain the negative components also seen in the GRACE observations (Fig. 2). There must be another mechanism causing the large negative signals in the GRACE observation.

We considered the internal mass redistribution (density change caused by dilatation of a compressible Earth) due to the earthquake. With the strains computed using the seismic model, we calculated the density changes by multiplying the sum of the normal strains (that is, the divergence of the displacement field) by the density at the corresponding depth. Assuming that there are two distinct densities for the crust and the mantle (fig. S1), the respective gravity changes due to density changes in the crust and the mantle were calculated separately (SOM). The negative gravity change in the crust (Fig. 3D) is primarily due to the expansion caused by horizontal (mostly in the east-west direction) and vertical motions of the sea floor. The gravity change caused by the compression in the mantle (Fig. 3E) is due to down-warping of the subsurface. The total gravity effect of the density change (Fig. 3F) shows negatives around the faults and smaller positives over the surrounding regions and variations along the strike.

The combined effects of uplift and subsidence and dilatation and compression from the seismically driven model (Fig. 4) yield excellent agreement (a correlation coefficient of 0.85) with the GRACE observations (Fig. 2).

In addition to our regional inversion of the overflight GRACE tracking data (Figs. 1 and 2), we also processed monthly mean GRACE gravity estimates expressed in terms of spherical harmonic (SH) coefficients (5). The global SH spectra are, however, less effective for modeling the regional gravity signals (such as earthquakes) because the spatially limited signals spread across the entire SH spectra (10). The GRACE SH coefficients have a good SNR limited only to low degree coefficients (that is, a long-wavelength spatial scale larger than 1300 km). Therefore, we applied Gaussian smoothing with an averaging radius of 800 km to reduce errors in higher degree coefficients (5). The months from February to May in 2003, 2004, and 2005 were used because they are available in common. We computed 4-month mean differences in various years, similar to Fig. 1. One, 2004–2003, (fig. S2A) shows nothing notable except the negative gravity change over the Mekong River; however, the pairs 2005–2003 (fig. S2B) and 2005–2004 (fig. S2C) show significant negative anomalies around the Malay Peninsula, Thailand. The magnitude of the anomaly is larger for the 2-year differenced pair (fig. S2B), and the location of the peak in 2005–2003 (fig. S2B) is moved toward the east from the north of the

Sumatra Islands, when compared to the prediction (fig. S2F). The mislocation of the peak signal is explained by the combined effects of the earthquake and hydrology in the Mekong river due to the smoothing of GRACE global spectra. At this low spatial resolution, we cannot isolate the earthquake anomalies from other signals. However, the gravity effects of vertical displacement (fig. S2D) and density change (fig. S2E) predicted by the seismic model still agree with the GRACE SH observations when combined and smoothed to the commensurate spatial resolution (fig. S2F). The 1-year difference pair (fig. S2C) was less affected by the Mekong hydrology and was in better agreement with the predicted gravity change from the seismic model (fig. S2F), in terms of strength and location of the peak.

Finally, we quantified the signal spectra sensitive to GRACE observations by analyzing the power spectral density (PSD) of predicted gravity changes from the seismic model (15). The PSD of the gravity changes due to uplift and subsidence from the model without smoothing (Fig. 5A) indicates that the dominant power is focused on spherical degree 40 in latitude and 100 in longitude (20). Higher degree components are found in longitude because the uplift and subsidence have a north-south elongated feature with variation of sign along longitude (fig. S3C). The power spectra of gravity changes induced by dilatation from the seismic model without smoothing (Fig. 5B) indicate that most

powers are at the low degrees. Unlike the uplift and subsidence, higher degree components are found in latitude because the dilatation has an east-west elongated feature with variation of sign along latitude (fig. S3F). Because of the poor SNR in the higher degrees (21, 22), GRACE is expected to provide reliable estimates that are limited to low degree components for uplift and subsidence (Fig. 5C) and for dilatation (Fig. 5D). Most of signals are within less than 40 to 50 degrees (on a spatial scale or resolution larger than 400 to 500 km). Although GRACE would miss the main power of the uplift and subsidence (out of the recoverable degrees), it successfully captures the main power of dilatation (within the recoverable degrees). According to the ratio between the total power of uplift and subsidence commensurate with GRACE resolution and the predicted power from the seismic model (table S1), it is found that GRACE retains only 2% of the power of uplift and subsidence signals. However, GRACE retains almost half of the power of dilatation signals. The seismic model predicts that the power of uplift and subsidence is 20 to 30 times larger than that of dilatation; however, for the band-limited GRACE observations, they are almost equal in magnitude. GRACE's sensitivity to low degree spectra only does not allow observations of a major portion of the coseismic uplift and subsidence, but the coseismic dilatation is well observed.

Like other shallow subduction earthquakes, the Sumatra-Andaman undersea earthquake has produced sparse geodetic measurements except for distant GPS measurements at surrounding islands. GRACE has mapped the coseismic mass redistribution directly above the faults with a resolution of approximately 400 to 500 km. Comparison with an independent seismic model and consideration of the fault mechanism with the geometry of subduction along the trench consistently indicate that the stronger negative gravity anomaly in the east of the Java trench observed by GRACE is due to substantial expansion of the seafloor crust. This unusual sensitivity to the coseismic dilatation suggests that GRACE can provide a new class of observational constraints on geophysical models of great subduction-zone earthquakes.

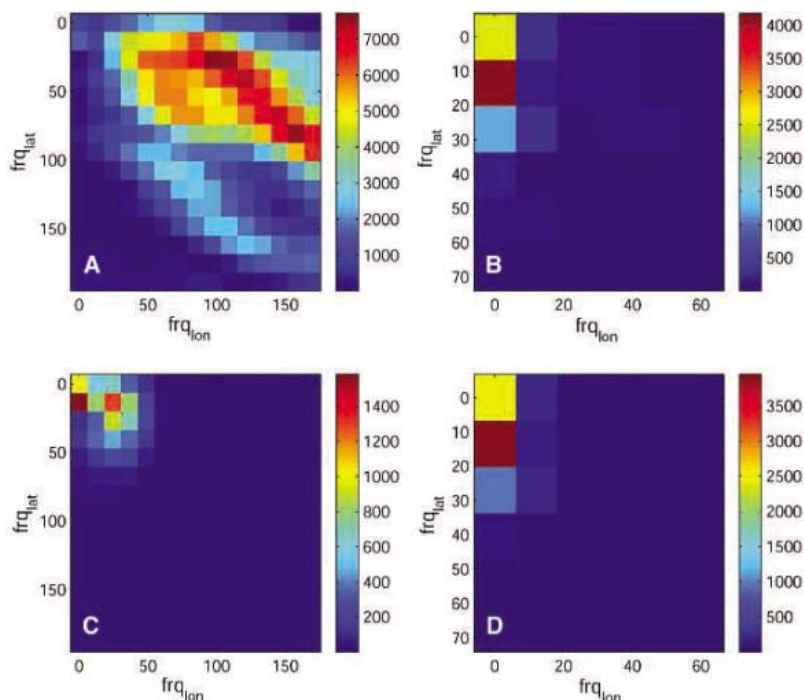


Fig. 5. (A) PSD of the gravity change of vertical displacement from the seismic model (15) (corresponds to fig. S3C). (B) PSD of dilatation (fig. S3F). (C) PSD of smoothed gravity changes due to vertical displacement (Fig. 3C). (D) PSD of smoothed gravity changes due to dilatation (Fig. 3F). The unit of measure is $\mu\text{Gal}^2/(\text{cycle}/\text{km})$. f_{lat} and f_{lon} are spherical degrees in latitude and longitude, respectively, and are defined in (20).

References and Notes

1. C. J. Ammon *et al.*, *Science* **308**, 1133 (2005).
2. T. Lay *et al.*, *Science* **308**, 1127 (2005).
3. J. Park *et al.*, *Science* **308**, 1139 (2005).
4. C. Vigny *et al.*, *Nature* **436**, 201 (2005).
5. B. D. Tapley, S. Bettadpur, J. Ries, P. Thompson, M. Watkins, *Science* **305**, 503 (2004).
6. B. D. Tapley, S. Bettadpur, M. Watkins, Ch. Reigber, *Geophys. Res. Lett.* **31**, L09607 (2004).
7. S. Bettadpur, *Level-2 Gravity Field Product User Handbook* (Report GRACE 327-734, Jet Propulsion Laboratory, Pasadena, CA, 2004).
8. D. Rowlands *et al.*, *Geophys. Res. Lett.* **32**, L04310 (2005).
9. J. Wahr, S. Swenson, V. Zlotnicki, I. Velicogna, *Geophys. Res. Lett.* **31**, L11501 (2004).
10. S. C. Han, C. K. Shum, C. Jekeli, D. Alsdorf, *Geophys. Res. Lett.* **32**, L07302 (2005).

11. D. Chambers, J. Wahr, S. Nerem, *Geophys. Res. Lett.* **31**, L13310 (2004).
12. S. C. Han, C. K. Shum, C. Jekeli, *J. Geophys. Res.* **111**, B04411 (2006).
13. S. C. Han, C. K. Shum, A. Braun, *J. Geodyn.* **39**, 11 (2005).
14. S. C. Han, C. K. Shum, K. Matsumoto, *Geophys. Res. Lett.* **32**, L20311 (2005).
15. C. Ji, a coseismic displacement model updated from Model III (1) for the Sumatra-Andaman (24 December 2004) earthquake and a model for the Nias (28 March 2005) earthquake. They are derived from a combination of seismic and geodetic observations and are formulated in terms of over 1000 slip (Burgers) vectors on seven rectangular dislocation patches using the uniform elastic half-space formalism (see fig. S4 for slip distribution).
16. Y. Okada, *Bull. Seismol. Soc. Am.* **75**, 1135 (1985).
17. Y. Okada, *Bull. Seismol. Soc. Am.* **82**, 1018 (1992).
18. The Moho depth is assumed to be 20 km below the sea floor, which is a roughly averaged value over the region on the basis of the CRUST2.0 model, which is an update of CRUST5.1.
19. S. C. Han *et al.*, *Geophys. J. Int.* **163**, 18 (2005).
20. The spatial frequency in the unit of (cycle/length) can be computed by using $f = n/2\pi R$, where f is frequency in (cycles/km), n is spherical degree, and R is Earth's mean radius. The corresponding spatial scale (resolution) in the unit of kilometers can be computed by $20,000/n$.
21. S. C. Han *et al.*, *Eos* **86**, G22A-05 (2005).
22. The GRACE regional estimates of time-variable gravity had full power up to a degree and order of approximately 40 (or a resolution of 500 km) when they were compared to the high-resolution terrestrial hydrology model Global Land Data Assimilation System.
23. Supported by grants from NASA (NNG04GN19G and NNG04GF01G) and from NSF's Collaboration in Mathematics and Geosciences Program (EAR0327633). Additional computing resources were provided by the Ohio Supercomputer Center. We acknowledge the

NASA/Geoforschungszentrum (GFZ) GRACE project for the GRACE data products distributed by the Jet Propulsion Laboratory (JPL) Physical Oceanography Distributed Active Archive Center. We thank S. Bettadpur, University of Texas, for providing higher sampled GRACE orbits and for helpful advice in GRACE L1B data processing; S. Okubo, University of Tokyo, and R. Gross, JPL, for valuable discussions; and two anonymous reviewers for helpful comments.

Supporting Online Material

www.sciencemag.org/cgi/content/full/313/5787/658/DC1
Materials and Methods
Figs. S1 to S4
Table S1
References

12 April 2006; accepted 15 June 2006
10.1126/science.1128661

Synthesis of Biaryls via Catalytic Decarboxylative Coupling

Lukas J. Gooßen,* Guojun Deng, Laura M. Levy

We present a safe and convenient cross-coupling strategy for the large-scale synthesis of biaryls, commercially important structures often found in biologically active molecules. In contrast to traditional cross-couplings, which require the prior preparation of organometallic reagents, we use a copper catalyst to generate the carbon nucleophiles *in situ*, via decarboxylation of easily accessible arylcarboxylic acid salts. The scope and potential economic impact of the reaction are demonstrated by the synthesis of 26 biaryls, one of which is an intermediate in the large-scale production of the agricultural fungicide Boscalid.

The biaryl substructure is a widely occurring component of biologically active and functional molecules (1–4). Its importance is reflected in the immense economic value of pharmaceuticals including Valsartan (5, 6) and Telmisartan (7, 8), agrochemicals such as Boscalid (9), and liquid crystals for LCD screens (10) (Fig. 1).

Over the past several decades, the mild and selective Suzuki coupling of nucleophilic arylboronic acids with aryl halides (11–14) has almost completely replaced classical methods of biaryl synthesis (15–18) and has become the method of choice for laboratory and industrial applications (19). More than 4000 publications (20) attest to the tremendous interest in improving this transformation. However, the Suzuki reaction still suffers from a fundamental drawback common to almost all catalytic couplings between aryl nucleophiles and electrophiles: It requires the use of stoichiometric amounts of an expensive organometallic compound, in this case a boronic acid, which must generally be prepared from sensitive precursors under elaborate anaerobic conditions (16).

Living organisms, which generally lack an air- and water-free environment, have long evolved to generate carbanion equivalents by straightforward

enzymatic decarboxylation of ubiquitously available carboxylic acid derivatives, including as an example the heteroarene carboxylic acid orotidine monophosphate (OMP, Fig. 2) (21–24). This biochemical transformation inspired us to adopt a loosely analogous approach for the chemical synthesis of biaryls, using carboxylate salts rather than organometallics as the source of carbon nucleophiles. However, whereas β -ketocarboxylic acids are capable of forming a six-membered cyclic transition state, lowering the activation barrier for decarboxylation (25, 26), metal salts of aromatic carboxylates require extreme temperatures to lose CO₂ (27–29), and under the reported conditions, the aryl-metal species are rapidly protonated by the surrounding medium to give the corresponding arenes. In mechanistic studies of such protodecarboxylation reactions, Nilsson proved the intermediacy of an

aryl-copper species in the pyrolysis of copper 2-nitrobenzenecarboxylate (250°C) by capturing it with excess iodobenzene and isolating 2-nitrobiphenyl along with nitrobenzene and several by-products (29).

Because of the intrinsic limitations of related copper-mediated Ullmann-type couplings (insufficient selectivity for the heterocoupling, stoichiometric use of copper), we saw little opportunity to turn this trapping experiment into a preparatively useful biaryl synthesis from arenecarboxylates. However, we envisioned that such a synthesis could be achieved with a bimetallic catalyst—a copper complex capable of mediating the strongly endothermic extrusion of carbon dioxide from arenecarboxylates, combined with a two-electron catalyst capable of catalyzing the cross-coupling with an aryl halide (Fig. 3). The copper derivative would thus initially coordinate to the carboxylate oxygen, then shift to the aryl π -system and insert into the C–C(O) bond under extrusion of CO₂ to form a stable aryl-copper intermediate (28). The two-electron catalyst (e.g., Pd) could then cross-couple this species with an aryl electrophile to form the desired biaryl and the corresponding metal halide.

To test our hypothesis and identify systems capable of mediating this highly desirable process, we chose as a model reaction the commercially important cross-coupling of 2-nitrobenzoic acid with 4-bromochlorobenzene to form the Boscalid intermediate **3a** (Fig. 4). Selected results from our screening experiments are summarized in table S1.

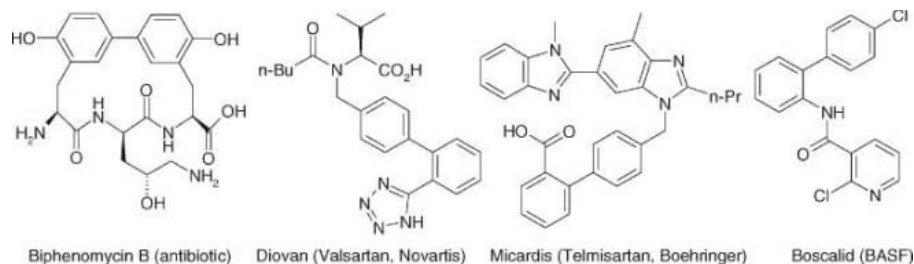


Fig. 1. Examples of top-selling biaryl products (31, 32). Worldwide sales: Diovan, US\$3.1 billion (2004); Micardis, US\$704 million (2004); Boscalid, EUR 150 million (projected).

Institut für Organische Chemie, Technische Universität Kaiserslautern, Erwin-Schrödinger-Straße, Building 54, D-67663 Kaiserslautern, Germany.

*To whom correspondence should be addressed. E-mail: goossen@chemie.uni-kl.de

As anticipated, biaryl formation was not observed when potassium 2-nitrobenzoate was heated with an aryl halide and a palladium/phosphine cross-coupling catalyst, nor when copper(II) 2-nitrobenzoate and the aryl halide were reacted in the absence of palladium. However, when the copper(II) and palladium catalysts were combined at a temperature as low as 120°C, we detected small amounts of the desired biaryl. The efficiency of the reaction was improved upon addition of potassium fluoride, presumably because of the formation of ArC(O)OCuF , which seems to lower the decarboxylation barrier. Further increases in the yield were obtained by continuous removal of the water by-product derived from the carbonate base (e.g., by azeotropic distillation or with molecular sieves), thus limiting the competing protonation of the aryl copper intermediate, and by optimization of the steric and electronic properties of the phosphine ligand coordinated to Pd. Quantitative decarboxylative cross-coupling to the desired biaryl was finally achieved with the use of $\text{Pd}(\text{acac})_2$, $\text{P}(i\text{-Pr})\text{Ph}_2$, CuCO_3 , KF , and mo-

lecular sieves in an *N*-methylpyrrolidine (NMP) solution (acac, acetylacetonate; Ph, phenyl).

Although this protocol for biaryl synthesis from carboxylic acids and aryl bromides is highly effective, it remains stoichiometric in the heavy metal copper. Following the proposed mechanism (Fig. 3), the copper salt is fully regenerated after each transmetalation step, so that a catalytic amount should theoretically suffice. However, the yields collapsed when we replaced most CuCO_3 by K_2CO_3 , an outcome we attribute to an irreversible reduction of Cu(II) to Cu(I). Clearly, an alternative protocol that is catalytic in both metals—as is required for industrial-scale applications—would only be possible with more stable but less effective Cu(I) complexes, at the expense of an increased reaction temperature.

We thus developed a second catalyst system comprising palladium acetylacetonate, copper(I) iodide, and bipyridine ligands, which proved at 160°C to be almost as active as the first system. With this new Cu(I)-based system, turnover was accomplished using substoichiometric amounts of

copper, and after further optimization, only 1% CuI, 0.5% $\text{Pd}(\text{acac})_2$, and 3% phenanthroline sufficed for near-quantitative coupling of potassium 2-nitrobenzoate with 4-bromochlorobenzene.

We found this protocol to be reliable and convenient for the preparation of **3a** not only on a milligram scale but also for multigram syntheses. It was successfully scaled up to molar quantities at Saltigo GmbH, with 20% toluene added to adjust the solvent boiling point to 160°C and allow azeotropic drying of the reaction mixture (30). Our catalytic system also allowed for replacement of the bromide electrophile with the less expensive (but generally far less reactive) 1,4-dichlorobenzene.

After optimizing the catalyst systems, we tested the generality of the reaction with regard to both coupling partners (Table 1). The two reaction protocols (Fig. 5) proved to be suitable for a wide array of aryl halides: Both electron-rich and electron-poor electrophiles were successfully converted across a range of steric demands and functional groups.

In principle, a process catalytic in both metals should be applicable to all aryl and vinyl carboxylic acids. However, although a notable range of carboxylic acids could be converted in the presence of stoichiometric amounts of copper, our first protocol involving catalytic copper initially remained limited to 2-nitrobenzoic acids (biphenyls **3a** to **3p**, Table 1).

This result prompted us to study the decarboxylation step separately from the cross-coupling step. We were delighted to find that at 160°C and within 24 hours, a catalytic amount (15%) of a copper(I) phenanthroline quinoline complex was able to protodecarboxylate aromatic, heteroaromatic, and vinylic carboxylates to the corresponding hydrocarbons (table S2). We also observed that added halide ions (which would be released in the transmetalation step; see Fig. 3) retarded this decarboxylation. Hence, instead of having encountered an inherent substrate limitation, the results suggest that the halides are in competition with the carboxylates for coordination sites at the copper. Therefore, a key to achieving a general process catalytic in both metals is to induce a stronger preference of the copper for carboxylate over bromide ions by tuning its ligand environment.

With stepwise improvements of the copper-phenanthroline catalysts, we were able to extend the scope of the protocol catalytic in both metals first to carboxylic acids with other strongly coordinating groups in *ortho*-position that increase the copper-ligating quality of the carboxylate substrate (2-acyl, 2-formyl), then to carboxylic acids with weakly coordinating *ortho*-substituents (2-fluorobenzoic acid, 2-cyanobenzoic acid), and finally to vinylic or heterocyclic derivatives (cinnamic acid, thiophenecarboxylic acid). This appears to be the performance limit of the simple copper-phenanthroline complexes: Stoichiometric amounts are still required for other benzoates.

Already at its early state of development, this decarboxylative biaryl synthesis has opened up

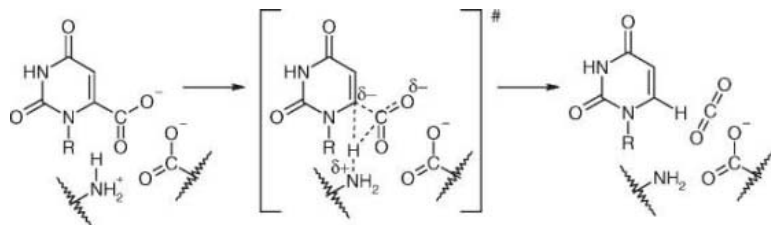


Fig. 2. Enzymatic decarboxylation of OMP, followed by protonation of the carbanion.

Fig. 3. Proposed mechanism for a decarboxylative biaryl synthesis. L can be phosphine, phenanthroline, or another ligand. See Table 1 for possible meanings of R and R'.

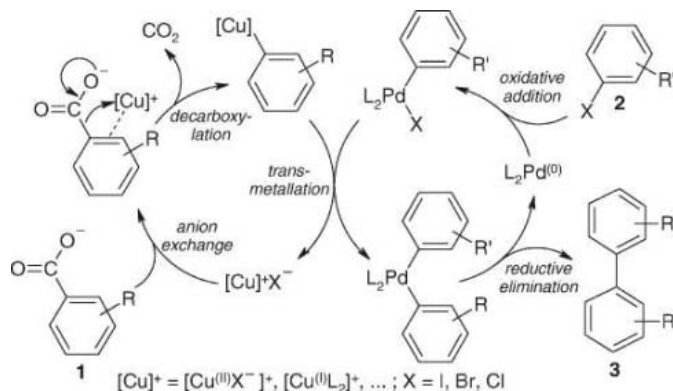


Fig. 4. Model reaction for the development of the reaction conditions.

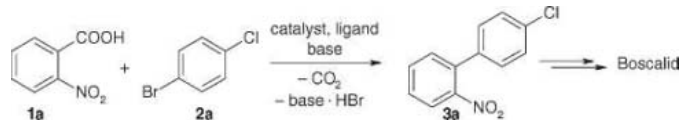


Fig. 5. Biaryl synthesis with excess copper (top) and catalytic copper (bottom).

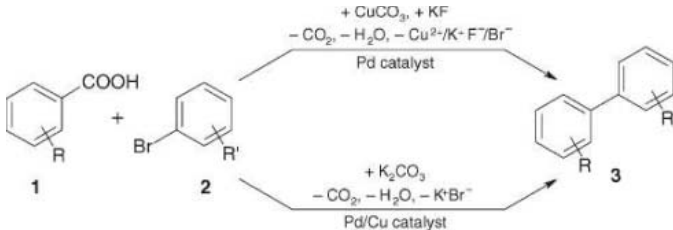
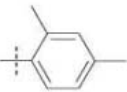
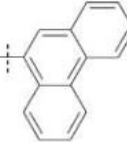
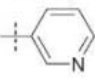
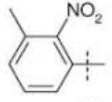
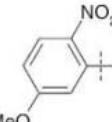
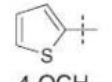
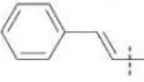


Table 1. Substrate scope of the cross-coupling reaction. Conditions with excess Cu: 1.0 mmol of aryl bromide, 1.5 mmol of carboxylic acid, 1.5 mmol of CuCO_3 , 1.5 mmol of KF, 0.02 mmol of $\text{Pd}(\text{acac})_2$, 0.06 mmol of $\text{P}(i\text{-Pr})\text{Ph}_2$, 500 mg of ground 3 Å molecular sieves (MS), and 3 ml of NMP, 120°C, 24 hours, isolated yields. Conditions with catalytic Cu: 1.0 mmol of aryl bromide, 1.5 mmol of carboxylic acid, 1.2 mmol of K_2CO_3 , 250 mg of ground 3 Å MS, and 1.5 ml of NMP, 160°C, 24 hours, isolated yields; catalyst system: 0.01 mmol of $\text{Pd}(\text{acac})_2$, 0.03 mmol of CuI, and 0.05 mmol of 1,10-phenanthroline.

ArCOOH	ArBr	Product	Yield (%) with excess Cu	Yield (%) with cat. Cu
2-NO ₂	4-Cl	3a	97	99
2-NO ₂	4-Cl [†]	3a		66
2-NO ₂	4-CN	3b	96	93
2-NO ₂	4-CN [†]	3b		96
2-NO ₂	4-CH ₃	3c	97	72
2-NO ₂	4-OCH ₃	3d	79	68
2-NO ₂	4-SCH ₃	3e	82	98 [†]
2-NO ₂	4-C(O)CH ₃	3f	86	
2-NO ₂	4-CO ₂ C ₂ H ₅	3g	97	96
2-NO ₂	4-CHO	3h	93	78
2-NO ₂		3i	93	
2-NO ₂	2-OCH ₃	3j	80	
2-NO ₂		3k	86	99
2-NO ₂	4-F	3l		97
2-NO ₂	4-CF ₃	3m		93
2-NO ₂		3n		98
	4-Cl	3o		74
	4-Cl	3p		77
	4-CH ₃	3q	53 [‡] (82 [§])	65
4-OCH ₃	4-CH ₃	3r	41 [‡]	
	4-CH ₃	3s	82 [‡]	91 ^{**}
2-CHO	4-CH ₃	3t	55 [§]	28 ^{**}
2-F	4-CH ₃	3u	82 [§]	67 ^{††}
2-C(O)CH ₃	4-CH ₃	3v	83 [§]	66 ^{**}
2-OCH ₃	4-CH ₃	3w	29 [§]	
2-NHC(O)CH ₃	4-CH ₃	3x	42 [§]	
2-NHC ₆ H ₅	4-CH ₃	3y	91 [§]	
2-SO ₂ CH ₃	4-CH ₃	3z	97 [§]	

*Starting from the aryl chloride. †0.1 mmol of copper catalyst. ‡160°C. §Alternative method with excess Cu: 1.0 mmol of aryl bromide, 1.3 mmol of carboxylic acid, 0.02 mmol of $\text{Pd}(\text{acac})_2$, 1.2 mmol of CuI, 0.1 mmol of 2,2'-bipyridine, 1.2 mmol of K_2CO_3 , 500 mg of ground 3 Å MS, 3 ml of NMP, 160°C, 24 hours, isolated yields. ||Catalyst system: 0.02 mmol of $\text{Pd}(\text{acac})_2$, 0.1 mmol of copper salt, and 0.1 mmol of 1,10-phenanthroline. ¶]5:1 mixture of 1,1- and 1,2-regioisomer. **1.2 mmol of Cs_2CO_3 as the base; catalyst system: 0.02 mmol of $\text{Pd}(\text{acac})_2$, 0.04 mmol of PPh_3 , 0.15 mmol of copper salt, 0.3 mmol of 1,10-phenanthroline, and 0.2 ml of toluene. ††1.2 mmol of Cs_2CO_3 as the base, 0.2 ml of toluene; catalyst system: 0.02 mmol of $\text{Pd}(\text{acac})_2$, 0.06 mmol of PPh_3 , 0.1 mmol of copper salt, and 0.2 mmol of 1,10-phenanthroline. See supporting online material for further details.

new opportunities for the industrial synthesis of high-value pharmaceutical intermediates. An extension of the catalytic protocol to the entire range of aromatic, vinylic, and heteroaromatic acids can be expected in the near future, from ligand generations designed to induce an even stronger affinity of copper for carboxylate ions.

References and Notes

- D. A. Horton, G. T. Bourne, M. L. Smythe, *Chem. Rev.* **103**, 893 (2003).
- G. Bringmann, C. Günther, M. Ochse, O. Schupp, S. Tasler, *Bianyls in Nature: A Multi-Faceted Class of Stereochemically, Biosynthetically, and Pharmacologically Intriguing Secondary Metabolites* (Springer-Verlag, New York, 2001).
- P. J. Hajduk, M. Bures, J. Praestgaard, S. W. Fesik, *J. Med. Chem.* **43**, 3443 (2000).
- G. W. Bemis, M. A. Murcko, *J. Med. Chem.* **39**, 2887 (1996).
- A. Markham, K. L. Goa, *Drugs* **54**, 299 (1997).
- K. F. Croom, G. M. Keating, *Am. J. Cardiovasc. Drugs* **4**, 395 (2004).
- M. Sharpe, B. Jarvis, K. L. Goa, *Drugs* **61**, 1501 (2001).
- S. Yusuf, *Am. J. Cardiol.* **89**, 18A (2002).
- M. E. Matheron, M. Porchas, *Plant Dis.* **88**, 665 (2004).
- E. Poetsch, *Kontakte* **1988**, 15 (1988).
- N. Miyaura, K. Yamada, A. Suzuki, *Tetrahedron Lett.* **20**, 3437 (1979).
- N. Miyaura, A. Suzuki, *Chem. Commun.* **1979**, 866 (1979).
- N. Miyaura, A. Suzuki, *Chem. Rev.* **95**, 2457 (1995).
- A. Suzuki, *J. Organomet. Chem.* **576**, 147 (1999).
- J. Hassan, M. Sevignon, C. Gozzi, E. Schulz, M. Lemaire, *Chem. Rev.* **102**, 1359 (2002).
- F. Diederich, P. J. Stang, Eds., *Metal-Catalyzed Cross-Coupling Reactions* (Wiley-VCH, Weinheim, Germany, 1998).
- J. Tsuji, *Palladium Reagents and Catalysts* (Wiley, Chichester, UK, ed. 2, 2004).
- N. Miyaura, *Top. Curr. Chem.* **219**, 11 (2002).
- A. M. Rouhi, *Chem. Eng. News* **82**, 49 (2004).
- CAS SciFinder keyword search for "Suzuki coupling" resulted in 4322 hits for the time period 1996–2006.
- H. Iding, P. Siegert, K. Mesch, M. Pohl, *Biochim. Biophys. Acta* **1385**, 307 (1998).
- T. P. Begley, S. E. Ealick, *Curr. Opin. Chem. Biol.* **8**, 508 (2004).
- R. J. Heath, C. O. Rock, *Nat. Prod. Rep.* **19**, 581 (2002).
- O. P. Ward, A. Singh, *Curr. Opin. Biotechnol.* **11**, 520 (2000).
- S. Lou, J. A. Westbrook, S. E. Schaus, *J. Am. Chem. Soc.* **126**, 11440 (2004).
- J. March, *Advanced Organic Chemistry* (Wiley, New York, ed. 4, 1985), pp. 627–630.
- T. Cohen, R. A. Schambach, *J. Am. Chem. Soc.* **92**, 3189 (1970).
- T. Cohen, R. W. Berninger, J. T. Wood, *J. Org. Chem.* **43**, 837 (1978).
- M. Nilsson, *Acta Chem. Scand. A* **20**, 423 (1966).
- L. J. Gooßen, G. Deng, patent pending, filing number PCT-DE2006-001014 (2005).
- For Valsartan and Micardis sales, see *Fifth Annual Contract Pharma Top Pharmaceutical & Biopharmaceutical Companies Report* (Rodman, Ramsey, NJ, 2005).
- BASF AG, *Shaping the Future, Financial Report 2005* (BASF, AG, Ludwigshafen, Germany, 2005).
- We thank H. Hugl, F. Rampf, and M. T. Reetz for helpful discussions, and B. Melzer and C. Linder for technical assistance. Supported by a Deutsche Forschungsgemeinschaft Heisenberg scholarship (L.J.G.), Saltigo GmbH, and Studiengesellschaft Kohle. Dedicated to my admired teacher K. P. C. Vollhardt on the occasion of his 60th birthday.

Supporting Online Material

www.sciencemag.org/cgi/content/full/313/5787/662/DC1
Materials and Methods
Tables S1 and S2

12 April 2006; accepted 29 June 2006
10.1126/science.1128684

Gender Differences in Patenting in the Academic Life Sciences

Waverly W. Ding,¹ Fiona Murray,² Toby E. Stuart^{3*†}

We analyzed longitudinal data on academic careers and conducted interviews with faculty members to determine the scope and causes of the gender gap in patenting among life scientists. Our regressions on a random sample of 4227 life scientists over a 30-year period show that women faculty members patent at about 40% of the rate of men. We found that the gender gap has improved over time but remains large.

The gender gap in academic science is a topic of ongoing policy and scholarly debate. Studies in fields as diverse as engineering and biology have found that women scientists suffer from an attainment gap along at least three important dimensions: productivity, recognition, and reward (1–4). Fortunately, some recent evidence provides cause for optimism. Especially in fields within the academic life sciences, the gender gap has narrowed (3, 5). Until recently, however, little research has explored an increasingly important source of non-salary remuneration for faculty: participation in commercial science (6). This omission is problematic given the growing opportunities for recognition and reward in the commercialization of scientific research. Although profiting from university research continues to generate controversy (7), the reality is that commercial activities including patenting, consulting, and scientific advisory board (SAB) membership have become commonplace (8). What limited evidence exists about “academic entrepreneurship” suggests a gender gap of considerable magnitude.

Here, we examine gender differences in one specific commercial activity—patenting. We conducted a longitudinal empirical analysis using a random sample of faculty in the life sciences employed in U.S. academic institutions. The analysis is complemented by interviews with life scientists at one prominent university. Although academic patents do not yield immediate financial returns to their inventors, frequently they serve as an avenue to a variety of rewards, such as royalty-bearing license agreements with established companies or startup formation with substantial equity participation. Although not the only route to commercial engagement, our interviews and previous research suggest that patents are an important precursor to opportunities in industry.

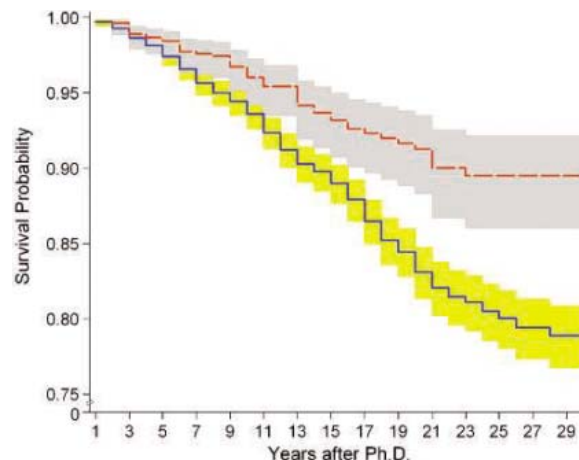
We began the quantitative analysis by drawing a random sample of 12,000 life scientists

from the UMI Proquest Dissertations database (9). We restricted the sample to those earning Ph.D.’s between 1967 and 1995 in the scientific fields that have most fostered the commercial life sciences. We then used the *Science Citation Index* (10) to collect the publications, coauthors, and employers of the individuals in the sample. Because our interest is in academic careers, we retained only the 4227 individuals with at least 5 years of post-Ph.D. publishing experience in academic institutions. We then obtained the patents on which the scientists in the sample are listed as inventors. With this information, we created a data set of scientist-year observations with covariates for the individual’s gender, annual publication activity, and annual patent count [supporting online material (SOM) text].

Of the scientists in our sample, 11.5% are listed as inventors on one or more patents. However, the full sample proportion masks a large gender difference: Of the 903 women in the sample, 5.65% held patents as of the last year of the data. By contrast, 13% of the 3324 male scientists in the data are listed on patents. Moreover, the 431 male patenters have amassed a total of 1286 patents in our data set. The 51 women patenters produced only 92 patents.

We structured the data archive to enable survival analyses. Figure 1 displays gender-specific nonparametric survivor plots that show the likelihood that a scientist in the data has not patented up to a given year of professional tenure. The plots show that, at all career stages,

Fig. 1. Gender-specific Kaplan-Meier estimates of the survivorship function of first patenting with confidence intervals. The likelihood that scientists (blue line for male and red dashed line for female) have not patented up to a given year of professional experience is shown. Both the stratified log-rank test and Wilcoxon test ($P < 0.01$) reject the hypothesis that the survival functions are equal.



the curve for male scientists is beneath that for women, and the gender gap in survival probabilities increases over time.

Similar to other areas of scientific attainment, patenting is affected by a range of individual, field, and institutional factors, many of which may differ systematically between the sexes (11–13). After constructing four mutually exclusive subsamples—male patent holders, female patent holders, men without patents, and women without patents—we observed considerable subsample differences in means (across levels of professional experience) in (i) number of papers, (ii) amount of NIH grants, and (iii) number of papers coauthored with researchers in industry (Fig. 2). Male patenters typically have the highest paper counts, the most NIH grant money, and along with the women patenters, the most coauthorships with industry scientists (table S1 provides significance tests).

Given evidence of these disparities between male and female scientists, it is important to determine the conditional effect of gender on patenting—its net effect after holding constant other measured attributes of scientists. Therefore, we estimated scientist-level regressions of the rate of patenting. Formally, let $\lambda_i(t)$ designate the instantaneous transition rate, where $t = 1, \dots, 35$ years (we assume that 35 years is the maximum time any scientist is at risk). We estimated Cox proportional hazards regressions. Letting $\lambda_0(t)$ indicate the baseline hazard, $X_i(t-1)$ indicate a vector of lagged, time-varying covariates, and V_i indicate a vector of time-independent covariates, we estimated $\lambda_i(t, X, V, \beta, \gamma) = \lambda_0(t) \times \exp[\beta'X_i(t-1) + \gamma'V_i]$.

We included a number of variables in the $X_i(t-1)$ vector. One attribute that influences patenting is a scientist’s research productivity. At the extreme, an unpublished scientist probably lacks novel findings to patent. Therefore, we included the number of articles each scientist has published in the previous 5-year period and the square of this variable. Those we interviewed suggested that scientists’ employers also influence patenting by providing support

¹Haas School of Business, University of California, Berkeley, CA 94720, USA. ²MIT Sloan School of Management, Massachusetts Institute of Technology, 50 Memorial Drive, Cambridge, MA 02142, USA. ³Harvard Business School, Soldiers Field Road, Boston, MA 02163, USA.

*All authors contributed equally to this work.

†To whom correspondence should be addressed. E-mail: tstuart@hbs.edu

for interactions with industry. To proxy for this workplace characteristic, we included the number of patents assigned to the scientist's employing university during the previous 5 years (excluding patents held by the focal scientist). We reasoned that universities with high patent counts will likely have an effective technology transfer office (TTO) and a culture that supports involvement in commercial endeavors.

Interviewees suggested that networks of colleagues influenced their patenting behavior, which is consistent with recent research on entrepreneurship (8, 14). Scientists (particularly male faculty) routinely mentioned consulting with coauthors, colleagues, and industry contacts for advice about the patent process. We captured faculty members' contacts with two variables. First, as a gauge of network reach,

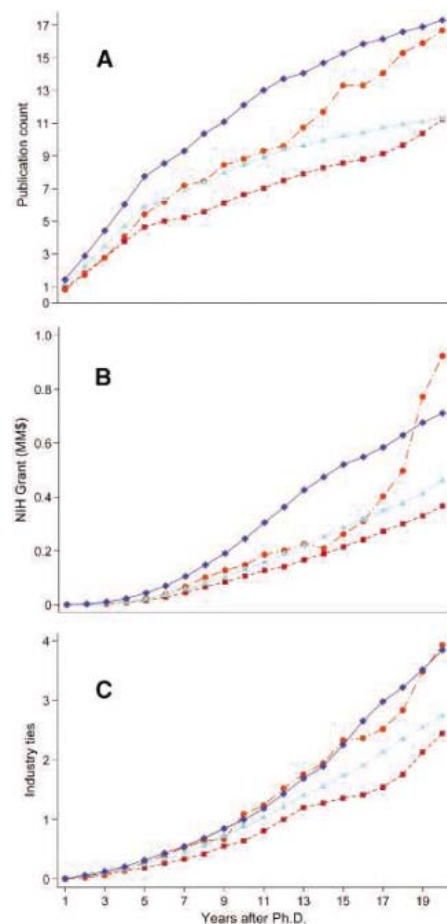


Fig. 2. Mean publication count (A), NIH grant totals (B), and number of jointly authored papers with industry researchers (C) during the first 20 years of scientists' careers. Groups are male patenters (dark blue squares), males without patents (light blue triangles), female patenters (light pink circles), and females without patents (dark pink squares). Although women patenters appear to have a higher mean grant total than male patenters beyond the 18th year of professional experience, this difference is not statistically significant. (Table S1 provides equality of means tests across categories.) MM\$, millions of dollars.

we included the average number of coauthors the scientist has had on previously published papers. Second, as a proxy for the richness of scientists' networks with industry, we included a dummy variable equal to one if a scientist has recently coauthored papers with one or more researchers in industry.

Figure 3 shows our regression findings (table S2). The parameter estimates suggest that an increase in the 5-year publication count of one standard deviation of the observed distribution (12.1 papers) multiplies the hazard rate of patenting by a factor of 1.81. Similarly, scientists that average a greater number of coauthors per paper, those that work at universities that promote patenting and those that have collaborative projects with scientists in industry, patent at a greater rate. There also are statistically significant scientific field effects. Relative to the omitted category (genetics) in the regression, molecular biologists, immunologists, and organic chemists patent at a substantially higher rate (Fig. 3 and table S2).

After accounting for the effects of productivity, networks, field, and employer attributes, what is the net effect of gender? There remains a large, statistically significant ($P < 0.001$) effect of being female. The parameter estimate implies that, holding constant productivity, social network, scientific field, and employer characteristics, comparable women life scientists patent at only 0.40 times the rate of equivalent male scientists. This finding leads to the question: What might cause such a large gender difference in patenting?

One possibility is that men and women do qualitatively different kinds of research. In particular, if women are risk averse in their research choices (15), there may be a gender difference in research "patentability." We believe such a difference would manifest in the extent of scholarly impact. To explore this possibility, we created a data set of the 23,436 articles published by the women in our sample and matched each paper (by publication year) with a randomly drawn article from the pool of male scientists' papers. This yields a sample of articles with a 1:1 gender ratio. We then ex-

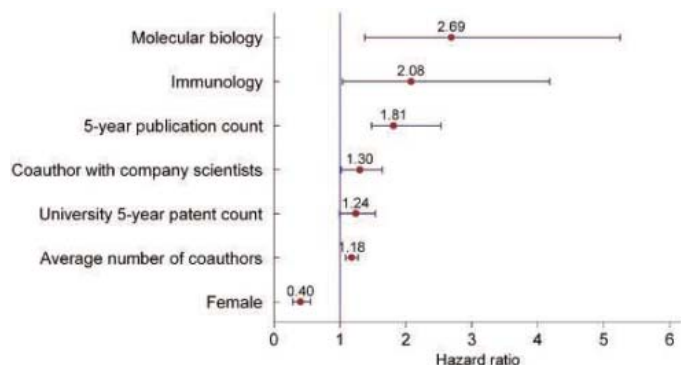
amined, by gender and year, the average number of citations and the journal impact factor (JIF) of these papers. We found that the per-article mean citation count for male scientists is very similar to that of women (table S3). Moreover, the gender gap in average JIF actually favors women (average JIF for male: 4.06; average JIF for female: 4.12). Overall, there is no evidence that women do less important work based on standard measures of scientific impact.

If there is no measurable gender difference in the scholarly influence of research, what else might cause such a large gender difference in patenting? For clues, we turned to our faculty interviews, in which two factors loomed large. The first is lack of exposure to the commercial sector. Most (but not all) women had few contacts in industry. Lacking these connections, women found it time-consuming to gauge whether an idea was commercially relevant. In contrast, men often described an industry contact as a precursor to patenting. Hampered by their narrow networks and concerned about the time it would take to "shop" a patent around, several female faculty were deterred from completing a patent filing. Thus, differences in the composition of professional networks meant that the time cost of patenting was higher for many women faculty.

Several women suggested a second hurdle: concern that pursuing commercial opportunities might hinder their university careers. The women we interviewed were more likely to describe the challenges associated with balancing multiple career elements: teaching, research, and commercialization. Unlike their male counterparts, who described their patenting decisions as unproblematic and driven by translational interests, female faculty expressed concern about the potentially negative impact that patenting might have on education, collegiality, and research quality.

Our interviews also uncovered two factors that reduced the perceived costs of patenting for female faculty: collegial support and institutional assistance. Compared with men, female faculty were much more likely to be encouraged in patenting by their (typically male) coauthors, who often drove the patenting process.

Fig. 3. Hazard ratios and 95% confidence intervals from Cox regression of time until patenting. Hazard ratio g implies that the probability of patenting changes by a factor of g for a unit (dichotomous variables) or standard deviation (continuous variables) change in the covariate value. Predictors are sorted by effect magnitude and are statistically significant if 1.0 falls outside of the confidence interval. (Full regression results are presented in table S2.)



Whereas men sought advice from their often broad-reaching networks, women frequently depended on close relationships with male collaborators to initiate the patenting process. Formal institutional sponsorship was also particularly important for women. Many women commented that their TTO provided industry contacts, advice, and encouragement to develop the commercial aspects of their research.

Our interviews also exposed differences between older and younger women scientists. Most senior female faculty we met perceived themselves as being excluded from industry relationships and therefore failed to develop an understanding of how commercial science works. Few made the transition to patenting. Some of the younger (but tenured) female life scientists had begun to incorporate patenting into their research strategy. Nonetheless, many still felt at a disadvantage to their male colleagues because of their limited experience at the academic-industry boundary. It is only among junior faculty that we found parity in attitudes, which were shaped by doctoral and postdoctoral experiences. Regardless of gender, those that experienced patenting during training were undaunted by the challenges of combining academic and commercial science.

Because our data spans 35 years, we can determine whether such generational distinctions are evident in the larger sample. For three Ph.D. cohorts (those earning degrees from 1967 to 1975, 1976 to 1985, and 1986 to 1995),

we examined gender-specific nonparametric cumulative hazard plots. For each cohort, we also calculated the male-to-female ratio of the cumulative hazards. For example, at the 10th year after scientists earned their Ph.D., the cumulative hazard of patenting for male scientists was 4.4 times as high as women in the 1967–1975 cohort, 2.1 times as high in the 1976–1985 cohort, and 1.8 times as high in the 1986–1995 cohort (fig. S1). Thus, consistent with our interview findings, the archival data indicate that the gender gap in patenting rates has been declining.

Our analyses suggest that patenting has become common in the academic life sciences, particularly for highly productive and networked faculty. Among the most senior faculty, a large gender gap persists, reinforced by women's limited commercial networks and traditional views of academic careers. Younger cohorts widely embrace patenting, although a gender gap remains. Increasingly, however, young female faculty are similar to their male colleagues: They view patents as accomplishments and as a legitimate means to disseminate research. If this trend continues, we may observe further declines in the magnitude of the gender gap in commercializing academic science.

References and Notes

1. J. R. Cole, S. Cole, *Social Stratification in Science* (Univ. Chicago Press, Chicago, IL, 1973).

2. J. S. Long, M. F. Fox, *Annu. Rev. Soc.* **21**, 45 (1995).
3. National Science Foundation, *Gender Differences in the Careers of Academic Scientists and Engineers* (NSF 04-323, Arlington, VA, 2004); available online (www.nsf.gov/sbe/srs/ns04323/pdf/front.pdf).
4. G. Sonnert, G. Holton, *Who Succeeds in Science? The Gender Dimension* (Rutgers Univ. Press, New Brunswick, NJ, 1995).
5. C. Holden, *Science* **294**, 396 (2001).
6. J. Thursby, M. Thursby, *J. Technol. Transfer* **30**, 343 (2005).
7. J. P. Walsh, W. M. Cohen, A. Arora, *Science* **299**, 1021 (2003).
8. T. E. Stuart, W. Ding, *Am. J. Soc.* **112**, 97 (2006).
9. UMI Proquest Dissertations database (<http://wwwlib.umi.com/dissertations/>).
10. *Science Citation Index* (<http://scientific.thomson.com/products/sci/>).
11. H. Etzkowitz, C. Kemelgor, M. Neuschatz, B. Uzzi, J. Alonzo, *Science* **266**, 51 (1994).
12. Y. Xie, K. A. Shauman, *Women in Science: Career Processes and Outcomes* (Harvard Univ. Press, Cambridge, MA, 2003).
13. P. D. Allison, J. S. Long, *Am. Soc. Rev.* **55**, 469 (1990).
14. S. Shane, T. Stuart, *Management Sci.* **48**, 154 (2002).
15. R. L. Fisher, *The Research Productivity of Scientists: How Gender, Organizational Culture and Problem Choice Processes Influence the Productivity of Scientists* (Univ. Press of America, Dallas, TX, 2005).
16. F.M. acknowledges financial support from the Cambridge-MIT Institute. T.E.S. acknowledges financial support from the Center for Entrepreneurial Leadership at the Ewing Marion Kauffman Foundation, Kansas City, MO. This material is partly based on work supported by the NSF under grant No. EEC-0345195 (T.E.S.).

Supporting Online Material

www.sciencemag.org/cgi/content/full/313/5787/665/DC1
Fig. S1
Tables S1 to S4

11 January 2006; accepted 13 June 2006
10.1126/science.1124832

Regulation of Sexual Development of *Plasmodium* by Translational Repression

Gunnar R. Mair,¹ Joanna A. M. Braks,¹ Lindsey S. Garver,² Joop C. A. G. Wiegant,³ Neil Hall,⁴ Roeland W. Dirks,³ Shahid M. Khan,¹ George Dimopoulos,² Chris J. Janse,¹ Andrew P. Waters^{1*}

Translational repression of messenger RNAs (mRNAs) plays an important role in sexual differentiation and gametogenesis in multicellular eukaryotes. Translational repression and mRNA turnover were shown to influence stage-specific gene expression in the protozoan *Plasmodium*. The DDX6-class RNA helicase, DOZI (development of zygote inhibited), is found in a complex with mRNA species in cytoplasmic bodies of female, blood-stage gametocytes. These translationally repressed complexes are normally stored for translation after fertilization. Genetic disruption of *pbdzi* inhibits the formation of the ribonucleoprotein complexes, and instead, at least 370 transcripts are diverted to a degradation pathway.

Translational repression (TR) of mRNAs in higher eukaryotes controls temporal expression of specific protein cascades or directs the location of translation within a cell, and is important after gamete fertilization (zygote formation) in the early embryo when de novo transcription of mRNA is restricted (1–5). The hallmark of repression is the assembly of certain mRNAs together with proteins into qui-

escent messenger ribonucleoprotein particles (mRNPs), where these transcripts are stored for translation at a later time. The DDX6 family of DEAD-box RNA helicases is tightly linked both to storage of mRNAs encoding proteins associated with progression through meiosis into translationally silent mRNPs and with the transport of mRNA to degradation centers in the cell (P-bodies). These helicases are found in orga-

nisms as diverse as yeast (e.g., Dhh1p) and humans (e.g., RCK/p54).

Earlier studies in *Saccharomyces cerevisiae* suggested that Dhh1p was localized to cytoplasmic P-bodies that contain both mRNA and enzymes central to the RNA degradation pathway (e.g., the decapping enzyme), implying that P-bodies harbor transcripts destined for degradation (6–8). More recently, it was proposed that mRNAs also exit P-bodies and re-engage polysomes for translation in a Dhh1p-dependent mechanism (9). With the exception of human RCK/p54, homologs of DDX6 helicases in metazoans have been found exclusively localized to mRNPs involved in TR (2–4).

TR has been described in *Plasmodium* (10–16) in the female gametocyte, the stable, blood-stream precursor cell of the female gamete, where two abundant transcripts are present but not translated. These mRNAs, *p25* and *p28*, en-

¹Department of Parasitology, Leiden University Medical Centre, 2333 ZA Leiden, Netherlands. ²Department of Molecular Microbiology and Immunology, Johns Hopkins School of Public Health, 615 North Wolfe Street, Baltimore, MD 21205, USA.

³Department of Molecular Cell Biology, Leiden University Medical Centre, 2333 ZA Leiden, Netherlands. ⁴The Institute for Genomic Research, 9712 Medical Center Drive, Rockville, MD 20850, USA.

*To whom correspondence should be addressed. E-mail: waters@lumc.nl

code proteins essential for zygote development and mosquito midgut invasion (17) and are kept in a translationally quiescent state. Translation is only initiated after these sexual forms have been activated during ingestion by a female mosquito, thus triggering gamete formation and subsequent fertilization. Later work showed that in gametocytes, TR most likely affected multiple transcripts and could be an important mechanism of gene regulation at this developmental time point involving mechanisms established in metazoans (16).

In the gametocyte sex-specific proteomes (18), we identified an RNA helicase (DOZI) that is highly up-regulated in female gametocytes and showed high sequence homology to the DDX6 family of RNA helicases. Sequence alignments showed that DOZI formed a specific clade within all annotated *Plasmodium falciparum* RNA helicases, their *P. berghei* and apicomplexan homologs that cluster specifically with several DDX6 helicases known to be involved in mRNP formation (figs. S1 to S3). DOZI appeared to be the only DDX6-family homolog present in *Plasmodium* and contained the domains involved in RNA-binding and RNA-unwinding activity (19).

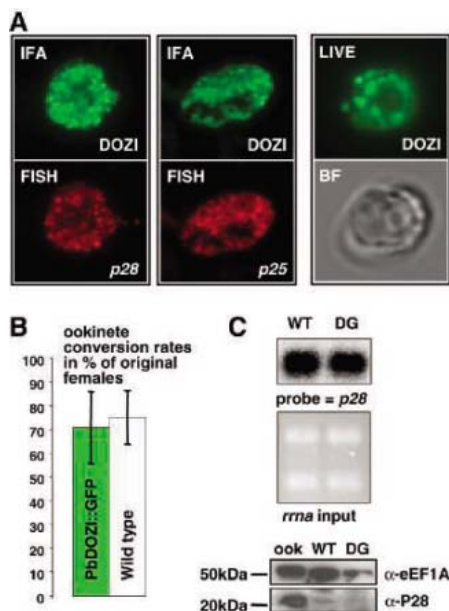


Fig. 1. PbDOZI::GFP, a modified *P. berghei* line expressing GFP-tagged DOZI, showed punctate localization in the cytoplasm of female gametocytes. Translational repression and zygote development were normal. (A) IFA and FISH analysis of female gametocytes showed a similar, punctate localization in the cytoplasm of DOZI::GFP and *p25* and *p28*. Live imaging also showing punctate localization. BF, bright field. (B) PbDOZI::GFP gametocytes showed wild-type development of zygotes into ookinetes. Data show the mean \pm SD. (C) Northern analyses of *p28* mRNA and Western analysis of P28 protein showed storage and translational repression of the transcript as in wild-type parasites. WT, wild type; DG, PbDOZI::GFP; ook, ookinetes.

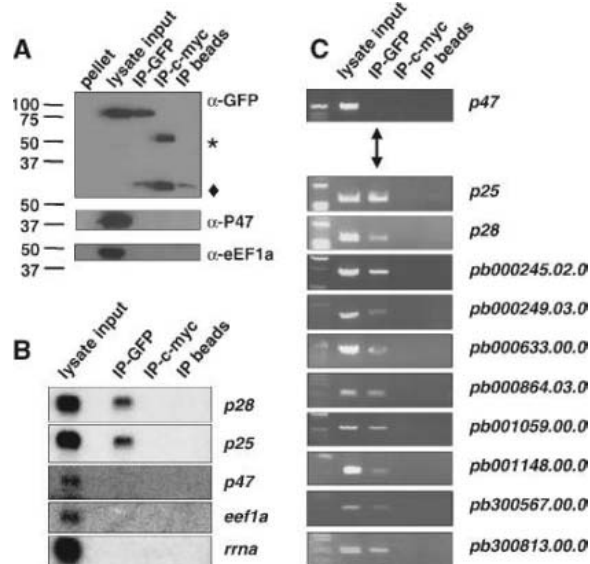
For cellular localization of DOZI, we generated a modified *P. berghei* line expressing a C-terminal green fluorescent protein (GFP) fusion of endogenous DOZI (DOZI::GFP) (Fig. 1, A to C; fig. S4). A punctate GFP-fluorescence pattern that appeared to be restricted to the cytoplasm of female gametocytes was observed in live and fixed cells after immunofluorescence assay (IFA) analysis with antibodies to GFP (anti-GFP) (Fig. 1A). These transgenic parasites showed wild-type fertilization rates and zygote/ookinete production (Fig. 1B). Steady-state levels and translational repression of *p28* mRNA were the same as those in wild-type parasites (Fig. 1C). Fluorescence in situ hybridization (FISH) analysis of the localization of *p28* and *p25* transcripts, combined with IFA for DOZI, showed that both transcripts were highly abundant in female gametocytes (Fig. 1A) with a punctate localization pattern comparable to that of the helicase. This suggested that the repressed transcripts and DOZI are distributed similarly in the cytoplasm and prompted an analysis of transcripts associated with DOZI.

Immunoprecipitations of the DOZI::GFP fusion protein from gametocyte lysates were made with monoclonal anti-GFP (GFP MAB). Eluates were analyzed for DOZI protein and transcript content. Western analysis of total gametocyte lysate input, as well as specific and control precipitates, identified DOZI::GFP only in the specific immunoprecipitates, whereas other control proteins (P47 and eEF1A) were only found in the input material (Fig. 2A). Northern analysis showed the presence of a substantial amount of *p25* and *p28* transcripts and not control RNA species in the GFP MAB eluate (Fig. 2B), suggesting that these mRNAs and DOZI occurred together in an mRNP. Additionally, reverse transcription-polymerase chain reaction (RT-PCR) analysis of the eluates demonstrated that many other transcripts that had been predicted to be translationally repressed (16) coelute with DOZI::GFP (Fig. 2C). Reverse transcription-quantitative polymerase chain reaction (RT-qPCR) analysis indicated that these same mRNA species were significantly enriched in the DOZI::GFP coeluate (fig. S5) and that they showed the punctate localization pattern in the cytoplasm (fig. S6).

P. berghei parasites were generated that lacked *pbdozi* (fig. S7). The *pbdozi*⁻ null mutants showed normal development of the asexual blood stages and normal production of gametocytes and gametes, but there was a total lack of development of fertilized female gametes (zygotes) into mature ookinetes (Fig. 3A). Normal development into ookinetes requires meiotic DNA replication in the zygote 2 to 3 hours after fertilization of female gametes (18). In *pbdozi*⁻ null mutants, all zygotes aborted development before meiosis. DOZI is also produced in males (18), although in much lower abundance than in females. We crossed the male and female gametes of *pbdozi*⁻ with gametes of mutant parasite lines that are defective in male (20, 21) or in female gamete production (22) (Fig. 3A). Such cross-fertilization assays revealed that male *pbdozi*⁻ gametes were able to fertilize wild-type DOZI-expressing female gametes, resulting in the development of ookinetes. By contrast, development of zygotes from *pbdozi*⁻ females fertilized by wild-type males was incomplete and similar to development of zygotes from the *pbdozi*⁻ line. These crosses demonstrate that the block in zygote/ookinete development is essentially due to a lack of DOZI of female gametocyte origin.

The phenotype of the *pbdozi*⁻ parasites might be expected from the predicted function of DOZI in the storage of translationally repressed mRNAs of P28 and P25 in the female gametocyte, and the later, essential, developmentally regulated use of these and other transcripts in postfertilization (zygote and ookinete devel-

Fig. 2. Immunoprecipitation (IP) experiments and localization of the transcripts *p25* and *p28* to complexes containing the DOZI::GFP fusion protein. (A) Western blot analyses of gametocyte lysates from IPs, with anti-GFP, anti-c-myc, or beads only, showed the presence of DOZI::GFP only in the specific (i.e., IP-GFP) fraction. No contamination with the control proteins P47 or eEF1A was observed; both were only present in the input lysate. Asterisk, anti-c-myc: diamond, protein G. (B) Northern blot analysis of RNA recovered from the IPs as shown in (A) identified *p25* and *p28* transcripts in the IP-GFP fraction. The transcripts of the controls *p47*, *eef1a*, and *rna* were not detected. (C) RT-PCR analyses of IP-eluates showed coelution with DOZI::GFP of *p25* and *p28* transcripts, and mRNAs predicted to be translationally repressed, but not of the control RNA *p47*.



opment) events. Northern analysis of mRNA showed not only a nearly complete loss of transcripts of *p25* and *p28* (Fig. 3B), explaining the absence of P28 and P25 (Fig. 3C), but also down-regulation of an additional three transcripts—*warp*, which encodes an ookinete-specific protein, as well as *pb000245.02.0* and *pb000633.00.0* (Fig. 3B), which earlier studies had predicted to be translationally repressed (16)—indicating a wider role of DOZI in mRNA maintenance.

The full extent of the effect of DOZI depletion on steady-state mRNAs of blood-stage, unactivated gametocytes was analyzed with an oligonucleotide microarray that consisted of 5283 *P. berghei* gene models (16, 23). We observed 370 transcripts to be significantly reduced by more than a factor of 2 in *pbdozi*⁻ as compared to wild-type gametocytes (table S1), including seven of nine genes previously shown to be translationally repressed (16). This subset also included groups of genes that ensure successful development of the parasite in the mosquito, e.g., genes linked to ookinete motility and invasion (table S2). Unexpectedly, transcripts of 92 genes were observed that concomitantly increased in abundance, which might reflect transcriptome responses to altered biological processes in the mutant or indicate a more complex role of DOZI in the regulation of mRNA abundance. These observations were confirmed by RT-qPCR analyses of selected transcripts (table S3, fig. S8).

Together, these data indicate that DOZI has a central role in the silencing and maintenance of steady-state levels of a population of gametocyte-specific transcripts. Furthermore, the loss of DOZI apparently severely affected the capacity of the parasite to store and stabilize a discrete subset of mRNAs in the female gametocyte, resulting

in a failure to synthesize specific proteins and to complete normal zygote development.

Translational repression in *Plasmodium* may function to specifically regulate gene expression during meiosis in the zygote. Posttranscriptional regulatory mechanisms of gene expression in *Plasmodium*, such as translational repression and mRNA homeostasis, might play a central role in development, because the annotation of *Plasmodium* genomes indicates a relative scarcity of transcription factors (24). Indeed, the timing of the appearance of proteins from transcripts that undergo TR in gametocytes can be quite different. For example, P25 and P28 are first detected about 2 hours after female gamete activation and fertilization, whereas WARP may only be detected in developing ookinetes 8 hours after fertilization (25).

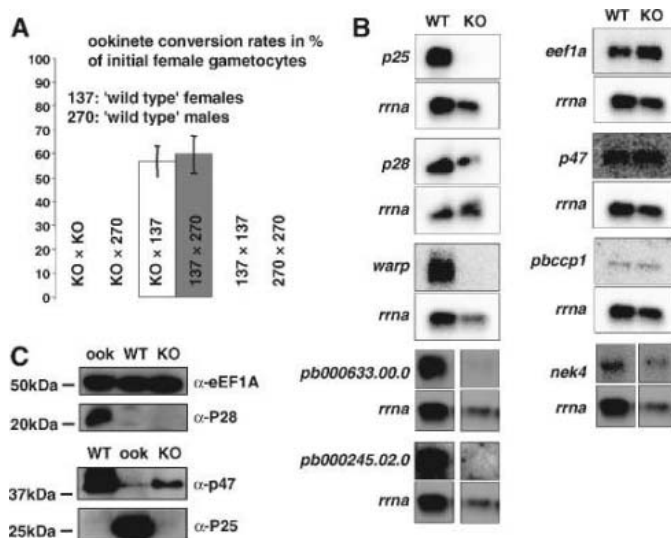
Until recently, DDX6 RNA helicases were implicated in mRNA storage in translationally silent mRNP complexes and in the transport of mRNA to P-bodies that serve as centers for mRNA degradation. More recently it has been shown that mRNA may be cycled to and from P-bodies in vegetative *S. cerevisiae* in a DDX6 helicase-dependent manner, at least in unicellular eukaryotes. DDX6 helicases are also expressed in germline cells and control the fate of mRNA species that are required for further development of the cell once it has been fertilized. Our data support a role for DOZI in the storage and silencing of mRNA species in *Plasmodium* gametocytes required after gamete fertilization (fig. S9). However, gametocytes in the blood circulation have a short half-life: The overwhelming majority fail to be transmitted to the mosquito and rapidly decay. Decaying gametocytes contain repressed transcripts that if translated, could produce proteins targeted

by transmission-blocking antibodies (10). Consequently, in decaying blood-borne gametocytes, DOZI may be involved in rapid destruction of the stored mRNAs. By contrast, in the activated female gamete in the mosquito, TR is relieved, allowing the coordinated production of proteins essential for the further development of the parasite and establishment of the infection in the mosquito vector.

References and Notes

1. L. J. Colegrove-Otero, N. Minshall, N. Standart, *Crit. Rev. Biochem. Mol. Biol.* **40**, 21 (2005).
2. N. Minshall, G. Thom, N. Standart, *RNA* **7**, 1728 (2001).
3. A. Nakamura, R. Amikura, K. Hanyu, S. Kobayashi, *Development* **128**, 3233 (2001).
4. M. Ladomery, E. Wade, J. Sommerville, *Nucleic Acids Res.* **25**, 965 (1997).
5. G. Almozni, A. P. Wolffe, *EMBO J.* **14**, 1752 (1995).
6. J. Collier, R. Parker, *Cell* **122**, 875 (2005).
7. U. Sheth, R. Parker, *Science* **300**, 805 (2003).
8. J. M. Collier, M. Tucker, U. Sheth, M. A. Valencia-Sanchez, R. Parker, *RNA* **7**, 1717 (2001).
9. M. Brenques, D. Teixeira, R. Parker, *Science* **310**, 486 (2005).
10. M. G. Paton *et al.*, *Mol. Biochem. Parasitol.* **59**, 263 (1993).
11. R. A. Vervenne, R. W. Dirks, J. Ramesar, A. P. Waters, C. J. Janse, *Mol. Biochem. Parasitol.* **68**, 259 (1994).
12. E. G. Abraham *et al.*, *J. Biol. Chem.* **279**, 5573 (2004).
13. M. del Carmen Rodriguez *et al.*, *Mol. Biochem. Parasitol.* **110**, 147 (2000).
14. M. K. Shaw, J. Thompson, R. E. Sinden, *Eur. J. Cell Biol.* **71**, 270 (1996).
15. J. Thompson, R. E. Sinden, *Mol. Biochem. Parasitol.* **68**, 189 (1994).
16. N. Hall *et al.*, *Science* **307**, 82 (2005).
17. I. Siden-Kiamos *et al.*, *J. Cell Sci.* **113**, 3419 (2000).
18. S. M. Khan *et al.*, *Cell* **121**, 675 (2005).
19. O. Cordin, J. Banroques, N. K. Tanner, P. Linder, *Gene* (2005).
20. O. Billker *et al.*, *Cell* **117**, 503 (2004).
21. M. R. van Dijk, personal communication.
22. M. R. van Dijk *et al.*, *Cell* **104**, 153 (2001).
23. www.genedb.org/genedb/pberghei/
24. M. J. Gardner *et al.*, *Nature* **419**, 498 (2002).
25. M. Yuda, K. Yano, T. Tsuboi, M. Torii, Y. Chinzei, *Mol. Biochem. Parasitol.* **116**, 65 (2001).
26. This research was supported by BIOMALPAR Network of Excellence Grant (G.R.M.), The Functional Genomics Initiative of the Wellcome Trust (G.R.M., J.A.M.B.), The Netherlands Organisation for Scientific Research (NWO) Genomics Initiative (S.M.K.), a NSF Graduate Research Fellowship (L.S.G.), and The Johns Hopkins Malaria Research Institute. We thank M. van Dijk for access to pbs47⁻ parasite mutants used in this study, and J. Ramesar for technical assistance. We thank the Johns Hopkins MRI Array Core Facility for providing the microarray equipment. This work has been supported by the NIH—National Institute of Allergy and Infectious Diseases 1R01AI061576-01A1, a Johns Hopkins School of Public Health Faculty Innovation Grant, and the Johns Hopkins Malaria Research Institute. The accession numbers to the array data submitted to the GEO-NCBI (Gene Expression Omnibus—National Center for Biotechnology Information) database (www.ncbi.nlm.nih.gov/projects/geo/) are GSM111868, GSM111871, GSM111872, GSM111873, GSM111874, GSM111875.

Fig. 3. The zygote development of *Pbdozi*⁻ null mutants was completely inhibited because of failure to store transcripts in gametocytes. (A) Analysis of zygote development in standard in vitro assays showing the lack of development of *pbdozi*⁻ null zygotes into ookinetes. *Pbdozi*⁻ null female gametes (KO) cross-fertilized with “wild type” males (270) did not develop into ookinetes, whereas “wild type” females (137) cross-fertilized with *pbdozi*⁻ null males (KO) showed normal ookinete development. Data show the mean ± SD.



(B) Northern blot analyses of gametocyte transcripts showed that *p25* and *p28* steady-state levels were substantially reduced in *pbdozi*⁻ null parasites. In addition, we showed transcripts that were also affected (left) or unaffected (right) by the lack of DOZI. (C) Western blot analyses of gametocyte lysates showing the absence of P28 and P25 in both wild-type (WT) and *pbdozi*⁻ null (KO) gametocytes. P28 and P25 were present only in ookinetes (ook). eEF1A and P47 were included as controls.

Supporting Online Material

www.sciencemag.org/cgi/content/full/313/5787/667/DC1
Materials and Methods
Figs. S1 to S9
Tables S1 to S4
References

19 January 2006; accepted 7 June 2006
10.1126/science.1125129

Anti-Inflammatory Activity of Immunoglobulin G Resulting from Fc Sialylation

Yoshikatsu Kaneko,* Falk Nimmerjahn,* Jeffrey V. Ravetch†

Immunoglobulin G (IgG) mediates pro- and anti-inflammatory activities through the engagement of its Fc fragment (Fc) with distinct Fcγ receptors (FcγRs). One class of Fc-FcγR interactions generates pro-inflammatory effects of immune complexes and cytotoxic antibodies. In contrast, therapeutic intravenous gamma globulin and its Fc fragments are anti-inflammatory. We show here that these distinct properties of the IgG Fc result from differential sialylation of the Fc core polysaccharide. IgG acquires anti-inflammatory properties upon Fc sialylation, which is reduced upon the induction of an antigen-specific immune response. This differential sialylation may provide a switch from innate anti-inflammatory activity in the steady state to generating adaptive pro-inflammatory effects upon antigenic challenge.

Immunoglobulin G (IgG) is the major serum immunoglobulin and is principally responsible for the recognition, neutralization, and elimination of pathogens and toxic antigens. It is a glycoprotein, composed of two identical heavy chains and two light chains, which in turn are composed of variable and constant domains.

The variable domains form the antigen recognition site, whereas the constant domains of the heavy chain form the effector arm of the molecule as an Fc domain. A single N-linked glycan is found at Asn²⁹⁷ in the Fc domain, and this covalently linked complex carbohydrate is composed of a core biantennary heptapolysaccharide

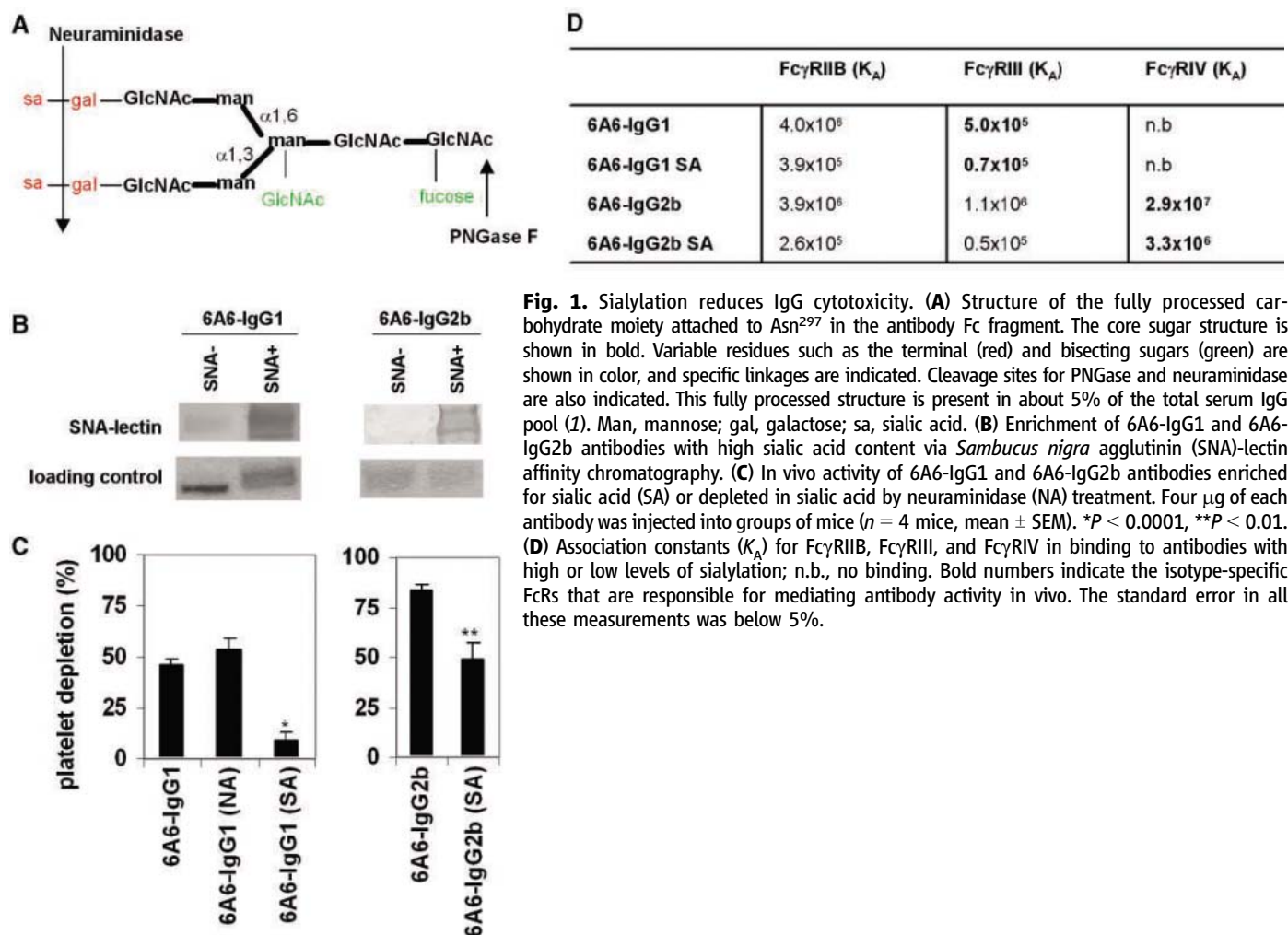
containing *N*-acetylglucosamine (GlcNAc) and mannose. Further modification of the core carbohydrate structure is observed in serum antibodies, with fucose, bisecting GlcNAc, galactose, and terminal sialic acid moieties being variably present (Fig. 1A). The fully processed form of the carbohydrate moiety exists in about 5% of the total serum IgG pool (1), and over 30 different covalently attached glycans have been detected at this single glycosylation site (1). Glycosylation of IgG is essential for binding to all Fcγ receptors (FcγRs) (2) through maintenance of an open conformation of the two heavy chains (3). This absolute requirement of IgG glycosylation for FcγR binding accounts for the inability of deglycosylated IgG antibodies to mediate in vivo triggered inflammatory responses (4).

The idea that individual glycoforms of IgG may contribute to modulating inflammatory responses has been suggested by the altered

Laboratory of Molecular Genetics and Immunology, The Rockefeller University, 1230 York Avenue, New York, NY 10021, USA.

*These authors contributed equally to this work.

†To whom correspondence should be addressed. E-mail: ravetch@rockefeller.edu



affinities for individual Fc γ R that have been reported for IgG antibodies containing or lacking fucose (5) and their consequential effects on cytotoxicity (6). In contrast, aglycosylated IgG retains FcRn binding and in vivo half-life (5). IgG glycosylation differs in patients with rheumatoid arthritis and several forms of autoimmune vasculitis with decreased Fc galactosylation and sialylation when compared to normal individuals (7–10). Variations in IgG glycoforms have also been reported to be associated with aging (11) and upon immunization (12). Thus, although it has been proposed that individual IgG glycoforms may play a role in modulating antibody effector function in vivo (13), an underlying mechanism that could account for the disparate observations is, as yet, lacking.

To determine whether specific glycoforms of IgG are involved in modulating the effector functions of antibodies, we explored the role of specific Asn²⁹⁷-linked carbohydrates in mediating the cytotoxicity of IgG monoclonal

antibodies of defined specificity. The antibodies to platelets, derived from the 6A6 hybridoma, expressed as an IgG1, IgG2a, or IgG2b switch variant in 293 cells as previously described (6, 14, 15), were analyzed by mass spectrometry to determine their specific carbohydrate composition (figs. S1 and S2). These antibodies contained minimal sialic acid residues, and because it has been suggested that antibodies with decreased levels of terminal sugar residues might be more pathogenic (7–10), we investigated the influence of sialic acid on antibody activity in vivo. Enrichment of the sialic acid-containing species by *Sambucus nigra* lectin affinity chromatography yielded antibodies enriched 60- to 80-fold in sialic acid content (Fig. 1B and fig. S2). Comparison of the ability of 6A6-IgG1 and 6A6-IgG2b antibodies to mediate in vivo platelet clearance revealed an inverse correlation with sialylation (Fig. 1C). Sialylation of 6A6-IgG antibodies resulted in a 40 to 80% reduction in biological activity, which could be

partially restored upon removal of these sialic acid moieties with neuraminidase (fig. S3). Surface plasmon resonance binding analysis revealed a 5- to 10-fold reduction in binding affinity for the sialylated forms of these antibodies to their respective activating or inhibitory Fc γ Rs as compared to their asialylated counterparts (Fig. 1D), whereas no differences in binding affinity for the antigen were observed (fig. S4). Thus, sialylation of the Asn²⁹⁷-linked glycan structure of IgG resulted in reduced binding affinities to the subclass-restricted Fc γ Rs and thereby reduced their in vivo cytotoxicity.

We next examined the role of N-linked glycans on the anti-inflammatory activity of immunoglobulins with established anti-inflammatory activity. Intravenous gamma globulin (IVIG) is a purified IgG fraction obtained from the pooled serum of 5000 to 10,000 donors that is widely used to treat inflammatory diseases through administration at high doses (16). The anti-inflammatory activity of IVIG therapy is a

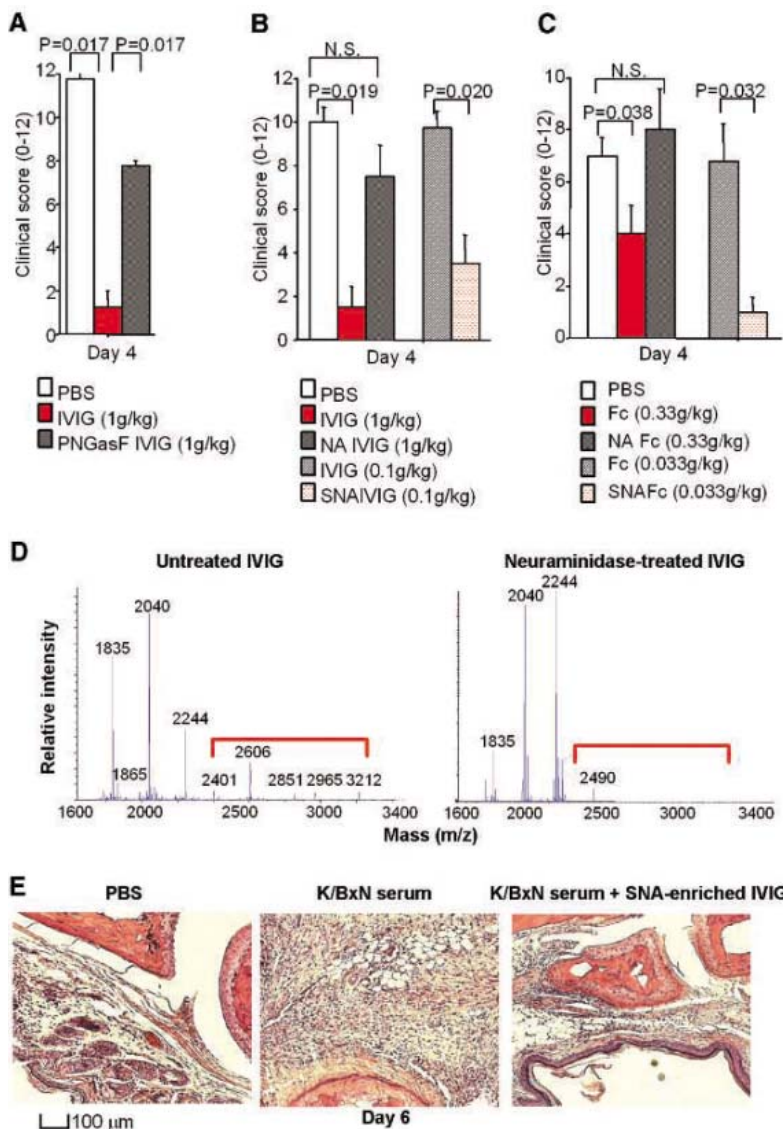


Fig. 2. The anti-inflammatory activity of IVIG requires sialic acid. **(A)** Clinical scores of K/BxN-serum-induced arthritis in mice treated with phosphate-buffered saline (PBS), IVIG, and PNGaseF-treated IVIG. **(B)** In addition to the treatment described in **(A)**, mice were treated with neuraminidase-treated IVIG (NA IVIG) or SNA-enriched IVIG (SNA IVIG). **(C)** Clinical scores of mice treated with the Fc fragment of IVIG, neuraminidase-treated Fc (NA Fc), or SNA-enriched Fc (SNA Fc) ($n = 4$, mean \pm SEM). **(D)** Carbohydrate profiles of IVIG preparations. MALDI-TOF mass spectrometry profiles of N-glycans derived from untreated or neuraminidase-treated IVIG are shown. Peaks that contain sialic acid residues are indicated (red brackets), and the carbohydrate composition of the peaks is presented in fig. S1. m/z , mass/charge ratio. **(E)** Representative hematoxylin/eosin staining of the ankle joints of control mice or mice with K/N-induced arthritis treated with or without SNA-enriched IVIG (0.1 g/kg). The extensive neutrophil infiltration observed in K/N-treated mice is absent from IVIG-SNA (0.1 g/kg)-treated mice. **(F)** Lectin blotting of the control Fc fragment of IVIG, neuraminidase-treated Fc (NA Fc), and Fc with high sialic acid content via SNA affinity chromatography (SNA Fc).

property of the Fc fragment (17) and is also protective in murine models of immunothrombocytopenia, rheumatoid arthritis, and nephrotoxic serum nephritis (18–20). To define the potential role of the glycan structure on the Fc in the anti-inflammatory activity of IVIG, these carbohydrates were removed with peptide N-glycosidase (PNGase) F, and the resulting ability to inhibit inflammatory responses was assessed in the K/N serum model of rheumatoid arthritis. Deglycosylated IVIG was unable to mediate anti-inflammatory activity in vivo (Fig. 2A). To further characterize this glycan requirement, IVIG was treated with neuraminidase to remove the terminal saccharides, and the composition of

the complete sugar removal was confirmed by mass spectrometry (Fig. 2D and fig. S1). These IgG preparations were then tested for their ability to protect mice from joint inflammation in the K/N serum arthritis model (21). Desialylation with neuraminidase abrogated the protective effect of the IVIG preparation in this model, at levels similar to those seen after removal of the entire glycan structure (Fig. 2B). This loss of activity was not the result of reduced serum half-life of the desialylated IgG preparations or the result of changes in the monomeric composition or structural integrity of the IgG (fig. S5). The unchanged FcRn binding affinity (5) and serum half-life of the

deglycosylated or desialylated IVIG variants strongly argue against a role for FcRn in the mechanism of IVIG action (fig. S5) (14).

The dependence of IVIG on sialic acid for its anti-inflammatory activity is distinct from the well-known property of sialic acid of masking structural determinants and rendering them inaccessible to ligand interactions (22). Rather, in this situation, sialic acid is responsible for the acquisition of new IgG activity in suppressing inflammation via the induction of inhibitory FcγRIIB expression (19). Because sialic acid appeared to be required for the anti-inflammatory activity of IVIG, we reasoned that the basis for the high doses [1 g per kilogram of body weight (g/kg)] needed for this anti-inflammatory activity might be the limiting concentration of sialylated IgG species in the total IVIG preparation (1, 7). We fractionated IVIG on an *Sambucus nigra* agglutinin (SNA)-lectin affinity column to obtain IgG molecules enriched for sialic acid–modified glycan structures and confirmed this idea using mass spectrometric analysis. In the K/N arthritis model, these sialic acid–enriched fractions showed a 10-fold enhancement in protection, so that equivalent protection was obtained at 0.1 g/kg of SNA-enriched IVIG as compared to 1 g/kg of unfractionated IVIG (Fig. 2, B and E). The protective activity was limited to the sialylated Fc fragment (Fig. 2, C and F). Serum half-life and IgG subclass distribution were equivalent in both fractions (fig. S6) and the anti-inflammatory effect was specific to IgG; sialylated N-linked glycoproteins such as fetuin or transferrin, with similar biantennary complex carbohydrate structures, had no statistically significant anti-inflammatory activity at equivalent or higher molar concentrations of IgG (fig. S7). Finally, the mechanism of protection of the sialylated IVIG preparation was similar to that of unfractionated IVIG in that it was dependent on FcγRIIB expression and resulted in the increased expression of this inhibitory receptor on effector macrophages (fig. S8). The high dose requirement for the anti-inflammatory activity of IVIG can be attributed to the minor contributions of sialylated IgG present in the total preparation. Thus, enhancing the sialylation of IgG may be an effective means of increasing the anti-inflammatory activity of IVIG. It remains to be determined whether both the 1,3 and 1,6 arms contribute equally to the anti-inflammatory property and whether preference for either the 2,3, 2,6 or 2,8 sialic acid–galactose linkages is involved in this activity.

Because passive immunization with IgG antibodies indicated that IgG can switch from a pro-inflammatory to an anti-inflammatory species by changing the extent of sialylation of the N-linked glycan on the Fc domain, we next determined whether IgG sialylation is regulated during an active immune response by using the nephrotoxic serum nephritis model (20). In this model, mice are presensitized with sheep IgG and then challenged with a sheep anti-mouse

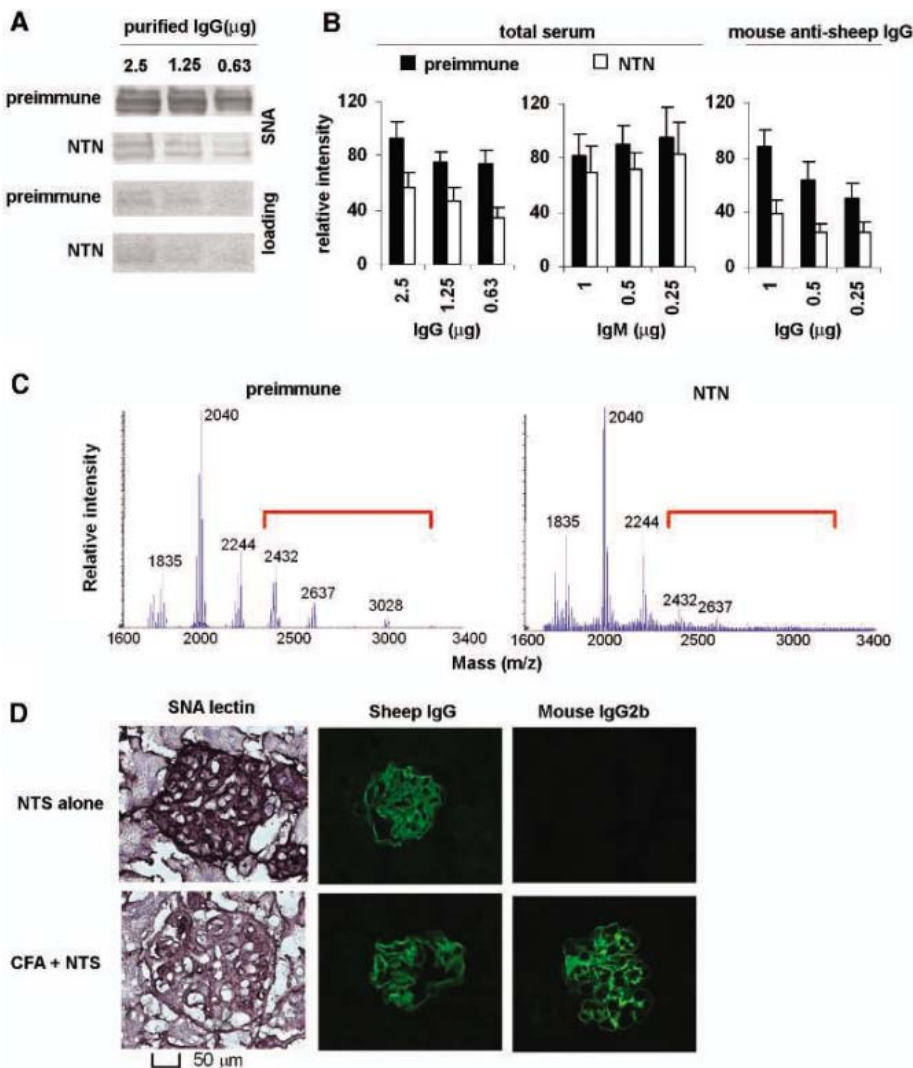


Fig. 3. Active immunization results in reduced IgG sialylation. (A) Serum IgG from untreated (preimmune) or mice with nephrotoxic nephritis (NTN) induced by immunization with sheep IgG and NTS was characterized for sialic acid content by blotting with SNA (14). (B) Quantitation of the level of sialylation of total serum IgG and IgM antibodies and sheep IgG–specific IgG antibodies in untreated and NTN mice (mean \pm SEM) as determined by densitometry. No detectable sheep IgG was present in the mouse antibody preparations. (C) MALDI-TOF analysis of sugar residues attached to IgG antibodies from untreated or NTN mice. Sialic acid–containing moieties are indicated (red brackets). The detailed carbohydrate composition of the individual peaks is shown in fig. S1. (D) Detection of sialic acid content in antibodies deposited in the glomeruli of mice injected with NTS with (NTS+CFA) or without (NTS alone) preimmunization with sheep IgG in Freund’s complete adjuvant (CFA).

glomerular basement membrane preparation [nephrotoxic serum (NTS)], thereby inducing a mouse IgG response. Serum IgG and IgM from preimmune and NTS-immunized mice were characterized for sialic acid content; total IgG sialylation was reduced on average by 40% in immunized mice as compared to the unimmunized controls (Fig. 3, A and B). The effect was specific for IgG; sialylation of IgM or transferrin was equivalent before and after immunization (Fig. 3B and fig. S9). This difference in sialylation was more pronounced when the anti-sheep-specific IgG fraction from mouse serum was analyzed, showing a 50 to 60% reduction in sialylation as compared to preimmune IgG (Fig. 3B), and these results were confirmed by matrix-assisted laser desorption/ionization-time-of-flight (MALDI-TOF) analysis (Fig. 3C). Finally, the mouse IgG2b antibodies to sheep that were deposited in the glomeruli (20) displayed reduced sialic acid content as compared to the preimmunized controls (Fig. 3D).

The regulated sialylation of IgG suggests a mechanism for ensuring that steady-state serum IgG antibodies maintain an anti-inflammatory

state. Upon antigenic challenge by a potential pathogen, the antigen-specific IgG antibodies can switch to a population with reduced sialic acid that is thus capable of mediating antigen clearance and a protective inflammatory response through the engagement of subclass-specific Fc γ Rs on effector cells.

References and Notes

1. F. H. Routier *et al.*, *J. Immunol. Methods* **213**, 113 (1998).
2. R. Jefferis, J. Lund, *Immunol. Lett.* **82**, 57 (2002).
3. P. Sondermann, J. Kaiser, U. Jacob, *J. Mol. Biol.* **309**, 737 (2001).
4. F. Nimmerjahn, J. V. Ravetch, *Immunity* **24**, 19 (2006).
5. R. L. Shields *et al.*, *J. Biol. Chem.* **277**, 26733 (2002).
6. F. Nimmerjahn, J. V. Ravetch, *Science* **310**, 1510 (2005).
7. R. B. Parekh *et al.*, *Nature* **316**, 452 (1985).
8. T. W. Rademacher, P. Williams, R. A. Dwek, *Proc. Natl. Acad. Sci. U.S.A.* **91**, 6123 (1994).
9. A. Matsumoto, K. Shikata, F. Takeuchi, N. Kojima, T. Mizouchi, *J. Biochem. (Tokyo)* **128**, 621 (2000).
10. M. Holland *et al.*, *Biochim. Biophys. Acta* **1760**, 669 (2005).
11. K. Shikata *et al.*, *Glycoconj. J.* **15**, 683 (1998).
12. G. C. Lastra, S. J. Thompson, A. S. Lemonidis, C. J. Elson, *Autoimmunity* **28**, 25 (1998).
13. A. Wright, S. L. Morrison, *Trends Biotechnol.* **15**, 26 (1997).
14. Materials and methods are available as supporting material on Science Online.

15. F. Nimmerjahn, P. Bruhns, K. Horiuchi, J. V. Ravetch, *Immunity* **23**, 41 (2005).
16. J. M. Dwyer, *N. Engl. J. Med.* **326**, 107 (1992).
17. P. Imbach *et al.*, *Lancet* **1**, 1228 (1981).
18. A. Samuelsson, T. L. Towers, J. V. Ravetch, *Science* **291**, 484 (2001).
19. P. Bruhns, A. Samuelsson, J. W. Pollard, J. V. Ravetch, *Immunity* **18**, 573 (2003).
20. Y. Kaneko, F. Nimmerjahn, F. M. P. Madaio, J. V. Ravetch, *J. Exp. Med.* **203**, 789 (2006).
21. H. Ji *et al.*, *Immunity* **16**, 157 (2002).
22. S. Han, B. E. Collins, P. Bengtson, J. C. Paulson, *Nat. Chem. Biol.* **1**, 93 (2005).
23. We thank M. Madaio for providing the NTS; C. Bertozzi for helpful discussions and suggestions; A. Datta for glycan analysis; and P. Smith, J. Clowney, A. Kim, and J. Pagan for technical assistance. These studies were supported by grants from NIH (J.V.R.). Y.K. was supported by fellowships from the Naito Foundation, the Kanoe Foundation for Life & Social-Medical Science, and the Uehara Memorial Foundation. F.N. is a fellow of the Cancer Research Institute.

Supporting Online Material

www.sciencemag.org/cgi/content/full/313/5787/670/DC1
Materials and Methods
Figs. S1 to S11
References

5 May 2006; accepted 20 June 2006
10.1126/science.1129594

N- to C-Terminal SNARE Complex Assembly Promotes Rapid Membrane Fusion

Ajaybabu V. Pobbati, Alexander Stein, Dirk Fasshauer*

Assembly of the soluble *N*-ethylmaleimide-sensitive factor attachment protein receptors (SNAREs) syntaxin 1, SNAP-25, and synaptobrevin 2 is thought to be the driving force for the exocytosis of synaptic vesicles. However, whereas exocytosis is triggered at a millisecond time scale, the SNARE-mediated fusion of liposomes requires hours for completion, which challenges the idea of a key role for SNAREs in the final steps of exocytosis. We found that liposome fusion was dramatically accelerated when a stabilized syntaxin/SNAP-25 acceptor complex was used. Thus, SNAREs do have the capacity to execute fusion at a speed required for neuronal secretion, demonstrating that the maintenance of acceptor complexes is a critical step in biological fusion reactions.

The three soluble *N*-ethylmaleimide-sensitive factor attachment protein (SNAP) receptors or SNAREs—syntaxin 1, SNAP-25, and synaptobrevin 2 (also referred to as VAMP2)—are key elements of the molecular machinery mediating the rapid exocytosis of synaptic vesicles in neurons (1, 2). Syntaxin and SNAP-25 are localized within the plasma membrane, and synaptobrevin resides in synaptic vesicles. In vitro, the three proteins assemble into a stable complex with equimolar stoichiometry. It consists of a tight bundle of four α helices aligned in parallel, in which the transmembrane regions of synaptobrevin and syntaxin lie at one end (3). SNARE assembly is thought to be

initiated at the N-terminal end and proceed toward the C-terminal membrane anchors (in a process referred to as zippering). In consequence, the membranes are pulled tightly together, overcoming the energy barrier for fusion (4–6).

Although the zipper hypothesis of SNARE function has received substantial support, the features of SNARE assembly in vitro are difficult to reconcile with the proposed role of SNAREs as catalysts of the final step in exocytotic membrane fusion. SNAREs are able to fuse liposomes, but the fusion rates are very slow, requiring hours for completion (7). Faster rates have been observed upon fusion of liposomes with planar membranes (8–10), but because these reactions do not require SNAP-25, the importance of these results remains questionable. On the other hand, neuronal exocytosis occurs at a submillisecond time scale (11). To resolve this major discrepancy, it has been proposed that, in primed fusion-ready vesicles, the

SNAREs are partially assembled in trans configuration bridging the fusing membranes (12, 13). However, the actual configuration of the SNARE machinery for rapid fusion has remained elusive.

SNARE assembly proceeds in an ordered fashion involving structurally defined intermediates (14, 15). In vitro, syntaxin and SNAP-25 readily form a stable four-helix bundle in 2:1 stoichiometry (16). Because the second syntaxin occupies the position of synaptobrevin (17, 18), the overall slow rate of SNARE assembly may primarily be due to competition between syntaxin and synaptobrevin for binding to a transient 1:1 syntaxin/SNAP-25 heterodimer (15), thus occluding the true reactivity of the final (and fusion-relevant) step in the assembly pathway.

We therefore investigated whether the formation of the 1:1 syntaxin/SNAP-25 heterodimer allowed subsequent binding of synaptobrevin at rates compatible with biological fusion reactions. We monitored the binding kinetics of fluorescently labeled synaptobrevin (19). To increase the concentration of the syntaxin/SNAP-25 heterodimer, we used a large excess of SNAP-25 over the SNARE motif of syntaxin [amino acids 180 to 262 (Syx180–262)]. When synaptobrevin was added, a rapid increase in fluorescence anisotropy was observed ($\sim 5 \times 10^5 \text{ M}^{-1} \text{ s}^{-1}$; Fig. 1A). Similarly fast binding was observed when the heterodimer was preformed with the entire cytoplasmic region of syntaxin (Syx1–262; Fig. 1B), demonstrating that syntaxin's autonomous N-terminal domain did not affect synaptobrevin binding (Fig. 1C).

Next, we attempted to stabilize the acceptor site for synaptobrevin in the 1:1 heterodimer. According to the zipper hypothesis, binding of synaptobrevin should initiate at the N-terminal end

Department of Neurobiology, Max-Planck-Institute for Biophysical Chemistry, Am Fassberg 11, 37077 Göttingen, Germany.

*To whom correspondence should be addressed. E-mail: dfassha@gwdg.de

of the complex. Consequently, nucleation should not be affected if only the C-terminal part of the binding site is occupied, leaving the N-terminal part free. We purified stable complexes with C-terminal fragments of synaptobrevin. When the binding of synaptobrevin (Syb) was measured, rapid binding was observed to complexes containing the fragments Syb60–96, Syb49–96, or Syb42–96 (Fig. 2A), whereas no binding was observed to complexes containing N-terminally longer fragments (Syb35–96 or Syb25–96). Thus, only a short N-terminal stretch is sufficient for fast synaptobrevin binding. Syntaxin was much less efficient in competing with synaptobrevin for binding to the Syb42–96 complex (fig. S2), suggesting that the N-terminal region was largely specific for synaptobrevin. Binding of synaptobrevin to complexes containing an N-terminal fragment of synaptobrevin was rather slow (Fig. 2A), indicating that the C-terminal end was not a preferred binding site.

We used circular dichroism (CD) spectroscopy to test whether fast binding of synaptobrevin to complexes containing C-terminal fragments was facilitated by a structured N-terminal region. Purified ternary complexes containing fragments corresponding to either one of the two halves of synaptobrevin, Syb1–59 or Syb60–96, exhibited a characteristic α -helical spectrum. Upon binding of Syb60–96 to the Syb1–59 complex, a major increase in α -helical structure was observed (Fig. 2B). Thus, the Syb1–59 complex is probably structured only N-terminally, whereas the remaining portion is mostly unstructured. In contrast, no change in α -helical content was observed upon binding of Syb1–59 to the Syb60–96 complex, suggesting that its N- and C-terminal regions are well structured. Because the speed of binding of synaptobrevin to complexes containing a C-terminal fragment was comparable to that observed for the syntaxin/SNAP-25 dimer, it seems that the binding sites for synaptobrevin are structurally very similar for both complexes. Indeed, their N-termini are of similar composition, containing only the N-terminal helices of SNAP-25 and syntaxin. In contrast, the C-terminal portion of the syntaxin/SNAP-25 heterodimer, such as the complex containing an N-terminal fragment of synaptobrevin, might be less structured. For the homologous heterodimer of Sso1p (equivalent to syntaxin) and Sec9p (equivalent to SNAP-25) from yeast, a similar structural configuration was determined by nuclear magnetic resonance (20): The N-terminal part consists of a three-helix bundle, whereas the C-terminal part is unstructured. Binding of Snc2p (equivalent to synaptobrevin) to the Sso/Sec9 complex is 100 times slower ($\sim 6000 \text{ M}^{-1} \text{ s}^{-1}$) (21) than the fast binding of synaptobrevin.

We then investigated whether the presence of the C-terminal synaptobrevin fragment would prevent complete zippering or whether the binding of intact synaptobrevin would displace the fragments. The peptide dissociated from the complex (Fig. 2C and fig. S3). To measure the rate of displacement, we formed a complex con-

taining labeled Syb49–96. The addition of Syb1–96 displaced this Syb49–96 fragment within 1 min (Fig. 2D). Thus, complexes containing a C-terminal fragment served as acceptors that allowed for SNARE complex formation at a much faster rate than hitherto observed.

Next we tested whether the Syb49–96 complex would accelerate liposome fusion. A moderate acceleration of liposome fusion occurs in the presence of a C-terminal peptide of synaptobrevin (Syb57–92) (22). We incorporated a Syb49–96 complex that contained the SNARE motif of syntaxin with a transmembrane region (TMR) into liposomes and monitored fusion with synaptobrevin liposomes. Lipid mixing was profoundly accelerated with liposomes containing the Syb49–96 complex [half-time ($t_{1/2}$) ≈ 1 min] when compared

to liposomes containing the syntaxin/SNAP-25 2:1 complex ($t_{1/2} \approx 20$ min) (Fig. 3). Because the presence of the C-terminal fragment of synaptobrevin will certainly retard fusion, we predict that the fusion kinetics with an unobstructed 1:1 complex as an acceptor would be even faster.

When we determined the stability of complexes containing synaptobrevin fragments, the Syb1–59 complex unfolded in a single transition at about 66°C , whereas the Syb60–96 complex was clearly less stable (melting temperature $\approx 44^\circ\text{C}$; Fig. 2B). This agrees with deuterium exchange experiments that had inferred a lower stability of the C-terminal region for the complex (23). A complex that contained both fragments (a Syb1–59:Syb60–96 complex) unfolded in two steps (Fig. 2B), demonstrating that both halves of the four-

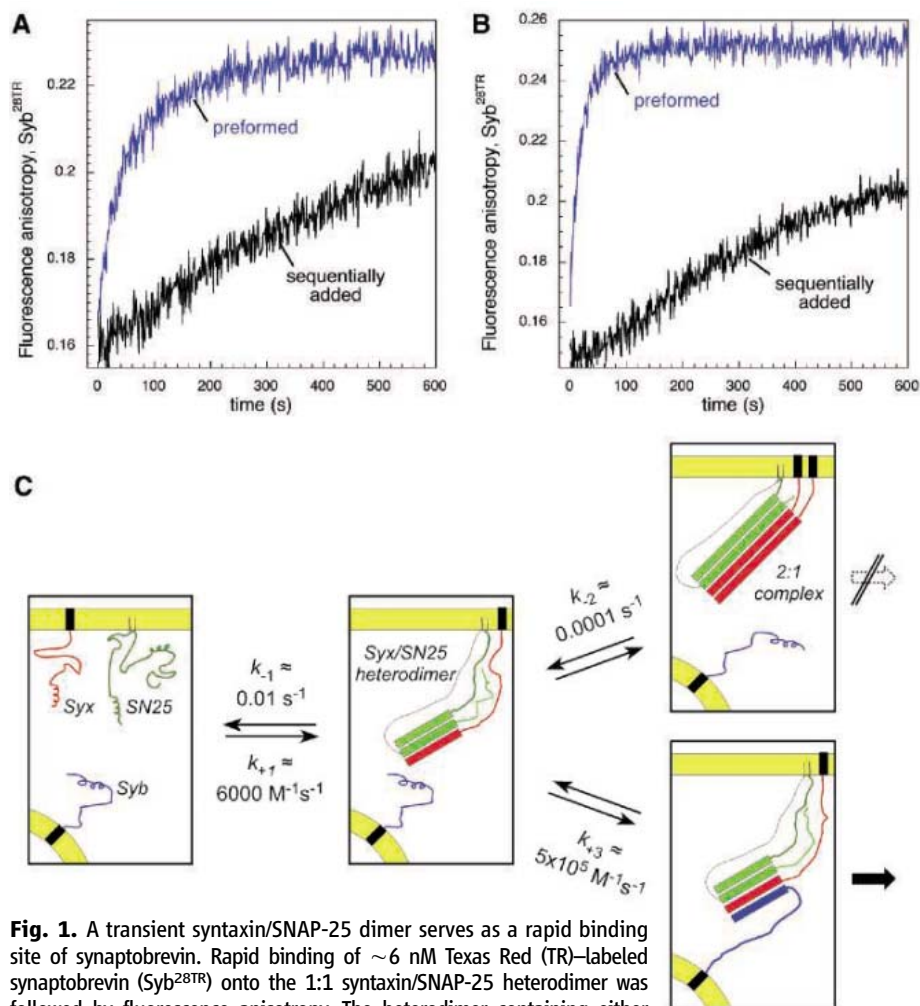


Fig. 1. A transient syntaxin/SNAP-25 dimer serves as a rapid binding site of synaptobrevin. Rapid binding of ~ 6 nM Texas Red (TR)-labeled synaptobrevin (Syb^{28TR}) onto the 1:1 syntaxin/SNAP-25 heterodimer was followed by fluorescence anisotropy. The heterodimer containing either (A) the SNARE motif of syntaxin (Syx180–262; 26 nM) or (B) the entire soluble domain of syntaxin (Syx1–262; 83 nM) was preformed by means of an excess of SNAP-25 (240 nM or 720 nM, respectively). When the proteins were added sequentially, a much slower binding of Syb^{28TR} was observed. (C) Kinetic model of the SNARE assembly pathway. The proteins are depicted between two fusing membranes; however, the rates were obtained with the use of the soluble portions of the SNAREs. First, syntaxin (Syx) and SNAP-25 (SN25) slowly assemble into a transient 1:1 heterodimer [$\sim 6000 \text{ M}^{-1} \text{ s}^{-1}$] (15) that provides a rapid binding site for synaptobrevin (Syb) or a second syntaxin molecule. Synaptobrevin does not actively replace the second syntaxin (15), indicating that the 2:1 complex is off-pathway. The off-rate of the second syntaxin from the 2:1 complex was $\sim 0.01 \text{ s}^{-1}$ (15, fig. S1A), and dissociation of the entire 2:1 complex occurred at $\sim 0.0001 \text{ s}^{-1}$ (fig. S1B). Assumed α -helical regions are boxed.

helix bundle were able to fold independently. A marked hysteresis in SNARE folding and unfolding (14) probably results from a kinetic barrier for the dissociation of synaptobrevin. It is conceivable that either fragment can dissociate and rebind as long as the remaining fragment holds the complex together. Thus, the first unfolding step of the Syb1–59:Syb60–96 complex may be reversible, whereas the second is not. Together, these data suggest that SNARE complex formation can be arrested halfway and that, in this configuration, the C-terminal part of an N-terminally anchored synaptobrevin can assemble reversibly.

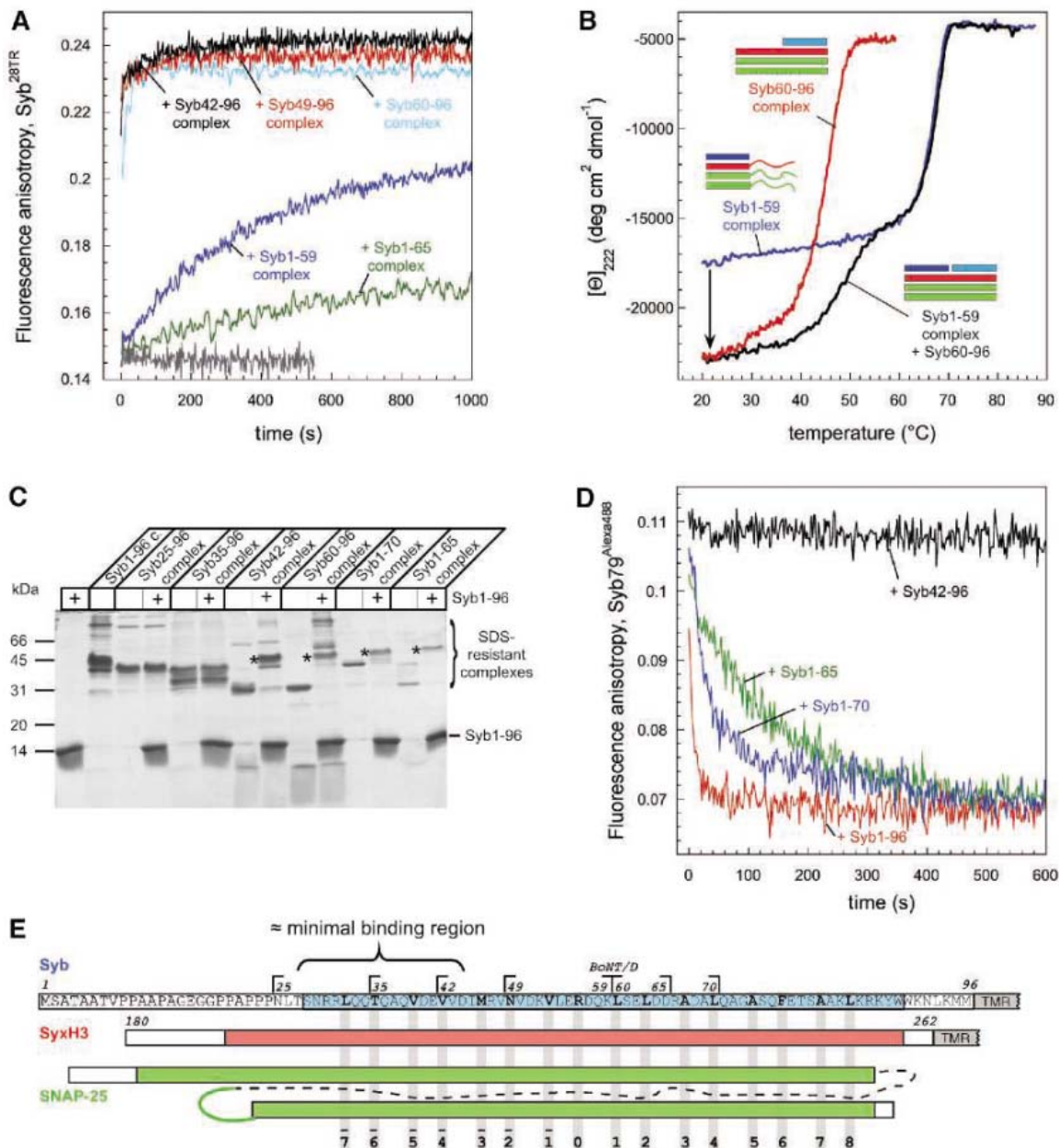
A partially assembled trans-SNARE configuration might be reached when the force generated by SNARE assembly and the repulsive force of the charged lipid headgroups balance each other. Such an equilibrium might be exploited by another protein to block further assembly, perhaps until its grip is released upon binding of Ca²⁺. Still, this factor would need to be able to sustain a strong SNARE assembly force. However, even a tightly fitting C-terminal synaptobrevin fragment was not able to arrest zippering between liposome membranes (Fig. 2D). Because the energetic barrier for membrane fusion is largely unknown, it remains

unclear whether SNAREs can be maintained in trans configuration. An energetically more favorable way to regulate SNARE assembly might be through the control of the nucleation process, in particular by restricting the first contact of synaptobrevin with the syntaxin/SNAP-25 acceptor.

Here we have shown that SNARE nucleation is restricted to the N-terminal portion and that zippering proceeds in an N- to C-terminal direction. In addition, synaptobrevin binds rapidly to a syntaxin/SNAP-25 acceptor. Stabilizing the syntaxin/SNAP-25 acceptor by a peptide allowed for fast liposome fusion. Thus, SNAREs have the capacity to execute

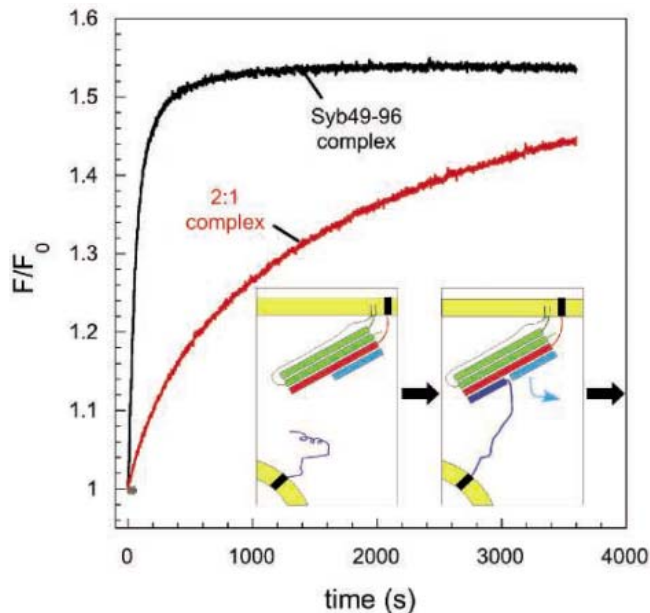
Fig. 2. Synaptobrevin fragments can be actively replaced from a ternary complex by the intact coil of synaptobrevin.

(A) Binding of synaptobrevin to SNARE complexes containing different fragments of synaptobrevin monitored by fluorescence anisotropy. Complexes (1 μM) were mixed with Syb^{28TR} (~200 nM). Binding was inhibited by preincubation with Syb1–96 (shown for the Syb49–96 complex as the gray curve). (B) Thermal unfolding of SNARE complexes containing synaptobrevin fragments monitored by CD spectroscopy. The Syb60–96 complex and the Syb1–59 complex unfolded in a single transition at ~45° and ~66°C, respectively, whereas a complex containing both fragments unfolded in two steps. The large increase in molar ellipticity upon binding of Syb60–96 to the Syb1–59 complex is indicated by an arrow. [Θ], molar ellipticity. (C) Replacement of synaptobrevin fragments visualized by SDS–polyacrylamide gel electrophoresis and Coomassie Blue staining. SNARE complexes containing different synaptobrevin fragments were incubated with Syb1–96. Upon replacement, a SDS-resistant complex containing Syb1–96 appeared (marked by asterisks). In the first two lanes, Syb1–96 and the SNARE complex containing Syb1–96 were loaded. (D) Fast displacement of Syb49–96 monitored by fluorescence anisotropy. A ternary complex containing Alexa488-labeled (~200 nM) Syb49–96 was incubated with different Syb fragments (1 μM).



Displacement led to a decrease in anisotropy. (E) Schematic depiction of synaptobrevin fragments used in the framework of the four-helix-bundle SNARE complex. The positions of the heptad repeat layers (–7 to +8) are indicated by gray vertical bars. The structured regions of the SNAREs are boxed (3).

Fig. 3. A complex containing a C-terminal synaptobrevin fragment greatly accelerates liposome fusion. A SNARE complex containing SNAP-25, the SNARE motif of syntaxin with TMR (Syx183–288), and Syb49–96 and a binary 2:1 complex containing Syx183–288 and SNAP-25 were purified and inserted into liposome membranes. Fusion with liposomes containing full-length synaptobrevin (Syb1–116) was monitored by lipid dequenching. At a final protein concentration of ~200 nM for both liposome populations, the liposomes containing the Syb49–96 complex fused very rapidly ($t_{1/2} \approx 1$ min) as compared to liposomes containing the 2:1 complex ($t_{1/2} \approx 20$ min).



The obtained rates are difficult to compare to published fusion rates, because other laboratories routinely use 5 to 10 μ M final protein concentrations, and their reactions usually do not reach saturation even after several hours of incubation. Additionally, graphical representations of their data are often expressed as rounds of fusion (7, 22, 25). F/F_0 relative fluorescence. (Insets) The N-terminal region of the Syb49–96 complex offers a free binding site for synaptobrevin. Upon complete zippering, the Syb49–96 fragment is displaced and lipid mixing can occur (drawing as in Fig. 1C).

fusion at a very high rate as required for neuronal exocytosis. It remains to be established at which state the SNAREs are arrested before fusion: at the level of a free 1:1 syntaxin/SNAP-25 acceptor or at a later stage when the N-terminal tip of synaptobrevin is already in contact with the acceptor complex, with further zippering being prevented by unknown mechanisms. The latter view is supported by the fact that mutations in C-terminal coiled-coil

residues of SNAP-25 selectively affect fusion triggering in vivo and also compromise the integrity of the C-terminal portion of the SNARE bundle (24).

References and Notes

1. D. Ungar, F. M. Hughson, *Annu. Rev. Cell Dev. Biol.* **19**, 493 (2003).
2. T. C. Sudhof, *Annu. Rev. Neurosci.* **27**, 509 (2004).
3. R. B. Sutton, D. Fasshauer, R. Jahn, A. T. Brunger, *Nature* **395**, 347 (1998).

4. H. R. Pelham, D. K. Banfield, M. J. Lewis, *Cold Spring Harbor Symp. Quant. Biol.* **60**, 105 (1995).
5. P. I. Hanson, J. E. Heuser, R. Jahn, *Curr. Opin. Neurobiol.* **7**, 310 (1997).
6. R. C. Lin, R. H. Scheller, *Neuron* **19**, 1087 (1997).
7. T. Weber *et al.*, *Cell* **92**, 759 (1998).
8. M. Fix *et al.*, *Proc. Natl. Acad. Sci. U.S.A.* **101**, 7311 (2004).
9. M. E. Bowen, K. Weninger, A. Brunger, S. Chu, *Biophys. J.* **89**, 690 (2004).
10. T. Liu, W. C. Tucker, A. Bhalla, E. R. Chapman, J. C. Weisshaar, *Biophys. J.* **89**, 2458 (2005).
11. B. L. Sabatini, W. G. Regehr, *Nature* **384**, 170 (1996).
12. D. Bruns, R. Jahn, *Pflug. Arch.* **443**, 333 (2002).
13. J. Rettig, E. Neher, *Science* **298**, 781 (2002).
14. D. Fasshauer, W. Antonin, V. Subramaniam, R. Jahn, *Nat. Struct. Biol.* **9**, 144 (2002).
15. D. Fasshauer, M. Margittai, *J. Biol. Chem.* **279**, 7613 (2004).
16. D. Fasshauer, H. Otto, W. K. Eliason, R. Jahn, A. T. Brünger, *J. Biol. Chem.* **272**, 28036 (1997).
17. M. Margittai, D. Fasshauer, S. Pabst, R. Jahn, R. Langen, *J. Biol. Chem.* **276**, 13169 (2001).
18. W. Xiao, M. A. Poirier, M. K. Bennett, Y. K. Shin, *Nat. Struct. Biol.* **8**, 308 (2001).
19. See supporting material on Science Online.
20. K. M. Fiebig, L. M. Rice, E. Pollock, A. T. Brunger, *Nat. Struct. Biol.* **6**, 117 (1999).
21. K. L. Nicholson *et al.*, *Nat. Struct. Biol.* **5**, 793 (1998).
22. T. J. Melia *et al.*, *J. Cell Biol.* **158**, 929 (2002).
23. X. Chen *et al.*, *Neuron* **33**, 397 (2002).
24. J. B. Sorensen *et al.*, *EMBO J.* **25**, 955 (2006).
25. F. Parlati *et al.*, *Proc. Natl. Acad. Sci. U.S.A.* **96**, 12565 (1999).
26. We thank M. Druminski for plasmid construction and W. Berning-Koch and U. Ries for purifying proteins. We are indebted to R. Jahn, A. Radakrishnan, K. Wiederhold, J. Sørensen, M. Holt, T. Siddiqui, and U. Winter for valuable comments on the manuscript. This work was supported by a grant from NIH (P01 GM072694).

Supporting Online Material

www.sciencemag.org/cgi/content/full/313/5787/673/DC1
Materials and Methods
Figs. S1 to S3
References

3 May 2006; accepted 15 June 2006
10.1126/science.1129486

A Clamping Mechanism Involved in SNARE-Dependent Exocytosis

Claudio G. Giraud, William S. Eng, Thomas J. Melia, James E. Rothman*

During neurotransmitter release at the synapse, influx of calcium ions stimulates the release of neurotransmitter. However, the mechanism by which synaptic vesicle fusion is coupled to calcium has been unclear, despite the identification of both the core fusion machinery [soluble N-ethylmaleimide-sensitive factor attachment protein receptor (SNARE)] and the principal calcium sensor (synaptotagmin). Here, we describe what may represent a basic principle of the coupling mechanism: a reversible clamping protein (complexin) that can freeze the SNAREpin, an assembled fusion-competent intermediate en route to fusion. When calcium binds to the calcium sensor synaptotagmin, the clamp would then be released. SNARE proteins, and key regulators like synaptotagmin and complexin, can be ectopically expressed on the cell surface. Cells expressing such “flipped” synaptic SNAREs fuse constitutively, but when we coexpressed complexin, fusion was blocked. Adding back calcium triggered fusion from this intermediate in the presence of synaptotagmin.

In the cell membrane, trafficking occurs constitutively. However, exocytosis—the fusion of vesicles containing stored secretory product—is tightly regulated by external signals

and is often highly synchronized. Nevertheless, regulated exocytosis and constitutive vesicle trafficking rely on the same machinery—cognate vesicle (v-) and target membrane (t-) SNARE

proteins. How, then, can fusion by a common mechanism be tightly triggered in one instance but occur spontaneously in another (1)?

It has been suggested that the fusion machinery is constitutively “on,” so that exocytosis—in which fusion is “off” in the absence of a signal for secretion—would require a protein “clamp” to block fusion in the basal state. Then, an additional protein “trigger” would be needed to reverse the clamp when a signal for secretion appears. Accumulation of fusion intermediates arrested at a discrete stage would create a synchronized and robust burst of secretion in response to urgent but transient physiological need. Isolated SNAREs can spontaneously fuse bilayers (2) on a time scale shorter than secretions can be stored—hours to days—but direct evidence for a clamp mechanism has been lacking.

Department of Physiology and Cellular Biophysics, Columbia University, New York, NY 10032, USA.

*To whom correspondence should be addressed. E-mail: jr2269@columbia.edu

Complexins are ~20 kD proteins associated with the SNARE complexes mediating exocytosis at neuronal synapses (3–5) and may represent candidates to act as fusion clamps. The human genome encodes four complexins that are broadly coexpressed in neuronal and neuroendocrine cells, of which two are soluble proteins and two are membrane-anchored by C-terminal prenylation (6). Whereas complexin binds tightly to the assembled exocytic SNARE complex in a 1:1 fashion, it binds weakly or not at all to its individual v- and t-SNARE subunits (4, 7–9). Complexin binds in the groove of the four-helix bundle of the SNARE complex (10) in its membrane-proximal half. If complexin could bind analogously to the zipper SNAREpins that drive fusion, it could potentially clamp fusion by arresting the fusion mechanism (11), but it could also promote fusion by stabilizing a key intermediate (12).

Genetic and physiological studies are difficult to interpret in this regard. Increasing the

concentration of complexin by presynaptic injection inhibits neurotransmission (13), but decreasing the concentration of complexin by knocking out two of the four complexins also blocks synchronous neurotransmitter release (14). Although complexins do not themselves appear to bind calcium (4), the phenotype of the double knockout can be bypassed simply by raising extracellular calcium (14).

Synaptotagmins I and II are the calcium sensors for synchronous synaptic transmission (15). Residing mainly in synaptic vesicles, they are members of a large family of neurally expressed proteins with two calcium-binding C2 domains (16). Knockout of mouse synaptotagmin I abolishes the fast synchronous component of calcium-mediated release (17). Mutations of synaptotagmin I reduce or eliminate the apparent cooperativity of calcium and alter the vesicle-release probability (18). Most important, defined mutations in synaptotagmin's calcium-binding site shift the calcium sensitivity of neuro-

transmission in a manner that reflects calcium binding by the isolated protein (19, 20).

The phenotypes of complexin and synaptotagmin deletions are virtually identical, suggesting that they cooperate in some fashion in calcium-triggered exocytosis (14, 17), whether directly or indirectly. Unfortunately, the complex nature of the phenotypes and the presence of multiple isoforms preclude further insights into molecular mechanism.

The outside of a cell normally lacks SNAREs and cytoplasmically located regulatory proteins, which can be added back—either directly to the medium or by expression on the cell surface with artificially added signal peptides—to test directly for function in regulating fusion.

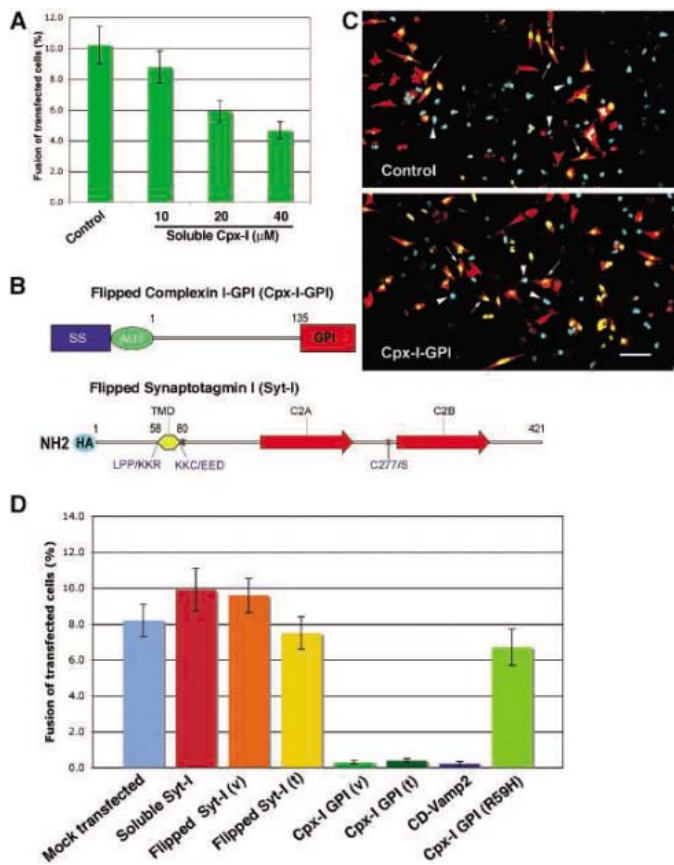
Here, we used fusion of intact cells mediated by flipped SNAREs–SNAREs ectopically expressed on the cell surface—to establish the functional capabilities of synaptotagmin and complexin in a biological context that is compositionally virgin (21).

To look for a direct modulatory role of complexin on fusion, we introduced bacterially expressed recombinant human complexin I into the flipped SNARE assay. Complexin inhibited the fusion of flipped-SNARE-expressing cells in a concentration-dependent manner (Fig. 1A), up to at least 56%. The complexin titration is not at a plateau, but we were unable to test higher concentrations. Thus, we sought to increase the local concentration of complexin I by “flipping” the protein and artificially anchoring it to the cell membrane by a glycerophosphatidylinositol (GPI) anchor (Fig. 1B). Under these conditions, residual fusion from cells expressing complexin-GPI (Cpx-I-GPI) was only 3% of the fusion observed in control cells (Fig. 1, C and D) and within the background level of fusion observed even in the presence of a competitive inhibitory VAMP2 fragment (CD-Vamp2) (Fig. 1D). Thus, SNARE-dependent fusion was completely abolished in Cpx-I-GPI-expressing cells. In contrast, a complexin point mutant with a critical VAMP2-binding residue mutated (R59H) (12, 22) was without effect (Fig. 1D). Cpx-I-GPI was an equally effective inhibitor when expressed on the v- or t-SNARE-expressing cells, suggesting that the 38 amino acid GPI linker provides the protein with sufficient conformational flexibility to behave essentially as a soluble protein.

We also developed a flipped variant of synaptotagmin I (Fig. 1B and fig. S1). In contrast to complexin, neither flipped synaptotagmin (Syt-I) nor a soluble C2A–C2B fragment produced a significant change in SNARE-mediated fusion (Fig. 1D). In the following experiments, only the membrane-embedded Syt-I was used, but indistinguishable results were obtained with soluble synaptotagmin.

Phosphatidylinositol-specific phospholipase C (PI-PLC) cleaves between the glycerol backbone and the phosphate group of GPI. Addition of PI-PLC to Cpx-I-GPI-expressing cells re-

Fig. 1. Complexin inhibits SNARE-mediated fusion. Cell fusion (21) was performed between HeLa cells stably expressing flipped t-SNAREs (and cyan fluorescent protein in the nucleus) (t-cells) and HeLa cells stably expressing flipped VAMP2 (and red fluorescent protein in the cytoplasm) (v-cells) in Dulbecco's modified media containing 1.8 mM calcium, unless otherwise noted. Proteins were either transiently transfected together with a cotransfection marker [a variant of yellow fluorescent protein bearing a nuclear localization signal (YFP-nls)] or exogenously added as recombinant protein to transient transfectants [see (36) for details]. Experiments were quantified as percentage of YFP-nls transfected cells with blue nuclei. These axes differ from previous publications (21, 30), where fusion was measured as a percent of “contacting v- and t-cells.” The absence of a cytosolic or membrane stain for t-cells prevented such a measurement here, and therefore the fusion efficiency should be considered an underestimate. Data are mean \pm SEM. (A) Recombinant complexin I was added at the indicated concentrations. (B) Domain structure of flipped regulatory proteins. The pre-prolactin signal sequence (SS) was fused to the N terminus of an AU1 epitope-tagged full-length human complexin I followed by a GPI anchoring motif. Flipped full-length synaptotagmin-I was generated by inverting the balance of charges around the transmembrane domain (TMD) (37). An N-terminal HA epitope was added, and cysteine was point-mutated to serine (C277S). (C) Cell fusion experiment between t-cells (cyan-nuclei, arrowheads), and v-cells (red cytoplasm) transiently transfected with YFP-nls (control) or YFP-nls plus Cpx-I-GPI. Fused cells have red cytoplasm and nuclei staining for both cyan and YFP (appears white; asterisks). Scale bar, 50 μ M. (D) Regulatory protein effects on cell fusion.



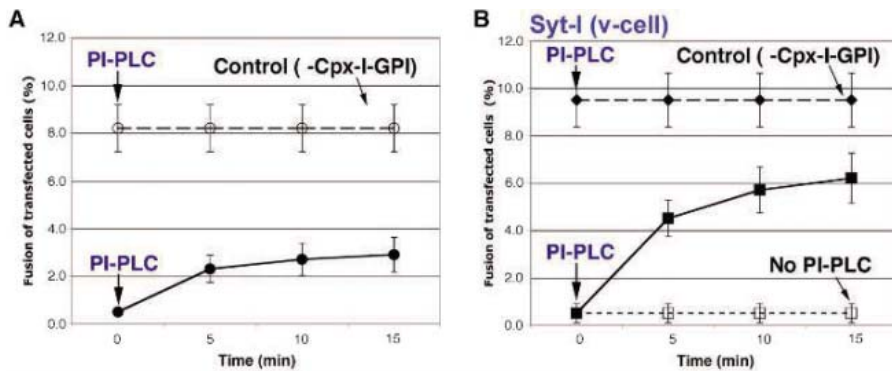
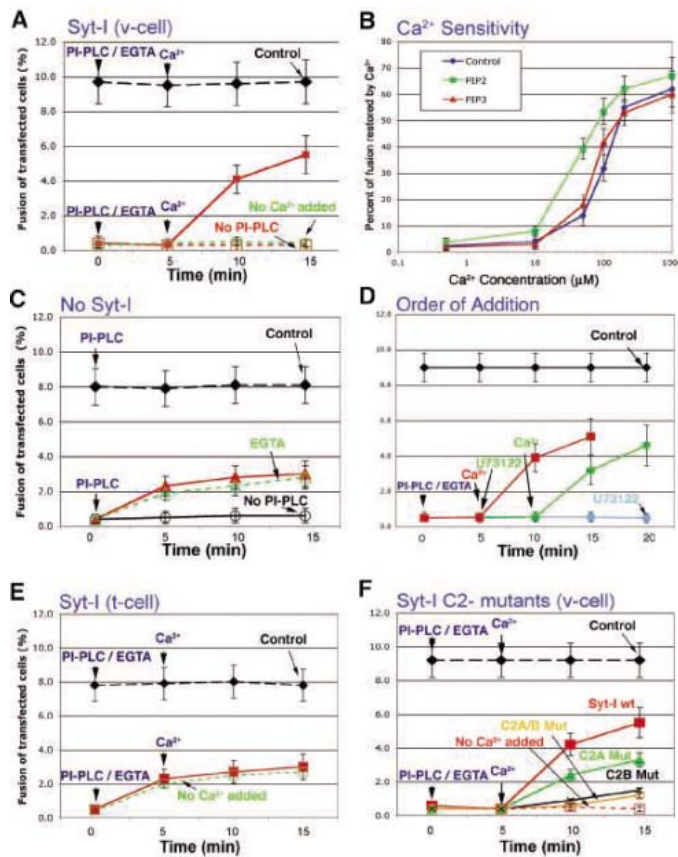


Fig. 2. Recovery of the cell fusion activity by PI-PLC cleavage of Cpx-I-GPI. *v*- and *t*-cells were incubated overnight before addition of 1 U/ml PI-PLC ($t = 0$, where indicated) to release the complexin GPI anchor. *v*-cells were transiently transfected with (A) Cpx-I-GPI or (B) Syt-1 and Cpx-I-GPI. Control curves have no Cpx-I-GPI. The resultant cell fusion activity was determined as in Fig. 1. The average percentage recovery to control values (from five independent experiments) at the 10-min time point was $34.2\% \pm 2.8\%$ for complexin alone and $68.8\% \pm 2.6\%$ for the samples containing synaptotagmin. Total free calcium equals 1.8 mM.

Fig. 3. Ca^{++} -dependent release of the complexin block. *v*- and *t*-cells were incubated overnight before addition of 1 U/ml PI-PLC and 1.8 mM EGTA ($t = 0$, where indicated) to release the complexin GPI anchor and reduce free calcium in the media to 10 μ M. At $t = 5$ min, free calcium was raised to 200 μ M (unless otherwise indicated). Control assays are without Cpx-I-GPI. Cells were fixed and data quantified as in Fig. 1. (A) Calcium dependence of synaptotagmin I mediated recovery. *v*-cells were transiently transfected with Cpx-I-GPI and Syt-1. (B) Calcium dependence of recovery of cell fusion. Cell fusion experiments as in (A), with *v*-cells expressing Cpx-I-GPI and Syt-1. Before starting the recovery, the cells were incubated for 3 hours in the presence of either buffer, 80 μ M PIP2 or 80 μ M PIP3. EGTA was introduced ($t = 0$) at 2 mM to give a free calcium concentration of 500 nM. After the 5-min EGTA/PI-PLC incubation, calcium was added to give the indicated free concentrations. Fusion recovery at 10 min is plotted as percent of the control fusion. (C) Recovery in the absence of Syt-1 is not calcium responsive. *v*-cells were transfected with Cpx-I-GPI. (D) The calcium-sensitive complex includes soluble complexin. As in (A), except a PI-PLC inhibitor (U73122) was included before calcium addition (green curve) or coincident with PI-PLC addition (blue curve). (E) Syt-1 does not stabilize clamp when expressed in the *t*-cells. Experiment is the same as 3A except Syt-1 is transiently transfected in *t*-cells. *v*-cells were transfected with Cpx-I-GPI. (F) Effect of synaptotagmin C2A and C2B mutants on the fusion recovery. *v*-cells were transiently transfected with Cpx-I-GPI plus wild-type Syt-1 (squares), C2A mutant (D178N) (triangles), C2B mutant (D303N,D309N) (crosses), or the double C2A/C2B mutant (D178N,D303N,D309N) (circles). Control experiments as squares but not transfected with Cpx-I-GPI (diamonds). Data for all panels are the mean \pm SEM of two independent experiments.



leased complexin from the cell surface (fig. S2, A and B). When PI-PLC was added to Cpx-I-GPI clamped fusion assays, there was a rapid recovery of fusion activity, accomplishing in 5 min what ordinarily takes several hours (Fig. 2A). The burst of fusion suggests that the SNAREs were at least partially assembled but could not complete fusion in the presence of Cpx-I-GPI. The burst plateaued at about 25% of overnight fusion, and the incomplete recovery could not be attributed to limiting concentrations of PI-PLC (fig. S2C). Instead, the relatively low recovery suggests that some complexin-SNARE clamped complexes remained associated even after GPI cleavage.

When full-length membrane-embedded Syt-I was present on the *v*-cell membrane, recovery from the clamped state by addition of PI-PLC was enhanced by a factor of 2 (Fig. 2B) (in cell culture medium containing 1.8 mM calcium). However, in the absence of PI-PLC, Cpx-I-GPI continued to completely clamp the fusion reaction. Thus, synaptotagmin may facilitate the removal of complexin but cannot overcome the very high local concentration of complexin maintained by the GPI anchor.

In the ideal recapitulation of synaptic vesicle exocytosis, the *v*- and *t*-cells would be incubated together (plus complexin and synaptotagmin) in the presence of very low calcium. In this context, we could most easily assess the role of calcium. A limitation of our assay system is that the cells require calcium to remain stably associated with the underlying glass support but tolerate low levels of calcium for ~ 40 min. Thus, we performed the following experiments with overnight incubations in the presence of calcium, followed by a transient EGTA [ethylene glycol bis-(2-aminoethyl ether)-N,N,N',N'-tetraacetic acid]-induced drop to 10 μ M free calcium. Under these conditions, PI-PLC cleavage could be carried out in the absence of calcium and before activation of synaptotagmin.

There was no recovery of fusion following the PI-PLC cleavage when Syt-1 was present but free calcium was kept low (10 μ M) (Fig. 3A). Reduction to 100 nM free calcium gave indistinguishable results (fig. S3). This synaptotagmin-containing intermediate recovered full fusogenicity upon addition of calcium (Fig. 3A) over a calcium range (~ 200 μ M) that promotes synaptotagmin binding to SNAREs (23) (Fig. 3B). Synaptotagmin binds the acidic lipid PIP2, but not PIP3, in a calcium-dependent manner (24). Likewise, recovery from the clamped state was stimulated by PIP2, but not PIP3 (fig. S4), and the half-maximal calcium concentration needed for stimulation is lower when the plasma membrane is enriched in PIP2 (but not PIP3) (Fig. 3B). Neither cleavage by PI-PLC (25) nor recovery from the complexin-block (in the absence of Syt-1) were calcium-sensitive (Fig. 3C). To eliminate the possibility that calcium-free Syt-1 was simply interfering with PI-PLC cleavage of Cpx-I-GPI, we carried out order-of-addition experiments,

with PI-PLC, a PI-PLC inhibitor, and calcium (Fig. 3D), confirming that both complexin and synaptotagmin were associated with the clamped complex in the absence of calcium.

When synaptotagmin was expressed on the t-cell (fig. S1B), neither the stabilization of the clamp nor the calcium-dependent enhancement of fusion recovery was maintained (Fig. 3E). Thus, flipped synaptotagmin maintains a topological restriction that is consistent with the principal synaptic vesicle localization of synaptotagmin and reminiscent of a topological restriction observed in liposomes (26). The calcium responsiveness was reduced when a conserved calcium-chelating aspartic acid residue was mutated in the Syt-I C2A domain and virtually eliminated when residues in the C2B domain were mutated (Fig. 3F), which parallels the consequences of mutating conserved aspartic acids *in vivo* (15).

The fast recovery kinetics implies the existence of a trans-SNARE clamped complex. Accessibility experiments with molecules that associate with different regions on the unstructured/uncomplexed individual SNAREs should reveal the extent of complex assembly. First, fusion appeared to be clamped after the initiation of SNAREpin assembly, because fusion proceeded after anchor cleavage even in the presence of the inhibitory v-SNARE cytoplasmic domain (fig. S5), which would bind and titrate out uncomplexed free t-SNAREs. Second, the clamped SNAREpin appeared not to be fully assembled, as assessed by neurotoxin treatment. Botulinum toxin B (BoNT/B) and Tetanus toxin each bind to free VAMP2 and cleave after the same amino acid (27), although Tetanus binds at a membrane distal position and BoNT/B binds more membrane proximal (28). When added to v cells prior to mixing with t-cells, each completely inhibited cell-cell fusion (Fig. 4A). When added to a cell-cell assay after accumulation of the clamped state, however, the toxins showed distinct effects. The assay remained complete-

ly resistant to the membrane-distally targeted tetanus but was partially susceptible to BoNT/B (Fig. 4B). Before nerve terminal activity, similar toxin accessibility differences are found in crayfish neuromuscular junctions (29). Fusion was clamped before a hemifusion intermediate, as judged by the lack of mixing of the ganglioside GM1 between cells (fig. S6), using an assay previously published (30). Thus, it is likely that the clamped trans-SNARE complex includes both calcium-free synaptotagmin and soluble complexin, a multi-component complex that may resemble the prestimulation configuration of presynaptic SNAREs.

Functional reconstitution has revealed a fundamental property of complexin: its ability to operate as a reversible molecular clamp. Clamping is enhanced by membrane anchoring of complexin, either by a GPI anchor (here), or, for some complexins, by prenylation (6). Clamping was observed whether complexin was anchored to the v- or t-SNARE-expressing cells, consistent with the behavior of a soluble protein, and was abrogated in a point mutant that also prevents overexpressed complexin from inhibiting exocytosis (22). Fusion was clamped after the initiation of SNAREpin assembly but before the t-SNAREs were fully zippered.

Synaptotagmin is a thoroughly studied protein whose role as the sensor for synchronous transmitter release is well established (15, 31). We suggest that another fundamental property of synaptotagmin may be the capacity to couple the calcium signal to SNAREs in a mechanism that requires complexin. Coupling of fusion to calcium is only reconstituted when synaptotagmin is added or expressed together with complexin. Synaptotagmin could couple from the v-side but not the t-side of the reaction, reflecting its primary location to synaptic vesicles *in vivo*. Mutation of residues in synaptotagmin's calcium-binding sites that are critical for calcium coupling *in vivo* also prevented reconstituted

coupling, and coupled fusion was enhanced by phosphoinositide.

The calcium sensitivity ($\sim 200 \mu\text{M}$) lies within the expected range of calcium microdomains (32) and physiologically is sufficient for some presynaptic terminals (31) but not others. Reintroduction of just one synaptotagmin-specific lipid (PIP2) increased our sensitivity to $\sim 40 \mu\text{M}$. Replenishment of the full spectrum of acidic lipids, including especially phosphatidylserine, may ultimately bring the assay into the low micromolar range. The lack of phosphatidylserine may also bear on a second partial discrepancy with other studies. Provision of synaptotagmin without complexin neither inhibited nor significantly stimulated fusion, even in the presence of calcium, showing that synaptotagmin is neither inherently a clamp nor a fusion protein. This characteristic differs from liposome reconstitutions, where Ca-synaptotagmin alone stimulates SNARE assembly and SNARE-mediated proteoliposome fusion (33, 34). However, each of these activities is strongly or entirely dependent on the presence of phosphatidylserine in the liposomes.

By their nature, reductionist systems that are compositionally defined are artificial, and *in vivo* studies will ultimately be required to confirm the physiological relevance of the inherent properties we have uncovered. To this end, the recent observation of increased spontaneous fusion events in cortical neuronal synapses derived from synaptotagmin knockout mice (35) is consistent with a negative (i.e., clamp-associated) role for synaptotagmin. To date, only autapses have been studied in complexin knockout mice (14), in which exocytosis was dramatically reduced, perhaps suggesting an additional positive role of complexin in stabilizing or activating the fusion machinery. The existing genetics are also confounded by the large number of potentially compensatory synaptotagmin and complexin isoforms.

Fusion triggered from clamped flipped SNAREs takes about 5 min in the reconstituted system as compared with milliseconds or less in synapses. It is possible that this difference reflects the kinetics of enzymatic cleavage of GPI-complexin (i.e., GPI-complexin bound to SNAREs is a poor substrate) or another property of GPI-complexin (perhaps arresting fusion at an earlier stage or perhaps the absence of other important factors from our defined system). However, we think a likely explanation may be that msec synaptic transmission requires only the transient opening of a fusion pore to allow egress of transmitter, whereas our assay measures macromolecular content mixing between cells, which will always be much slower than the initial fusion pore.

Non-neuronal exocytosis, needed for the diverse forms of intercellular communication and physiological response in the body, may also rely on a similar clamping principle—although using different clamps—and similar triggering mecha-

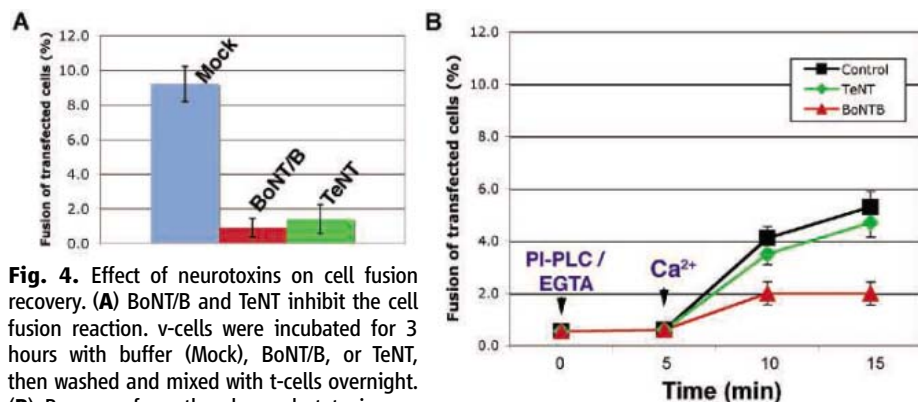


Fig. 4. Effect of neurotoxins on cell fusion recovery. **(A)** BoNT/B and TeNT inhibit the cell fusion reaction. v-cells were incubated for 3 hours with buffer (Mock), BoNT/B, or TeNT, then washed and mixed with t-cells overnight. **(B)** Recovery from the clamped state is partially sensitive to BoNT/B. Cell fusion was performed as in Fig. 3A, using v/Cpx-1-GPI/Syt-1-cells. Before starting the recovery, the cells were incubated for 3 hours in the presence of buffer (control) (squares), BoNT/B (triangles), or TeNT (diamonds). Cells were washed, then incubated with EGTA and PI-PLC (at $t = 0$) to give baseline free calcium of $10 \mu\text{M}$. At $t = 5$ min, Ca^{++} ($200 \mu\text{M}$ free final) was added to the reaction. The extent of fusion was quantified as in Fig. 1.

nisms to govern the common and constitutive engine for membrane fusion, SNARE proteins.

References and Notes

1. T. Sollner *et al.*, *Nature* **362**, 318 (1993).
2. T. Weber *et al.*, *Cell* **92**, 759 (1998).
3. S. Takahashi *et al.*, *FEBS Lett.* **368**, 455 (1995).
4. H. T. McMahon, M. Missler, C. Li, T. C. Sudhof, *Cell* **83**, 111 (1995).
5. T. Ishizuka, H. Saisu, S. Odani, T. Abe, *Biochem. Biophys. Res. Commun.* **213**, 1107 (1995).
6. K. Reim *et al.*, *J. Cell Biol.* **169**, 669 (2005).
7. S. Pabst *et al.*, *J. Biol. Chem.* **277**, 7838 (2002).
8. K. Hu, J. Carroll, C. Rickman, B. Davletov, *J. Biol. Chem.* **277**, 41652 (2002).
9. H. Tokumaru *et al.*, *Cell* **104**, 421 (2001).
10. R. B. Sutton, D. Fasshauer, R. Jahn, A. T. Brunger, *Nature* **395**, 347 (1998).
11. A. Bracher, J. Kadlec, H. Betz, W. Weissenhorn, *J. Biol. Chem.* (2002).
12. X. Chen *et al.*, *Neuron* **33**, 397 (2002).
13. S. Ono *et al.*, *Eur. J. Neurosci.* **10**, 2143 (1998).
14. K. Reim *et al.*, *Cell* **104**, 71 (2001).
15. T. W. Koh, H. J. Bellen, *Trends Neurosci.* **26**, 413 (2003).
16. M. S. Perin, V. A. Fried, G. A. Mignery, R. Jahn, T. C. Sudhof, *Nature* **345**, 260 (1990).
17. M. Geppert *et al.*, *Cell* **79**, 717 (1994).
18. J. T. Littleton, M. Stern, M. Perin, H. J. Bellen, *Proc. Natl. Acad. Sci. U.S.A.* **91**, 10888 (1994).
19. R. Fernandez-Chacon *et al.*, *Nature* **410**, 41 (2001).
20. J. S. Rhee *et al.*, *Proc. Natl. Acad. Sci. U.S.A.* **102**, 18664 (2005).
21. C. Hu *et al.*, *Science* **300**, 1745 (2003).
22. D. A. Archer, M. E. Graham, R. D. Burgoyne, *J. Biol. Chem.* **277**, 18249 (2002).
23. A. F. Davis *et al.*, *Neuron* **24**, 363 (1999).
24. G. Schiavo, Q. M. Gu, G. D. Prestwich, T. H. Sollner, J. E. Rothman, *Proc. Natl. Acad. Sci. U.S.A.* **93**, 13327 (1996).
25. D. W. Heinz, L. O. Essen, R. L. Williams, *J. Mol. Biol.* **275**, 635 (1998).
26. L. K. Mahal, S. M. Sequeira, J. M. Gureasko, T. H. Sollner, *J. Cell Biol.* **158**, 273 (2002).
27. G. Schiavo *et al.*, *Nature* **359**, 832 (1992).
28. R. Pellizzari *et al.*, *J. Biol. Chem.* **271**, 20353 (1996).
29. S. Y. Hua, M. P. Charlton, *Nat. Neurosci.* **2**, 1078 (1999).
30. C. G. Giraudo *et al.*, *J. Cell Biol.* **170**, 249 (2005).
31. G. J. Augustine, *Curr. Opin. Neurobiol.* **11**, 320 (2001).
32. R. Llinas, M. Sugimori, R. B. Silver, *Science* **256**, 677 (1992).
33. W. C. Tucker, T. Weber, E. R. Chapman, *Science* **304**, 435 (2004).
34. A. Bhalla, M. C. Chicka, W. C. Tucker, E. R. Chapman, *Nat. Struct. Mol. Biol.* (2006).
35. Z. P. Pang, J. Sun, J. Rizo, A. Maximov, T. C. Sudhof, *EMBO J.* **25**, 2039 (2006).
36. Materials and methods are available as supporting material on Science Online.
37. J. P. Beltzer *et al.*, *J. Biol. Chem.* **266**, 973 (1991).
38. We thank M. Wiedmann for helpful comments, T. Balla for providing His-PLC δ 1-PH-GFP and YFP-GRP1-PH plasmids, and J. Dannenberg and T. Sollner for providing the CD-syt-1 plasmid. This work is supported by an NIH grant to J.E.R.

Supporting Online Material

www.sciencemag.org/cgi/content/full/1129450/DC1
Materials and Methods

Figs. S1 to S6

Table S1

References

2 May 2006; accepted 12 June 2006

Published online 22 June 2006;

10.1126/science.1129450

Include this information when citing this paper.

Anaphase Inactivation of the Spindle Checkpoint

William J. Palframan,¹ Janet B. Meehl,² Sue L. Jaspersen,³ Mark Winey,² Andrew W. Murray^{1*}

The spindle checkpoint delays cell cycle progression until microtubules attach each pair of sister chromosomes to opposite poles of the mitotic spindle. Following sister chromatid separation, however, the checkpoint ignores chromosomes whose kinetochores are attached to only one spindle pole, a state that activates the checkpoint prior to metaphase. We demonstrate that, in budding yeast, mutual inhibition between the anaphase-promoting complex (APC) and Mps1, an essential component of the checkpoint, leads to sustained inactivation of the spindle checkpoint. Mps1 protein abundance decreases in anaphase, and Mps1 is a target of the APC. Furthermore, expression of Mps1 in anaphase, or repression of the APC in anaphase, reactivates the spindle checkpoint. This APC-Mps1 feedback circuit allows cells to irreversibly inactivate the checkpoint during anaphase.

Chromosome segregation and cell cycle progression are coordinated. Before mitotic chromosome segregation, sister chromatids are held together by cohesin (1). To segregate properly, a pair of sister chromatids must be bioriented, with the two sister kinetochores attached to and pulled toward opposite poles of the spindle. Cohesin resists these pulling forces, which produces tension between the sister kinetochores (2). The spindle checkpoint detects chromosomes that are not bioriented, by monitoring both tension at kinetochores and the presence of kinetochores that are unattached to spindle microtubules (3–5). As mitosis proceeds and sister chromatid pairs biorient, the

number of kinetochores lacking tension falls. The spindle checkpoint is sensitive enough to detect a single unattached kinetochore (6) or a single chromosome whose sisters are attached to the same pole (mono-orientation) (7, 8) and delays cell cycle progression until biorientation is complete.

Activation of the spindle checkpoint inhibits the onset of anaphase, arresting cells in mitosis until all chromosomes are bioriented (9). The target of the spindle checkpoint is Cdc20, an accessory subunit of the anaphase-promoting complex (APC) (10). Cdc20 induces the mitosis-specific form of the APC (APC^{Cdc20}). The ubiquitin ligase activity of APC^{Cdc20} targets securin (Pds1) for destruction, relieving the inhibition of separase (Esp1), a protease that cleaves the cohesin subunit Scc1 (1). Thus, when all chromosomes are bioriented, the spindle checkpoint is satisfied and the cohesin linkage is eliminated, which allows sister chromatids to separate.

Anaphase kinetochores are no longer under tension; they lack a sister chromatid to pull

against, and once they reach the spindle pole, any drag forces created by movement through a viscous medium disappear. However, the cell cycle does not arrest as a result of chromosome segregation, which suggests that the spindle checkpoint is inactivated as cells enter anaphase. Cdc15 is a part of the mitotic exit network in budding yeast (*Saccharomyces cerevisiae*); *cdc15-2* strains proliferate at 23°C and arrest in late anaphase at 37°C (11). To confirm that the checkpoint cannot be activated during anaphase, we arrested *cdc15-2* cells at 37°C and transferred them to medium containing the microtubule poison nocodazole, a known activator of the spindle checkpoint (4). The stability of epitope-tagged Pds1, an APC^{Cdc20} target, was measured to monitor the checkpoint's activity (12). Anaphase-arrested cells treated with nocodazole did not stabilize Pds1, which showed a lack of spindle checkpoint activity (Fig. 1A). In contrast, Pds1 was stable in cells that had been arrested in metaphase with nocodazole at 37°C (Fig. 1A). Pds1 was also stabilized in anaphase-arrested cells in which Cdc20 expression had been inhibited, which confirmed that the anaphase instability of Pds1 was due to the activity of APC^{Cdc20}, the target of the spindle checkpoint (Fig. 1A).

Spindle checkpoint signaling in anaphase matters only because Cdc20 is required after the metaphase-to-anaphase transition. Although inhibiting APC^{Cdc20} stabilizes Pds1 and arrests cells in metaphase (10), stable Pds1 also keeps cells from leaving anaphase (13, 14), and repressing Cdc20 in anaphase leads to the accumulation of Pds1 (Fig. 1B). This shows that Cdc20 activity is required to destabilize Pds1 in anaphase cells, which corroborates the finding that APC^{Cdc20} is needed for anaphase exit (15) and suggests that activating the spindle checkpoint in anaphase cells would prevent mitotic exit.

¹Department of Molecular and Cellular Biology, Biological Laboratories, Harvard University, 16 Divinity Avenue, Cambridge, MA 02138, USA. ²MCD Biology, UCB 347, University of Colorado, Boulder, CO 80309, USA. ³Stowers Institute for Medical Research, 1000 East 50th Street, Kansas City, MO 64110, USA.

*To whom correspondence should be addressed. E-mail: amurray@mcb.harvard.edu

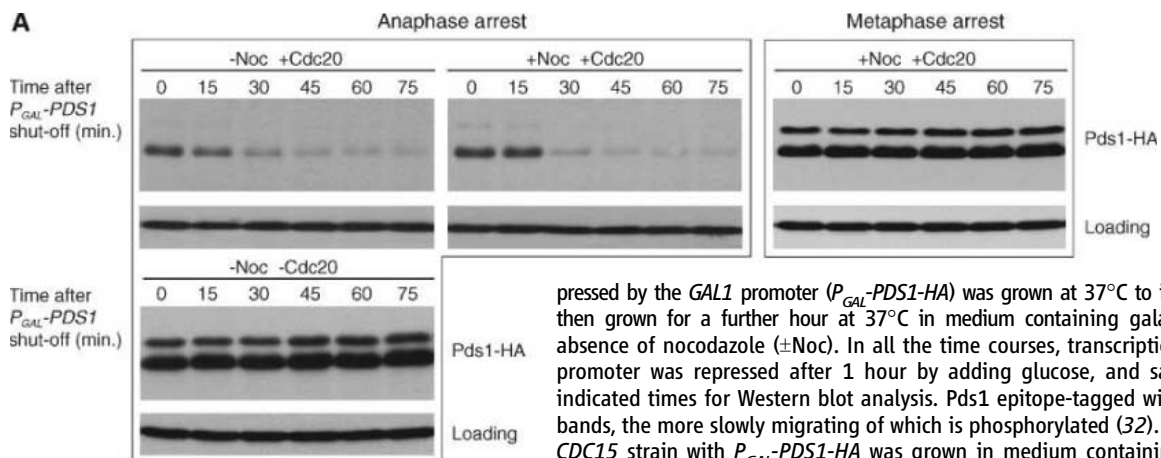
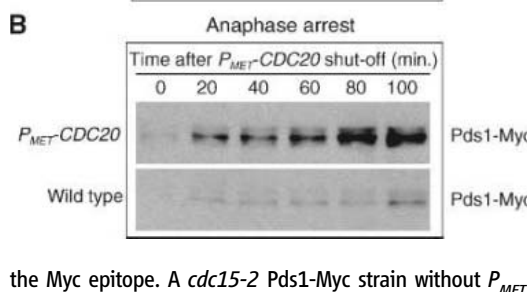


Fig. 1. Lack of tension at the kinetochore fails to activate the spindle checkpoint in anaphase, and APC^{Cdc20} activity is necessary for Pds1 degradation in anaphase. (A) (Top, left) A *cdc15-2* strain with hemagglutinin (HA) epitope-tagged Pds1 expressed



by the *GAL1* promoter (*P_{GAL}-PDS1-HA*) was grown at 37°C to induce anaphase arrest, and then grown for a further hour at 37°C in medium containing galactose in the presence or absence of nocodazole (±Noc). In all the time courses, transcription of Pds1 from the *GAL1* promoter was repressed after 1 hour by adding glucose, and samples were taken at the indicated times for Western blot analysis. Pds1 epitope-tagged with HA runs as two distinct bands, the more slowly migrating of which is phosphorylated (32). (Top, right) As a control, a *CDC15* strain with *P_{GAL}-PDS1-HA* was grown in medium containing nocodazole at 37°C to induce a metaphase arrest, and then grown for a further hour at 37°C in medium containing galactose and nocodazole. (Bottom) A *cdc15-2* strain with *P_{GAL}-PDS1-HA* and Cdc20 expressed under the control of the repressible *MET3* promoter (*P_{MET}-CDC20*) was grown at 37°C in medium lacking methionine to induce an anaphase arrest and then grown for a further hour at 37°C in complete synthetic medium (CSM) + galactose + methionine to selectively repress the expression of Cdc20. Equal loading was confirmed using actin (top panels) and Cdc28 (bottom). (B) A *cdc15-2* strain with epitope-tagged Pds1 expressed under the endogenous promoter (*Pds1-Myc*) and *P_{MET}-CDC20* was grown at 37°C without methionine to induce an anaphase arrest and then transferred to methionine-containing medium to repress the expression of Cdc20; samples were taken at the indicated times for Western blot analysis with antibodies to the Myc epitope. A *cdc15-2* Pds1-Myc strain without *P_{MET}-CDC20* (wild type) was grown under the same conditions as a control.

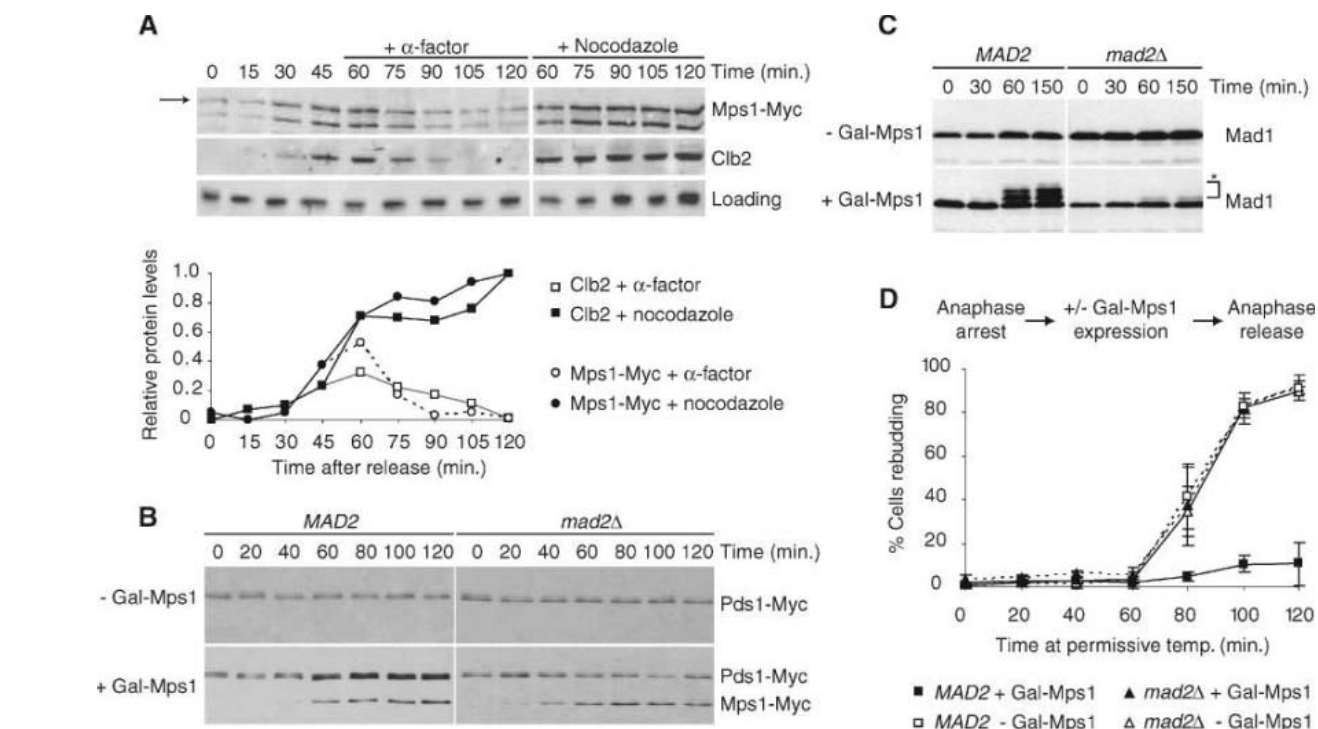


Fig. 2. Mps1 is a cell cycle-regulated protein, and expression of Mps1 in anaphase reactivates the spindle checkpoint. (A) A strain with epitope-tagged Mps1 (Mps1-Myc) under the control of the endogenous *MPS1* promoter was released from α -factor arrest and then arrested at either the subsequent metaphase (with nocodazole) or G₁ (using α factor). Samples were taken at the indicated times for Western blot analysis with antibodies to the Myc epitope and Clb2 protein. Full-length Mps1-Myc is indicated with an arrow, and the lower band is a degradation product. The relative levels of the different proteins were quantified over the time course. (B, C, and D) *MAD2* and *mad2Δ* strains with epitope-tagged Pds1 (Pds1-Myc) and

MPS1 driven by the *GAL1* promoter (*P_{GAL}-MPS1-myc*) were released from a G₁ (α factor) block to an anaphase (*cdc15-2*) arrest at 37°C in the absence of galactose. The anaphase-arrested cells were transferred to medium containing either raffinose to maintain Mps1 repression (– Gal-Mps1) or galactose to induce Mps1 expression (+ Gal-Mps1); at the indicated times after the transfer, samples were taken for Western blot analysis with antibodies to the Myc epitope (B) and antibody to Mad1 to monitor Mad1 phosphorylation (C). (D) After 120 min, the cells were transferred to the permissive temperature for *cdc15-2* (23°C), and samples were taken at the indicated times to monitor rebudding as a measure of cell cycle arrest.

We asked how the spindle checkpoint is kept inactive during anaphase. Mps1 is a protein kinase whose activity is essential for spindle checkpoint signaling (16), and Mps1 overexpression arrests cells in metaphase by activating the checkpoint (17). Mps1 mRNA levels show little change during the cell cycle (18). In contrast, Mps1 protein abundance varied during the cell cycle (Fig. 2A), rising and falling with those of the mitotic cyclin Clb2, which accumulates as cells enter mitosis and is degraded as they leave it (15). This fall does not occur in cells released from G₁ and then arrested at metaphase, which suggests that Mps1 is degraded after the metaphase-to-anaphase transition (Fig. 2A).

As cells enter anaphase, Mps1 levels fall, and the spindle checkpoint is turned off. This coincidence prompted us to ask if the checkpoint could be reactivated in anaphase by overexpressing Mps1 from the *GAL1* promoter. Synchronized *cdc15-2* cells were released from G₁, arrested in anaphase at 37°C, and then treated with galactose to induce Mps1 expression. Spindle checkpoint reactivation, even in the absence of microtubule disruption, was demonstrated by an increase in Pds1 stability, Mad1 phosphorylation, and the inability of cells to rebud after they were returned to the permissive temperature (Fig. 2, B, C, and D). Pds1 stabilization and Mad1 phosphorylation

are hallmarks of spindle checkpoint activation (19). Checkpoint reactivation depended on Mad2, an essential component of the spindle checkpoint (4). We ruled out a role for the Bub2-dependent spindle-positioning checkpoint, which keeps cells from leaving anaphase until one spindle pole body has entered the daughter cell (20) (fig. S1, A and B). The dependence on Mad2 indicates that Mps1 overexpression reactivates the spindle checkpoint and that all the components of this pathway downstream of Mps1 are functional in anaphase. The result also suggests that reducing the level of Mps1 helps to inactivate the checkpoint in anaphase.

The amount of Mps1 fell by about 50% as synchronized cells went from metaphase to anaphase (Fig. 3A, 140-min time point). If *Cdc20* expression was then repressed while the cells were kept in anaphase, Mps1 accumulated, which indicated a role for APC^{Cdc20} in reducing Mps1 stability during anaphase (Fig. 3A, 140-min to 220-min time points).

The destruction box (D-box) is a recognition site for APC^{Cdc20} and APC^{Cdh1}, the form of the APC active in G₁ (21). There are three putative D-boxes (RXXL) in the noncatalytic N-terminal half of the Mps1 protein (fig. S2) (22). We fused the N-terminal portion of Mps1 (Mps1N, amino acids 1 to 450) to *Escherichia coli* β-galactosidase (LacZ), mutated the putative

Mps1 D-boxes, and expressed the protein from the *GAL1* promoter. By using this noncatalytic fragment, we avoided the complication that increasing Mps1 expression would activate the checkpoint and would reduce APC^{Cdc20} activity. Mps1N-LacZ expression was induced for 2 hours before transcription was shut off by the addition of glucose. In metaphase-arrested cells, Mps1N-LacZ was largely stable for the duration of the experiment (Fig. 3B). In contrast, in cells arrested in anaphase or G₁, this fusion protein was unstable (Fig. 3B). Mutation of the three D-box motifs (267RELL, 319RRAL, 356REVL) together was effective in stabilizing the protein construct in anaphase and G₁ (Fig. 3B). Mutation of the 356REVL D-box alone substantially increased the stability of the fusion protein in anaphase and G₁, which suggested that this motif is particularly important for regulating Mps1 stability. Deletion of *CDH1* or repression of the APC subunit *Cdc16* in G₁ also stabilized full-length, wild-type Mps1 (fig. S3). These results suggest that Mps1 is a substrate for APC^{Cdc20}- and APC^{Cdh1}-dependent destruction in anaphase and G₁, respectively.

The observations that a spindle checkpoint protein is a target of the APC and that APC^{Cdc20} is inhibited by the checkpoint suggest that these two activities oppose each other in a double-negative feedback loop (Fig. 4A). In this model, the checkpoint inhibits the APC before chromo-

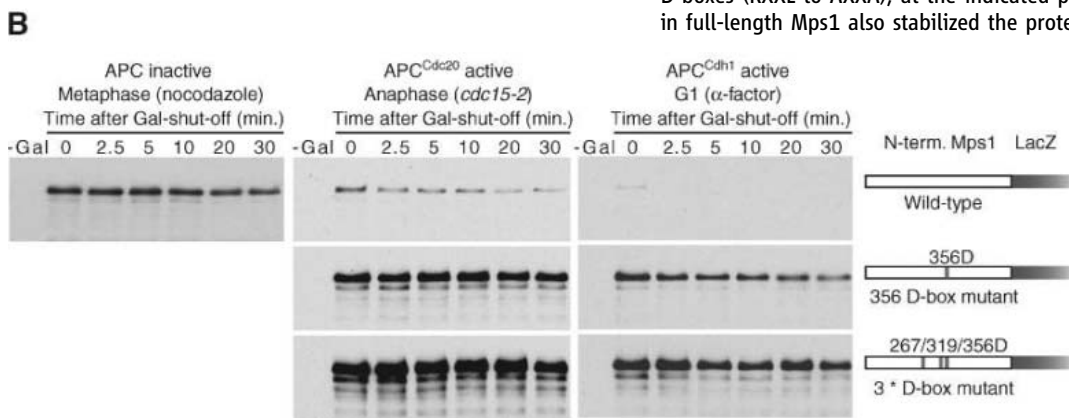
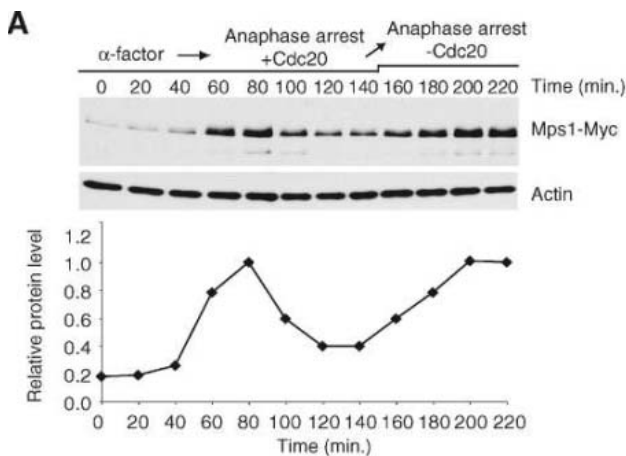


Fig. 3. Mps1 protein abundance falls in anaphase, and Mps1 stability is regulated by the APC. **(A)** Cells containing epitope-tagged Mps1 (Mps1-Myc) and *P_{MET}-CDC20* were released from a G₁ (α -factor) arrest to an anaphase (*cdc15-2*) arrest at 37°C in medium without methionine. After 140 min, 4',6'-diamidino-2-phenylindole (DAPI) staining revealed that 97% of the cells had arrested in anaphase with separated chromosomes. At this time, the anaphase-arrested cells were transferred to medium containing methionine to repress expression of *Cdc20*. At the indicated times, samples were taken for Western blot analysis with antibodies to the Myc epitope, and a calibration curve was used to quantify Mps1 levels. **(B)** Strains containing Mps1N-LacZ fusion proteins expressed under the *GAL1* promoter (*P_{GAL}-MPS1N-LacZ*) were arrested in metaphase (nocodazole), anaphase (*cdc15-2*), or G₁ (α factor), and then transferred to medium containing galactose for 2 hours to induce expression of the fusion protein. Glucose and cycloheximide were added to shut off Mps1 transcription and translation; samples were taken at the indicated times for Western blot analysis with antibody to β -galactosidase. Proteins contained the wild-type Mps1 N-terminal fragment, or fragments with mutation of putative D-boxes (RXXL to AXXA), at the indicated positions. Mutation of the 356D-box in full-length Mps1 also stabilized the protein (fig. S5).

some biorientation, and this inhibition stabilizes Mps1 and potentiates the checkpoint. Once the chromosomes are aligned, the checkpoint's activity is reduced, the APC becomes more active, and Mps1 is degraded, which prevents subsequent reactivation of the checkpoint.

To test whether this feedback loop depends on the presence of other checkpoint components, such as Mad2, we measured the stability of Mps1 after a period of high Mps1 expression from the *GAL1* promoter in either *MAD2* or *mad2Δ* cells arrested in anaphase. Mps1 was present in greater amounts at steady state and was more stable in *MAD2* cells than in *mad2Δ* cells, which indicated that the feedback loop was activated in the *MAD2* cells but not in the checkpoint mutant (Fig. 4B). The stabilized Mps1 in *MAD2* cells was highly phosphorylated, consistent with the observation that the stability

of Mps1 is influenced by its phosphorylation state (23, 24).

If Mps1 and APC activity form a feedback loop, transient expression of Mps1 should be able to switch the circuit into a state of sustained Mps1 stability and APC inactivity; this state should not be dependent on continued *MPS1* transcription. Furthermore, because the checkpoint depends on the kinase activity of Mps1, it should be possible to switch the feedback circuit to its original state by inhibiting this activity. We tested these hypotheses by transiently expressing a repressible allele of Mps1 (*mps1-as1*) in anaphase. The kinase activity of this allele can be specifically inhibited with 4-amino-1-*tert*-butyl-3-(1'-naphthylmethyl)pyrazolo[3,4-*d*]pyrimidine (1NM-PP1), an inhibitor of genetically manipulated protein kinases (25). *mps1-as1* was expressed in anaphase-arrested, *cdc15-2*

cells; the cells were shifted to 23°C; and Mps1 expression was shut off with glucose in the presence or absence of the inhibitor. We measured the ability of the checkpoint to maintain the "on" state by monitoring the time taken for cells to rebud and the stability of epitope-tagged Pds1 and Mps1 (Fig. 4C and fig. S4). In the absence of 1NM-PP1, prolonged checkpoint activation was observed in *MAD2* cells, but not in checkpoint (*mad2Δ*) mutant cells. Treatment with 1NM-PP1 reduced the duration of checkpoint activation in *MAD2* cells. Although continued kinase activity was essential, continued Mps1 expression was not required to prolong checkpoint signaling and delay rebudding. This suggests that transient Mps1 expression reduces APC activity below the threshold at which Mps1 is sufficiently stable to maintain the feedback circuit in the "checkpoint on" state.

If Mps1 stability regulates checkpoint activity in anaphase, increasing the stability of Mps1 should reactivate the spindle checkpoint, without overexpressing the protein. Repression of Cdc20 in anaphase stabilizes Mps1 (Fig. 3A), and we tested whether this repression was sufficient to activate the spindle checkpoint. Cdc20 expression was repressed in anaphase-arrested (*cdc15-2*) cells for 45 min at 37°C before transfer to 23°C to reactivate Cdc15. We compared rebudding time in checkpoint-proficient (*MAD2*) and checkpoint-deficient (*mad2Δ*) cells (Fig. 4D). The *MAD2* cells stayed arrested for the duration of the experiment, whereas the checkpoint-deficient mutant cells and control cells in which Cdc20 expression had never been repressed rebudded (Fig. 4D). We found high levels of Mad1 phosphorylation and reduced Cdc20 abundance in the checkpoint-proficient cells, consistent with checkpoint activation (19, 26) (fig. S6). The simplest interpretation of these results is that a small amount of Cdc20 remains in checkpoint-deficient cells after a short period of Cdc20 repression, which allows exit from anaphase. In the checkpoint-proficient cells, repressing Cdc20 stabilizes checkpoint components, which allows the absence of tension at anaphase kinetochores to reactivate the checkpoint. Checkpoint activation further inhibits and destabilizes Cdc20 (26), which initiates a positive-feedback loop that makes it difficult for cells to exit mitosis, even after Cdc15 activity has been restored at the permissive temperature. We argue that the cell cycle engine in these cells has switched to a metaphase-like state. This result suggests that the anaphase stabilization of Mps1, and potentially other checkpoint components, permits the reactivation of the spindle checkpoint. We propose that it is the destabilization of these components that inactivates the checkpoint in anaphase in a normal cell cycle.

The regulation of other spindle checkpoint or kinetochore components likely plays a role in anaphase checkpoint inactivation. The budding yeast aurora kinase, Ipl1, activates the spindle checkpoint by creating unattached kinetochores,

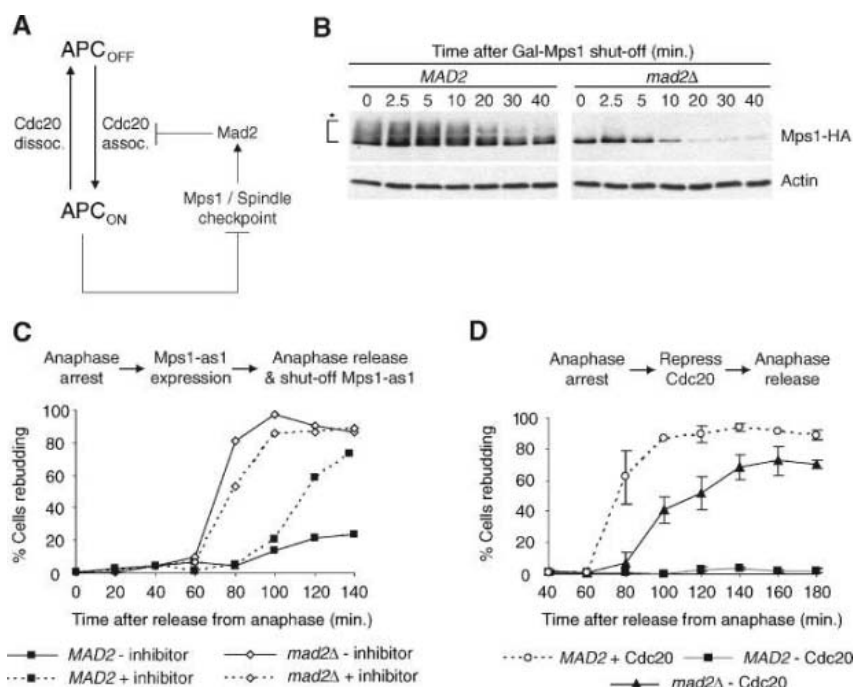


Fig. 4. Mps1 and the APC mutually inhibit each other to create a double-negative feedback loop. (A) A model for Mps1 acting via the spindle checkpoint pathway to inhibit APC^{Cdc20} activity, thereby increasing Mps1 stability. (B) Mps1 stability in anaphase-arrested (*cdc15-2*) cells with *P_{GAL1}-MPS1-HA* grown in galactose to induce expression of Mps1 for 1 hour. Glucose was added to the medium, and samples were taken at the indicated times for Western blot analysis with antibodies to HA epitope. Mps1 stability in anaphase was Mad2-dependent, and Mps1 phosphorylation (clearly visible when Mps1 is tagged with the HA epitope) results in a shift of the Mps1-HA band (indicated with an asterisk) that largely depends on the presence of Mad2. (C) Anaphase-arrested (*cdc15-2*) *MAD2* and *mad2Δ* cells with Pds1-Myc and a kinase-repressible epitope-tagged Mps1 protein expressed under the *GAL1* promoter (*P_{GAL1}-mps1-as1-myc*) were transiently grown in galactose to induce Mps1 expression. After 2 hours, the cells were shifted to the permissive temperature (23°C) in medium containing glucose, with or without the 1NM-PP1 kinase inhibitor. Rebudding of cells was measured at the indicated times and the samples were used for Western blot analysis with antibody to the Myc epitope (see fig. S4). (D) Checkpoint activation without Mps1 overexpression, in anaphase-arrested (*cdc15-2*) *MAD2* and *mad2Δ* cells with *P_{MET}-CDC20-HA* grown in medium containing methionine to repress Cdc20 expression. After 45 min, the cells were shifted to the permissive temperature for anaphase release (23°C), and samples were taken at the indicated times to measure rebudding and used for Western blot analysis with antibodies to Mad1 and the HA epitope (see fig. S6). A strain containing Cdc20 expressed under the endogenous promoter was grown under the same conditions as a control.

and Ipl1 moves from kinetochores to spindle microtubules shortly after the initiation of anaphase (5, 27, 28). Microtubule attachment to kinetochores in anaphase may be stabilized by the loss of Ipl1, helping to keep the checkpoint inactive. However, Ipl1 mutants respond to treatment with nocodazole, whereas anaphase-arrested cells do not (Fig. 1A), which suggests that additional factors, such as Mps1 degradation, have turned off the checkpoint in anaphase (29). The organization of other “chromosomal passenger proteins” also changes as cells enter anaphase (30), as do spindle microtubule dynamics (31), and these factors may also influence checkpoint behavior in anaphase. Finally, the checkpoint destabilizes Cdc20, as well as inhibits its activity, which reinforces the mutual antagonism between the checkpoint and APC^{Cdc20}.

We have presented evidence for a mechanism that inactivates the spindle checkpoint as yeast cells enter anaphase. When mitosis starts, the APC is off, the checkpoint is on, and checkpoint proteins are stable. As long as one chromosome has not aligned, the checkpoint inhibits the APC. When this chromosome biorients, a threshold is crossed, the APC becomes active, cells enter anaphase, and the destruction of Mps1 (and possibly other checkpoint proteins) permanently inactivates the checkpoint. The opposing activities of the checkpoint and the APC let cells

switch rapidly between prometaphase, when they can sensitively monitor chromosome alignment, and anaphase, when they are irreversibly committed to entering the next cell cycle, despite the lack of tension at the kinetochores.

References and Notes

1. K. Nasmyth, *Science* **297**, 559 (2002).
2. R. B. Nicklas, C. A. Koch, *J. Cell Biol.* **43**, 40 (1969).
3. M. A. Hoyt, L. Totis, B. T. Roberts, *Cell* **66**, 507 (1991).
4. R. Li, A. W. Murray, *Cell* **66**, 519 (1991).
5. B. A. Pinsky, C. Kung, K. M. Shokat, S. Biggins, *Nat. Cell Biol.* **8**, 78 (2006).
6. C. L. Rieder, A. Schultz, R. Cole, G. Sluder, *J. Cell Biol.* **127**, 1301 (1994).
7. X. Li, R. B. Nicklas, *Nature* **373**, 630 (1995).
8. W. A. Wells, A. W. Murray, *J. Cell Biol.* **133**, 75 (1996).
9. A. Musacchio, K. G. Hardwick, *Nat. Rev. Mol. Cell Biol.* **3**, 731 (2002).
10. L. H. Hwang *et al.*, *Science* **279**, 1041 (1998).
11. S. L. Jaspersen, J. F. Charles, R. L. Tinker-Kulberg, D. O. Morgan, *Mol. Biol. Cell* **9**, 2803 (1998).
12. O. Cohen-Fix, J. M. Peters, M. W. Kirschner, D. Koshland, *Genes Dev.* **10**, 3081 (1996).
13. M. Shirayama, A. Toth, M. Galova, K. Nasmyth, *Nature* **402**, 203 (1999).
14. O. Cohen-Fix, D. Koshland, *Genes Dev.* **13**, 1950 (1999).
15. F. M. Yeong, H. H. Lim, C. G. Padmashree, U. Surana, *Mol. Cell* **5**, 501 (2000).
16. E. Weiss, M. Winey, *J. Cell Biol.* **132**, 111 (1996).
17. K. G. Hardwick, E. Weiss, F. C. Luca, M. Winey, A. W. Murray, *Science* **273**, 953 (1996).
18. C. A. Ball *et al.*, *Nucleic Acids Res.* **28**, 77 (2000).
19. K. G. Hardwick, A. W. Murray, *J. Cell Biol.* **131**, 709 (1995).
20. R. Li, *Proc. Natl. Acad. Sci. U.S.A.* **96**, 4989 (1999).
21. M. Glotzer, A. W. Murray, M. W. Kirschner, *Nature* **349**, 132 (1991).
22. Single-letter abbreviations for the amino acid residues are as follows: A, Ala; C, Cys; D, Asp; E, Glu; F, Phe; G, Gly; H, His; I, Ile; K, Lys; L, Leu; M, Met; N, Asn; P, Pro; Q, Gln; R, Arg; S, Ser; T, Thr; V, Val; W, Trp; Y, Tyr; and X, any amino acid.
23. S. L. Jaspersen *et al.*, *Dev. Cell* **7**, 263 (2004).
24. See supporting data on *Science* Online.
25. M. H. Jones *et al.*, *Curr. Biol.* **15**, 160 (2005).
26. J. Pan, R. H. Chen, *Genes Dev.* **18**, 1439 (2004).
27. S. Buvelot, S. Y. Tatsutani, D. Vermaak, S. Biggins, *J. Cell Biol.* **160**, 329 (2003).
28. G. Pereira, E. Schiebel, *Science* **302**, 2120 (2003).
29. S. Biggins, N. Bhalla, A. Chang, D. L. Smith, A. W. Murray, *Genetics* **159**, 453 (2001).
30. P. Vagnarelli, W. C. Earnshaw, *Chromosoma* **113**, 211 (2004).
31. T. Higuchi, F. Uhlmann, *Nature* **433**, 171 (2005).
32. O. Cohen-Fix, D. Koshland, *Proc. Natl. Acad. Sci. U.S.A.* **94**, 14361 (1997).
33. We thank S. C. Schuyler and B. Stern for their support and technical assistance, the members of the Murray and Winey labs for their helpful comments and suggestions, K. Hardwick for providing antibodies, and A. Wenger for his efforts. Supported by NIH grants GM43987 (A.W.M.) and GM51312 (M.W.). S.L.J. is a Leukemia and Lymphoma Society Special Fellow.

Supporting Online Material

www.sciencemag.org/cgi/content/full/1127205/DC1
SOM Text
Figs. S1 to S6
Table S1

9 March 2006; accepted 30 May 2006
Published online 6 July 2006;
10.1126/science.1127205
Include this information when citing this paper.

Frames, Biases, and Rational Decision-Making in the Human Brain

Benedetto De Martino,* Dharshan Kumaran, Ben Seymour, Raymond J. Dolan

Human choices are remarkably susceptible to the manner in which options are presented. This so-called “framing effect” represents a striking violation of standard economic accounts of human rationality, although its underlying neurobiology is not understood. We found that the framing effect was specifically associated with amygdala activity, suggesting a key role for an emotional system in mediating decision biases. Moreover, across individuals, orbital and medial prefrontal cortex activity predicted a reduced susceptibility to the framing effect. This finding highlights the importance of incorporating emotional processes within models of human choice and suggests how the brain may modulate the effect of these biasing influences to approximate rationality.

A central tenet of rational decision-making is logical consistency across decisions, regardless of the manner in which available choices are presented. This assumption, known as “extensionality” (1) or “invariance” (2), is a fundamental axiom of game theory (3). However, the proposition that human decisions are “description-invariant” is challenged by a wealth of empirical data (4, 5). Kahneman and Tversky originally described this deviation from

rational decision-making, which they termed the “framing effect,” as a key aspect of prospect theory (6, 7).

Theories of decision-making have tended to emphasize the operation of analytic processes in guiding choice behavior. However, more intuitive or emotional responses can play a key role in human decision-making (8–10). Thus, when taking decisions under conditions when available information is incomplete or overly complex, subjects rely on a number of simplifying heuristics, or efficient rules of thumb, rather than extensive algorithmic processing (11). One suggestion is that the framing effect results from systematic biases in choice behavior arising from an affect heuristic under-

written by an emotional system (12, 13). However, despite the substantial role of the framing effect in influencing human decision-making, the underlying neurobiological basis is not understood.

We investigated the neurobiological basis of the framing effect by means of functional magnetic resonance imaging (fMRI) and a novel financial decision-making task. Participants (20 university students or graduates) received a message indicating the amount of money that they would initially receive in that trial (e.g., “You receive £50”). Subjects then had to choose between a “sure” option and a “gamble” option presented in the context of two different frames. The “sure” option was formulated as either the amount of money retained from the initial starting amount (e.g., keep £20 of the £50; “Gain” frame) or as the amount of money lost from the initial amount (e.g., lose £30 of the £50; “Loss” frame). The “gamble” option was identical in both frames and was represented as a pie chart depicting the probability of winning or losing (Fig. 1) (14).

The behavioral results indicated that subjects’ decisions were significantly affected by our framing manipulation, with a marked difference in choices between the two frames (Fig. 2A). Specifically, and in accordance with predictions arising from prospect theory, subjects were risk-averse in the Gain frame, tending to choose the sure option over the gamble option

Wellcome Department of Imaging Neuroscience, Institute of Neurology, University College London, 12 Queen Square, London WC1 3AR, UK.

*To whom correspondence should be addressed. E-mail: b.martino@fil.ion.ucl.ac.uk

[gambling on 42.9% of trials; significantly different from 50% ($P < 0.05$, $t_{19} = 1.96$)], and were risk-seeking in the Loss frame, preferring the gamble option [gambling on 61.6% of trials; significantly different from 50% ($P < 0.005$, $t_{19} = 3.31$)]. This effect of frame was consistently expressed across different probabilities and starting amounts (fig. S1).

Reaction times for decisions were not affected by frame [Gain frame, 1895 ms; Loss frame, 1884 ms ($P > 0.1$)]; this result provides evidence that difficulty was well matched between the two frames. Moreover, subjects performed highly accurately on “catch” trials (14) (fig. S2) where the expected outcomes of the sure and gamble options were unbalanced,

indicating their continued engagement with the task throughout the experiment. Despite the marked though variable impact of the frame on subjects’ choice behavior (Fig. 2B), the majority (16/20) of subjects seemed unaware of any biasing effect when specifically questioned in a debriefing session that followed the experiment.

Subjects performed the behavioral task inside an fMRI scanner, allowing us to obtain continuous measures of regional brain activity. The subjects’ individual decisions during the entire fMRI experiment were recorded and used to construct four regressors of interest: sure decisions in the Gain frame (G_{sure}), gamble decisions in the Gain frame (G_{gamble}), sure decisions in the Loss frame (L_{sure}), and gamble decisions in the Loss frame (L_{gamble}).

Given that the frame effect relates to subjects’ asymmetrical pattern of decisions across frames, the key experimental contrast of interest is the interaction between the decision to gamble (or not) and the valence of the frame: $[(G_{\text{sure}} + L_{\text{gamble}}) - (G_{\text{gamble}} + L_{\text{sure}})]$. It is noteworthy that this interaction contrast is balanced with respect to both decision type and frame valence. Consequently, we could identify brain areas that were more active when subjects chose in accordance with the frame effect (i.e., $G_{\text{sure}} + L_{\text{gamble}}$), as opposed to when their decisions ran counter to their general behavioral tendency ($G_{\text{gamble}} + L_{\text{sure}}$). This contrast revealed significant activation in the bilateral amygdala (Fig. 3, A and B). To ensure that this activation in the amygdala was not being driven by a significant effect in one frame alone (e.g., Loss frame), we conducted an independent analysis for each frame. This confirmed that robust activation in the amygdala was equally observed for simple effects of decision type (sure or gamble) in each frame separately. Thus, amygdala activation was

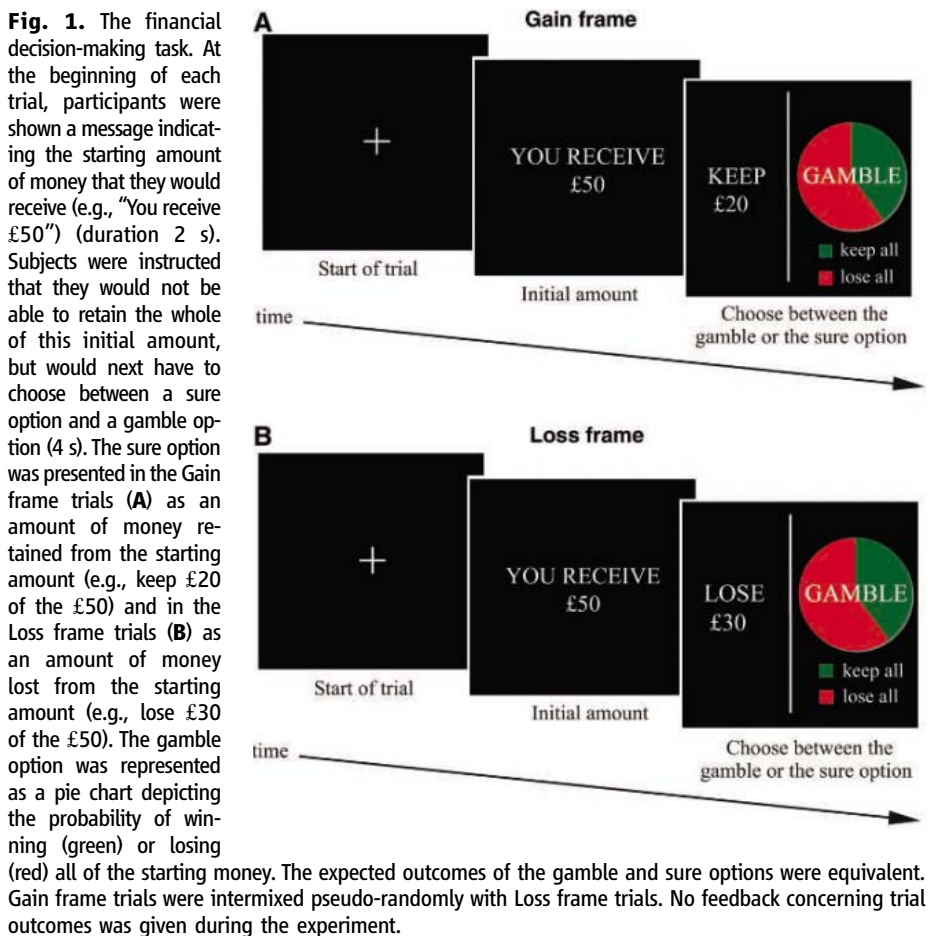
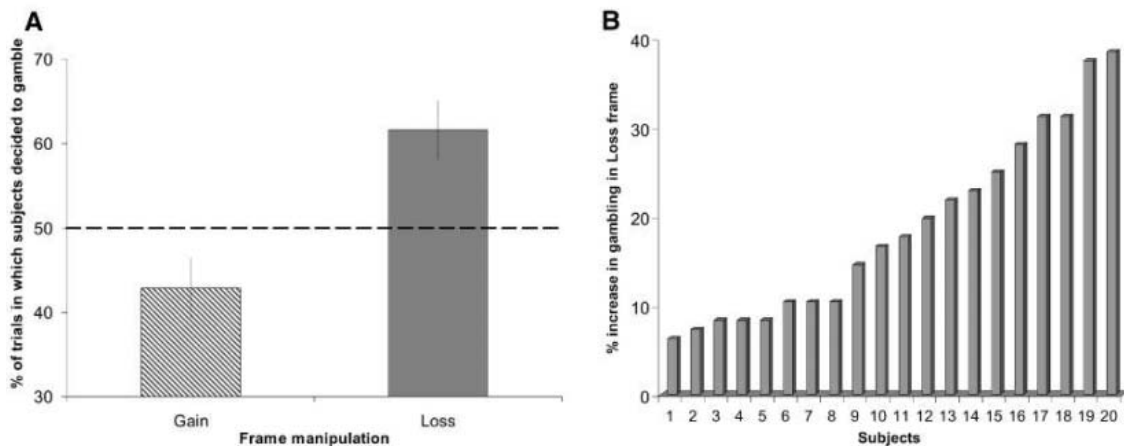


Fig. 2. Behavioral results.

(A) Percentages of trials in which subjects chose the gamble option in the Gain frame and the Loss frame. Subjects showed a significant increase in the percentage of trials in which the gamble option was chosen in the Loss frame with respect to the Gain frame [61.6% > 42.9% ($P < 0.001$, $t_{19} = 8.06$)]. The dashed line represents risk-neutral behavior (choosing the gamble option in 50% of trials). Error bars denote SEM. (B) Each bar represents, for each individual subject, the percentage difference between how often subjects chose the gamble option in the Loss frame as compared to the Gain frame. A hypothetical value of zero represents a complete indifference to the framing manipulation (i.e., fully “rational” behavior). All participants, to varying degrees, showed an effect of the framing manipulation.



significantly greater when subjects decided to choose the sure option in the Gain frame [$G_{\text{sure}} - G_{\text{gamble}}$] [Montreal Neurological Institute (MNI)

space coordinates (x, y, z) 18, -4, -24; Z score = 4.0], and the gamble option in the Loss frame [$L_{\text{gamble}} - L_{\text{sure}}$] [MNI space coordinates -16, 0,

-26; Z score = 3.80; 12, 2, -22; Z score = 4.67], in keeping with a central role in mediating the frame effect.

A different pattern of brain activation was identified when subjects made decisions that ran counter to their general behavioral tendency. In this reverse interaction contrast [$(G_{\text{gamble}} + L_{\text{sure}}) - (G_{\text{sure}} + L_{\text{gamble}})$], we observed enhanced activity in the anterior cingulate cortex (ACC) (Fig. 3, C and D) (and to a lesser extent in the bilateral dorsolateral prefrontal cortex at an uncorrected threshold of $P < 0.005$; fig. S3) when subjects chose the gamble option in the Gain frame and the sure option in the Loss frame.

In light of the substantial intersubject variability in behavioral susceptibility to the frame, we next identified subject-specific differences in neural activity associated with their decision bias (that is, the decision \times frame interaction) (Fig. 2A). Using the overall susceptibility of each subject to the frame manipulation as a between-subjects statistical regressor, operationalized as a “rationality index” (14), we found a significant correlation between decreased susceptibility to the framing effect and enhanced activity in the orbital and medial prefrontal cortex (OMPFC), specifically in the right orbitofrontal cortex (R-OFC; $r = 0.8$, $P < 0.001$) and the ventromedial prefrontal cortex (VMPFC; $r = 0.75$, $P < 0.001$) (Fig. 4). In summary, those subjects who acted more rationally exhibited greater activation in OMPFC associated with the frame effect.

Our data provide a neurobiological account of the framing effect, both within and across individuals. Increased activation in the amygdala was associated with subjects’ tendency to be risk-averse in the Gain frame and risk-seeking in the Loss frame, supporting the hypothesis that the framing effect is driven by an affect heuristic underwritten by an emotional system. The amygdala plays a key role in value-related prediction and learning, both for negative (aversive) and positive (appetitive) outcomes (15–17). Furthermore, in simple instrumental decision-making tasks in animals, the amygdala appears to mediate decision biases that come from value-related predictions (18). In humans, the amygdala is also implicated in the detection of emotionally relevant information present in contextual and social emotional cues (19). It was previously shown that activation in the amygdala during the passive viewing of surprised faces is significantly modulated by the valence of preceding verbal contextual information (20). Our data extend the role of the amygdala to include processing the type of contextual positive or negative emotional information communicated by the frame in the context of a decision-making task.

In our study, activation of the amygdala was driven by the combination of a subject’s decision and the frame in which it took place, rather than by the valence of the frame per se. Consequently, our findings indicate that frame-related

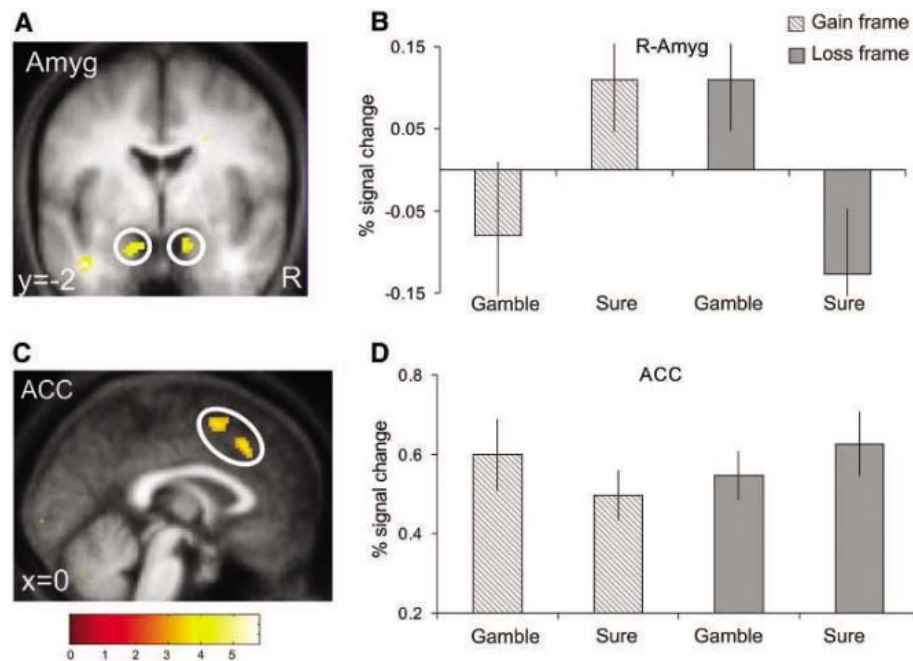
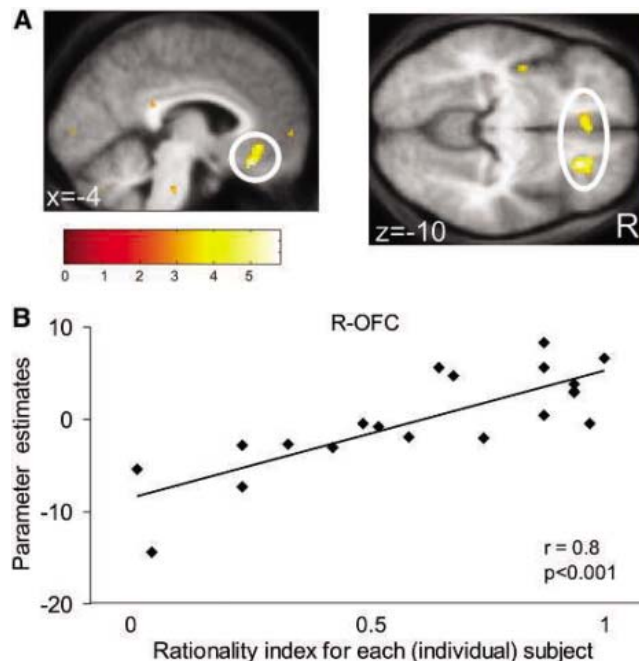


Fig. 3. fMRI results. (A) Interaction contrast [$(G_{\text{sure}} + L_{\text{gamble}}) - (G_{\text{gamble}} + L_{\text{sure}})$]: brain activations reflecting subjects’ behavioral tendency to choose the sure option in the Gain frame and the gamble option in the Loss frame (i.e., in accordance with the frame effect). Bilateral amygdala (Amyg) activation [MNI space coordinates (x, y, z)]: left hemisphere, -14, 2, -24 (peak Z score = 3.97); right hemisphere, 12, 2, -20 (Z score = 3.82). (C) Reverse interaction contrast [$(G_{\text{gamble}} + L_{\text{sure}}) - (G_{\text{sure}} + L_{\text{gamble}})$]: brain activations reflecting the decision to choose counter to subjects’ general behavioral tendency. Anterior cingulate cortex (ACC) activation: 2, 24, 44 (Z score = 3.65); -2, 8, 56 (Z score = 3.78). Effects in (A) and (C) were significant at $P < 0.001$; for display purposes they are shown at $P < 0.005$. (B and D) Plots of percentage signal change for peaks in right amygdala (12, 2, -20) (B) and ACC (2, 24, 44) (D). Error bars denote SEM.

Fig. 4. Rationality across subjects: fMRI correlational analysis. Regions showing a significant correlation between rationality index [between-subjects measure of susceptibility to the framing manipulation; see (14)] and the interaction contrast image [$(G_{\text{sure}} + L_{\text{gamble}}) - (G_{\text{gamble}} + L_{\text{sure}})$] are highlighted. (A) Orbital and medial prefrontal cortex (OMPFC) [MNI space coordinates (x, y, z)]: VMPFC (left panel), -4, 34, -8 (Z score = 4.56); OMPFC and R-OFC circled in right panel [R-OFC: 24, 30, -10 (Z score = 5.77)]. Effects were significant at $P < 0.001$; for display purposes they are shown at $P < 0.005$. (B) Plot of the correlation of parameter estimates for R-OFC with the rationality index for each subject ($r = 0.8$, $P < 0.001$).



valence information is incorporated into the relative assessment of options to exert control over the apparent risk sensitivity of individual decisions. The observation that the frame has such a pervasive impact on complex decision-making supports an emerging role for the amygdala in decision-making (21, 22).

When subjects' choices ran counter to their general behavioral tendency, there was enhanced activity in the ACC. This suggests an opponency between two neural systems, with ACC activation consistent with the detection of conflict between predominantly "analytic" response tendencies and a more "emotional" amygdala-based system (23, 24).

Previous descriptions of the frame effect have been predominantly confined to between-subjects investigations. Our experimental design allowed us to distinguish the anatomical bases of the frame effect, both within and between subjects. Interestingly, amygdala activity did not predict the substantial intersubject difference in terms of susceptibility to the frame effect. Instead, subjects' tendency to be susceptible to the frame showed a robust correlation with neural activity in the OMPFC. It is noteworthy that there are strong reciprocal connections between the amygdala and the OMPFC (25), although each may contribute to distinct functional roles in decision-making (26). Lesions of the OMPFC cause impairments in decision-making; these are often characterized as an inability to adapt behavioral strategies according to the consequences of decisions, leading to impulsivity (27, 28). It is thought that the OMPFC, incorporating inputs from the amygdala, represents the motivational value of stimuli (or choices), which allows it to integrate and evaluate the incentive value of predicted outcomes in order to guide future behavior (29, 30). Our data raise an intriguing possibility that more "rational" individuals have a better and more refined representation of their own emotional biases that enables them to modify their be-

havior in appropriate circumstances, as for example when such biases might lead to suboptimal decisions. As such, our findings support a model in which the OMPFC evaluates and integrates emotional and cognitive information, thus underpinning more "rational" (i.e., description-invariant) behavior.

Our findings suggest a model in which the framing bias reflects an affect heuristic by which individuals incorporate a potentially broad range of additional emotional information into the decision process. In evolutionary terms, this mechanism may confer a strong advantage, because such contextual cues may carry useful, if not critical, information. Neglecting such information may ignore the subtle social cues that communicate elements of (possibly unconscious) knowledge that allow optimal decisions to be made in a variety of environments. However, in modern society, which contains many symbolic artifacts and where optimal decision-making often requires skills of abstraction and decontextualization, such mechanisms may render human choices irrational (31).

References and Notes

1. K. J. Arrow, *Econ. Inq.* **20**, 1 (1982).
2. A. Tversky, D. Kahneman, *J. Bus.* **59**, S251 (1986).
3. J. von Neumann, O. Morgenstern, *Theory of Games and Economic Behavior* (Princeton Univ. Press, Princeton, NJ, 1944).
4. D. Kahneman, A. Tversky, *Choices, Values, and Frames* (Cambridge Univ. Press, New York, 2000).
5. B. J. McNeil, S. G. Pauker, H. C. Sox Jr., A. Tversky, *N. Engl. J. Med.* **306**, 1259 (1982).
6. D. Kahneman, A. Tversky, *Econometrica* **47**, 263 (1979).
7. A. Tversky, D. Kahneman, *Science* **211**, 453 (1981).
8. H. Damasio, T. Grabowski, R. Frank, A. M. Galaburda, A. R. Damasio, *Science* **264**, 1102 (1994).
9. J. Greene, J. Haidt, *Trends Cogn. Sci.* **6**, 517 (2002).
10. G. F. Loewenstein, E. U. Weber, C. K. Hsee, N. Welch, *Psychol. Bull.* **127**, 267 (2001).
11. T. Gilovich, D. W. Griffin, D. Kahneman, Eds., *Heuristics and Biases: The Psychology of Intuitive Judgment* (Cambridge Univ. Press, New York, 2002).
12. P. Slovic, M. Finucane, E. Perers, D. MacGregor, in *Heuristics and Biases: The Psychology of Intuitive Judgment*, T. Gilovich, D. W. Griffin, D. Kahneman, Eds. (Cambridge Univ. Press, New York, 2002), pp. 397–421.
13. X. Gabaix, D. Laibson, in *The Psychology of Economic Decisions, Vol. 1: Rationality and Well-Being*, I. Brocas, J. D. Carrillo, Eds. (Oxford Univ. Press, Oxford, 2003), pp. 169–183.
14. See supporting material on Science Online.
15. M. G. Baxter, E. A. Murray, *Nat. Rev. Neurosci.* **3**, 563 (2002).
16. J. E. LeDoux, *The Emotional Brain* (Simon & Schuster, New York, 1996).
17. J. J. Paton, M. A. Belova, S. E. Morrison, C. D. Salzman, *Nature* **439**, 865 (2006).
18. L. H. Corbit, B. W. Balleine, *J. Neurosci.* **25**, 962 (2005).
19. R. Adolphs, *Brain Res.* **1079**, 25 (2006).
20. H. Kim *et al.*, *J. Cogn. Neurosci.* **16**, 1730 (2004).
21. M. Hsu, M. Bhatt, R. Adolphs, D. Tranel, C. F. Camerer, *Science* **310**, 1680 (2005).
22. B. W. Balleine, S. Killcross, *Trends Neurosci.* **29**, 272 (2006).
23. M. M. Botvinick, T. S. Braver, D. M. Barch, C. S. Carter, J. D. Cohen, *Psychol. Rev.* **108**, 624 (2001).
24. E. K. Miller, J. D. Cohen, *Annu. Rev. Neurosci.* **24**, 167 (2001).
25. D. G. Amaral, J. L. Price, A. Pitkanen, S. T. Carmichael, in *The Amygdala: Neurobiological Aspects of Emotion, Memory, and Mental Dysfunction*, J. P. Aggleton, Ed. (Wiley-Liss, New York, 1992), pp. 1–66.
26. C. A. Winstanley, D. E. Theobald, R. N. Cardinal, T. W. Robbins, *J. Neurosci.* **24**, 4718 (2004).
27. A. Bechara, A. R. Damasio, H. Damasio, S. W. Anderson, *Cognition* **50**, 7 (1994).
28. E. T. Rolls, J. Hornak, D. Wade, J. McGrath, *J. Neurol. Neurosurg. Psychiatry* **57**, 1518 (1994).
29. G. Schoenbaum, B. Setlow, M. P. Saddoris, M. Gallagher, *Neuron* **39**, 855 (2003).
30. G. Schoenbaum, M. R. Roesch, T. A. Stalnaker, *Trends Neurosci.* **29**, 116 (2006).
31. K. Stanovich, F. West, in *Heuristics and Biases: The Psychology of Intuitive Judgment*, T. Gilovich, D. W. Griffin, D. Kahneman, Eds. (Cambridge Univ. Press, New York, 2002), pp. 421–440.
32. Supported by a Wellcome Trust Programme Grant (R.J.D.) and a Wellcome Trust studentship (B.D.M.). We thank H. Spiers, P. Sterzer, and J. Hughes for helpful discussions during the analysis of the study and P. Bossaerts for useful comments on the manuscript.

Supporting Online Material

www.sciencemag.org/cgi/content/full/313/5787/684/DC1

Materials and Methods

Figs. S1 to S3

Tables S1 to S3

References

5 April 2006; accepted 12 June 2006

10.1126/science.1128356

Q

Who's delivering science to every corner of the world?



Dr. Dinah Davidson



Steve Cook



Chris Bernau

AAAS

“ With only one issue of *Science* to go around our remote research camp in Brunei, we've worked out a plan as systematic as the ants we're studying. On the boat to and from town, in a treetop, or on the deck after dinner, we all get our chance to catch up on what's new in the world of science. ”

AAAS members Dr. Dinah Davidson, Steve Cook, and Chris Bernau, researchers at the Kuala Belalong Field Studies Center (run by the University of Brunei Darussalam)

AAAS is committed to advancing science and giving a voice to scientists around the world. We work to improve science education, promote a sound science policy, and support human rights.

Helping our members stay abreast of their field is a key priority for AAAS. One way we do this is through *Science*, which features all the latest breakthroughs and groundbreaking research, and keeps scientists connected wherever they happen to be. Members like Steve, Chris, and Dinah find it essential reading.

To join the international family of science, go to www.aaas.org/join.

To see other member photos, please visit:
<http://promo.aaas.org/membpics.shtml>



ADVANCING SCIENCE, SERVING SOCIETY

www.aaas.org/join

Does your next career step need direction?

*For a career in science,
I turn to Science*

*With thousands of job postings,
it's a lot easier to track down a
career that suits me*

*I got the offer I've been
dreaming of*

Now what?



*I have a great new research idea.
Where can I find more grant options?*

*I want a career,
not just a job*

*You know, ScienceCareers.org
is part of the non-profit AAAS*

*That means they're putting
something back into science*



There's only one place to go for career advice if you value the expertise of *Science* and the long experience of AAAS in supporting career advancement - ScienceCareers.org. The pages of *Science* and our website ScienceCareers.org offer:

- Thousands of job postings
- Career advice articles and tools
- Funding information
- Networking opportunities

www.sciencecareers.org

Science

MAGAZINE'S

STATE OF THE PLANET 2006-2007

DONALD KENNEDY
and the Editors of *Science*

AAAS



Science Magazine's **State of the Planet 2006-2007**

Donald Kennedy, Editor-in-Chief,
and the Editors of *Science*

The American Association for
the Advancement of Science

The most authoritative voice in American science, *Science* magazine, brings you current knowledge on the most pressing environmental challenges, from population growth to climate change to biodiversity loss.

COMPREHENSIVE • CLEAR • ACCESSIBLE



ISLANDPRESS

Science

AAAS

islandpress.org



Reagent Cooler

A new reagent cooler is a custom-fit companion for VistaLab 100mL reagent reservoirs. It maintains fluid temperatures at less the 5°C for up to 2 hours. Manufactured with non-toxic gel encased in heavy-duty PVC (polyvinyl chloride), these bright blue coolers chill or freeze quickly, are reusable, and provide full and consistent reservoir cooling without the contamination risks or inconvenience of ice baths. VistaLab reagent reservoirs have been redesigned with trimmed base corners and deeper pour-off spouts for spill-free emptying, and feature a unique deep-well design that maximizes reagent recovery with minimal waste.

VistaLab For information 302-832-8266 www.vistalab.com

Chromatography Systems

Cell separation and protein purification sequences in the laboratory are critical components of process development for new therapies. They require multiple steps that are often labor-intensive and time-consuming. A new benchtop system automates the process, significantly improving laboratory efficiency and cutting down drug development by weeks or even months. The new PKL Chromatography System enables operations on a 24-hour continuous basis. This flexible tool performs process optimization for new drugs used in clinical trials and small-scale production. It also provides a roadmap for easy drug production scale-up.

Pall Corp For information 212-529-4500
www.pall.com

Avian Flu Detection

The Avian Flu Detection Sampler Set contains four polyclonal antibodies against hemagglutination and neuraminidase from a Southeast Asian strain of H5N1 influenza isolated in 2004. These antibodies can be used for the detection of the H5N1 hemagglutinin and neuraminidase proteins in bodily fluid, tissue, or cultured cell lines. They have been designed to have minimal cross-reactivity to other influenza strains. Immunogenic peptides are included as positive controls and to determine protein concentration.

ProSci Inc For information 888-513-9525
www.ProSci-inc.com

Signal Transduction Protein Array

The Panorama Human Signal Transduction Protein Array contains 259 full-length proteins that are involved in key cellular processes, including proliferation, differentiation, and apoptosis. This array makes use of a unique fusion tag that has been shown to confer protein functionality and that also serves to select, tether, and uniformly

orient proteins on a streptavidin-coated glass slide. This technology offers the unique advantage of allowing proteins to behave in a sterically unencumbered manner, thereby increasing the potential for acquiring data that is more closely representative of native physiological states. Signal transduction describes cellular response to external or internal stimuli and often results in fundamental cellular changes such as regulating gene expression or controlling cell proliferation.

Sigma-Aldrich For information
+44 (0) 1260 296505 www.sigma-aldrich.com

Conical Filter Units

Nalgene 50 mL Conical Filter Units, featuring Pall Supor machV polyethersulfone (PES) membranes, provide rapid vacuum filtration of biological sample volumes ranging from 20 mL to 50 mL. The filter is attached to a 50-mL centrifuge tube for faster, easier preparation of tissue and cell samples with reduced risk of contamination or spills. The Supor machV PES membrane, with a 0.2- μ m pore size, has been shown to accelerate flow rates up to 50 percent, while exhibiting low protein binding of cell culture media and other solutions. These filters can be used for even the most difficult-to-filter fluids, such as serum.

Nalge Nunc International For information
800-625-4327 www.nalgenunc.com

Mixer

The MixMate is for mixing and vortexing of aqueous solutions and suspensions in various micro test tubes and plates. It has five preset programs for the optimized mixing of 0.2-ml polymerase chain reaction (PCR) tubes to 2.0-ml micro test tubes; 96-well and 384-well PCR plates; and shallow and deep-well plates at a maximum mixing frequency of up to 3000 rpm. MixMate is suitable for controlled mixing of enzymatic reactions; controlled incubation of absorption; blocking or

reaction preparations; resuspension of DNA, RNA, protein, or cell pellets in tubes and plates; and vortexing in micro test tubes.

Eppendorf For information 800-645-3050
www.eppendorfna.com

Reporter-Tagged Genes

A variety of mouse and human genes that express reporter-tagged proteins are available for studies in cultured cells and transgenic animals. Unlike complementary DNAs, these clones carry complete native gene sequences, including sequence elements required for natural regulation of gene expression and alternative splicing. Reporters include epitope-tags, green fluorescent proteins, and luciferase.

SpectraGenetics For information 412-488-9350
www.spectragenetics.com

For more information visit **Product-Info**, **Science's new online product index** at <http://science.labvelocity.com>

From the pages of Product-Info, you can:

- Quickly find and request free information on products and services found in the pages of *Science*.
- Ask vendors to contact you with more information.
- Link directly to vendors' Web sites.

Newly offered instrumentation, apparatus, and laboratory materials of interest to researchers in all disciplines in academic, industrial, and government organizations are featured in this space. Emphasis is given to purpose, chief characteristics, and availability of products and materials. Endorsement by *Science* or AAAS of any products or materials mentioned is not implied. Additional information may be obtained from the manufacturer or supplier by visiting www.science.labvelocity.com on the Web, where you can request that the information be sent to you by e-mail, fax, mail, or telephone.

Classified Advertising



Get the Experts Behind You.

For full advertising details, go to www.sciencecareers.org and click on For Advertisers, or call one of our representatives.

United States & Canada

E-mail: advertise@sciencecareers.org
 Fax: 202-289-6742

JILL DOWNING

(CT, DE, DC, FL, GA, MD, ME, MA, NH, NJ, NY, NC, PA, RI, SC, VT, VA)
 Phone: 631-580-2445

KRISTINE VON ZEDLITZ

(AK, AZ, CA, CO, HI, ID, IA, KS, MT, NE, NV, NM, ND, OR, SD, TX, UT, WA, WY)
 Phone: 415-956-2531

KATHLEEN CLARK

Employment: AR, IL, LA, MN, MO, OK, WI
 Canada; Graduate Programs; Meetings & Announcements (U.S., Canada, Caribbean, Central and South America)
 Phone: 510-271-8349

DARYL ANDERSON

(AL, IN, KY, MI, MS, OH, TN, WV)
 Phone: 202-326-6543

GABRIELLE BOGUSLAWSKI

(U.S. Recruitment Advertising Sales Director)
 Phone: 718-491-1607

Europe & International

E-mail: ads@science-int.co.uk
 Fax: +44 (0) 1223-326-532

TRACY HOLMES

Phone: +44 (0) 1223-326-525

HELEN MORONEY

Phone: +44 (0) 1223-326-528

CHRISTINA HARRISON

Phone: +44 (0) 1223-326-510

SVITLANA BARNES

Phone: +44 (0) 1223-326-527

JASON HANNAFORD

Phone: +81 (0) 52-789-1860

To subscribe to Science:

In U.S./Canada call 202-326-6417 or 1-800-731-4939
 In the rest of the world call +44 (0) 1223-326-515

Science makes every effort to screen its ads for offensive and/or discriminatory language in accordance with U.S. and non-U.S. law. Since we are an international journal, you may see ads from non-U.S. countries that request applications from specific demographic groups. Since U.S. law does not apply to other countries we try to accommodate recruiting practices of other countries. However, we encourage our readers to alert us to any ads that they feel are discriminatory or offensive.



POSITIONS OPEN



TEXAS A&M
HEALTH SCIENCE CENTER
 COLLEGE OF MEDICINE

FACULTY POSITIONS

The Department of Molecular and Cellular Medicine (MCM) in the College of Medicine invites applications from individuals with Ph.D., M.D., or equivalent degrees for several tenure-track faculty positions at the ASSISTANT, ASSOCIATE, or FULL PROFESSOR rank. The Department is principally located on the Texas A&M campus in College Station. Research in the Department spans a wide range of biological processes, from the structure and function of biomolecules to cell physiology (see web page for more information). Senior applicants should have a vigorous extramurally funded research program and junior applicants will need to develop a research program that is highly competitive for extramural funding. The successful candidates will also be expected to participate in both medical and graduate student instruction and training. Applicants for junior positions should submit their curriculum vitae and descriptions of research and teaching philosophy and have three letters of references e-mailed or sent to: **Junior Faculty Search, Molecular and Cellular Medicine, 1114 Texas A&M University, College Station, TX 77843-1114**. Applicants for the senior position are invited to send their information to **Senior Faculty Search** at the same address. Electronic applications are encouraged. Review of applicants will begin immediately and interviews will be scheduled starting in November 2006.

E-mail: mcm@medicine.tamhsc.edu. Website: http://medicine.tamhsc.edu/basic_sciences/MCM.

The Texas A&M Health Science Center is an Affirmative Action/Equal Opportunity Employer.

SAN DIEGO, CALIFORNIA, NEUROPATHOLOGIST AT THE UNIVERSITY OF CALIFORNIA, SAN DIEGO (UCSD). The Department of Pathology (website: <http://medicine.ucsd.edu/pathology>) seeks a Neuropathologist for an appointment at the rank of Assistant (tenure-track) or Associate/Full Professor (tenured), as appropriate. We seek an outstanding person with the drive to develop an independent research program in oncology or developmental neuropathology, while sharing clinical and teaching responsibilities. Clinical duties will involve both UCSD teaching hospitals, Hillcrest and Thornton, with responsibility for neuropathologic autopsies and review of biopsies from brain, muscle, and nerve. The Division of Neuropathology has a fully accredited residency training program in Neuropathology for which the successful candidate will share responsibility. Salary will be consistent with established UCSD pay scales. Applicants must be Board-certified in anatomic and neuropathology, and have, or be eligible for, a California medical license. Review of applications will begin September 22, 2006, and will continue until the position is filled. Interested applicants should submit a letter of interest, curriculum vitae, and names/addresses of at least three references to: **Henry C. Powell, M.D., D.Sc., FRCPath, Search Committee Chair, c/o Ms. Catherine Schumacher, Search Coordinator, Department of Pathology 0717, University of California San Diego School of Medicine, 9500 Gilman Drive, La Jolla, CA 92093-0717**. Applications by e-mail are acceptable to e-mail: cdschumacher@ucsd.edu. UCSD is an Affirmative Action/Equal Opportunity Employer with a strong institutional commitment to excellence through diversity.

FACULTY POSITIONS OF ASSISTANT PROFESSOR AND ABOVE
 National Central University

The Department of Life Sciences at the National Central University is seeking candidates for several Tenure-Track Faculty positions. The duty of these positions will include research and teaching in selected postgraduate as well as undergraduate subjects. Persons with an outstanding record of academic and scholarly accomplishment in life sciences are encouraged to apply. For further information, please visit our website at website: <http://www.ncu.edu.tw/~ls>.

POSITIONS OPEN

FACULTY POSITIONS IN PHARMACEUTICAL SCIENCES
 School of Pharmacy
 University of Missouri, Kansas City

The Division of Pharmaceutical Sciences in the School of Pharmacy at the University of Missouri, Kansas City (UMKC) invites applications for multiple 12-month tenure-track positions at the ASSISTANT/ASSOCIATE PROFESSOR level. At least one position will be in the area of pharmaceuticals and one in the area of medicinal chemistry, both broadly defined. Research resources include state-of-the-art instrumentation such as an ABI Q-Trap liquid chromatography/mass spectrometry, a Finnegan Ion Trap nano-LCMS, a Nikon confocal microscope, and real time PCR as well as cell culture and comprehensive manufacturing laboratories. Current strengths within the Division are drug delivery, formulation development, bioorganic chemistry, functional genomics, and chemical biology. The selected candidates will be provided competitive salaries and startup support, and will be expected to develop extramurally funded research programs. Participation in undergraduate, professional, and graduate courses is expected.

UMKC is a comprehensive research university exemplifying the values of education first, innovation, accountability, diversity, and collaboration. More information about UMKC is at website: <http://www.umkc.edu/strategicplan>, or go to website: <http://www.umkc.edu/pharmacy>.

Please submit curriculum vitae and a statement of research interests, and arrange for three letters of recommendation to be sent to:

Professor Ashim K. Mitra, Chair
 Division of Pharmaceutical Sciences
 School of Pharmacy
 University of Missouri, Kansas City
 5100 Rockhill Road
 Kansas City, MO 64110-2499

Review of applications will begin August 1, 2006, and will continue until the positions are filled.

UMKC is an Affirmative Action/Equal Opportunity Institution.

DIRECTOR OF VISION RESEARCH CENTER
 at University of South Carolina

The Department of Ophthalmology, University of South Carolina (USC) School of Medicine is accepting applications for an **ENDOWED CHAIR** and the position of Director of the Vision Research Center at USC. This full-time basic science faculty candidate must be knowledgeable in all areas of vision research with emphasis on cell and molecular biology, wound healing, and gene modulation and expression. An interest in biomedical engineering applications is desirable. As Director, the successful candidate will conduct his/her own funded research as well as support the development of other researchers, and coordinate research activity and productivity leading to new funding opportunities such as program project grants, and tech-transfer opportunities. The successful candidate will have a joint appointment in an appropriate basic science department and will receive a substantial setup package. Support will also be available for seed programs for pilot projects. USC School of Medicine is able to provide well-equipped laboratory space and access to many core facilities.

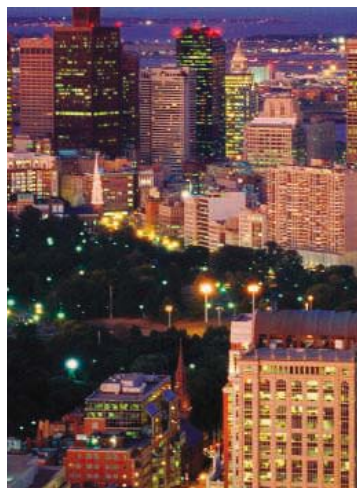
Requirements: Ph.D. in biological science, chemistry, or engineering with experience in eye research and current NIH funding.

Contact: **Dr. Richard M. Davis, M.D.** Telephone: 803-434-7062.

UNDERGRADUATE TENURE-TRACK FACULTY POSITIONS
 Genetics and Molecular Biology
 or Ecology and Biodiversity

Samford University, Birmingham, Alabama

For complete job descriptions, see website: <http://www.samford.edu/biology>. Review begins October 15, 2006. Equal Opportunity Institution.



FOCUS ON CAREERS

New England Region of Renowned Research

For scientists who can cope with the region's weather, New England offers a remarkable density of top research institutions, a comfortable lifestyle, and myriad opportunities to perform high quality work. BY PETER GWYNNE

It's no coincidence that researchers know the Boston-Cambridge area as "Genetown." Its combination of research universities, research institutions, biotechnology firms, and pharmaceutical companies' research arms makes it a prime destination for top-notch life scientists. But other locations in New England, from the Boston suburbs to clusters in the region's other five states, have developed their own centers for academic and industrial life science.

The region in the country's extreme Northeast boasts a long history, a variety of attractive scenery from coast to mountains, an abiding love of the Boston Red Sox baseball team, and – even outside Genetown – a concentrated wealth of top-flight academic, commercial, and nonprofit research institutions. As a result, the location has established itself as a key hub of American science in general and life science in particular. "I would say the two most sought-after locations in academic science are California and New England," says Robert Alpern, dean of the Yale University School of Medicine.

New England doesn't suit everyone. Its weather can be cold, and so can its people. But many local employers agree with the comment of Jill Rapp, human resources manager at Amgen's Massachusetts site: "It is a very positive environment for recruitment." Here we discuss New England's attractions and occasional disadvantages with representatives of two companies – one in Cambridge and the other in a suburb of Boston – and of two long-established institutions farther from the region's cultural, commercial, and academic center.



ROBERT ALPERN

Geographic Advantage

New England's greatest advantage stems from geography: Within a relatively small area it contains a huge number of major research organizations. "We have some of the best hospitals and academic institutions, which allows for a nice level of integration and the ability to attract talent as interns," says Andrew Suchoff, vice president of human resources at Serono, Inc., in Rockland, about half an hour south of Boston. "I've been building an institute for oncology," adds his colleague Steve Arkinstall, head of research at the Serono Research Institute. "We've found that the area produces scientists with expertise in protein engineering, chemistry, and antibody technologies, and an understanding of drug discovery. We

research collaborations," he says. "Twenty percent of oncology clinical trials take place in the Boston area. We also have the MIT and Harvard cancer research centers. I would say it's as good as any other area in the world for enabling you to access the best expertise."

The geographic benefit applies to much of New England. "The advantage is clearly the density of academic institutions," says Alpern of Yale, which is based in New Haven, Connecticut. "We also have a number of big pharmaceutical companies with large organizations in Connecticut. And being located between Boston and New York City is important. We're in a very rich academic environment; one can travel between institutions without having to get on an airplane."

Even the Woods Hole Oceanographic Institution, based in the picturesque Cape Cod village of Woods Hole, exists in the **CONTINUED** »

Amgen

<http://www.amgen.com>

Serono Research Institute

<http://www.serono.com>

Woods Hole Oceanographic Institution

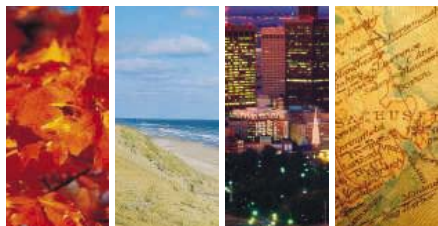
<http://www.whoi.edu>

Yale University School of Medicine

<http://www.yale.edu>

have a ready source of really excellent people on our doorstep."

The concentration offers more than well-trained recruits. "There is amazing brain power in this area, with all the local universities and research organizations, which provides the opportunity for continued collaborations," Amgen's Rapp says. Arkinstall agrees. "This area has been incredibly useful in facilitating



FOCUS ON CAREERS

New England

midst of a scientific hub that includes the Marine Biological Laboratory and the National Oceanic and Atmospheric Administration's Northeast Fisheries Science Center. "Our small town has five other institutions to offer our scientists a shared experience," says Jim Yoder, the oceanographic institution's vice president for academic programs and dean.



STEVE ARKINSTALL

Positives and Negatives

Lifestyle also plays a role in attracting scientists to New England. "New England offers great historical locations, numerous cultural opportunities, excellent school systems, a good public transportation system, and plenty to do for both families and young professionals," Amgen's Rapp explains. "People enjoy living in New England," Yoder adds.

"It's a beautiful part of the country and there are lots of activities." Alpern expands on that point. "Living in New England is really nice because you can get to New York City or Boston in less than two hours and can purchase a few acres of land at a reasonable cost," he says.

However, the price of housing works as a disadvantage in some parts of the region, and particularly close to Boston. "The cost of living is a concern for many who chose to come to Boston from lower-cost-of-living areas," says Amgen's Rapp. "We have made some improvements in our relocation package to deal with those challenges."

Recruiters who want to persuade scientists to move to New England from points south and west also face a meteorological challenge. "The major disadvantage is the winter; it's too cold and it lasts so long," Alpern says. "The weather is an issue," Yoder echoes. "People who have been on the West Coast tend to stay there."

Alpern points to one other difficulty for organizations outside the Boston-Cambridge area. "The major disadvantage in our area compared to Boston is finding jobs for spouses, especially if the spouse is an academic," he points out. "If they can't get a job at Yale, there's not much for them. But if they're not academics, they have the opportunity to find a job with numerous companies."



JILL RAPP

Breadth of Opportunities

Regional institutions certainly offer plenty of opportunities to scientists. Amgen, for example, announced in March its intention to expand the work force at its Cambridge location. "We currently have 175 employees, up from about 90 a year ago," Rapp reports. "We're growing rapidly. Our newest additions include groups in pathology and a focus on several therapeutic areas, including hematology/oncology, neuroscience, and metabolic disorders. We plan to be close to 200 employ-



ANDREW SUCHHOFF

ees by the end of this year and to grow to around 400 in the longer term. This will include expansion in our new groups along with our previously existing functions – chemistry, pharmacokinetics and drug metabolism, and pharmaceuticals. There will also be growth in some of our operational functions to support the research growth."

Serono, which has had a presence on the south shore of Massachusetts for two decades, currently has about 450 employees in its Rockland laboratories, which opened in 2002. "We've been hiring scientists with expertise in cancer for about 18 months," Arkinstall says. "We're looking for a mixture of people." The company emphasizes collegiality among the several aspects of the pharmaceutical field. "Often, drug discovery scientists are divorced from other things going on in the company. That's not the case here," Arkinstall says. "Our facility is all inclusive, with the research institution, clinical trials groups, and a commercial organization that supports the business," Suchhoff says. Serono also gives its scientists the chance to move beyond the laboratory. "There are opportunities for people to take on managerial roles and get a diversity of experience," Suchhoff adds.

For academics, who need to impress students as well as faculty members with the virtues of New England, seeking scientists is a non-stop task. "We're always recruiting," says the Woods Hole Oceanographic Institution's Yoder. "With retirements and departures, we lose about 10 scientists every year." The institution recruits worldwide, but finds many of its new faculty already on the premises. "One of our best recruiting tools is our postdoctoral program; we have about 60 postdocs in residence," Yoder says. That program contains many of the best and the brightest. "Our postdoctoral scholars program is very competitive," Yoder continues. "We choose about 10 out of more than 100 applicants each year. They are often chosen later as faculty because they have been through the pressure."



JIM YODER

High Standards

The Yale School of Medicine has equally high standards. "Most of our departments are recruiting faculty almost every year," Alpern says. "They aim very high, recruiting for the top two or three scientists in their discipline each year."

What attracts top scientists to the region? The critical mass of colleagues plainly plays a key role in the Boston-Cambridge area and beyond. "The name Yale definitely helps, but I don't think it would replace 'what have you done for me lately?'" Alpern explains. "The major factor that recruits look for is the other scientists already here. We also invest a lot of money in core resources that support the sciences. Scientists understand the importance of having those facilities available."

Visit www.sciencecareers.org and plan to attend upcoming meetings and job fairs that will help further your career.

A former science editor of Newsweek, Peter Gwynne (pgwynne767@aol.com) covers science and technology from his base on Cape Cod, Massachusetts, U.S.A.

OPEN TO

EXPLORE

Each individual brings new possibilities for innovation. We invite you to join our mission of lifesaving drug discovery.

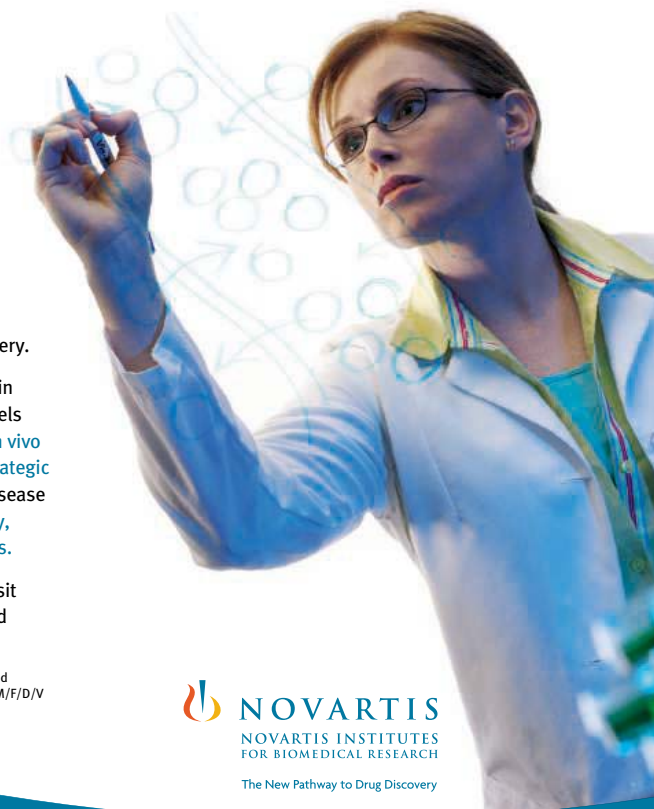
At the Novartis Institutes' cutting-edge research facilities in Cambridge, MA, we now have multiple openings at all levels (BS/MS/PhD) in areas such as **chemistry, biochemistry, in vivo pharmacology, cellular/molecular biology, epigenetics, strategic alliances, communications, and IT**, and in the following disease areas: **cardiovascular, diabetes & metabolism, oncology, ophthalmology, infectious diseases, and muscle disorders.**

To view descriptions of all open positions and to apply, visit www.nibr.novartis.com and follow the links to Careers and Job Opportunities.

Novartis is committed to embracing and leveraging diverse backgrounds, cultures, and talents to achieve competitive advantage. Novartis is an equal opportunity employer. M/F/D/V



www.nibr.novartis.com
©2006 Novartis AG



UNIVERSITY OF MASSACHUSETTS LOWELL

**Postdoctoral Fellow in Biology
Job Reference # AP09020601**

The University of Massachusetts has an immediate opening for a Postdoctoral Fellow to conduct research in the field of mammalian limb regeneration and wound healing. Expertise in either electrochemistry and applied electrical potentials or protein microarray, cytokines and molecular biology techniques desired. Applicant must have a Ph.D. or equivalent and a strong background in biochemistry or cell biology. Position includes competitive salary, fringe benefits, and the opportunity to work in a dynamic research environment in the Boston Area.

Apply to :

**Dr. Susan Brauhn, Department of Biological Sciences
C/O Human Resources
University of Massachusetts Lowell
883 Broadway Street, Room 101
Lowell, MA 01854**

or submit cover letter and resume via e-mail to:
jobs@uml.edu

Please indicate job reference number AP09020601 in subject line of e-mail.



The University of Massachusetts Lowell is an Equal Opportunity/Affirmative Action, Title IX, H/V, and ADA 1990 Employer.



Scientific Curators

Professional positions are available as Scientific Curators with the Mouse Genome Informatics Program at The Jackson Laboratory, working with the Mouse Genome Database, Mouse Tumor Biology Database, and MusCyc Database. Successful candidates will primarily be responsible for data acquisition and analysis, evaluating and annotating data to be incorporated into the databases, integrating information from disparate sources, and interacting with research laboratories and genome centers to facilitate data transfer. In addition, Curators take part in database and interface design by contributing biological perspectives to new data content and displays. Areas of preferred expertise are 1) mammalian genetics, phenotype analysis, development; 2) gene annotation and analysis of gene sets based on biological data; 3) tumor biology, cancer genetics, mouse models, 4) metabolic pathways, functional gene/protein annotation, biochemistry. Other desirable attributes include excellent writing/communication skills and the ability to work effectively in a team environment. Ph.D. degree in Life Sciences or M.S. with extensive experience required.

The Jackson Laboratory is one of the world's foremost centers for mammalian genetics research. Located in Bar Harbor, ME, the lab is adjacent to Acadia National Park. Mountains, ocean, forests, lakes, and trails are all within walking distance. If you love high-tech challenges but you're looking for a more natural environment, this could be the opportunity you've been searching for.

Interested applicants should apply online, checking off job requisition #SC-05. Please submit cover letter and resume as one document.

The Jackson Laboratory is an Equal Opportunity/Affirmative Action Employer.

www.jax.org

University of Nebraska-Lincoln and Iowa State University

Cooperative Program in Veterinary Medical Education

The University of Nebraska-Lincoln (UNL), through the Institute of Agriculture and Natural Resources and its College of Agricultural Sciences and Natural Resources, seeks applications to fill six full-time, tenure-track professorial positions for an innovative Cooperative Program in Veterinary Medical Education between UNL and the Iowa State University, College of Veterinary Medicine (ISU CVM). The first two years of the veterinary medical curriculum will be offered to Nebraska resident students on the UNL campus. These students will then transfer to the ISU CVM where they will complete the remaining two years of the curriculum. The program will offer successful candidates a unique opportunity to participate in building an innovative system for veterinary medical education. Five of the six positions will be located at UNL. The Veterinary Epidemiologist will be located at the Great Plains Veterinary Educational Center near Clay Center, NE.

UNL and ISU are recognized as outstanding Association of American Universities Land Grant Institutions, and both are located in states where livestock populations are some of the largest in the world.

Through this partnership, UNL and ISU CVM will build on historic strengths, leverage resources, anticipate opportunities and future directions, and build bridges with veterinarians, the livestock industries, and companion animal owners in new and unique ways. This program will facilitate collaboration between teaching, research and extension faculties at the two institutions and will combine expertise to address regional, national and global issues important to our stakeholders and to veterinary medicine.

Outstanding candidates are sought for the following positions:

- Veterinary Gross Anatomist (Req. #060564)
- Veterinary Epidemiologist (Req. #060562)
- Neurobiologist (Req. #060557)
- Veterinary Pathologist (Req. #060560)
- Immunologist (Req. #060559)
- Veterinary Surgery and Anesthesiology (Req. #060561)

The successful candidates will be considered at the ranks of Assistant, Associate or Full Professor. Salary and rank will be commensurate with accomplishments and experience. Successful candidates will join 26 faculty members, including board-certified and board-eligible specialists, in the UNL Department of Veterinary and Biomedical Sciences. Successful candidates will also have opportunities to collaborate with accomplished faculty members throughout the University of Nebraska System and Iowa State University.

To view the complete job details and make application for a position, go to the web site at: <http://employment.unl.edu>. Click on "Search Job Openings." Enter the requisition number, view the job details and make application according to the instructions. Complete the faculty academic administrative information form and attach a letter of application, curriculum vitae, and contact information for 3 professional references for each position.

Review of applications will begin on **September 15, 2006**, and continue until the positions are filled or the search is closed.

The University of Nebraska is committed to a pluralistic campus community through Affirmative Action and Equal Opportunity and is responsive to the needs of dual career couples. We assure reasonable accommodation under the Americans with Disabilities Act. Contact Mrs. Pat Martinez at 402-472-8539 (e-mail: pmartinez1@unl.edu) for assistance.

VERTEX

Small Molecules. Huge Discoveries.

Vertex Pharmaceuticals Incorporated is a global biotechnology company focused on the discovery, development and commercialization of breakthrough drugs for a range of serious diseases. Our business strategy is to commercialize major new drugs both independently and in collaboration with other pharmaceutical companies. We currently have the following opportunities available:

Protein Biochemistry

Become a part of our cutting-edge exploration into the biochemistry of membrane proteins.

Research Scientist I, 4050-01B
Research Scientist II, 4050-02B

Cellular and Molecular Biology

Cell & Molecular Biology is looking for a Research Scientist I, targeted to support the implementation of cellular assay systems for drug discovery efforts in neuroinflammation and axonal degeneration associated with Multiple Sclerosis.

Research Scientist I, 4120-03B

Biomarker Research and Translational Pharmacology

Biomarker Research and Translational Pharmacology is looking for an energetic and interactive individual to operate a core FACSARIA.

Sr. Research Associate, 4200-01B

We provide a highly stimulating working environment coupled with a high level of professional and intellectual challenge. In addition to competitive salary and benefits, we also offer equity participation and participation in a stock purchase program. No agencies, please. Apply online at: www.vrtx.com.
EOE



We Enjoy a Big Lead in Small Molecules.



NATIONAL ECOLOGICAL OBSERVATORY NETWORK

Project Manager

The National Ecological Observatory Network office (NEON: www.neoninc.org), managed by the nonprofit NEON Corporation (NEON Inc.), has an immediate opening for a full-time Project Manager (PM) to manage the construction phase of the NEON facility from its offices in Washington DC. Funded as a Major Research Equipment and Facilities Center project of the National Science Foundation (NSF), NEON is a continental scale research instrument consisting of geographically distributed and networked infrastructure, including lab and field instrumentation, site-based experimental infrastructure, biodiversity archive facilities and/or computational, analytical and modeling capabilities.

Job Description: The Project Manager reports to the NEON Inc. CEO. The CEO is the Principal Investigator (PI) for the NSF funding. Together, the PM and PI are accountable to NSF and to the NEON Inc. Board of Directors for their project's performance and fiduciary and compliance responsibilities.

The PM will be involved in all phases of planning, organizing, conducting, and documenting project management of NEON in development and construction, and annual or periodic validation review for its operation. The PM exercises primary responsibility for the business aspects of construction, maintenance and operation of the NEON facility, including planning coordination; serving as the interface with the relevant communities; preparing documentation for program review and approval; preparing funding requests for operations, maintenance and related programmatic activities; and overseeing the project. The PM works closely with a variety of NEON scientists, engineers, technologists, and contractors as well as NEON's business office staff.

The PM is responsible for leading the NEON project team to develop the Preliminary and Final Design plans. Additionally, the PM, subject to favorable construction funding commitments, will be responsible for executing the NEON (MREFC) Project Construction scope within budget and on schedule. During the Readiness Stage, the PM's responsibilities include:

- Managing the overall budget and schedule according to the project reporting and financial guidelines required by NSF. Allocating resources amongst the project tasks and authorizing financial commitments and payments within established limits, and presenting and recommending, as appropriate, commitments and payments beyond these limits to the Board of Directors and NSF when costs exceed established thresholds.
- Coordinating, communicating, and negotiating with the NSF BIO Directorate and the NSF Large Facilities Office in a cooperative teaming arrangement.
- Developing the NEON PMO and project management team by identifying the necessary staff, office resources, infrastructure requirements and other services needed to fully prepare NEON Inc. to: (1) receive NSF awards; (2) complete the requisite deliverables; and (3) demonstrate the ability to execute the NEON Project construction within scope, cost and schedule.
- Formulating a detailed plan to complete the final NEON Project Execution Plan (PEP).
- Establishing both schedule and budget reserves for the Project Development Plan (PDP), and recommending to the Board of Directors the appropriate level of contingency allocation throughout the lifetime of the Readiness Stage.
- Ensuring that the PDP and technical approaches adopted and implemented in the Preliminary Design / Readiness Stage are consistent with the NEON Science Requirements, and identifying to the Board of Directors where implementation of these requirements may conflict with the allocated project resources. The PM has the responsibility for decisions affecting capability, schedule, cost, and risk and for providing the rationale to the Board of Directors for approval of such decisions.
- Preparing a comprehensive cost and schedule baseline plan, including the necessary software tools, configuration and change control processes and procedures, skilled Earned Value Management personnel, and training of the technical management to support the implementation and construction of the NEON Project.
- Preparing and organizing formal management and technical reviews of the Preliminary Design and major milestones, ensuring compliance with the Science Requirements, schedule, and budget.
- Working with the NEON participating collaborators and partner institutions to ensure effective oversight and management of work tasks undertaken by the partners.

Skills, Experience and Qualifications: The successful NEON Project Manager candidate will possess the following qualifications:

- Significant knowledge and experience with large project management and oversight. Specific familiarity with the following topics: Budget and budget contingency estimation and methodology, Project Management Plans, Project Management Control Systems, Earned Value Management Reporting, Development of a project's critical path, Risk management, Development and management of a project baseline.
- Strong leadership skills, decision-making abilities, effective communicator, and effective motivator. Extensive management knowledge gained in a research and / or education-related setting and the ability to provide sound advice and policy recommendations. Extensive skill planning, organizing, and directing teams conducting reviews, developing and negotiating implementation of recommendations for changes and improvements with NSF and awardee management.
- Hold a MS or PhD in a field of science (preferably related to the ecology, biology, chemistry or other earth sciences) or engineering. Other MS or PhD degrees will be considered.
- Willingness to perform extensive travel. Occasionally, work may be required in remote sites, on-board research vessels, or in areas that will expose the incumbent to all kinds of occupational (e.g., construction sites) and environmental (e.g., extreme hot or cold, high altitudes) conditions. Willingness to make a 7 to 8 year commitment to the construction project.

To apply: This is a full-time, salaried position at the NEON offices in Washington, DC, subject to the continuing availability of NSF funding. Benefits include healthcare, paid vacation, and retirement plan. Send cover letter, resume, salary history, and salary requirements to: **NEON Administrative Director, attn. NEON Project Manager Search, AIBS, 1444 Eye St. NW, Suite 200, Washington, DC 20005, FAX; 202-628-1509, bwec@aibs.org.**



RAPID ACCESS TO PREVENTIVE INTERVENTION DEVELOPMENT "RAPID" PROGRAM

National Cancer Institute

The National Cancer Institute announces the ongoing initiative: Rapid Access to Preventive Intervention Development (RAPID). RAPID will make available to academic investigators the preclinical and early clinical drug development contract resources of NCI's Division of Cancer Prevention. In some instances resources will be provided to the investigator. The goal of RAPID is the rapid movement of novel molecules and concepts from the laboratory to the clinic for clinical trials of efficacy. RAPID will assist investigators who submit successful requests by providing any (or all) of the pre-clinical and phase 1 clinical developmental requirements for phase 2 clinical efficacy trials. These include, for example, preclinical pharmacology, toxicology, and efficacy studies; bulk supply, GMP manufacturing, and formulation; and regulatory and IND support and phase 1 clinical studies. Suitable types of agents for RAPID may range from single chemical or biological entities to defined complex mixtures with the potential to prevent, reverse, or delay carcinogenesis. For more detailed information, visit the web site, <http://cancer.gov/prevention/RAPID>

Requests for RAPID resources are to be submitted as described in the web site. Written requests will be evaluated by a specially constituted RAPID panel, consisting of outside experts from academia and industry. Requests must be received on or before **November 1, 2006**. Applications should be submitted directly to the office listed below. Inquiries are encouraged, and the opportunity to clarify issues or questions is welcome. Please contact:

RAPID Program Official, Executive Plaza North, Room 2117, 6130 Executive Blvd., Bethesda, MD 20892, Rockville, MD 20852 (for express/courier service), Telephone: (301) 435-5011, Email: kapetani@mail.nih.gov, Or Telephone: (301) 594-0459, Email: jc94h@nih.gov, Fax: (301) 402-0553.



Laboratory of Signal Transduction National Institute of Environmental Health Sciences Research Triangle Park, North Carolina

Postdoctoral Position in Stress Induced Signaling Pathways Elizabeth Murphy, Ph.D.

The Cell Biology group is investigating the cellular response to stress. One area of research involves the study of stress induced signaling pathways which protect against subsequent injury. Our lab is studying preconditioning, a process in which brief intermittent periods of stress reduce lethal injury during a subsequent prolonged period of stress such as ischemia. We are investigating these protective mechanisms in perfused hearts and isolated cells. A second area of research involves investigating signaling pathways involved in apoptosis. Our laboratory is particularly interested in alterations in calcium homeostasis and its role in apoptosis.

TO APPLY: Submit a cover letter, curriculum vitae, bibliography and the names of three references to: **Dr. Elizabeth Murphy, National Institute of Environmental Health Sciences, Laboratory of Molecular Carcinogenesis, P.O. Box 12233 (D2-03), Research Triangle Park, NC 27709, murphy1@niehs.nih.gov (919)541-3873, Fax: (919)541-7880**



National Institute of General Medical Sciences Office of Scientific Review SCIENTIFIC REVIEW ADMINISTRATOR

The National Institute of General Medical Sciences (NIGMS), a major research component of the National Institutes of Health (NIH) and the Department of Health and Human Services (DHHS), is seeking applications from exceptional scientists to serve as **Scientific Review Administrator in the Office of Scientific Review**. The individual selected will organize and manage the comprehensive scientific and technical merit review of applications for research programs and/or research training and career development grants through interaction with established scientists in a variety of fields. Scientific Review Administrators are responsible for assuring the fairness and consistency of the scientific peer review process, and for providing technical guidance on peer review policies and procedures and review criteria to applicants, reviewers, and Institute staff.

Qualifications: The successful individual will possess a Ph.D., M.D. or equivalent degree in a field relevant to the position, have research experience in biochemistry, cell and molecular biology, pharmacology, or biophysics (or a closely related area), an in-depth knowledge of biological processes, leadership and managerial skills, and strong oral and written communication skills. Applicants must be U.S. citizens.

Salary: The current salary range is \$65,048 - \$118,828, depending on experience and accomplishments; a full Civil Service package of benefits (including retirement, health, life and long term care insurance, Thrift Savings Plan participation, etc.) is available.

How to Apply: Position requirements and detailed application procedures are provided in vacancy announcement **NIGMS-06-129154**, which can be obtained by accessing the NIGMS website at <http://www.nigms.nih.gov>. All applications and supplemental information must be received no later than **August 18, 2006**. For additional information, contact **Ms. Eric Bandak at (301) 594-2035**.



Chief, Neural System Psychopathology Program

The National Institute of Mental Health (NIMH), National Institutes of Health (NIH), Department of Health and Human Services (HHS), is seeking candidates for Chief, Neural Systems Psychopathology Program, within the Clinical Neuroscience Research Branch, Division of Adult Translational Research (DATR). This program supports research that seeks to understand the neural basis of psychopathology at a systems neuroscience level. The Research focuses on how the integration of multiple neural signals, circuits and/or structures leads to symptoms or symptom complexes that are characteristic of mental disorders. This position will provide leadership and guidance within the area of Neural Systems Psychopathology across multiple grant and contract funding programs within the Branch, and will play important roles in establishing goals and directions of therapeutics initiatives and activities within the Branch and Division. The scientific and technical background appropriate for these positions could come from any of a large number of areas, including, but not limited to: psychiatry, neurology, human clinical trials, neuropharmacology, clinical pharmacology, clinical neuroscience, neuroimaging, genetics, molecular neurobiology, etc. While not a requirement, regulatory and/or industry experience in CNS clinical development would be desirable. Candidates must have at least an M.D. and/or Ph.D. Individuals filling this position will work closely with the Branch Chief, Clinical Neuroscience Research Branch, DATR. The ability to work both independently and collaboratively is required. Strong scientific, analytic, communication, and organizational skills are also required. Salary will be commensurate with experience. Send CV and bibliography by email to **Steven J. Zalcman, M.D., at szalcman@mail.nih.gov (Tel: 301-443-1692) by October 1, 2006**. With nationwide responsibility for improving the health and well being of all Americans, the Department of Health & Human Services oversees the biomedical research programs of the National Institutes of Health (<http://www.os.dhhs.gov>).



WWW.NIH.GOV



Health Scientist Administrator

Are you interested in an exciting, meaningful and challenging career working with some of the most outstanding scientists in the world? Then the National Institute of Mental Health (NIMH), a major research component of the National Institutes of Health (NIH) and the Department of Health and Human Services, invites you to apply for the position of Health Scientist Administrator in the Division of Extramural Activities, Extramural Review Branch (ERB).

The NIMH mission is to reduce the burden of mental illness and behavioral disorders through research on mind, brain, and behavior. The ERB is responsible for the initial review of the scientific merit of grant applications (e.g., research and training grants, fellowship applications, cooperative agreement concepts and applications), contracts and for concept review of Research and Development contracts. The successful candidate will join a highly interactive and diverse group of scientists and will be responsible for all aspects of planning, coordinating, directing, and implementing peer reviews of all applications and proposals focusing on the area listed in the mandatory selection criteria (see below). You will have the opportunity to meet and work with top scientists in the country and participate in the process of implementing state-of-the-art research in mental health.

Experience is required in the professional knowledge of principles, theories, and research methods pertaining to the neurobiology, diagnosis, treatment and prevention of HIV/AIDS (e.g., etiology, epidemiology, assessment, development/efficacy/effectiveness of psychosocial and/or pharmacological interventions).

In order to qualify for this career position you should have a doctoral degree in a relevant field of biomedical and /or behavioral science and appropriate clinical experience. Salary will be commensurate with experience and expertise.

Your letter of interest for this position, including a brief description of career interests, a curriculum vitae and a bibliography, should be submitted to: **Dr. Henry Haigler, NIMH, NIH c/o Ms. Amita Patel, 6001 Executive Blvd., Room 6166, Bethesda, MD 20892-9609; Tel. (301) 443-8865; FAX:(301) 480-3402; e-mail: apatel@mail.nih.gov**. For information concerning the nature of the job, contact **Dr. Henry Haigler at (301) 443-7216 or e-mail hhaigler@mail.nih.gov**. The Institute has a strong commitment to the diversity of its workforce and a biomedical research environment that reflects the diversity of the American population (<http://oeo.od.nih.gov/>).



Director, Division of Pediatric Translational Research and Treatment Development

The National Institute of Mental Health, a major research component of the National Institutes of Health (NIH) and the Department of Health and Human Services (DHHS), is seeking exceptional candidates for the position of Director, Division of Pediatric Translational Research and Treatment Development (DPTR). This position provides overall scientific, programmatic, and administrative leadership for an extramural grants and contracts portfolio of approximately \$138 million and manages a staff of 22 individuals (<http://www.nimh.nih.gov/dptr/dptr.cfm>). The DPTR Director is responsible for developing a vision for research and training to bridge basic science into a better understanding of pediatric psychopathology from a developmental perspective, resulting in the discovery of novel treatment and prevention strategies. The Director should also have a keen appreciation for developing a grants and contracts portfolio that guides the national agenda for research on mental illnesses in children.

Applicants must possess an M.D. with a specialty in psychiatry or pediatrics and/or a Ph.D. in neuroscience, psychology, or related discipline with broad senior-level research experience and experience in direct administration of a research program. Applicants should be known and respected within their profession, both nationally and internationally, as distinguished individuals of outstanding scientific competence. Salary is commensurate with experience and accomplishments.

Interested candidates should send a letter of interest, including a brief description of research experience, contact information for at least three references, and a curriculum vitae and bibliography to: **Dr. Daniel Pine, Chair, Search Committee for Director, DPTR at NIMHsearch@mail.nih.gov or at 6001 Executive Blvd. Room 8235, MSC 9669, Bethesda, MD 20893 (Rockville, MD 20852 for express or courier service)**. Review of applications will begin on **August 15, 2006**, but applications will continue to be accepted and considered until the position is filled.

The NIH encourages the application and nomination of qualified women, minorities, and individuals with disabilities.



**Chief, Laboratory of Bacterial Diseases
National Institute of Allergy and Infectious Diseases
National Institutes of Health**

The National Institute of Allergy & Infectious Diseases (NIAID), Division of Intramural Research (DIR) is seeking an outstanding individual to head the newly established Laboratory of Bacterial Diseases (LBD) in Bethesda, Maryland. The laboratory is to be located in the new C.W. Bill Young Center for Biodefense and Emerging Pathogens located on the NIH campus in Bethesda, Maryland.

The mission of the LBD will be to study basic and applied aspects of bacterial diseases related to biodefense or emerging and re-emerging pathogens, focusing on pathogenic bacteria. Exceptional scientists with research interests in basic, translational or clinical aspects of bacterial pathogenesis are encouraged to apply. The long-term goals of the Institute include supporting research that enables the development of new diagnostics, vaccines, and therapeutics.

This position requires an M.D., Ph.D. or equivalent with proven leadership abilities and a strong independent research program. Preference will be given to candidates with a documented record of accomplishment in bacterial disease research, and those whose program(s) are consistent with the mission of the NIAID.

The Laboratory Chief will have independent resources to conduct basic and clinical research and will supervise other Principal Investigators with independent research programs. The successful candidate is expected to lead a strong research program in laboratory and/or clinical research. Committed resources include space, support personnel and an allocated annual budget to cover service, supplies, animals and related resources and salaries. A Laboratory Chief in the DIR is equivalent to a Department Chair in a University or Medical School. Applicants must be U.S. citizens or permanent residents and be eligible for the appropriate security clearance under the CDC Select Agent Program. Salary will be commensurate with experience and qualifications.

Interested candidates may contact **Dr. Karyl Barron, Deputy Director, DIR, NIAID at 301/402-2208 or email (kbarron@niaid.nih.gov)** for additional information about the position and/or infectious diseases research at the NIH.

To apply for the position, candidates must submit curriculum vitae, bibliography, a detailed statement of research interests, and reprints of up to three selected publications, preferably via Email to: Lynn Novelli at novelli@niaid.nih.gov. In addition, the names of three potential references must be sent to **Dr. Steven M. Holland, Chair, NIAID Search Committee, c/o Ms. Lynn Novelli, DIR Committee Manager, 10 Center Drive, MSC 1356, Building 10, Room 4A26, Bethesda, Maryland 20892-1356**. Completed applications **MUST** be received by **Monday, September 25, 2006**. Please refer to **AD#004** on all correspondence. Further information on this position and guidance on submitting your application is available on our website at: <http://healthresearch.niaid.nih.gov>



**Chief, Laboratory of Human Bacterial Pathogenesis
National Institute of Allergy and Infectious Diseases
National Institutes of Health**

The National Institute of Allergy & Infectious Diseases (NIAID), Division of Intramural Research (DIR) is seeking an outstanding individual to head the Laboratory of Human Bacterial Pathogenesis (LHBP) in Hamilton, Montana.

The mission of the LHBP is to study human bacterial diseases related to emerging and re-emerging pathogens. The research to be conducted in the LHBP is to include; 1) the molecular basis of host-pathogen interactions, 2) the genetic basis of bacterial virulence and pathogenesis, 3) the use of animal modeling to define host defense mechanisms and biology and immunology of host-pathogen interactions, and 4) development of novel and improved intervention strategies to control bacterial infectious diseases. The ultimate goal is to develop diagnostics, vaccines, and therapeutics for emerging and re-emerging infectious diseases.

This position requires a Ph.D. and/or M.D. or equivalent with proven leadership abilities and a strong independent research program. Preference will be given to candidates with a documented record of accomplishment in bacterial disease research, and especially to those whose program(s) are consistent with the mission of the NIAID to study emerging and re-emerging bacterial pathogens.

The Laboratory Chief will have independent resources to lead and conduct laboratory research and translational/clinical research, as appropriate. Mechanisms are available to conduct clinical studies at the Bethesda campus and/or to obtain clinical samples through contract mechanisms at non-NIH institutions. The individual will supervise other Principal Investigators with independent research programs investigating the pathogenicity of Staphylococcus and Streptococcus species. Committed resources include space, support personnel, animal resources and an allocated annual budget to cover service, supplies and salaries. A Laboratory Chief in the DIR is equivalent to a Department Chair in a University or Medical School. Salary is dependent on experience and qualifications.

Interested candidates may contact **Dr. Karyl Barron, Deputy Director, DIR, NIAID at (301) 402-2208 or email (kbarron@niaid.nih.gov)** for additional information about the position. To apply for the position, candidates must submit a curriculum vitae, bibliography, a detailed statement of research interests, and reprints of up to three selected publications preferably via email to: **Felicia Braunstein at braunsteinf@niaid.nih.gov or by US Mail to: Ms. Felicia Braunstein, DIR Committee Manager, 10 Center Drive MSC 1349, Building 10, Rm. 4A-30, Bethesda, Maryland 20892-1349**. In addition, the names of three referees must be sent to **Dr. Tom Schwan, Chairperson, NIAID Search Committee, c/o Ms. Felicia Braunstein, DIR Committee Manager, 10 Center Drive MSC 1349, Building 10, Rm. 4A-30, Bethesda, Maryland 20892-1349**. Please note search #005 when sending materials. Completed applications **MUST** be received by **October 6, 2006**. Further guidance on submitting your application is available on our website at: <http://healthresearch.niaid.nih.gov>.



The Argonne Named Postdoctoral Fellowship Program

The Director's Office initiated these special postdoctoral fellowships at Argonne, to be awarded internationally on an annual basis to outstanding doctoral scientists and engineers who are at early points in promising careers. The fellowships are named after scientific and technical luminaries who have been associated with Argonne and its predecessors, and the University of Chicago, since the 1940's.

Candidates for these fellowships must display superb ability in scientific or engineering research, and must show definite promise of becoming outstanding leaders in the research they pursue. Fellowships are awarded for a two-year term, with a possible renewal for a third year, and carry a stipend of \$72,000 per annum with an additional allocation of up to \$20,000 per annum for research support and travel.

Requirements for Applying for an Argonne Named Postdoctoral Fellowship:

The following documents must be sent via **e-mail** to: fellowships@anl.gov by **October 13, 2006**.

- Letter of Nomination (Recommendation from individual who supports your candidacy for the fellowship.)
- Curriculum Vitae (Include the names of the Nominator and two additional reference names.)
- Two letters of reference (It is the candidate's responsibility to arrange that the two reference letters are sent to Argonne via **e-mail** prior to the **October 13, 2006** deadline.)
- Bibliography of publications
- Bibliography of preprints
- Description of research interests to be pursued at Argonne (We encourage applicants to contact Argonne staff in their areas of interest in order to explore possible areas of research.)
- Name(s) of Argonne Division(s) in which you would like to work.

All correspondence should be addressed to Argonne Named Postdoctoral Fellowship Program. One application is sufficient to be considered for all named fellowships.

For additional details, visit the Argonne web site at <http://www.anl.gov>. Argonne is an equal opportunity employer and we value diversity in our workforce.

Argonne is a U.S. Department of Energy laboratory managed by The University of Chicago.



David Croll Professor of Sustainable Energy Systems

Cornell University's College of Engineering has identified sustainable energy systems as a priority area for growth in research and education. We seek an individual for the newly established David Croll Professorship of Sustainable Energy Systems. The David Croll Professor will be expected to lead research and teaching efforts for this strategic priority (<http://www.engineering.cornell.edu/explore/strategic-planning/>).

We will accept applications from persons with distinguished academic and research backgrounds in any of the engineering and scientific disciplines which contribute to knowledge in the energy field. The individual we are seeking must have an outstanding record of engineering and scientific accomplishment in an area critical to energy systems, and vigorous current activity in an energy system suitable to a sustainable future. The successful candidate must possess a clear and broad vision of the central issues of energy and its environmental impacts; a firm grasp of what universities can contribute; and the ability to develop and provide leadership to a multi-disciplinary, university-wide, research and education program devoted to energy and its environmental impacts.

The incumbent will have an appointment in one of the departments of the College. Disciplines in the college currently contributing to energy and environmental impacts research are environmental engineering, chemical engineering, mechanical engineering, electrical engineering, materials science and engineering, and earth and atmospheric sciences.

**Applications should be addressed to
Professor Michael Spencer, Associate Dean of Engineering
241 Carpenter Hall, Cornell University, Ithaca, NY 14853
or by email to Engr_ORGSPE@cornell.edu
Review of applications will begin on September 1, 2006,
and continue until the position is filled.**

Cornell University is an equal opportunity, affirmative action educator and employer.



Cornell University



MRC Laboratory of Molecular Biology, Cambridge International Postdoctoral Fellowships at LMB

The MRC Laboratory of Molecular Biology (LMB) invites applications for a new international postdoctoral fellowship scheme.

The LMB has always welcomed postdoctoral fellows with their own fellowships, funded from the many worldwide funding agencies. The Laboratory is now expanding the opportunities for postdoctoral research at LMB by offering up to four 3-year postdoctoral fellowships per annum. These are open to postdoctoral scientists of any nationality to work in an area of molecular biology at LMB, and are intended to support exceptional, highly motivated and independent individuals at an early stage in their career. The Laboratory provides excellent training in a multi-disciplinary environment and has a distinguished history of hosting postdoctoral fellows who have gone on to become world-leading scientists (see <http://www2.mrc-lmb.cam.ac.uk/archive/pastmem.html>).

Before submitting a formal application, applicants must discuss their proposal with, and be supported by an LMB group leader who is willing to accommodate the research proposed within their available laboratory space. However, the fellowship will be awarded to the applicant as an individual and not to the group they will be joining. Descriptions of the current research interests of the 60 research groups can be found on the LMB website at <http://www2.mrc-lmb.cam.ac.uk> or in the laboratory brochure (copy can be requested from lmbpostdoctoralfellowships@mrc-lmb.cam.ac.uk).

For details of the fellowships, eligibility and how to apply, please go to <http://www2.mrc-lmb.cam.ac.uk/LMBpostdoctoralfellowships.html>. The closing date for applications is October 31st 2006, for a start date between March and December 2007. LMB postdoctoral fellows will have the status of MRC Career Development Fellows, with a salary in the range of £25,000 - £30,000 per annum and access to the optional MRC final salary pension scheme as well as on-site childcare, sports and social facilities.

This is a No Smoking site.
For further information about MRC, visit www.mrc.ac.uk
The Medical Research Council is an Equal Opportunities Employer.
'Leading Science for Better Health'

PENN STATE



Head, Department of Biochemistry and Molecular Biology

Penn State is seeking an individual with an outstanding research record and excellent interpersonal skills who can provide energetic and creative leadership for its Department of Biochemistry and Molecular Biology. The Department has 38 faculty members with interests that include gene regulation, genomics and bioinformatics, biophysics and structural biochemistry, microbiology, virology, cell biology and developmental biology. A number of additional faculty appointments are anticipated over the next few years. The research programs in the Department are currently supported by annual grant awards exceeding \$12 million. The Department has vigorous undergraduate and graduate educational programs and participates in a number of interdisciplinary graduate programs. The Department also plays a major role in the broader life sciences community in the Eberly College of Science and across Penn State. Further detailed information may be found at the Department's Web site at <http://www.bmb.psu.edu>. The position is available for Fall 2007. Credentials appropriate to the rank of tenured full professor are required. Review of applications and nominations will begin October 1, 2006 and will continue until the position is filled. Applications, including curriculum vitae and the names of three references, and nominations may be submitted via email to mlb1@psu.edu or mailed to:

BMB Head Search Committee
Eberly College of Science, 517 Thomas Building
The Pennsylvania State University
University Park, PA 16802

Penn State is committed to affirmative action, equal opportunity and the diversity of its workforce.

PENN STATE Making Life Better



**Initiative in Global
Environmental
Change and
Conservation Biology**

The College of Agricultural and Environmental Sciences, University of California, Davis, is participating in an initiative in the area of global environmental change and conservation biology that includes the recruitment of six new positions. Three of these positions will be recruited now and three will be recruited during the next year. All positions will be tenure-track at the **ASSISTANT PROFESSOR** level (unless otherwise stated below), with the possibility of an appointment in the California Agricultural Experiment Station.

The positions currently being recruited include:

QUANTITATIVE ANIMAL CONSERVATION ECOLOGIST – We are especially, but not exclusively, interested in candidates who research how large-scale environmental change will affect the abundance, distribution, and role in ecosystem functioning of fishes or amphibians. To ensure consideration applications must be submitted by September 22, 2006.

ECOSYSTEM BIOGEOCHEMICAL MODELER – We are interested in an ecosystem biogeochemical modeler who has strong skills and interests in understanding and forecasting ecosystem dynamics in the context of global and regional environmental change. To ensure consideration applications must be submitted by September 22, 2006.

BIOECONOMIC MODELER – This position is being recruited at the Associate and Full Professor ranks, with tenure. The selected candidate will be expected to have skills and interests in integrating concepts from economics and ecology into quantitative bioeconomic models. To ensure consideration applications must be submitted by November 1, 2006.

Recruitments that will follow these first three include (1) GLOBAL CHANGE INFORMATICS: This position will focus on assessing the impacts of global change using databases at a large scale. **(2) CONSERVATION VALUATION ANALYST:** This position will explore society's views of species, ecosystem services, and intrinsic value of wilderness areas by combining methods from cognitive psychology, survey design, statistics, and econometrics to address hypothetical trade-off scenarios. **(3) QUANTITATIVE PLANT CONSERVATION ECOLOGIST:** This position will focus on quantitative landscape and plant population models needed to forecast best practice strategies for maintenance of biodiversity and to shape the agricultural economy of the state.

Please visit <http://recruitments.caes.ucdavis.edu/> for additional information about these positions and the Global Environmental Change and Conservation Biology initiative at UC Davis, and for application requirements. If you experience problems with the website, please contact us at recruitments@caes.ucdavis.edu.

The University of California is an Affirmative Action/Equal Opportunity Employer.



National Institute on Aging

NATIONAL INSTITUTE ON AGING
NATIONAL INSTITUTES OF HEALTH
DEPARTMENT OF HEALTH AND HUMAN SERVICES



CHIEF, LABORATORY OF EXPERIMENTAL GERONTOLOGY

The Intramural Research Program (IRP) of the National Institute on Aging (NIA), Baltimore, Maryland is seeking a Tenured Senior Investigator for the position of Chief, Laboratory of Experimental Gerontology (LEG).

The Chief, LEG will be responsible for a wide-ranging intramural laboratory program of research in experimental models focused on the in vivo biology of aging and interventions that retard aging processes. One of the major ongoing projects is a longitudinal study of the potential beneficial effects of calorie restriction on aging in nonhuman primates. An interest in interventions to alleviate or prevent aging-related deficits would be valuable.

The LEG is an intramural Laboratory, with at least three principal investigators including the Chief. In addition to the NIA Primate Aging Study, the Laboratory includes current members organized into two units: Aging, Metabolism, and Nutrition Unit (AMNU) and the Functional Genomics Unit (FGU). The AMNU applies whole body physiological and tissue-specific molecular approaches to investigate effects of nutritional interventions on basic mechanisms of aging and age-related diseases. The goal of the Functional Genomics Unit (FGU) is to understand molecular and cellular mechanisms of aging with focus on characterizing the molecular changes associated with aging and how these changes might be prevented.

The ideal candidate will have a doctoral degree and will have shown a productive interest in the study of aging and/or age-related diseases or processes and a proven record of excellence in laboratory and/or clinical research, as demonstrated by publication in the highest quality peer-reviewed journals, participation in invited national and international meetings, and receipt of research awards. Furthermore, consistent with the priorities of the NIH, an established track record of success in mentoring scientists-in-training, will contribute to the evaluation process. Compensation (which may include a recruitment or retention incentive up to 25% of pay) and resources are commensurate with research experience and accomplishments. A full package of benefits (including retirement, health, life and long-term care insurance) is available. To apply, please send a cover letter, curriculum vitae, bibliography, and three letters of recommendation to: Peggy Grothe, Intramural Program Specialist, Office of the Scientific Director (Box 09); **Vacancy #IRP-06-06**; National Institute on Aging, 5600 Nathan Shock Drive, Baltimore, MD 21224-6825. Position will remain open until **September 30, 2006**. If additional information is needed, please call 410-558-8012 or email: grothep@grc.nia.nih.gov.

Additional information regarding the NIA IRP and the LEG is available at the following websites: <http://www.grc.nia.nih.gov>; <http://www.nih.gov/nia>; and <http://www.grc.nia.nih.gov/branches/leg/leg.htm>



DHHS and NIH are Equal Opportunity Employers



Argonne
NATIONAL
LABORATORY

Assistant Ecologist

The Environmental Science Division of Argonne National Laboratory, one of America's premier science/technology R&D centers located 25 miles southwest of Chicago, Illinois, is seeking qualified applicants to conduct environmental studies on the effects of human activities (especially energy developments) on terrestrial or aquatic ecosystems. Responsibilities include collecting, analyzing, and evaluating data; developing approaches for investigating the effects of human activities on terrestrial or aquatic ecosystems; developing monitoring, mitigation, or cleanup strategies; and effectively documenting the results of the work. Strong communications skills and the ability to work effectively with a multidisciplinary team of scientists and engineers are a must.

Candidates with a Ph.D. and one or two years of postdoctoral experience are preferred, although others with advanced degrees will be considered.

Postdoctoral Appointment

The Environmental Science Division of Argonne National Laboratory has an immediate opening for a postdoctoral appointee in the area of aquatic or terrestrial ecology. The successful candidate will assist Argonne scientists in evaluating the effects of human disturbances (especially energy developments) on aquatic or terrestrial ecosystems; collecting, analyzing, and evaluating data to characterize the impacts of development on ecosystems; designing and implementing studies to inventory and monitor ecosystems; and preparing reports and publications.

A Ph.D. in aquatic ecology, terrestrial ecology, environmental biology, or other natural science discipline, received not more than three years prior to the start of the appointment is required. This is a one-year position with a possibility of additional one- to two-year extension.

We offer a comprehensive compensation and benefits package. Interested candidates should submit a detailed resume and salary history through the Argonne web site at <http://www.anl.gov/jobs> under job search for requisition number EVS 310594 (Assistant Ecologist) or EVS 310649 (Post doc). Candidates for the postdoctoral appointment should include a list of publications, and the names and addresses of three references.

A U.S. Department of Energy laboratory managed by The University of Chicago. *Argonne is an equal opportunity employer, and we value diversity in our workforce.*



**Department of Health and Human Services (DHHS)
National Institutes of Health (NIH)
National Heart, Lung and Blood Institute (NHLBI)**

Medical Officer Vacancy

The Department of Health and Human Services and the National Institutes of Health announce a Medical Officer vacancy to serve in the Division of Blood Diseases and Resources, National Heart, Lung and Blood Institute. The position is located in the Thrombosis and Hemostasis Program. The incumbent will utilize clinical expertise and skills in reviewing clinical research protocols, monitoring and oversight of performance and evaluating clinical outcomes and data. The Medical Officer will be part of a team that directs and manages a national program in thrombosis and hemostasis and will share leadership responsibilities in research grants administration, reporting progress, and identifying opportunities in future research, especially clinical research.

Qualifications: An M.D. with some research experience in hematology/cardiology, especially in clinical protocol development, monitoring and management. Desirable qualifications: peer-reviewed publications, research experience in any area of blood coagulation or thrombosis, ability to communicate and function as a team. U.S. citizenship required.

Appointment will be made at the GS-14 or GS-15 grade level (\$91,407 to \$139,774). A Physician's Comparability Allowance (PCA) up to \$30,000 will be paid. The grade and amount of PCA will be based on the requirements of the position and the selectee's experience and qualifications. A Recruitment Incentive may be paid. Position offers health, life, retirement and personal leave benefits.

How to apply: Detailed vacancy information and application instructions can be found at <http://www.usajobs.opm.gov> under announcement number **NHLBI-06-136508**. All applications must be received by the closing date **August 31, 2006**. For additional information contact: Christopher Duggan at 301-402-8028.



DHHS and NIH are Equal Opportunity Employers





Molecular FOUNDRY
A USER FACILITY FOR NANOSTRUCTURED MATERIALS
MATERIALS SCIENCE DIVISION • LAWRENCE BERKELEY NATIONAL LABORATORY

Scientific Positions at the Molecular Foundry

The Molecular Foundry is seeking highly accomplished and innovative scientists to fill 15 positions in its six facilities.

- Imaging and Manipulation of Nanostructures:**
Scanning probe, electron, and optical microscopy
- Organic and Macromolecular Synthesis:**
Design, synthesis, and characterization
- Inorganic Nanostructures:**
Synthesis and characterization of nanotubes, nanowires, and nanocrystals
- Biological Nanostructures:**
Synthesis, conjugation, and characterization
- Nanofabrication:**
Beam and imprint lithography
- Theory of Nanostructured Materials:**
Theory and computation of nanoscale phenomena

These scientists will design and lead a vigorous individual research program in an area of relevance to the Foundry mission and devote equal effort to collaborating with outside users on peer-reviewed projects.

Particularly accomplished scientists who have also demonstrated successful management of large groups of investigators will be considered for "Lead Scientist" positions, with operational and managerial responsibility for one of the six facilities.

Scientists will generally be appointed to 5-year term positions which, with continued positive performance and current DOE funding projections, we anticipate will become career (indefinite) positions. "Lead Scientist" positions may be filled at the career level. Appointees are employees of the University of California. More detailed position descriptions/application requirements:
<http://foundry.lbl.gov/index.html>

Lawrence Berkeley National Laboratory is an AA/EEO employer, committed to a diverse workforce.



The Molecular Foundry at Lawrence Berkeley National Laboratory (LBNL) is a newly constructed, state-of-the-art Department of Energy "user facility" for the design, synthesis, and characterization of materials with nanometer dimensions. Its programs are tightly linked to the breadth of world class research activities at LBNL and the UC Berkeley campus. Its charter defines two primary missions:

- 1) Conduct outstanding research across the breadth of nanoscience, and
- 2) Collaborate with scientists who visit to use its state-of-the-art instruments, techniques, and expertise to further their own research efforts.

FACULTY POSITIONS IN PLANT AND MICROBIAL BIOLOGY

The Institute of Plant and Microbial Biology, Academia Sinica, Taipei is enthusiastically inviting applications for two or more faculty positions in the research areas of 1) microbiology (including mycology, bacteriology and virology) related to plants, and 2) biochemistry, cellular biology and genetics of plants.

These positions are at the level of Assistant Research Fellow (equivalent to Assistant Professor in universities), however applications for more senior levels are also welcome. Excellent facilities and starter grants will be provided for these positions.

For details of the Institute and Academia Sinica, please visit the website at <http://ipmb.sinica.edu.tw/>. Applicants are expected to have a PhD degree plus postdoctoral training.

Chinese language skills are NOT required and international scientists are encouraged to apply. The application folder should include curriculum vitae, a statement of research accomplishments, and future research plans.

The application folder and at least three letters of recommendation should be sent to:

**Dr. Tuan-hua David Ho, Director,
Institute of Plant and Microbial Biology,
Academia Sinica, Academia Rd, Nankang,
Taipei, Taiwan 11529
FAX: (+886)2-2782-1605
e-mail: thdh@sinica.edu.tw**

The review of applications will start on Oct 1, 2006 until the positions are filled.

GOLDBELT RAVEN LLC

Due to continued growth, Goldbelt Raven, LLC, has an immediate need for experienced research personnel for positions in the Frederick, MD and Fort Bragg, NC areas.

If you're interested in joining the Goldbelt Raven team and think you may qualify for one of the positions listed below, please fax your resume to our **HR Department** at **301-695-5403**.

- Sr. Research Physician-Frederick, MD**
- P/T Sr. Research Physician-Frederick, MD**
- Lead Research Physician-Frederick, MD**
- Sr. Management Analyst-Frederick, MD**
- P/T Sr. Management Analyst-Frederick, MD**
- Clinical Research Coordinator-Frederick, MD**
- Clinical Research Study Coordinator-Frederick, MD**
- Biomedical Research Laboratory Technician-Frederick, MD**
- Medical Technical Writer-Frederick, MD**
- Staff Scientist-Frederick, MD**
- Clinical Research Study Nurse-Fort Bragg, NC**
- 2-Licensed Practical Nurses-Fort Bragg, NC**

All positions require U.S. Citizenship

What's your next career move?

Get help from the experts.

www.sciencecareers.org

- Job Postings
- Job Alerts
- Resume/CV Database
- Career Advice from Next Wave
- Career Forum
- Graduate Programs
- Meetings and Announcements

ScienceCareers.org

We know science



Microbial Ecology Positions

POSITION SUMMARY: This position is for a Microbial Ecologist at the Staff Scientist or Senior Scientist level (Ph.D. plus eight or more years of postdoctoral experience), who will work within an innovative microbial ecology and environmental engineering department. The level of the position will be determined upon experience and number of years of postdoctoral experience. Molecular microbial ecology of groundwater, vadose zone, soil, and water contamination (organics and metals), and air should be the primary research focus. To learn more, please visit <http://www-esd.lbl.gov>.

DUTIES: The qualified individual will conduct research associated with soil microbiology, microbial ecology, in situ bioremediation, environmental biotechnology, bioreactors for remediation, and environmental monitoring associated with surface and subsurface habitats at the United States Department of Energy's (DOE) legacy sites and California. The successful applicant is expected to work on existing projects with staff scientists at the Center for Environmental Biotechnology at LBNL and develop their own research program in the area of molecular microbial ecology. Collaboration with the Virtual Institute for Microbial Stress and Survival (Genomes to Life Program) and the Joint Genome Institute are also strongly encouraged. Emphasis will be placed on research studies on the natural and engineered biodegradation of organics (e.g. PAHs, PCBs, nitroaromatics, and solvents) and metals (e.g. Cr, Se, U, and Hg), carbon sequestration, climate change, and environmental issues related to homeland security.

QUALIFICATIONS: Applicants should be senior level Ph.D.s with eight or more years of postdoctoral experience and an established record of publications and competitive research funding from DOE and other federal agencies for the staff scientist level. For the Senior Scientist position, the applicant must have an internationally recognized scientific reputation in the area of molecular microbial ecology with fifteen plus years of postdoctoral experience. A distinguished record of publication in high impact scientific journals is expected. Generally the applicant's expertise should be in the area of microbial ecology, soil microbiology, environmental biotechnology, or molecular microbiology. Hands-on experience with field studies of bioremediation is highly desirable. It is also required that the applicant make use of molecular techniques in their research, e.g. microarray technology. The candidate should have strong interpersonal and organizational capabilities related to large-scale studies, as well as demonstrated ability to direct large research programs successfully. The applicant's research must be compatible with the DOE's Genomes to Life program. The successful applicant should be focused on solving environmental industrial problems through innovative research and development activities, as well as developing a niche of innovative research addressing the DOE's environmental needs.

NOTE: There are potentially multiple positions open for well qualified candidates.

A letter of interest, resume, and names of three references are required for application. For fastest consideration, apply online at: <http://jobs.lbl.gov>, select "Search Jobs", and enter 016449 in the keyword search field. Inquiries may be directed to Dr. Terry Hazen at TCHazen@lbl.gov.

LBNL is an Affirmative Action/Equal Opportunity Employer committed to the development of a diverse workforce.

For more information about LBNL and its programs, visit <http://www.lbl.gov>.



Lawrence Berkeley National Laboratory (LBNL) is located in the San Francisco Bay Area on a 200-acre site in the hills above the University of California's Berkeley campus and is managed by the University. A leader in science and engineering research for more than 75 years, Berkeley Lab is the oldest of the U.S. Department of Energy's National Laboratories.

Yong Loo Lin School of Medicine
Department of Physiology



Programme in Cell and Molecular Physiology

The Department of Physiology, Yong Loo Lin School of Medicine, National University of Singapore, invites applications for full time tenure-track faculty positions.

The department has strengths in Cell and Molecular Physiology. We are looking for a Principal Investigator at the level of senior Asst Professor or Assoc Professor to strengthen the department in the area of Cell Death and Survival, with emphasis on apoptosis, cellular differentiation, proliferation and cell motility. Candidates must demonstrate a good track record in research achievements and teaching. Having a basic degree in medicine (MD or MBBS) will be advantageous. Candidates are expected to apply for independent research funding in Singapore and are required to participate in undergraduate and / or graduate level teaching. Salary will be commensurate with qualifications and experience.

Please submit full curriculum vitae, description of research interests and the names of six referees with full contact details by 12 October 2006 to:

**Head, Recruitment Committee,
Department of Physiology, Yong Loo Lin School of
Medicine, National University of Singapore, Block MD9,
2 Medical Drive, Singapore 117597.
Email: phstmn@nus.edu.sg
Fax: +65 6778 8161**

Only shortlisted candidates will be notified.



College of Life Science,
Peking University (PU)



**Temasek Life Sciences Laboratory Limited,
National University of Singapore (TLL)**

A Joint Zebrafish Development Biology Laboratory

Principal Investigator position is open for outstanding individuals to establish their independent research program based in the new lab. Candidates are expected to have a record of excellent and internationally recognized research accomplishments in areas related to Zebrafish Developmental Biology. The successful applicant will be a Faculty member of the College of Life Sciences, Peking University. Internationally competitive salary, start-up fund and experiment facilities will be provided by PU and TLL.

Applications, including a full CV, a list of publications, further research plans, and at least three names of referees should be submitted before September 30th, to:

**Dr. Wei Dong,
Center of Developmental Biology and Genetics,
College of Life Sciences,
Peking University, Beijing 100871, P. R. CHINA.**

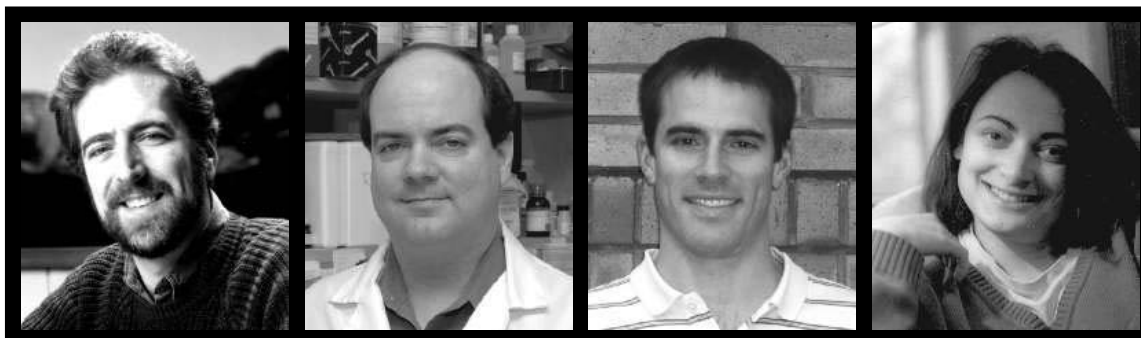
For further information, please contact directly by
telephone: **+86 10 62756185**, or
email: dongwei@pku.edu.cn

NEW ADVISERS
from Industry & Academia

Science Careers Forum

- How long should it take to get my Ph.D.?
- Academia or industry?
- What will make my resume/cv stand out?
- How do I negotiate a raise?

Connect with Experts



Moderator Dave Jensen
Industry Recruiter

Mr. Jensen has over 20 years of experience in human resource consulting and staffing for the biotechnology and pharmaceuticals industry.

Kevin Foley, Ph.D.
Associate Director of In Vivo Pharmacology Synta Pharmaceuticals

Kevin Foley's research focuses on the discovery and preclinical development of small molecule drugs. He has served as an NIH grant reviewer and as a member of the Scientific Advisory Board for a biotechnology startup company. He has worked in the biotechnology industry since 1998.

Andrew Spencer, Ph.D.
Scientist PDL Biopharma, Inc.

Andy Spencer has a B.S. in chemistry, and a Ph.D. in biochemistry from Michigan State. As a grad student and postdoctoral fellow, Andy spent over ten years in university research labs before moving to the biotechnology industry in 2003.

Kelly Suter, Ph.D.
Assistant Professor University of Louisville School of Medicine

Kelly Suter has a B.S. in Chemistry, a B.A. in Biology, a Master's in Physiology, and a Ph.D. in Physiology. She did a postdoc at Colorado State University and was a postdoctoral fellow and research assistant professor at Emory University.

www.sciencecareers.org
and click on Career Forum

ScienceCareers.org

We know science



SOLEIL SYNCHROTRON

General Director and Research Directors

SOLEIL is the French synchrotron radiation facility which is going to start its operation for users in January 2007. The source is a third generation storage ring operating at 2.75 GeV. The experimental program includes 24 beamlines among which 11 will start operation in 2007. SOLEIL is expected to be one of the world leaders in the field of synchrotron radiation science and technology and will be open to the international scientific community. More information on SOLEIL and its scientific program can be found on the website <http://www.synchrotron-soleil.fr>

SOLEIL calls for applications for three positions in the directorate which all require scientists with outstanding research experience who can bring scientific vision to the posts. Though not mandatory, an experience in synchrotron radiation methods will be appreciated.

■ **General Director** : he/she will provide leadership in defining and coordinating the scientific and technical development of the facility (beamlines and light source) to ensure that SOLEIL remains at the forefront of the world activity in the field of synchrotron radiation. He/she will have to promote SOLEIL in a national and international context. He/she will also be responsible for the efficient operation of the facility for the users. As the Chief Executive Officer of the SOLEIL non trading company (350 staff members and a yearly budget of about 50 M€), he/she should possess recognized management abilities. He/she will report to the Council whose members are the shareholders of the company, the CNRS and the CEA. He/she will represent SOLEIL at the national and international levels as well as in any legal issue. He/she will be assisted by a senior management team with four associate directors (light source, science and administration) and two division leaders (computing and technical services).

■ **2 Research Directors** : they will be in charge of shaping the scientific program to bring it at the forefront of science in the worldwide competition, taking into account the specificities of the SOLEIL light source. They should therefore have a recognized expertise in one or several of the following fields: physics, material sciences (hard and soft matter), chemistry, life sciences, earth and environmental sciences, and have some background in other ones. They are also expected to boost the development of industrial applications as well as the use for societal needs. As responsibilities will be shared amongst them, their exact duties will be defined by the General Director depending on their experience and field of expertise. They both will be in charge of managing the Science Division (150 people among which 72 scientists). Together with the General Director, they will be responsible for the beam time allocation to users' proposals.

The three positions are for five years and the successful candidates are expected to take up their positions in summer 2007. The working place is in Saint Aubin which is located 25 km south of Paris. A working knowledge of both French and English is desirable. If you wish to be considered for one of these positions, please submit a full CV and covering letter detailing your vision of the post and your suitability for it, and a list of four references. Applications and requests for information should be sent to: Dr. Denis RAOUX, General Director, Synchrotron SOLEIL, Orme des Merisiers, Saint Aubin, BP 48, 91192 Gif sur Yvette, France; telephone +33(0)169359010 or email denis.raoux@synchrotron-soleil.fr. All applications should be returned by October 15th 2006.



SCRIPPS
FLORIDA
THE SCRIPPS RESEARCH INSTITUTE

Tenure-Track Positions in Regenerative Medicine

The Scripps Research Institute Florida campus is seeking applicants for two tenure-track faculty positions (PhD or MD/PhD) in a newly formed Department of Regenerative Medicine. This department will focus on a multi-disciplinary approach to cell and tissue generation and regeneration, which may include neuronal, epithelial, hematopoietic, mesenchymal, or germ cell lineages. Emphasis will be placed on individuals who can take advantage of an existing cutting-edge technology infrastructure that includes genomics and cell based screening, proteomics, informatics and significant capabilities in drug discovery. Appointments may be made at any level.

Interested persons should submit a curriculum vitae, two-page statement of research interests, and complete contact information for at least three professional references to:

Chair
Regenerative Medicine Search Committee
c/o Human Resources
Scripps-Florida Research Institute
5353 Parkside Drive
Jupiter, FL 33458

Pharmacology

TENURE-TRACK ASSISTANT/ASSOCIATE PROFESSOR In Pharmacology/Toxicology

The University of Texas at El Paso

The Department of Biological Sciences and the Border Biomedical Research Center at the University of Texas at El Paso (UTEP) is seeking a tenure-track Assistant or Associate Professor starting January 2007 for its expanding research emphasis in pharmacology and toxicology. Candidates that focus on mechanisms of pharmacology/toxicology as related to human disease, small molecule pharmacology, or high-throughput screening are particularly invited, although all areas of pharmacology and toxicology will be considered. In the fall of 2006, the Department ([website: http://academics.utep.edu/biology](http://academics.utep.edu/biology)) will occupy a new state-of-the-art facility, which includes mammalian and aquatic animal facilities, and core facilities in tissue culture, molecular biology, protein chemistry, microscopy, and DNA sequencing. The successful candidate will develop and maintain a strong independent and extramurally funded research program and contribute to both undergraduate and graduate education.

Qualifications Required: Applicants must have a Ph.D. or M.D., and relevant postdoctoral research experience.

Application Procedure: Applications should be sent to: **Dr. Lisa Bain, Department of Biological Sciences, The University of Texas at El Paso, 500 W. University Avenue, El Paso, TX 79968-0519**, and should include curriculum vitae, a statement of research interests, copies of three publications, and contact information for three references. Applications will be reviewed beginning September 1, 2006.

OUR TIME  IS NOW

THE UNIVERSITY OF TEXAS AT EL PASO DOES NOT DISCRIMINATE ON THE BASIS OF RACE, COLOR, NATIONAL ORIGIN, SEX, RELIGION, AGE, DISABILITY, VETERAN STATUS OR SEXUAL ORIENTATION IN EMPLOYMENT OR IN THE PROVISION OF SERVICES.

www.utep.edu

Careers & Graduate Programs for B.S. & M.S. Scientists

Advertising Supplement



Be sure to read this special ad supplement devoted specifically to opportunities for scientists holding B.S. and M.S. degrees, in the upcoming **25 August issue of *Science***.

Find B.S. and M.S. job listings, graduate program listings, and other career resources online at **www.sciencecareers.org**.

Get the experts
behind you.

**Hundreds of BS/MS
job opportunities in print
and online**

For advertising information, contact:

U.S. Daryl Anderson,
phone: 202-326-6543,
e-mail: danderso@aaas.org

Europe and International,
Tracy Holmes, phone: +44 (0) 1223 326 500,
e-mail: ads@science-int.co.uk

Japan Jason Hannaford,
phone: +81 (0) 52 789-1860,
e-mail: jhannaford@sciencemag.jp

ScienceCareers.org

We know science



NEUROIMMUNOLOGY POSTDOCTORAL FELLOWSHIP AT UNC-CHAPEL HILL

The Neuroimmunology Program at the University of North Carolina, Chapel Hill is offering a research fellowship position. Our laboratory is focusing on the cellular and molecular pathogenesis of multiple sclerosis and the translational research leading to new therapies for autoimmune diseases. The main projects in the laboratory are addressing T-cell activation threshold and TCR degeneracy repertoire in patients with MS and other autoimmune diseases. Additionally, we are also focusing on preclinical testing of statins involving cellular assays and gene expression analyses to characterize the immunomodulatory effects of statins. Applicants should have extensive experience in cellular and molecular immunology, lab techniques including tissue culturing, T cell cloning, flow cytometry, ELISA, immunoblotting, and gene expression analysis. The Neuroimmunology laboratory is fully integrated in the Department of Immunology and Microbiology graduate program. Our laboratory is located in the Neuroscience research building, which hosts a gene array and confocal/electron microscopy core facility and is equipped with a flow cytometer, harvester, counter, and all the equipment needed for molecular biology experiments. Close collaborations with Department of Immunology and Microbiology provide stimulative intellectual and collegial environment.

Interested candidates should forward CV and letter of interest to: **Silva Markovic-Plese, M.D., Associate Professor of Neurology, UNC Department of Neurology, CB# 7025, Chapel Hill, NC 27599** or email markovics@neurology.unc.edu. *EOE*



INSTITUTE FOR ADVANCED RESEARCH, NAGOYA UNIVERSITY 15 Tenure-Track Positions (Designated Associate/ Assistant Professors) in All Fields of the Natural Sciences



(Duration of Appointment: November 1, 2006 ~ March 31, 2011)

In recognizing the value of creative research in providing intellectual assets for the future, Nagoya University established the Institute for Advanced Research (IAR) in April 2002 as a research base for achieving the highest level of academic research. IAR's founding director is Dr Ryoji Noyori, the 2001 Nobel Prize Laureate in Chemistry. IAR is the first academic institution in Japan that intensively promotes highly creative research in all academic disciplines. IAR's "Special Rearing Plan for Researchers (Tenure-Track Positions)" has been selected as part of the "Supporting Young Researchers with Fixed-term Appointments" program. This program has been commissioned by the Japanese Ministry of Education, Culture, Sports, Science and Technology (MEXT) and is financially supported by the Special Coordination Fund for Promoting Science and Technology for the financial year of 2006. IAR is inviting applications from young researchers from all over the world for 15 tenure-track positions in all fields of the natural sciences at an associate/assistant professor level. Appointees selected by the IAR Tenure-Track Position Selection Committee will be appointed as designated Associate/Assistant Professors of Nagoya University. Appointees will be provided with an outstanding research environment and will be expected to commit to the highest standards of scholarship and professionalism. Upon completion of the appointment, the appointee may be granted a tenured position (tenured positions at Nagoya University have a compulsory retirement age) if the research undertaken during his/her period of appointment proves to have met the standards agreed upon at the start of the term.

Requirements: A PhD degree in any fields of natural sciences granted within the past 10 years (as of November 1, 2006).

Interested candidates should apply online at: <http://www.iar.nagoya-u.ac.jp/SRPR/index.html>. The closing date is **August 17, 2006**. Offers will be made in late September, 2006. Additional information about IAR and the program can be found at <http://www.iar.nagoya-u.ac.jp/>. Inquiries are handled by email only. Email Address: SRPR_inquiry@iar.nagoya-u.ac.jp.

Nagoya University is an Equal Opportunity Employer.

Creighton UNIVERSITY Medical Center

School of Medicine
Department of Medical Microbiology
and Immunology

Faculty Position in Microbial Pathogenesis

As part of ongoing expansion, the Department of Medical Microbiology and Immunology in the School of Medicine at Creighton University Medical Center invites applications for a tenure-track position at the Assistant, Associate or full Professor level depending on qualifications and experience. Investigators interested in microbial pathogenesis especially in the context of host immune response are encouraged to apply. The appointee will be expected to conduct a vigorous independent research program, with an interest and aptitude for teaching graduate and professional (e.g., medical, dental, and other allied health) students. Generous laboratory space with equipment, competitive start-up funding, and ongoing support with state-of-the-art core facilities will be provided. Applicants should have a Ph.D., M.D., or M.D./Ph.D. degree and postdoctoral training and experience denoting significant research accomplishment and scholarly promise. Senior applicants should have a demonstrated potential to maintain peer-reviewed research funding.

A curriculum vitae, brief summary of research plans and teaching interests, and three letters of recommendation should be sent to: **Richard V. Goering, Ph.D., Professor and Chair, Department of Medical Microbiology and Immunology, Creighton University Medical Center, 2500 California Plaza, Omaha, NE 68178**. Applications will be screened immediately and will continue to be accepted until the position is filled.

*Creighton University is an
Affirmative Action/Equal Opportunity Employer.*

Neuroscience

TENURE-TRACK ASSISTANT/ASSOCIATE PROFESSOR NEUROSCIENCE THE UNIVERSITY OF TEXAS AT EL PASO

The Department of Biological Sciences and the Border Biomedical Research Center at the University of Texas at El Paso (UTEP) is seeking a neuroscientist, with interests in immunology, pharmacology, or toxicology, for a tenure-track Assistant or Associate Professor level position. Candidates able to interface with the infectious disease and/or toxicology units of the Border Biomedical Research Center are encouraged to apply. Preference will be given to those with demonstrated potential for conducting quality, extramurally-funded research, and a commitment to teaching physiology at the undergraduate and graduate levels. A new, state-of-the-art facility containing core facilities for molecular biology, DNA sequencing, tissue culture, protein chemistry and microscopy will house the Department (website: <http://academics.utep.edu/biology>) beginning Fall 2006.

Qualifications Required: Applicants must have a Ph.D. or M.D., and relevant postdoctoral experience. Review of applications will begin August 1, 2006, for an anticipated start date of January 1, 2007.

Application Procedure: Send curriculum vita, statement of research interests and teaching philosophy, copies of three publications and contact information for three references to: Chair, Neuroscience Search Committee, Department of Biological Sciences, University of Texas at El Paso, 500 W. University Ave., El Paso, TX 79968-0519. Questions may be directed to kgosselink@utep.edu



THE UNIVERSITY OF TEXAS AT EL PASO DOES NOT DISCRIMINATE ON THE BASIS OF RACE, COLOR, NATIONAL ORIGIN, SEX, RELIGION, AGE, DISABILITY, VETERAN STATUS OR SEXUAL ORIENTATION IN EMPLOYMENT OR IN THE PROVISION OF SERVICES.

www.utep.edu

Get the experts behind you.



www.ScienceCareers.org

now part of
ScienceCareers.org

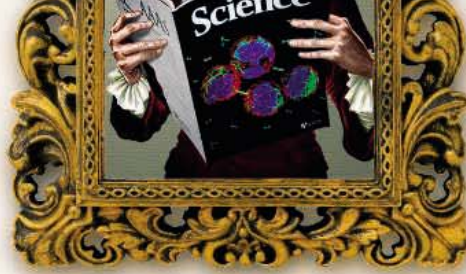
- Search Jobs
- Career Forum
- Next Wave
- Career Advice
- Job Alerts
- Meetings and Announcements
- Resume/CV Database
- Graduate Programs

All features on ScienceCareers.org are **FREE** to job seekers.

ScienceCareers.org

We know science





Career advice, insight and tools.

Turn to the experts for the big picture.
Visit www.ScienceCareers.org



Your career is too important to leave to chance. So to find the right job or get career advice, turn to the experts. At ScienceCareers.org we know science. And we are committed to helping take your career forward. Our knowledge is firmly founded on the expertise of *Science*,

the premier scientific journal, and the long experience of AAAS in advancing science around the world. Put yourself in the picture with the experts in science. Visit www.ScienceCareers.org.

ScienceCareers.org

We know science



POSITIONS OPEN

TENURE-TRACK ASSISTANT PROFESSOR
in Marine Phycology

The Department of Botany, University of British Columbia (UBC) ([website: www.botany.ubc.ca](http://www.botany.ubc.ca)), seeks applications for a tenure-track position in marine phycology. All areas of marine phycology will be considered, but preference will be given to candidates with a strong field-based component to their research and expertise in macroalgal marine biodiversity. The successful applicant will be expected to develop a strong research program and teach courses in phycology and other areas in the UBC Biology Program. Interests in teaching and research at the Bamfield Marine Sciences Centre ([website: www.bms.bc.ca](http://www.bms.bc.ca)) are desirable, and the candidate will interact with the UBC Biodiversity Research Centre ([website: http://www.biodiversity.ubc.ca](http://www.biodiversity.ubc.ca)). Salary will be commensurate with experience. Appointment will be at the Assistant Professor level and is subject to final budgetary approval.

Applicants should send curriculum vitae, a summary of research interests, a statement of teaching philosophy, reprints of key publications, and should arrange to have three letters of reference sent directly to the Department. Applications should be addressed to the: **Chair, Phycology Search, Department of Botany, University of British Columbia, 6270 University Boulevard, Vancouver, BC, Canada, V6T 1Z4**. Electronic applications to e-mail: phycolog@interchange.ubc.ca are preferred, but paper applications will be accepted. Application deadline is October 1, 2006.

The University of British Columbia hires on the basis of merit and is committed to employment equity. All qualified applicants are encouraged to apply; however, Canadian citizens and permanent residents of Canada will be given priority.

POSTDOCTORAL TRAINING GRANT
POSITION

Positions are available for individuals interested in joining an expanding interdisciplinary prostate and urologic cancer program, focusing on androgen receptor intracellular trafficking and the roles of a novel tumor suppressor in prostate cancer. *The applicant should be a U.S. citizen or green card holder.* Applicants should send a letter describing their research interest, curriculum vitae, and the names of at least three persons from whom references can be obtained to: **Vinnette Sommariva, University of Pittsburgh School of Medicine, Department of Urology, Shadyside Medical Center, 5200 Centre Avenue, Suite G40, Pittsburgh, PA 15232. Fax: 412-623-3904.** *The University of Pittsburgh is an Affirmative Action, Equal Opportunity Employer.*

The Department of Molecular Genetics at Ochsner Clinic Foundation, New Orleans, Louisiana, seeks candidates for ASSISTANT RESEARCH SCIENTIST and ASSOCIATE RESEARCH SCIENTIST positions. Applicants must have an M.D. or Ph.D., or alternatively a Master's degree with three years of research experience.

Candidates with strong backgrounds in molecular biology and molecular genetics are encouraged to send their curriculum vitae and references to: **Julia Cook, Ph.D., Department of Molecular Genetics, Ochsner Clinic Foundation, 1516 Jefferson Highway, New Orleans, LA 70121; e-mail jcook@ochsner.org.**

CAREER OPPORTUNITY

This unique program offers the candidate with an earned doctorate in the life sciences the opportunity to obtain the Doctor of Optometry (OD) degree in 27 months (beginning in March of each year). Employment opportunities exist in research, education, industry, and private practice. Contact the Admissions Office, telephone: 800-824-5526 at The New England College of Optometry, 424 Beacon Street, Boston, MA 02115. Additional information at [website: http://www.neco.edu](http://www.neco.edu), e-mail: admissions@neco.edu.

POSITIONS OPEN

INTERDISCIPLINARY: VETERINARY
MEDICAL OFFICER/RESEARCH
MICROBIOLOGIST

GS-0701/0403-12/13/14/15
Salary Range of \$62,291 to \$133,850

The U.S. Department of Agriculture, Agricultural Research Service (USDA/ARS), Arthropod-Borne Animal Diseases Research Laboratory in Laramie, Wyoming, is seeking a permanent, full-time Veterinary Medical Officer/Research Microbiologist to develop research on pathogenic mechanisms, control, and the epizootic cycles of arbovirus diseases. Investigates clinical, virological, serological, immunological, and pathological responses of arboviruses from animals to insects to animals (cycle of infection); the isolation and identification of arboviruses from vectors and animals; and the development and implementation of control strategies for bluetongue, vesicular stomatitis, rift valley fever, and other arbovirus diseases of livestock. To have a printed copy of the vacancy announcement mailed to you, call **Bobbie Bobango** at telephone: 307-766-3606 or access information online at [website: http://www.afm.ars.usda.gov/divisions/hrd/index.html](http://www.afm.ars.usda.gov/divisions/hrd/index.html). Send applications for announcement ARS-X6W-0154R to: **USDA, Agricultural Research Service, Human Resources Division, Attn: Keli A. Martin, 5601 Sunnyside Avenue, Stop 5106, Beltsville, MD 20705-5106, fax: 301 504-1535; e-mail: scirecruit@ars.usda.gov.** Applications must be marked ARS-X6W-0154R and postmarked by September 11, 2006. *Citizenship is required.*

USDA/ARS is an Equal Opportunity Employer and Provider.

ASSISTANT PROFESSOR
Department of Neurobiology and Anatomy
Wake Forest University School of Medicine

The Department of Neurobiology and Anatomy invites applications for the position of Assistant Professor. Applicants should have proven teaching capabilities in multiple components of a human structure course (gross anatomy, histology, embryology) and proven research productivity in sensory physiology. The position will be available January 1, 2007. Candidates should send curriculum vitae, statement of research interest, and three letters of recommendation to: **Search Committee for Human Structure Position, Department of Neurobiology and Anatomy, Wake Forest University School of Medicine, Winston-Salem, NC 27157-1010.** For more information on the Department and areas of research emphasis, visit our [website: http://www.wfubmc.edu/nba](http://www.wfubmc.edu/nba). *Wake Forest University School of Medicine is an Affirmative Action/Equal Opportunity Employer.*

NEUROBIOLOGY RESEARCH-TRACK (FACULTY) AND POSTDOCTORAL POSITIONS.

Available immediately to investigate neural mechanisms of taste representation in the mammalian brainstem. There are three open positions requiring experience with: (1) in vivo electrophysiology, (2) patch clamp electrophysiology, or (3) neuroanatomy. Positions include highly competitive salary and fringe benefits, grant opportunities, and interaction with neuroscientists in the Department ([website: http://www.utm.edu/anatomy-neurobiology/](http://www.utm.edu/anatomy-neurobiology/)) and the Neuroscience Program ([website: http://cns.utm.edu/](http://cns.utm.edu/)). Applicants must have a Ph.D. or M.D. Send applications (curriculum vitae and names of three references) to: **John Boughter (e-mail: jboughter@utm.edu), Department of Anatomy and Neurobiology, University of Tennessee Health Science Center, 855 Monroe Avenue, Suite 515, Memphis, TN 38163.** *University of Tennessee is an Affirmative Action/Equal Employment Opportunity/ADA Employer.*

POSITIONS OPEN

ASSISTANT PROFESSOR, MICROBIOLOGY
University of Washington

The Department of Microbiology is initiating a search for an Assistant Professor whose research interests employ the power and logic of genetics to address complex microbiological problems. The position is a 12-month tenure-track position in the School of Medicine. In addition to research, all University of Washington faculty engage in teaching and service. Possible research areas include, but are not limited to, bacterial development, phage biology, microbial evolution, host-microbe interactions, chromosome mechanics, and regulatory mechanisms.

Applicants with a minimum of two years of post-doctoral experience should send their curriculum vitae, a statement of up to two pages of research interests, and names and contact information for three letters of reference to: **Chair, Search Committee, Department of Microbiology, P.O. Box 357242, HSC Room G-328, University of Washington, 1959 N.E. Pacific Street, Seattle, WA 98195.** Application deadline: October 1, 2006. Salary and benefits are competitive and commensurate with qualifications and experience.

The University of Washington is an Affirmative Action, Equal Opportunity Employer and is building a culturally diverse faculty. Applications from female and minority candidates are strongly encouraged.

SUPERVISORY RESEARCH FISHERY
BIOLOGIST/ECOLOGIST

Vacancy announcement: NMFS-SEFSC-2006-0047/NMFS-SEFSC-2006-0050.

At [website: http://www.usajobs.opm.gov/](http://www.usajobs.opm.gov/).

Title: Chief, National Oceanic and Atmospheric Administration Fisheries, Sustainable Fisheries Division, Miami, Florida. Job Summary: performs scientific work and guides scientific staff who collect data and provide analyses to support the development, conservation, and management of fishery resources. Scientific work includes the evaluation of the impact of human activities (such as fishing, coastal development, and offshore natural resource exploitation) and environmental factors on fishery resources and their habitat.

Open period: Friday, July 21, 2006, to Thursday, August 24, 2006.

FACULTY POSITION IN ECOLOGY

Ithaca College seeks applicants for tenure-eligible ASSISTANT PROFESSOR position in ecology starting August 2007. Research emphasis on animals. Candidate expected to develop active research program with undergraduates, teach general ecology, or an upper level ecology course, and contribute to introductory biology and nonscience major courses. Involvement in environmental studies/science program and prior teaching experience are desirable. More information at [website: http://www.ithaca.edu/biology](http://www.ithaca.edu/biology). Screening of applications begins October 1, 2006; position will remain open until filled. *Ithaca College is an Equal Opportunity/Affirmative Action Employer. Members of underrepresented groups (including people of color, persons with disabilities, veterans, and women) are encouraged to apply.*

ASSISTANT/ASSOCIATE PROFESSOR

One long-term contract FACULTY POSITION. Begin January 2008 preferably, otherwise August 2008. Ph.D. required, primary teaching responsibility anatomy/physiology along with freshman biology courses. Experience in small college preferred. Liberal arts environment. Responsibilities include academic advising, committee work, expected to engage in research with undergraduates, to write grants, and to publish. Strong record of teaching excellence and scholarship desirable. Send letter stating interest, complete resume, transcripts, and three letters of reference to: **Sr. John Karen Frei, Dean, School of Natural and Health Sciences, Barry University, 11300 N.E. Second Avenue, Miami Shores, FL 33161** by October 15, 2006.

2 Great Career Events

Science Career Fair

Science Careers is hosting our annual Boston career fair in conjunction with the upcoming DDT meeting. Come meet recruiters face to face and explore career opportunities for all levels of scientists.

For information on exhibiting, please contact Daryl Anderson at (202) 326-6543.

10 August 2006
11:00 am – 4:00 pm

Seaport Hotel
Plaza Ballroom
Boston, MA



Drug Discovery
Technology™
2006

For more information on these events visit
www.sciencecareers.org/boston

Making the Most of Your Career Fair

If you'll be attending the career fair, maximize your experience by first coming to our free seminar.

8 August 2006
6:00 pm – 7:00 pm
reception to follow
The Conference Center
at Harvard Medical



ScienceCareers.org

We know science



Faculty Careers 2

A Science Advertising Supplement

Looking for a faculty position?

Be sure to read this special ad supplement devoted to faculty career opportunities in the **8 September issue of Science**.

Find faculty position listings and other career resources online at www.sciencecareers.org.

For advertising information, contact:

U.S. Daryl Anderson
phone: 202-326-6543
e-mail: danderso@aaaas.org

Europe and International
Tracy Holmes
phone: +44 (0) 1223 326 500
e-mail: ads@science-int.co.uk

Japan Jason Hannaford
phone: +81 (0) 52 789-1860
e-mail: jhannaford@sciencemag.jp

ScienceCareers.org

We know science



CONFERENCE

• International Conference •

Physiological and Pathological Importance of Gap Junctions

A conference to present the rapid advances in understanding roles of connexins and gap junctional cell-cell communication in normal physiology and pathological mechanisms.

November 20-22, 2006

Auditorium of Amway Japan Limited, Tokyo Japan

Invited speakers:

K. Willecke (Bonn), R. Bruzzone (Paris), X. Gong (Berkeley), D. Kelsell (London), P. Lampe (Seattle), D. Laird (Ontario), J. Saffitz (Boston), D. Spray (New York), G. Van Camp (Antwerp), R. Weingart (Bern), J. Trosko (East Lansing), M. Asamoto (Nagoya), T. Kojima (Sapporo), M. Oyamada (Kyoto), T. Yano (Tokyo)

Topics:

Control of Connexin Functions, Role in Cancer - Mechanisms and Prevention, Cardiovascular Function and Diseases, Role in Nervous System Function and Diseases, and Sensory Organs (Skin Disease, Cataract and Deafness)

Registration/Abstract submission details:

<http://www.gap-junction.jp/>

For further details contact:

Hiroshi Yamasaki, Kwansei Gakuin University, Sanda, Japan
(miyabi@ksc.kwansei.ac.jp)

Organized and Sponsored by:

Japan Connexin Research Group, School of Science & Technology of Kwansei Gakuin University, Nitrilite Health Institute, Amway Japan Limited, The Pharmaceutical Society of Japan

POSITIONS OPEN

MEMORIAL SLOAN-KETTERING
CANCER CENTER

POSTDOCTORAL POSITIONS available for highly motivated candidates with background in genetics and/or molecular/cellular biology to join a research group interested in signaling in thyroid cells and in mechanisms of thyroid carcinogenesis. The projects will encompass the development and refinement of transgenic models of thyroid cancer caused by mutations of mitogen-activated protein kinase effectors, and their inactivation by genetic and pharmacological approaches (see *Cancer Res.* **63**: 1454-7, 2003; *Cancer Res.* **65**: 4238-45, 2005; *Cancer Res.* **65**: 2465-73, 2005; *J. Clin. Invest.* **115**: 94-101, 2005; *Clinical Cancer Research* **12**:1785-93, 2006). Successful candidates will join a laboratory with extensive experience in studying the genetics and biology of thyroid cancer. Applicants should hold a Ph.D. and/or M.D. degree and have strong laboratory and analytical skills. Experience in cell signaling would be very helpful. Informal inquiries may be made to **Dr. James Fagin** at e-mail: fagin@mskcc.org. Applications should be submitted to: **James A. Fagin, M.D., Chief, Endocrinology Service, Memorial Sloan-Kettering Cancer Center, 1275 York Avenue, New York, NY 10021**, to the attention of **Ms. C. Murray-Marone**.

Memorial Sloan-Kettering Cancer Center is an Equal Opportunity Employer with a strong commitment to enhancing the diversity of its faculty and staff. Women and applicants from diverse racial, ethnic, and cultural backgrounds are encouraged to apply.

TENURE-TRACK FACULTY POSITION
Microbiology and Immunology

The Department of Molecular Biology and Immunology invites applications for a full-time tenure-track appointment at the rank of **ASSISTANT PROFESSOR OR HIGHER**. Candidates must hold a Ph.D. and relevant postdoctoral experience with a strong record of excellence in research. The start date is negotiable. Although the research area in molecular biology and immunology is open, preferences will be given to applicants with significant experience in bacterial pathogenesis or molecular virology, infectious disease, or immune response to infection. The successful candidate will be expected to develop and expand an independent, externally funded research program. The individual is also expected to participate in teaching both graduate and medical students.

To insure full consideration, please apply online at **website: <http://www.unthscjobs.com>** and include the following information: (1) current curriculum vitae and list of publications and grant support; (2) brief statement of research interests; and (3) contact information for three references.

University of North Texas Health Science Center is an Equal Opportunity/Affirmative Action Employer. Hiring is contingent upon eligibility to work in the United States. Women and minorities are especially encouraged to apply.

POSTDOCTORAL FELLOW

A Postdoctoral Fellow position is available at Blood Systems Research Institute (BSRI), in San Francisco, California. The position is to study aspects of developmental stem cell biology and immunology related to prenatal therapy (see **Muench and Barcena, *Cancer Control* **11**:2, 105-18, 2004**). BSRI is a research institute dedicated to the science of transfusion medicine, **website: <http://www.bsrif.org>**. Candidates must possess a Ph.D. or equivalent, and a strong background in cell biology, molecular biology, and/or immunology. Send curriculum vitae by August 18, 2006, to e-mail: bsricareers@bloodsystems.org or: **Human Resources, Blood Systems Research Institute, 270 Masonic Avenue, San Francisco, CA 94118**. Fax: 415-775-3859. *Pre-employment drug screen required. Equal Opportunity Employer, Minorities/Females/Persons with Disabilities/Veterans.*

POSITIONS OPEN



POSTDOCTORAL FELLOW POSITION in neuroscience at the Department of Biomedical Sciences of Ohio University College of Osteopathic Medicine. Competitive salary and benefits package offered. This position requires a Ph.D. or M.D. and professional experience in whole-cell or single-channel electrophysiology of brain slice. Candidate with experience in cell/molecular biology with biochemistry or fluorescence imaging technique are also considered. We are looking for a self-motivated individual to join our team effort to study zinc homeostasis and zinc signaling in the brain. For more information on research, visit our **website: <http://www.oucom.ohiou.edu/dbms-li/>**.

This position is available immediately. For full consideration apply by September 1, 2006. Apply online at **website: <http://www.ohiouniversityjobs.com/applicants/Central?quickFind=51678>**.

A statement of research interests and three reference letters should be mailed to: **Dr. Yang Li, Department of Biomedical Sciences, Ohio University College of Osteopathic Medicine, 346 Irvine Hall, Athens, Ohio 45701**, or e-mailed to e-mail: li@oucom.ohiou.edu. We seek a candidate with a commitment to working effectively with students, faculty, and staff from diverse backgrounds. Ohio University is located in a picturesque college town in the rolling foothills of the Appalachian Mountains in southeastern Ohio. *Ohio University is an Affirmative Action, Equal Opportunity Employer with a Dual Career Network (website: <http://www.ohio.edu/dual>).*

POSTDOCTORAL RESEARCH ASSOCIATE
MOLECULAR VIROLOGIST

A Postdoctoral Research Associate position is available immediately to study the latency-reactivation cycle of alpha-herpesviruses, bovine herpesvirus 1 (BHV-1) and herpes simplex virus type 1 (HSV-1). The functional analysis of proteins encoded by transcripts abundantly expressed in latently infected neurons will be pursued. Ph.D. candidates or graduates with a technical background in molecular biology, cell culture, and virology are encouraged to apply. The ability to conduct independent research and supervise students is important. Review of applications will begin August 28, 2006, and continue until position is filled or closed. To apply, access the **website: <http://employment.unl.edu>**. Search for requisition 060548. Complete the Academic Administrative Information Form, attaching application letter, curriculum vitae, and list of three references. *The University of Nebraska is committed to a pluralistic campus community through Affirmative Action and Equal Opportunity. We assure reasonable accommodation under the Americans with Disabilities Act; contact Pat Martinez for assistance at telephone: 402-472-8539.*

POSTDOCTORAL POSITION
Columbia University

We are seeking a highly motivated and talented Postdoctoral for a research project in the area of cellular aging in normal and disease states. Our research objectives focus on the molecular and cellular pathogenesis of premature aging diseases.

Requirements: Ph.D./M.D. degree, at least four years of full-time research experience, fluency in spoken and written English. Applicants should have strong experience in proteomics (including proteome profiling by 2 D gel analysis, database search). Additional experience in molecular and cellular biology techniques is desirable.

Applications should contain your curriculum vitae, a short letter indicating prior research/future goals, and two letters of recommendation; please send by electronic mail only to **Karima Djabali at e-mail: kd206@columbia.edu**.

Columbia University is an Affirmative Action/Equal Opportunity Employer.

POSITIONS OPEN

The United States Department of Agriculture (USDA), division of Animal and Plant Health Inspection Services welcomes applications for a **POSTDOCTORAL FELLOWSHIP** in the Foreign Animal Disease Diagnostic Laboratory located at the Plum Island Animal Disease Center (PIADC), Plum Island, New York. This is a term position funded through the APHIS Science Fellows Program for a period of two years, extendable to four years. The incumbent will conduct research on the development of microarrays for the discovery and diagnoses of emerging viral diseases of animals. Skills in molecular biology and bioinformatics are highly desirable as is a background in virology. The PIADC offers a rich scientific environment with government, industry, and academic collaborations. The PIADC has BSL3 facilities equipped with state-of-the-art equipment for microarrays, virus isolation, molecular cloning, sequencing, electron microscopy, confocal and laser capture microscopy, and large animal studies. *Minimum requirements include U.S. citizenship and a doctoral degree in the life sciences with experience in basic molecular biology techniques. A comprehensive benefits package is included and minimum starting salary is \$56,799. New employees will be subject to a federal background check.* Application for this opportunity should be made electronically by August 28, 2006, deadline to an online application system at the following **website: <http://www.usajobs.opm.gov/>**. The announcement number is 24VS-2006-0071. Follow the instructions as outlined in the vacancy announcement or e-mail: michael.t.mcintosh@aphis.usda.gov for further information. *The USDA is an Equal Opportunity Employer and all qualified candidates are encouraged to apply.*

POSTDOCTORAL RESEARCH SCIENTIST
or ASSOCIATE RESEARCH SCIENTIST
Columbia University Institute for Cancer Genetics

Positions are available at the Postdoctoral research scientist or Associate research scientist level, to study the genetics and epigenetics of human leukemias and the molecular genetics of Down syndrome. Ph.D. or M.D. and related research experience required.

Please send statement of research interests, curriculum vitae, availability, and names of references to: **Dr. Benjamin Tycko, Institute for Cancer Genetics, Columbia University, 1130 St. Nicholas Avenue, New York, NY 10032**. Fax: 212-851-5284; e-mail: bt12@columbia.edu. *Columbia University is an Equal Opportunity/Affirmative Action Employer.*

We deliver —
customized job alerts.

ScienceCareers.org
We know science 

MARKETPLACE

Modified Oligos

@
Great Prices

Get the Details
www.oligos.com

The Midland Certified Reagent Co., Inc.
3112-A West Cuthbert Avenue
Midland, Texas 79701
800-247-8766

SCIENCE THIS ADVANCED ISN'T SUPPOSED TO BE SO EASY.

OLYMPUS IX81 + SPINNING DISK CONFOCAL



5



LOOK CLOSER

Clear, continuous, confocal 4D imaging with improved signal-to-noise and optical sectioning makes the IX81 with DSU Spinning Disk Confocal the workhorse of your lab toolbox.

5 SEE CLEARER

From 10x to 100x, the IX81 with DSU offers five interchangeable disks to match your objective's numerical aperture and specimen type.

+ DO MORE

An incredibly flexible and fully automated setup, the IX81 with DSU makes live cell imaging easier than ever.



OLYMPUS IX81 with DSU
FLEXIBLE, POWERFUL... AND SECOND TO NONE
www.olympusamerica.com/microscopes 800 446 5967

© 2005 Olympus America Inc.

OLYMPUS

Your Vision, Our Future